

Fatigue Damage in the Orthotropic Steel Deck with respect to the Trough-to-Deck Plate Joint in between the Crossbeams



Fatigue damage in the orthotropic steel deck with respect to the trough-to-deck plate joint in between the crossbeams



Delft University of Technology
The Netherlands
Faculty of Civil Engineering and Geosciences
Department of Design & Construction
Section of Structural Engineering



Rijkswaterstaat
Ministerie van Infrastructuur en Milieu

Ministry of Infrastructure and the Environment
Directorate-General for Public Works and Water Management
Construction Department – Infrastructure
Steel & Mechanical Installations

Graduation committee:

Prof. Ir.	A.C.W.M. Vrouwenvelder	(TU-Delft)
Dr.	M.H. Kolstein	(TU-Delft)
Dr. Ir.	P.C.J. Hoogenboom	(TU-Delft)
Ir.	F.J. van Dooren	(Rijkswaterstaat)
Ir.	L.J.M. Houben	(TU-Delft)

Name student: Jingyi Liao
Student number: 1293370
Date: September 2011

"If I have seen further it is by standing on the shoulders of giants"

Isaac Newton

Acknowledgements

This paper presented is the thesis of my master graduation project in the Faculty of Civil Engineering and Geosciences the Delft University of Technology. The study was carried out in cooperation with the Ministry of Infrastructure and the Environment which locates in Utrecht. It was there I performed most of the work. The study focuses on the fatigue damage of orthotropic steel bridges. The objective is to predict the fatigue damage of the bridge deck with respect to the trough-to-deck plate joint.

The starting point of this study is my internship about fatigue in the orthotropic steel bridge. The Internship was also carried out in the Ministry of Infrastructure and the Environment. After the internship, a further analysis on the subject was found to be necessary in order for the maintenance of the old steel bridges and designing of the new steel bridges. Under this circumstance, I was able to continue with this study as my graduation project. In the whole process, all the parties involved provided me with great help. Therefore, I would like to take this chance to thank my supervisor, Ir. Frank van Dooren, who gave me this opportunity and guided me from the initiation to the final stage and helped me to develop an understanding of the subject. Furthermore, I owe my deepest gratitude to Prof. A.C.W.M. Vrouwenvelder, Dr. M.H. Kolstein and Dr. P.C.J.Hoogenboom. Without their supervising and advices would this thesis not be accomplished. Both their knowledge and their rigorous high degree of professionalism encouraged and guided me.

Also, I wish to express my gratitude to my colleagues who supported me during the research. They provided me not only with their academic knowledge but also with their enthusiasm. I really enjoyed the last months working there.

Finally, I would like to thank my parents for giving me the opportunity to perform my study in the Delft University of Technology. Last not least a special thanks to Jason Yan for supporting me during the last years.

Jingyi Liao
Delft, September 2011

Summary

Fatigue damage in the orthotropic steel deck with respect to the trough-to-deck plate joint in between the crossbeams

Orthotropic steel decks are widely applied in long span bridges, movable bridges and shorter span road and rail bridges due to its favorable properties. These properties are low deadweight, lots of plastic reserve in case of overload and aesthetic advantage.

Since 1955, lots of orthotropic steel bridges were constructed in the Netherlands. At that time, the engineers underestimated the increase of the traffic intensity and the traffic weight. Therefore, in the last decades several fatigue cracks have been detected in orthotropic steel decks. The fatigue crack can initiate in different locations. The most frequently observed crack occurs in the longitudinal weld between the trough and the deck plate. This kind of crack will not only jeopardize the cooperation between the trough and the deck plate, but also endanger the safe operation of the bridge.

There are two objectives of this study. First of all, it is necessary to get a better understanding of the influence factor of the crack in the trough-to-deck plate joint. Secondly, based on the knowledge of the mechanical behavior of the orthotropic deck, a simplified approach is developed for the fatigue design with respect to the trough-to-deck plate joint.

The first part covers the study of the fatigue crack in the trough-to-deck plate joint by means of finite element modeling of a part of the orthotropic steel deck with assumptions based on the Eurocodes and Dutch national annexes (loads and classifications). The models are used to find out which factors influence the stress in the trough-to-deck plate joint. The comparison is carried out between models with different geometries. It turns out that the thickness of the wearing surface, the thickness of the trough web and the thickness of the deck plate play a significant role in determining the stress level in the trough-to-deck plate joint. Furthermore, the wheel-load print and the location of the wheel load can also influence the stress level in the trough-to-deck plate joint.

From the first part of the study, it turns out that the 3D finite element modeling and the evaluation of the stress ranges in the trough-to-deck plate joint are really complex and followed by a time consuming post-processing. Not only for new bridges but also for old bridges there is an urgent need for simplifying the fatigue assessment procedure. Based on the knowledge gained from the first part, a simplified 2D beam model with respect to

the stress in the trough-to-deck plate joint is developed in the second part. By analyzing the results of the 3D plate models, it shows that the maximum transverse stress range occurs at the mid-span of the trough. For this reason, the simplified model should be able to simulate the mechanical characteristics of the cross-section of the orthotropic deck at the mid-span. With this precondition in mind, the simplified model consists of two levels. Both levels have the same cross-sections as the 3D plate model. They are connected to each other by rigid links which ensures that both of them have the same deflections. The bottom level represents the part of the orthotropic deck at the mid-span which is directly loaded by the wheel load. Therefore, the width (in the longitudinal direction) depends on the length of the wheel print. In this way, this level simulates the transverse stiffness of the loaded part of the deck. The top level in the simplified 2D beam model represents the cross-section which is not directly loaded by the wheel load. But it plays a role in transverse spreading of the wheel loads over the troughs. Approximately, the width of this level equals to the half of the trough span minus the length of the wheel print. The longitudinal bending stiffness of these two levels is simulated by vertical spring which is added on each trough web in the bottom level. The spring stiffness of each trough is equal to unit load at mid-span divided by resulted displacement at mid-span according to Hook's law.

The results of the simplified 2D beam model can be compared with those of the 3D plate model. There are, however, some adjustments that need to be applied to the simplified model. At the level of the deformation, the differences between these two models are transparent. As the ends of the trough span are fully constrained, there is horizontal deformation at the mid-span which is caused by the distortion. The distortion is due to the eccentricity of the wheel load. However, there is no horizontal constraint on the trough bottom in the simplified 2D model. This means that the original simplified 2D model needs to be adjusted to simulate the deformation in the trough caused by the distortion. A fixed horizontal support is applied on each trough bottom as compensation. However, this adjustment is not able to simulate the extra deformation in the 3D plate model completely correctly. As the deformation is dependent on the geometries of the the trough, it can be hardly simulated by a fixed support. This indicates that the stress range derived from the improved simplified 2D model is still not accurate enough. Therefore, it is necessary to apply an adjustment factor on the simplified model trough web results to improve the accuracy of its results. According to this study, the difference between the results of these two models is mainly dependent on the distortion. Based on this fact the adjustment factor is given as the ratio between the 3D plate model's result and the simplified 2D model's result. Since the distortion has little influence on the stress in the deck plate of the bottom level, an adjustment factor of 1 can be applied there. In the top level, the stress in the deck plate of the simplified model is about twice as large as the stress obtained from the finite element model. In this case, the adjustment factor is equal to 0.5. Compared with the stress in the deck plate, the stress in the trough web is much more sensitive to the distortion. Consequently, the adjustment factor is related to some parameters of the orthotropic deck which affect the degree of the distortion. The main parameters are the thickness of the deck plate t_{deck} , the thickness of the trough

t_{trough} and the shape of the trough $\frac{b_{trough}}{h_{trough}}$. The formula for calculating the adjustment

factor α evolved from this study is $\alpha = \frac{b_{trough}}{h_{trough}} + 0.31 \cdot \frac{t_{deck}}{t_{trough}} \geq 1$. This adjustment factor

should be applied on both levels.

To verify the improved simplified 2D model and the adjustment factors, a fatigue assessment of the trough-to-deck plate joint is executed. This fatigue assessment is carried out for an orthotropic steel deck model with asphalt layer. It has a deck plate thickness of 18 mm and an 8 mm thick, 350 mm height and 150 mm bottom width trough. Base on the Eurocode + NB fatigue load model 4 long distance for highway bridges (2 million trucks a yaer for a 100 years) and the transverse spreading of the trucks according to the Eurocode, lifetime fatigue damage calculations are made for both the deck plate crack and the longitudinal weld crack. Using the reservoir method, the stress ranges spectrum got from the finite element model and from the simplified model can be changed into the lifetime damage. No lifetime damage is observed in the deck from both models. In the trough web, the fatigue damage is observed. It is found that the choice of the transverse location of the central line along which the wheels pass the bridge and the transverse spreading around that line has a large influence on the fatigue damage. And the wheel load location of the maximum stress is not necessary to be the location of the maximum fatigue damage. The fatigue damage is mainly related to the stress ranges amplitude and also the detail category of the joint.

In general, the results obtained from the simplified 2D model with adjustment factors are comparable to the results of the 3D plate model. Based on the comparison made for three welding categories, the simplified model appears to be sufficiently reliable in defining the fatigue damage in the trough-to-deck plate joint according to the Eurocodes.

Contents

Acknowledgements	1
Summary	2
1 Introduction	8
1.1 History	8
1.2 Orthotropic steel deck's development in the Netherlands	10
1.3 Internship subject and conclusions	11
1.4 Problem formulation	12
1.4.1 Problem statement	12
1.4.2 Objective of this thesis	13
1.4.3 Trough-to-deck plate joint	14
1.5 Fatigue according to NEN-EN 1993-1-9	17
1.5.1 Natural of fatigue	17
1.5.2 S-N curve	18
1.5.3 Determination of stresses	20
1.5.4 Fatigue sensitive spots in orthotropic steel deck	21
1.6 Fatigue loads according to NEN-EN 1991-2	22
1.6.1 Fatigue load model 1	22
1.6.2 Fatigue load model 2	24
1.6.3 Fatigue load model 3	26
1.6.4 Fatigue load model 4	27
1.6.5 Fatigue load model 5	28
1.7 Damage calculation	28
1.7.1 The Rainflow Method	28
1.7.2 The Reservoir Method	32
1.7.3 Fatigue damage accumulation	34
2 Literature review	36
2.1 Research by J. Janss	36
2.2 Research by M. S. Pfeil, R. C. Battista, A. J. R. Mergulhão	39
2.3 Research by S. YA and K. YAMADA	47
2.4 Research by Z.G. Xiao, K. Yamada, S. Ya and X.L. Zhao	50
2.5 Research by Y.L. Zhang, Y.S. Li and D.Y. Zhang	53
2.6 Research by M.H. Kolstein	55
2.7 Evaluation of the literature study	60
3 Finite element model	62
3.1 Geometry	62
3.2 Object joint	66
3.3 Mesh density	67
3.4 Boundary conditions	68
3.5 Wheel loads	69
3.6 Type of analyses and results to be computed	73
3.7 Comparison with site measurement	74
3.7.1 Description of the Scharsterrijn Bridge	75

3.7.2 Object locations	77
3.7.3 Wheel loads	78
3.7.4 Comparison results with site measurement	81
3.8 Results	83
3.8.1 Longitudinal influence line	83
3.8.2 Transverse influence line	86
3.9 Comparison between different models.....	89
3.9.1 Stress range in the exterior trough web	89
3.9.2 Stress range in the exterior deck plate	90
3.10 Conclusions	92
4 2D model in MIDAS Civil.....	93
4.1 The original 2D model.....	93
4.1.1 The vertical spring stiffness	93
4.1.2 Two-level model.....	94
4.2 Improved 2D model.....	95
4.3 Verification of the improved 2D model	99
4.4 Conclusions of 2D model.....	101
5 Simplification of the 3D model results	102
5.1 Analysis of the influence line at section D.....	102
5.2 Comparison between 3D model and improved 2D model	108
5.3 Conclusions	112
6 Adjustment of the improved 2D model results.....	113
6.1 Adjustment factor for the trough web result	113
6.1.1 Boundary condition	113
6.1.2 Distortion.....	114
6.1.3 Parameters	117
6.1.4 Empirical stress factor equation.....	118
6.2 Adjustment factor for the deck plate results	120
6.3 Conclusion	121
7 Verification of improved 2D model	122
7.1 Fatigue assessment procedure.....	122
7.2 Comparison of the lifetime fatigue	126
7.3 Conclusions	134
8 Application of the improved 2D model.....	136
8.1 General	136
8.2 Results	137
8.3 Conclusions for fatigue calculation for a movable bridge (model D).....	142
9 Conclusions and recommendations	143
9.1 Conclusions	143
9.2 Recommendations/future study	144
10 References.....	145
Literature.....	145
College lecture books	147
Standards.....	147

Websites	148
Software	148
Appendices	149

1 Introduction

A steel deck plate which is supported in two mutually perpendicular directions is called an orthotropic steel deck. The support system consists of crossbeams in the transversal direction and stiffeners in the longitudinal direction. In other words, it can also be named as ORTHOGonal anisoTROPIC plate since the deck plate is stiffened in the horizontal plane. However, the desirable stiffness's in the two perpendicular directions can be arranged separately.

1.1 History

The use of such deck plate was due to the requirement of minimizing the dead load of the bridge and saving the labour cost. In the 1920's, the American engineers reduced the dead load of movable bridges by using steel plate riveted to steel beam. Later they came up with the idea of "battledeck floor" which was also the origin of the modern orthotropic steel deck. As what has been shown in figure 1.1, the floor consists of a steel deck plate, supported by longitudinal stringers. The deck plate carries only the traffic load and transfers it to the stringers. This is an early model of the orthotropic steel deck.

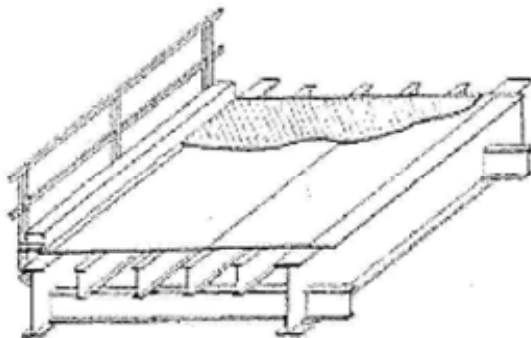


Figure 1.1 Battledeck floor (De Bakker, [1])

Later, German engineers developed a steel deck structure with inverted T-beam stiffeners in the longitudinal and transversal directions. See figure 1.2

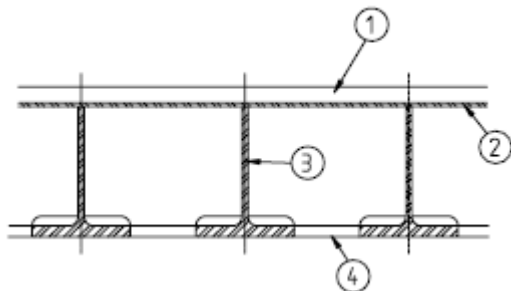


Figure 1.2 Deck plate stiffened by inverted T-beam (De Bakker, [1])

As the T-beam in two directions was welded to the deck plate, there were too many connections and the deck plate had to act as the top flange in these two directions. Therefore, such structure was not an economical solution.

Open stiffeners

In order to meet the requirement of an economic solution and reduction of labour, the orthotropic steel decks with open stiffeners were applied after the World War II. In figure 1.3, the most common used open stiffeners are strips, bulb profiles and angles which are still used in the ship building industry. Two sides of a stiffener are welded to the deck plate with fillet welds in the longitudinal direction. However, the completion of all the fillet welds requires an extensive labour work and results an uneconomical solution. A simpler method would be the stiffener passes through the crossbeam in cut-outs which are the parts removed from the crossbeams. In order to make the fitting of the stiffeners easier, the size of the cut-out is a little larger than that of the stiffener which is called cope hole. In this case, the rotational stiffness is reduced in this location. Compared with the modern stiffeners, the open stiffeners can only span a shorter distance of 2 to 3 meter. In addition, they are relatively inefficient in taking bending stresses. Due to these disadvantages, they are no longer used in the steel bridges.

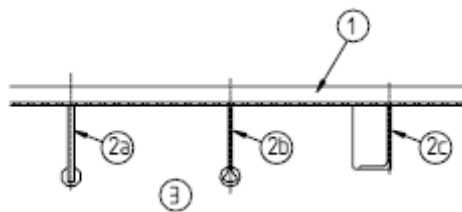


Figure 1.3 Typical section with open stiffeners. 1) wearing course; 2a) strip stiffener; 2b) bulb stiffener; 2c) angle stiffener; 3) crossbeam web (De Jong, [2])

Closed stiffeners

Compared with open stiffeners, closed stiffeners are more popular nowadays. The most widely applied closed stiffeners are shown in figure 1.4. They are V-shaped, V-shaped with an extension, U-shaped and trapezoidal cross-section. These stiffeners require only one sided fillet weld per leg which reduces the connections. The requirements of the labour extent are reduced. Due to their shapes, a larger static strength and stiffness than open stiffeners can be achieved. Therefore it can span distances of 3 to 5 meter and results in the reduction of the number of crossbeams and elements. The U-shaped and trapezoidal shaped stiffeners are most used in the existing bridges. And in modern bridges, only trapezoidal stiffeners are applied.

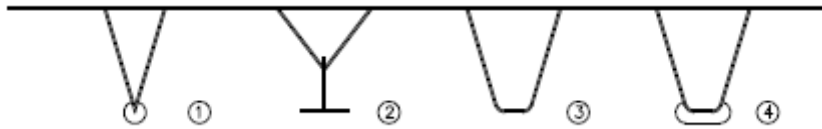


Figure 1.4 Sections with closed stiffeners (De Jong, [2])

The main reason which impelled the development of orthotropic steel deck was the lack of material and the needs for the rebuilding of the country after World War II. German engineers developed the modern orthotropic steel deck which provided a considerable low weight structure, saving material and site construction time. The Kurpfalz Bridge over the river Neckar in Mannheim, Germany in 1950 is the first welded orthotropic deck. It is a three-span bridge of 56+75+56 meters built with continuous beams and web girders.

1.2 Orthotropic steel deck's development in the Netherlands

The first generation of the orthotropic steel bridge in the Netherlands was built between 1955 and 1965. And it was widely applied between 1960 and 1980. After 1980, due to the development of concrete bridges, the use of orthotropic steel deck bridges has decreased. Today orthotropic steel deck bridges are used for long span, specific shape or architectural reasons and in movable bridges, for example the stay cable part and the movable part of the Erasmusbrug and the Hongersdijckbrug.



Figure 1.5 Erasmusbrug (left) and Hongersdijckbrug (right)

1.3 Internship subject and conclusions

This graduation project is an extension of the previous internship which was carried out by Rijkswaterstaat. During the internship, the study of the fatigue behaviour of the orthotropic steel deck and the sensitive spots in the bridge cross section was carried out. Besides, the fatigue damage in the bottom flange of the trough was investigated in details. By means of a set of Excel Programs developed by Rijkswaterstaat, the fatigue assessment was analyzed in three locations (trough to crossbeam joint, one eighth of the trough span and one fourth of the trough span) along the length of the trough span (the set of Excel Programs are attached in appendix C). The influence line derived from each set of Excel Programs was verified with the help of MIDAS Civil. The verification showed that the set of Excel Programs has a reliable and conservative estimation on the stress in the object joint [31].

After confirming the reliability of the set of Excel Programs, it was applied in the fatigue assessment in several fixed and movable orthotropic steel bridges. Several conclusions were derived. First of all, it proves that a larger trough profile and a better detail fatigue category can reduce the fatigue damage in the object joint sufficiently. The orthotropic steel bridge can benefit more from the larger section modulus of the larger trough profile. Also a better fatigue resistance can be achieved by a better detailing. Secondly, the crossbeams distance and the stiffness of the crossbeam have also influence on the fatigue life of the orthotropic deck. In general, the fatigue damage could be increased by enlarging the crossbeams distance. This is because in case of larger crossbeam distance, the stiffness of the orthotropic deck is less. Similarly, smaller crossbeam stiffness can cause larger fatigue damage also in the span of the trough. Because when the stiffness of the support is weak, the field moment in the trough would be large. But if the crossbeam is stiff, the most of the moment would be attracted to the crossbeam and cause large fatigue damage in the trough to crossbeam joint. Thirdly, since the bending moment varies along the length of the trough, the fatigue damage in the bottom flange of the trough also varies in the longitudinal direction.

In the research, the fatigue damage in the three locations along the trough span was also studied. It is found out that the trough splice can be better put in the one eighth of the trough span rather than in the one fourth of the trough span. The later is a traditional place for the usual trough splice.

In addition, a check of the form of the trough to crossbeam joint was carried out. In this check, a comparison was made between two kinds of trough to crossbeam joint. One is that the trough passes the crossbeam continuously. Another one is that the trough passes the crossbeam continuously with an extra cut-out. The investigation shows that the later one has a longer fatigue life than the first one with regarding to cracks in the troughs. By means of the cut-out which varies from 60mm to 100mm, the bottom flange of the trough to crossbeam joint is left open. The bottom trough flange can be considered not to be rested on the crossbeam. Due to the linear distribution of the stress over the

height of the trough, the stress in the trough to crossbeam joint is decreased. Therefore, the trough to crossbeam joint with an extra cut-out has a better performance than the one without extra cut-out.

Another conclusion extracted from the research is that the type of axel load, traffic intensity and the type of fatigue load model can lead to different fatigue lifetime damages in the object joints. Therefore, the engineer should bear it in mind when designing a new bridge.

Details regarding to this research can be found in the report of the internship [31] and thus are not further illustrated here.

1.4 Problem formulation

From the internship, it can be derived that the fatigue cracks of the orthotropic steel deck have been largely influenced by the slenderness of its components, the geometric details adopted for welded joints and the increasing of the traffic load and intensity. Most of the cracks are initiated in the welds. After the initiation, the cracks can grow into other structural components. When the crack length exceeds certain value it will threaten the safety of the structure. At this moment, Rijkswaterstaat is busy with the detection, reparation and renovation of the existing steel bridges in the Dutch highways. According to the forecast, the traffic intensity will keep increasing. It means more cracks are expected in the coming years.

1.4.1 Problem statement

The fatigue problem occurs only at the joints where high stress ranges or high stress concentration exists. Due to the complex network of longitudinal troughs, crossbeams and the deck plate there are many sensitive spots in the orthotropic steel deck, for example the trough splice joint and the trough-to-crossbeam joint. Many researches show that the cracks in these kinds of joints can decrease the stiffness of the deck. The most detective cracks occur in the longitudinal weld between the trough and the deck plate. These locations are shown in figure 1.6. This kind of crack can endanger the running safety of the bridge.

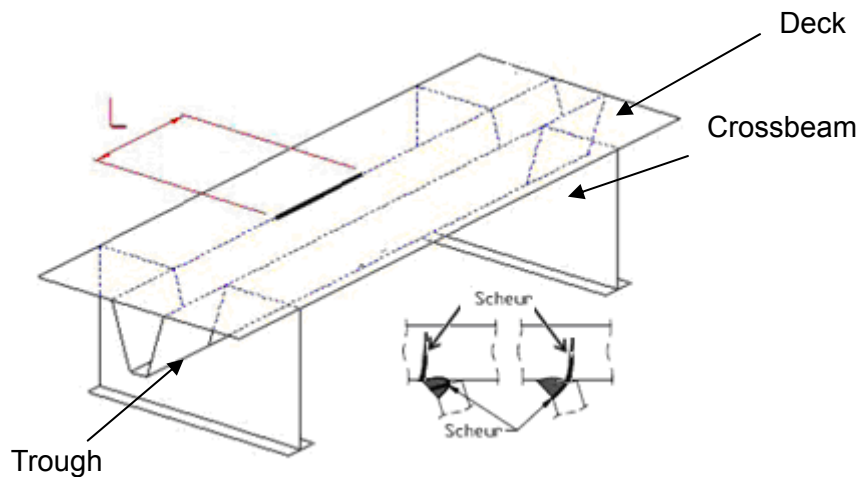


Figure 1.6 Fatigue in the trough-to-deck plate joint

This thesis focuses on the trough-to-deck plate joint since this detail is crucial in the highway bridges. In these places, the high load concentration of increased traffic intensity will cause extremely high stress ranges and load cycles. Besides, this detail is often decisive for the fatigue behavior of the entire orthotropic steel deck.

1.4.2 Objective of this thesis

Some decades ago, the older bridges were designed and built without taking fatigue damage into account. Nowadays the fatigue design is already an important issue which has been formulated in the Eurocodes. For new bridges, the Eurocodes give rules for the fatigue verification of bridges loads in NEN-EN 1991-2 [N1], fatigue strength in NEN-EN 1993-1-9 [N2] and NEN-EN 1993-2 [N3] partially based on the dissertation of the Kolstein, M.H. *Fatigue classification of welded joints in orthotropic steel bridge decks* (Kolstein, M.H., [3]) and the dissertation of de Jong, F.B.P. *Renovation techniques for fatigue cracked orthotropic steel bridge decks* (De Jong, F.B.P., [2]).

According to the Eurocodes, the stress ranges evaluation has to be performed for the new design steel bridges. But the evaluation of the stress ranges in the longitudinal welds between the trough and the deck plate is rather complex and can only be done with the aid of a complex FEM-model, followed by a time consuming post-processing. The whole process is needed in order to find out if the chosen construction geometry has a sufficient lifetime.

The first objective of this thesis is to analyze the influence of different factors on the crack in the trough-to-deck plate joint by means of FEM-modelling of a part of an orthotropic steel deck with assumptions based on the Eurocodes (loads and classifications).

The second objective of this work is to work out a simplified approach which is

convenient and sufficient to be used for the design of steel bridges with respect to fatigue life requirement. The starting point for this simplified approach is a set of Rijkswaerstaat Excel Programs developed for the fatigue calculation of the bottom side of the troughs. The aim is to be able to calculate the fatigue damage in the trough-to-deck plate joint for both old and new bridges and in future to incorporate the simplified approach in the National Annex.

1.4.3 Trough-to-deck plate joint

As described in section 1.1, there are two kinds of stiffeners. One is the open stiffener, e.g. strip, bulb and angle. This kind of stiffener has to be welded with two sided fillet welds to the deck plate. This kind of welding technology leads to an increase of the production cost. Another kind of stiffener is the closed trough which is widely applied in the orthotropic steel deck nowadays. Due to its geometry the trough requires only one sided weld per web which reduces the connections and the length of the welds extremely. But at the same time, the one sided welding of the trough also raises technological problem. As the welding can only be performed from the outside, the connection of the inside trough to the deck plate is often less sufficient. Furthermore the longitudinal weld between the closed trough and the deck is more prone to the fatigue failure than that between the open stiffener and the deck. It is because that the closed trough constraints the transversal deformation of the deck plate while the open stiffener does not or less. Therefore, special attention has to be paid on this weld.

As shown in the figure 1.7, the deck plate can be considered as a beam which is multiply supported by the trough webs in the transversal direction. The deck is comparable to a continuous beam in sense of bending moment distribution. In practice, the distance of the trough web is 300 mm. When the wheel load is put centrally above one trough as shown in figure 1.7, the trough span between the two trough webs which is under direct load will move downwards. The spans next to these two trough webs will deform in the opposite direction. Due to the rigid joint between the trough webs and the deck plate, a bending moment will be generated in the webs.

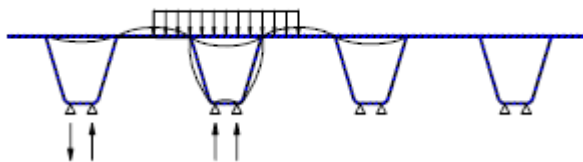


Figure 1.7 Effect of local wheel loads (NEN-EN 1993-2, [N3])

At the same time, the deck plate also deforms in the vertical direction due to the bending of the troughs in between the crossbeams (figure 1.8). This deflection is determined not only by the stiffness of the trough itself but also by the crossbeam distance and the stiffness of the crossbeam. The maximum deformation is expected at the location of the

wheel load. As the deflection is aroused due to this global deformation in the trough, the bending moment is also increased in the trough web and result in the increasing of the stresses in the trough web. These two kinds of deformation together lead to the crack in the longitudinal weld of the trough-to-deck plate joint.

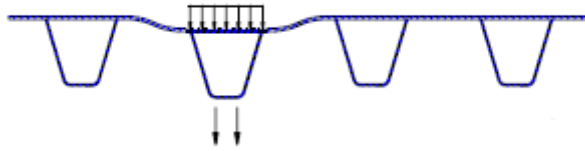


Figure 1.8 Effect of the differential deflections of troughs (NEN-EN 1993-2, [N3])

Due to the geometry of the welding, there are four potential spots around the weld where the fatigue cracks may initiate, see figure 1.9.

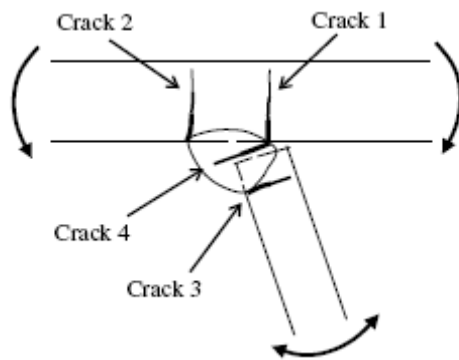


Figure 1.9 Fatigue cracks in the trough-to-deck plate joint (Xiao, Z.G., Yamada, K., et al, [4])

Crack 1 initiates in the weld root and propagates through the deck plate

Crack 2 initiates in the weld toe in the deck plate and propagates through the deck plate

Crack 3 initiates in the weld toe in the trough web and propagates through the trough web

Crack 4 initiates in the weld root and propagates through the weld throat.

Crack 1 and crack 2 have a similar fatigue mechanism (figure 1.10). As described in the previous section, the deck plate can be considered as continuous supported beam by the trough web. A wheel load, which is working centrally above a trough, causes a deflection of the deck plate under it and also deformation in the spans next to it. Due to the flexural stress, the fatigue crack will initiate in the weld toe or the weld root where the high stress concentration exists. When the crack grows through the thickness of the deck plate and reaches a certain length in the longitudinal direction, it will threaten not only the running safety of the traffic but also the integrity of the deck structure.

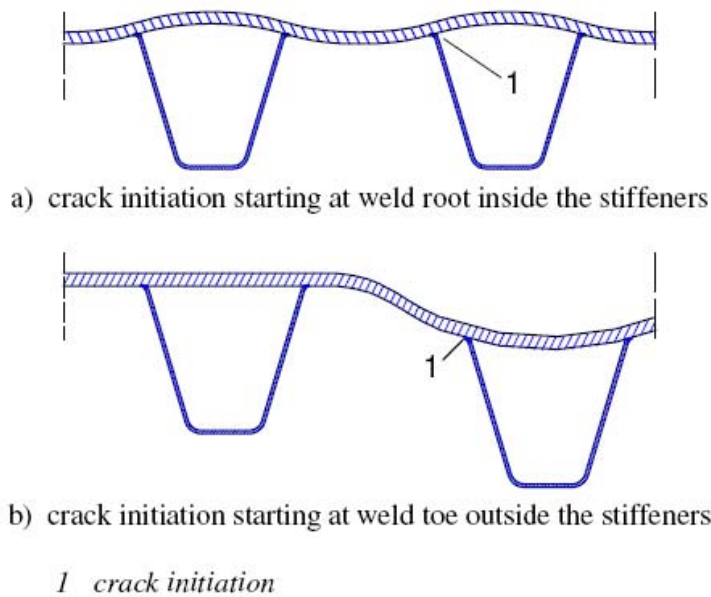


Figure 1.10 Fatigue crack in the deck plate (NEN-EN 1993-2, [N3])

Crack 3 and crack 4 are mainly caused by the transverse bending moment in the trough web (figure 1.11). Due to the rigid joint between the trough and the deck plate, the web of the trough has to deform together with the deck plate. In this case, the bending moment in the web will arise. The bending moment in the trough web together with the welding connection result in stress and stress concentration in the weld toe in the trough web. After cyclic loading of the traffic, crack 3 and crack 4 will be observed.

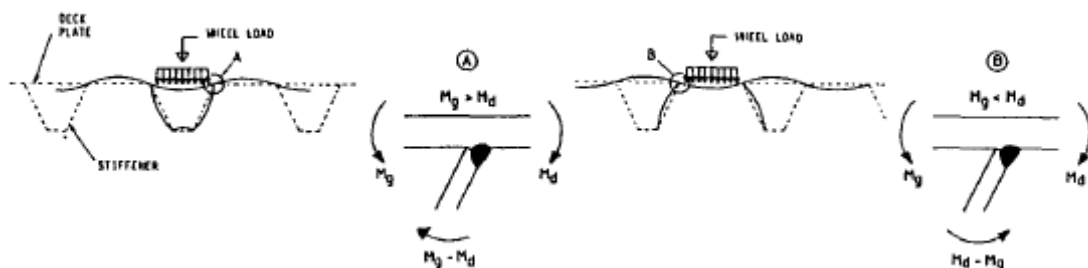


Figure 1.11 Transverse bending moment in the cross section (Janss, J., [5])

From previous fatigue test (Kolstein, M.H., [3]), it is known that this type of crack can be prevented by applying sufficient or full penetration. Furthermore, the pre-weld gap between trough profile and the bottom surface of the deck plate has also influence on the fatigue life of this weld (Kolstein, M.H., [6]).

In the NEN-EN 1993-1-9 [N2], the fatigue strength categories of the trough-to-deck plate joint are given in table 1.1:

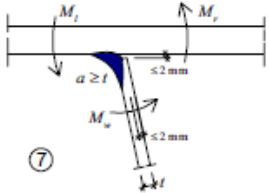
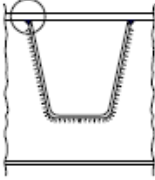
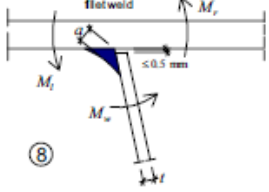
71		$\Delta\sigma = \frac{\Delta M_w}{W_w}$ 	<u>Weld connecting deck plate to trapezoidal or V-section rib</u> 7) Partial penetration weld with $a \geq t$	7) Assessment based on direct stress range from bending in the plate.
50			8) Fillet weld or partial penetration welds out of the range of detail 7)	8) Assessment based on direct stress range from bending in the plate.

Table 1.1 Detail classification of longitudinal weld of trough-to-deck plate joint (NEN-EN 1993-1-9, [N2])

1.5 Fatigue according to NEN-EN 1993-1-9

In the past several decades, the traffic intensity and the wheel loads have been increased considerably. Therefore cracks were detected in the orthotropic steel deck bridges caused by fatigue due to high stress ranges. Fatigue, as what is defined in the NEN-EN1993-1-9 [N2] “*the process of initiation and propagation of cracks through a structural part due to action of fluctuating stress.*”, becomes a well known phenomenon of the orthotropic decks of steel bridge.

1.5.1 Natural of fatigue

What is the nature of fatigue? Fatigue is the mechanism whereby cracks initiate and grow under fluctuating stresses. Final failure generally occurs in regions of tensile stress where the reduced area of cross section has insufficient capacity to carry the total load. This phenomenon does not occur in every kind of structure. Many kinds of structures, such as building frames, carry mainly the permanent load. It means that they do not have any problem with the fluctuating stresses. But in others, such as bridges, cranes and offshore structures, fatigue due to the fluctuating stresses should be taken into account.

The fatigue failure can be divided into the following stages:

- crack initiation
- propagation of crack
- final fracture

The crack initiation in metals is always associated with the accumulation of irreversible plastic strain. The accumulation of plastic strain results in surface ridges and troughs which also called extrusions and intrusions, see figure 1.12. The crack would initiate likely at the changes in the section or at the notches where the stress concentrates.

Generally, the fatigue life depends on the shape of the changes and notches. After the stage of initiation the crack would grow incrementally under cyclic loads. For fatigue, the applied loading may be well below the elastic limit of the material. Therefore the important thing of fatigue analysis is to find out how much the crack would grow under each cycle of applied loading. With this information the calculation of how many cycles will lead to failure could be done.

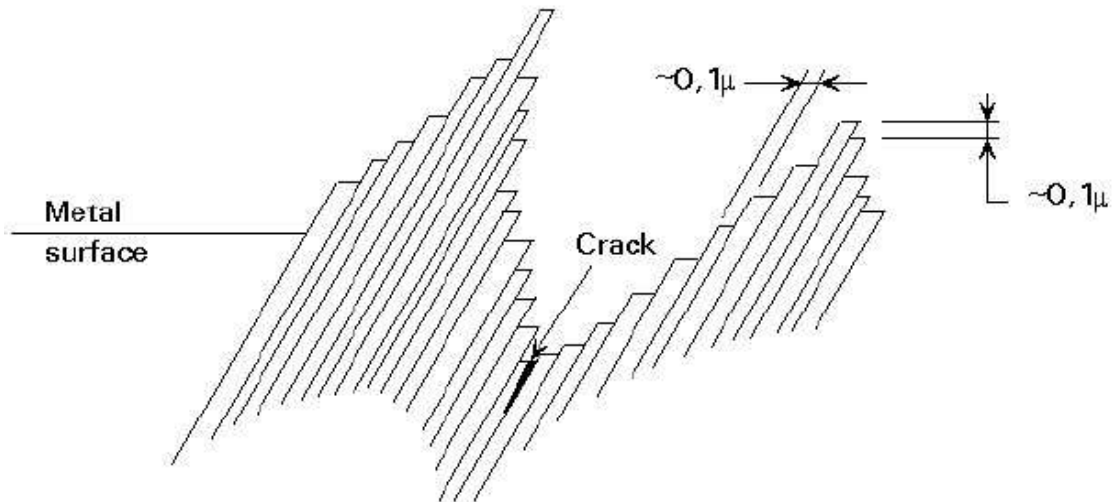


Figure 1.12 Slip band with extrusions and intrusion formed on the surface of a grain subjected to cyclic stress. Crack nucleation at intrusion (ESDEP, [W1])

1.5.2 S-N curve

Since fatigue is caused by the fluctuating stresses, the fatigue strength is defined as the stress range $\Delta\sigma_R$ which fluctuates at the location of crack initiation and causes failure of the component after a specified number of cycles N . The stress range equals to the difference between the maximum stress and the minimum stress. The number of cycles N is called the fatigue life.

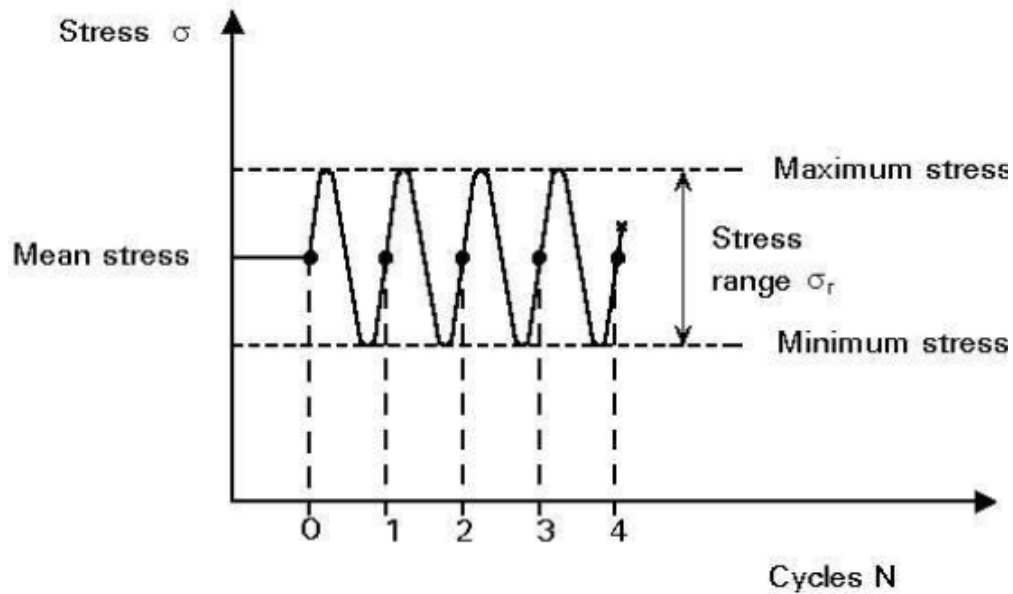


Figure 1.13 Constant amplitude stress history (ESDEP, [W1])

In the Eurocodes, the relationship between the stress ranges and the cycles N is represented by a series of $\log \Delta\sigma_R - \log N$ curves which is called S-N curves (figure 1.14). The S-N curve gives the information of the fatigue strength and fatigue life corresponds to typical detail categories. The designations of the detail categories indicate the fatigue strength of the details when the number of the cycles equals to 2 million. These detail categories are indicated with line 1 in figure 1.14 at. There are two kinds of lines after line 2 at 5 million cycles. The horizontal dot line gives the constant amplitude fatigue limit of 5 million cycles. It is a compromise between the 2 million cycles for good details and the 10 million cycles for details which create severe notch effect. But if the detail is under the working of variable amplitude stress, its fatigue limit will be lower. And the decrease of the fatigue limit is represented by the inclined line between line 2 and line 3. After the knee point at line 3 (cut-off limit), the line keeps horizontal. It means that the stress range below this limit does not contribute to the fatigue damage.

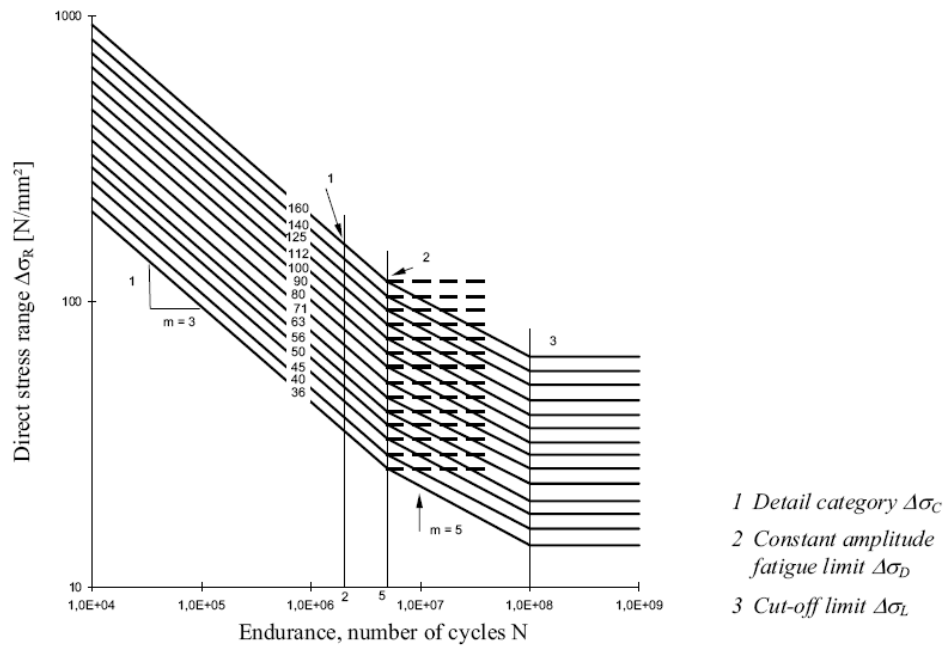


Figure 1.14 S-N curve (NEN-EN 1993-1-9, [N2])

1.5.3 Determination of stresses

The S-N curve defined in the Eurocodes is based on the nominal stress ranges which are determined with material elasticity. Therefore, the nominal stress excludes the stress concentrators and residual stresses effects which are resulted from the geometry of the component, the weld geometry, the welding process and etc. If the structural detail contains an additional stress concentrator, the modified stress should be applied. The stress concentrator could be introduced by misalignment, abrupt changes of section in the vicinity of a weld and etc. These two definitions could be illustrated with the help of figure 1.15.

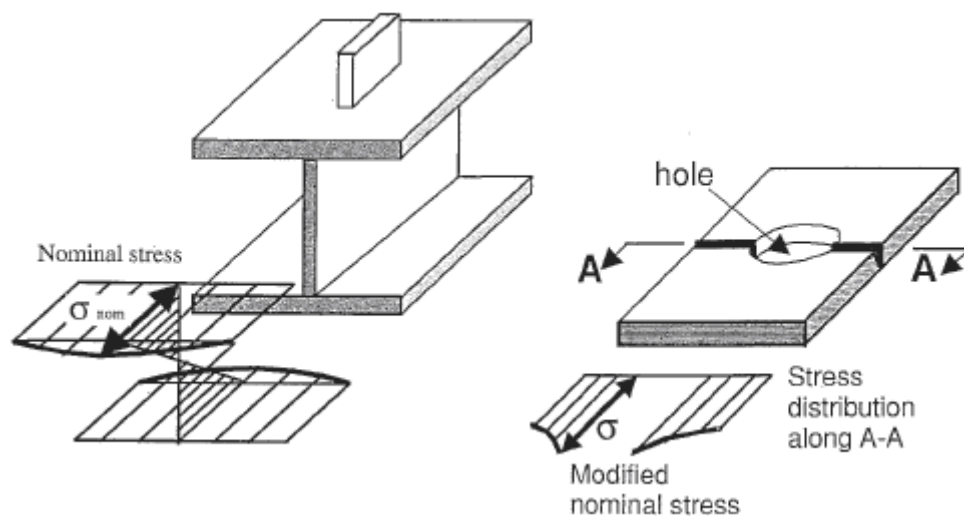


Figure 1.15 Nominal stress distribution in I beam with flange attachment (left), modified nominal stress in detail combining butt weld and hole (middle) (European convention for constructional

steelwork, [N4])

In practice, the welded joints are hardly to be classified due to complicated geometric effects. In this case, the geometric stress is recommended for the analysis. Geometric stress which is also called structural stress includes the stress concentrating effects due to the structural discontinuities, but the local nonlinear stress peak caused by the notch at the weld toe is ignored, see figure 1.16. The value of geometric stress at the weld toe is called the hot spot stress. The structural hot spot stress approach is recommended for welded joints where there is no clearly defined nominal stress due to complicated geometric effects, and where the structural discontinuity is not comparable to a classified structural detail (Hobbacher, A., [7]).

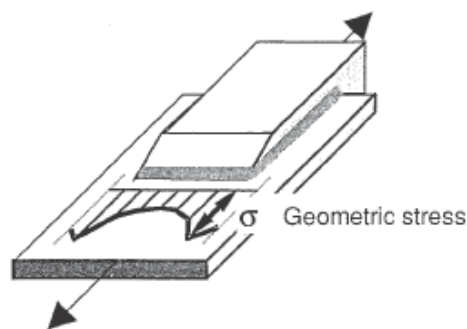


Figure 1.16 Geometric stress at bar-plate connection (European convention for constructional steelwork, [N4])

1.5.4 Fatigue sensitive spots in orthotropic steel deck

As mentioned before, the cracks in steel structure are most probably initiated at the weld due to the discontinuities, material property changes and imperfection at this location. The critical area to fatigue in the orthotropic steel deck is given in the following figure (figure 1.17). As a sum up, the cracks could be divided into the following categories:

- cracks in the deck plate
- cracks in the longitudinal weld between deck plate and trough
- cracks in the trough splice joint
- cracks in the connection between trough and crossbeam

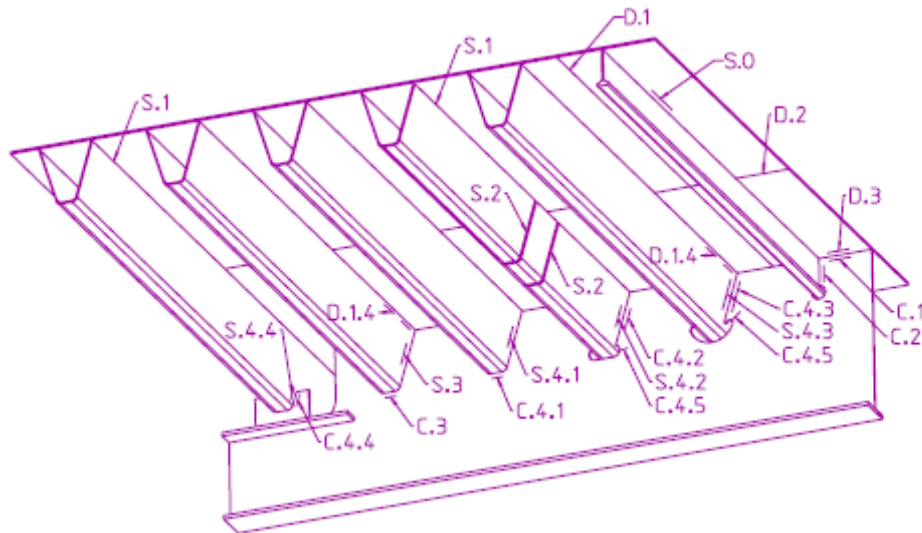


Figure 1.17 Susceptible locations for fatigue in orthotropic steel bridge decks (Leendertz, J.S., [8])

1.6 Fatigue loads according to NEN-EN 1991-2

In order to design the steel bridge taking account of the fatigue phenomena, there are five fatigue load models for fatigue design which are prescribed in NEN-EN 1991-2 [N1]. In fatigue analyses, only the vertical forces are taken into account, since they cause the governing fatigue stress in the steel bridge. Fatigue load models 1, 2 and 3 which are appropriate for typical heavy traffic and intended to be used to determine the maximum and minimum stresses resulting from the possible load arrangements on the bridge of any of these loads. Fatigue load model 4 and 5 are intended to be used to determine stress range spectra resulting from the passage of trucks on the bridge. For steel bridge design, the Dutch National Annex only allows using fatigue load model 4 for calculating the fatigue damage in the Dutch highway bridges, unless otherwise agreed in the specific project.

1.6.1 Fatigue load model 1

Fatigue load model 1 is similar to the static load model which is intended for the determination of road traffic effects associated with ultimate limit state verifications and with particular serviceability verifications. It consists of two partial loading systems which are double-axle concentrated loads (TS) and uniformly distributed loads (UDL). Table 1.2 shows the value of the loading systems for static load model. For this fatigue load model, the axle loads should be multiplied with a factor of 0.7 and the UDL should be multiplied with 0.3. The details of fatigue load model 1 are illustrated in figure 1.18.

Location	Tandem system <i>TS</i>	<i>UDL</i> system
	Axle loads Q_{ik} (kN)	q_{ik} (or q_{ik}) (kN/m ²)
Lane Number 1	300	9
Lane Number 2	200	2,5
Lane Number 3	100	2,5
Other lanes	0	2,5
Remaining area (q_{ik})	0	2,5

Table 1.2 Load model 1: characteristic values (NEN-EN 1991-2, [N1])

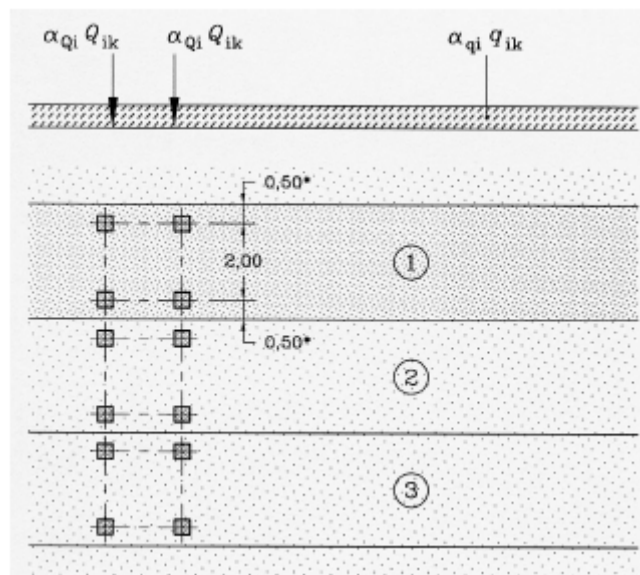


Figure 1.18 Application of fatigue load model 1 (NEN-EN 1991-2, [N1])

In order to avoid excessively conservative traffic loads, the adjustment factors should be applied on the traffic categories defined in table 1.3. As what has been defined in the national annex, the adjustment factor for the traffic in the Netherlands is 1. This is an exception for the traffic categories 3 and 4 in the urban area which has a primarily residential function. In this area, the adjustment factor has a value of 0.85. Furthermore, the maximum and minimum stresses should be determined from all the possible load arrangements of the model on the bridge. Table below indicates the categories and numbers of the heavy vehicles of the traffic.

Traffic categories		N_{obs} per year and per slow lane
1	Roads and motorways with 2 or more lanes per direction with high flow rates of lorries	$2,0 \times 10^6$
2	Roads and motorways with medium flow rates of lorries	$0,5 \times 10^6$
3	Main roads with low flow rates of lorries	$0,125 \times 10^6$
4	Local roads with low flow rates of lorries	$0,05 \times 10^6$

Table 1.3 Indicative number of heavy vehicles expected per year and per slow lane (NEN-EN 1991-2, [N1])

1.6.2 Fatigue load model 2

Fatigue load model 2 consists of a set of frequent trucks. The number of axels and the axle spacing, the load of each axle and the wheel contact areas and the transverse distance between wheels are defined in NEN-EN 1991-2 [N1]. See also table 1.4. The wheel types are given in table 1.5. The maximum and minimum stresses should be determined from the most severe effects of different trucks. They should be separately considered, travelling alone along the appropriate lane.

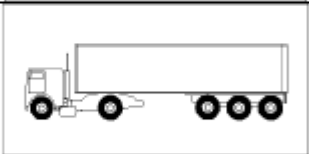
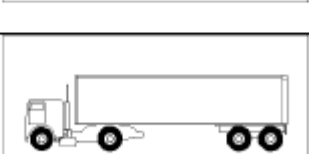
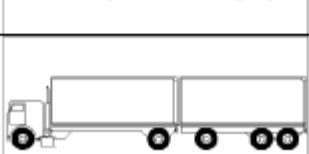
1		2	3	4
LORRY SILHOUETTE		Axle spacing (m)	Frequent axle loads (kN)	Wheel type (see Table 4.8)
		4,5	90 190	A B
		4,20 1,30	80 140 140	A B B
		3,20 5,20 1,30 1,30	90 180 120 120 120	A B C C C
		3,40 6,00 1,80	90 190 140 140	A B B B
		4,80 3,60 4,40 1,30	90 180 120 110 110	A B C C C

Table 1.4 Set of "frequent lorries" (NEN-EN 1991-2, [N1])

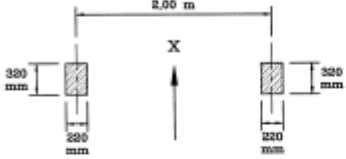
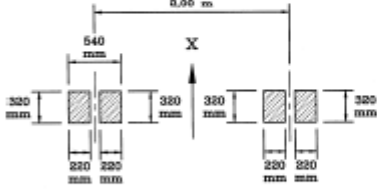
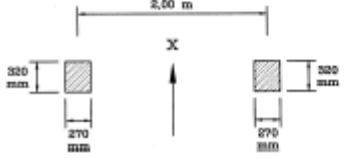
WHEEL/ AXLE TYPE	GEOMETRICAL DEFINITION
A	
B	
C	

Table 1.5 Definition of wheels and axles (NEN-EN 1991-2, [N1])

1.6.3 Fatigue load model 3

Unlike fatigue load model 1 and 2 which are used to check whether the fatigue life may be considered as unlimited, fatigue load model 3, 4 and 5 are intended to be used for fatigue life assessment. By using a material-dependent adjustment factor in fatigue load model 3, the influence of the annual traffic volume and of some dimensions can be taken into account. This model concerns single vehicle model (see figure 1.19). The weight of each axle is equal to 120 kN. When relevant, two vehicles in the same lane should be taken into account. When using this fatigue load model, the maximum and minimum stresses and the stress ranges for each cycle of stress fluctuation resulting from the transit of the model along the bridge should be calculated.

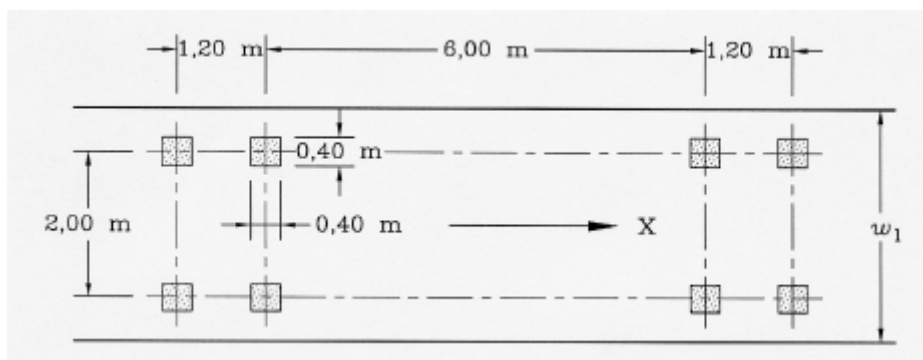
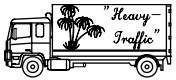
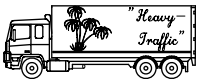


Figure 1.19 Fatigue load model 3 (NEN-EN 1991-2, [N1])

1.6.4 Fatigue load model 4

Fatigue load model 4 consists of sets of standard trucks. In the norm, the number of axles and the axle spacing, the equivalent load of each axle, the wheel contact areas and the transverse distances between wheels are specified. See table 4.7 of national annex [N5]. The percentage of each standard lorry in the traffic flow can also be found in the same table. Thereby the total number of vehicles per year for the whole carriageway can be defined. Depending on the specific requirements of individual project, different vehicle types and traffic types can be verified. In order to define the fatigue damage, the Rainflow or the Reservoir counting method should be applied. These two methods take not only the difference between maximum and minimum stress, but also every stress cycle caused by the passage of the truck or axles into account. Details of these two methods are given in section 1.7.

Type voertuig			Verkeerstype			Wiel type
Afbeelding van de vrachtwagen	Afstand tussen de assen m	Gelijkwaardige aslast kN	Lange afstand % ¹	Middel-lange afstand % ¹	Lokaal verkeer % ¹	
	4,5	70 130	20,0	50,0	80,0	A B
	4.20 1,30	70 120 120	5,0	5,0	5,0	A B B
	3,20 5,20 1,30 1,30	70 150 90 90 90	40,0	20,0	5,0	A B C C C
	3,40 6,00 1,80	70 140 90 90	25,0	15,0	5,0	A B C C
	4,80 3,60 4,40 1,30	70 130 90 80 80	10,0	10,0	5,0	A B C C C

¹ Percentage vrachtwagens

Table 1.6 Set of equivalent lorries, wheel types refer to table 1.5 (NEN-EN 1991-2/NB, [N5])

1.6.5 Fatigue load model 5

Different from the other four fatigue load models, fatigue load model 5 is the most general model which is based on the recorded road traffic data. Nowadays, this model is mainly used for the calculation of fatigue for exciting bridges in highways. For old cases, automatic counting records for the number of trucks are used. The loads are derived from 4 weights in motion locations on the Dutch highways.

For the assessment of local action effects, the models should be centered on notional lanes which are assumed to be located anywhere on the carriage way. However, when the transverse location of the vehicles for fatigue load models 3, 4 and 5 has significant influence on the results, a statistical distribution of this transverse location should be considered. This distribution is shown in figure 1.20 as an example.

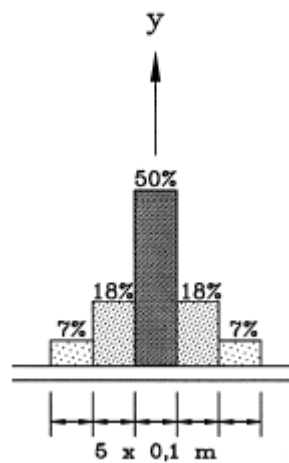


Figure 1.20 Frequency distribution of transverse location of central line of vehicle (NEN-EN 1991-2, [N1])

1.7 Damage calculation

After getting the history of the stresses, a suitable counting method is needed in order to evaluate stress ranges, their numbers of cycles and the mean stresses where necessary. The NEN-EN1993-1 [N2] recommends two cycle counting methods:

The Rainflow Method

The Reservoir Method.

1.7.1 The Rainflow Method

The Rainflow Method was developed by the Japanese researchers Tatsuo Endo and M.Matsuishi in 1968. It was named after the process of rain falling off a pagoda roof. Before the developing of the method, the available methods were not good at the range counting or range-mean counting. Since the stress-strain history was not taken into account, the methods led to unreasonable results especially for hysteretic materials. As

one of such material, the stress and strain in the steel, not only are related to the working load on it, but also depend on the previously developed stresses and strains. In the Rainflow Method, the Japanese's were successful to count the stress-strain hysteresis loops. A more detail description of the theory of this method is given as below.

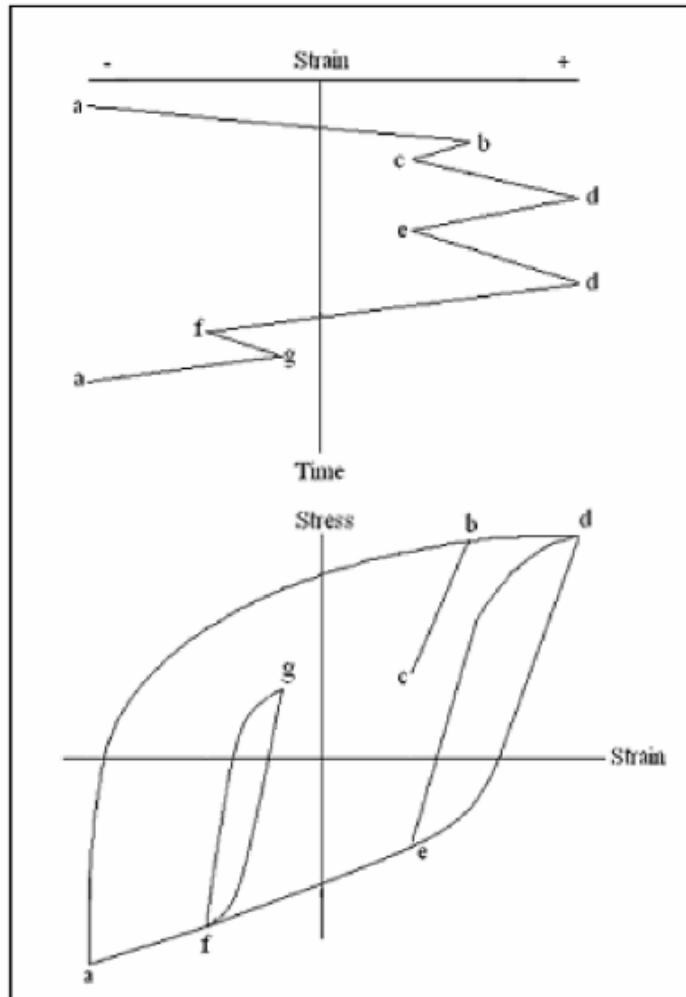


Figure 1.21 Load history (ESDEP, [W1])

The upper part of figure 1.21 is a simplified loading history which has been rotated by 90 degree. It reduces a spectrum of varying stress into a set of simple stress reversals and has a shape of the Japanese pagoda. Below it, the resulting deformation, stresses and strains are drawn. We could identify four cycles in the lower part of the figure. The most outside curve is the largest cycle. On the left hand side of the coordinate system, there is a small cycle. Further there are two more cycles on the opposite. Each of the cycles has its own stain range and mean stress. The interpretation of the deformation process is:

Starting at a, the minimum strain, the material is uploaded to b. At point b, the load is reduced to point c. Then the load is reapplied from c to d, the material deforms elastically to b and remembers its prior history, i.e. from a to b, and the deformation continues along path a to d as if event b-c never occurred.

The Rainflow Method is based on the theory which is explained in the previous paragraphs. In the following, the Rainfolw Method will be illustrated with several figures:

As what could be seen from the first figure, the stress cycle diagram is turned 90 degrees to illustrate as the pagoda. When the water or rain falls on the top of the roof, it would flow along the pattern of the stress cycle. For each leg of the roof, the imaginary rain flow would start from its highest point as shown by the dots in figure 1.22.

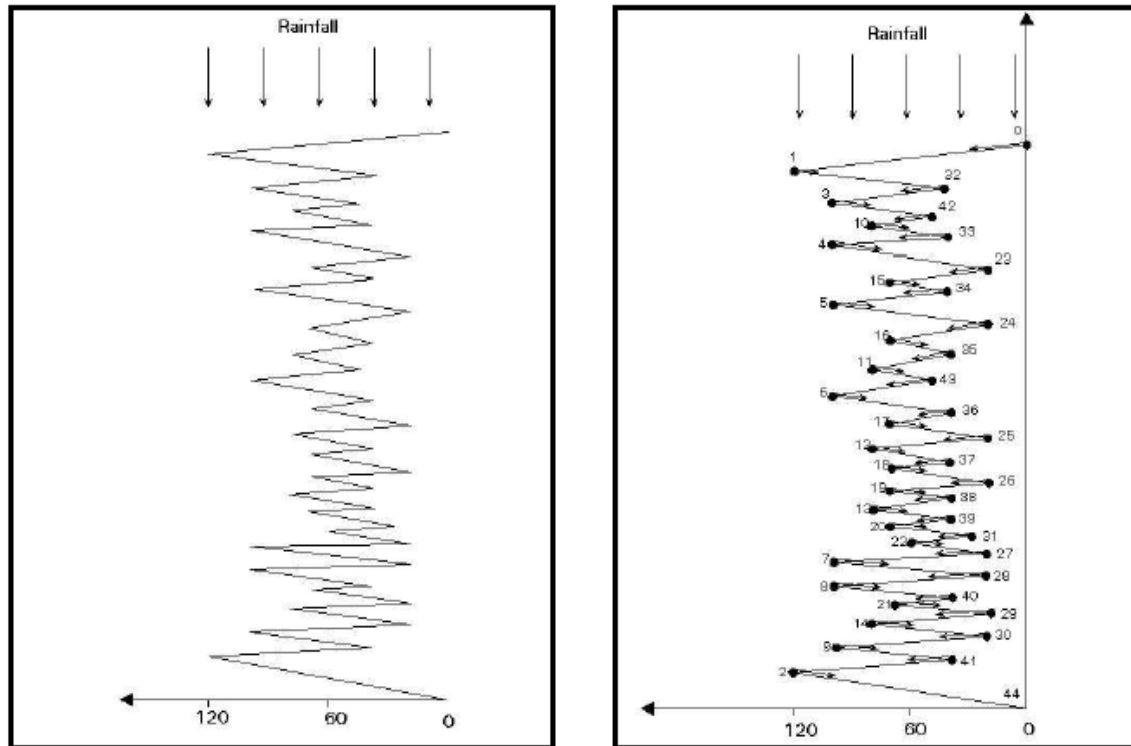


Figure 1.22 Initial trace for rainflow cycle counting (left) Rainflow introduced at dot positions from outside sequence (right) (ESDEP, [W1])

First start at each tensile peak, the water comes from the peak and flows follow the stress pattern. The flow will stop if the opposing peak is larger than its origin (figure 1.23). When the water drop meets the flow from a previous peak it will also terminate. The drop can fall on another roof and continue to slip according to the previous two situations. Each valley generates one half cycle. The magnitude of each half cycle is equal to the stress difference between its start and termination.

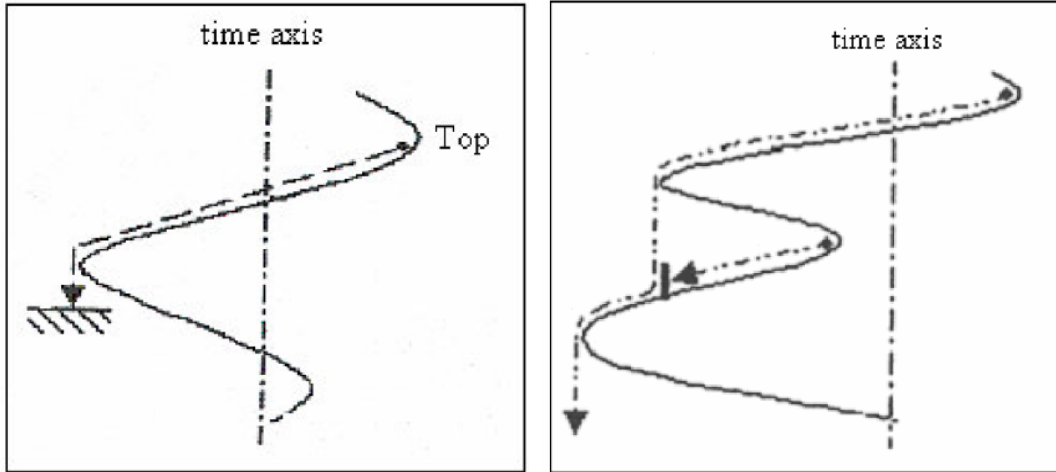


Figure 1.23 Cycle counting (ESDEP, [W1])

And secondly, the process is repeated in reverse with valley-generated rainflow paths. The complete rainflow diagram is shown in figure 1.24.

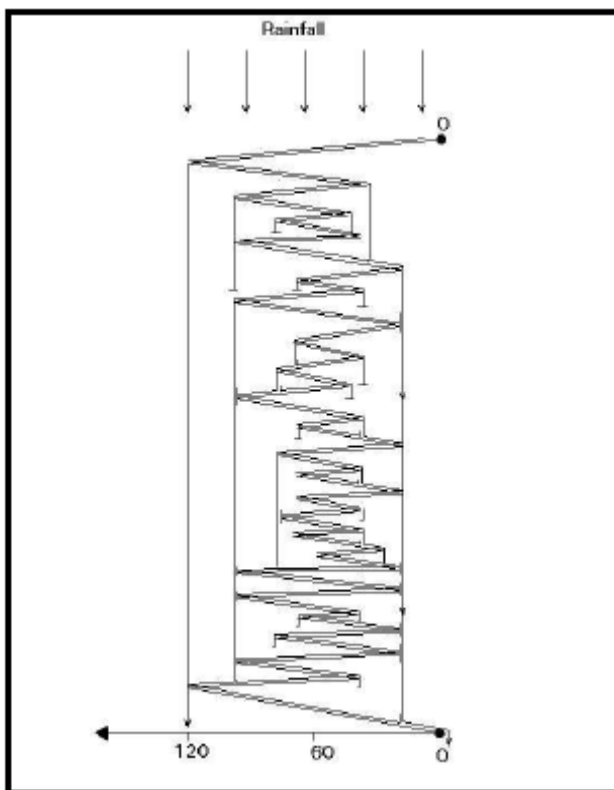


Figure 1.24 Complete rainflow diagram (ESDEP, [W1])

By paring up the half cycles of identical magnitude with opposite sense, a whole cycle of the stress range can be achieved.

1.7.2 The Reservoir Method

An alternative method of counting the cycle is the Reservoir Method. This method is recommended in the British Standard Bridge Design Code which is suitable for short stress histories produced by individual loading events. Different from the Rainflow Method, it counts the complete cycles in stead of the half cycle.

To use this method, the records of a long enough period is necessary in order to get the same peak value at the start point and finish point, for example figure 1.25. Firstly, a line has to be drawn between these two stress peaks. Then the region between is filled with water, as shown in figure 1.26, to form a reservoir. After the reservoir has been formed, open a tap in the lowest trough to drain the trough T1 while the other troughs are still tapped with water, see figure 1.27. As shown in figure 1.28, the draining of the trough T1 corresponds to the cycle of stress range S1. Again a tap is opened in the next lowest trough T2. The decrease of the water level in this trough corresponds to another cycle of stress range S2. The draining is continued sequentially through each next lowest trough and it builds up series of stress ranges.

The important principle of the Reservoir Method is the recognition that by taking the difference between the lowest and highest stress levels (trough and peak) it is ensured that the greatest possible stress range is counted first, and this procedure is repeated sequentially so that the highest ranges are identified as the random fluctuations take place. The Reservoir Method procedure does ensure that practical combinations of minima and maxima are considered together whereas this is not always the case in other stress cycle counting procedures.

Another way of counting the cycles with the Reservoir Method is to turn the diagram upside down (figure 1.29). The result is not different from the previous procedure, but its advantage is that it takes the major cycle of stress from zero to maximum and back.

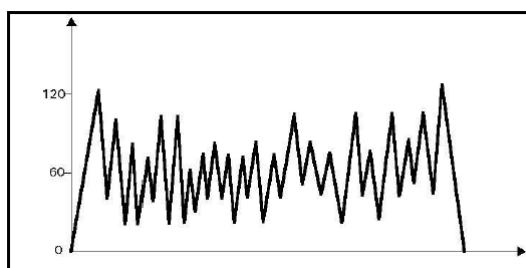


Figure 1.25 Schematic stress time history (ESDEP, [W1])

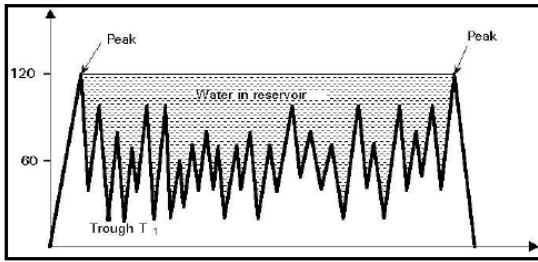


Figure 1.26 Forming reservoir for stress-time history of figure 4.5 (ESDEP, [W1])

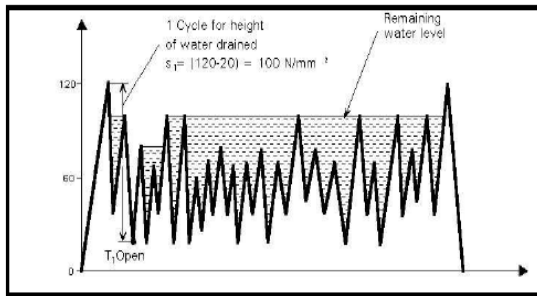


Figure 1.27 Open a tap in the lowest trough (ESDEP, [W1])

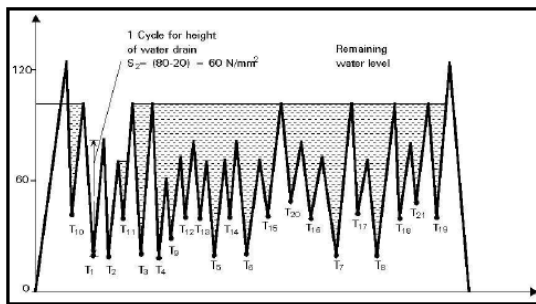


Figure 1.28 Open another tap in the next lowest trough (ESDEP, [W1])

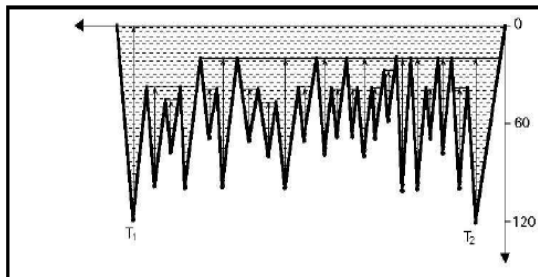


Figure 1.29 Inverse reservoir method (ESDEP, [W1])

1.7.3 Fatigue damage accumulation

In Eurocode 3, the Palmgren-Miner rule has been chosen to be the method of the fatigue damage accumulation. It was first proposed by A. Palmgren in 1924. In 1945, M.A. Miner popularized the rule. In this rule, the structure is assumed under variable amplitude fatigue loadings. These loadings are simplified into a manageable number of bands with different stress ranges (figure 1.30).

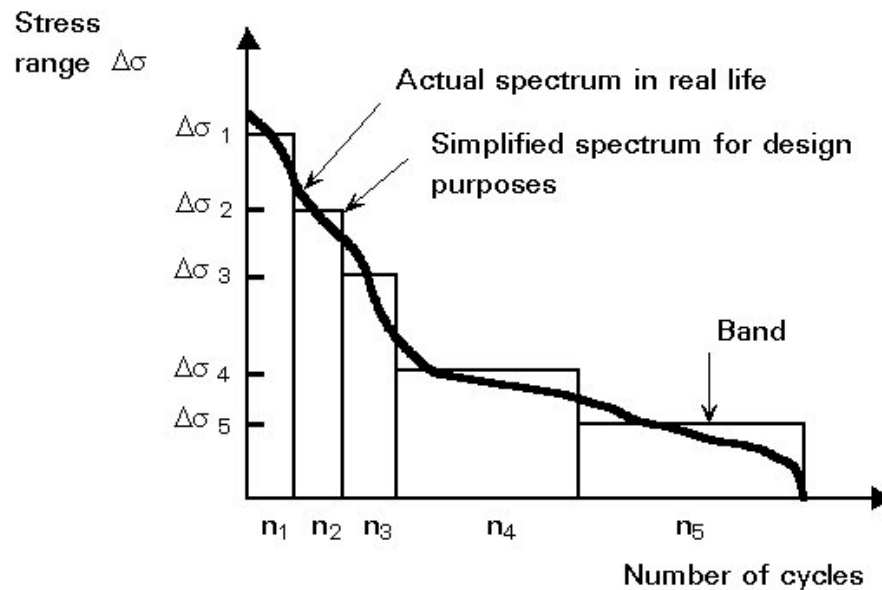
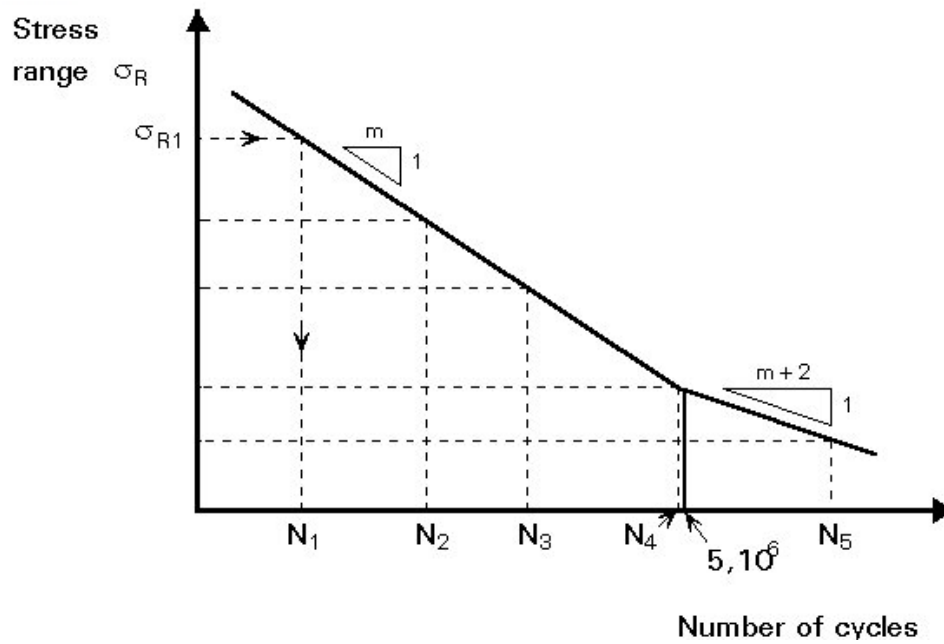


Figure 1.30 Simplification of stress spectrum (ESDEP, [W1])

The total fatigue damage is the linear summation of the damage of each individual stress range. In the calculation of individual damage, it is done by dividing the existing number of stress cycles of each stress range n_i by the allowed number of stress cycles N_i according to the S-N diagram (figure 1.31).



$$\frac{n_1}{N_1} + \frac{n_2}{N_2} + \dots + \frac{n_n}{N_n} \leq 1$$

Figure 1.31 Determination of endurance for each band (ESDEP, [W1])

Although that the Palmgren-Miner rule is the most popular and useful summation of the fatigue damage, it still has some major disadvantages. As could be seen from the procedure of the summation, the Palmgren-Miner rule takes no consideration of the sequence effects of the fatigue loading. Actually these effects really exist. For example, the cycles of low stress followed by high stress cause more damage than the prediction. And the high stress followed by low stress may have less damage because of the presence of compressive residual stress. (ESDEP, [W1])

2 Literature review

Before starting with the investigation of the fatigue behaviour of the trough-to-deck plate joint, it is very important to do a literature review. By doing the literature review, information about what is known and what is interesting to do in the further research can be collected. This literature study is based on the work which was done in the past decades. The literature is listed in chronological order. In the end, a summary of the findings will be given. At the same time, it leads also to a conclusion on what kinds of study are still needed on the same subject.

This study focuses on the fatigue of the trough-to-deck plate joint. The literature related to this subject, can be divided into two groups. These two groups are:

- The welding technology
- The geometrical configuration of steel bridge

2.1 Research by J. Janss

Due to the lack of knowledge, the requirement of the longitudinal weld between the trough web and the deck plate is very rigorous in many countries which results in a high cost of the manufacture of the orthotropic steel deck. Therefore, in 1988 Janss carried out a research concerns the influence of loosened fabrication conditions on the fatigue behaviour of those welded connections. Specially, he analyzed the effect of important lacks of penetration and/or the absence of any preparation of the longitudinal edges of the trough.

The research was carried out on small test specimens. The dimensions of the specimens are shown in figure 2.1. These specimens were manufactured according to the following principles:

- The longitudinal edges of the troughs were 'as received' without any preparation such as grinding or chamfering;
- Manual welding of the trough to deck plate joint. No limitation was provided for the lack of penetration of the welds. The actual lack of penetration has been measured for each specimen;
- The tack welds were integrated in the final weld without any special care.

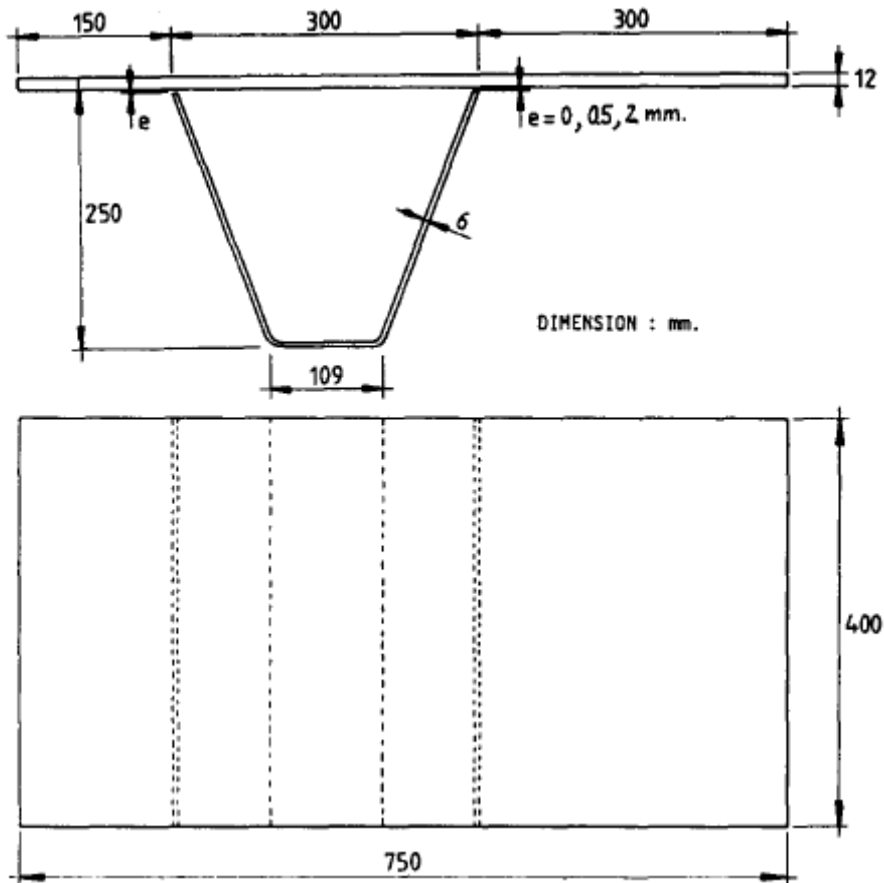


Figure 2.1 Dimensions of the specimens (Janss, J., [N5])

Moreover, there were two particular prescriptions for the fabrication of the test pieces:

- The fit (e , see figure 2.1) between the trough web and the deck plate had different values: 0.2 and 0.5 mm.
- The welding position was horizontal or overhead.

The arrangement of the specimen and the loads is shown in figure 2.2. The stresses were measured by the strain gauges around the welds. The locations of the strain gauges are shown in figure 2.3. By doing the measurements, the limits of the fatigue load, stress and the stress range of the transverse bending stress at the weld toe in the trough can be determined. As a sum up, the results of the tests are listed in table 2.1:

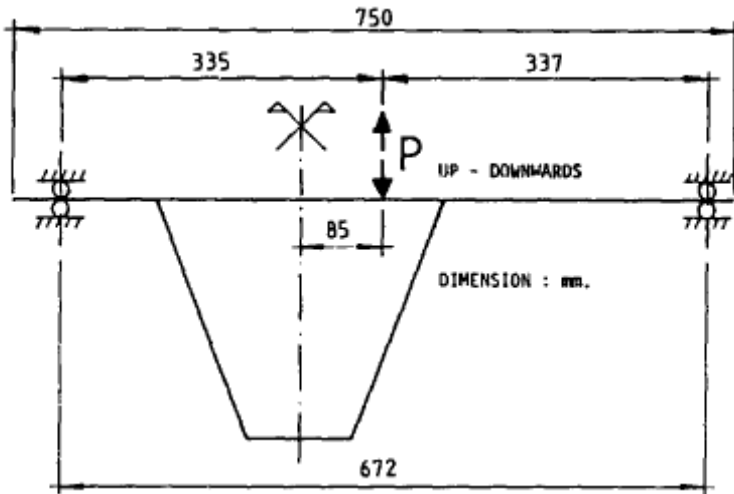


Figure 2.2 The setup of the test (Janss, J., [N5])

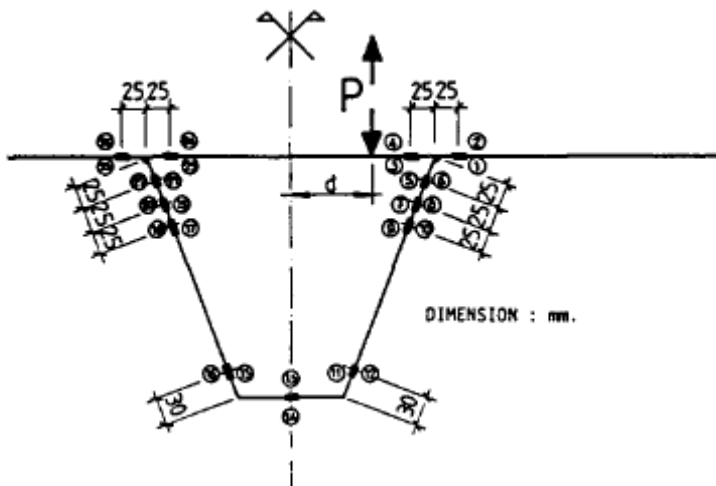


Figure 2.3 The arrangement of the tensors (Janss, J., [N5])

No.	Welding	e (mm) (N/mm ²)	$\Delta\sigma_s$	σ_{min} σ_{max} (s)	No. of cycles to failure $\times 10^3$	Position of crack	r (mm)	p (mm)
							(see Fig. 2)	
1			172.2	-1.52	215	Weld	3.5	4.7
2			169.2	-1.53	284	Weld	4.2	4.2
3			206.9	-1.56	255	Weld	4.0	4.0
4			110.4	-1.53	908	Weld	3.5	4.5
5	Horiz.	0	137.0	-1.53	402	Weld	3.5	4.5
6			133.4	-1.14	515	Weld	3.5	4.5
7			98.3	-1.12	+2 000	No crack	—	4.5
8			149.2	-1.14	410	Weld	4.0	4.5
9			135.1	-1.15	862	Weld	3.7	4.5
10			120.1	-1.13	1 740	Weld	4.5	4.7
11			164.2	-1.57	119	Weld	4.5	—
12			152.3	-1.50	255	Weld	—	—
13			187.2	-1.46	59	Weld	—	—
14			112.6	-1.54	759	Weld	3.6	3.0
15	Horiz.	2	137.7	-1.55	273	Weld	—	—
16			134.8	-1.14	364	Weld	3.5	2.0
17			105.7	-1.14	629	Weld	5.0	1.5
18			145.8	-1.14	724	Weld	4.5	2.2
19			133.5	-1.15	406	Weld	4.2	2.0
20			119.6	-1.14	354	Weld	3.5	3.0
21	Horiz. ^a	0	68.5	-1.70	5 722	Weld	—	4.0
22			68.3	-1.43	+4 000	No crack	—	3.0
23	Horiz. ^a	2	69.7	-1.13	+2 000	No crack	—	2.5
24			70.1	-1.71	1 200	Weld	4.0	3.0
25			166.3	-1.56	276	Plate	—	3.0
26	Overhead	0	196.8	-1.59	133	Plate	—	1.0
27			110.6	-1.63	903	Plate	—	3.9
28			166.0	-1.61	109	Plate	—	1.5
29	Overhead	2	210.2	-1.65	42	Plate	—	1.5
30			110.0	-1.62	1 239	Plate	—	3.2
31			83.5	-1.55	1 790	Weld	3.1	4.0
32	Horiz.	0.5	168.0	-1.57	254	Weld	3.0	3.8
33			105.1	-1.53	1 533	Weld	2.9	4.0
<i>Complementary tests</i>								
34			81.7	-1.77	+2 250	No crack	—	2.0
35	Autom.	0.5	120.2	-1.65	+2 700	No crack	—	2.5
36			220.6	-1.55	4 200	Weld	—	4.0

^aSmall initial cracks in the longitudinal edge of the stiffener

Table 2.1 Test's data (Janss, J., [N5])

The result shows that a costly preparation of trough web can not provide a better fatigue strength of the joint. Janss also concluded that when the gap between the trough web and the deck plate is smaller than 0.5 mm and the thickness of the trough and the deck plate are respectively 6mm and 12 mm, the stress range at two million cycles of the transverse stress at the weld toe in the trough is equal to 80 N/mm². In this case, the lack of penetration of the weld could be up to 4 mm and the thickness of the resistant section of the weld may be equal to 4 mm.

2.2 Research by M. S. Pfeil, R. C. Battista, A. J. R. Mergulhão

In this paper, they addressed the question of the stress distribution and concentration at the trough-to-deck plate joint by using a numerical model of an orthotropic steel deck.

Based on the result of the numerical model, a parametric analysis which can lead to a rational design of the orthotropic steel deck was carried out.

The numerical model, which is shown in figure 2.4 (d), is modelled according to the Rio-Niterói bridge deck (figure 2.4 (a), (b), (c)). The dimensions of the model are collected in table 2.2. In order to simulate the distortion and out-of-plane bending of the trough, the four-node shell element which combines separate membrane and plate bending behaviour of the element was used. The wheel load pressure was modelled at the mid span in two situations without considering the distribution effect of the wearing surface. One was soft contact and the other was hard contact. These were simulated by modifying the pneumatic stiffness of the tyres.

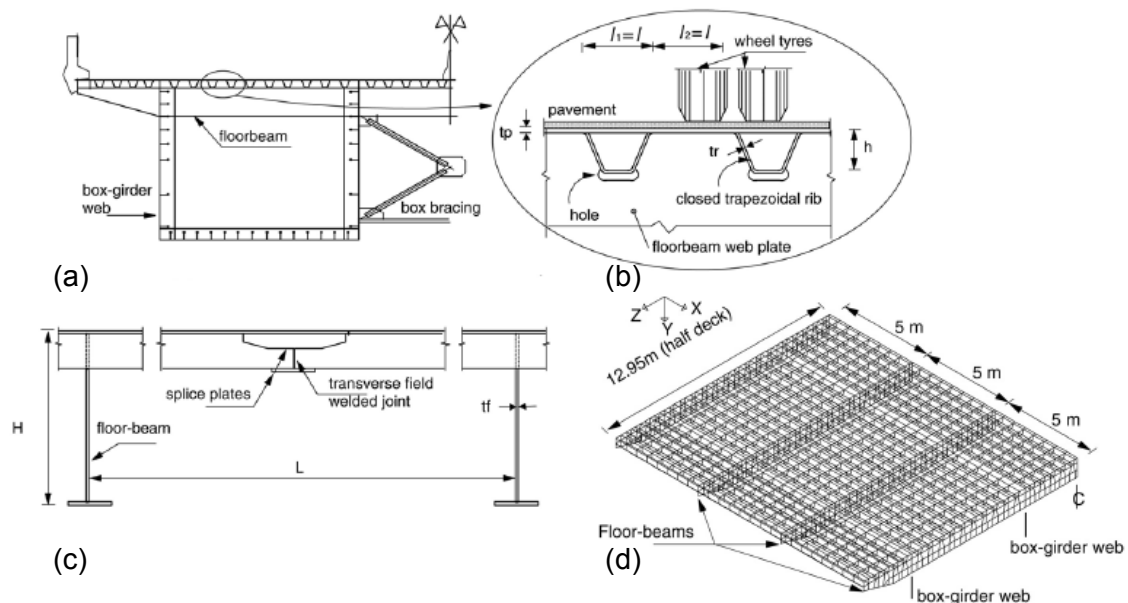


Figure 2.4 Steel orthotropic deck of Rio-Niterói bridge (a) Bridge steel box-girder with orthotropic deck; (b) Detail of the cross section of the Rio-Niterói bridge deck; (c) Longitudinal section of the Rio-Niterói bridge deck; (d) The finite element model (Pfeil, M.S., et al, [9])

Indication	Dimension [mm]
h	250
t_p	10
t_r	8
t_f	10
l	327
H	1000
L	5000

Table 2.2 Dimensions of the finite element model

This numerical analysis shows that the model deforms in the transversal direction. It is

illustrated in figure 2.5 (a). This effect due to the working of the wheel load is kept locally at the mid span. This phenomenon can also be illustrated by the influence line. In figure 2.5 (b), the influence line at the trough-to-deck plate joint (point r) is plotted. The influence line indicates that a shift of the center of the wheel load transversely as small as 150 mm can induce a remarkable change in the transverse bending moment, for example from zero to the maximum absolute value (M_r).

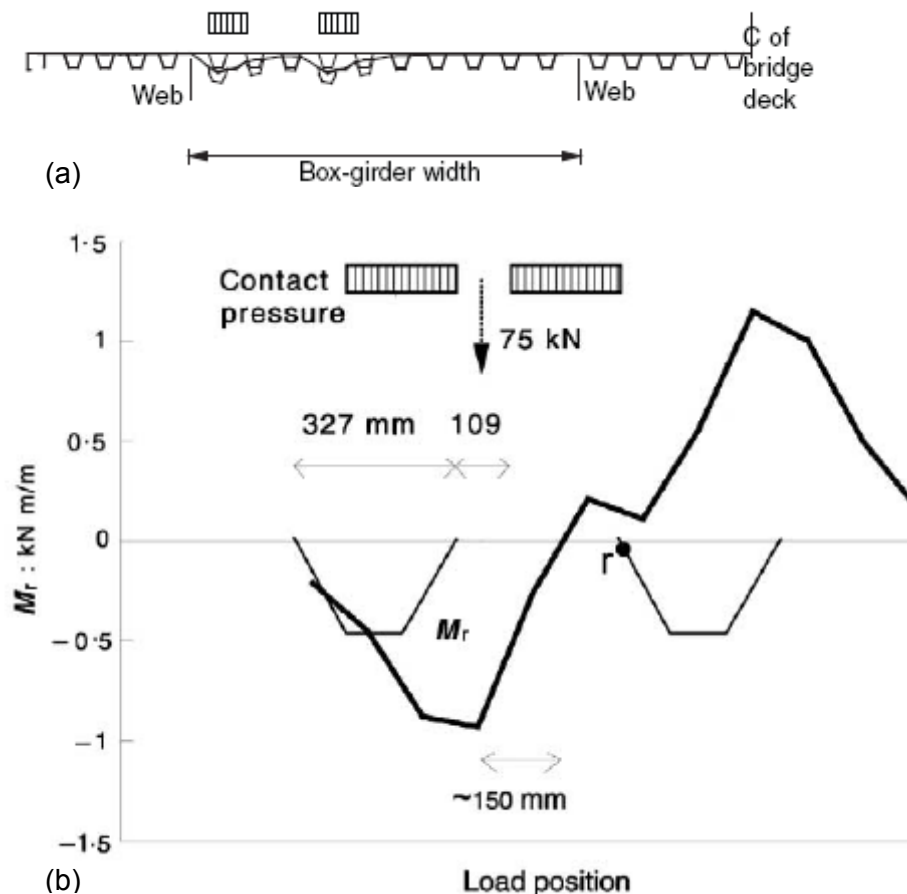


Figure 2.5 (a) Local transversal deformation of the orthotropic deck under wheel loading; (b) Influence line of the transverse bending moment at the trough-to-deck plate joint (Pfeil, M.S., et al, [9])

At the same time, a prototype scale model was built up in order to have a better understanding of the behaviour of the local transverse bending stress in the trough and to calibrate the numerical model. This prototype scale model was already reinforced with a concrete slab on top of a thin layer of visco-elastic material (figure 2.6). The model had an area of 10 by 10 m² which represents the portion of the deck between the webs of one box-girder plus the adjacent cantilever (figure 2.4 (a)) with two spans between the crossbeams. A twin-axle truck wheel load was applied on the deck plate by a self-equilibrated system. The wheel load areas were measured, the initial area, under the working of the truck dead load 150 kN, and the final area for additional 150 kN axle load (see figure 2.7). With the help of the strain gauges and the displacement transducers (figure 2.8) the extensive strain and the displacement measurement were

carried out.

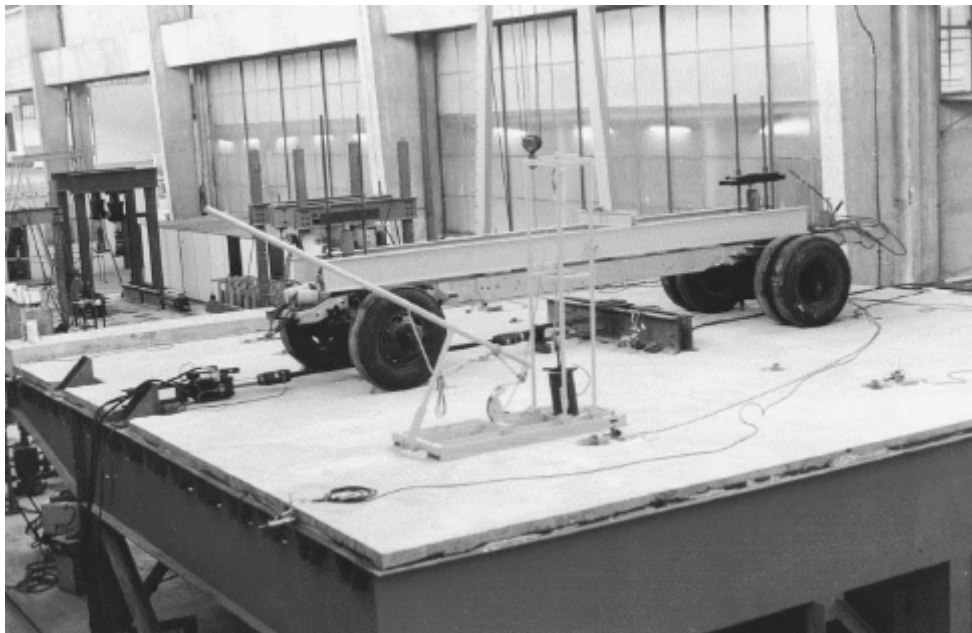


Figure 2.6 The prototype model is reinforced by a concrete slab on top of a visco-elastic layer (Pfeil, M.S., et al, [9])

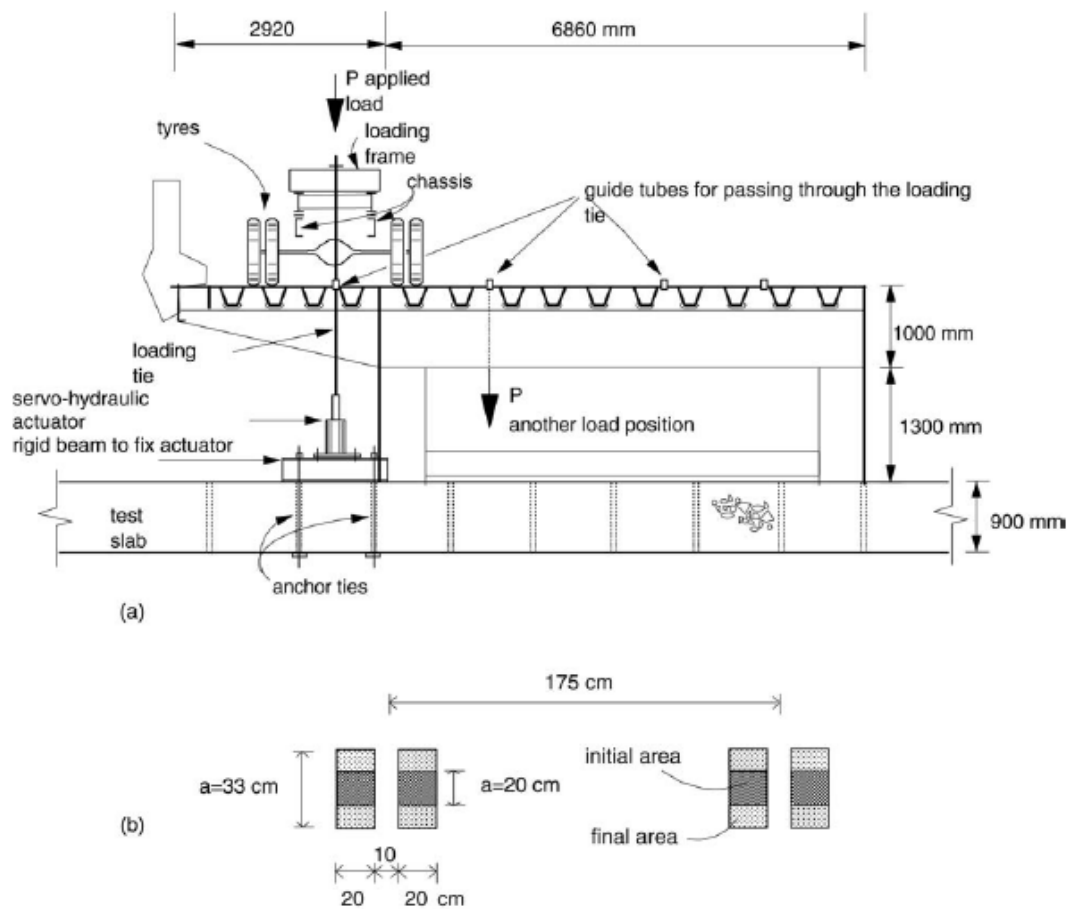


Figure 2.7 (a) Setup of the experiment; (b) The applied wheel load area (Pfeil, M.S., et al, [9])

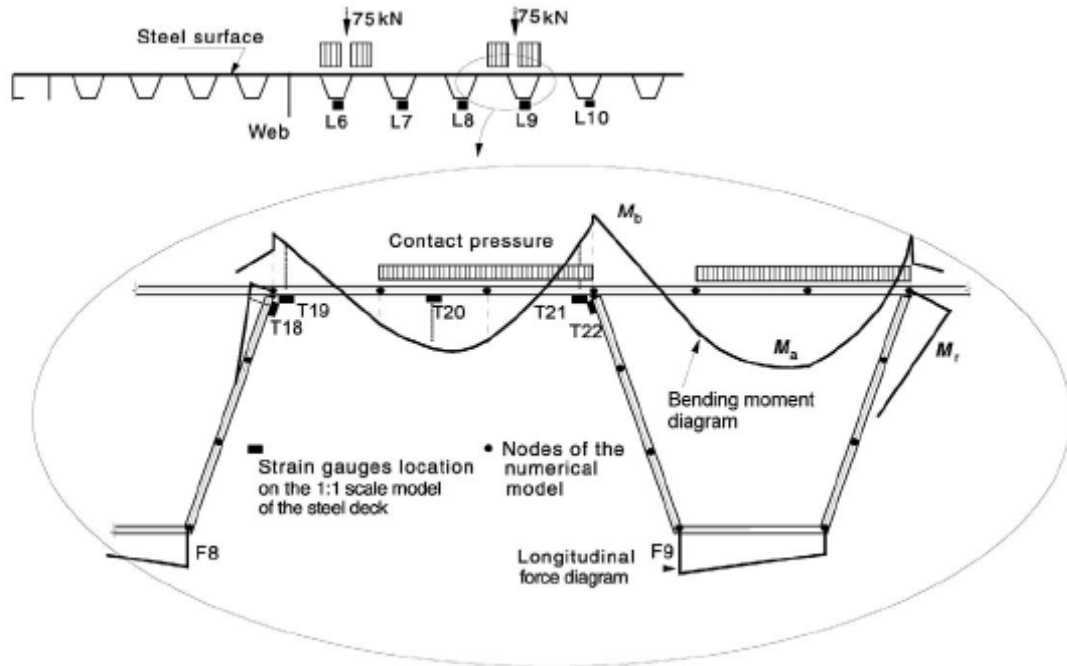


Figure 2.8 Location of the tensors and the bending moment in the trough and the deck plate in the cross section of at the mid span (Pfeil, M.S., et al, [9])

First of all, the calibration was done by comparing the results of the numerical model and the experiment. The results measured at the mid span are listed in table 2.3. In table 2.3, it is shown that the difference between the experimental and theoretical results is small. Especially the stress under the hard contact loading, it is close to the experiment's result. The stress value in table 2.4 indicates that the contact area of the wheel load has influence on the fatigue strength of the orthotropic steel deck as well. By having a larger load distribution area the stresses generated in the orthotropic steel deck will be reduced. Furthermore, the result also shows that locations T20, T21 and T22 are more sensitive to the load area than the other locations. The stress changes in percentage are larger in these locations, as given in table 2.4.

Analysis	Stress values (MPa) at strain-gauges locations					
	T18	T19	T20	T21	T22	
Experimental	-73	-111	119	-79	-30	
Theoretical	Soft contact	-76	-96	156	-99	-9
Theoretical	Hard contact	-73	-93	120	-75	-12

Table 2.3 Results of the experiment and the numerical model (Pfeil, M.S., et al, [9])

Wheel tyres contact area	Stress values (MPa) at strain-gauges locations				
	T18	T19	T20	T21	T22
20 × 20 cm ²	-74	-105	144	-93	-15
20 × 33 cm ²	-73	-93	120	-75	-12

Table 2.4 Results of two wheel loads area (Pfeil, M.S., et al, [9])

Besides the contact area of the wheel load, the location of the wheel load also determines the stress in the trough web. Figure 2.9 shows that the maximum normal force and the bending moment in the trough web occur when the wheel loads are in different locations. By adding up the stresses resulting from these two reaction forces, it turns out that the bending moment is dominant.

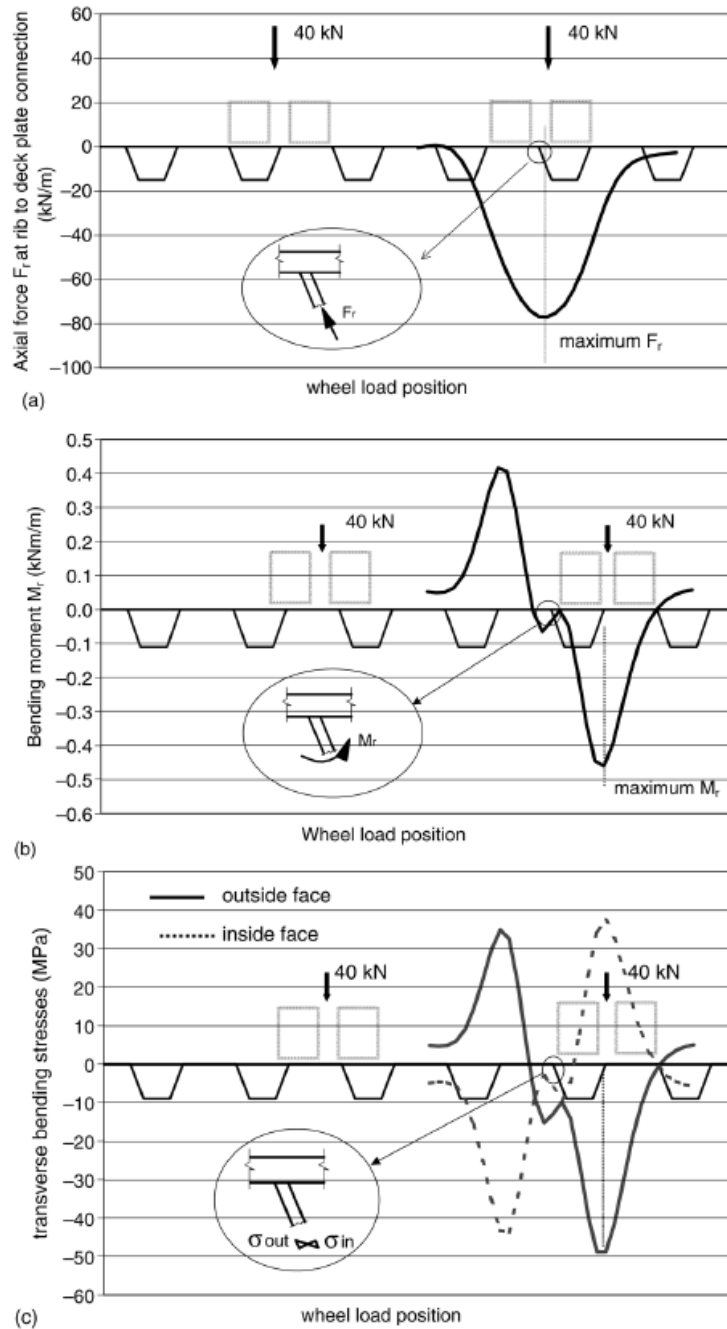


Figure 2.9 Variation of the normal force and bending moment in the trough web at the mid span of the deck panel due to different transverse location of the wheel loads. (a) Normal force in the trough web; (b) Bending moment in the trough web; (c) Resultant stresses in the trough web. (Pfeil, M.S., et al, [9])

Based on these conclusions, the Brazilian researchers took out a parametric study of the relevant geometric dimensions which have influence on the stress (σ_r) in this joint. They calculated the stress in the joint with different combinations of the trough thickness, the deck plate thickness (t_r and t_p) and the trough height (h). The distance between the trough web I and the axle load P are kept as constants ($l=327$ mm, $P = 80$ kN). By summarizing the results, they found out that the stress in the joint is related to the

transverse bending moment in the trough web M_r and also the bending moment in the deck plate M_p . The transverse bending moment M_r in the trough web is related to G which is named as the trough relative slenderness:

$$G = \frac{t_r^3 / h^*}{t_p^3 / l_1 + t_p^3 / l_2 + t_r^3 / h^*}$$

in which h^* is the width of the inclined trough web; l is equal to the largest value of l_1 or l_2 . The bending moment M_p is proportional to l^3 .

The same conclusion can be found in AASHTO (American Association of State Highway and Transportation Officials) and written as the following formula:

$$\alpha_r \propto \frac{t_r}{t_p^3} \frac{l^3}{h^*} = S$$

In figure 2.10, the results of the parametric study are plotted. The curves represent the variations of stress with the non-dimensional parameter S .

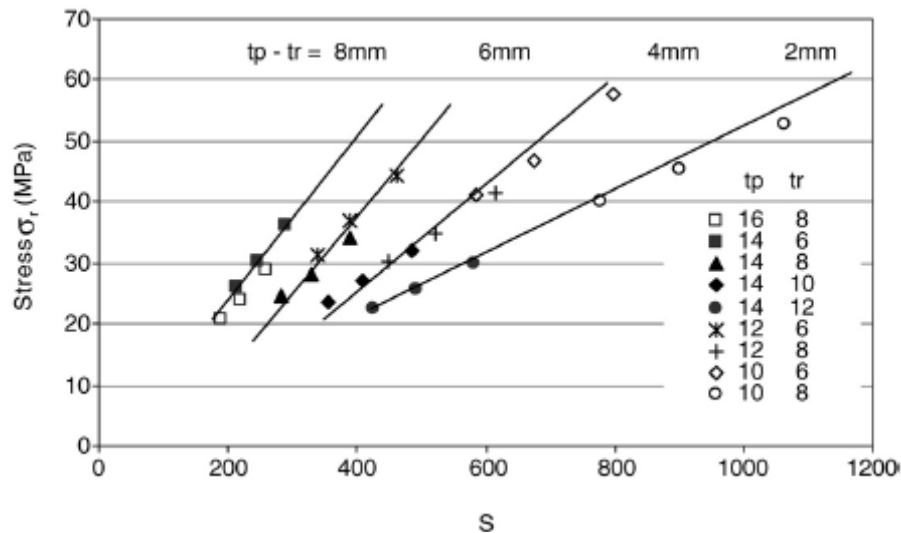


Figure 2.10 Maximum stresses sorted by parameter S and the thickness of the deck plate and trough (Pfeil, M.S., et al, [9])

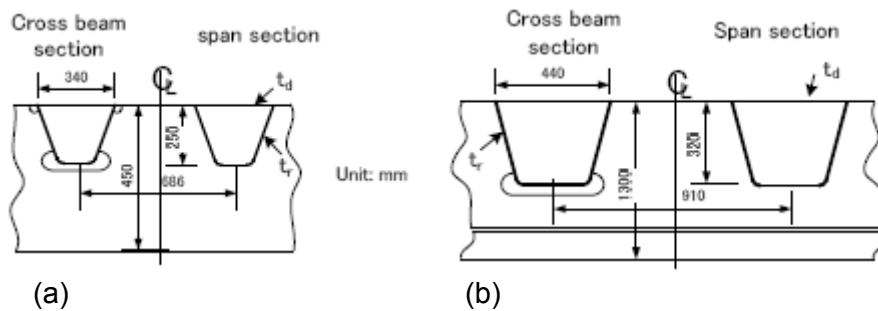
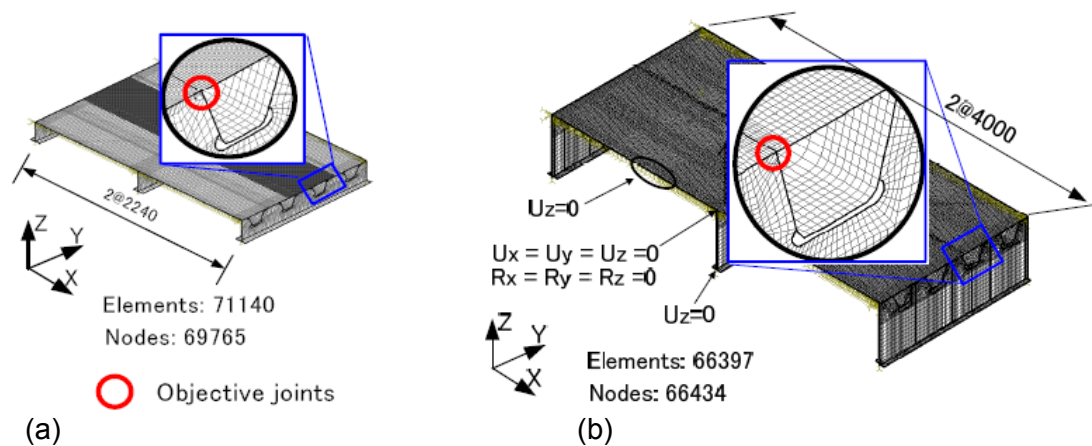
Some conclusions can be drawn from this figure:

- A lower stress can be achieved by applying thicker deck plate and trough.
- When a deck plate thickness is determined, a thinner trough can be used. This is because the stresses are not much increased when reducing the trough thickness. Furthermore, by using a thinner trough, the weight of the structure can be reduced.

When applying the second conclusion drawn from the literature, it is noticeable that it is true only with regarding to the fatigue crack in the trough-to-deck plate joint. That is because the crack can not only initiate in the trough-to-deck plate joint, but also in the bottom flange of the trough. By considering the fatigue cracks in the trough bottom flange, it is not possible to reduce the trough web thickness.

2.3 Research by S. YA and K. YAMADA

In the dissertation of S, YA and K. YAMADA, 'Fatigue Durability Evaluation of Trough to Deck Plate Welded Joint of Orthotropic Steel Deck', the failure at the weld toe in deck plate was investigated. The analysis was carried out by using the finite element models. These models can be divided into two categories: the standard-deck model and the large-trough-deck model (figure 2.11 and figure 2.12). The large-trough-deck model's span is twice as big as the standard-deck model's span. Furthermore, the large-trough-deck models have also larger cross sections. Detail information is collected in table 2.5.



Model	t_d	t_r	Trough span	Model types
GD12R6	12	6	2240	Standard-deck models
GD12R8	12	8		
GD14R6	14	6		
GD14R8	14	8		
GD16R6	16	6		
GD16R8	16	8		
GD18R9	18	8	4000	Large-rib-deck models
GD18R9	18	9		

Table 2.5 Dimensions of the finite element model (mm) (Ya, S., Yamade, K., [10])

Although the asphalt pavement was not included in the finite element model, the load cases of with and without load distribution were modified in order to find out the influence of the asphalt pavement on the result (figure 2.13). The three wheel load positions were applied on the model, see figure 2.14.

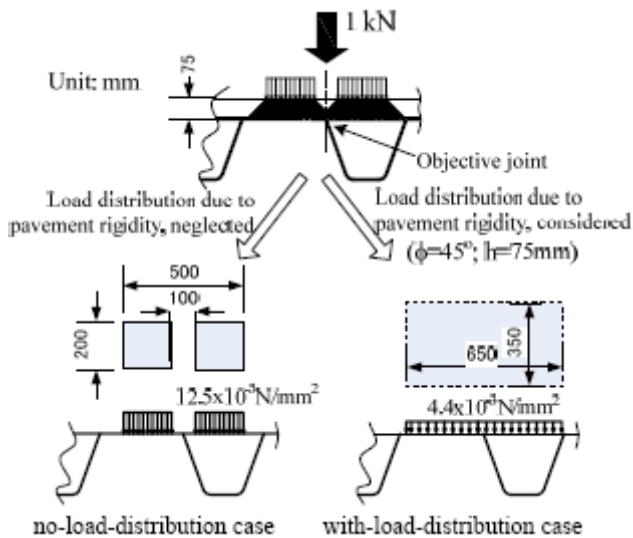


Figure 2.13 Modeling of the distributed wheel load (Ya, S., Yamade, K., [10])

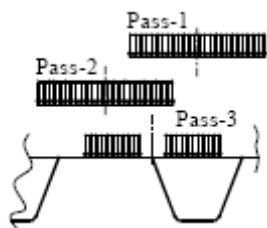
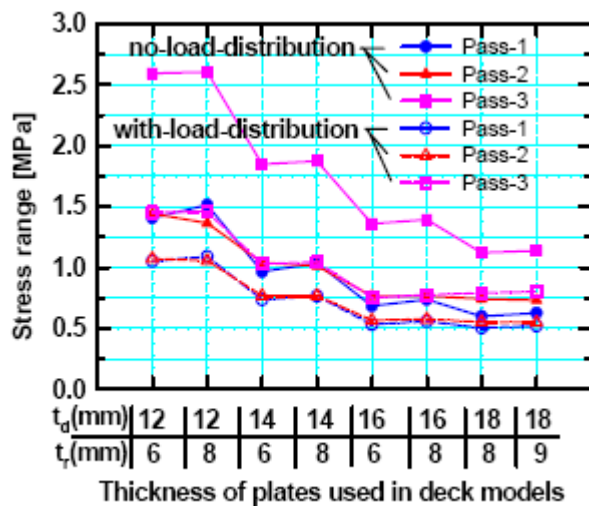
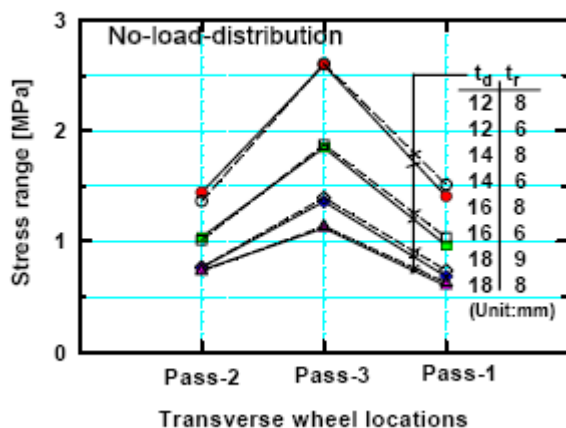


Figure 2.14 Three different load patterns (Ya, S., Yamade, K., [10])

Since the S-N curve for the fatigue analysis is based on the nominal stress, the nodal stress at the bottom surface of the deck plate at 10 mm away from the intersection of the trough-to-deck plate joint is considered as the nominal stress for this investigation. In the figure below, the nominal stress at halfway of the span is plotted for different deck dimensions. It turns out that the load case without load distribution results in a larger stress range than the other cases. When the models are under the same load distribution case, the model with larger dimensions generates a smaller stress range. In addition, the load case Pass-3 results in the largest stress in the object joint which is decisive among the three passes.



(a) Stress ranges vs. plate thickness



(b) Stress ranges vary with transverse wheel passage

Figure 2.15 Stress ranges at halfway of the trough span (Ya, S., Yamade, K., [10])

The comparison of the stress ranges was also made among three different locations along the trough span, see figure 2.16. It can be concluded from the figure that the stress range at one quarter of the span is the largest in standard-deck model. The stress range can be decreased by using thicker deck plate. But in the large-deck model it is possible that the first crack will appear at the CCB (central cross beam). Using a thicker trough in these two kinds of model has little influence on the fatigue life of the joint.

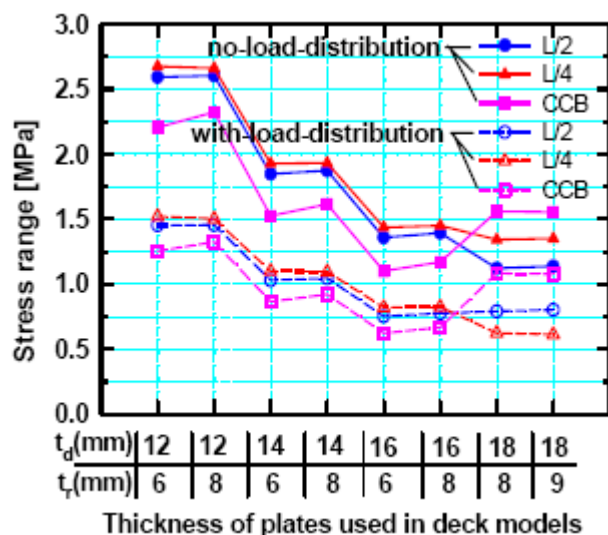


Figure 2.16 Comparison of the stress ranges at 1/2, 1/4 of the trough span and at the crossbeam under Pass-3 (Ya, S., Yamada, K., [10])

2.4 Research by Z.G. Xiao, K. Yamada, S. Ya and X.L. Zhao

In order to study the different crack mechanisms at the trough-to-deck plate joint, Z.G. Xiao, K. Yamada, S. Ya and X.L. Zhao took out a study about the transverse stress distribution within the joint region by using finite element programs. First of all, a finite element model was created as figure 2.17. As what is shown in the figure, the deck plate is supported by four trapezoidal troughs in the transversal direction and five crossbeams in the longitudinal direction. Since the two troughs in the middle and the deck plate between them are the object area, a finer mesh density is applied in this region. The length of the element is around 20 mm. The dimensions of the components are collected in table 2.6.

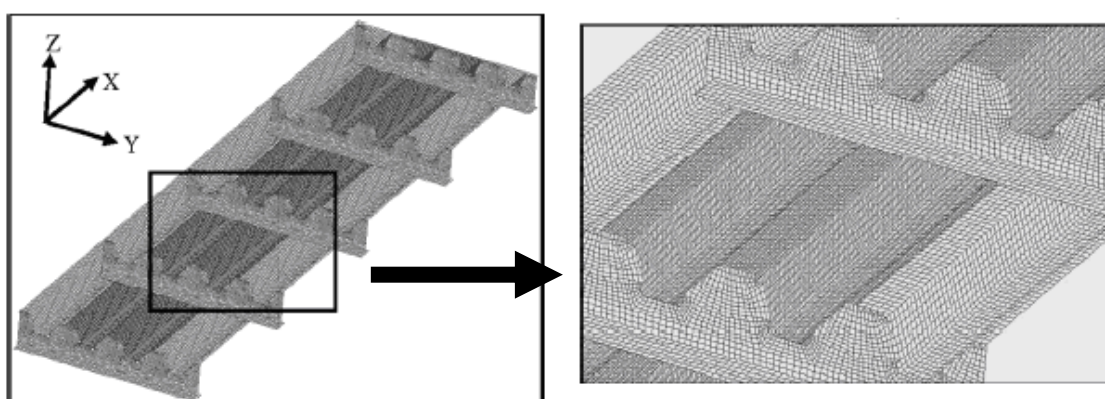


Figure 2.17 Finite element model (Xiao, Z.G., et al, [4])

Structural components		Abbreviations	Dimensions[mm]
Deck plate	Thickness	t_{dp}	12
	Length	L_{dp}	9600
	Width	B_{dp}	2560
Trough	Thickness	t_t	8
	Width upper	B_{tu}	320
	Height	H_t	250
	Distance	D_t	640
Crossbeam	Distance	D_c	2400

Table 2.6 Dimensions of the finite element model

According to the Japanese standard, a wheel load of 100 kN with an area of 200 by 500 mm² is applied on the deck plate as shown in figure 2.18 a. Due to the existing wearing surface (thickness equals to 70 mm), the wheel load is distributed over a larger area of 340 by 640 mm². As indicated in figure 2.18, the interior joint of a middle trough is chosen as the object joint. The stress at this joint is studied in five cross sections. Since the origin of the coordinate system is set in the interior crossbeam, these five cross sections locate at $x= 0, -300, -600, -900, -1200$ mm, respectively. The wheel load, which is running in the longitudinal direction, is applied in three transverse locations. Figure 2.18 b, c and d present the over trough, in-between-trough and riding trough-web positions of the wheel load, respectively.

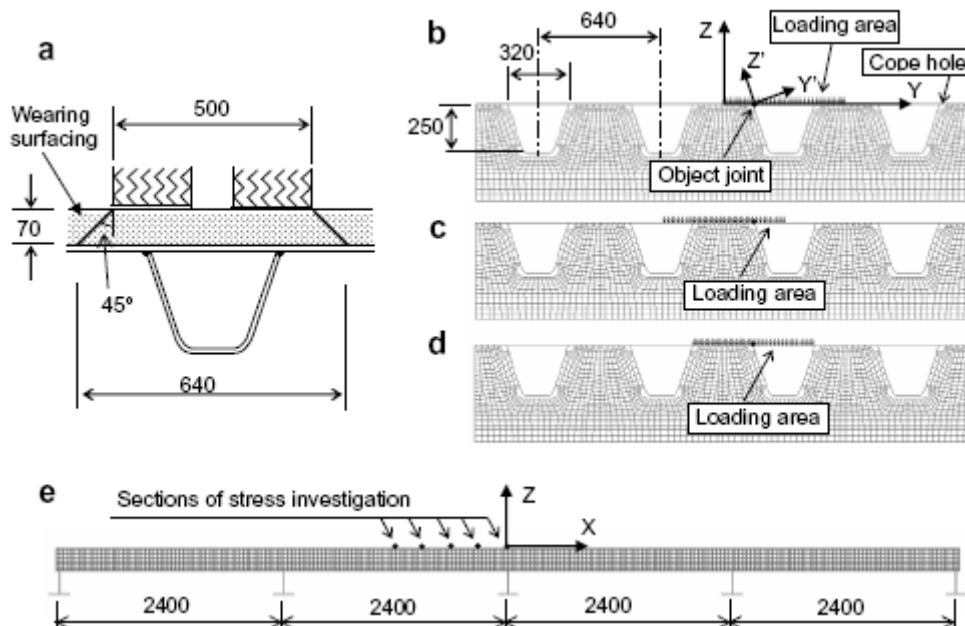


Figure 2.18 (a) Load distribution on the deck plate; (b) Over-trough loading; (c) in –between-troughs loading; (d) Riding-trough web loading; (e) sections of stress investigation [mm] (Xiao, Z.G., et al, [4])

In table 2.7, the results are collected for three sections around the trough-to-deck plate joint. It is clear that the riding-trough web load generates the maximum stress range in

section A and B. The maximum stress rang in section C is reached when the in-between-trough load is applied. Besides that, it is also observed that the stress range in the deck plate is much larger than that in the trough web.

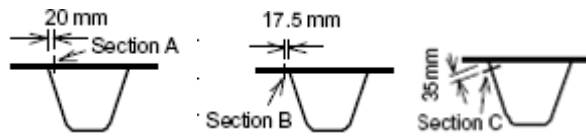


Figure 2.19 Three object sections (Xiao, Z.G., et al, [4])

Location of stress investigation		Over-rib loads	In-between-ribs loads	Riding-rib wall loads
Section A (Bottom face)	$X=0$	94.7	47.4	91.0
	$X = -300 (L/8)$	77.3	74.6	104.8
	$X = -600 (L/4)$	76.2	73.2	103.6
	$X = -900 (3L/8)$	74.3	72.1	101.6
	$X = -1200 (L/2)$	72.1	71.5	99.8
Section B (Bottom face)	$X = -300 (L/8)$	86.3	88.7	118.3
	$X = -600 (L/4)$	84.9	87.4	117.5
	$X = -900 (3L/8)$	82.2	86.8	115.2
	$X = -1200 (L/2)$	79.1	86.5	113.0
Section C (Outside face)	$X = -300 (L/8)$	9.1	34.9	22.6
	$X = -600 (L/4)$	14.7	39.7	23.4
	$X = -900 (3L/8)$	18.1	40.9	21.7
	$X = -1200 (L/2)$	18.1	40.8	20.1

Table 2.7 Range of transverse stress (Mpa) under the action of 100 kN wheel load (Xiao, Z.G., et al, [4])

By gathering the results of the computational models (table 2.8), it turns out that many factors will influence the fatigue life of the trough-to-deck plate joint. From the fourth and seventh column, it can be concluded that the stress range can be significantly reduced by distributing the wheel load over a large area. It is also true that increasing the deck plate can reduce the stress range. However, a thicker trough does not guarantee a small stress range. The last column shows that a larger-trough model can provide with a longer fatigue life. In this case the larger-trough model means a combination of a larger trough and a larger spacing between troughs and the crossbeams. In this way, the weight of the structure is less and the welding lengths are shorter. This indicates the cost can also be reduced.

Location of stress investigation		Stress range (MPa)					
		Basic model	Without surfacing	6 mm Rib	14 mm Deck	Single wheel	Large rib
Section A (Bottom face)	$X = 0$	91.0	134.0(1.47)	85.6(0.94)	63.2(0.69)	108.8(1.20)	59.9(0.66)
	$X = L/8$	104.8	158.7(1.51)	106.4(1.02)	76.6(0.73)	122.2(1.17)	78.1(0.74)
	$X = L/4$	103.6	156.3(1.51)	104.9(1.01)	75.2(0.73)	118.1(1.14)	76.6(0.74)
	$X = 3L/8$	101.6	153.5(1.51)	102.0(1.00)	73.2(0.72)	114.3(1.13)	73.8(0.73)
	$X = L/2$	99.8	151.5(1.52)	99.4(1.00)	71.4(0.72)	111.4(1.12)	72.7(0.73)
Section B (Bottom face)	$X = L/8$	118.3	181.4(1.53)	119.3(1.01)	87.0(0.74)	141.1(1.19)	85.8(0.73)
	$X = L/4$	117.5	180.1(1.53)	118.0(1.00)	85.9(0.73)	138.9(1.18)	84.9(0.72)
	$X = 3L/8$	115.2	177.3(1.54)	115.4(1.00)	83.9(0.73)	135.4(1.18)	82.1(0.71)
	$X = L/2$	113.0	174.5(1.54)	112.8(1.00)	81.8(0.72)	131.8(1.17)	81.2(0.72)

Note: Numbers in parentheses are ratios of stress range to the basic model.

Table 2.8 Stress ranges of trough-to-deck plate joint under riding-trough web loads (100kN) (Xiao, Z.G., et al, [4])

2.5 Research by Y.L. Zhang, Y.S. Li and D.Y. Zhang

In China, the fatigue of steel bridge was not taken into consideration in the past design code. This leads to an insufficient design in sense of fatigue resistance. In this circumstance, a study was carried out to gain knowledge of the behaviour of the trough-to-deck plate joint. In this study, the deck structure of a suspension bridge was modelled in ANSYS (figure 2.20). And the dimensions of the components are shown in figure 2.21 and table 2.9.



Figure 2.20 Finite element model (Zhang, Y.L., et al [11])

Structural components		Abbreviations	Dimensions[mm]
Deck plate	Thickness	t_{dp}	12
	Length	L_{dp}	12200
	Width	B_{dp}	1860
Trough	Thickness	t_t	8
	Width upper	B_{tu}	310
	Height	H_t	260
	Distance	D_t	620
Crossbeam	Distance	D_c	4000

Table 2.9 Dimensions of the finite element model

On the structure, a 70 kN wheel load with a contact area of 200 mm by 600 mm is applied. By considering the wearing surface on the deck plate, the wheel load is distributed over a larger area of 380 mm by 780 mm. In this research, three locations of the wheel load in the transversal direction were studied (riding-rib wall loading, over-rib loading and in-between-ribs loading). In the longitudinal direction, two locations were under investigation, see figure 2.21.

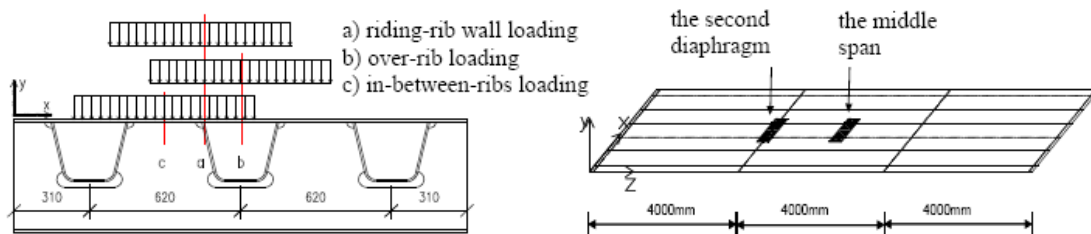


Figure 2.21 (a) Transverse loading cases; (b) Longitudinal load cases (Zhang, Y.L., et al [11])

The results of the transverse stress distribution in the deck plate at the second crossbeam and at the middle span are plotted in the figure 2.22 and figure 2.23. It is clear that the loading area suffers from larger stress than the rest. And the influential area at the middle span is larger than that at the second cross beam. The stress curve is sharp when the investigated trough-to-deck plate joint is under the load area. It means that the stress concentrates at this point. By comparing the stress ranges generated by these three transverse loading locations, it can be concluded that the riding-trough web loading is the most critical load case.

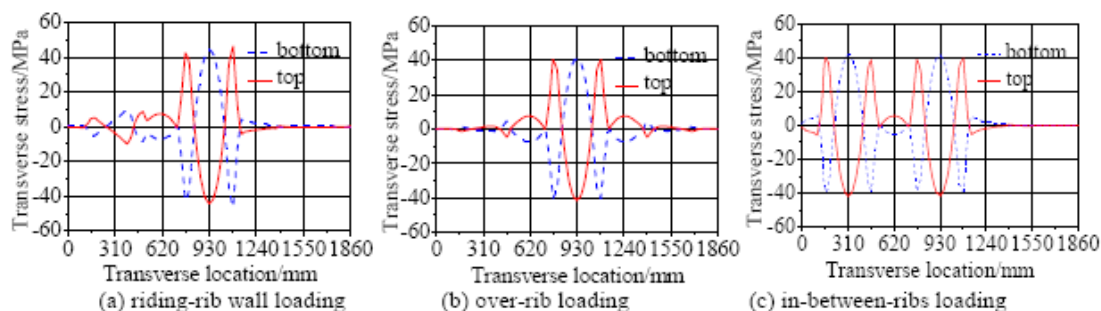


Figure 2.22 Transverse stress distribution in the deck plate at the second crossbeam (Zhang, Y.L., et al [11])

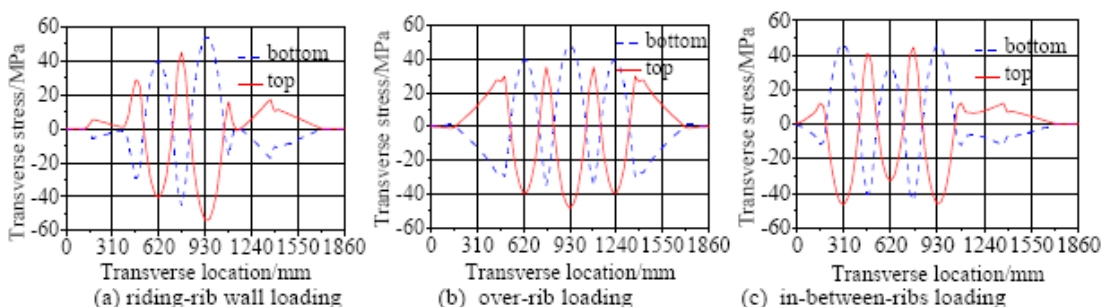


Figure 2.23 Transverse stresses distribution in the deck plate at the middle span (Zhang, Y.L., et al [11])

In the figure below, the longitudinal stress influence lines at the bottom surface of the object joint are plotted for five locations A, B, C, D and E. It is clear to see that the maximum stress at each location appears when the wheel load is running over the object location. Moreover, under the three transverse loading locations, the maximum stress ranges appear at section B. In addition, the riding-rib web loading has the largest stress

range. It means that this transverse loading location is the most unfavourable loading situation.

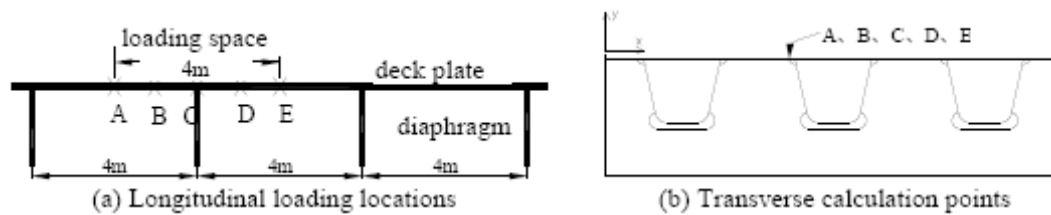


Figure 2.24 The object points and sections (Zhang, Y.L., et al [11])

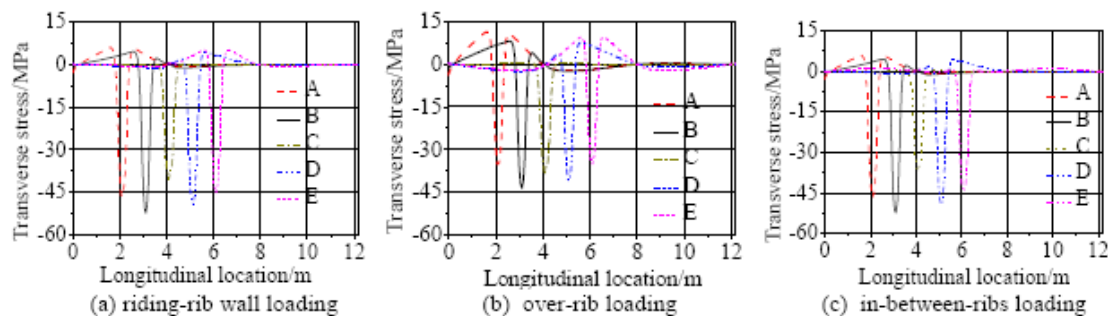


Figure 2.25 Longitudinal influence line at the deck bottom in the object joints (Zhang, Y.L., et al [11])

2.6 Research by M.H. Kolstein

In the dissertation of M.H. Kolstein, '*Fatigue Classification of Welded Joints in Orthotropic Steel Bridge Decks*', attention was also paid on the trough-to-deck plate joint. The test program and the data were divided according to the following weld types:

- Fillet welded joint-manual welding
- Partial penetration welded joint-manual welding
- Partial penetration welded joint-automatic welding

Within the joint categories, the subdivision was made according to the modes of failure. There are three potential modes:

- Crack initiates in the weld toe in the deck plate
- Crack initiates in the weld root through the throat
- Crack initiates in the weld toe on the trough

The results of the fatigue tests on the fillet welded joints carried out by Maddox, Thonnard and Kolstein are shown in the same figure. All tested joints failed in the weld. All the test results fall in the same scatter and are larger than the specified classification in the Eurocodes. Therefore it is suggested to upgrade the classification from 50 to 63 for the manual fillet welded joint.

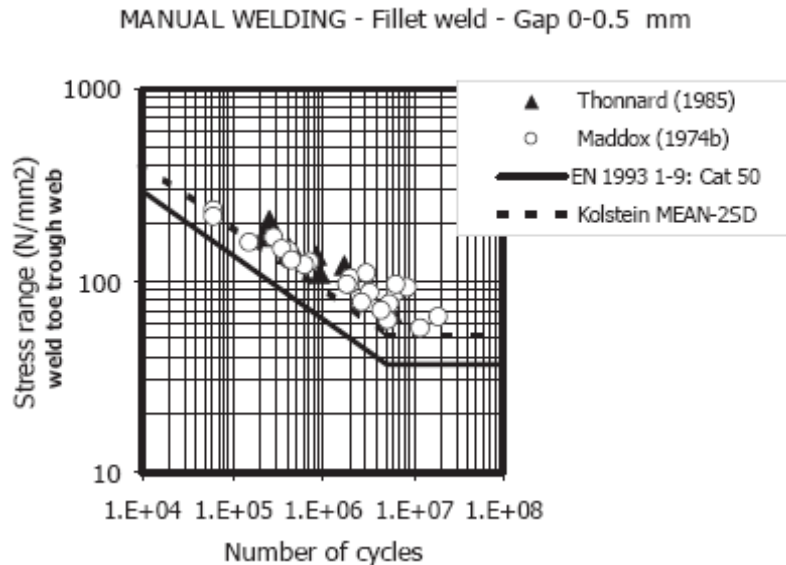


Figure 2.26 Fillet welded joint with 0 to 0.5 mm gap (Kolstein, M.H., [3])

Thonnard carried out the fatigue tests on the manual partial penetration welding with a gap of 2 mm. Most of the tests failed in the trough web. By comparing the tests' results and the defined S-N curve in the Eurocodes (figure 2.27) it can be concluded that the classification of the manual partial penetration welding can be kept as 50 as what has been defined in the Eurocodes.

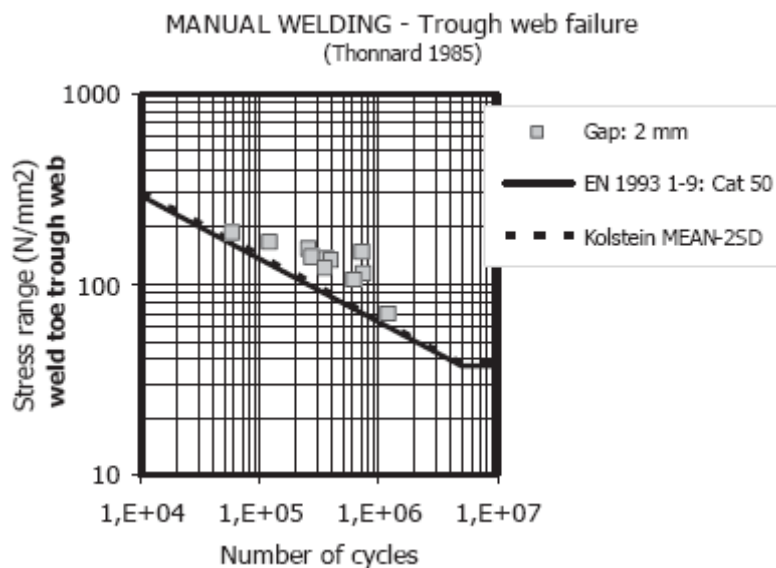


Figure 2.27 Penetration welded joint with 2 mm gap; failure in the trough web (Kolstein, M.H., [3])

The test on the trough-to-deck plate joint was also carried out by Bruls in 1990. The trough web and the deck plate were connected with an automatic partial penetration weld and the gap between them was smaller than 0.5 mm. This type of joint failed in the weld throat when the stress range is about 100 N/mm^2 .

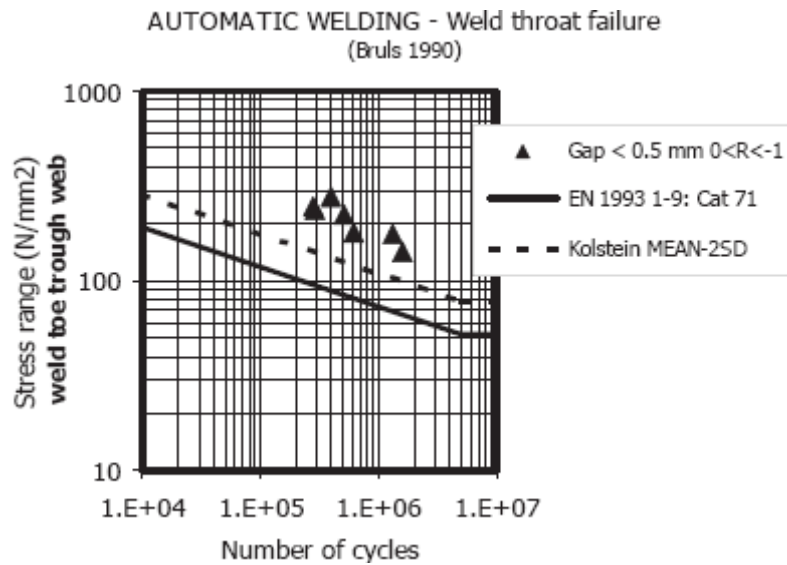


Figure 2.28 Partial penetration welded joint, gap<0.5 mm, failure in the weld throat (Kolstein, M.H., [3])

The automatic partial penetration welds with a 0-2 mm gap were tested by Dijkstra and Bignonnet. The failures were found in the deck plate. The results of these two independent test sets are similar to each other (figure 2.29). This approach leads to a design stress range of 140 N/mm² at 2E+06 cycles. But by considering the reproducibility of this joint, it is recommended to lower the classification to category 125. Even though, a strict requirement of the weld and the plate material is a precondition.

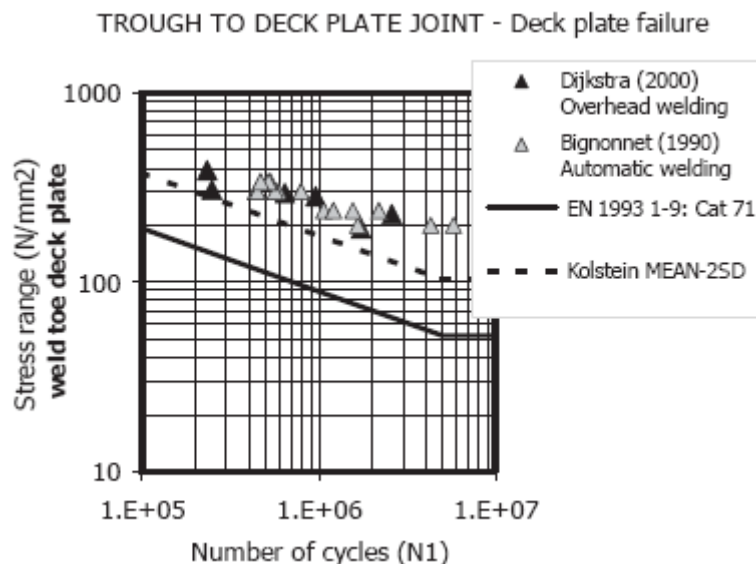


Figure 2.29 Automatic welding with a gap of 0-2 mm between trough and deck plate with deck plate failure (Kolstein, M.H., [3])

Based on these test results and the given detail category in NEN-EN 1993-1-9 and by considering the reproducibility of the welds, M.H. Kolstien proposed the new detail

categories of the trough-to-deck plate joint as followed.

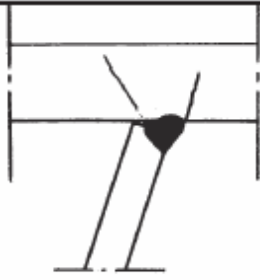
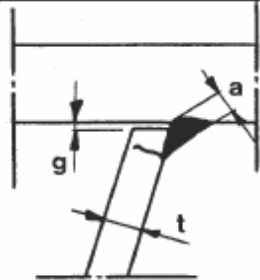
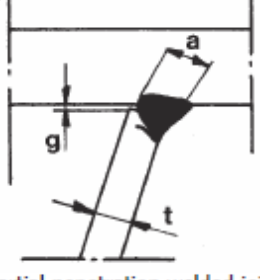
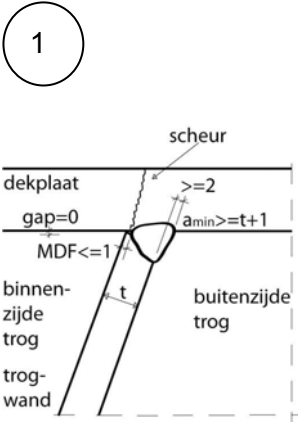
Detail category	Constructional detail	Description	Requirements
125	 Deck plate crack	1) For cracking in the deck plate. Smooth transition of the weld and plate material	1) Assessment based on the nominal stress range $\Delta\sigma$ in the deck plate at the location of the trough.
63	 Fillet welded joint	2) For cracking in the weld or trough web.	2) Assessment based on the nominal stress range $\Delta\sigma$ in the trough web at the deck.
		2a) Fillet weld. gap ≤ 0.5 mm throat \geq web thickness	2a) The trough web must be shaped parallel to the deck plate
50	 Partial penetration welded joint	2b) Partial penetration weld. $0.5 \text{ mm} < \text{gap} \leq 2 \text{ mm}$ throat \geq web thickness	2b) Nominal penetration 80%, minimum 50%
90		2c) Penetration weld. gap ≤ 0.5 mm.	2c) Nominal penetration 80%, minimum 50%. Overhead welding yearly inspection.
100		2d) Partial penetration weld. gap ≤ 0.5 mm.	2d) Automatic welding. Nominal penetration 80%, minimum 50%

Table 2.10 Proposal detail categories for trough to deck plate joints (Kolstein, M.H., [3])

Based on the proposal of M.H. Kolstein, NEN-EN 1993-2/NB gives more detail descriptions of the categories.

Detail-categorie	Constructiedetail	Beschrijving	Eisen

Detail-categorie	Constructiedetail	Beschrijving	Eisen
125		<p>Locatie Scheur in de dekplaat op een locatie tussen de dwarsdragers</p> <p>Scheurtype Scheur geïnitieerd vanuit de las tussen de dekplaat en de verstijvers; kan aan beide zijden ontstaan</p> <p>scheurgroei Door de dikte van de dekplaat vanuit de las.</p>	<p>$\Delta\sigma$ berekend als nominale lokale spanning aan de onderzijde van de dekplaat op het scheurinitiatiepunt, berekend met een 3D model</p> <p>amin t+1 mm</p> <p>Vorbewerking ; Verstijverbeen afschuiven tot een lasopeningshoek van 50°. Bij O.P. lassen tot t ≤ 6mm geen afschuiving</p> <p>spleet 0 mm; over 10% van de lengte is < 0,5 mm toegestaan</p> <p>MDF ≤ 1,0 mm</p> <p>NDO visueel: 100%; MT: alle lasaanzetten + 10% van de laslengte als steekproef te kiezen op basis van de visuele inspectie</p> <p>Lasgeometrie: De las moet vloeiend aanliggen aan het dek en het verstijverbeen.</p>
100 bij automatisch lasproces 90 bij handlassen		<p>Locatie Las tussen het verstijverbeen en de dekplaat op een locatie tussen de dwarsdragers</p> <p>Scheurtype Scheur geïnitieerd vanuit de las</p> <p>Scheurgroei</p>	<p>$\Delta\sigma$ berekend als lokale nominale spanning in het verstijverbeen, berekend met een 3D model</p> <p>amin t+1 mm</p> <p>Vorbewerking ; Verstijverbeen afschuiven</p>

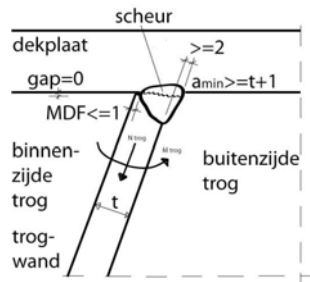
Detail-categorie	Constructiedetail	Beschrijving	Eisen
		Door de dikte van de las vanuit de wortel of de teen van de las.	<p>tot een lasopeningshoek van 50°. Bij O.P. lassen tot $t \leq 6\text{mm}$ geen afschuining</p> <p>spleet 0 mm; over 10% van de lengte is < 0,5 mm toegestaan.</p> <p>MDF $\leq 1,0$ mm</p> <p>NDO visueel: 100%; MT: alle lasaanzetten + 10% van de laslengte als steekproef te kiezen op basis van de visuele inspectie</p> <p>Lasgeometrie: De las moet vloeiend aanliggen aan het dek en het verstijverbeen.</p>

Table 2.11 Detail classification of longitudinal weld of trough-deck plate joint (NEN-EN 1993-2/NB, [N6])

2.7 Evaluation of the literature study

Although the previous sections present the results of different independent researches, the conclusions are direct and obvious. It turns out that the stress in the trough-to-deck plate joint is greatly dependent on the dimensions of the structure itself and the distribution area of the wheel load. The location of the wheel load also determines where the peak value of the stress will occur in the component. If the center of the wheel load is above the trough wall, the maximum stress occurs in the deck plate. The maximum stress in the trough web is generated when the center of the wheel load is in between two troughs. The precise load location depends also on in which surface (in- or exterior surface of the trough web) the stress is under study. Furthermore, the stress in the joint can be reduced by using a thicker deck plate and a thicker wearing surface. But a thicker trough web has hardly any influence on the fatigue life of the joint.

Based on the previous research, detail information and category of the welds are given in the National Annex. But there is still a lack of knowledge on how to determine the stresses in the trough-to-deck plate correctly and sufficiently. Though a large cross section (trough spacing stays the same) can reduce the stress in the joint, it increases

the weight of the structure and therefore leads to an uneconomical solution. The objective of this thesis is to develop a simplified approach which can be used for the design of steel bridges with respect to fatigue resistance.

3 Finite element model

In this chapter, the 3D finite element models are created for the fatigue analysis of the steel bridges. These models are built with the help of finite element program MIDAS Civil [S1]. Different loads are applied on the model according to the Eurocodes. At last, results of the calculation are given.

3.1 Geometry

The analysis of the trough-to-deck plate joint is done with the help of 3D finite element model. In this study, the stresses from the crossbeams and the main girders are neglected. Only the local effects of the orthotropic deck are taken into account. Therefore, a partial structure (the orthotropic deck) is modeled instead of the whole bridge structure. To find out the influence of the geometry on the stress in the trough-to-deck plate, two types of orthotropic steel deck are considered. One type is the orthotropic deck with asphalt layer on the deck plate. The influence of the asphalt layer is taken into account by a spreading of the wheel load with an angle of 45° (the asphalt layer is assumed to have no stiffness). The other is without this wearing surface. Under each type of orthotropic deck, two models are created. In these models, different trough and deck plate thicknesses are applied. The geometries and main dimensions of these models are given in table 3.1.

Structural component		Model type			
		Orthotropic deck with asfalt (60mm)		Orthotropic deck without asfalt (8mm epoxy layer)	
		Model A	Model B	Model C	Model D
Crossbeam	Height(H_c)	1250	1250	1250	1250
	Length(L_c)	4200	4200	4200	4200
	Distance(D_L)	3500	3500	3500	3500
	Thickness(t_c)	12	12	12	12
Deck plate	Length(L_d)	21000	21000	21000	21000
	Width(B_d)	4200	4200	4200	4200
	Thickness(t_d)	12	18	12	22
Trough	Height(h_t)	325	350	325	350
	Width upper(b_{top})	300	300	300	300
	Width bottom(b_{bot})	105	150	105	150
	Thickness(t_t)	6	8	6	8
	Distance(d_t)	600	600	600	600

The unit of the dimension is mm

Table 3.1 Dimensions of the orthotropic deck models

In general, the model consists of seven trapezoidal troughs which are supported by seven crossbeams (figure 3.1). The model has a $21000 \times 4200 \text{ mm}^2$ deck plate. The seven crossbeams divide the deck into six spans. The spacing between the trough webs is 300 mm and the spacing between the crossbeams is 3500 mm. The crossbeam is modeled as a vertical plate which is 1250 mm high and 12 mm thick.

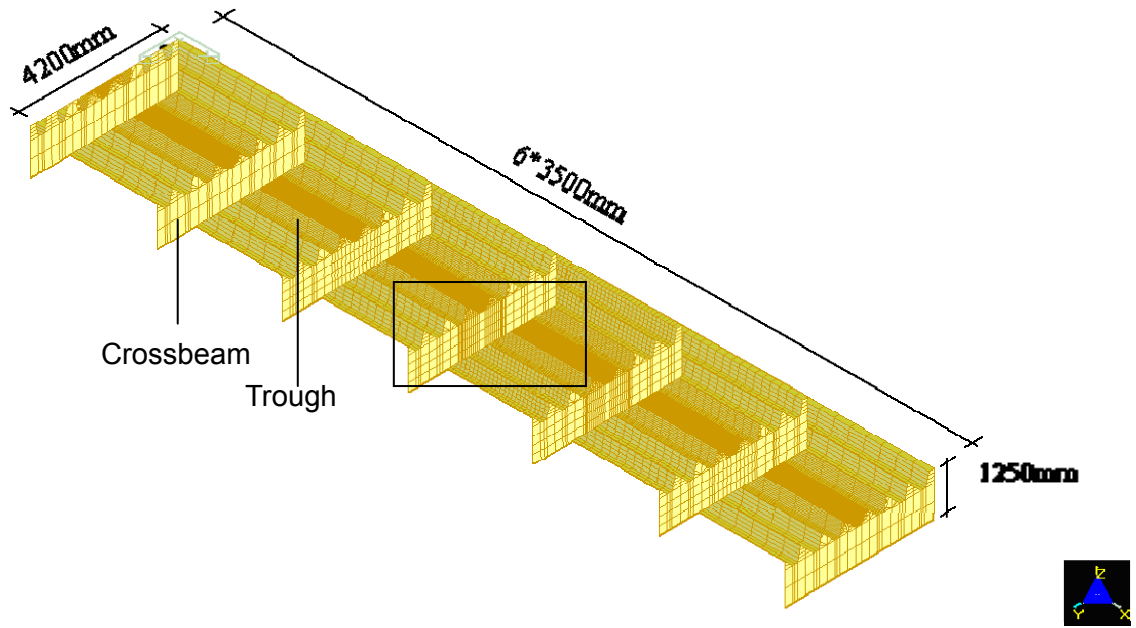


Figure 3.1 Orthotropic deck 3D model in MIDAS Civil

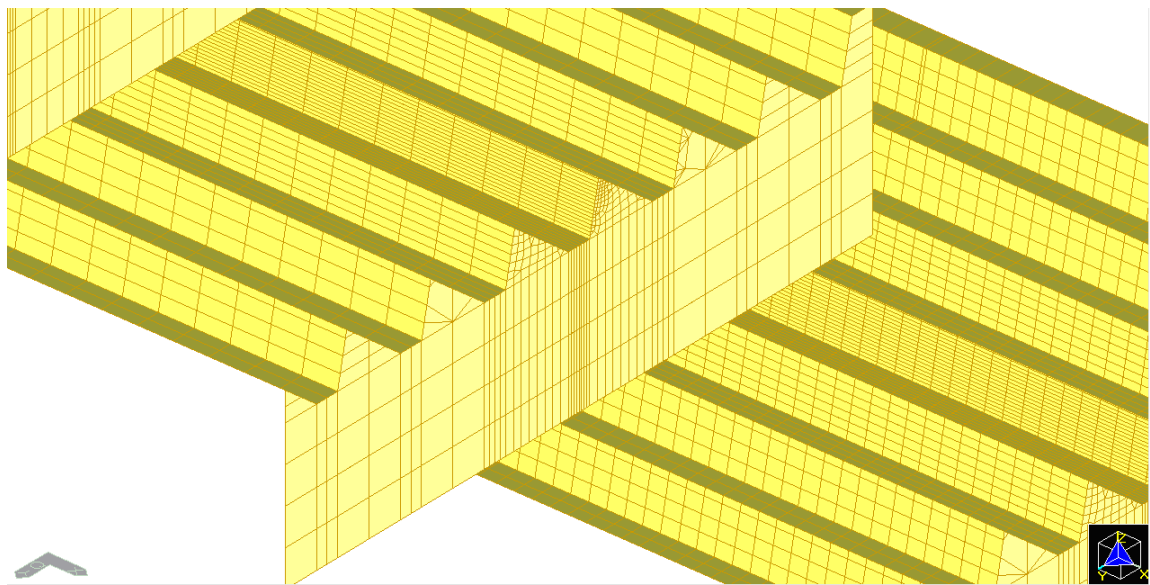


Figure 3.2 Detail of the orthotropic deck model

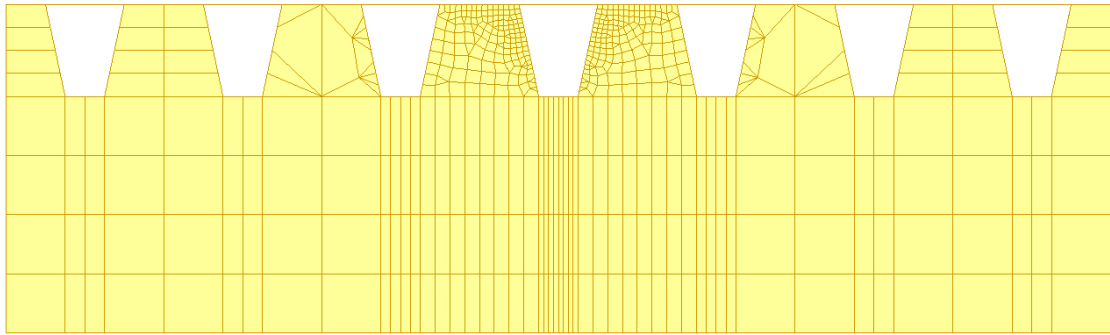


Figure 3.3 Cross-section of the orthotropic deck model

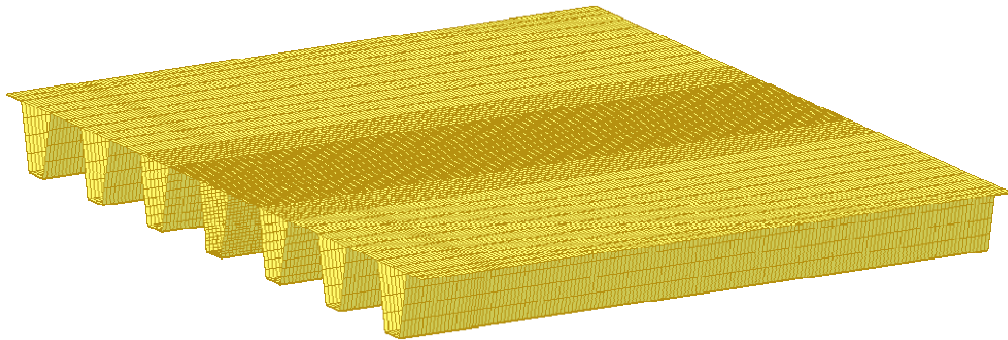


Figure 3.4 Perspective view of the fourth span

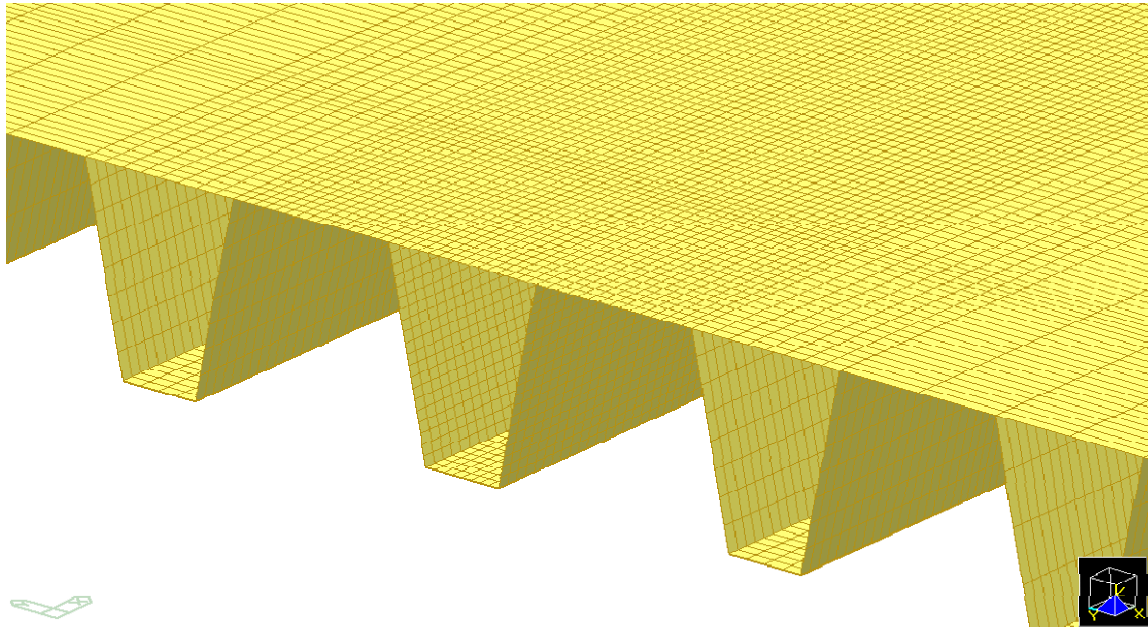


Figure 3.5 Detail view of the fourth span

The element used in this 3D finite element modeling is plate element. It is also called shell element in MIDAS Civil. Four nodes placed in the same plane define a plate element. The element is capable of counting for in-plane tension/compression, in-plane/out-of-plane shear and out-of-plane bending behaviors. Therefore, the plate element is permitted to model the retaining walls, bridge decks, building floors and mat foundations. In each node of the element, there are five degrees of freedom which are the translational degrees of freedom in x, y and z-directions, and rotational degrees of freedom in x and y-axes in the element coordinate system, see figure 3.6.

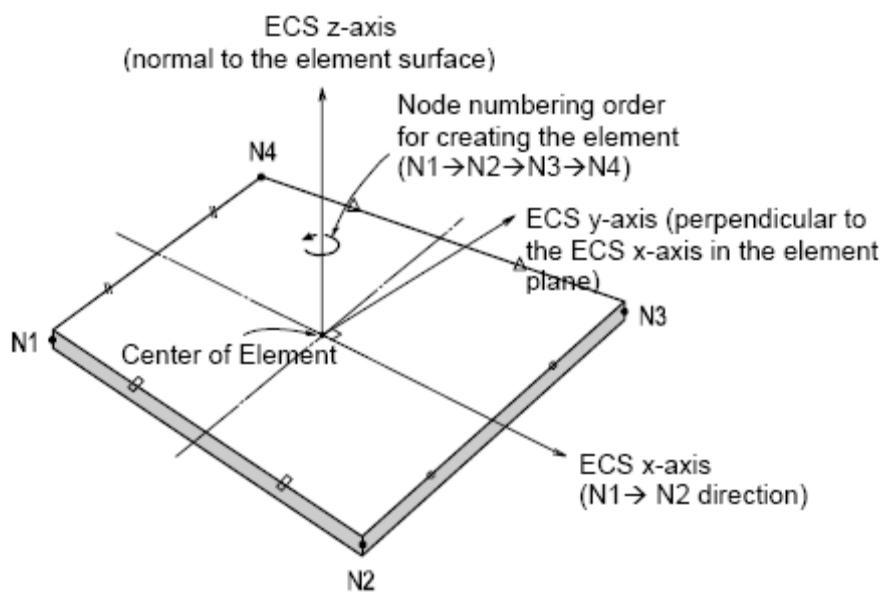


Figure 3.6 Arrangement of plate element and its element coordinate system (Manual MIDAS Civil, [12])

3.2 Object joint

As this study focuses on the trough-to-deck plate joint in between the crossbeams, the object joint is on the left-hand trough web of the middle trough (see figure 3.7). The stress in this object joint is investigated in four different cross-sections in the trough span between the fourth and the fifth crossbeams. They are indicated with section A, B, C and D in figure 3.8. When the wheel load is centrally above section A, the edge of the wheel print should be exactly above the third crossbeam. Therefore, its location depends on what kind of wheel print is put on the deck plate. Section B, C and D are at one eighth, one quarter and halfway of the fourth trough span. The coordinates of the object joints are listed in Table 3.2.

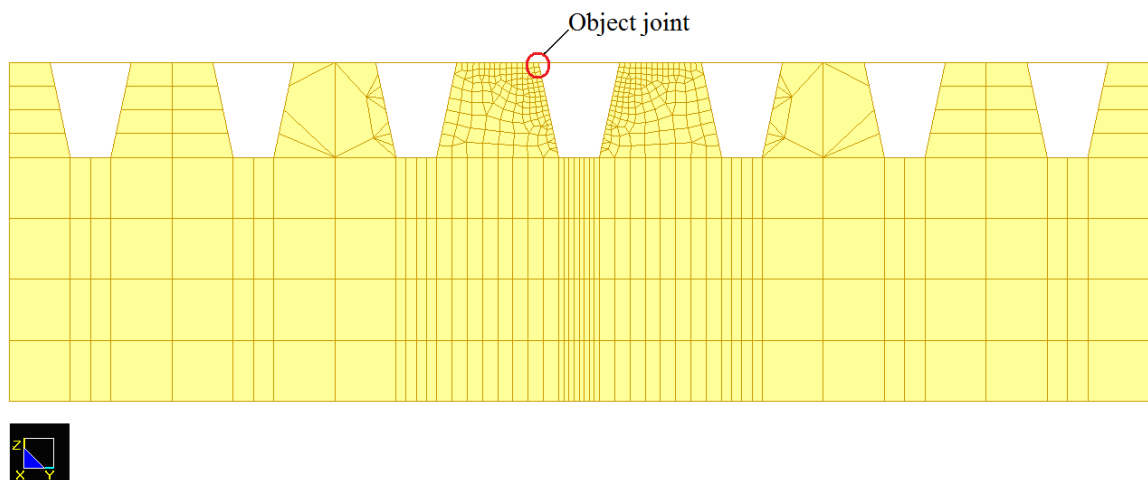


Figure 3.7 Cross-section of the orthotropic deck and the object joint

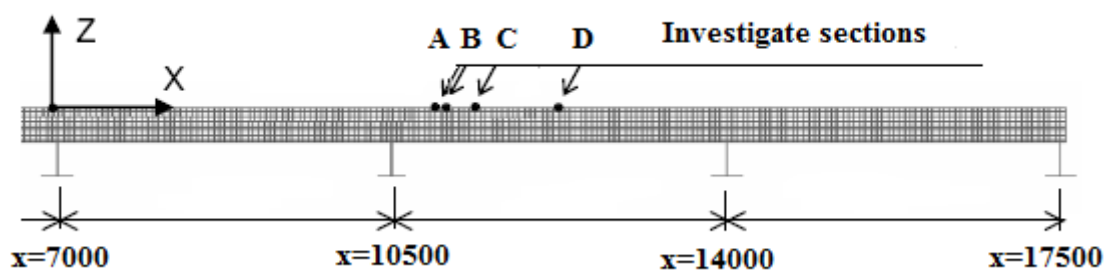


Figure 3.8 Object sections along the length of the trough span

Object joints	X-coordinates [mm]	Y-coordinates [mm]	Z-coordinates [mm]
A	(depending on wheel print)	2250	0
B	10937.5	2250	0
C	11375	2250	0
D	12250	2250	0

Table 3.2 Coordinates of the object joints

3.3 Mesh density

Using a proper mesh density is important for finding out the reliable result. If an inappropriate course mesh is applied, the model may miss important data for an accurate result. On the other hand, if a too dense mesh is used, the program will take a long unnecessary time for calculating. To get an accurate result and save time in modeling, different mesh density should be applied according to the requirement of the research. In this study, the elements which are under investigation or nearby the object joint are dense meshed. In figure 3.9, one may see that the elements around the middle trough and in the fourth span are much smaller than the others. In this area, the element has a length of 20mm. The width of the element in the central part of the cross section has a length of 20mm (see figure 3.10). Outside of this region, the further the element is away from the object span and trough, the courser the mesh is.

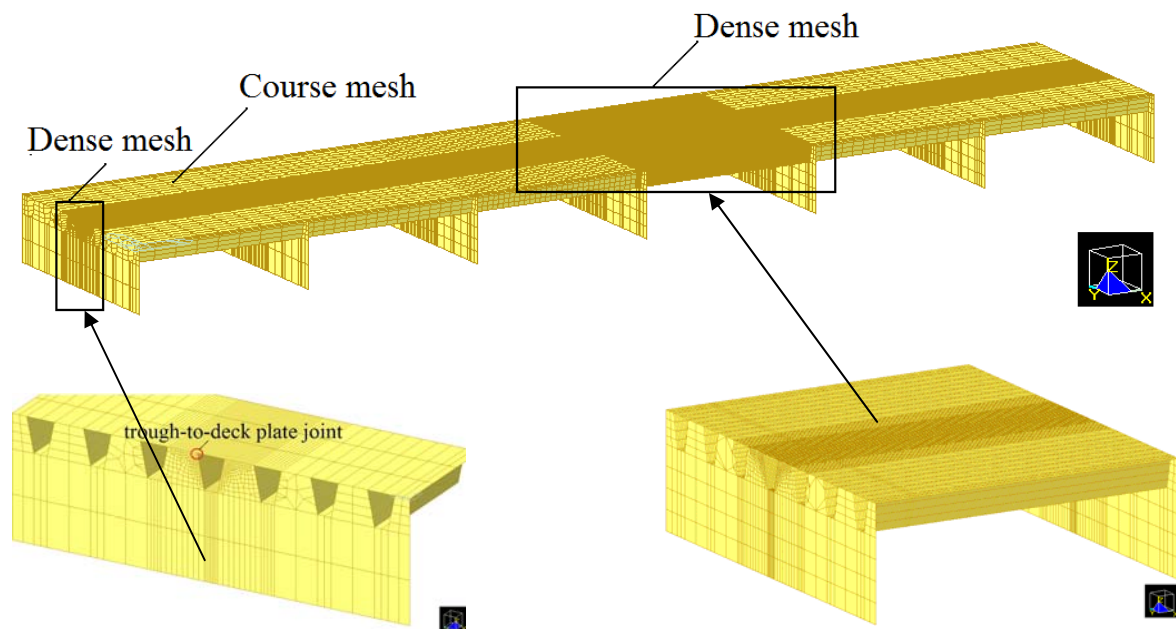


Figure 3.9 Mesh density in the finite element model

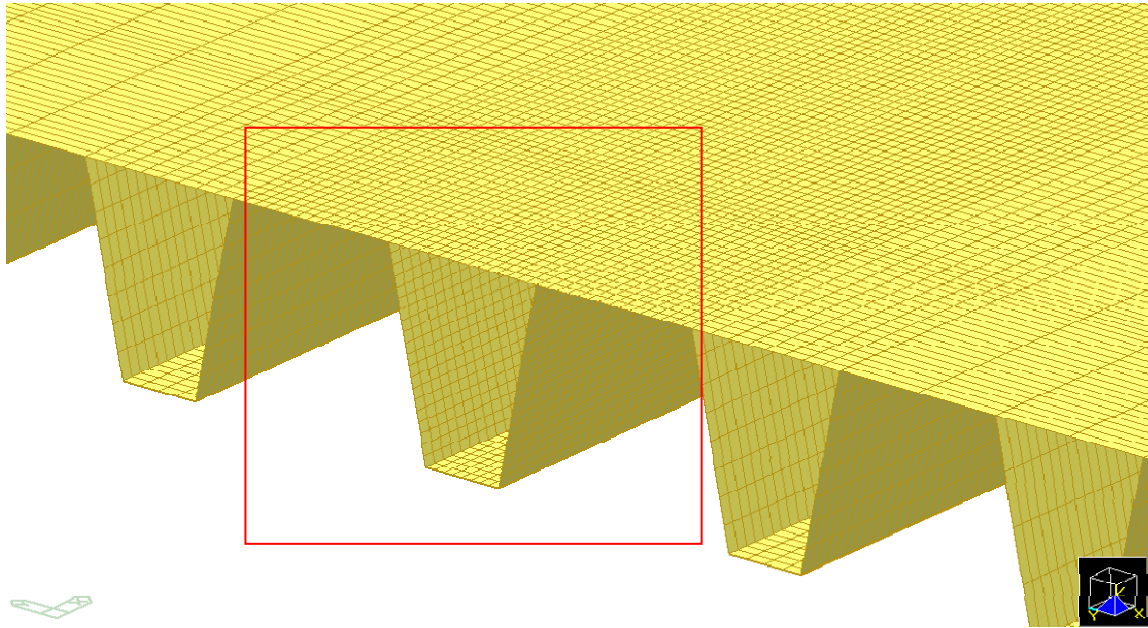


Figure 3.10 The central part of the cross-section which has a mesh of 20mm*20mm

3.4 Boundary conditions

The bottoms of the crossbeams are constrained in the vertical direction (z direction). Among them, the bottom of the left crossbeam (support) is constrained also in x direction (longitudinal direction). In order to avoid transversal movement of the bridge, all nodes at $y=0$ (at the bottom of the crossbeams) are fixed in the y direction (transversal direction) as well (figure 3.11). A top view of the boundary conditions is presented in figure 3.12

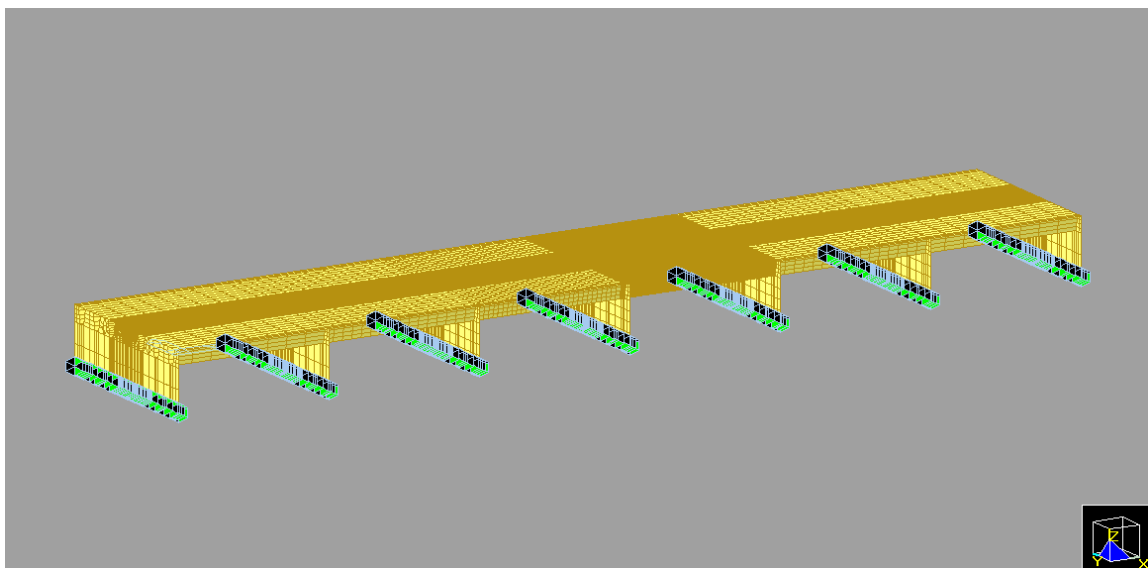


Figure 3.11 Perspective view of the orthotropic deck with boundary conditions

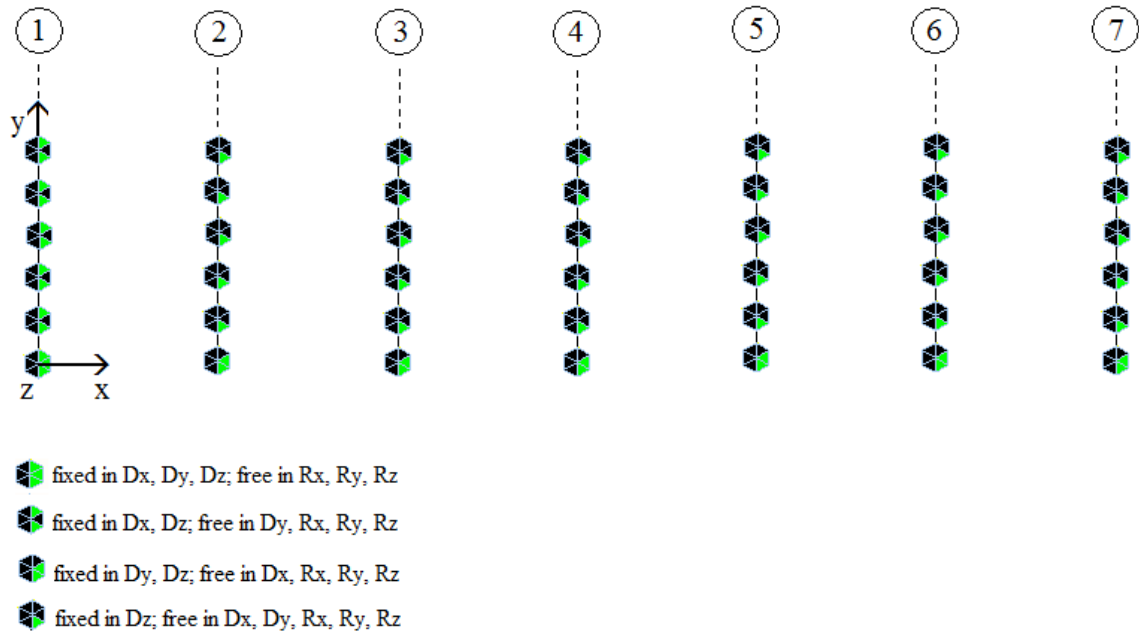


Figure 3.12 Schematic diagram of boundary conditions

3.5 Wheel loads

The loads applied here are the uniformly distributed single wheel load of 50kN. They represent the axles A, B and C as defined in NEN-EN 1991-2-2003 (table 3.3). The wheel load print on the deck plate is enlarged by taking the spreading of the wearing surface into account. There are two kinds of typical wearing surfaces. The first one is asphalt wearing surface which has a thickness of 60mm. The second is 8mm epoxy layer without asphalt applicable on top of the bridge deck. Suppose the wheel load spreads with an angle of 45° within the wearing surface (see figure 3.13 and figure 3.14).

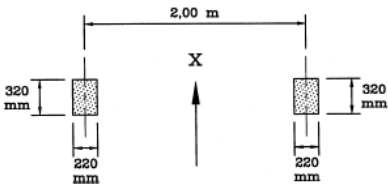
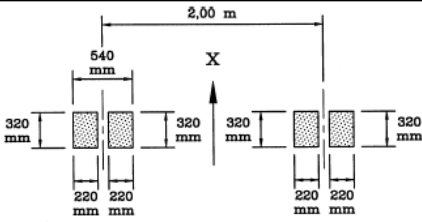
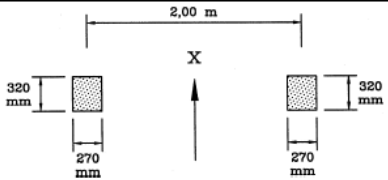
WHEEL/ AXLE TYPE	GEOMETRICAL DEFINITION
A	
B	
C	

Table 3.3 Definition of wheels and axles (NEN-EN 1991-2, [N1])

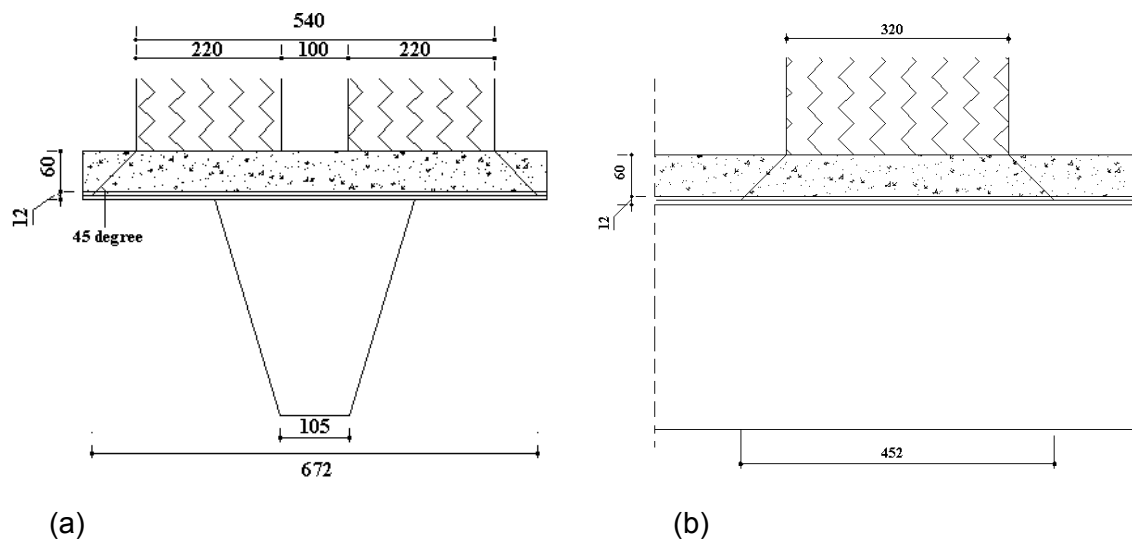


Figure 3.13 Axle B distribution over the wearing surface (a) Distribution over the width of the wheel; (b) Distribution over the length of the wheel

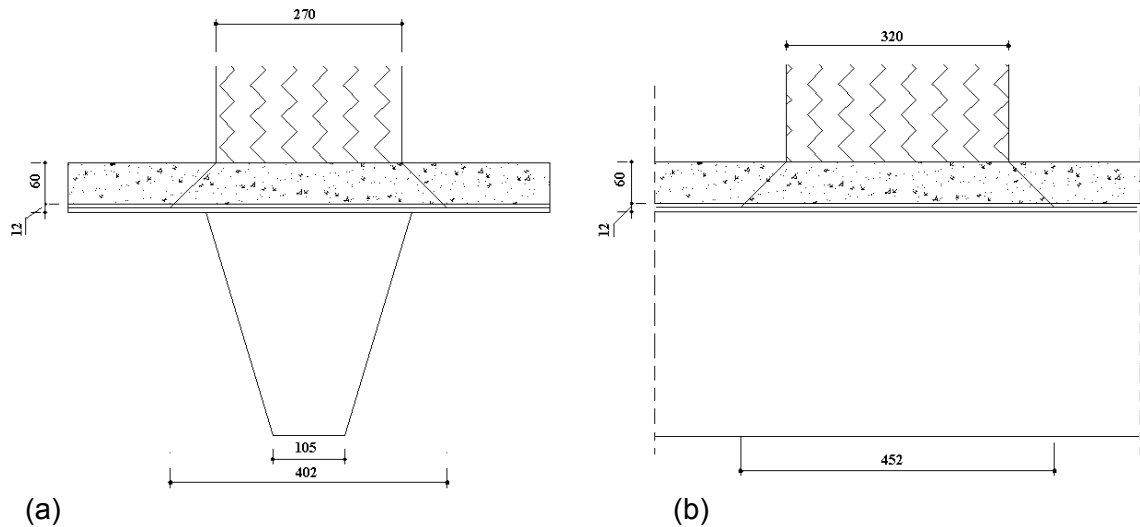


Figure 3.14 Axle C distribution over the wearing surface (a) Distribution over the width of the wheel; (b) Distribution over the length of the wheel

The distributed wheel loads are:

$$q_A = \frac{F}{b * h} = \frac{50000}{352 * 452} = 0.314 N / mm^2$$

$$q_B = \frac{F}{b * h} = \frac{50000}{672 * 452} = 0.165 N / mm^2$$

$$q_C = \frac{F}{b * h} = \frac{50000}{402 * 452} = 0.275 N / mm^2$$

in which F : the single axle wheel load

b : the width of the wheel print

h : the length of the wheel print

As a sum up, the area of the axle load and the uniformly distributed wheel load on different models due to axle A, axle B and axle C are presented in the following tables:

Axle type	Wheel load area $b * h$ [mm ²]			
	Model A	Model B	Model C	Model D
Axle A	352*452	358*458	245*348	258*358
Axle B	672*452	678*458	568*348	578*358
Axle C	402*452	408*458	298*348	308*358

Table 3.4 Wheel load print

Axle type	Wheel load [N/mm ²]			
	Model A	Model B	Model C	Model D
Axle A(q_A)	0.314	0.305	0.586	0.541
Axle B(q_B)	0.165	0.161	0.253	0.242
Axle C(q_C)	0.275	0.268	0.482	0.453

Table 3.5 Uniformly distributed wheel load

For the finite element analyses, two kinds of load array are applied on the deck plate. One of the load arrays simulates the situation the moving of truck on the bridge. Totally, 31 load steps are applied on the deck representing the movement of an axle load between the third and sixth crossbeam of the interval of each step is 350 mm. In this case, there are nine load patterns along which the axle load is running. The center of these nine load patterns are arranged from -400mm away from the left-hand side of the middle trough to 400mm on the other side of the trough. The interval between the load patterns which are next to each other is 100mm.

Load case	Y-coordinates of the load center[mm]	With respect to the center of the middle trough [mm]
1to31	1700	-400
32to62	1800	-300
63to93	1900	-200
94to124	2000	-100
125to155	2100	0
156to186	2200	100
187to217	2300	200
218to248	2400	300
249to279	2500	400

Table 3.6 Locations of the longitudinal load patterns

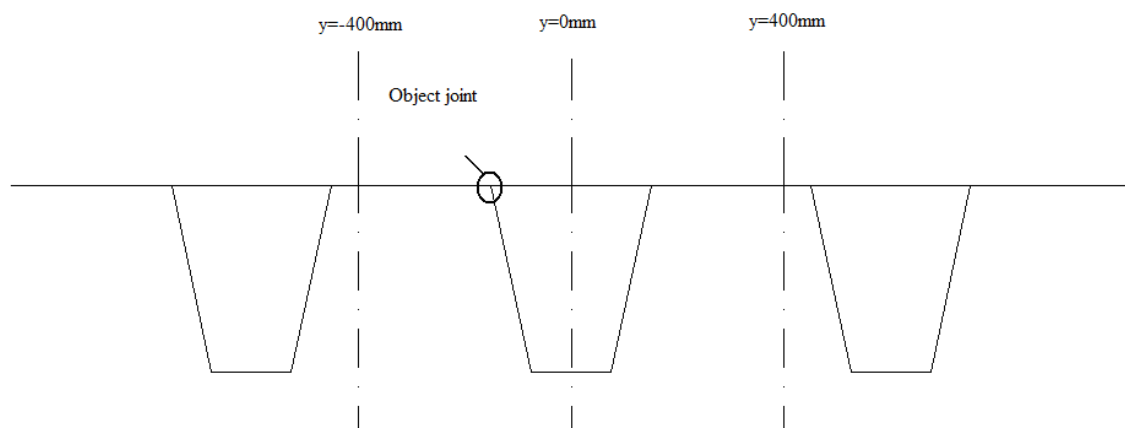


Figure 3.15 Longitudinal running loads' patterns

Another load array simulates the transverse spreading of the wheel load over the cross-section of the deck plate. It assumed, in stead of moving in the longitudinal

direction, the wheel load is moving in the transverse direction. Totally, 25 load cases are generated in the transversal direction along the four object joints between $Y=1500$ mm and $Y=2700$ mm. They have an interval of 50 mm.

Load case	X-coordinates of the load center [mm]
280to304	Section A
305to329	Section B($x=10937.5$ mm)
330to354	Section C($x=11375$ mm)
355to379	Section D($x=12250$ mm)

Table 3.7 Load cases of the transverse load patterns

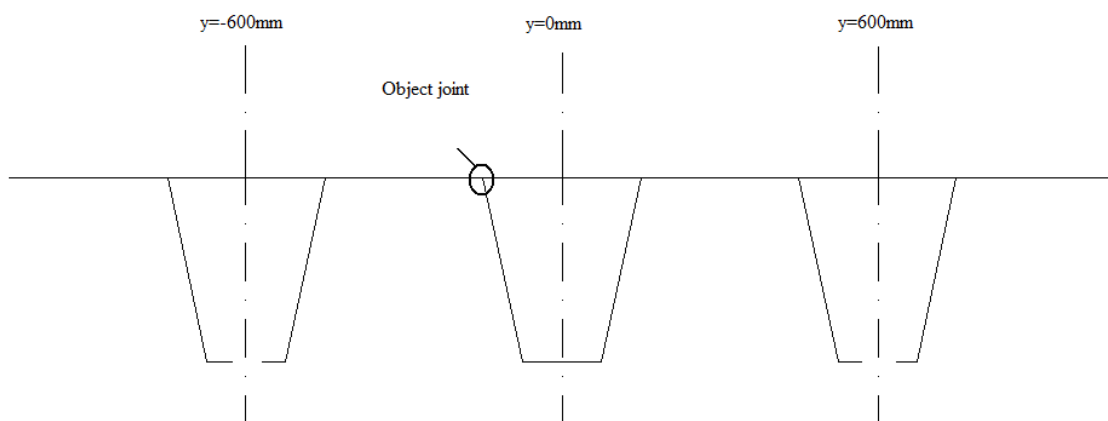


Figure 3.16 Transverse running loads' region

3.6 Type of analyses and results to be computed

A linear static analysis is performed to calculate the stresses in the 3D finite element model. It means that both the material and geometry of the model are linear. The wheel load generates stresses in the deck plate and also in the trough web. Due to the different crack mechanisms in this joint, the stresses of four locations are picked out for investigation. They are the stresses in the exterior and interior surface of the trough web and the stresses in the bottom surface of the exterior and interior deck plate. These locations are indicated in figure 3.17. Furthermore, the local coordinating systems of the deck plate and the trough web are indicated in figure 3.18. The transverse stresses plotted in the influence lines for the deck plate and the trough web are the normal stresses σ_y in the local coordinate system.

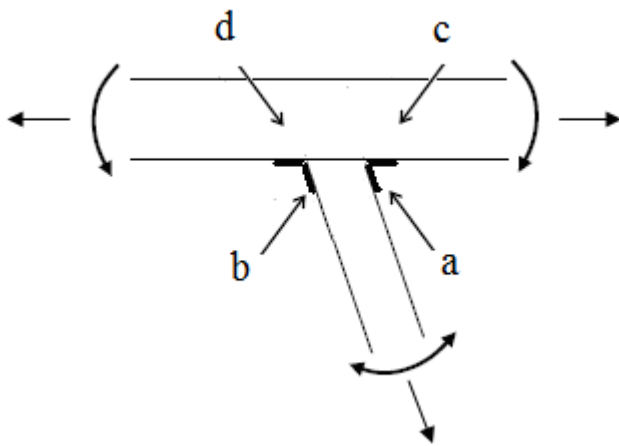


Figure 3.17 The object locations in the trough to deck plate joint a) exterior surface of the trough web; b) interior surface of the trough web; c) bottom surface of the exterior deck plate; d) bottom surface of the interior deck plate

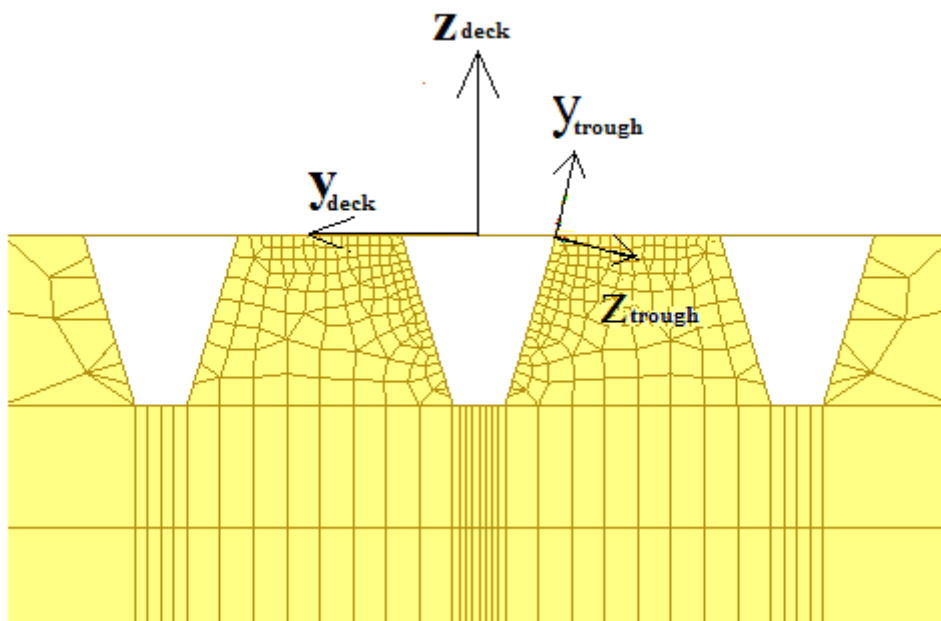


Figure 3.18 Local coordinate system of the deck plate and the trough web

3.7 Comparison with site measurement

Firstly a comparison is performed to analyze whether the model and the computational results are correct. A report regarding to the site measurements performed on Scharsterrijn bridge is available for comparison (De Freitas. S.T., [22]). The report records the measurement results based on a short term monitoring. The monitoring was carried out by the Stevin Laboratory of the Faculty of Civil Engineering and Geosciences at the Delft University of Technology by order of the Takke LSBV brugdekken VOF.

3.7.1 Description of the Scharsterriijn Bridge

Scharsterriijn bridge is in the highway A6 in Friesland, a northern province of the Netherlands. The bridge consists of two parts: a fixed part and a movable part. The monitoring was carried out on the orthotropic steel deck in the movable part of bridge. The orthotropic deck consists of a 12mm thick deck plate, 6mm thick 250mm height and 300mm wide U-shaped trough. The movable part can be further divided into three parts each 2530mm in the longitudinal direction by four crossbeams. A 7mm thick epoxy layer is applied on the deck plate. In March 2009, rehabilitation was carried out on the deck plate. During the rehabilitation, the existing orthotropic deck was stiffened by bonding a second steel plate of 6mm on it. The second steel plate has a length of 8200mm and a width of 4200mm. In this study, the computed results are compared to the site measurement results before rehabilitation. The drawing of the cross-section is shown in the following figure.



Figure 3.19 Scharsterriijn bridge (fixed part on left side and movable part on the right side) (left); Orthotropic deck of the movable part (right) (Freitas, S.T., et al , [22])

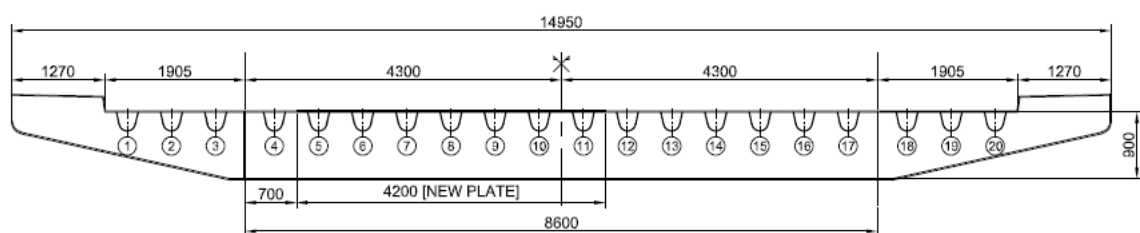


Figure 3.20 General cross-section of Scharsterriijn movable bridge and new plate position (dimensions in mm) (Freitas, S.T., et al , [22])

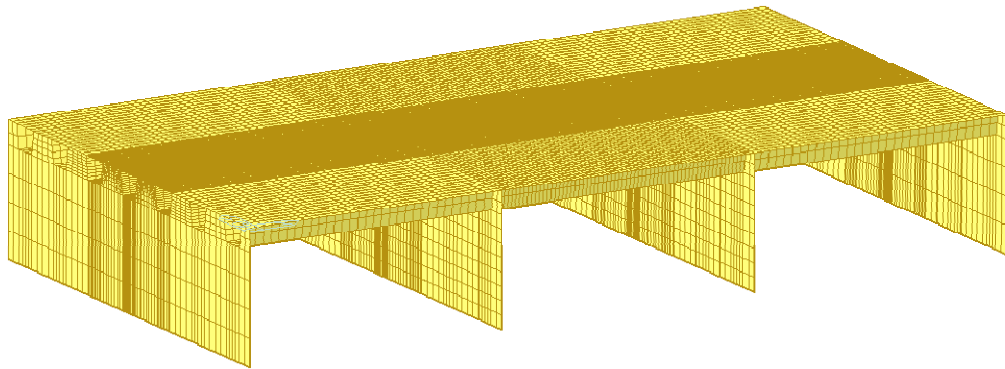


Figure 3.21 3D model in MIDAS Civil

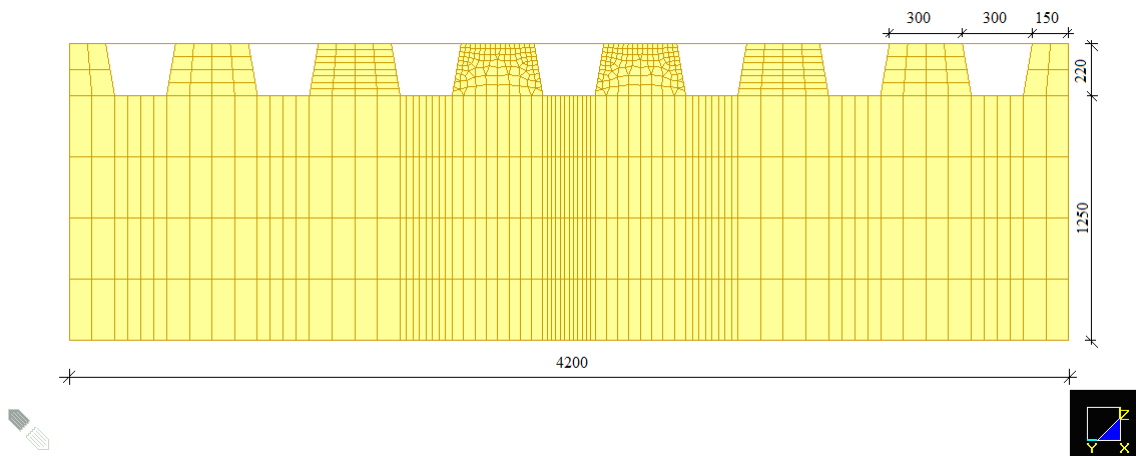
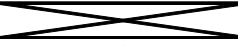


Figure 3.22 Cross-section of the 3D model in MIDAS Civil

The geometry of the orthotropic steel deck (before rehabilitation) is translated into a 3D model made in MIDAS Civil (table 3.8). For the simplicity, the U-shape trough is modeled as a trapezoidal trough.

Structural component		3D model	Scharsterriijn bridge
Deck plate	Span	2530	2530
	Width	4200	8600
	Thickness	12	12
Trough	Span	2530	2530
	Height	220	250
	Width upper	300	300
	Width bottom	225	
	Thickness	6	6
	Distance	600	600
Epoxy layer	Thickness(t_a)	7	7

The unit of the dimension is mm

Table 3.8 Dimensions of the orthotropic decks

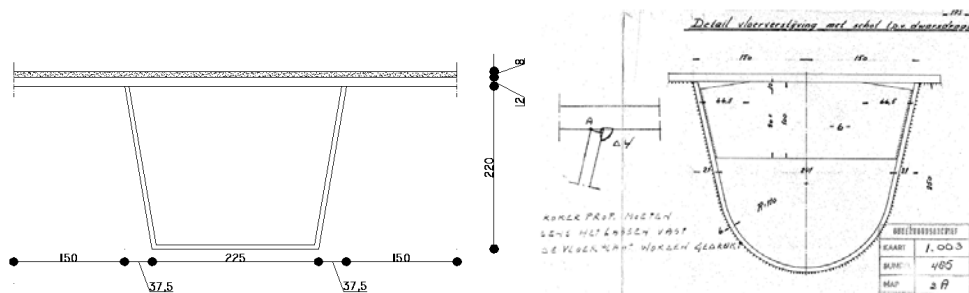


Figure 3.23 Trapezoidal trough in the 3D model (left); U-shaped trough in Scharsterriijn bridge (right); unit in mm

Furthermore, the boundary conditions between these two models are different. As described before, the crossbeams in the 3D model are supported in their bottom edges. It is assumed that the crossbeams are stiff enough that no deflection can take place in the crossbeams. On the contrary, the orthotropic deck of Scharsterriijn bridge is supported by the main girders which are 3175mm away from the edge of the bridge (see figure 3.20). In this case, the deflection of the crossbeam may have influence on the stress in the deck.

3.7.2 Object locations

The site measurements were carried out in the middle cross-section of the middle span (section 1' in figure 3.24). At this section, a total of 16 strain gauges were applied (figure 3.25).

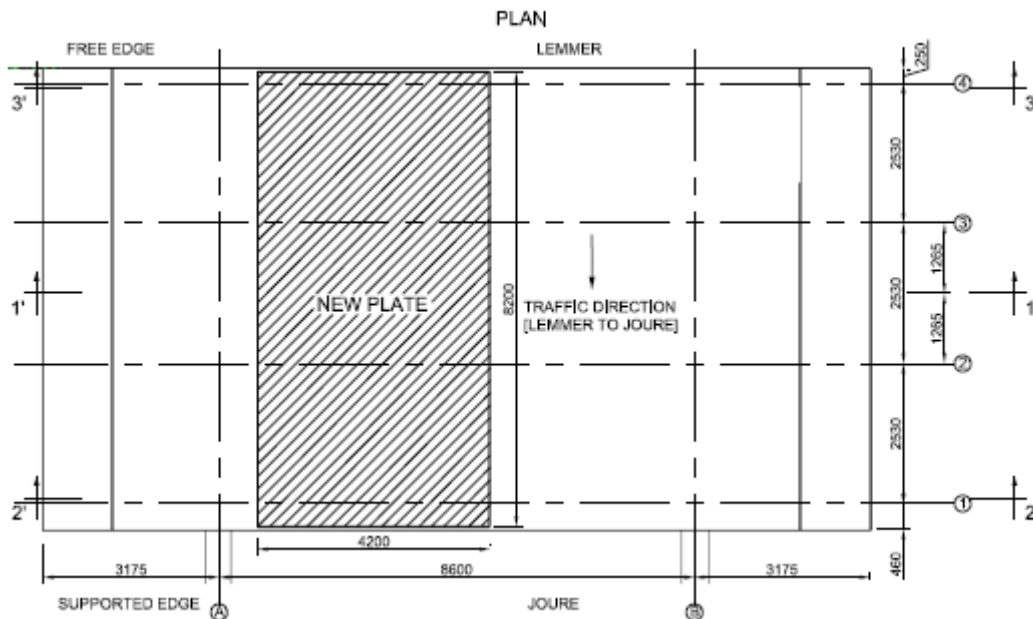


Figure 3.24 Plan view Scharsterrijn movable bridge (dimensions in mm) (Freitas, S.T., et al, [22])

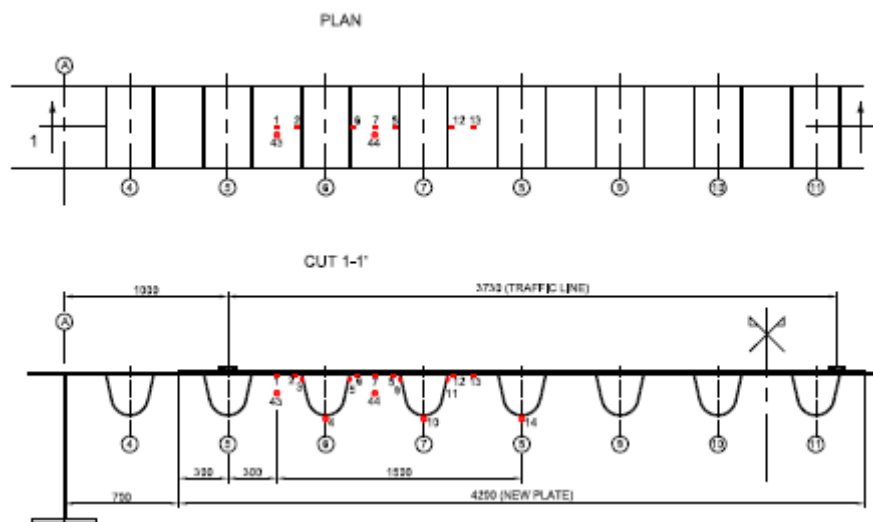


Figure 3.25 Transverse location of the strain gauges for the short term monitoring at cross-section halfway between crossbeam 2 and 3 (dimensions in mm) (Freitas, S.T., et al, [22])

Strain gauges 2, 3, 5, 6, 8, 9, 11 and 12 were positioned 15mm from the weld toe of the trough-to-deck plate joint in the middle cross-section and measured the transverse strains. They are relevant to the object joint of this study (figure 3.17), especially strain gauges 8 and 9 which are on the middle trough.

3.7.3 Wheel loads

The investigated strain gauges measured the strains due to a calibrated truck when no traffic was running on the bridge. The truck was placed at 15 transverse positions on the deck plate. Based on the measurements, the stress influence lines in the object joint can

be drawn which are comparable to the computed results in MIDAS Civil.

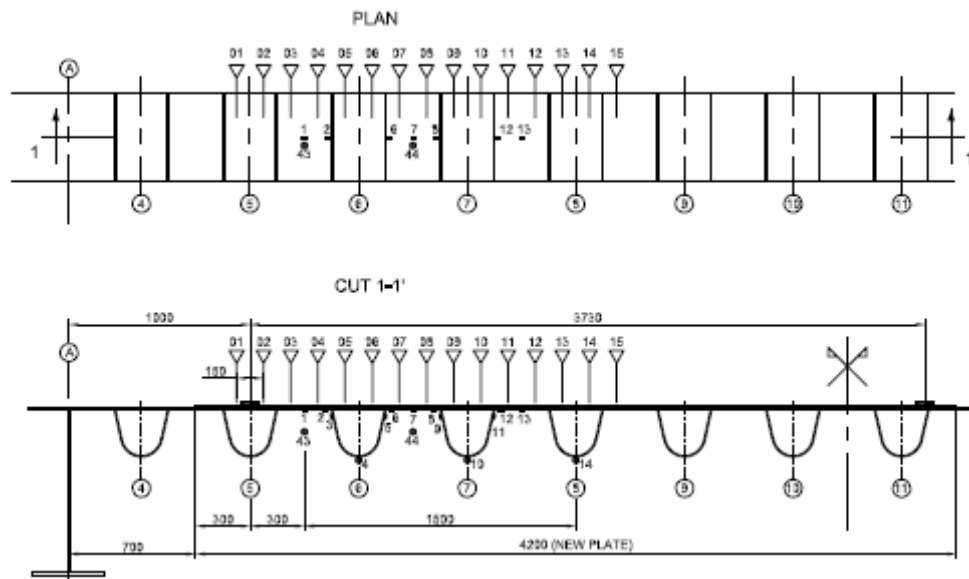


Figure 3.26 Middel span cross-section 1-1': 15 wheel load positions and strain gauges positions (Freitas, S.T., et al, [22])

The truck applied on the deck was a four axle lorry, with one axle at the front side with single tyres and three axles at the back side with double tyres.



Figure 3.27 Calibrated truck used for the strain measurement (Freitas, S.T., et al, [22])

The measurements were carried out for the front and rear wheel. For each kind of wheel, the measurements were performed twice (before rehabilitation and after rehabilitation), see table 3.9. It has been mentioned before, that only the measurements before the rehabilitation are relevant to this study. The wheel loads' properties are presented here below.

Wheel	Wheel loads before	Wheel print	Wheels distance	Axles distance
Front Wheel (single tyre)	38.5kN	270mm*320mm	2155mm	5320mm

Table 3.9 Wheel loads' properties

The same wheel load is also applied on the 3D model. The wheel load is applied on the deck plate from $y=1250\text{mm}$ to $y=2950\text{mm}$ in 12 steps (figure 3.28). The distance between each load step is 150mm. In this way, the results obtained from the 3D model

are comparable to the results obtained from the site measurements.

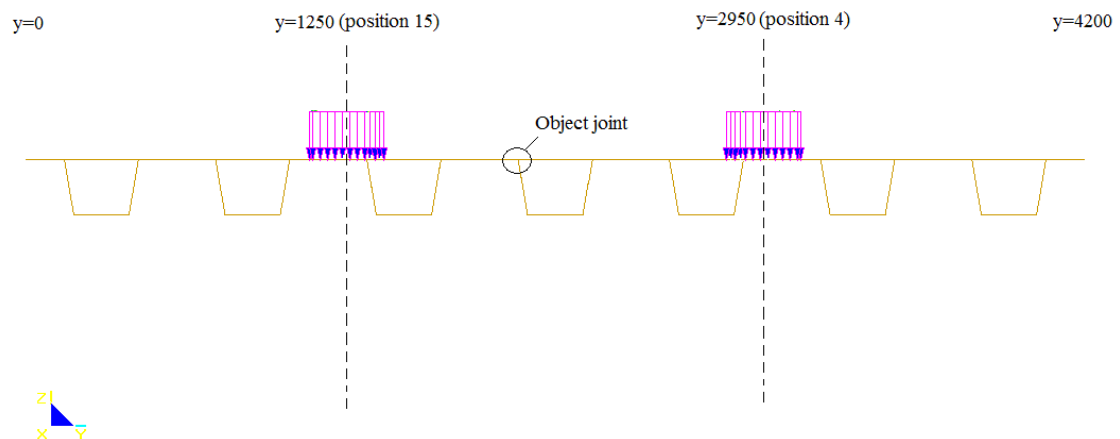


Figure 3.28 Wheel load pattern in the 3D model

Besides the differences in the geometry between these two models, another difference is the wheel load. The wheel load applied on the finite element model is modeled as uniformly distributed area load on the deck plate. But according to the research done by Groenendijk (cited by De Jong, F.B.P., [2]), it is not the case in the reality. Groenendijk concluded that the wheel load mainly governs the stresses at the tyre edges and the tyre pressure mainly governs the stresses around the centre of the tyre. As an example, a measured 3D stress pattern of the wheel load done with the VRSPTA system is presented here below.

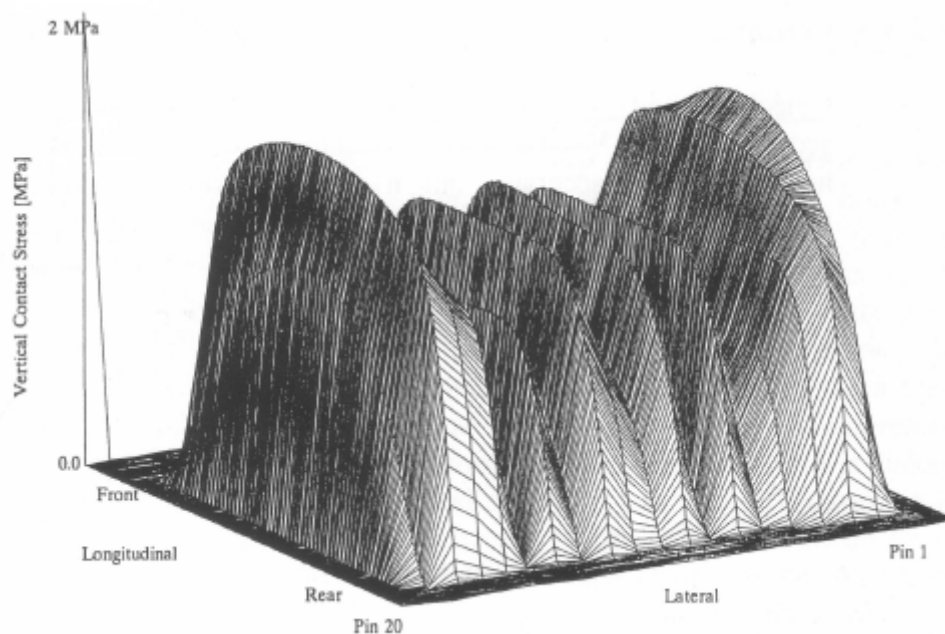


Figure 3.29 Example of measurement result VRSPTA (De Jong, F.B.P.,[2])

Based on the findings of Groenendijk, De Jong performed further analysis on the wheel print measurements. In his research, he found out that the single axle load has a significant influence on the wheel print. As an example, he compared the wheel print of

axle B under different axle load (figure 3.30). It is clear to see that when the axle load is increased, the wheel print becomes larger.

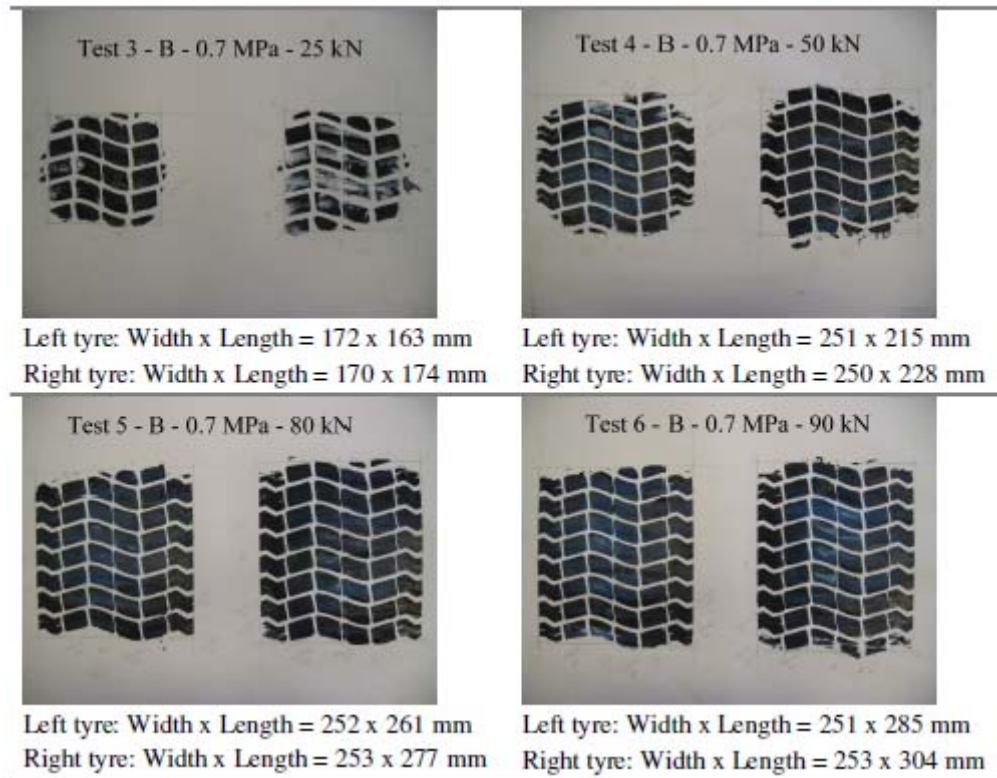


Figure 3.30 Results wheel print measurements double (type B) at 0.7 MPa inflation pressure

3.7.4 Comparison results with site measurement

The transverse influence line in the exterior deck plate of Scharsterrijn bridge is generated from stain gauge 8 (between position 8 and 9) which is 15mm away from the wheel toe. Due to the mesh density and model's property, the transverse influence line of the 3D model is generated from the node which is 12mm away from the trough-to-deck plate joint.

In general, the shapes of these two influence lines are similar to each other. Both of them have a W shape. When the wheel load moves from the left hand side of the object joint to the right hand side, the influence line begins with a mere zero stress. At position 7, the influence line reaches an extreme value of the stress. After that, the stress increases until wheel load is at position 8. When the wheel load moves towards position 10, another extreme value in the influence line would appear. By moving the wheel load from position 10 to position 12, the influence line would reach its maximum value of stress. After that, the influence line fluctuates around zero. However, there are some differences between these two curves. General speaking, the magnitude of stress in the 3D model is larger than the magnitude of stress in Scharsterrijn bridge. This has to do with the form of the wheel load. Furthermore, the shape of the trough has also influence on the computed results.

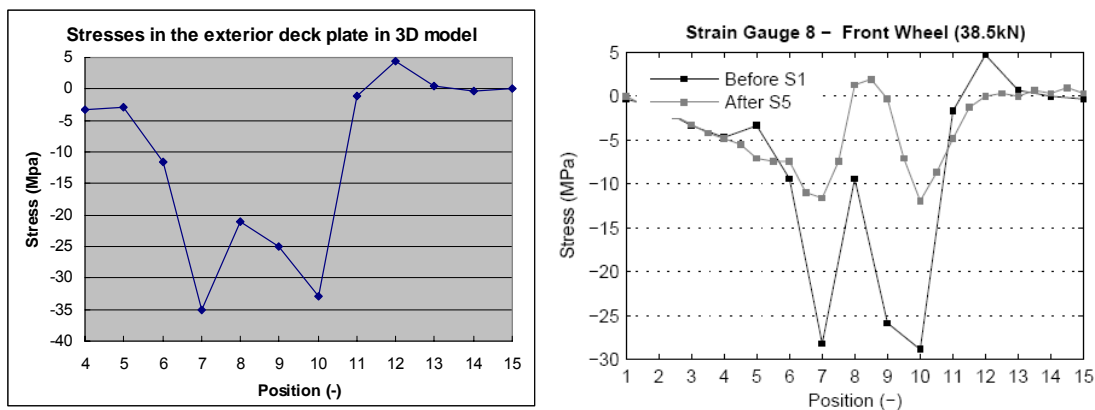


Figure 3.31 Comparison results in the exterior deck plate with the site measurements at strain gauge 8: the computed results in MIDAS Civil (left), the site measurements on Scharsterrijn bridge (right)

The comparison is also made between the influence lines in the exterior trough web of these two models.

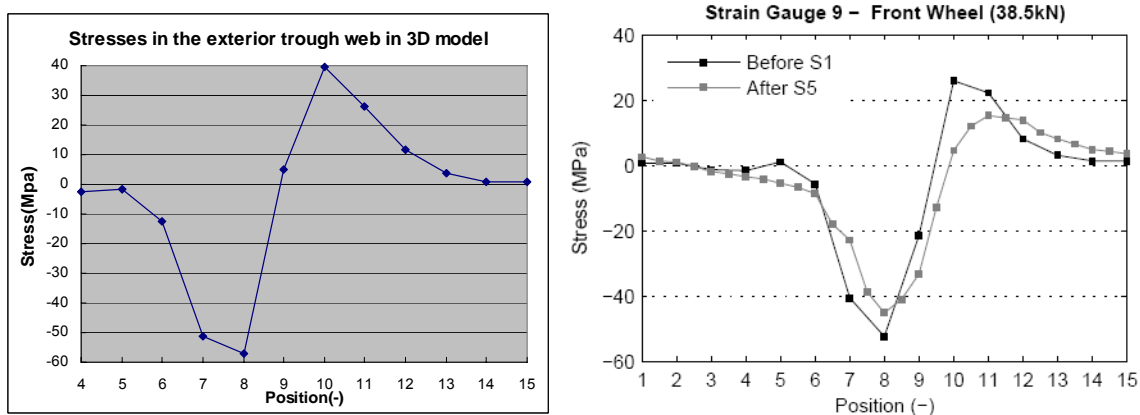


Figure 3.32 Comparison results in the exterior trough web with the site measurements at strain gauge 9: the computed results in MIDAS Civil (left); the site measurements on Scharsterrijn bridge (right)

The influence line obtained from the 3D model is similar to the influence line obtained from the site measurement between position 4 and position 15. Both of them begin with a smaller value of stress at position 4. By moving the wheel load away from position 4, the influence line would decrease. At position 8 which is nearby the stain gauge 9, the influence line reaches its smaller value. After that, the influence line increases remarkably and reaches its maximum value at position 10. Soon after, the influence line decreases again. The same as the influence lines in the deck plate, the magnitude of the stress obtained from the 3D model is also larger than the result obtained from the site measurement. This is mainly due to the form of the applied wheel load and also the differences between the 3D model and Scharsterrijn bridge (form of the trough and the boundary conditions).

Based on the comparisons, it can be found out that the results obtained from the 3D

model are comparable to the results obtained from the site measurement. It means that the way of making model in MIDAS Civil is correct. This study can be continued by using the 3D models. And the results of the 3D models made in this way should be dependable.

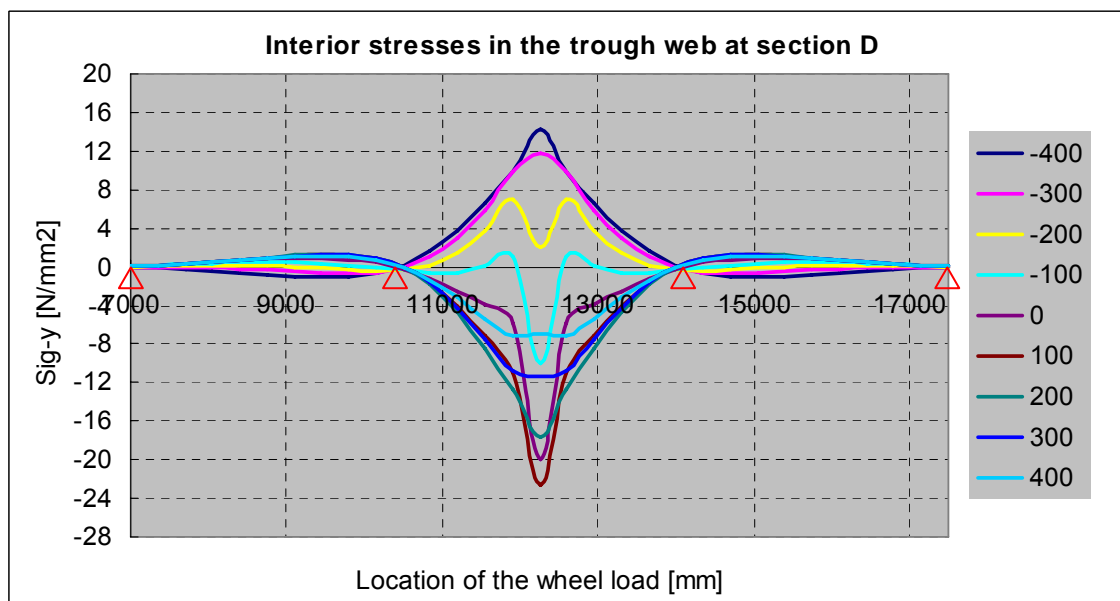
3.8 Results

In this paragraph, the results calculated by MIDAS Civil will be presented in the form of longitudinal and transverse influence lines. Furthermore the comparison between the four different orthotropic decks will be made. In the end the stress range which is decisive for the fatigue calculation will be given.

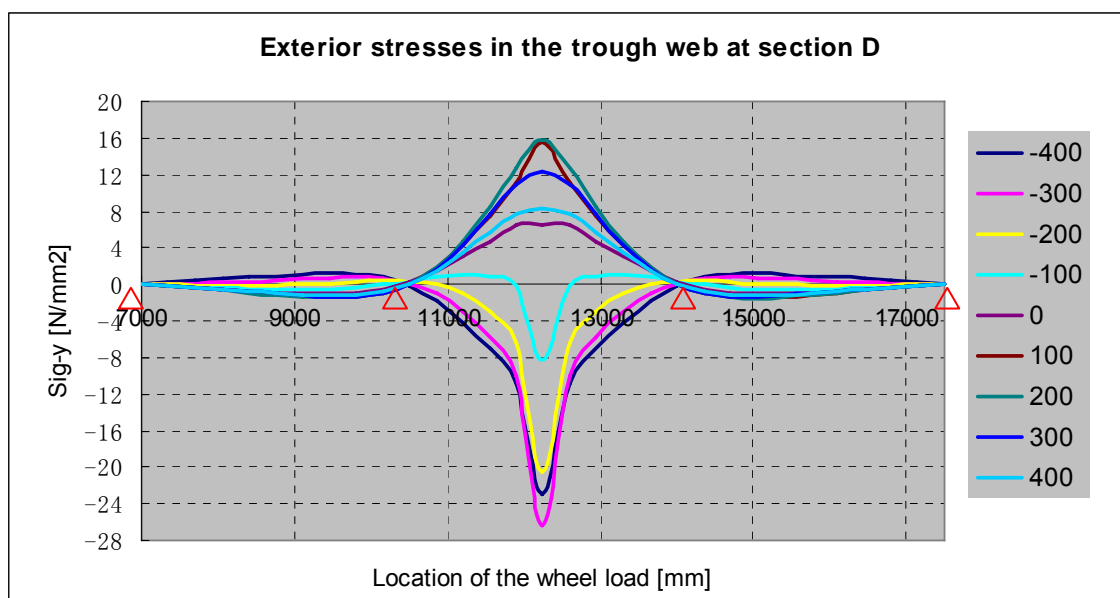
3.8.1 Longitudinal influence line

The longitudinal influence lines are generated for the longitudinal load patterns. Due to these nine axle load patterns which are indicated in section 3.5, nine different longitudinal influence lines can be drawn for the interior and exterior surface of the trough web and the bottom surface of the interior and exterior deck plate in four different models. Since that there are many consistencies in the influence lines among the four different models, only the longitudinal influence lines in model B under axel C are presented in this chapter for the simplicity. Furthermore, the interpretation of the longitudinal influence lines is valid for every model unless otherwise noted

The longitudinal influence lines of the four object joints are calculated and plotted in figures. As an example the vertical stresses in the trough web for section D at the halfway of the trough span are plotted in the following figures. The red triangle indicates the location where the crossbeam exists. The longitudinal influence lines for the other sections are given in appendix A.



(a)



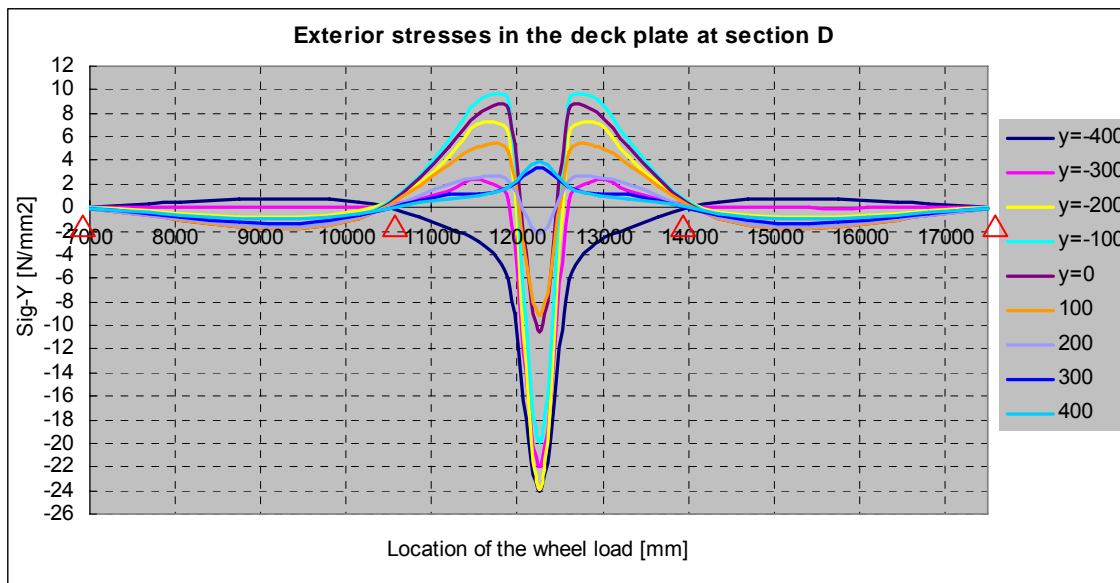
(b)

Figure 3.33 Model B under axle C: longitudinal influence lines in the trough web at section D (a) Interior stresses in the trough web; (b) Exterior stresses in the trough web

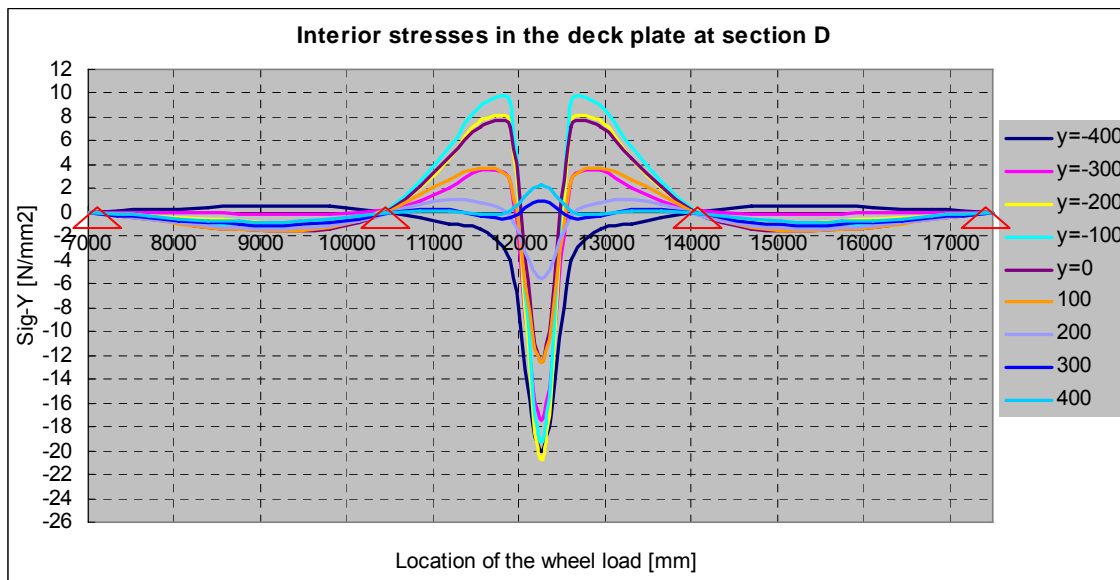
It seems that, in all cases, the stress reaches its maximum value as the wheel load is precisely applied on the section of the investigation. And the transverse stresses can only be excited when the wheel load is close to it. Therefore, greater change in the stress only takes place in the middle span between $x=10500\text{mm}$ and $x=14000\text{mm}$. The further the wheel load away from the object joint is, the smaller the stresses are generated. This conclusion is not only valid in the longitudinal direction but also in the transversal direction (see section 3.8.2). The stress outside the range of the middle span is small which can be neglected. The maximum stress range in object joint a (interior surface of

the trough web) occurs when the wheel load is moving around $y=100$ mm in the longitudinal direction. For object joint b (exterior surface of the trough web) the maximum stress range appears when the wheel load is moving around $y=-300$ mm. This conclusion coincides with the previous researches' results that the riding-between troughs wheel load is the most critical load pattern for the trough web.

The longitudinal influence lines are also drawn for the bottom surface of the interior and exterior deck plate at the trough-to-deck plate joint (point c and d in figure 3.17).



(a)



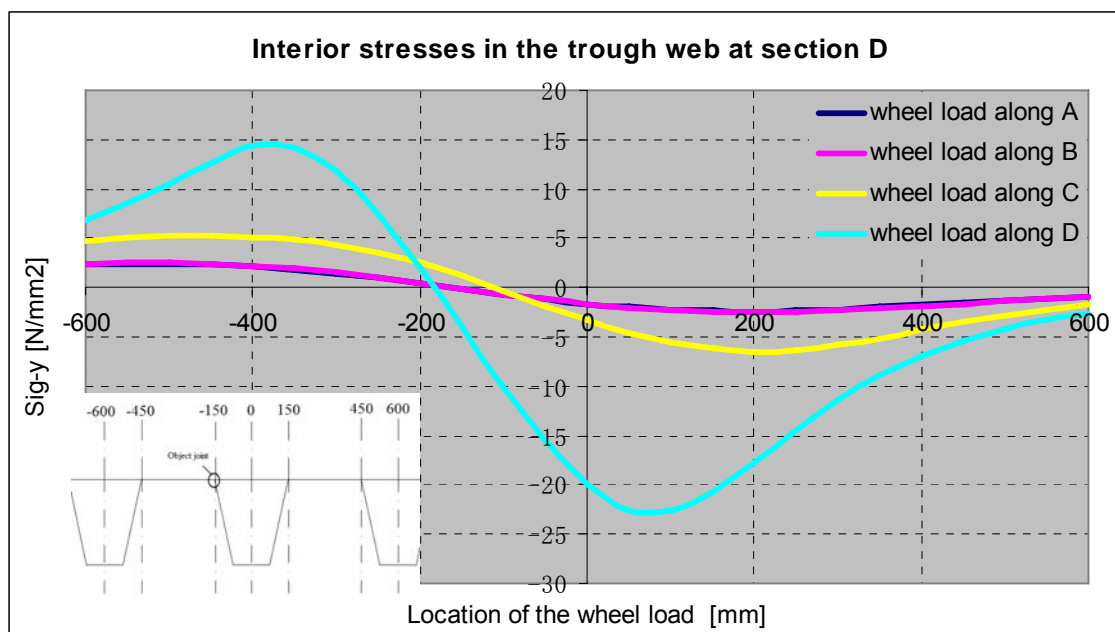
(b)

Figure 3.34 Longitudinal influence line in the deck plate at section D (a) Interior stresses in the deck plate; (b) Exterior stresses in the deck plate

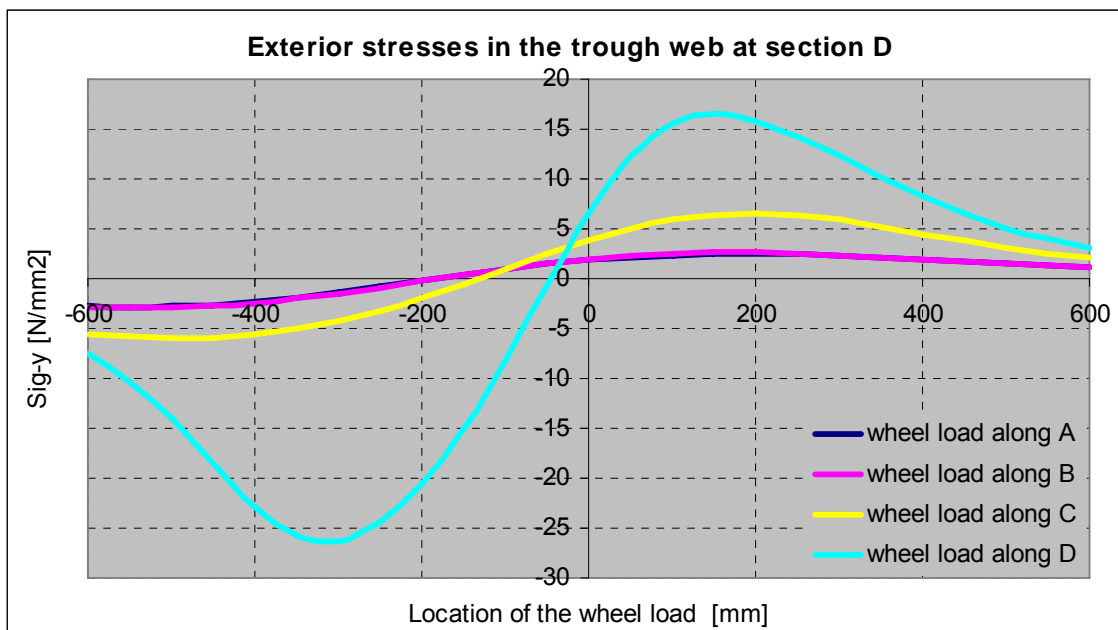
Figure 3.34 indicates that the maximum stress in the deck plate also appears when the wheel load is running between the middle two crossbeams. The further the axle is away from the object joint, the smaller the influence of the axle load on the stress in the object joint is. This conclusion is valid for results in both longitudinal and transversal directions. A large portion of each influence line in the interior and also exterior deck plate is in compression. Generally, only the tension stress can cause fatigue cracking. However, high tensile residual stress and constraint stress exist in the welding detail. In this case, it is reasonable that the residual tensile stress may shift the compression stress in the object location into tension stress. Additionally, the change of the stress from compression into tension contribute to the fatigue damage calculation.

3.8.2 Transverse influence line

Besides the longitudinal load patterns, there are also transverse load patterns applied along the four sections. As an example, the transverse influence lines at section D for model B under axle C are presented in this section. For the transverse influence lines in the rest of the sections, please refer to appendix A.



(a)



(b)

Figure 3.35 Model B under axle C: transverse influence line in the trough web at section D (a) Interior stresses in the trough web; (b) Exterior stresses in the trough web

From these figures, it can be observed that only the wheel load above section D has the most important influence on the stress in the object joint. The wheel loads above the other sections can hardly generate any significant stress in the object joint. It becomes clear that the further the wheel load away from the object joint is, the smaller the stress in the object joint is. In figure 3.35 (a), the maximum (negative) stress in the interior trough web appears around $y=50\text{mm}$. Since the most part of the wheel load is on the right-hand side of the object joint in this situation, the moment generated in the interior side reaches its maximum value (point a in figure 3.36). The negative stress under this load case is due to the bending moment and the normal force in the interior trough web. The same tendency is observed in the influence line in the exterior trough web. But the maximum (negative) stress in this object location occurs under axle load at $y=-300\text{mm}$.

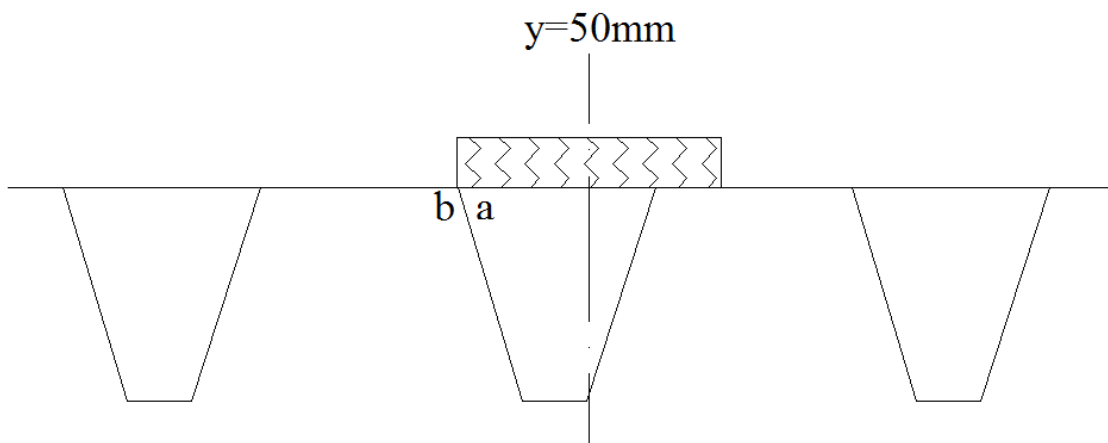
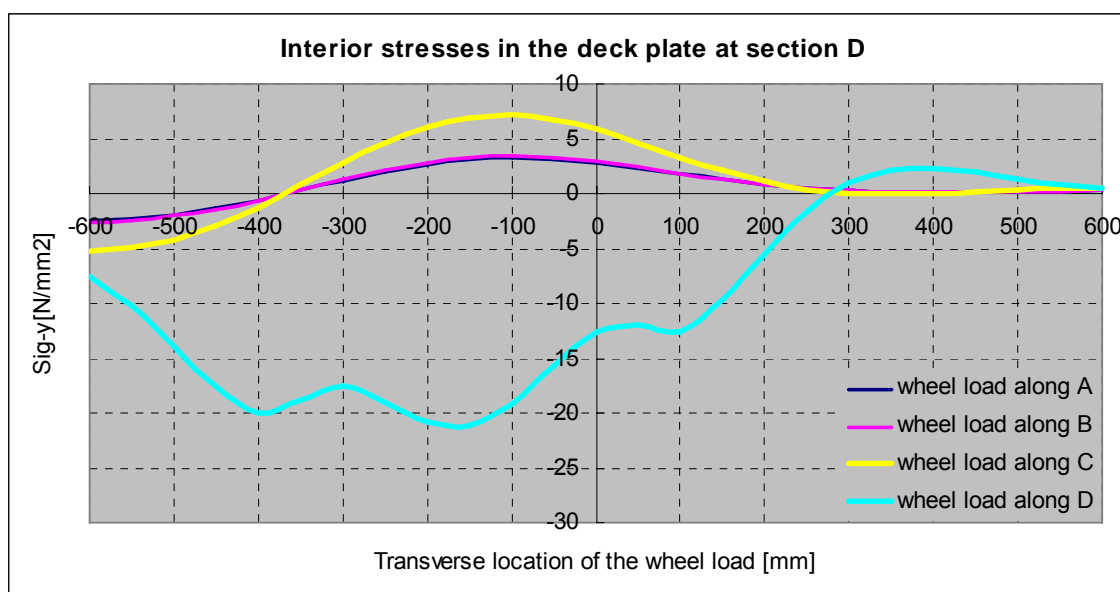
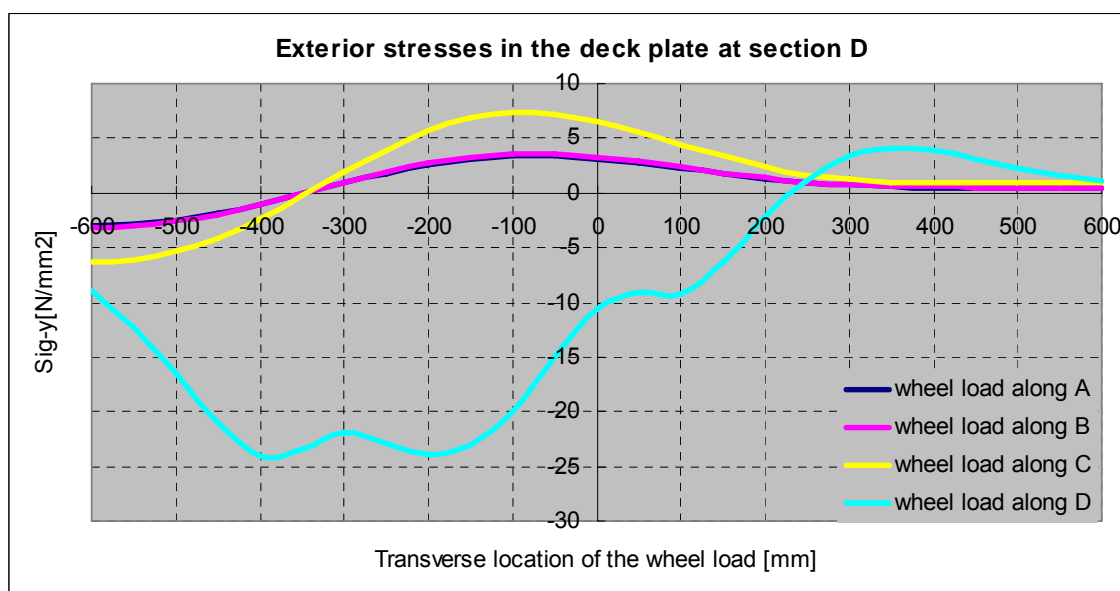


Figure 3.36 Wheel load centrally above $y=50\text{mm}$

The result in the deck plate using the same wheel load in the same model is presented here below. As expected, the wheel load array at section D gives the largest stress in the deck plate at section D. Furthermore, the deck plate is under compression in this case. Conversely, when the wheel load is working at the other sections, a large portion of the influence line has a positive value (tension stress). But the magnitude of the stress in section D is much larger than the stress in the other sections. As expected, the extreme stress takes place when the wheel load is riding over trough web ($y=-150\text{mm}$) at section D.



(a)



(b)

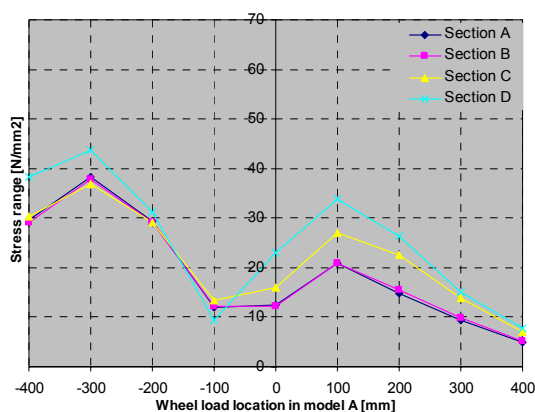
Figure 3.37 Model B under axle C: transverse influence line in the deck plate at section D (a) Interior stresses in the deck plate; (b) Exterior stresses in the deck plate

3.9 Comparison between different models

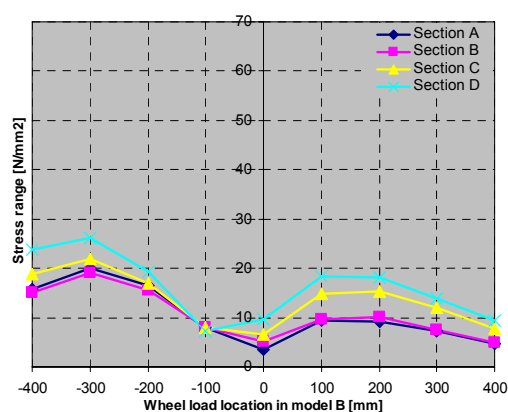
As discussed above, four different orthotropic deck models are simulated in the finite element model. They are two models with asphalt layer and two models without the layer. In the previous section, the plots of the longitudinal and transverse influence lines are also given. It is shown that the influence lines of above-mentioned models have a similar shape, meaning that the shapes of the influence line and the locations where the maximal and minimal stresses occur are the same. In this chapter, the differences of the influence lines are addressed. This is done by comparing the stress ranges in these models. Since the stress range is the dominating factor in the fatigue calculation, the stress ranges are presented in the following graphs. The stress range equals to the difference between the maximum stress and the minimum stress of the longitudinal influence line.

3.9.1 Stress range in the exterior trough web

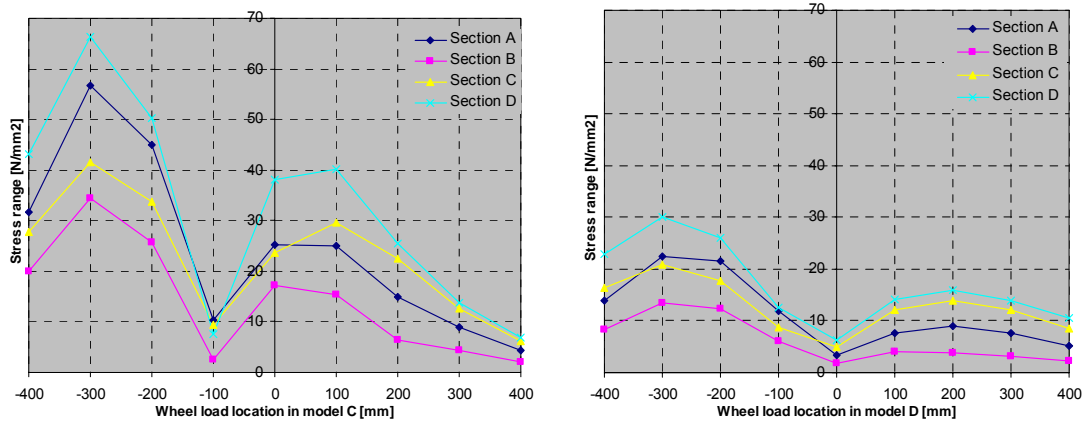
The stress ranges are derived from the longitudinal influence lines and presented for nine different transverse locations of the wheel load patterns. As an example, the stress ranges in the exterior trough web under axle C are compared for all four models. Since the interior surface of the trough web is symmetrical to the exterior surface of the trough web, the bending moment in the trough web can cause a same magnitude stress with different sign in these two surfaces of the trough web. In a way, the stress range curve in the interior trough web is similar to that in the exterior trough web. In this case, the explanation of the stress range in the exterior trough web can also be used for the interior trough web. For the simplicity, the stress ranges under other load conditions are presented in appendix A.



(a)



(b)



(c)

(d)

Figure 3.38 Stress ranges in the exterior trough web under axle load C (a) Stress ranges in model A; (b) Stress ranges in model B; (c) Stress ranges in model C; (d) Stress ranges in model D

It can be concluded that the stress range curves have a similar shape. The maximum stress range is generated by the load pattern when the axle load is running above $y=-300\text{mm}$. This conclusion has also been proven by the literature research. After this peak value, the stress range decreases when the axle load moves towards the center of the middle trough ($y=0\text{mm}$). Between $y=-100\text{mm}$ and $y=0\text{mm}$ the stress range reaches its minimal value. After this point it increases again.

It is also shown in the figures that the stress ranges in small cross-section model A or model C are generally larger than those in respectively model B and model D (larger cross-section). The stress range decreases as the deck plate and the trough web become thicker. With the same cross section (model A and model C), model A with a 60mm thick asphalt layer has a smaller stress range than model C. This is due to the contribution of the asphalt layer on the wheel load print on the steel deck plate. In other words, a larger wheel load distributed area will result in a smaller stress range in the trough web. Furthermore, one may note that the stress ranges in section D (halfway of the trough span) are larger than in the other sections.

3.9.2 Stress range in the exterior deck plate

Similar to the comparison of the stress ranges in the trough web, only the stress ranges in the bottom surface of the exterior deck plate under axle C are compared here. The rest can be found in appendix A.

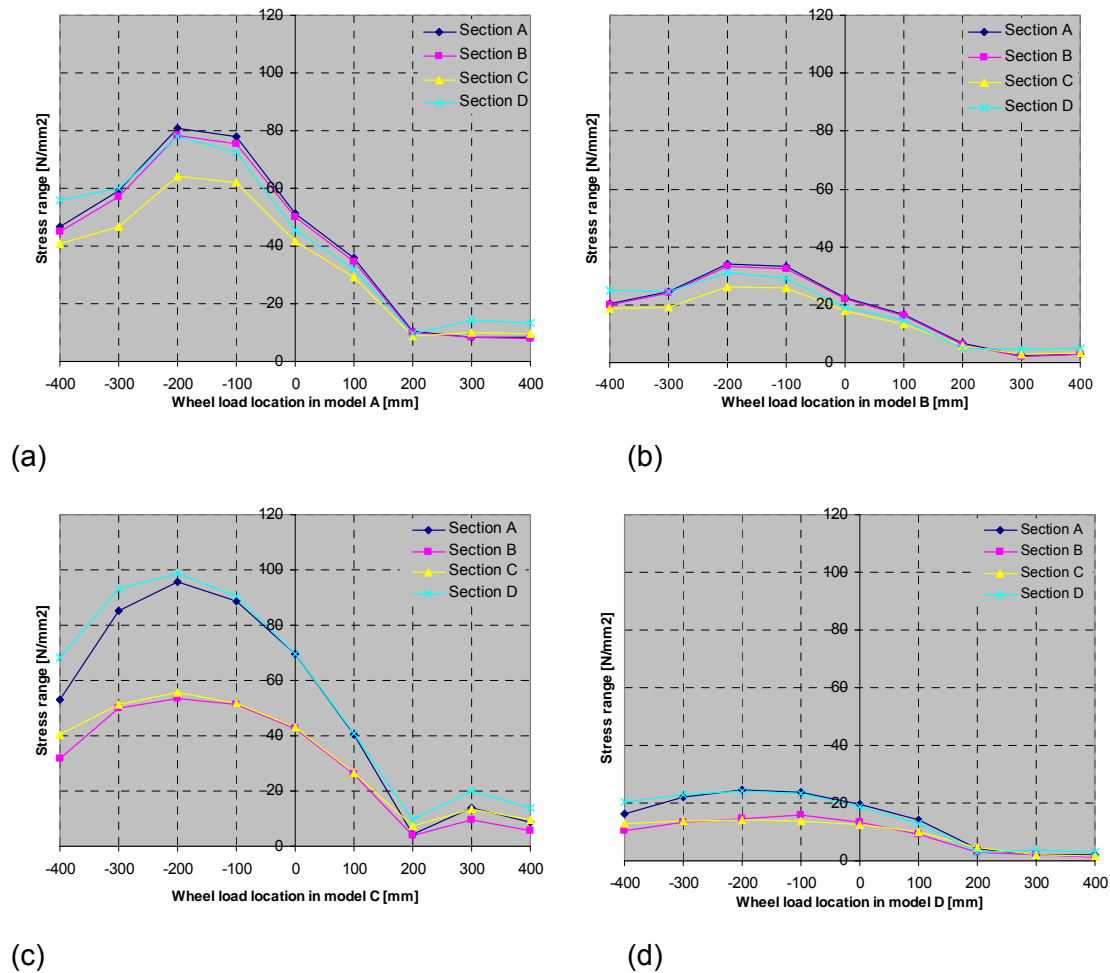


Figure 3.39 Stress ranges in exterior deck plate under axle load C (a) Stress ranges in model A; (b) Stress ranges in model B; (c) Stress ranges in model C; (d) Stress ranges in model D

In figure 3.39, the stress ranges in different models are similar to each other. By moving the central line of the wheel load from $y=-400\text{mm}$ towards $y=-200\text{mm}$, the stress range increases. Within the region of $y=-200\text{mm}$ and $y=-100\text{mm}$, the stress range reaches its maximum value. After that, it decreases as the center of the wheel load moves away towards the other side of the object joint ($y=-150\text{mm}$).

As expected, the stress range in the small cross-section is generally larger than that in the large cross-section (model A compared to model B, model C compared to model D). This is true, because that a larger deck thickness and trough web thickness can result in a smaller stress in the object locations. In the models without asphalt layer, the stress range in section D is the largest. In the models with asphalt layer, the stress range in section D is not the largest. But because that the difference in stresses under these wheel load locations between section A, B and D is small, section D is considered from here on.

3.10 Conclusions

By analyzing the influence lines and comparing the influence lines between different models, the following conclusions can be drawn:

- The stresses in the trough web are largely influenced by the deck plate thickness, the presence of an asphalt layer and the thickness of the trough web.
In the old bridges with a 12mm thick deck plate, applying an asphalt layer can reduce the stresses in the trough web by 30%.
By increasing the deck plate thickness in the fixed bridges with asphalt layer from 12mm (past situation) to 18mm (present and future situation), the stresses in the trough web can be reduced by 30%.
By increasing the trough web thickness from 6mm to 8mm can reduce the stress in the trough web by 15%, which is not significant compared to the others.
- The stresses in the deck plate are largely influenced by the deck plate thickness and the presence of an asphalt layer.
By increasing the deck plate thickness in the fixed bridges with asphalt layer from 12mm (past situation) to 18mm (present and future situation), the stresses in the deck plate can be reduced by 60%.
In the old bridges with a 12mm thick deck plate, applying an asphalt layer can reduce the stresses in the deck plate by 25%.
By applying an asphalt layer on the modern bridge with an 18mm thick deck plate, the stresses in the deck plate can also be reduced by 25%.
The stresses in the deck plate are hardly affected by the dimensions and thickness of the trough.
- The stresses in the deck plate and the trough web are largely influenced by the exact location of the wheel load and the contact area of the wheel load.
- For nearly all geometries investigated, the largest stress range in the deck plate in case of the passing of one axle load occurs in the middle of the trough span (section D in the models). There is only one exception that for one set of geometries the stress range at the location nearby the crossbeam is governing. For all geometries investigated, the largest stress range in the trough web in case of the passing of one axle load occurs in the middle of the trough span (section D in the models).

4 2D model in MIDAS Civil

Orthotropic steel deck is a complex structure in which the deck plate, longitudinal trough and crossbeam working together to carry the traffic load running on the bridge. Due to the large number of the connections between different structural components the orthotropic steel deck is sensitive to fatigue. The trough-to-deck plate joint is especially critical for this kind of damage. This chapter focuses on developing a simplified method for calculating the stresses in this joint based on a simplified mechanics 2D model of an orthotropic deck programmed in Excel sheet developed by Rijkswaterstaat. In this chapter, attention is paid on the trough-to-deck plate joint at the halfway of the trough span. The highest stress concentration and stress range are generated in this detail which is always determinate for the design of the orthotropic deck.

4.1 The original 2D model

The orthotropic steel deck is stiffened in two directions, namely the longitudinal direction and the transversal direction. The traffic load is firstly transferred by the deck plate to the troughs which are supported by the crossbeams. This configuration ensures a sufficient and effective stress distribution in the whole structure. During the internship, the 2D model built in the Excel Program was used to find out the stresses in the longitudinal direction. In this model, springs are applied under the trough. This is to simulate the vertical stiffness of the trough itself. It is obvious that the spring stiffness is determined by the force-deflection curve of the troughs. This 2D model is accurate enough for the study of the vertical behavior of the structure (vertical resistance). It has been proven by the research carried out during the internship. The excel sheets of the original 2D model are attached in appendix C. The manual of these excel sheets can also be found in that appendix.

4.1.1 The vertical spring stiffness

The vertical spring stiffness is calculated with the help of the model of a single trough crossing over multiple crossbeams, see figure 4.1. It is assumed that a certain width of the deck plate together with the trough cross section carry the vertical wheel load and the bending moment. A reasonable assumption would be the deck plate width is the trough top width plus half of the trough top width on each side of the trough. By applying a point load F on the halfway of the trough span, displacement u takes place in this location. Therefore the vertical stiffness of this single trough is incorporated into the hooke's law, wherein k_z is the spring constant of the vertical bending stiffness in the longitudinal direction.

$$k_z = \frac{F_z}{u}$$

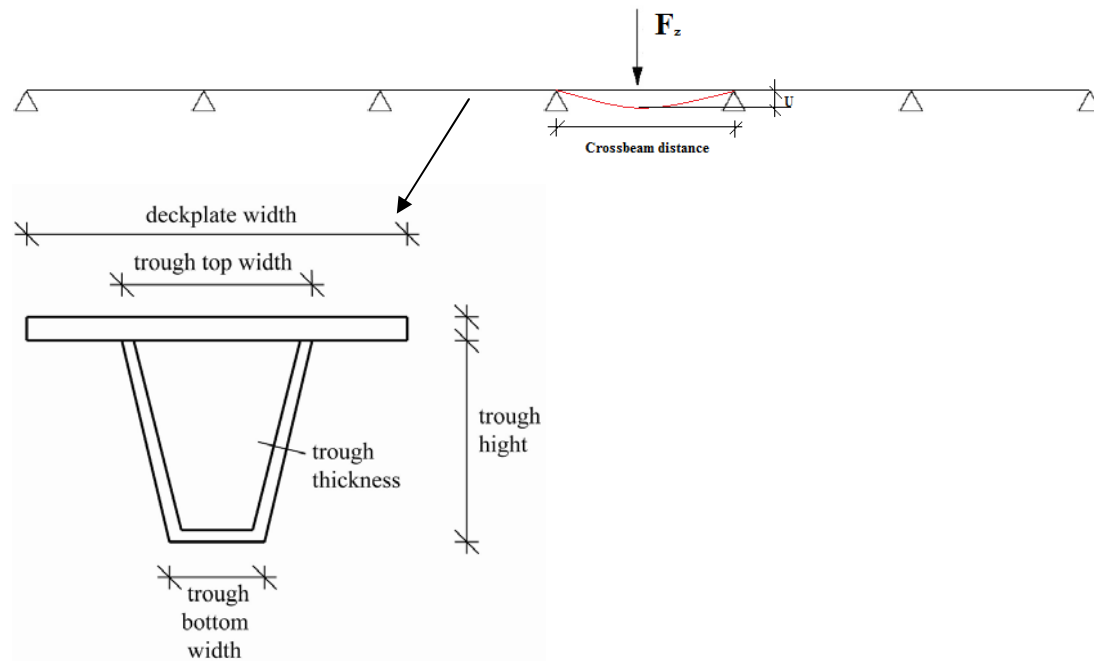


Figure 4.1 Beam model for calculating the vertical spring constant

4.1.2 Two-level model

In this section a 2D beam model consisting of 2 levels will be described. Each level consists of seven troughs with deck plate. The bottom level represents the directly loaded cross-section of the deck plate and the troughs. It has an assumed width (=length in the direction of the trough) of the length of the wheel load. At the bottom flange of the trough, each trough web is supported by a vertical spring which represents the vertical stiffness of a trough due to its own bending in longitudinal direction. The value of the spring stiffness is equal to half of k_z which has been found out in section 4.1.1. The top level represents the cross-section of the not directly loaded part of the orthotropic steel deck. When the point load is working at the halfway of the trough span, the deflection along the trough span varies from the maximum in the middle of the span to zero at the crossbeam. It means that the spreading of the wheel load in the transversal direction due to the transverse bending stiffness also varies from the maximum in the middle of the trough span to zero at the crossbeam. This total effective width of the cross-section which helps the spreading of the wheel load in the transversal direction is assumed to be 50% of the trough span. Therefore, the cross-section of the top level has a width (=length in the direction of the trough) of 50% of the trough span minus the width of the bottom level. The top sides of the trough webs of these two levels are connected with rigid link which ensures that they have the same deflection.

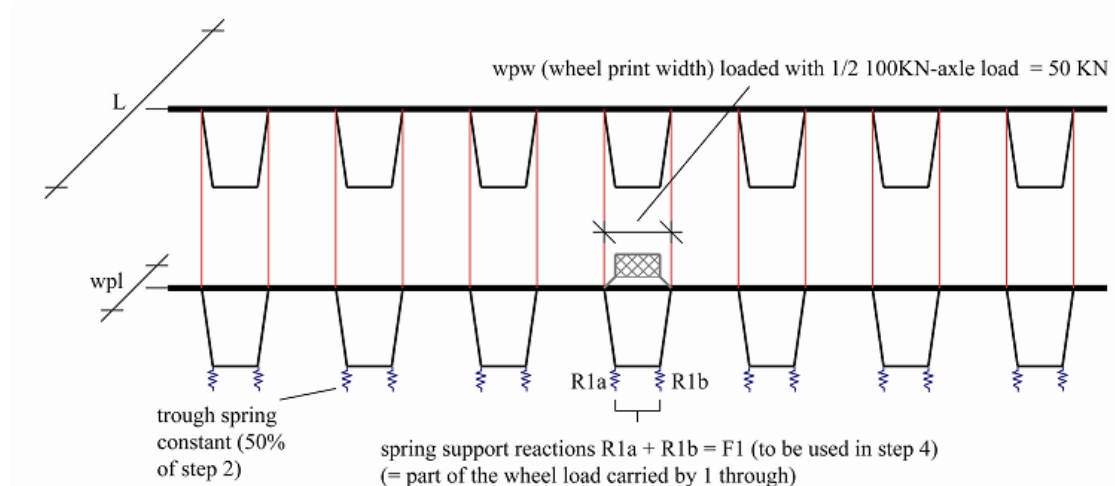


Figure 4.2 2D beam model

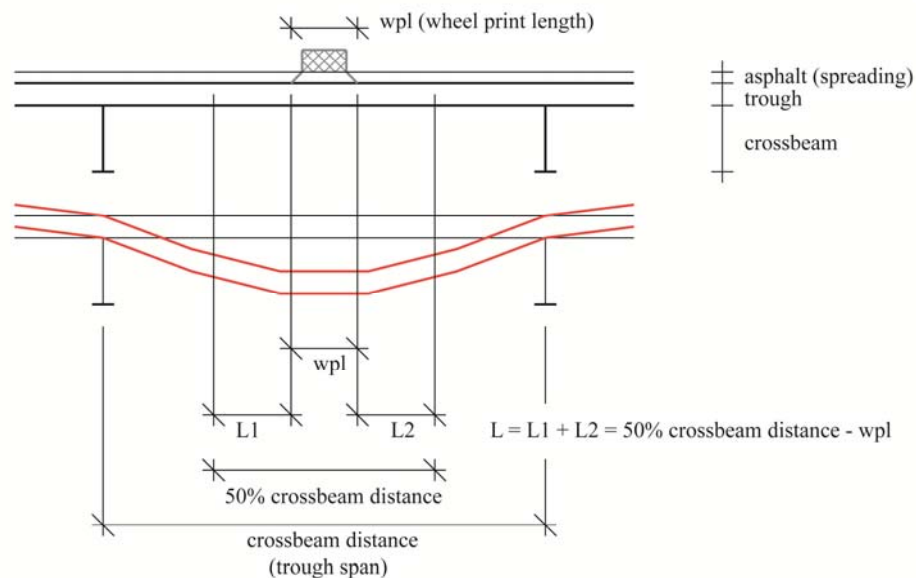


Figure 4.3 The directly loaded part and the load dispersal part

4.2 Improved 2D model

This 2D model in section 4.1 is accurate enough for the study of the bending stresses on the bottom side of the troughs (vertical resistance). This has been proven by the internship. However, this model overlooks the torsional stiffness effects of the trough. In this circumstance, the simplification made in the internship model will lead to an inaccurate result in the study of the local stresses in the trough-to-deck plate joint of the orthotropic steel deck. As an example, when the wheel load is working in between two troughs, the calculated transverse displacement of the bottom flange of the trough derived from the internship 2D model is in the opposite direction of the displacement of the 3D model (see figures below). Therefore, finding out a more appropriate boundary condition in the transversal direction is necessary to improve the original 2D model.

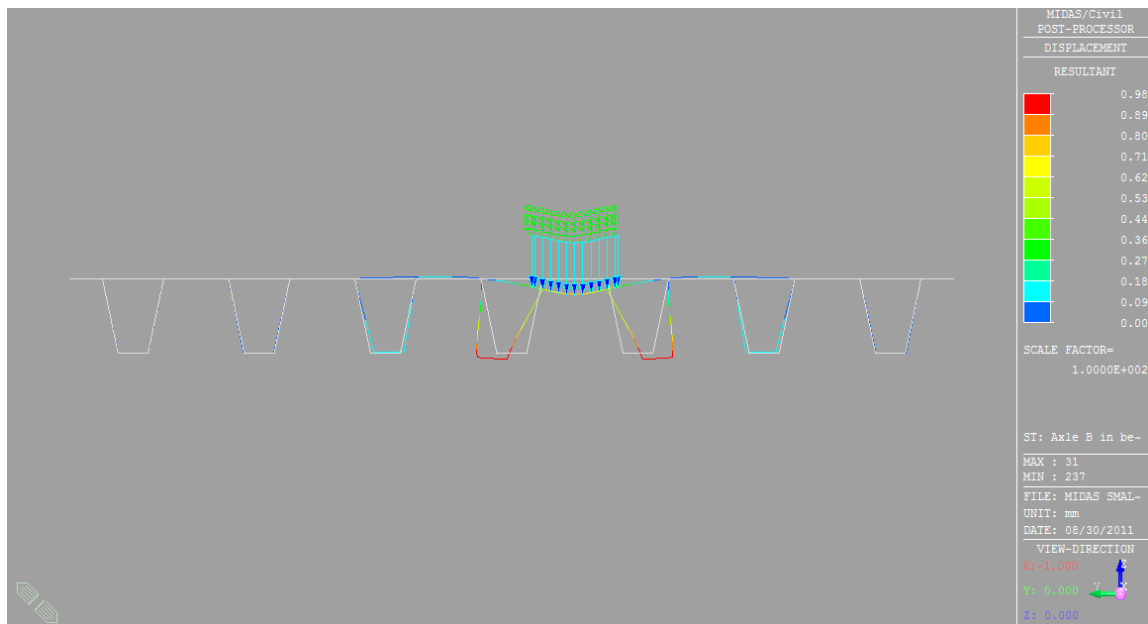


Figure 4.4 Deformation in the original 2D beam model of model B under axle C

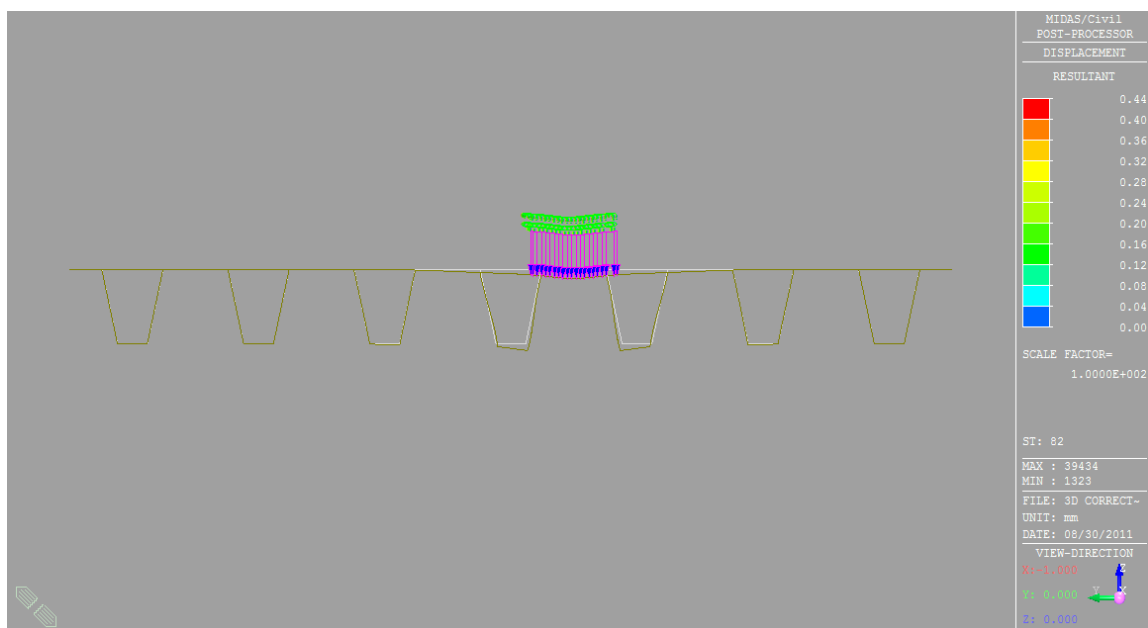


Figure 4.5 Deformation in the 3D model of model B under axle C

For this reason two kinds of alternative horizontal supports for the trough bottom flange are added. Calculations are performed with each support scenario respectively in the following chapters. These support scenarios are:

- Trough without horizontal support (the original internship 2D model)(Figure 4.6 a)
In this model, no horizontal support on the trough bottom flange is added. It means that the bottom flange of trough can freely deform in the transversal direction.
- Trough with fixed support (Figure 4.6 b)
In this model, the transverse displacement of the trough bottom flange is restricted.
- Trough with spring (Figure 4.6 c)
In this model, a horizontal spring is added on the bottom flange of the trough. The

calculation of the spring stiffness is described in the following paragraph.

In the figure below, the object joint is indicated with a red circle. Furthermore, the troughs are numbered from one to seven.

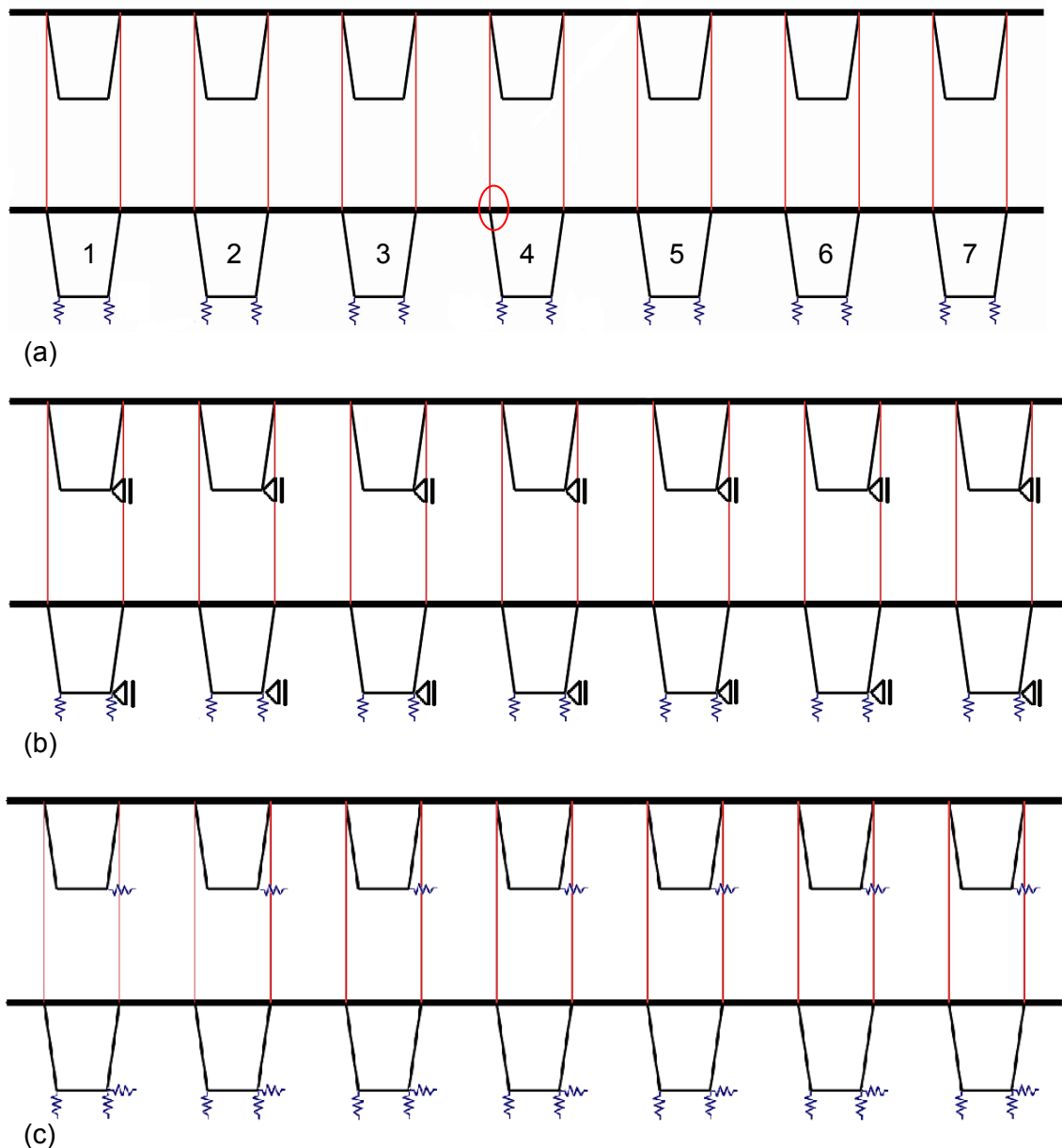


Figure 4.6 Beam models (a) the original beam model without horizontal support; (b) improved beam model with horizontal support; (c) improved beam model with spring horizontal support

For the calculation of the horizontal spring stiffness an assumption is made. The assumption is that only the bottom part of the trough cross-section with a certain height contributes to the transverse stiffness of the trough bottom. This cross-section is used in a beam element model which has six spans over seven supports, see figure 4.7. By applying a point load F_y at the halfway of the fourth span in the horizontal direction, a horizontal displacement of w occurs at this location. According to the Hooke's law the horizontal spring stiffness of each single trough can be calculated as follows:

$$k_y = \frac{F_y}{w}$$

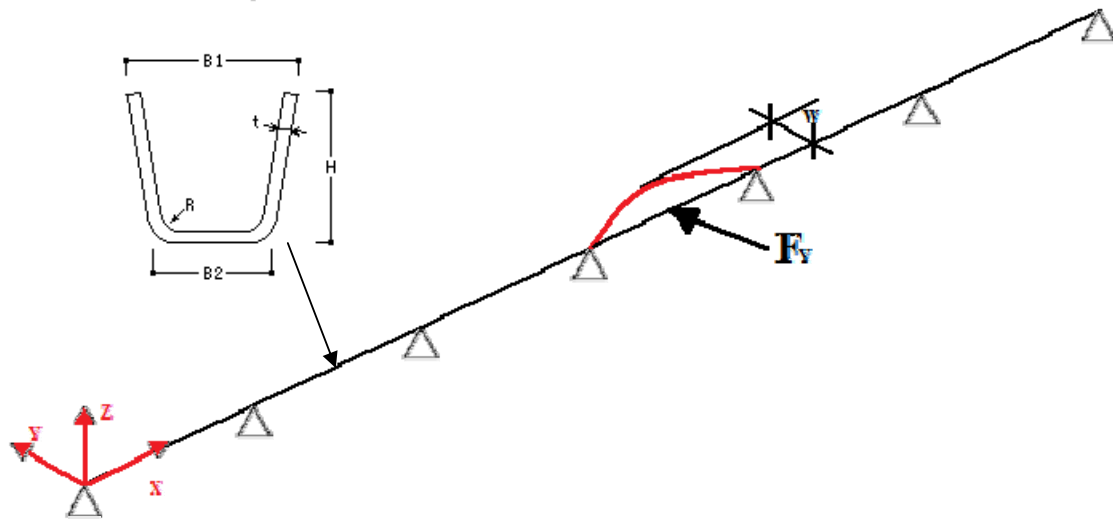


Figure 4.7 Beam model for calculating horizontal spring constant

This spring is used in the third model as horizontal support. It is applied on the trough bottom flange of the bottom level as well as on the top level (Figure 4.6 c).

Load cases

A single wheel load of 50 kN is applied on the deck plate of the bottom level of the two-level model. It is added as a uniformly distributed line load. There are two kinds of axle loads, one is axle B and the other is axle C as defined in NEN-EN 1991-2-2003 (Table 3.3). Since the beam element is defined as line element in the MIDAS Civil, the wheel load is also presented as line beam load on the elements. In this circumstance, the wheel loads working on the model are:

$$q_A = \frac{F}{W_A} = \frac{50000}{W_A}$$

$$q_B = \frac{F}{W_B} = \frac{50000}{W_B}$$

$$q_C = \frac{F}{W_C} = \frac{50000}{W_C}$$

in which, W_A , W_B and W_C are the width of the wheel print axel A, axle B and axle C including the spreading of the wearing surface, respectively.

For each kind of axle, three calculations are performed regarding to three different load locations.

- Wheel load centrally above the middle trough (trough 4)
- Wheel load on the object trough web of the middle trough

- Wheel load in between the trough 3 and 4

4.3 Verification of the improved 2D model

These 2D models are verified by comparing the results with those of the 3D models and the Excel Programs. The stresses are listed in table 4.1 and table 4.2.

Wheel load location	Object joint	3D	Excel Programs	without horizontal support	with horizontal support	with horizontal spring	
Axle B above the trough	trough web	Interior	-16.10	-18.90	-17.90	-12.56	-18.10
		Exterior	0.00	0.70	1.00	-2.16	-3.24
	deck plate	Interior	-37.00	-48.50	-45.80	-40.84	-44.56
		Exterior	-36.10	-47.40	-46.60	-40.28	-43.65
Axle B on trough web	trough web	Interior	-8.64		-25.63	-5.44	-15.20
		Exterior	-9.95		8.45	-10.36	-2.01
	deck plate	Interior	-50.40		-46.50	-53.05	-48.66
		Exterior	-52.00		-43.25	-55.30	-50.18
Axle B in-between troughs	trough web	Interior	1.24		-18.43	2.44	-10.61
		Exterior	-18.30		10.84	-16.16	-2.93
	deck plate	Interior	-45.20		-32.53	-44.04	-35.59
		Exterior	-49.00		-27.64	-48.36	-35.66
Axle C above the trough	trough web	Interior	-39.20	-40.20	-39.00	-37.28	-39.02
		Exterior	20.10	20.50	20.45	20.12	21.36
	deck plate	Interior	-39.60	-53.60	-50.44	-44.97	-47.04
		Exterior	-32.80	-47.40	-43.90	-39.04	-42.49
Axle C on trough web	trough web	Interior	-8.51		-41.24	-1.32	-20.87
		Exterior	-18.80		23.56	-18.68	2.64
	deck plate	Interior	-63.60		-57.75	-66.47	-56.95
		Exterior	-66.90		-50.03	-70.14	-60.23
Axle C in-between troughs	trough web	Interior	22.70		-26.65	31.12	-1.23
		Exterior	-43.20		9.74	-46.68	-25.46
	deck plate	Interior	-47.40		-30.17	-46.85	-36.21
		Exterior	-57.80		-30.61	-57.76	-41.30

Table 4.1 Stresses in the object joints of model A (small cross-section with asphalt layer)

Wheel load location	Object joint	3D	Excel Programs	without horizontal support	with horizontal support	with horizontal spring	
Axle B above the trough	trough web	Interior	-10.10	-11.60	-9.42	-8.40	-9.52
		Exterior	-1.22	-1.10	-1.78	-1.78	-1.28
	deck plate	Interior	-13.10	-19.10	-16.39	-15.84	-16.01
		Exterior	-12.80	-18.60	-17.70	-15.61	-17.21
Axle B on trough web	trough web	Interior	-4.33		-16.58	-3.01	-9.55
		Exterior	-8.76		5.82	-8.05	-1.73
	deck plate	Interior	-18.50		-17.63	-20.48	-18.35
		Exterior	-19.60		-17.30	-21.50	-19.67
Axle B in-between troughs	trough web	Interior	2.32		-17.73	2.50	-6.92
		Exterior	-14.40		9.07	-12.38	-2.82
	deck plate	Interior	-17.00		-12.14	-17.08	-13.46
		Exterior	-19.30		-10.90	-19.07	-14.91
Axle C above the trough	trough web	Interior	-20.00	-20.00	-19.46	-17.82	-19.50
		Exterior	6.47	6.40	6.94	6.18	7.30
	deck plate	Interior	-12.60	-20.60	-17.45	-16.15	-17.15
		Exterior	-10.60	-18.60	-17.10	-14.36	-16.68
Axle C on trough web	trough web	Interior	-4.01		-24.61	-2.44	-13.18
		Exterior	-15.00		12.39	-11.10	-0.18
	deck plate	Interior	-21.10		-19.49	-24.48	-20.93
		Exterior	-23.10		-17.90	-25.93	-22.04
Axle C in-between troughs	trough web	Interior	11.80		-15.90	12.12	-0.60
		Exterior	-26.30		6.50	-23.28	-10.34
	deck plate	Interior	-17.50		-10.41	-17.92	-12.36
		Exterior	-22.00		-9.73	-21.98	-15.38

Table 4.2 Stresses in the object joints of model B (small cross-section with asphalt layer)

It is shown in the tables that the results of the 3D plate model and the 2D beam model with horizontal support have the best fit. The difference of the results for the load cases resulting in the maximum stresses in either the deck plate or the trough is not very large

but can be improved. Therefore, it can be concluded that the beam model with horizontal support fits the result of the 3D plate model better. As a result, the improved 2D model (made in MIDAS Civil) is presented in figure 4.8. Different from figure 4.2 which shows the two levels of the simplified model are above each other, figure 4.8 presents the two levels on the same height. The two levels in figure 4.2 are connected with rigid bars which insure that both levels have the same vertical deflection. In MIDAS Civil, this situation is achieved with the help of a rigid vertical connection as shown in figure 4.8.

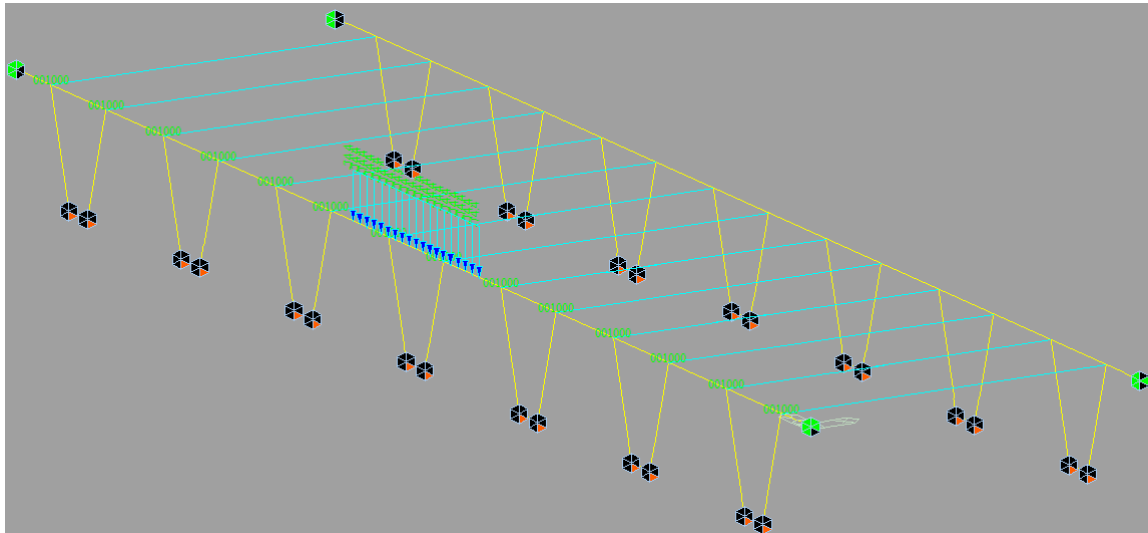


Figure 4.8 Final intermediate 2D model in MIDAS Civil

Although the 2D beam model with horizontal support fits the result of the 3D plate model better than the other two, it is still not a perfect match. First of all, in the beam model the distortion of the troughs is ignored. The distortion of the trough has influence on the load distribution area, and therefore the distribution of the bending moment. Secondly, the element type has also influence on the results. In the 2D model, the beam element is applied. As one-dimensional element, the analysis results in the 2D model are not affected by the size of its width (=length in the direction of the trough explained in section 4.1.2) In this case, the width of the model which is actually the length of the trough is assumed to be dimensionless and no stress distribution is found along the width of the model. The figures below show the stress distribution in the trough web in the longitudinal direction when the axle C is working on the trough web. It is obvious that the trough web in the 2D beam model can only be divided in the vertical direction. Due to that the beam element is dimensionless in its cross section, on variation of the stress along the width of the beam element (which is also the length of the trough) can be observed. In the 3D plate model the trough web is divided not only in the vertical direction but also in the longitudinal direction. The plate element can lead to the stress distribution in the trough web. Therefore, the stresses in the 2D beam model are uniformly distributed in the longitudinal direction of the element. On the contrary, the stresses distribution in the 3D plate element is non-uniform.

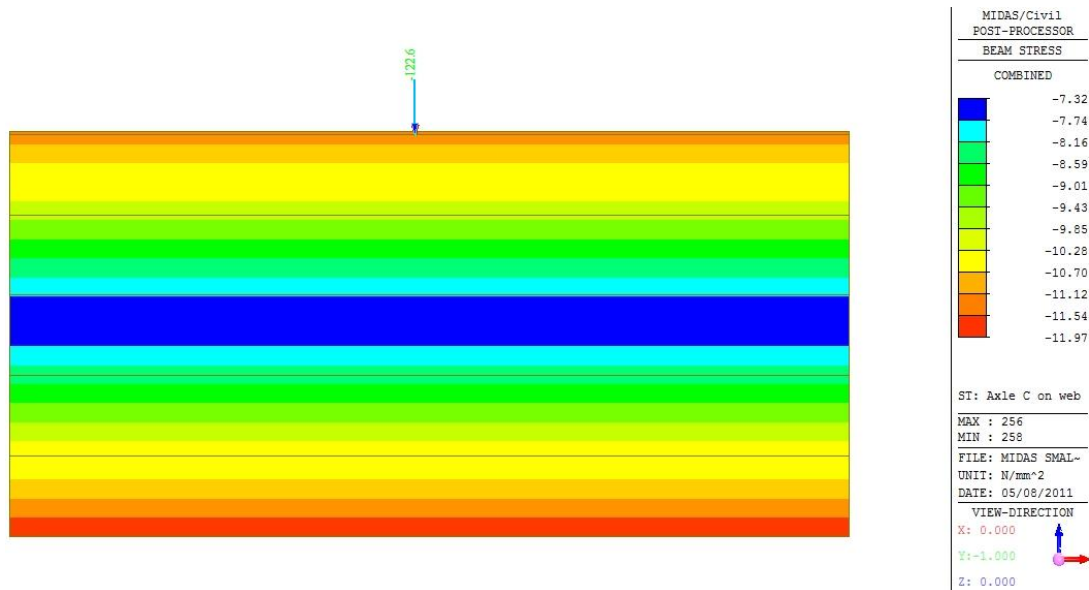


Figure 4.9 Stresses distribution in the trough web in the beam model

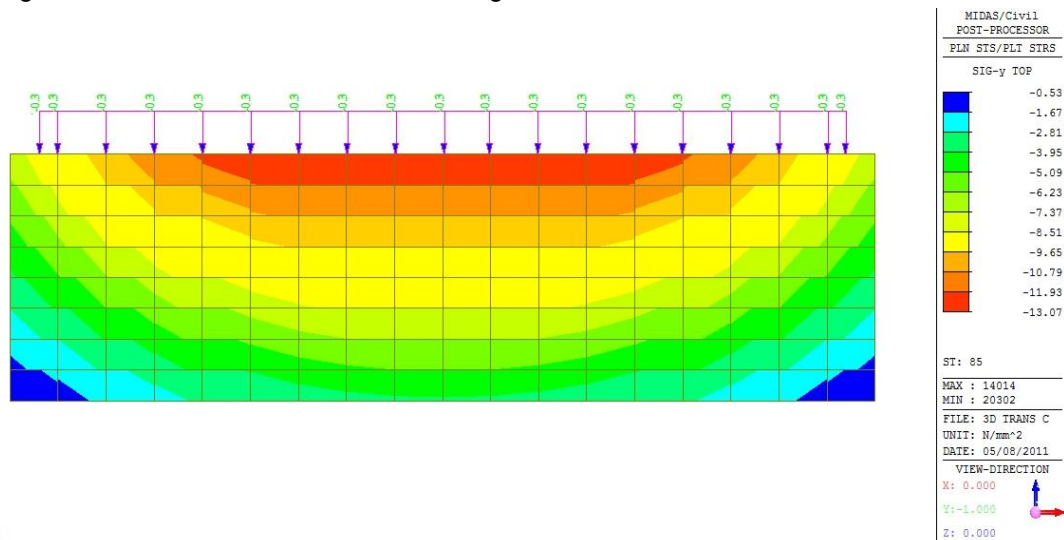


Figure 4.10 Stresses distribution in the trough web in the 3D plate mode

4.4 Conclusions of 2D model

- The original 2d model is not applicable for calculating the transverse stress in the trough-to-deck plate joint. By adding a horizontal support in the bottom flange of the trough, the results obtained from 2D model fit the results of 3D model better. The 2D model with horizontal support is considered from here on.
- There is still difference between the 2D model with horizontal support and the 3D model. The difference is mainly caused by distortion.

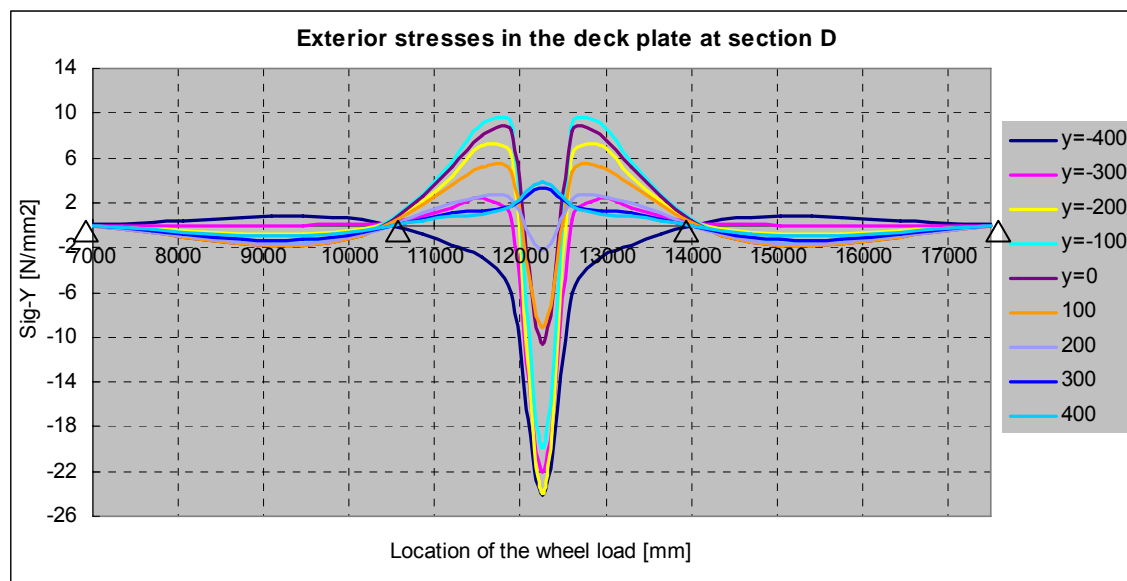
5 Simplification of the 3D model results

As what has been presented in the previous chapter, the 2D model has some limitations which can lead to a less accurate result in the stress calculation. In order to improve the accuracy of the 2D beam model, results modification should be made to the model results. In section 5.1, the influence lines derived from the 3D model are presented. Based on the influence lines, comparison between the 3D and modified 2D models is made. In the end, the recommendation over the modification of the 2D model is given.

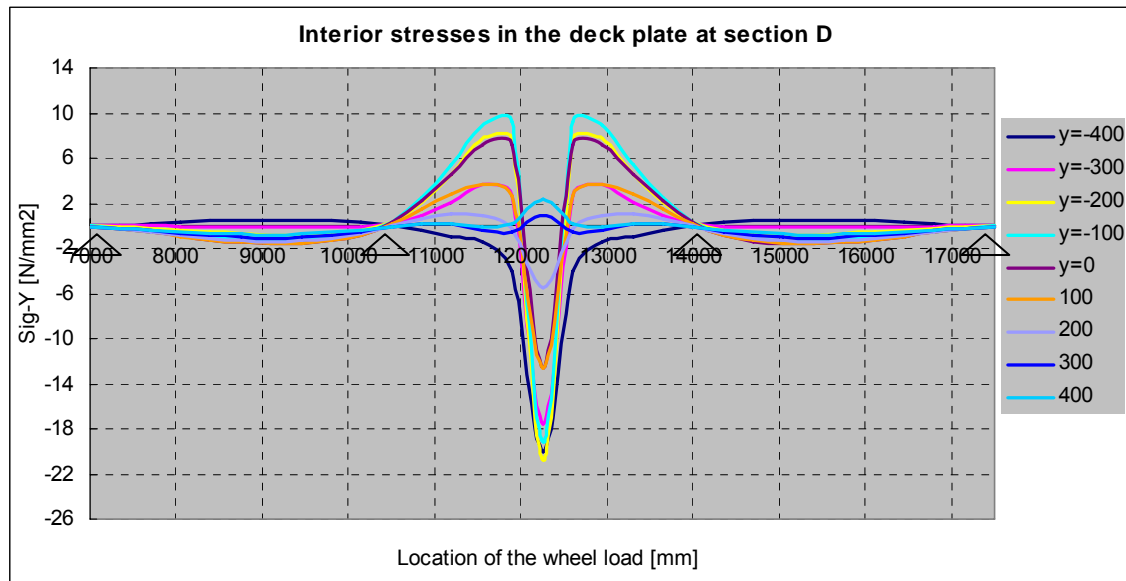
5.1 Analysis of the influence line at section D

The longitudinal and transverse influence lines of the transverse stress in the trough-to-deck plate joint are the basis for the fatigue calculation of this joint. Longitudinal influence lines are plotted for four different sections, and it is discovered that the influence line at section D which is at the mid-span of the trough is decisive for the fatigue calculation. Because that the stress range at this section is usually larger than that in the other sections. For simplicity, the influence line got from model B (large cross-section with asphalt layer) under axle C is mainly presented in this thesis. The rest of the influence lines can be found in appendix A. The conclusions derived are generally applicable for all models.

First of all, the results of the 3D finite element model are given again for the specific scenario. Each plot in the following figure presents the longitudinal influence lines in the deck plate for nine transverse locations from $y=-400\text{mm}$ to $y=400\text{mm}$.



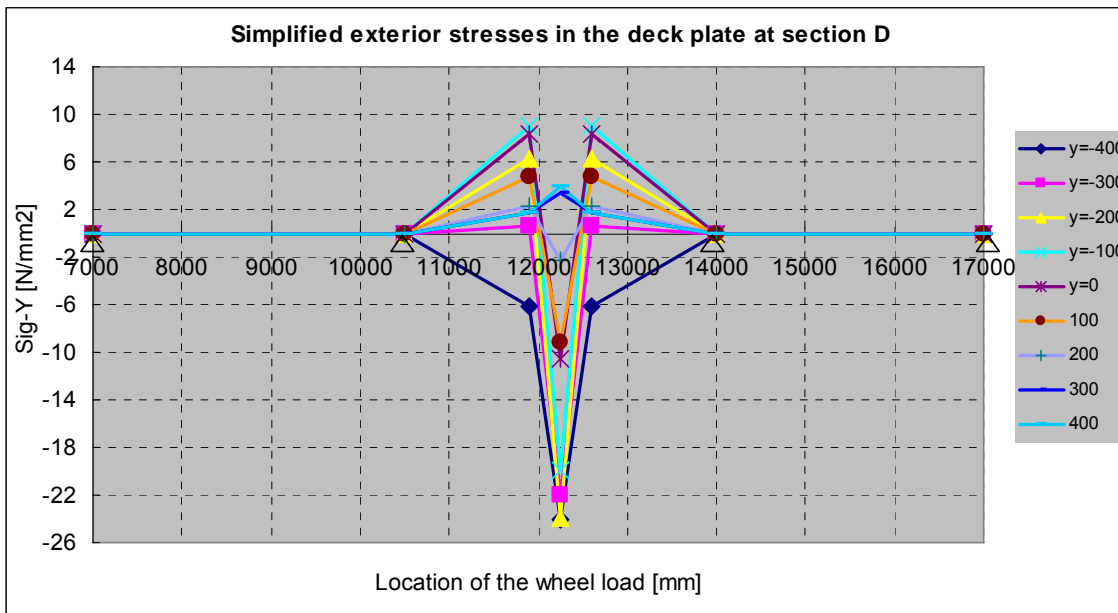
(a)



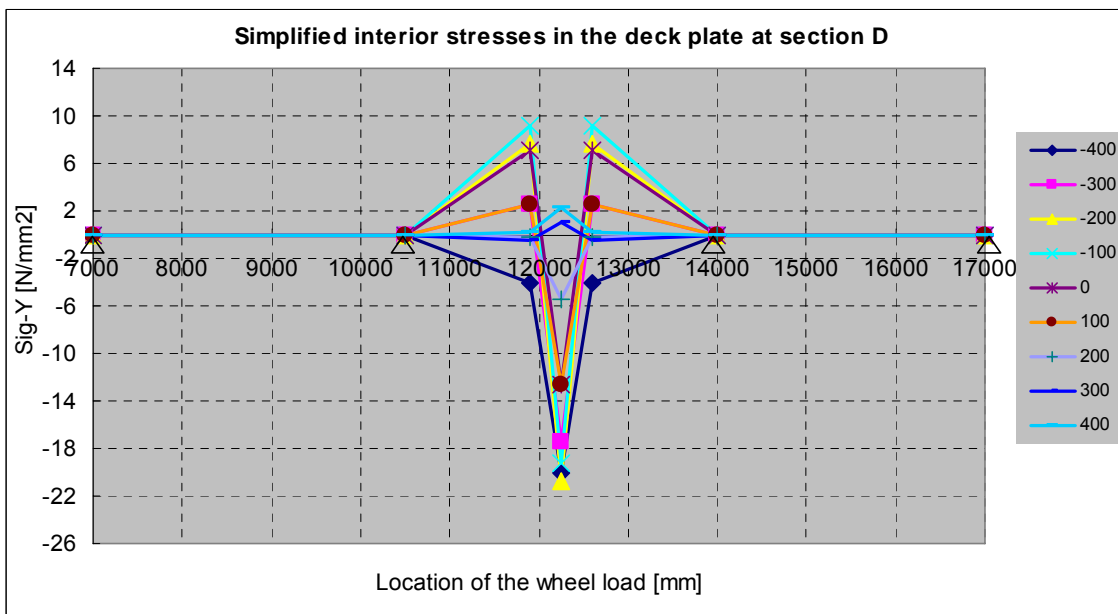
(b)

Figure 5.1 Model B under axle C: longitudinal influence line of the stress in the deck plate at section D (a) Exterior stresses in the deck plate at section D; (b) Interior stresses in the deck plate at section D

The stress reaches its peak value when the axle wheel load moves over section D. The further the axle load away from the section is, the smaller the stress generated by the wheel load is. Therefore, the fluctuation of the stresses in the deck plate when the wheel load is running in the middle span (from $x=10500\text{mm}$ to 14000mm) is interesting for the fatigue calculation. When the axle wheel load acts outside the range of $x=10500\text{mm}$ to 14000mm , the stress in the deck plate generated by this wheel load can be ignored. Under the axle load in the mid-span, the influence lines have several characters in common. In general, the influence line reaches its extreme value when the axle load is precise on section D. When the axle load is moving away from section D, the stress will decrease or increase very quickly. And around section $D\pm 350\text{mm}$, an inflection point appears in the influence line. Moreover, the stresses at $x=10500\text{mm}$ and 14000mm are very small which can be considered as zero. With these five characteristic values of stress (three peak values and two zeros), the longitudinal influence line in the deck plate can be simplified as follows:



(a)



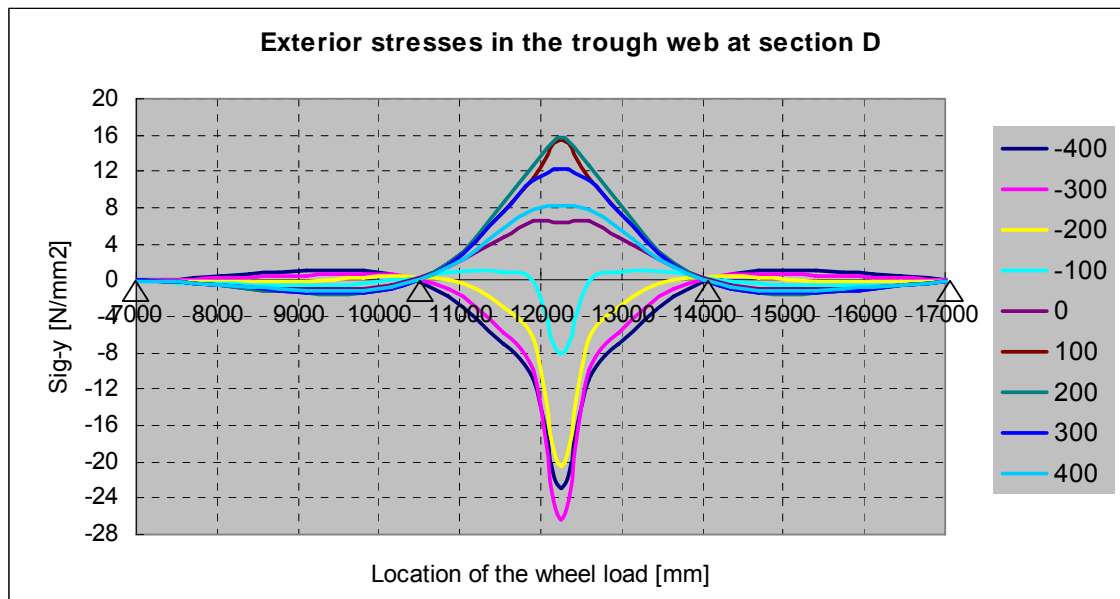
(b)

Figure 5.2 Model B under axle C: simplified longitudinal influence line of the stress in the deck plate at section D (a) Exterior stresses in the deck plate at section D; (b) Interior stresses in the deck plate at section D

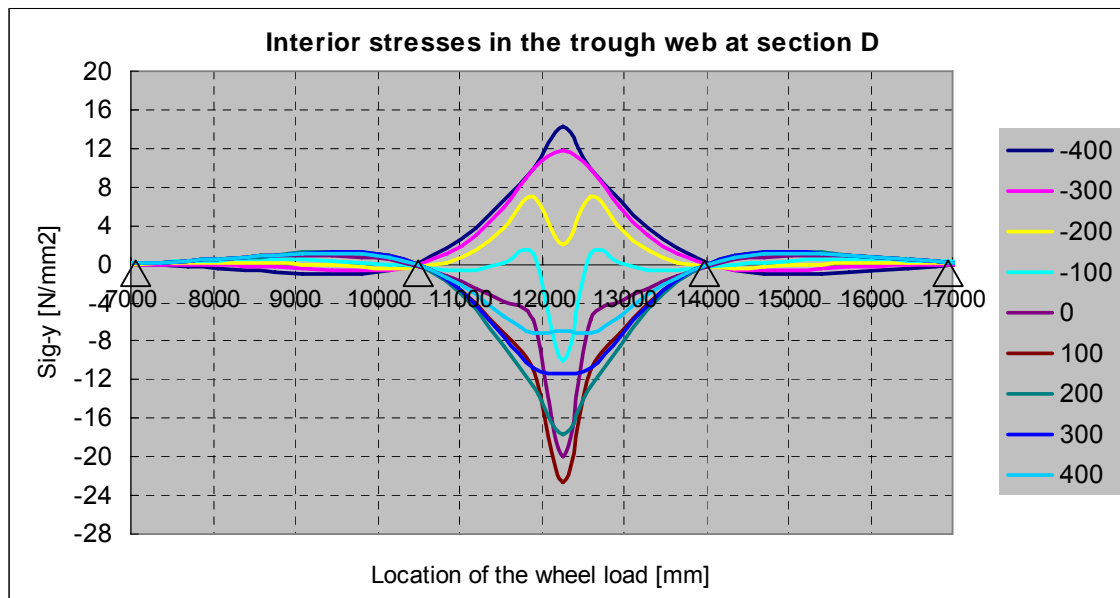
These simplified influence lines are used for the later comparison with the results of the 2D models. In this way, the comparison is more explicit. Details are given in the next sector. Another advantage of these simplified influence lines is that they are more convenient to be used for the fatigue check. This check is done in the next chapter, thus is not discussed here.

From figure 5.2 it is clear that the simplified influence lines have the same tendency as the normal influence lines presented in figure 5.1. The fluctuation of all the influence lines begins at $x=10500\text{mm}$ and ends at $x=14000\text{mm}$ where the middle span is supported by two crossbeams (indicated with triangular in black). The middle specific point ($x=12250\text{mm}$) indicates the extreme value of the influence line. The two points next to the middle one are the inflection point of the influence line.

The following figure presents the longitudinal influence lines in the trough web at section D.



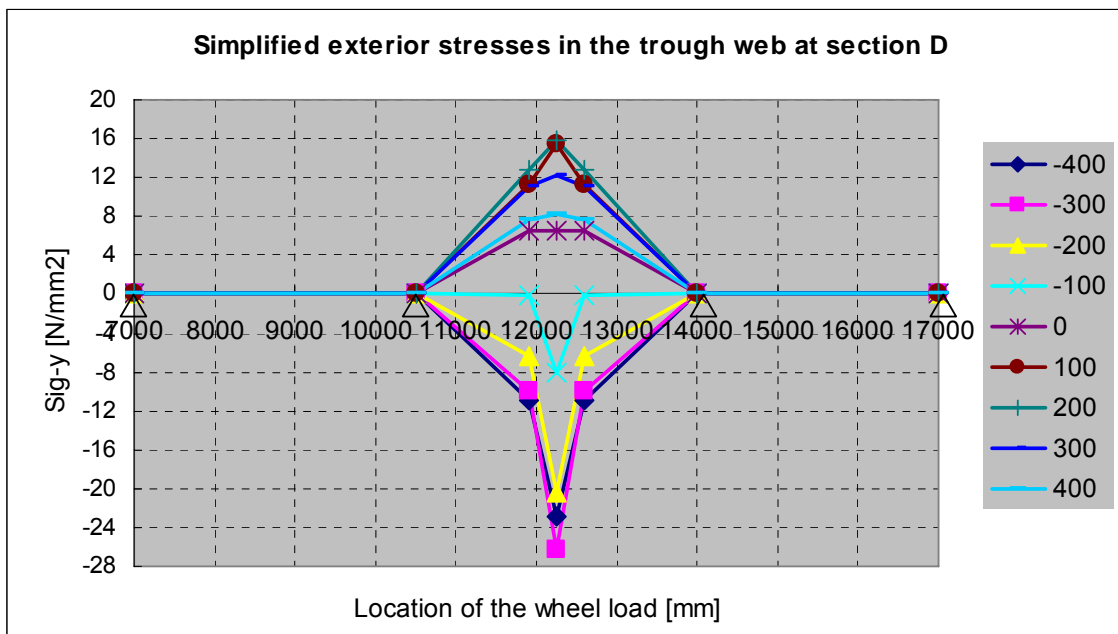
(a)



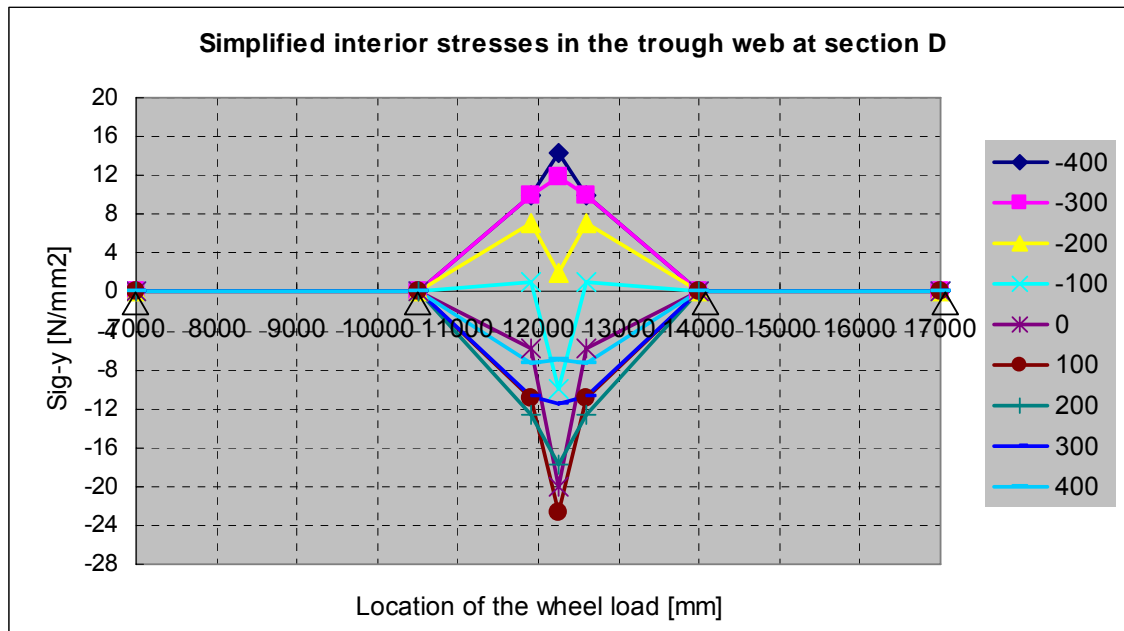
(b)

Figure 5.3 Model B under axle C: longitudinal influence line of the stress in the trough web at section D (a) Exterior stresses in the trough web at section D; (b) Interior stresses in the trough web at section D

Similarly, attention is paid to the central part of the influence line (from $x=10500\text{mm}$ to 14000mm). When the wheel load is moving towards the center of the middle span, the stress in the trough web fluctuates moderately. Until the wheel load passes a cross-section which is 350mm away from the section D, the stress increases or decrease significantly. It is discovered that the stress will reach a peak or trough value in the center of middle span. Therefore, a conclusion can be made for the analysis that the longitudinal influence line in the trough web can also be simplified by five characteristic points, see figure 5.4.



(a)



(b)

Figure 5.4 Model B under axle C: simplified longitudinal influence line of the stress in the trough web at section D (a) Exterior stresses in the trough web at section D; (b) Interior stresses in the trough web at section D

As what has been shown in the plots that the influence line is simplified by connected the points which represent the characteristic value of stress generated by the moving axle load.

The results of the improved 2D models are presented below for comparison.

As discussed above, the longitudinal influence line was simplified into straight lines with five characteristic values based on the results got from the 3D finite element model. Actually, these five characteristic values can also be calculated by the simplified model. This approach provides a straight forwards analytical calculation of the stress range for the fatigue assessment.

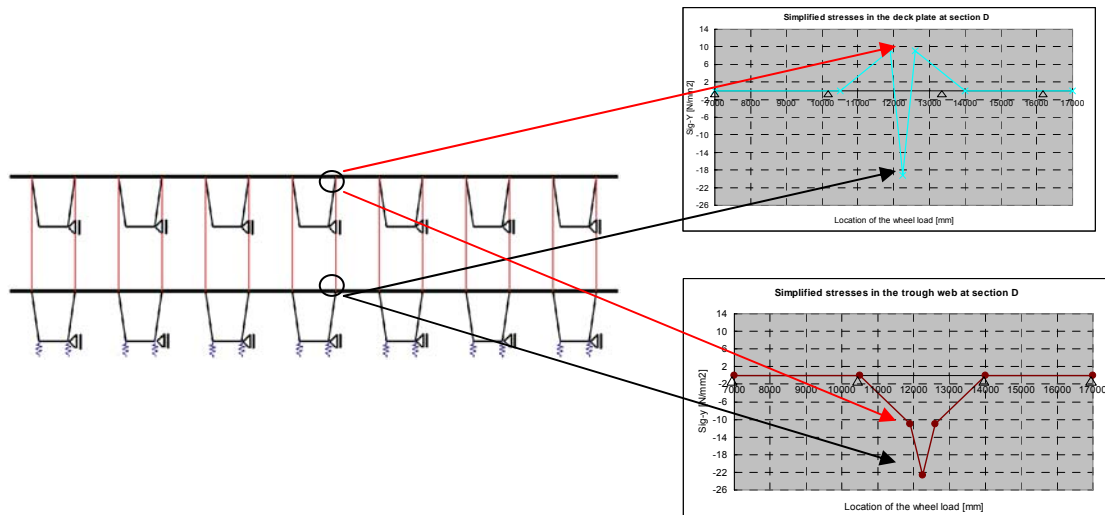


Figure 5.5 Simplification influence line

In the improved 2D beam model, the bottom level represents the direct loaded section at the halfway of the middle span. Therefore, a global deformation (due to bending and deflection of the trough) as well as a local deformation (due to local deflection of the directly loaded deck plate) takes place at this part. As a result, a maximum stress in the model is generated at this level. This value should compare to the trough value in the simplified influence line. Since the orthotropic deck is a continuous structure, the not directly loaded part will also deflect representing the effects in a cross-section of the trough (with deck plate and trough web) just before and after the location of the wheel load (location of the inflection point). Therefore, by considering the mechanical behavior of the simplified model in the previous chapter, the stress generated in the top level is able to represent the stress at the inflection point. In this way, the results of the improved 2D models have the form of the simplified influence lines of the 3D model as well.

5.2 Comparison between 3D model and improved 2D model

Although the longitudinal influence line can be simplified by using two characteristic values got from the two-level 2D beam model, it has been shown that the 2D model has a less accurate result. As discussed before, the most possible solution is by multiplying the stress with an adjustment factor. In order to find out the applicable adjustment factor, comparison of the characteristic value should be made between the 3D model and the 2D model. To make the adjustment factor universalism, two more models are made.

The comparison is made for six different models. The new models are indicated with yellow color.

Structural component		Model type					
		Orthotropic deck with asphalt (60mm)			Orthotropic deck without asphalt (8mm epoxy layer)		
		Model A	Model B	Model E	Model C	Model D	Model F
Crossbeam	Height(H_C)	1250	1250	1250	1250	1250	1250
	Length(L_C)	4200	4200	4200	4200	4200	4200
	Distance(D_L)	3500	3500	3500	3500	3500	3500
	Thickness(t_c)	12	12	12	12	12	12
Deck plate	Length(L_d)	21000	21000	21000	21000	21000	21000
	Width(B_d)	4200	4200	4200	4200	4200	4200
	Thickness(t_d)	12	18	18	12	22	18
Trough	Height(h_t)	325	350	350	325	350	350
	Width upper(b_{top})	300	300	300	300	300	300
	Width bottom(b_{bot})	105	150	150	105	150	150
	Thickness(t_t)	6	8	6	6	8	6
	Distance(d_t)	600	600	600	600	600	600

The unit of the dimension is mm

Figure 5.6 Geometry of the orthotropic deck models

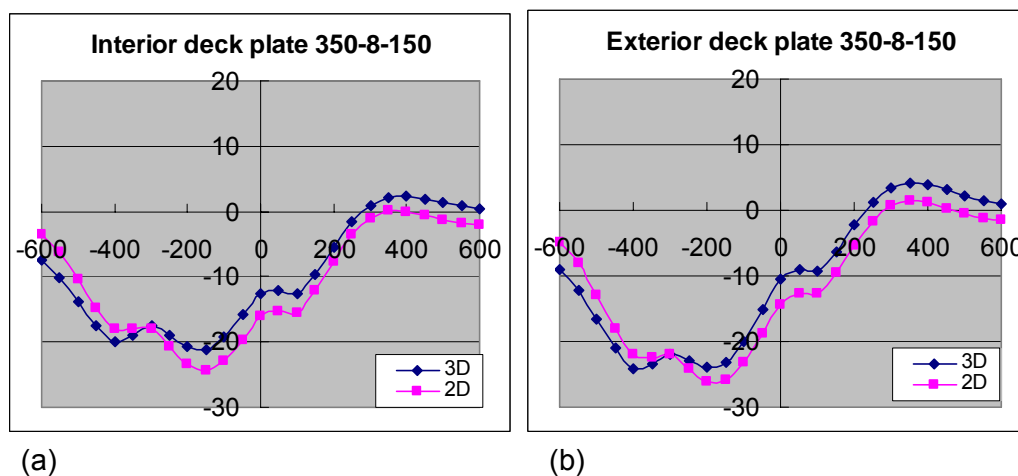
Axle type	Wheel load area $b \cdot h$ [mm ²]					
	Model A	Model B	Model E	Model C	Model D	Model F
Axle B	672*452	678*458	678*458	568*348	578*358	574*354
Axle C	402*452	408*458	408*458	298*348	308*358	304*354

Figure 5.7 wheel load print

Axle type	Wheel load [N/mm ²]					
	Model A	Model B	Model E	Model C	Model D	Model F
Axle B(q_B)	0.165	0.161	0.161	0.253	0.242	0.246
Axle C(q_C)	0.275	0.268	0.268	0.482	0.453	0.465

Figure 5.8 Uniformly distributed wheel load

As an example, the comparison of the transverse influence line in model B under wheel load axle C is presented here. The plots of the other models are given in appendix B.



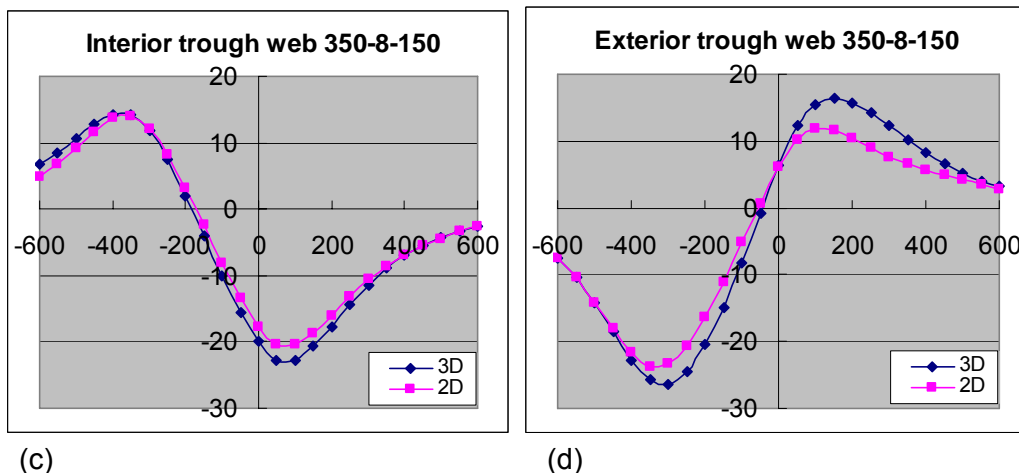


Figure 5.9 Comparison transverse influence line of bottom level in modal B under axle C (a) Influence line in interior deck plate; (b) Influence line in exterior deck plate; (c) Influence line in interior trough web; (d) Influence line in exterior trough web

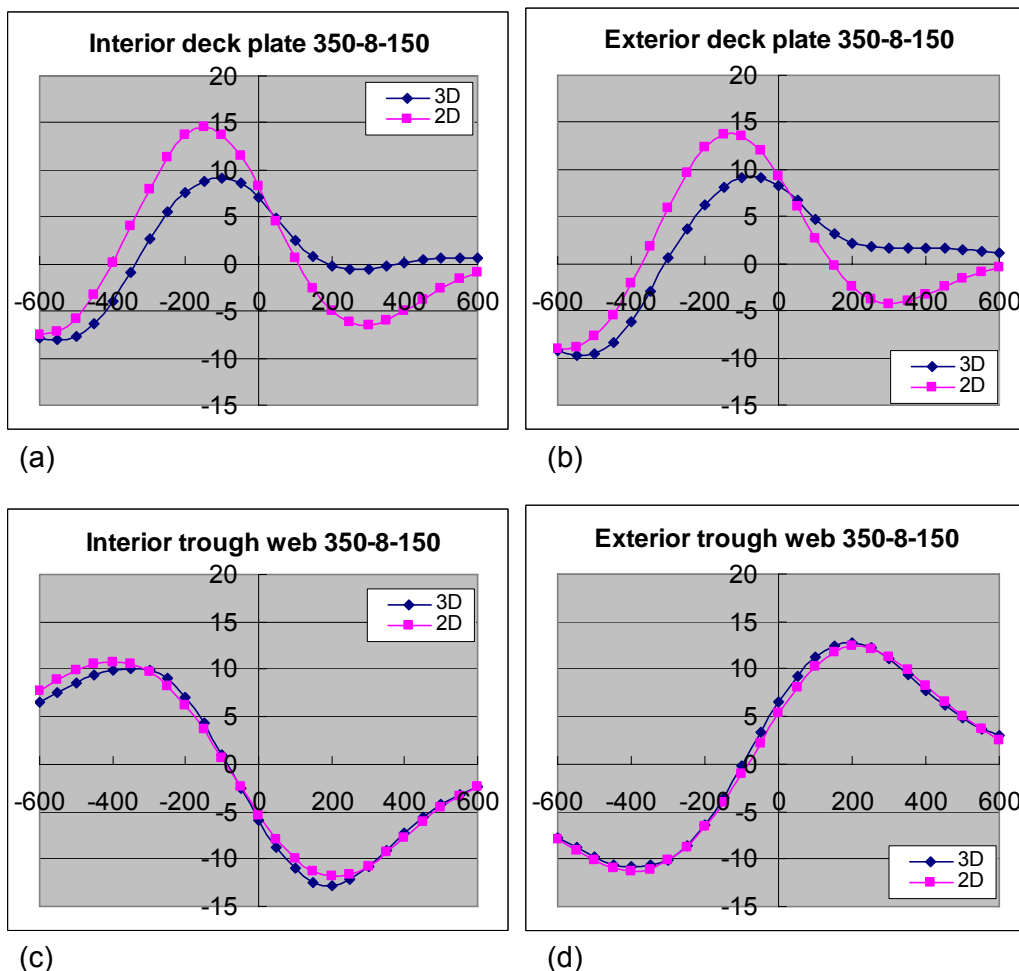


Figure 5.10 Comparison transverse influence line of top level in modal B under axle C (a) Influence line in interior deck plate; (b) Influence line in exterior deck plate; (c) Influence line in interior trough web; (d) Influence line in exterior trough web

The transverse influence lines of the deck plate at $y=-150\text{mm}$ and the interior trough web at $y=100\text{mm}$, exterior trough web at $y=-300\text{mm}$ obtained with the 2D model are compared with the results of the 3D model. From the comparison made in model B under axle C, it shows that the results in the trough web for both bottom and top level in the 2D model have the same shape compared to the 3D model. But the 2D model shows slightly non-conservative simulation. The results in the deck plate for both bottom and top level in the 2D model is also similar to the results of 3D model. In most load cases, the 2D model gives conservative results. In the bottom level, the deck plate stress in 2D model is 10%-20% larger than the 3D model results. The difference is larger in the top level, it is about 50%.

To have a proper understanding of the correlation of the stress between these two models, the results of the comparison for the four models are summarized in the following table. In this table, “ok” means that the conformity is really high between these two models thus no further adjustment is needed. “C” means that the result of the simplified model is conservative. ‘NC’ means that the result of the simplified model is smaller than the finite element model.

Comparison		Deck plate				Trough web			
		Interior deck plate		Exterior deck plate		Interior trough web		Exterior trough web	
		Axle B	Axle C						
Bottom level	Model A	ok/c	ok/c	ok/c	ok/c	nc	ok/c	nc	ok/c
	Model B	ok/c	ok/c	ok/c	ok/c	nc	ok/nc	nc	ok/nc
	Model E	ok/c	ok/c	ok/c	ok/c	nc	nc	nc	nc
	Model C	ok/c	ok/c	ok/c	ok/c	ok	ok/c	ok	ok/c
	Model D	ok/c	ok/c	ok/c	ok/c	nc	ok/nc	nc	ok/nc
	Model F	ok/c	ok/c	ok/c	ok/c	nc	nc	nc	nc
Top level	Model A	c	c	c	c	c	c	c	c
	Model B	c	c	c	c	ok	ok	ok	ok
	Model E	c	c	c	c	nc	nc	nc	nc
	Model C	c	c	c	c	c	c	c	c
	Model D	c	c	c	c	ok	ok	ok	ok
	Model F	c	c	c	c	nc	nc	nc	nc

ok:no adjustment factor is needed
 c:conservative
 nc:non-conservative

Table 5.1 Comparison of the stress in the simplified model and the finite element model

The comparison result is straight forward. For the deck plate in the bottom level which is governing the fatigue damage in the deck plate, the results got from the simplified model are ok or conservative (10%-20% larger than the 3D model result). In this case, no adjustment factor is needed. In the trough web bottom level, the results are sometimes conservative and sometimes non-conservative. In order to ensure that the simplified model can make a safe fatigue calculation, an adjustment factor should be applied here. For the deck plate in the top level, the results of the simplified model are always in the safe side. But too much conservative will result into an uneconomic design. Therefore, it is necessary to find out a reduction factor for the deck plate top level. In the trough web

top level, the comparison shows that the simplified model needs the adjustment factor to simulate the actual stress in the orthotropic steel deck. A brief overview of the comparison between 3D model and 2D model is presented here below:

Comparison	Deck plate	Trough web
Bottom level	OK	OK/C/NC
Top level	C	OK/C/NC

OK: no adjustment factor is needed

C: conservative

NC: non-conservative

Table 5.2 Brief overview of the comparison

From the comparison it also shows that there are variations in the stress of the 3D model to improved 2D model ratio. Therefore, determining the value of the adjustment factor requires more parametric analysis. In the following analysis, the influence of the geometry of the structure will be studied.

5.3 Conclusions

- The transverse stresses and the stress ranges in the deck plate and the vertical stresses and the stress ranges in the trough web (for the trough-to-deck plate joint in between the crossbeams) only depend on loads in between the adjacent crossbeams. Loads in the next trough spans do not or hardly have influence on the stresses. Because of this, the longitudinal influence line is equal to the crossbeam distance (normally 3 to 4 m, 3.5m in the case of this study). It means that the stresses and the stress ranges not only depend on the axle or wheel dimensions, but also total configuration of the trucks.
- The 2D model with horizontal support on the bottom flange of the trough is still not accurate for calculating the stress in the object joint. Therefore, adjustment factor should be applied on the results obtained from the 2D model with horizontal support.

6 Adjustment of the improved 2D model results

The fatigue damage depends on the stress ranges spectrum which varies between the simplified model and the finite element model. In this case, it is possible that the design made with the help of the improved 2D model is too conservative or optimistic. To this end, the adjustment factor should be applied on the simplified model. The adjustment factor is a widely used concept in the civil engineering's world, especially when dealing with the design load or stress.

To have a proper adjustment factor which can indicate the relation between the stresses got from 3D model and those of the improved 2D model, it is necessary to find out what kind of parameters have influence on the adjustment factor. Concerning the trough web-to-deck plate joint, some parameters influencing the stress in this object joint are discussed in the following.

6.1 Adjustment factor for the trough web result

As presented in the previous section, the comparison shows that the stress in the trough web is much sensitive to the distortion than the stress in the deck plate. In this section, the research of the adjustment factor for the trough web result is carried out.

6.1.1 Boundary condition

Based on these two kinds of model, it is clear that the boundary conditions between these two models are different. As what can be seen in the following graph, the boundary conditions in the 3D model are applied on the bottom edge of the crossbeams. The crossbeams are fixed in x-, y- and z-direction. And the trough passes continuously through the crossbeam. The trough is welded along its edge to the crossbeam. Since the trough is constrained only at the crossbeam, the part of the trough which is far away from the crossbeam will displace not only vertically but also horizontally.

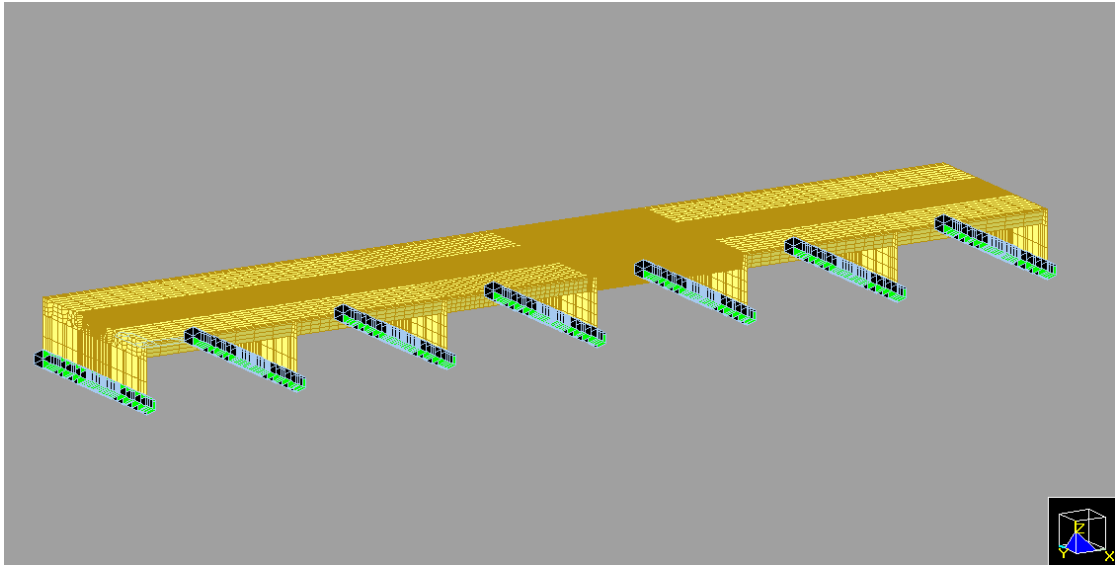


Figure 6.1 Finite element model with boundary conditions

However, this displacement is different in the improved 2D model. In the simplified model, the constraints are applied on the bottom flange of the trough in both levels. On the top level, a fixed horizontal support is added on the bottom flange of the trough. On the bottom level, two kinds of supports are added on the bottom flange. In the vertical direction a spring is added on each trough web and the spring stiffness indicates the vertical bending stiffness of the trough in the longitudinal direction (see section 4.1.1). In the horizontal direction, a fixed support is applied which restricts the horizontal displacement of the trough (based on the results of section 4.2)

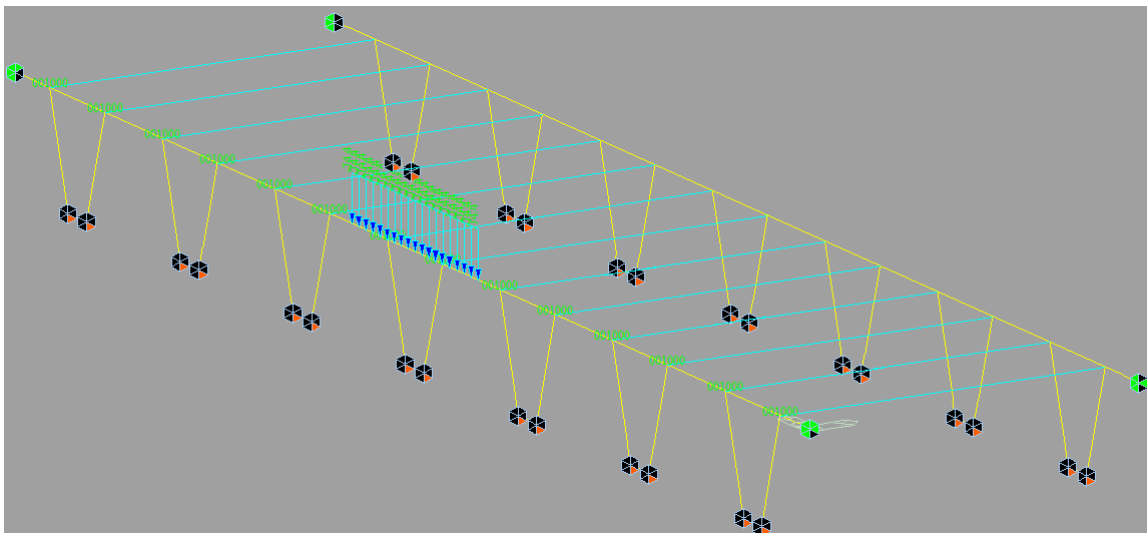


Figure 6.2 Simplified model with boundary conditions

6.1.2 Distortion

The deformation of the trough is different with different boundary conditions. This difference occurs in the vertical as well as in the horizontal direction. As presented in the

previous chapters, in the 2D model, springs are attached at the bottom of the trough to simulate the longitudinal bending stiffness of the trough. In the horizontal direction, the trough is fixed. These constraints will result in a difference of deformation between the two models. An example is given below: the trough has a thickness of 8mm. The height of the trough is 350mm and the width of the bottom flange is 150mm. A single axle load of 50 kN with 408mm wide and 458mm long is applied on top of two troughs (see the figure below).

The maximum horizontal displacement in the finite element model occurs in the bottom flange of the trough web. This lateral displacement of the bottom flange of the trough is mainly caused by distortion. On the contrary, there is no horizontal displacement in the bottom flange in the simplified model. In other words, it can be concluded that there is no distortion in the simplified model. The deformations of the orthotropic deck models are presented in the following figures. The values are enlarged with a scaling factor of 200.

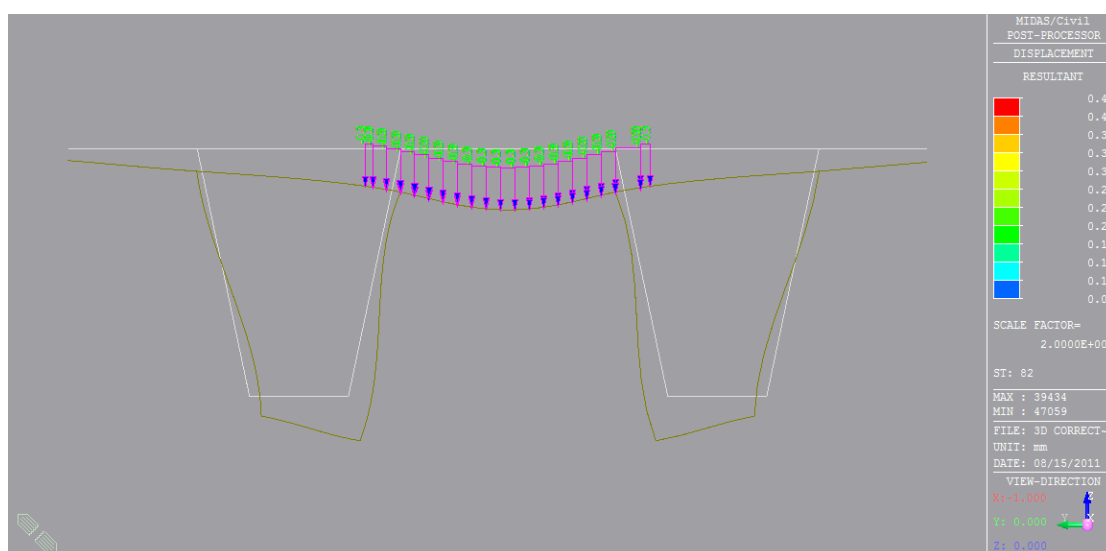


Figure 6.3 Deformation in the 3D model under in-between trough running wheel load

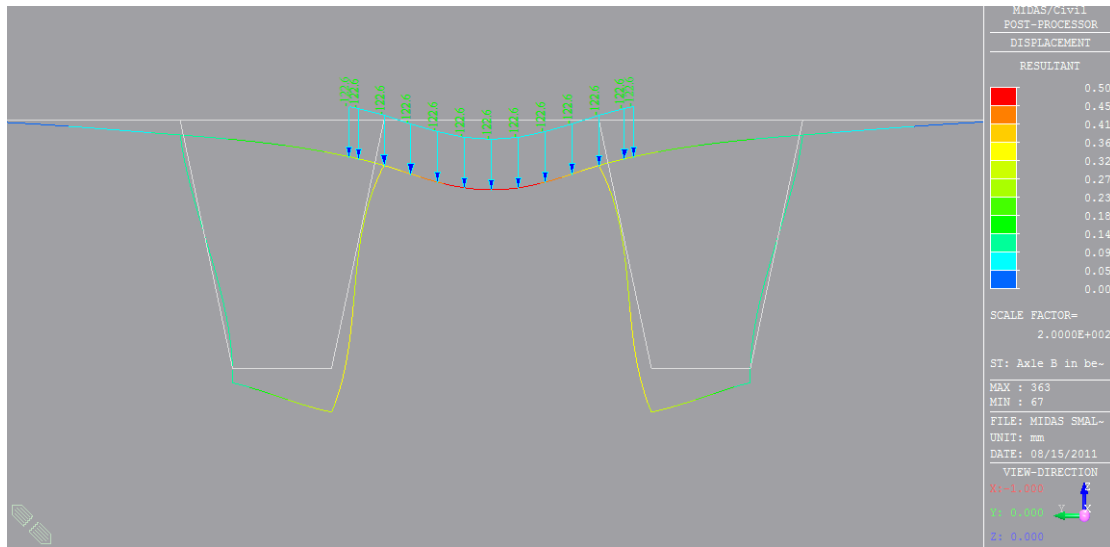


Figure 6.4 Deformation in the improved 2D model under in-between trough running wheel load

In figure 6.5, the horizontal deformation in the trough web is presented. The difference between these two models is clearly distinguished. There is no distortion in the 2D model. Therefore, the wheel load spreading over the deck plate is better and the deformation of the trough web is constraint. They lead to a smaller normal force and the bending moment in the trough web. In contrast to the simplified model, the distortion exists in the finite element model which makes the trough web deforms further towards the center of the wheel load. Hence the bending moment also increases in the trough web. In addition to this, the normal force is also increased. Because the more the orthotropic deck distorts, the worse the wheel load spreading is over the deck plate. In a word, the distortion and the distortion degree have an influence on the stress in the orthotropic deck.

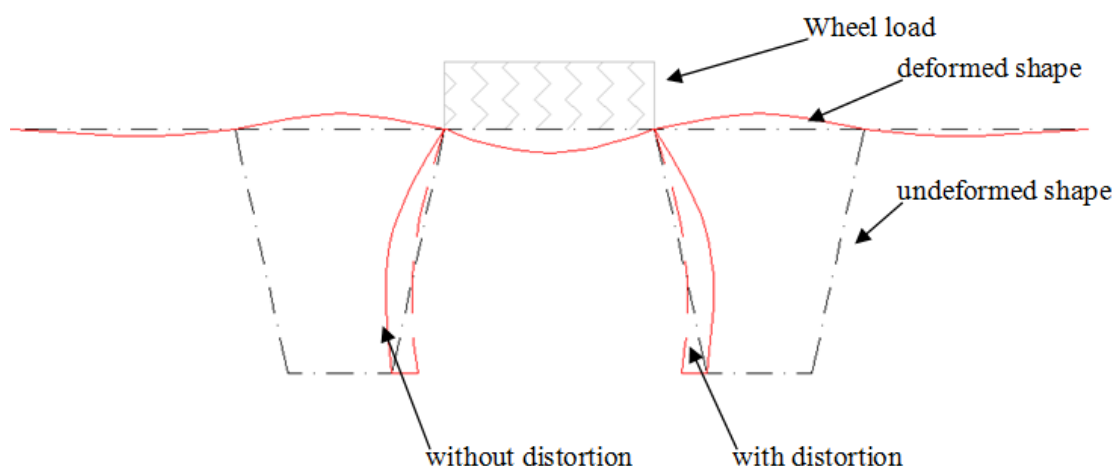


Figure 6.5 Horizontal deformation in the trough web.

6.1.3 Parameters

From the previous sections, it has been shown that the stress level also depends on the torsional properties of the trough in the orthotropic deck. And the difference between the two models is mainly due to the distortion. Thus, a parametric study is carried out here below.

The research carried out by Dr. Delesie ([15], [16], [17]) focuses on the effect of trough distortion of orthotropic bridge deck on load dispersal behavior and stress concentrations. In the research, the experimental and numerical results are both analyzed to find out the stress concentration in the orthotropic bridge deck induced by trough distortion. The results confirmed that a larger trough height results in lower distortion-related stresses in the trough web. Furthermore, the deformation in the mid-span is related to the shape of the trough. In general, the more triangular the trough is shaped, the less it distorts. The same conclusion can also be found in the work of Cullimore and Smith ([18]). In their research, a finite element analysis was performed on orthotropic steel deck models. One is with trapezoidal trough and the other one is with a triangular trough. The comparison results show that the bending moments in the web of the trough with trapezoidal trough are considerably greater than those in the triangular trough. In a word, the stress in the orthotropic deck with trapezoidal trough is larger than that of similar geometry with triangular trough. The increase of stress is caused by distortion which is more likely to happen in a trapezoidal trough.

A similar comparison is also made in this study in order to see the influence of the trough shape on the distortional deformation. Table 6.1 records the horizontal displacement of the trough bottom flange dy in four different models under the same wheel load axle C in-between troughs.

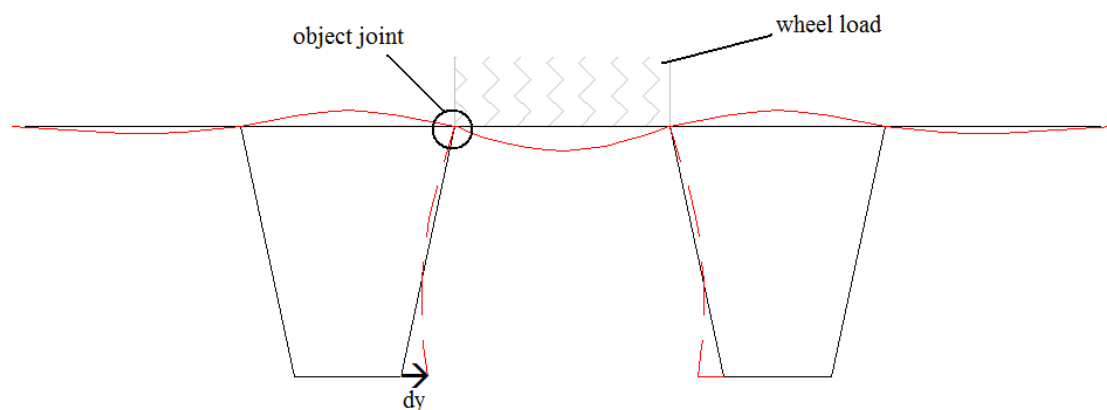


Figure 6.6 Horizontal displacement in the trough bottom flange dy

Orthotropic deck with asphalt	Displacement d_y	Orthotropic deck without asphalt	Displacement d_y
Model A($t_d=12;t_t=6;b_{bot}/h_t=0.32$)	0.05	Model C($t_d=12;t_t=6;b_{bot}/h_t=0.32$)	0.06
Model B($t_d=18;t_t=8;b_{bot}/h_t=0.43$)	0.09	Model D($t_d=22;t_t=8;b_{bot}/h_t=0.43$)	0.11
Model E($t_d=18;t_t=6;b_{bot}/h_t=0.43$)	0.25	Model F($t_d=18;t_t=6;b_{bot}/h_t=0.43$)	0.25

Table 6.1 Horizontal displacement in trough bottom flange (unit: mm)

The first and the third column of this table indicate the type of model and the geometry of the model. The first column collects the models with a 60mm thick asphalt layer on the deck plate. The models without asphalt layer are collected in the third column. t_d is the deck plate thickness. t_t is the trough web thickness. b_{bot} is the width of the bottom flange. h_t is height of the trough. Factor b_{bot}/h_t represents the shape of the trough. The smaller the factor is, the more triangular the trough is shaped.

It can be seen in the table that when the cross-sections of the orthotropic decks are the same, the displacements caused by the distortion in the model with and without asphalt layer are similar to each other. This means that the stress due to distortion in the deck is not much influenced by the dimension of the wearing surface.

Another factor is the thickness of the deck plate. These are model B and model D. Model B and model D have the same trough dimensions, as presented in the table above. But the deck plate thickness in model D is larger than that in model B. In such circumstance, Model D has a larger displacement, which indicates a larger stress in the trough web. Thus a conclusion can be made that the deck plate thickness is an importance factor in determining the magnitude of distortion and a thick deck plate has an increasing effect on the stresses in the troughs related to the distortions. But in general, related to bending in the orthotropic deck, a thicker deck plate gives lower stress in the trough.

Another comparison is made between model B and model E in order to study the influence of the trough web thickness on the distortion while the factor b_{bot}/h_t and the deck plate thickness are kept the same for the two models. The web in model B has a thickness of 8 mm, while this value is 6mm in model E. It is shown in the results that the displacement of model B is 0.09mm. This is much smaller than the displacement in model E. In other words, the distortional effects of the trough would be increased more with a thinner web.

Another factor is b_{bot}/h_t . It has also influence on the displacement in the trough bottom flange. Generally, when the factor is increased the displacement is increased.

Here above, the factors that may influence the fatigue life of a bridge are presented. With these factors, modifications to the 2D model can be made. This is dealt with below.

6.1.4 Empirical stress factor equation

As discussed above, the factors that may influence the fatigue behavior of the trough

consist of b_{bot}/h_t , the deck plate thickness and the trough web thickness. With these factors, an empirical equation can be found in order to relate the results of the 2D model to those of 3D model. This equation is able to provide appropriate adjustment factors which can be applied on the results of the 2D model. These adjustment factors can be used to correct the trough web results in 2D model for distortional effect. With this approach, the results of the 2D model would fit better the results of 3D model which are considered to be accurate. Attention should be paid that in most cases, the adjustment factors are larger than 1.0. This means that stresses are underestimated in the 2D model. However, this is not always the case. In some circumstances, the factors can be less than 1.0, which means that the stresses are overestimated. To find out the equation, a linear extrapolation is made here according to the table presented below.

The adjustment factors for the trough web are presented in the table below:

Orthotropic deck mdels	Bottom level				Top level			
	Interior trough web		Exterior trough web		Interior trough web		Exterior trough web	
	Axle B	Axle C						
Model A	1.14	1	1.14	1	0.76	0.8	0.64	0.7
Model B	1.1	1.1	1.1	1.1	1.1	1.1	1.1	1.1
Model E	1.25	1.25	1.35	1.35	1.37	1.37	1.35	1.35
Model C	1	1	1	1	0.75	0.8	0.7	0.7
Model D	1.15	1.13	1.2	1.2	1.12	1.17	1.12	1.13
Model F	1.2	1.15	1.3	1.35	1.37	1.37	1.35	1.33

Table 6.2 Adjustment factors in the trough web according to the numerical results

On the basis of the numerical results and the parametric analysis, an empirical equation for the adjustment factor in the trough web is determined as below:

$$\alpha = \frac{b_{bot}}{h_t} + 0.31 * \frac{t_d}{t_t} \geq 1$$

in which b_{bot} : width of the trough bottom flange

h_t : height of the trough

t_d : thickness of the deck plate

t_t : thickness of the trough web

The adjustment factor equation presented herein can be used for correcting the lack of distortion in the simplified model in case that the distortion has a negative effect on the fatigue resistance. This equation is an empirical equation. In order to verify this equation, comparison is made between the equation predicted factors and the listed factors (see table 6.3 and table 6.4).

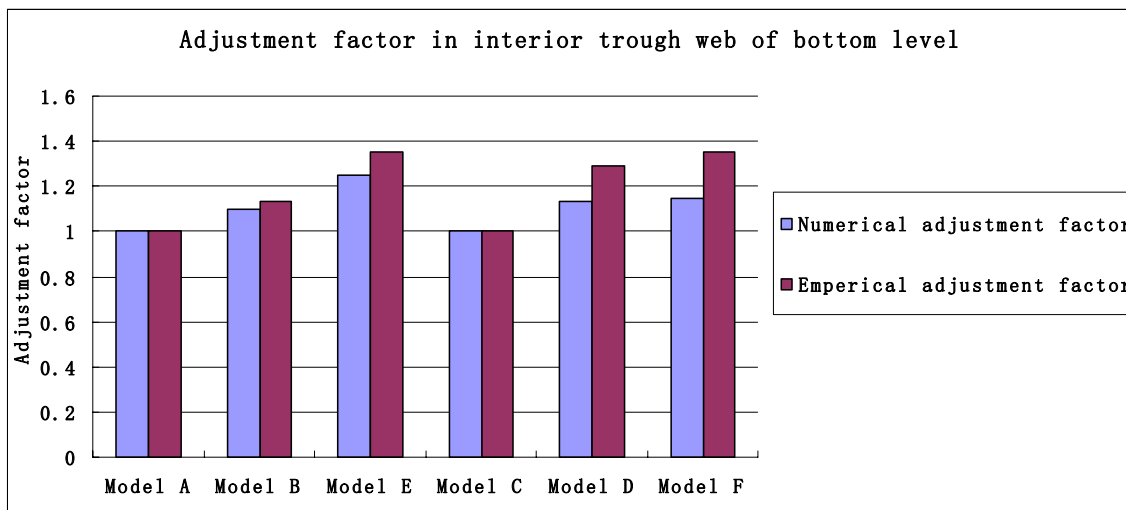


Table 6.3 Comparison between the numerical adjustment factor and the empirical adjustment factor in the interior trough web bottom level

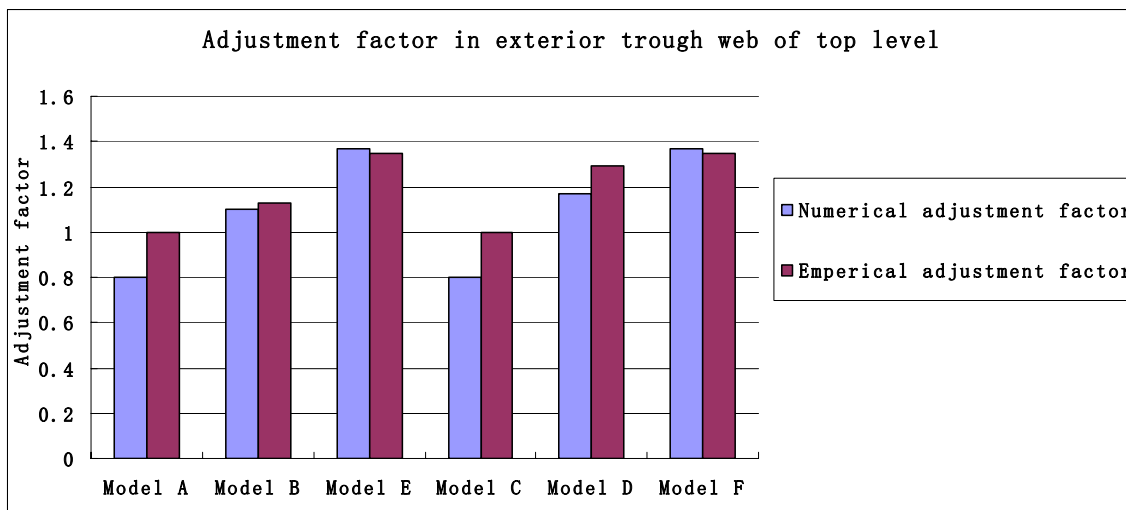


Table 6.4 Comparison between the numerical adjustment factor and the empirical adjustment factor in the exterior trough web top level

6.2 Adjustment factor for the deck plate results

Unlike the stress in the trough web, the stress in the deck plate is less sensitive to the distortion in the trough. Table 6.5 collects the adjustments factor for the deck plate results.

Orthotropic deck mdels	Bottom level				Top level			
	Interior deck plate		Exterior deck plate		Interior deck plate		Exterior deck plate	
	Axle B	Axle C						
Model A	1	1	1	1	0.78	0.45	0.97	0.56
Model B	0.9	0.9	0.9	0.9	0.75	0.63	0.9	0.67
Model E	0.9	0.8	0.9	0.85	0.73	0.71	0.82	0.7
Model C	0.9	0.9	0.9	0.9	0.67	0.62	0.84	0.7
Model D	0.75	0.9	0.85	0.95	0.81	0.82	0.86	0.84
Model F	0.8	0.9	0.85	0.95	0.78	0.83	0.82	0.81

Table 6.5 Adjustment factors in the deck plate according to the numerical results

The stresses in the deck plate of the 2D model are similar to or larger than the stresses found in the 3D model. In the bottom level, the influence lines derived from the results of these two models are almost identical. Therefore, an adjustment factor of 1.0 can be applied here. But on the stress in the top level, an adjustment factor of less than 1.0 should be applied. As the results got from the simplified model are considerably larger than those of the 3D model, a smaller factor is preferable in order for an economical design. Considering all the available data, 0.5 is an appropriate and conservative value in the deck plate of the top level.

6.3 Conclusion

- From this research, it shows that the distortion does exist in the trough under eccentric load. The distortion results in the increase of the transverse stress in the trough-to-deck plate joint. Comparison between different geometries of the trough shows that the distortion depends on the shape of the trough. For the distortional deformation at the mid-span, the more the trough triangular shaped, the less is the trough prone to distortional deformations.
- Compared to the results obtained from the trough web, the stress in the deck plate is less sensitive to the distortion in the trough.
- As a sum up, the adjustment factors for the results in the improved 2D model are shown in the following table:

<i>Trough-to-deck plate joint</i>	<i>Adjustment factor</i>	
	Bottom level	Top level
Trough web	$\alpha = \frac{b_{bot}}{h_t} + 0.31 * \frac{t_d}{t_t} \geq 1$	$\alpha = \frac{b_{bot}}{h_t} + 0.31 * \frac{t_d}{t_t} \geq 1$
Deck plate	1	0.5

Table 6.6 Adjustment factors on the simplified model

7 Verification of improved 2D model

In chapter 6, the improved 2D model results are compared with the results of the 3D model. Besides this, modification is applied on the 2D model in order to achieve a better simulation of the real stress.

In order to prove the accuracy of the improved simplified model, a fatigue assessment is carried out in this chapter. The fatigue assessment described in this chapter is to check whether the improved 2D model together with the adjustment factors can lead to accurate lifetime damage. According to the National Annex, only the fatigue load model 4 is applicable for the fatigue assessment of steel bridges. Therefore, as an example, the fatigue assessment in this chapter is carried out for orthotropic deck model B (large cross-section with asphalt layer) with fatigue load model 4 according to the NEN-EN 1993-2:NB. Fatigue load model 4 is the only applicable fatigue load model for the Dutch highway bridge defined in the NEN-EN 1993-2/NB.

7.1 Fatigue assessment procedure

With the help of the finite element program MIDAS Civil and the Excel Program the fatigue assessment in the trough to deck plate joint can be carried out. A complete overview of the relationship between these two programs and the aspects to be dealt with in the procedure are presented in the following table:

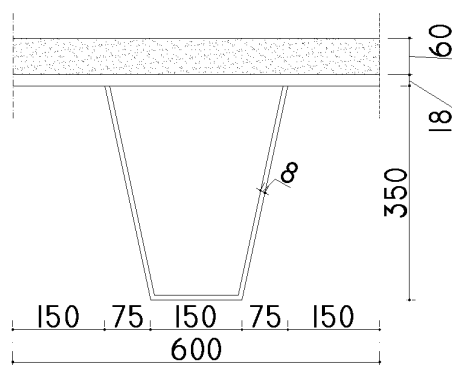
Procedure	Aspect	Method
Step 1: General	Input: Structural Geometries Output: 3D/2D models	<ul style="list-style-type: none"> • 3D model • Improved 2D model
Step 2: Loads	Input: <ul style="list-style-type: none"> • Axle loads • Wheel prints Output: Influence lines of single axle load	<ul style="list-style-type: none"> • 3D model • Improved 2D model
Step 3: Influence lines	Input: <ul style="list-style-type: none"> • Influence lines of single axle load • Axle load transverse distribution • Fatigue load model 4 long distance for highway bridges(2 million trucks a year for a 100 	<ul style="list-style-type: none"> • Excel Program

	years) • Adjustment factors Output: Stress histories	
Step 4: Fatigue damage assessment	Input: • Stress histories • Detail categories Output: Lifetime fatigue damage	• Reservoir method • Palmgren-Miner rule

Table 7.1 Fatigue assessment procedure

In step 1, the orthotropic deck can be modeled by defining the material property, structural component geometry and boundary condition in the 3D model in MIDAS Civil or in the 2D model in MIDAS Civil or in the Excel Program (the manual and the excel sheet of the 2D model in the Excel Program can be found in appendix D).

In order to verify the accuracy of the simplified model and the adjustment factor, a fatigue assessment is carried out for orthotropic deck model B (large cross-section with asphalt layer). The structure consists of the following components. For information regarding to how the model is constructed in MIDAS Civil and in the Excel Program, please refer to section 3 and section 4.



Structural component		Model B
Crossbeam	Height(H_C)	1250
	Length(L_C)	4200
	Distance(D_L)	3500
	Thickness(t_C)	12
Deck plate	Length(L_d)	21000
	Width(B_d)	4200
	Thickness(t_d)	18
Trough	Height(h_t)	350
	Width upper(b_{top})	300
	Width bottom(b_{bot})	150
	Thickness(t_t)	8
	Distance(d_t)	600
Asphalt	Thickness(t_a)	60

The unit of the dimension is mm

Table 7.2 Dimensions of orthotropic deck model B

Step 2 comprises defining the single wheel load and the wheel print on de deck plate according to NEN-EN 1991-2: 2003. The loads are applied on the models developed in

the two programs. The way of how to modeled load depends on the type of model (refer to section 4.4).

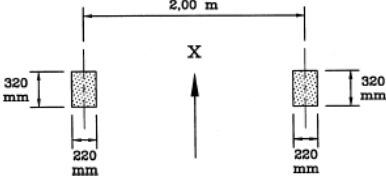
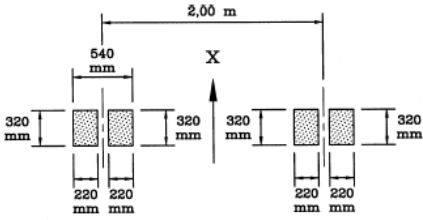
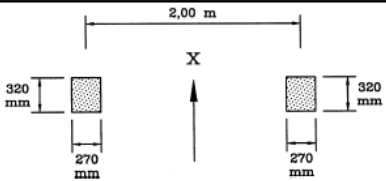
WHEEL/ AXLE TYPE	GEOMETRICAL DEFINITION
A	
B	
C	

Table 7.3 Definitions of wheels and axles

By running the post-processing of MIDAS Civil or the Excel Program, results are delivered in different aspects. The most important aspect for fatigue behavior is the stress influence line in the object point. Therefore the transverse and longitudinal influence lines due to the single axle load are picked out for further analysis.

In step 3, the influence line of single wheel load is transferred into the influence line due to a set of passing axle loads representing complete group of trucks. All the trucks used belong to the five standard trucks defined by the fatigue load model 4 in NEN-EN1991-2 + NB. One hundred trucks (fatigue load model 4 of NEN-EN1991-2 + NB) travel along the bridge one after another. The axle loads of trucks are spread in the transverse direction over the deck plate. The Eurocode defines the transverse distribution in 5 blocks each 100mm width with 7,18,50,18 and 7 percent (figure 7.1). In this assessment, the central line of the transverse Eurocode's wheel distribution (as shown in figure 7.1) can therefore be located at every transverse deck location in between $y=-400\text{mm}$ and $y=+400\text{mm}$. This means that the load pattern may cover the range from -650mm to $+650\text{mm}$. This step gives the stress history of the object joint.

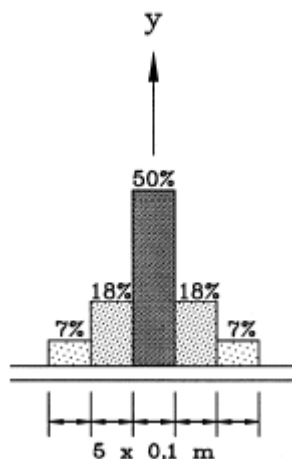


Figure 7.1 Transverse wheel distribution at tyre center

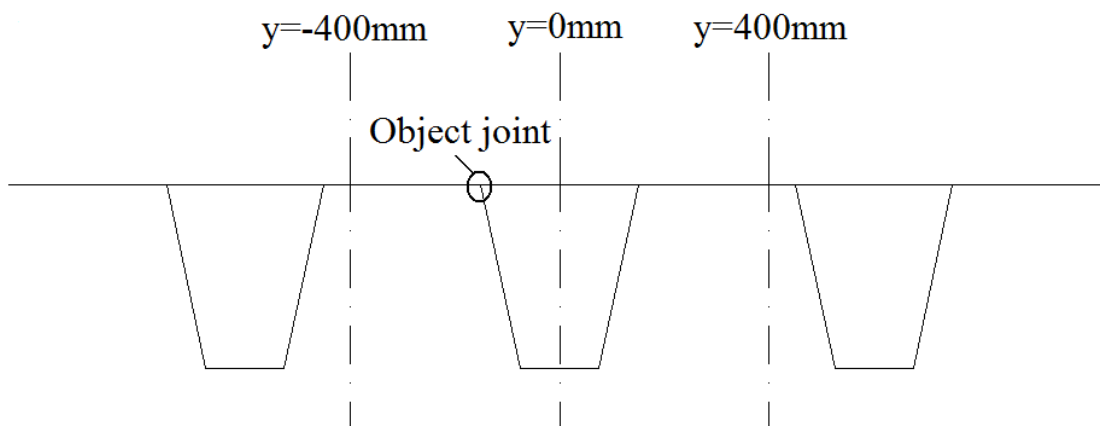


Figure 7.2 Axle load working area

Depending on the model used (the 2D model), stress adjustment factor should be applied. As what has been discussed in section 5.2, there is difference between the results of 3D model and the 2D model. For reference to the result got from the 3D model, the adjustment factor has to be applied on the result of the 2D model. According to the research carried out in chapter 6, the adjustment factor depends on several parameters. As a sum up, the adjustment factor is listed in table. For a more complete description of how to find out the adjustment factor, please refer to chapter 6.

<i>Trough-to-deck plate joint</i>	<i>Adjustment factor</i>	
	Bottom level	Top level
Trough web	$\alpha = \frac{b_{bot}}{h_t} + 0.31 * \frac{t_d}{t_t} \geq 1$	$\alpha = \frac{b_{bot}}{h_t} + 0.31 * \frac{t_d}{t_t} \geq 1$
Deck plate	1	0.5

Table 7.4 Adjustment factors on the 2D model

With the help of the Reservoir Method, the stress history is converted into stress ranges

spectrum in step 4 (for the simplicity, the stress spectra are presented in appendix E). The stress ranges spectrum, their number and the detail category are the input of Palmgren-Miner rule and result in the fatigue life of the object joint. For explanation of the Reservoir Method and the Palmgren-Miner rule, please refer to section 1.7.

7.2 Comparison of the lifetime fatigue

The lifetime fatigue damage is calculated for the interior and exterior surface of the trough web and the bottom surface of the interior and exterior deck plate at the trough-to-deck plate joint, show in figure 7.3. The result obtained by the simplified 2D model with adjustment factor is compared to the result of the 3D model. The detail classifications are taken from NEN-EN 1993-2 for new bridges (classification 100 is for automatic weld (MDF=1); classification 90 is for the hand welded welds (MDF=1)). In addition, a fillet weld with classification 50 is checked. (Please refer to section 2.6 for information of the detail category).

The first series of comparison is done for the interior surface of the trough web indicated with a in figure 7.3.

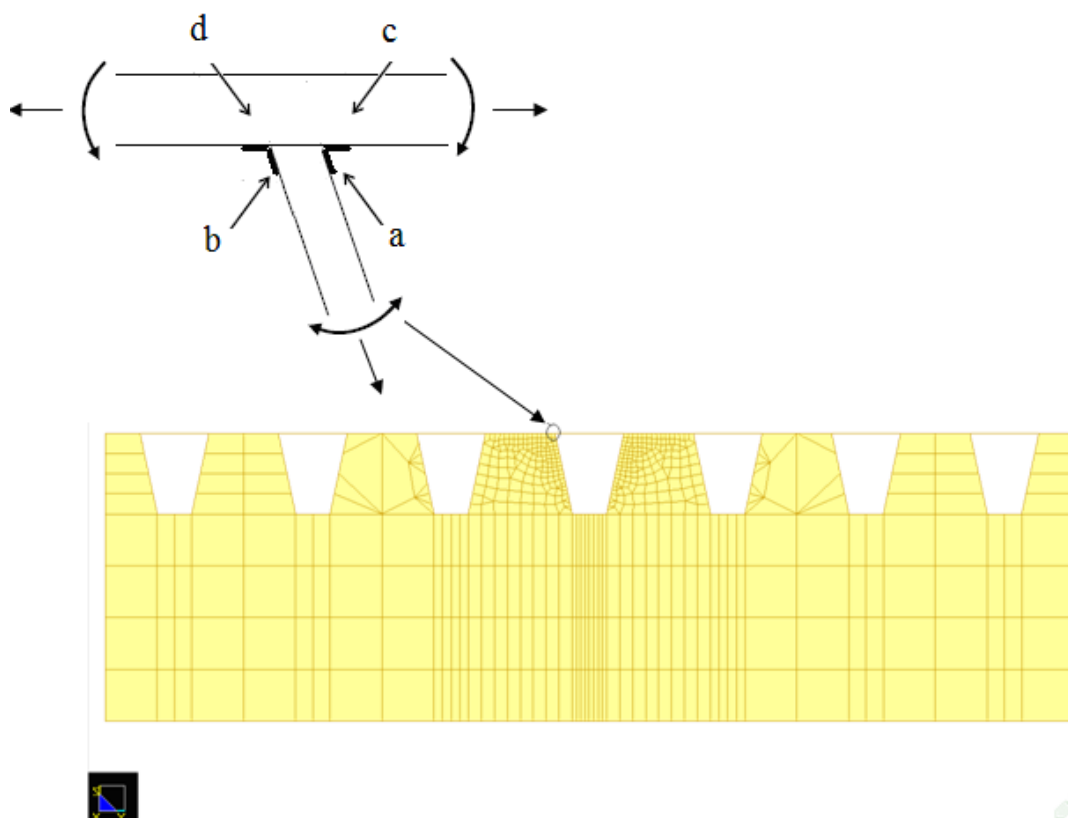


Figure 7.3 Object joint at the cross-section of the orthotropic deck at halfway of the trough span

The comparison of the fatigue damage in the interior surface of the trough web is shown in table 7.5. Generally, figure 7.4, figure 7.5 and figure 7.6 show good agreement between the results of the simplified 2D model and those of the 3D model. Furthermore,

the fatigue damage calculated from simplified 2D model keeps conservative as expected.

Lifetime damage interior trough web		Central load location [mm]																
		-400	-350	-300	-250	-200	-150	-100	-50	0	50	100	150	200	250	300	350	400
Category 100	Finite element model	0.00	0.00	0.00	0.00	0.07	0.12	0.11	0.06	0.02	0.00	0.00	0.00	0.00	0.00	0.00	0.00	
	Simplified model	0.00	0.00	0.00	0.02	0.09	0.18	0.13	0.07	0.03	0.00	0.00	0.00	0.00	0.00	0.00	0.00	
Category 90	Finite element model	0.00	0.00	0.00	0.05	0.12	0.23	0.22	0.13	0.07	0.04	0.00	0.00	0.00	0.00	0.00		
	Simplified model	0.00	0.00	0.00	0.07	0.16	0.31	0.27	0.14	0.08	0.04	0.00	0.00	0.00	0.00	0.00		
Category 50	Finite element model	0.21	0.41	0.75	1.28	1.91	3.63	4.03	3.28	3.48	2.77	4.55	5.04	4.14	2.93	1.60	0.77	0.41
	Simplified model	0.42	0.56	1.14	1.50	2.30	4.20	4.38	3.41	3.71	2.97	5.13	5.54	5.18	3.37	2.27	0.90	0.64

Table 7.5 Fatigue damage comparison in interior trough web

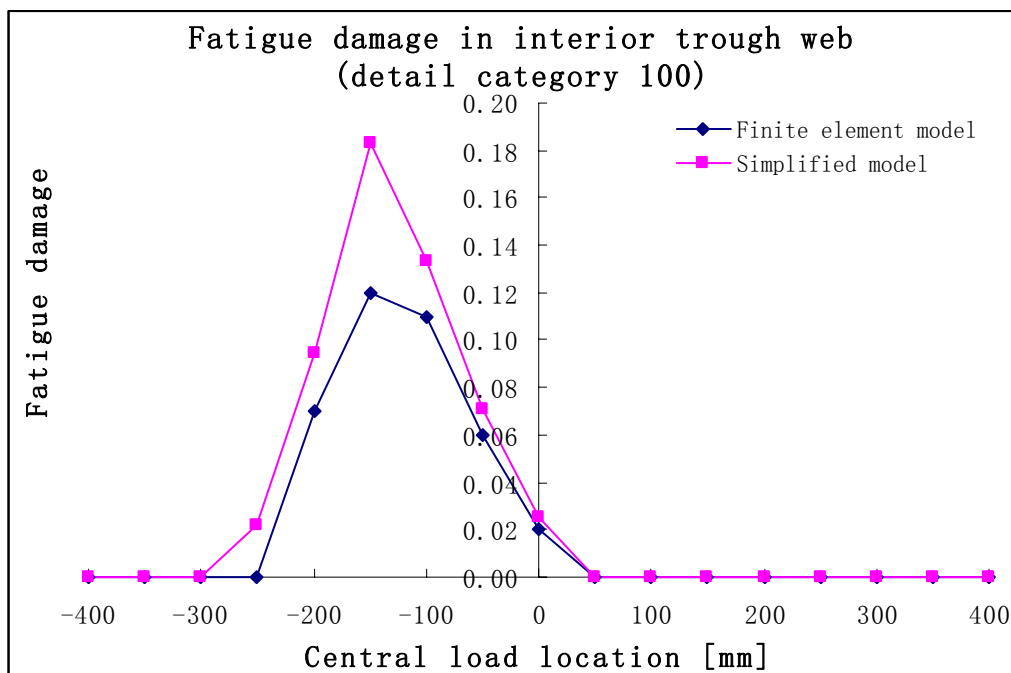


Figure 7.4 Lifetime damage in interior trough web in highway bridge dimensions with asphalt layer; automatic welding with MDF=1

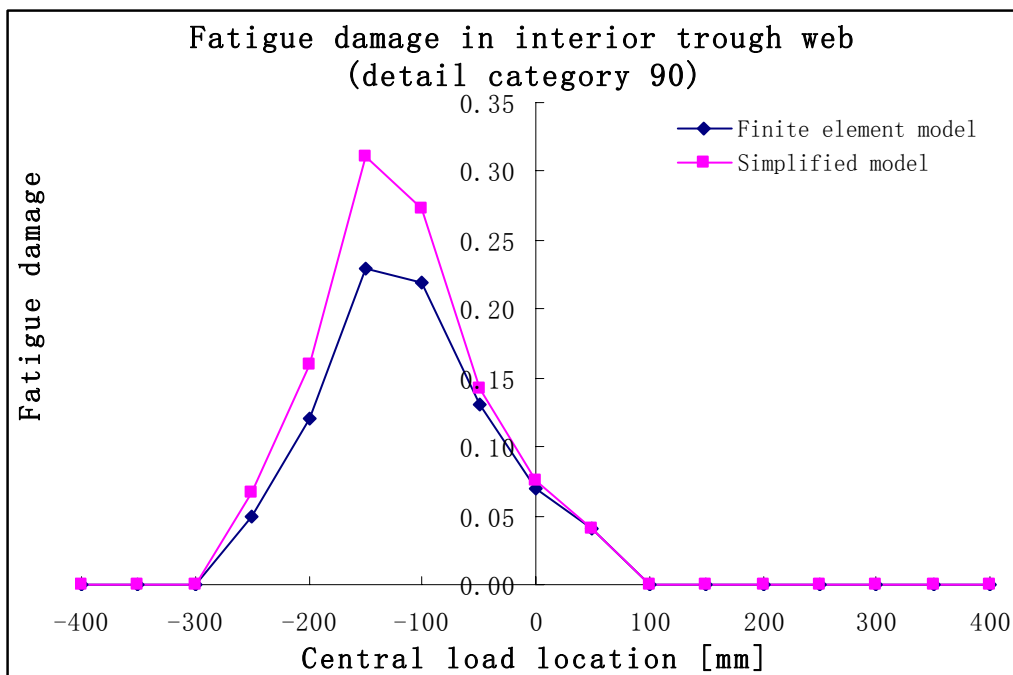


Figure 7.5 Lifetime damage in interior trough web in highway bridge dimensions with asphalt layer; hand welded with MDF=1

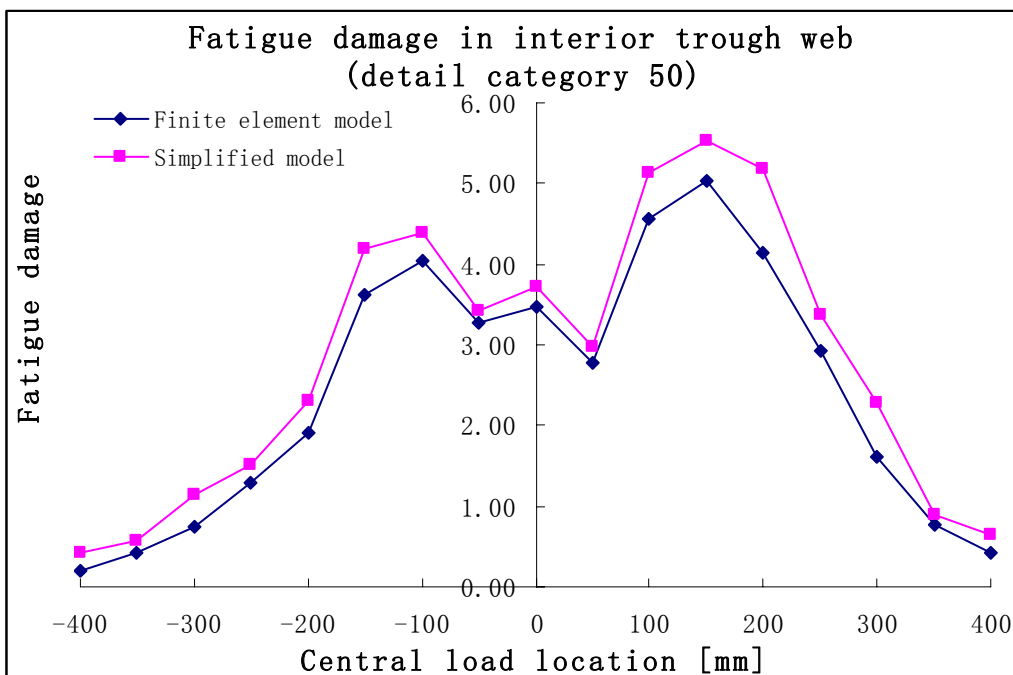


Figure 7.6 Lifetime damage in interior trough web in highway bridge dimensions with asphalt layer ; fillet weld

Table 7.5 records the fatigue damage in the interior trough web calculated by the finite element model and by the simplified model. In general, the fatigue damage is grouped by the detail category. It can be noted from the table that detail category 100 has the smallest fatigue damage in the interior trough. When the detail category decreases, the

fatigue damage increases. Further, the fatigue damage calculated by the simplified model after adjustment is similar to the fatigue damage in the finite element model. It can also be observed from figure 7.4, figure 7.5 and figure 7.6. The fatigue damage curves fit each other well in different detail categories. As shown in figure 7.4 and figure 7.5, the maximum damage occurs when the central line of the wheel load is running above the object trough web ($y=-150\text{mm}$). But there is no fatigue damage in the interior trough when the center of the wheel load is far from the object joint. However, it is not the case for the fatigue damage of detail category 50. The shape of the fatigue damage in this detail category is different from the other two categories. Here, the maximum fatigue damage is generated by the wheel load central above $y=150\text{mm}$. Furthermore, the fatigue damage is observed in a larger range (from $y=-400\text{mm}$ to $y=400\text{mm}$). This has to do with the design S-N curves and also the detail category. When a lower detail category is applied in the structure, smaller stress ranges have to be taken into account for the fatigue damage calculation as they may cause severe damage as well. That is also why the trough-to-deck plate joint with a lower detail category has larger fatigue damage in it. It should be marked that detail category 50 is not often used in the modern design due to its low fatigue resistance. Thus it is avoided whenever possible.

In addition, the fatigue damage curve is presented together with the transverse influence line. This is to show the relationship between these two most importance aspects in the fatigue calculation. In figure 7.7, the fatigue damage curve of detail category 100 and the transverse influence line under axle C are presented.

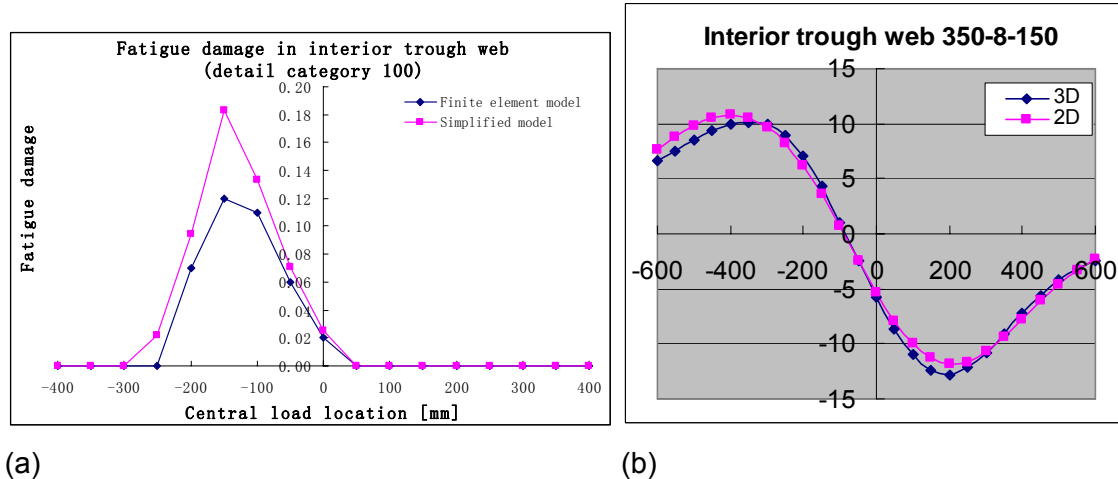


Figure 7.7 (a) Fatigue damage in the interior trough web (detail category 100); (b) Transverse influence line in the interior trough web

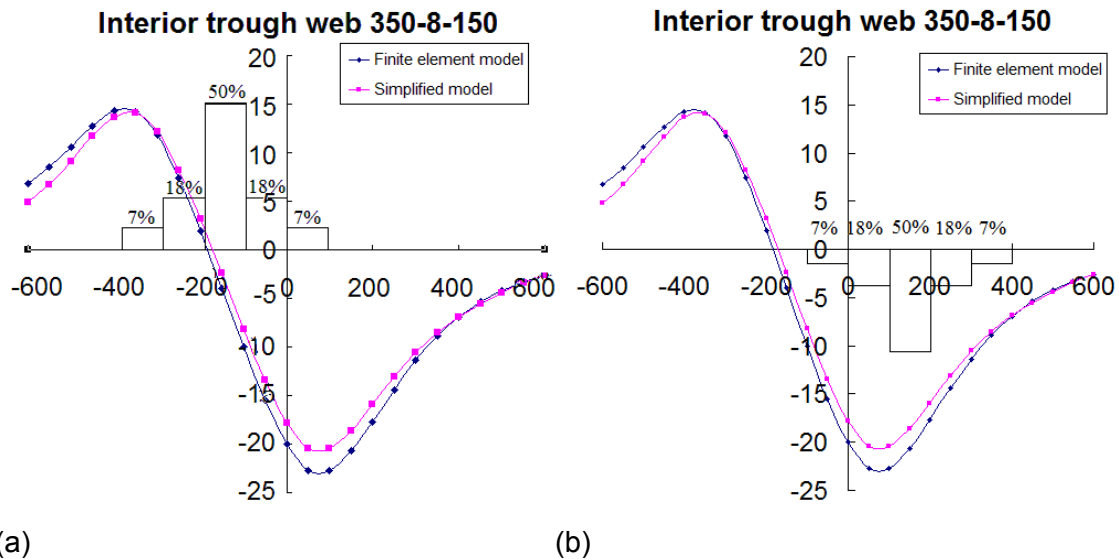


Figure 7.8 Transverse influence line with wheel load distribution (a) Central line of the wheel load distribution at $y=-100\text{mm}$; (b) Central line of the wheel load distribution at $y=150\text{mm}$

As shown in the figure, there is contrast between these two curves. Where the stress is maximal, the fatigue damage is zero. However the stress at $y=-150\text{mm}$ is small, the fatigue damage is the largest among all the load cases. This phenomenon can be explained with the help of the frequency distribution of transverse location of central line of vehicle considering the fatigue damage is largely dependent on the stress variation but not the absolute stress level. This distribution is added in the transverse influence line. As shown in figure 7.8 (a), one may see that the variation of the stress within the area of the distribution is large, and the region of the wheel load distribution covers from the minimum (negative) stress to the maximum (positive) stress. When the center line of the trucks is at $y=150\text{mm}$ where the influence line reaches its extreme value, the distribution of the wheel is presented figure 7.8 (b). It is for sure that the magnitude of the stress is big in this region, but the stress range is smaller than the previous situation. By translating the stress under single axle load into the stress history produced by one hundred trucks, the difference becomes more obvious (figure 7.9 and figure 7.10). The stress history under center line of trucks at $y=150\text{mm}$ is dense. Because that there is seldom distinct change in the stress. On the other hand, the stress history under center line of trucks at $y=-150\text{mm}$ gives a significant fluctuation of stress in the interior trough web. As a result, it has larger stress ranges which are taken into account for the fatigue damage calculation. The same conclusion can also be drawn by comparing the stress spectra. For the simplicity, the stress spectra are presented in appendix E.

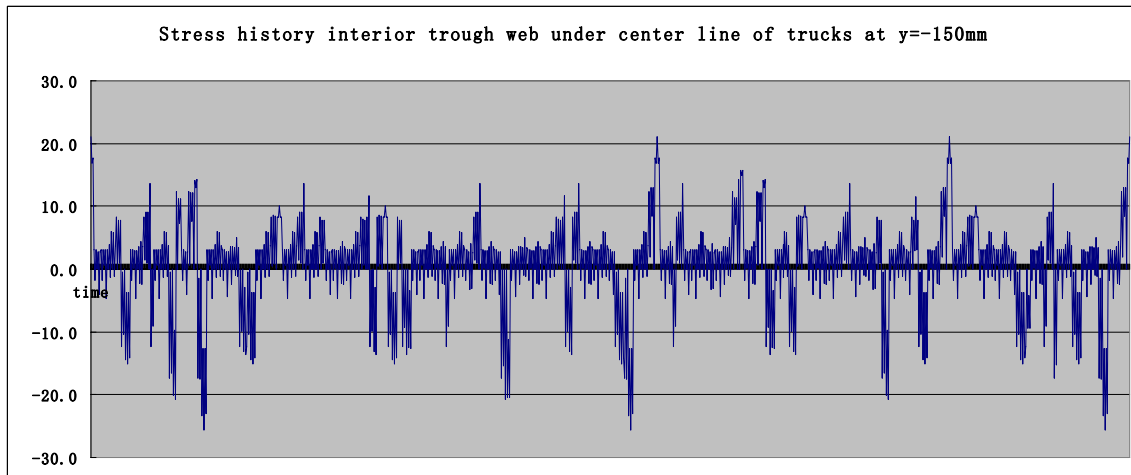


Figure 7.9 Stress history in the interior trough web under center line of trucks at $y=-150\text{mm}$

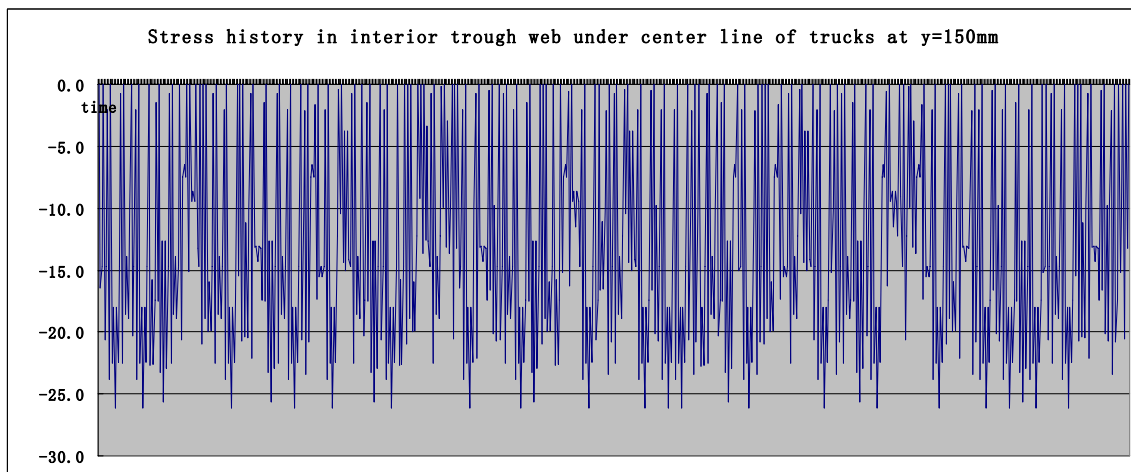


Figure 7.10 Stress history in the interior trough web under center line of trucks at $y=150\text{mm}$

In addition, one more conclusion can be given from the stress history (figure 7.9 and figure 7.10). These two figures record the stress influence lines in the object location due to one hundred trucks passing over the orthotropic deck. It means that the shape of the stress influence line is determined not only by the axle load, but also by the arrangement of the trucks. Fatigue model 4 in the Eurocode defines the type of trucks and the percentage of each type in the traffic flow. There is no specific definition of the arrangement of the trucks.

The fatigue damage calculation is also done for the exterior trough web. The fatigue damage in this detail is listed in table 7.6. Based on these data, figures are also drawn.

Lifetime damage exterior trough web		Central load location [mm]															
		-400	-350	-300	-250	-200	-150	-100	-50	0	50	100	150	200	250	300	350
Category 100	Finite element model	0.00	0.00	0.00	0.00	0.09	0.10	0.19	0.13	0.06	0.05	0.00	0.00	0.00	0.00	0.00	0.00
	Simplified model	0.00	0.00	0.00	0.00	0.10	0.11	0.14	0.10	0.04	0.00	0.00	0.00	0.00	0.00	0.00	0.00
Category 90	Finite element model	0.00	0.00	0.00	0.08	0.16	0.23	0.36	0.22	0.09	0.09	0.00	0.00	0.00	0.00	0.00	0.00
	Simplified model	0.00	0.00	0.00	0.09	0.16	0.21	0.24	0.16	0.11	0.05	0.00	0.00	0.00	0.00	0.00	0.00
Category 50	Finite element model	8.09	8.38	6.30	5.77	4.41	3.85	5.27	3.22	1.57	1.91	1.86	0.80	0.53	0.80	0.25	0.23
	Simplified model	9.79	9.87	7.94	5.70	4.20	3.46	3.28	2.64	1.97	2.01	1.23	0.58	0.60	0.38	0.63	0.24

Table 7.6 Fatigue damage comparison in exterior trough web

From table 7.6, it can be observed that the fatigue damages calculated by these two kinds of models are close to each other. Only at a few locations, the damages in the simplified model are smaller than those in the finite element model. The data in the table are translated into curves in figure 7.11, figure 7.12 and figure 7.13. The blue curve indicates the fatigue damage in the finite element model. The pink one indicates the fatigue damage in the simplified model.

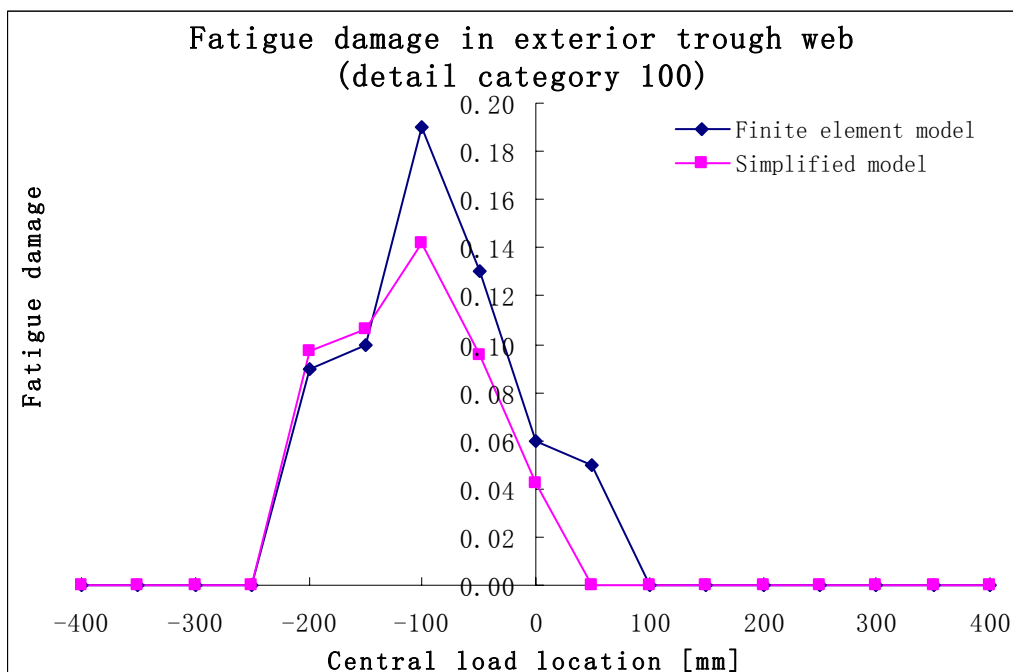


Figure 7.11 Lifetime damage in exterior trough web in highway bridge dimensions with asphalt layer; automatic welding with MDF=1

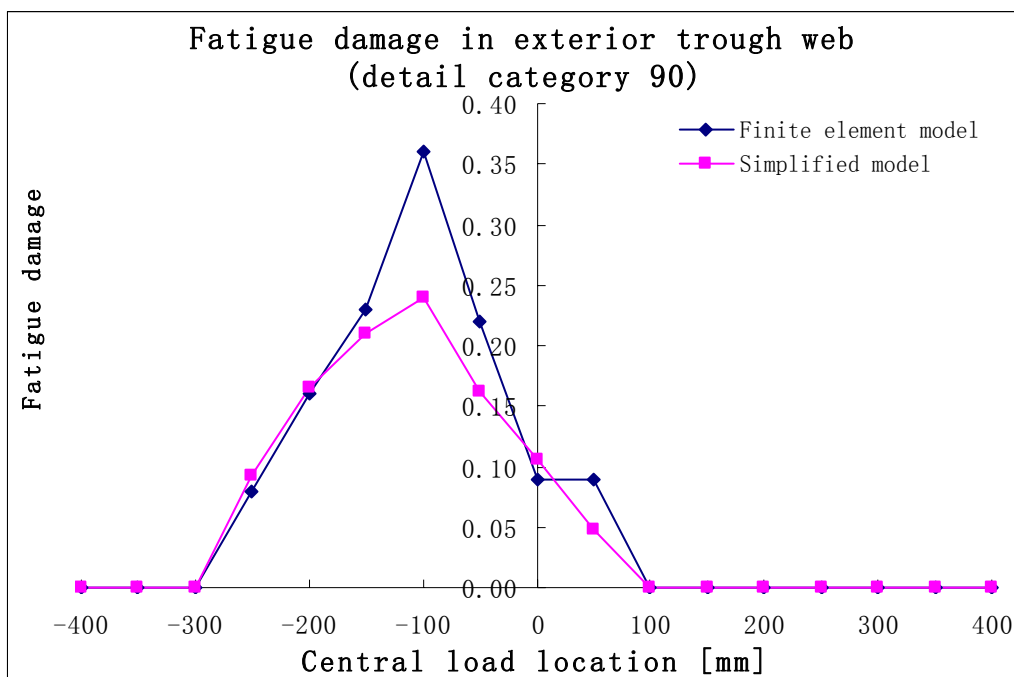


Figure 7.12 Lifetime damage in exterior trough web in highway bridge dimensions with asphalt layer; hand welded with MDF=1

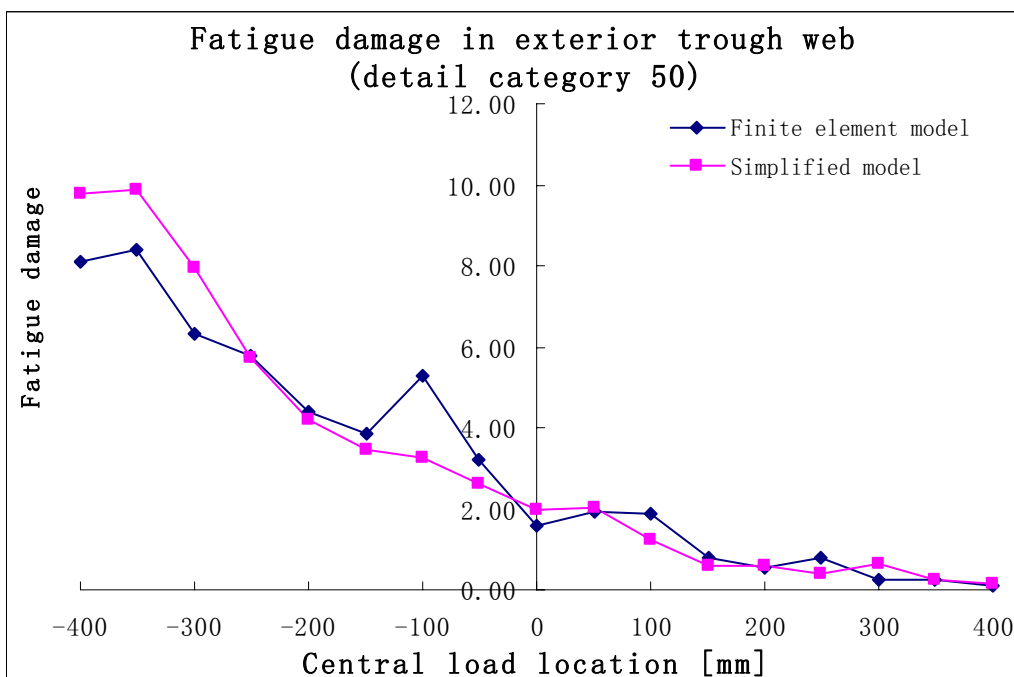


Figure 7.13 Lifetime damage in exterior trough web in highway bridge dimensions with asphalt layer ; fillet weld

These figures show a satisfied similarity in the shape between these two kinds of curves. For detail category 100 and 90, the maximum fatigue damage occurs when the wheel load is above $y=-100\text{mm}$. When the center of the wheel load moves further away from $y=-100\text{mm}$, the fatigue damage decreases. As expected, the lower the detail category of

the trough-to-deck plate joint belongs to, the larger the area is under the fatigue damage curve in the figure. That is because, by decreasing the detail category, smaller stress ranges should be taken into account for the fatigue damage calculation as well. In general, this fatigue assessment in the exterior trough web shows a good fit between these two kinds of models.

Besides the fatigue assessment in the trough web, the fatigue damage calculation is also done according to the stress in the deck plate of the object joint.

lifetime damage exterior deck	Central load location [mm]																
	-400	-350	-300	-250	-200	-150	-100	-50	0	50	100	150	200	250	300	350	400
Finite element model	0.00	0.00	0.00	0.00	0.00	0.00	0.00	0.00	0.00	0.00	0.00	0.00	0.00	0.00	0.00	0.00	0.00
Simplified model	0.00	0.00	0.00	0.00	0.00	0.00	0.00	0.00	0.00	0.00	0.00	0.00	0.00	0.00	0.00	0.00	0.00

Detail category 125

Table 7.7 Fatigue damage comparison in exterior deck plate

lifetime damage interior deck	Central load location [mm]																
	-400	-350	-300	-250	-200	-150	-100	-50	0	50	100	150	200	250	300	350	400
Finite element model	0.00	0.00	0.00	0.00	0.00	0.00	0.00	0.00	0.00	0.00	0.00	0.00	0.00	0.00	0.00	0.00	0.00
Simplified model	0.00	0.00	0.00	0.00	0.00	0.00	0.00	0.00	0.00	0.00	0.00	0.00	0.00	0.00	0.00	0.00	0.00

Detail category 125

Table 7.8 Fatigue damage comparison in interior deck plate

The results got from the bottom surface of the exterior and interior deck plate show a satisfied agreement between both models. It is because the influence lines in the deck plate are similar between these two models, as previously discussed. The most interesting phenomenon is that no fatigue damage in the bottom surface of the deck plate during its lifetime is found. This has to do with the high detail category of the welding at this joint. Besides, the stress ranges amplitude in the deck plate play also an important role in the fatigue life of the structure. Therefore, the fatigue damage in the trough web is decisive for the trough-to-deck plate joint. As the fatigue damage in the exterior trough web is larger than the interior trough web, the first crack may initiate in the weld toe in the trough.

7.3 Conclusions

By carrying out the fatigue assessment and performing the comparison between the fatigue damage calculated by the finite element model and the adjusted simplified model, the following conclusions can be drawn.

- Using the Eurocodes + NA (National Annex) fatigue load model 4 long distance for highway bridges (2 million trucks a year for a 100 year) and the transverse spreading of the trucks according to the Eurocode, lifetime fatigue damage calculations are made for both the deck plate crack and the longitudinal weld crack. Fatigue calculations were made for an orthotropic deck with troughs of 350mm height and 8mm thick and an 18mm thick deck plate with asphalt layer for fixed bridge. It shows no damage in the deck plate (classification 125) and a damage smaller than 1 in the

longitudinal weld between the deck plate and the trough (classification 100 or 90).

- The maximum stress in the interior trough web is caused by the wheel load around $y=100\text{mm}$; the maximum stress in the exterior trough web is caused by the wheel load around $y=-300\text{mm}$. But these wheel load locations are not necessary to be the locations of the maximum fatigue damage in the trough web. The choice of the transverse location of the central line along which the wheels pass the bridge and the transverse spreading around the line has large influence on the fatigue damage.
- The fatigue assessment results of model B show that a lower detail category of the trough-to-deck plate joint can reduce the fatigue life of the orthotropic steel deck. Due to the higher stress ranges and lower detail category in the trough web, the first crack in the trough-to-deck plate joint may initiate in the weld toe in the trough web.
- This chapter is mainly used for the verification of the adjusted 2D model. It proves that the simplified model can lead to an accurate result in the fatigue assessment. Furthermore, the simplified model is user-friendly. It can save lots of time not only on the pre-processing but also on the post-processing. In addition, it takes less computing time and does not require much storage space as the 3D model.

8 Application of the improved 2D model

In chapter 7, the improved 2D model has been verified by doing the fatigue assessment on model B. By comparing the results obtained from the improved 2D model with the results from 3D model, it shows that the improved 2D model has a satisfied accuracy in finding out the influence line and calculating the lifetime fatigue damage in the object joint.

In addition, an application of the improved 2D model is carried out in this chapter. Based on the results obtained from the assessment, recommendations would be given on the design of the orthotropic deck with respect to the trough-to-deck plate joint in-between the crossbeams.

8.1 General

This application is performed on orthotropic deck model D. This kind of orthotropic steel deck is usually applied on movable bridge in which the troughs do not pass the crossbeam but welded in between the crossbeams.

In order to keep the self weight of the orthotropic steel deck low, a thinner epoxy layer of 8 mm is applied on the deck plate in stead of the asphalt layer. The deck plate thickness is 22mm and the trough web thickness is 8mm. Furthermore, the shape of the trough is kept the same as in the fixed bridge. The table on the right hand side of the cross-section drawing collects the general dimensions of model D.

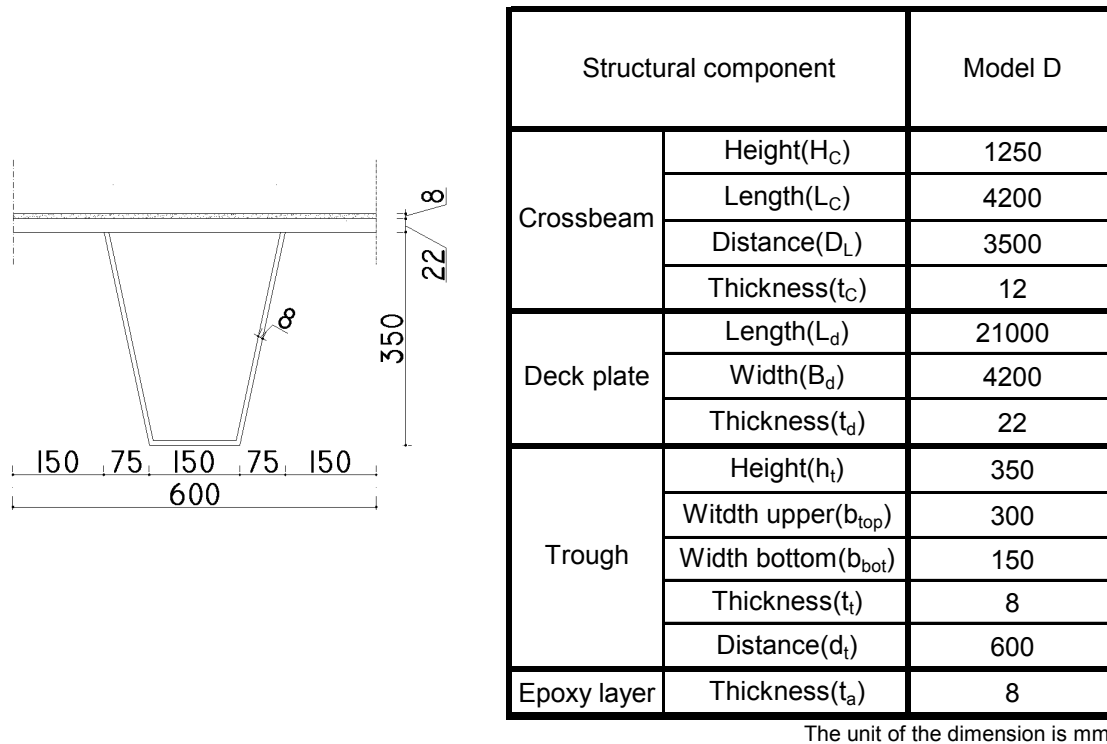


Figure 8.1 Cross-section of trough with deck plate in model D (left); Dimensions of model D (right)

The traffic loads on model D are also derived from NEN-EN 1991-2:2003. Applying the loads on the deck plate should take the spreading of the epoxy layer into account. As a sum up, the wheel load print on the deck plate and the uniformly distributed wheel load are presented in table 8.1.

Model	Wheel load area $b \cdot h$ [mm^2]		
	Axle A	Axle B	Axle C
Model D	258*358	578*358	308*358

Model	Wheel load [N/mm^2]		
	Axle A	Axle B	Axle C
Model D	0.541	0.242	0.453

Table 8.1 Wheel load print on model D (left); uniformly distributed wheel load on model D (right)

The fatigue loads are derived from fatigue load model 4 defined in NEN-EN 1991-2:2003 and National Annex. For detail information of the assessment procedure based on fatigue load model 4, please refer to section 7.1.

8.2 Results

In this section, the lifetime fatigue damage in the object joint is only based on the influence lines and the stress spectra (see appendix E) generated by the improved 2D model. The detail classifications are taken from NEN-EN 1993-2 which can also be found in section 2.6 and section 7.2.

The first series of result obtained from the fatigue assessment is the lifetime fatigue

damage in the interior surface of the trough web.

Lifetime damage interior trough web	Central load location [mm]																
	-400	-350	-300	-250	-200	-150	-100	-50	0	50	100	150	200	250	300	350	400
Category 100	0.00	0.00	0.00	0.06	0.18	0.21	0.22	0.10	0.06	0.00	0.00	0.00	0.00	0.00	0.00	0.00	0.00
Category 90	0.00	0.00	0.00	0.10	0.31	0.41	0.42	0.30	0.10	0.06	0.00	0.00	0.00	0.00	0.00	0.00	0.00
Category 50	0.70	0.76	1.40	2.26	5.17	6.11	6.67	5.89	5.57	6.02	6.74	9.08	7.32	4.93	3.18	1.64	0.82

lifetime fatigue damage in one hundred years

Table 8.2 Lifetime fatigue damage during one hundred years in the interior surface of the trough web in model D

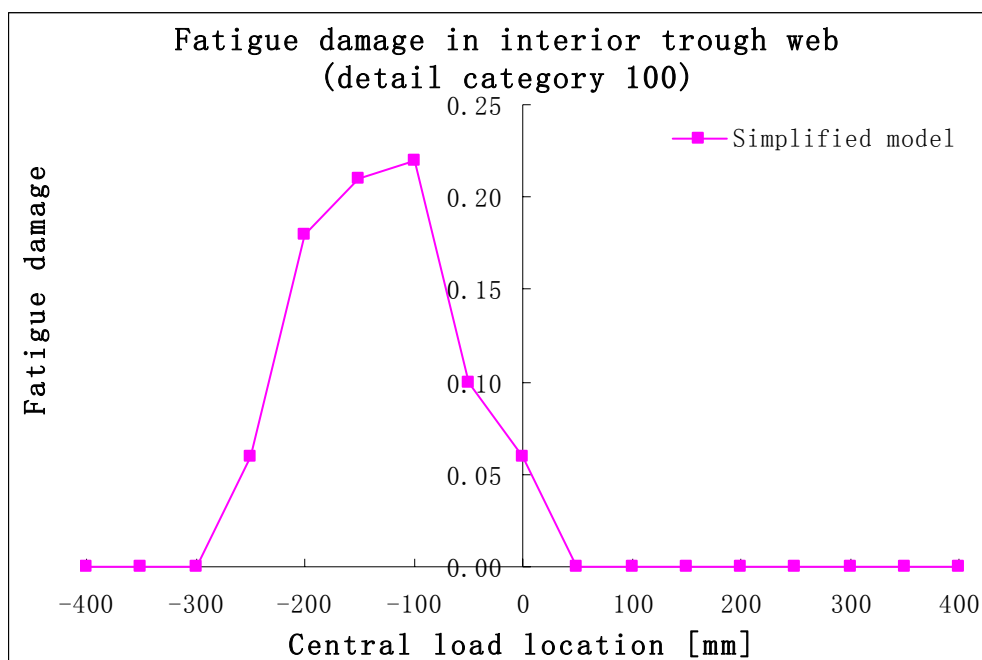


Figure 8.2 Lifetime damage during one hundred years in the interior surface of the trough web in model D; automatic welding with MDF=1

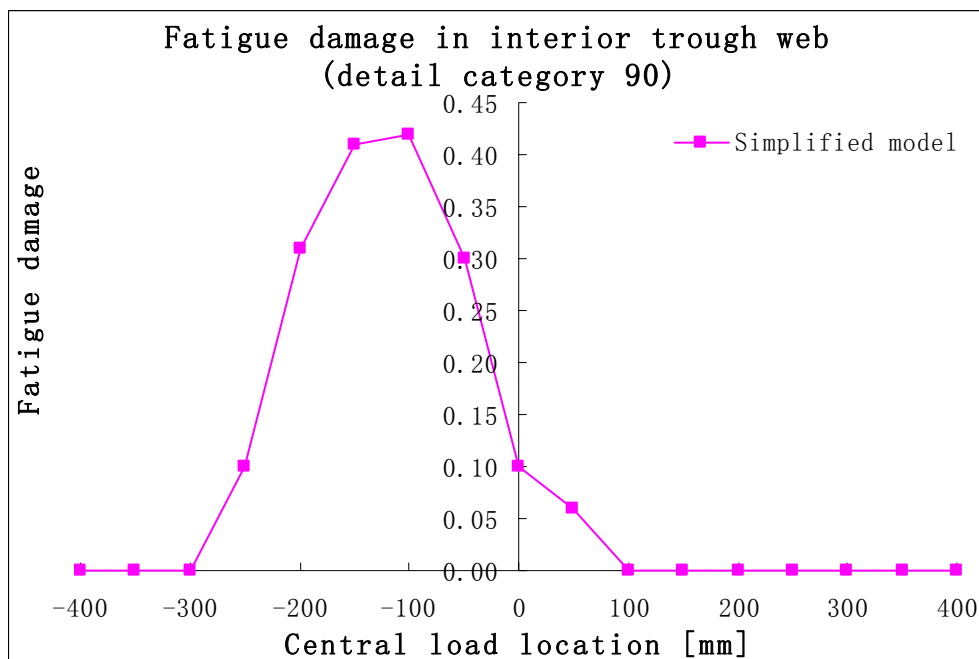


Figure 8.3 Lifetime damage during one hundred years in the interior surface of the trough web in model D; hand welded with MDF=1

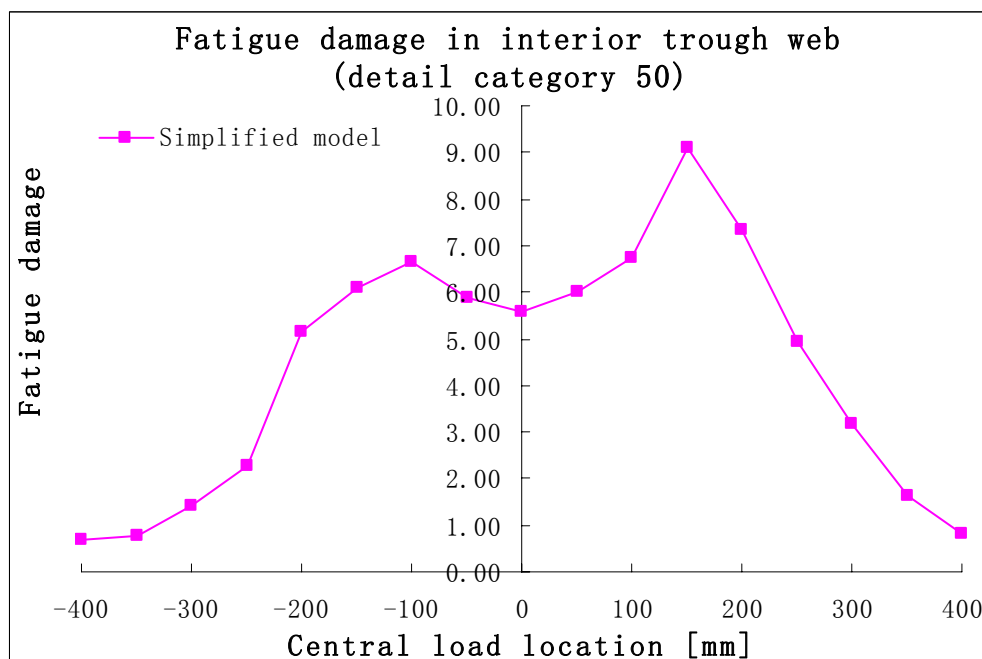


Figure 8.4 Lifetime damage during one hundred years in the interior surface of the trough web in model D; fillet weld

The lifetime fatigue damages for different detail categories under the same fatigue load model show that the decrease of the detail category in the trough-to-deck plate joint can lead to larger fatigue damage in the interior surface of the trough web. Looking at the shape of the fatigue damage curves in detail category 100 and 90, it can be observed

that they are very similar to each other. When the central line of the transverse distribution of wheel load is on the left hand side of $y=-300\text{mm}$, no fatigue damage happens under these two detail categories. By moving the central line of the wheel load towards $y=-100\text{mm}$, the damages increase and reach the peak values at $y=-100\text{mm}$. As mentioned in the verification of the 2D model, the maximum damage caused here is due to the large stress range under central line at $y=-100\text{mm}$. After $y=-100\text{mm}$, the damage curves decrease when the central line of the wheel load moves away. The fatigue damage curve under detail category 50 is different from the other two. It has two peaks in the curve. The first one is at $y=-100\text{mm}$ and the second one is at $y=150\text{mm}$ which is also the maximum damage. This kind of phenomena has also come up in section 7.2. The same explanation can be applied here.

The lifetime fatigue damages in the exterior surface of the trough web are also presented here in the same way. The fatigue damage in this detail is listed in table 8.3. Based on these data, figures are also drawn (figure 8.5, figure 8.6 and figure 8.7).

Lifetime damage exterior trough web	Central load location [mm]																
	-400	-350	-300	-250	-200	-150	-100	-50	0	50	100	150	200	250	300	350	400
Category 100	0.00	0.00	0.00	0.07	0.18	0.17	0.21	0.16	0.10	0.06	0.00	0.00	0.00	0.00	0.00	0.00	0.00
Category 90	0.12	0.39	0.44	0.12	0.30	0.34	0.38	0.33	0.20	0.10	0.06	0.00	0.00	0.00	0.00	0.00	0.00
Category 50	19.17	20.05	18.05	13.60	9.16	6.23	5.43	4.41	3.20	2.94	1.71	0.86	0.59	0.95	0.78	0.30	0.26

lifetime fatigue damage in one hundred years

Table 8.3 Lifetime fatigue damage during one hundred years in the exterior surface of the trough web in model D

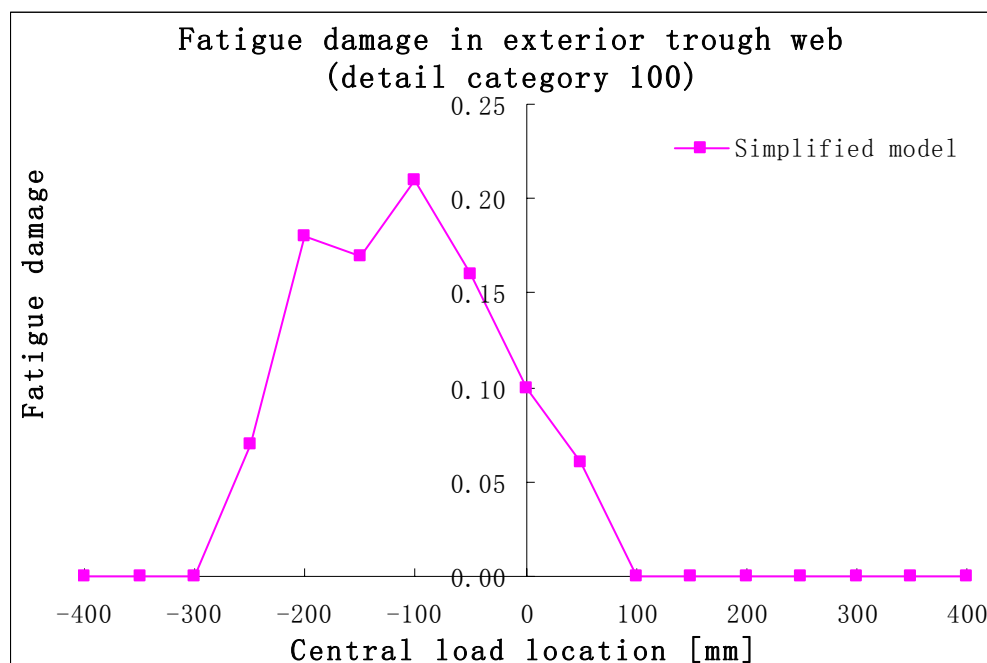


Figure 8.5 Lifetime damage during one hundred years in the exterior surface of the trough web in model D; automatic welding with $MDF=1$

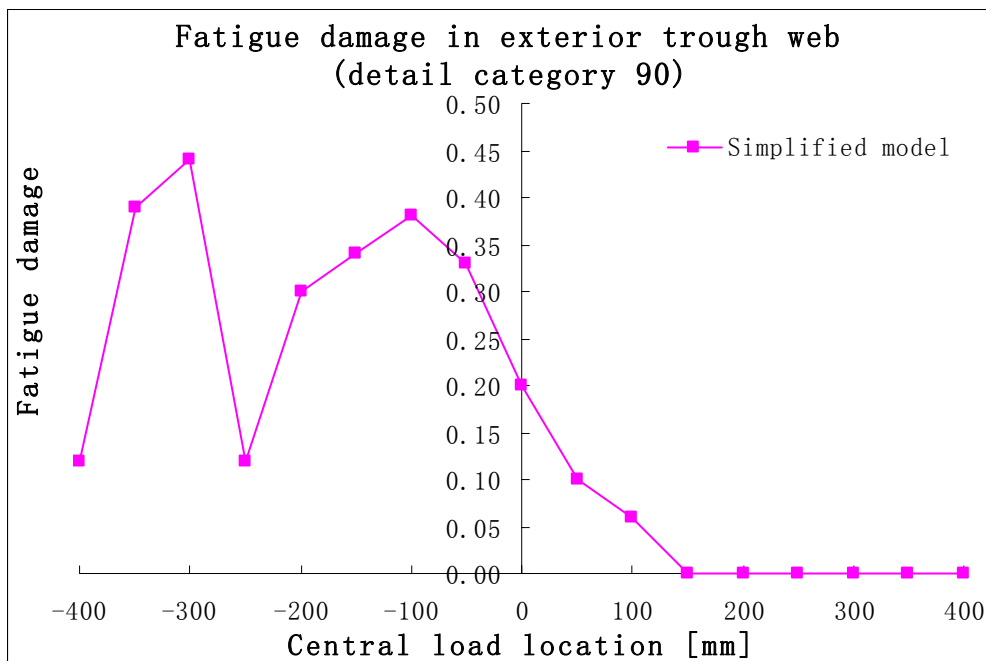


Figure 8.6 Lifetime damage during one hundred years in the exterior surface of the trough web in model D; hand welded with MDF=1

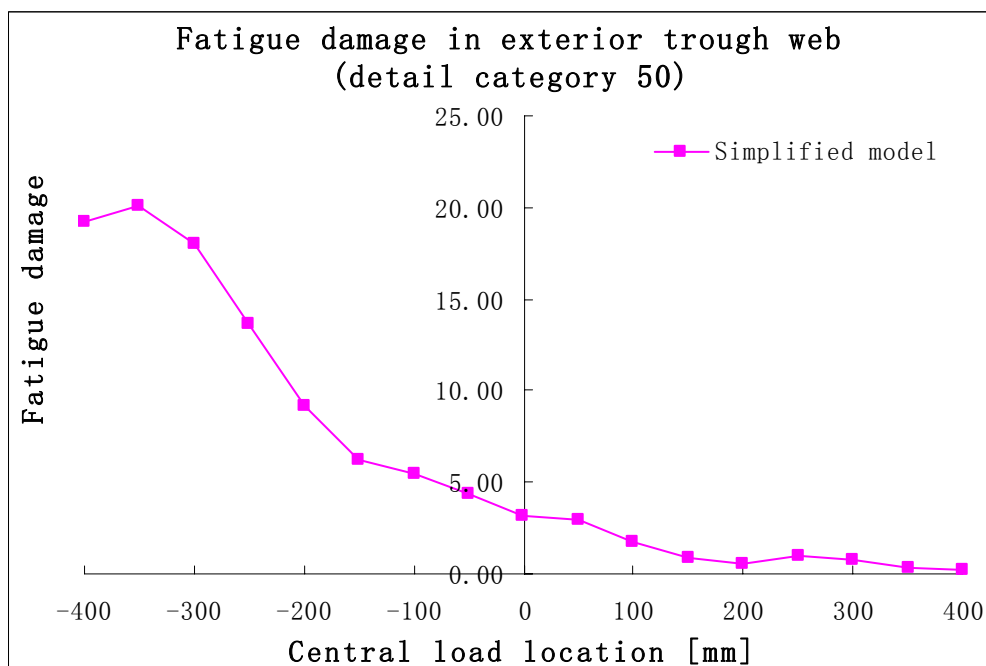


Figure 8.7 Lifetime damage during one hundred years in the exterior surface of the trough web in model D; fillet weld

As expected, the lower the detail category of the trough-to-deck plate joint belongs to, the larger the fatigue damage in the exterior trough web. That is because, by decreasing the detail category, smaller stress ranges can also cause fatigue damage in this case. Comparing to the fatigue damage curves in the interior trough web, the similarity among

these three fatigue damage curves in the exterior trough web is small. It is obvious that the largest fatigue damage does not occur under the same wheel load case. This has to do with the stress ranges taken into account by the calculation.

The fatigue damage in the deck plate is also presented here below (table 8.4 and table 8.5).

lifetime damage interior deck	Central load location [mm]																
	-400	-350	-300	-250	-200	-150	-100	-50	0	50	100	150	200	250	300	350	400
Simplified model	0.00	0.00	0.00	0.00	0.00	0.00	0.00	0.00	0.00	0.00	0.00	0.00	0.00	0.00	0.00	0.00	0.00

Detail category 125

Table 8.4 Lifetime fatigue damage during one hundred years in bottom surface of the interior deck plate in model D

lifetime damage exterior deck	Central load location [mm]																
	-400	-350	-300	-250	-200	-150	-100	-50	0	50	100	150	200	250	300	350	400
Simplified model	0.00	0.00	0.00	0.00	0.00	0.00	0.00	0.00	0.00	0.00	0.00	0.00	0.00	0.00	0.00	0.00	0.00

Detail category 125

Table 8.5 Lifetime fatigue damage during one hundred years in bottom surface of the exterior deck plate in model D

The same as what has been found in the fatigue calculation in model B, no fatigue damage in the deck plate is found.

8.3 Conclusions for fatigue calculation for a movable bridge (model D)

- From the fatigue calculation for a 22mm deck without asphalt for movable bridge model D (the plate thickness is proposed in the National Annex of the NEN-EN 1993-2 for movable bridge in highways in case of troughs passing through the crossbeam based on the fatigue calculations of the deck plate at the intersection of the deck plate, the trough webs and the crossbeam), it shows no fatigue damage in the deck plate (classification 125) and a damage smaller than 1 in the longitudinal weld between the deck plate and the trough (classification of 100 or 90).
- When the troughs do not pass the crossbeam but are welded in between the crossbeams, the deck plate thickness might be decreased.

9 Conclusions and recommendations

In this last chapter, an overview of the conclusions extracted from the study regarding to the objectives proposed in section 1.4 is given. In addition, recommendations for the subject are provided, which might worth a further study in the future.

The main objectives of this thesis are:

1. Gain insight into the behavior of the orthotropic steel deck, the influencing factor of the crack in the trough-to-deck plate joint in the deck;
2. Developing a simplified model for the fatigue design of steel bridges with respect to the trough-to-deck plate joint according to the Eurocodes

9.1 Conclusions

1. Based on the research results described in section 3.9, it turns out that the stress in the trough-to-deck plate joint is largely dependent on the geometry of the structure and the type of the wheel load. The stresses in the deck plate are largely influenced by the deck plate thickness and the presence of an asphalt layer. By increasing the deck plate thickness and the wearing surface layer, the transverse stress in the deck plate can be reduced. The stresses in the deck plate are hardly affected by the dimensions and the trough thickness. The same as the stress in the deck plate, the stress in the trough web can be reduced by using a thicker deck plate, wearing surface and a larger trough (larger trough web, larger trough cross-section).

Stress range is the most important factor which influences the fatigue crack in the orthotropic deck. For nearly all the investigated geometries, the largest stress range in the trough-to-deck plate joint occurs in the middle of the trough span (section D in the models). Therefore, the orthotropic deck design with respect to the trough-to-deck plate joint in between the crossbeams can base on the lifetime fatigue damage in section D.

2. A relatively simple 2D beam model, developed for stress and fatigue calculation of the bottom side of the troughs, can also be used to calculate the longitudinal and the transverse influence lines in the trough-to-deck plate joint in between the crossbeams. Compared to the model used for the calculation of the stresses on the bottom side of the troughs (the original simplified 2D beam model), the boundary conditions have to be changed and a modification factor on the results in the trough

web has to be applied. The change of the boundary conditions and the modification factor are necessary because the original simplified 2D model is not capable of handling the distortional effects of the trough in the same way as the 3D model. After changing the boundary conditions in the model and applying the adjustment factors on the results, the results of the 2D model and the 3D model have a good match for the geometries studied.

In the verification stage, the results obtained from the 2D model are compared with the results obtained from the 3D model. And the comparison shows that a relatively simple 2D beam model can be used for the fatigue damage calculations of the trough-to-deck plate joint in between the crossbeams in an orthotropic steel deck (and following from a study performed during the internship can also be used for the fatigue damage calculations of the bottom side of the troughs). In future, the model might be the basis of a design tool in the National Annex of the NEN-EN 1993-2.

9.2 Recommendations/future study

In this section, some recommendations regarding to this study are given:

1. Based on conclusion 1, the effect of the asphalt layer is of great importance. Eurocode + NB allows to take a spreading of 45 degrees into account and does not allow to take the corporation between the steel deck plate and the asphalt layer into account. The stress ranges and therefore the fatigue life greatly depend on those assumptions.
2. It is believed that Eurocode fatigue load model 4 (to be used for steel bridges in the Netherlands) should represent the actual future traffic in a good way. The fatigue calculation results for the details studied here prove to be sensitive for wheel print dimensions and transverse spreading of the loads.
3. Based on conclusion 1, it is suggested to run a check on the stress in the deck plate near the crossbeam in the simplified 2D beam model in which the troughs are fixed in the vertical direction.
4. More explicit study into the empirical stress adjustment factor for the trough web results is suggested along with a check of the simplified 2D beam model for different trough spans and deck plate spans.
5. Further research about the influence of the extra cut-out underneath the trough in the crossbeam on distortional effect is suggested.
6. Experimental results or on-site measured stresses should be available for the verification of the simplified 2D model results. Due to the lack of experimental data, the scope of application of the simplified 2D model is restricted.
7. The effect of torsion on the stress needs further investigation. The research carried out by Dr. Delesie ([15], [16], [17]), focusing on the effect of trough distortion of orthotropic bridge deck on load dispersal behavior and stress concentrations, is still in processing.

10 References

Literature

- [1] De Backer, H., *Optimalisatie van het vermoeiingsgedrag van het orthotroop brugdekconcept door verbeterde dispersie van de verkeersbelasting* (dissertation Universiteit Gent), Gent, 2006
- [2] De Jong, F.B.P., *Renovation techniques for fatigue cracked orthotropic steel bridge decks* (dissertation TU-Delft), Delft, 2006
- [3] Kolstein, M.H., *Fatigue Classification of Welded Joints in Orthotropic Steel Bridge Decks* (dissertation TU-Delft), Delft, 2007
- [4] Xiao, Z.G., et al, *Stress Analyses and Fatigue Evaluation of Rib-to-deck Joints in Steel Orthotropic Decks*, International Journal of Fatigue 30 (2008), 1387-1397
- [5] Janss, J., *Fatigue of Welds in Orthotropic Bridge Deck Panels with Trapezoidal Stiffeners*, Journal of Constructional Steel Research 9 (1988), 147-154
- [6] Kolstein, M.H., Wardenier, J., *Fatigue Strength of Welded Joints in Orthotropic Steel Bridge Decks*, *Welding in the World/Le Soudage dans le Monde*, Vol. 38 (1996), page 175/194
- [7] Hobbacher, A., *Recommendations for Fatigue Design of Welded Joints and Components*, International Institute of Welding, Paris, 2003
- [8] Leendertz, J.S., *Fatigue Behaviour of Closed Stiffener to Crossbeam Connections in Orthotropic Steel Bridge Decks* (dissertation TU-Delft), Delft, 2008
- [9] Pfeil, M.S., et al, *Stress Concentration in Steel Bridge Orthotropic Decks*, Journal of Constructional Steel Research 61 (2005), 1172-1184
- [10] Ya, S., Yamada, K., *Fatigue Durability Evaluation of Trough to Deck Plate Welded Joint of Orthotropic Steel Deck*, Doboku Gakkai Roundunshuu A, Vol.64 NO.3, 603-616, July 2008
- [11] Zhang, Y.L., et al, *Fatigue Life Estimation of Rib-to-Deck Joints in Orthotropic Steel Deck*, Advanced Materials Research, Vol.163-167, p410-416, 2011
- [12] Manual of MIDAS Civil, *MIDAS/Civil Getting Started*, MIDASoft Inc. 2010

- [13] Wang, C.S., et al, *Fatigue Damage Evaluation and Retrofit of Steel Orthotropic Bridge Decks*, Advance Material Research, Vol.163-167, p3511-3516, 2011
- [14] De Backer, H., et al, *Analytical Calculation of Internal Forces in Orthotropic Plated Bridge Decks Based on the Slope-Deflection Method*, Journal of Constructional Steel Research 64 (2008) 1530-1539
- [15] Delesie, C., Van Bogaert, P., *Modeling Stiffener Distortion in Orthotropic Bridge Decks with FEM Using Superelements*, Conference Proceedings 11th Nordic Steel Construction Conference, Malmö, 2009
- [16] Delesie, C., et al, *The Effect of Stiffener Distortion of Orthotropic Bridge Decks on Load Dispersal Behavior and Stress Concentrations*, Proceedings International Orthotropic Bridge Conference, Sacramento, 2008
- [17] Delesie, C., Van Bogaert, P., *Experimental and Numerical Simulation of Stress Concentrations in Orthotropic Bridge Decks Induced by Stiffener Distortion*, Proceedings Eurosteel 2011 conference, August 31-September 2, 2011, Budapest, Hungary
- [18] Cullimore, M.S.G., Smith, J.W., *Local Stresses in Orthotropic Steel Bridge Decks Caused by Wheel Loads*, Journal of Constructional Steel Research, Vol.1 NO.2, January 1981
- [19] Tang, M.C., *A New Concept of Orthotropic Steel Bridge Deck*, Structure and Infrastructure Engineering, Vol.7, Nos. 7-8, July-August 2011, 587 595
- [20] Otte, A., *Proposal for Modified Fatigue Load Model Based on EN 1991-2*, (Master thesis, TU-Delft), Delft, July 2009
- [21] Van Pol, P., *Effect of Cope Holes in the Crossbeam of Orthotropic Steel Bridge Decks*, (Master thesis, TU-Delft), Delft, December 2009
- [22] Freitas, S.T., et al, *Orthotropic Deck Renovation of the Movable Bridge Scharsterrijn*, Conference Proceedings 11th Nordic Steel Construction Conference, Malmö,, 2009
- [23] Fisher, J.W., *Fatigue of Steel Bridge Infrastructure*, Structure and Infrastructure Engineering, Vol.7, p457-475, April 2011
- [24] Biehn, B., et al, *Fatigue Crack Propagation Analysis for Welded Joint Subjected to Bending*, International Journal of Fatigue, Vol.33, p746-758, 2011

- [25] Li, Z.X., et al, *Determination of Effective Stress Range and Its Application on Fatigue Stress Assessment of Existing Bridges*, International Journal of Solids and Structures, Vol.39, p2401-2417, 2002
- [26] van Dooren, F., et al, *Project Renovation Steel Bridge*, (presentation), Rijkswaterstaat
- [27] Leendertz, J.S., et al, *Fatigue Aspects of Orthotropic Steel Decks*, (presentation), Rijkswaterstaat
- [28] *Design of Bridges: Guide to Basis of Bridge Design Related to Eurocodes Supplemented by Practical Examples*, Leonardo Da Vinci Pilot Project CZ/02/B/F/PP-134007, Pisa, October 2005
- [29] Maljaars, J., *Vermoeiingsscheuren in de las tussen de deckplaat en de trog*, (presentation), TNO
- [30] Friedrich, H., *Repair and Strengthening of Orthotropic Bridge Deck in Germany*, (presentation), Federal Highway Research Institute
- [31] Liao, J., *Trough Fatigue Analysis in Orthotropic Steel Bridge Decks*, (internship report, TU-Delft), Delft, 2010

College lecture books

- [C1] Kolstein M.H. Steel Bridges CT5125, lecture book TU-Delft, Faculty CiTG, November 2011
- [C2] Romeijn, A., Fatigue CT5126, lecture book TU-Delft, Faculty CiTG, September 2006
- [C3] Bijlaard, F.S.K., Steel structure 2 CT4115, lecture book TU-Delft, Faculty CiTG, 2006
- [C4] Wardenier, J., Hollow sections in structural applications, published by Bouwen met Staal, 2002

Standards

- [N1] NEN-EN 1991-2 *Traffic loads on bridges*, publication of CEN (Comité Européen de Normalisation), Brussel, October 2003

- [N2] NEN-EN 1993-1-9 *Fatigue*, publication of CEN (Comité Européen de Normalisation), Brussel, January 2006
- [N3] NEN-EN 1993-2 *Design of steel structures, part 2: Steel bridges*, publication of CEN (Comité Européen de Normalisation), Brussel, July 2007
- [N4] European Convention for Constructional Steelwork, *Good Design Practice, A Guideline for Fatigue Design*, Lanusanne, 2000
- [N5] NEN-EN 1991-2/NB, *National Annex to NEN-EN 1991-2 : Traffic loads on bridges*, Nederlands Normalisatie Instituut, Delft, July, 2010
- [N6] NEN-EN 1993-2/NB, *National Annex to NEN-EN 1993-2 : Design of steel structures, part 2: Steel bridges*, Nederlands Normalisatie Instituut, Delft, July, 2010

Websites

- [W1] European Steel Design Education Programme
<http://www.fgg.uni-lj.si/kmk/ESDEP/master/toc.htm>
- [W2] Ministerie van Infrastructuur en Milieu (Intranet Rijkswaterstaat)
<http://corporatie.intranet.rws.nl/>
- [W3] eFatigue 'A trusted source for fatigue analysis'
www.efatigue.com
- [W4] Stalen Bruggen
www.platformstalenbruggen.nl
- [W5] Wikipedia 'The free encyclopedia'
www.wikipedia.org

Software

- [S1] MIDAS Civil 2010, MIDASoft Inc.
- [S2] Excel program, Microsoft
- [S3] Excel Program developed by Rijkswaterstaat

Appendices

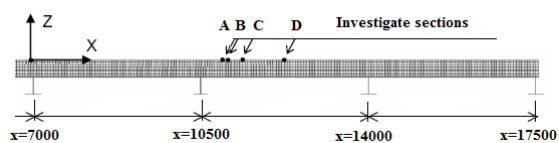
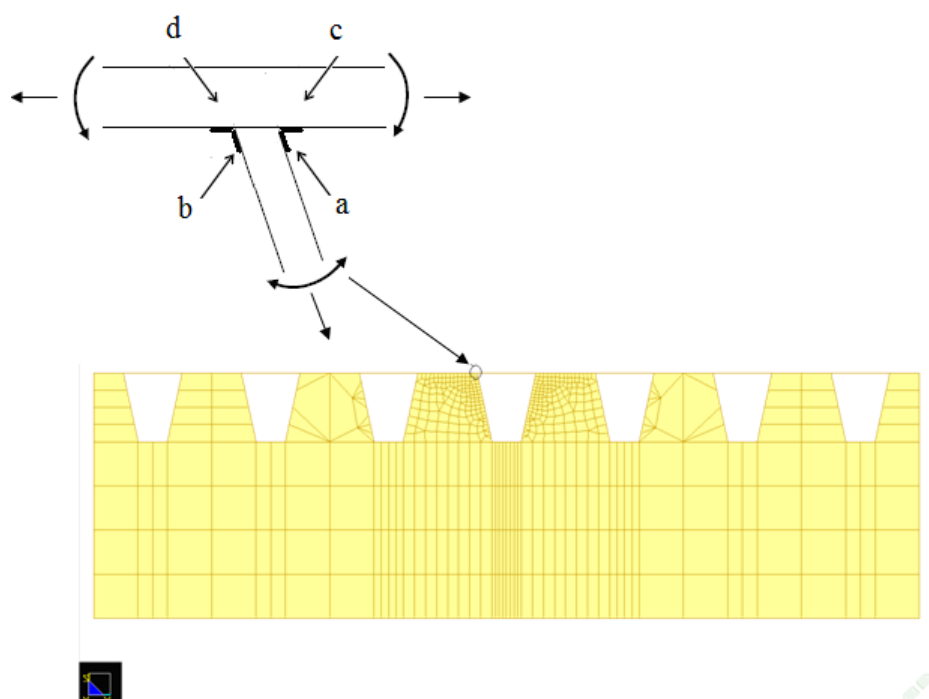
Appendix A Stress in 3D finite element model MIDAS Civil

Appendix A Stress in 3D finite element model MIDAS Civil.....	1
1. Influence lines in model A.....	3
2. Influence lines in model B.....	8
3. Influence lines in model C.....	16
4. Influence lines in model D.....	24
5. Stress ranges in model A.....	31
6. Stress ranges in model B.....	34
7. Stress ranges in model C.....	36
8. Stress ranges in model D.....	38

Due to the limitation of the space in the thesis, only a few influence lines are showed in the thesis. The rest influence lines and the stress ranges in the object joints will be presented in this part of the appendix. The general explanation of the influence lines and the stress ranges can be found in the thesis.

1. Influence lines in model A

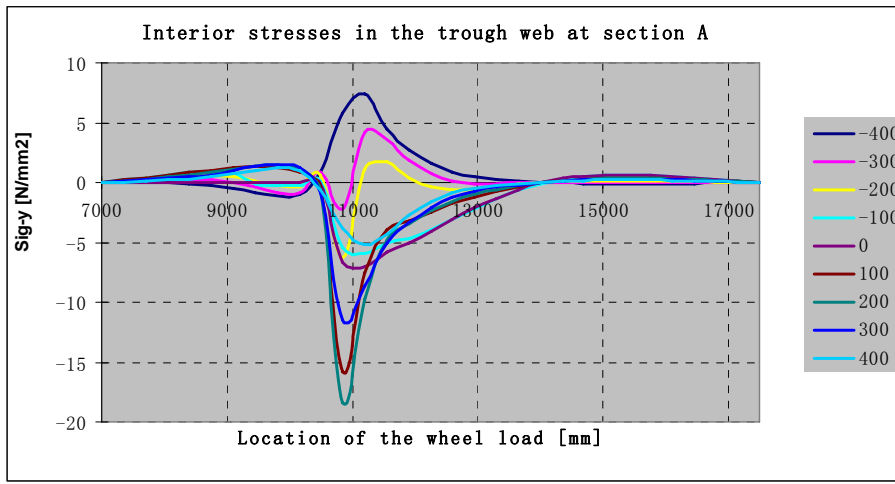
This chapter presents the influence lines of location a (interior), b (exterior) in the trough web and c(interior), d(exterior) deck plate at sections A, B, C and D in model A. The working of the running wheel load is simulated by load cases in Midas Civil. First of all, the longitudinal influence lines are given for the object locations. And then the transverse influence lines will be given.



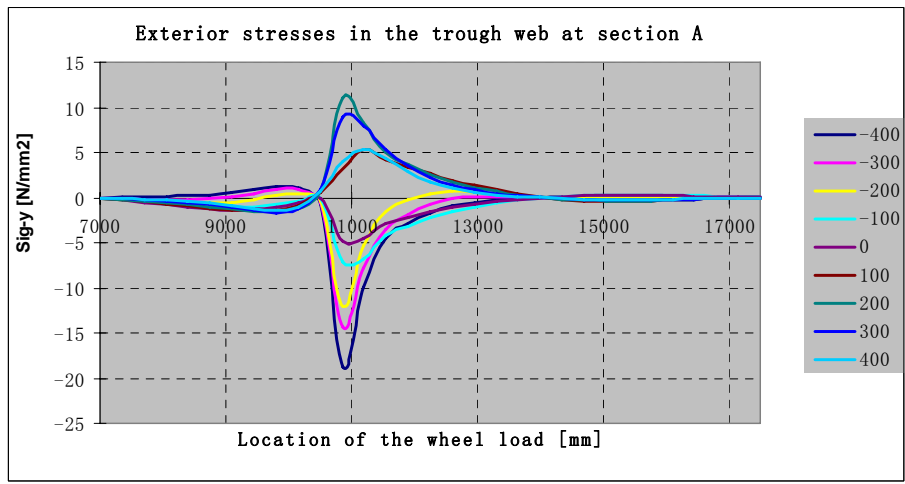
Object joints	X-coordinates [mm]	Y-coordinates [mm]	Z-coordinates [mm]
A	(depending on wheel print)	1950	0
B	10937.5	1950	0
C	11375	1950	0
D	12250	1950	0

Longitudinal influence line under wheel load B

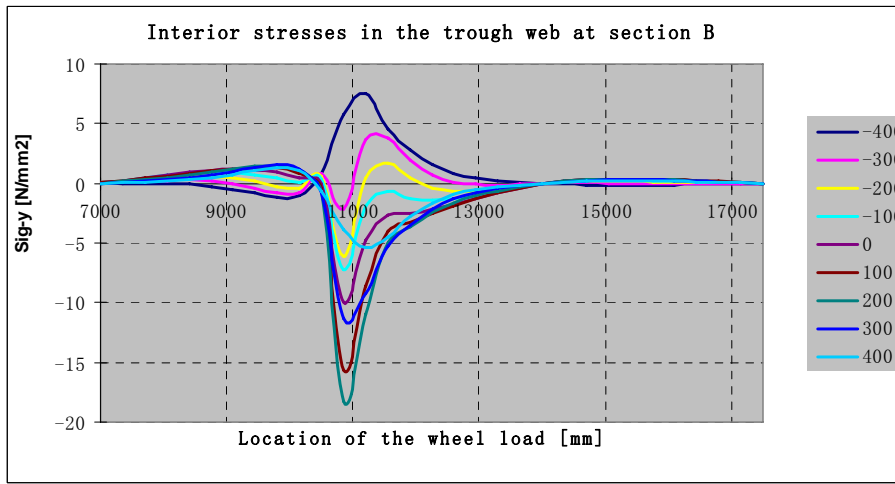
Longitudinal influence line in the trough web



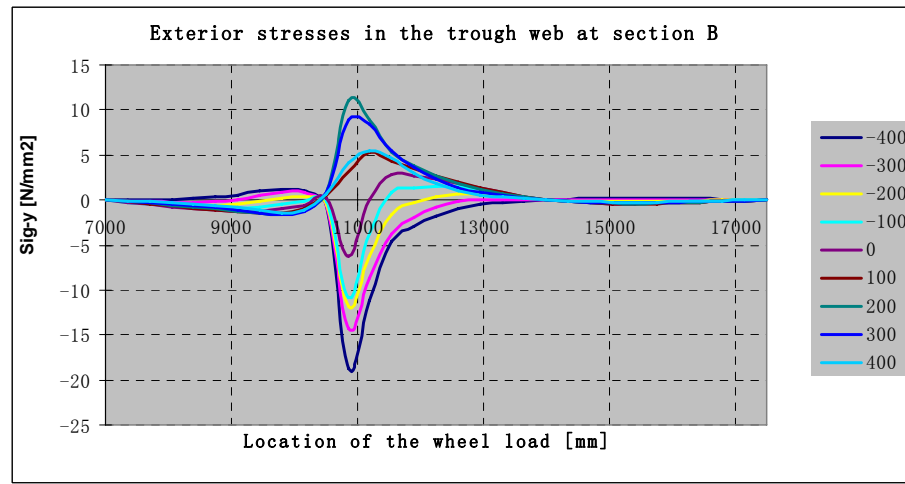
(a) Longitudinal influence line in the interior trough web at section A



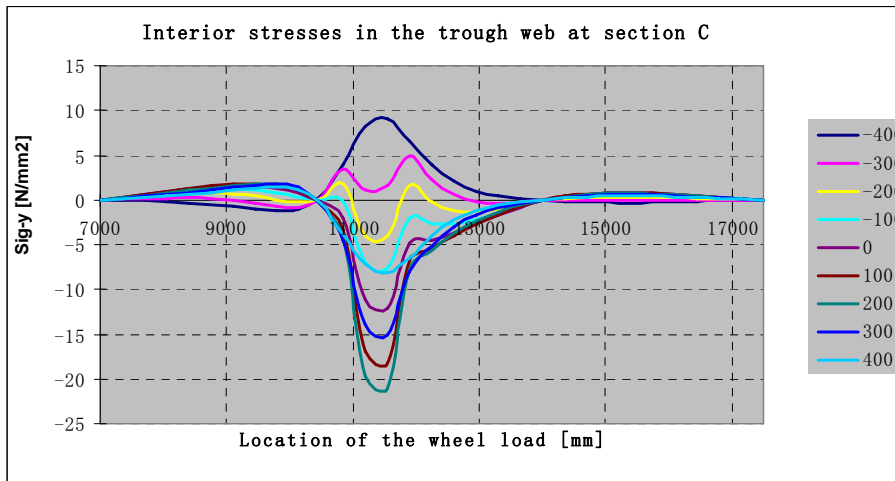
(b) Longitudinal influence line in the exterior trough web at section A



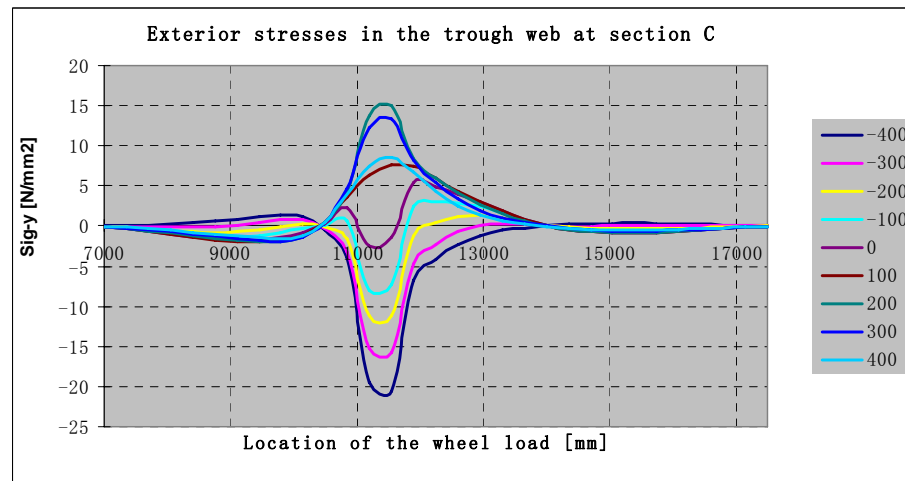
(c) Longitudinal influence line in the interior trough web at section B



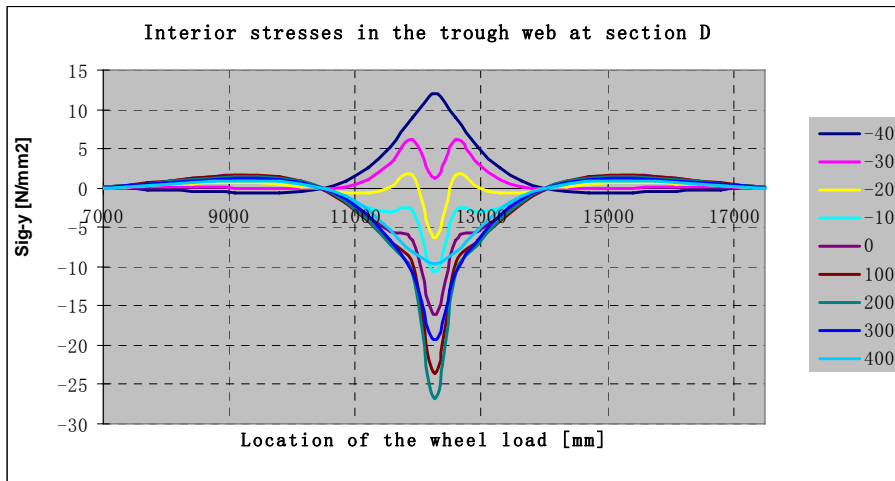
(d) Longitudinal influence line in the exterior trough web at section B



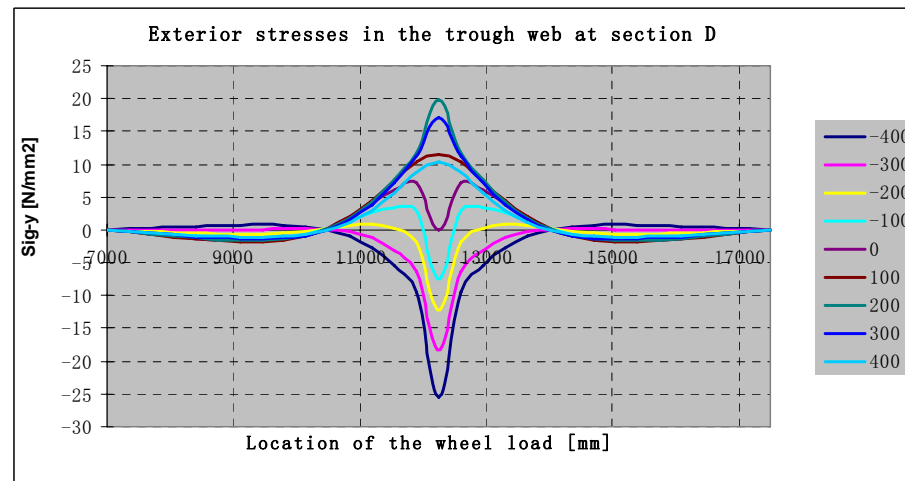
(e) Longitudinal influence line in the interior trough web at section C



(f) Longitudinal influence line in the exterior trough web at section C

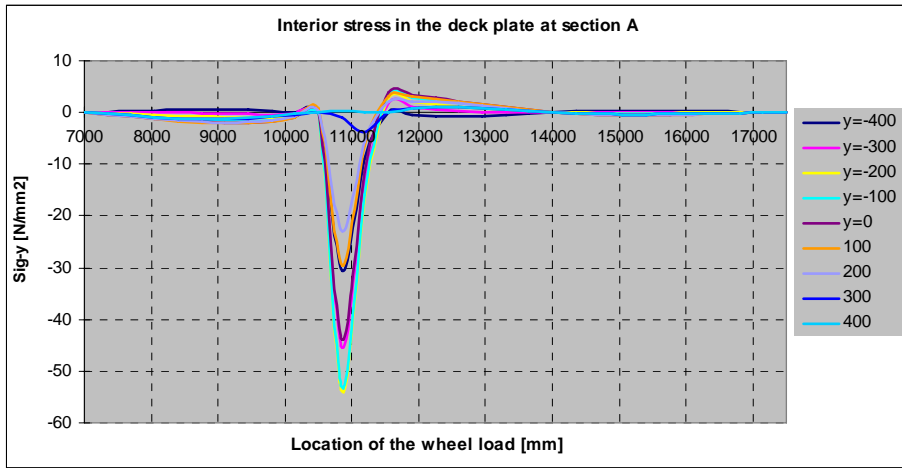


(g) Longitudinal influence line in the interior trough web at section D

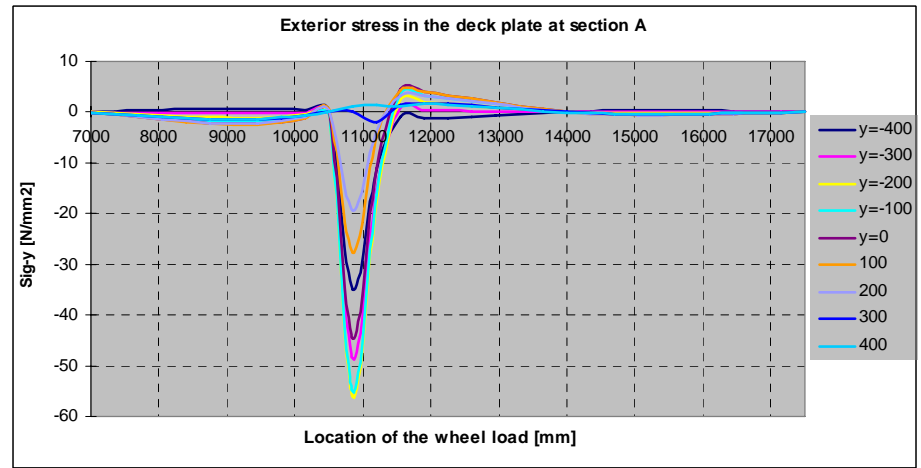


(h) Longitudinal influence line in the exterior trough web at section D

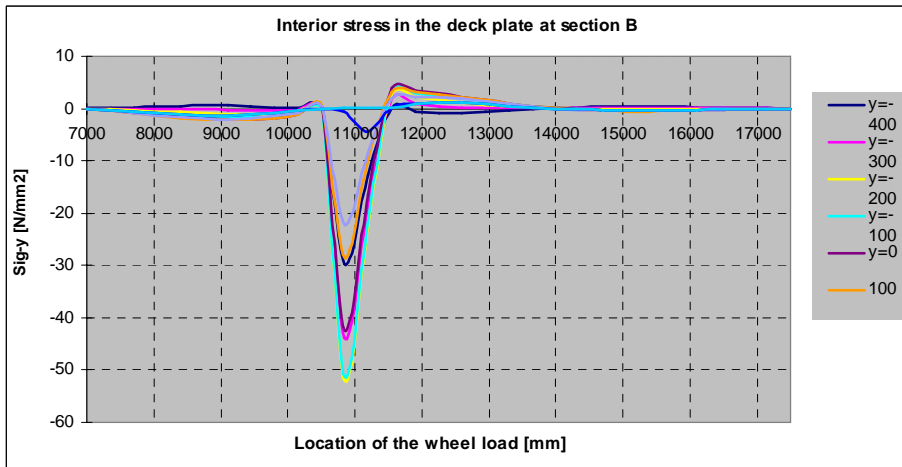
Longitudinal influence line in the deck plate



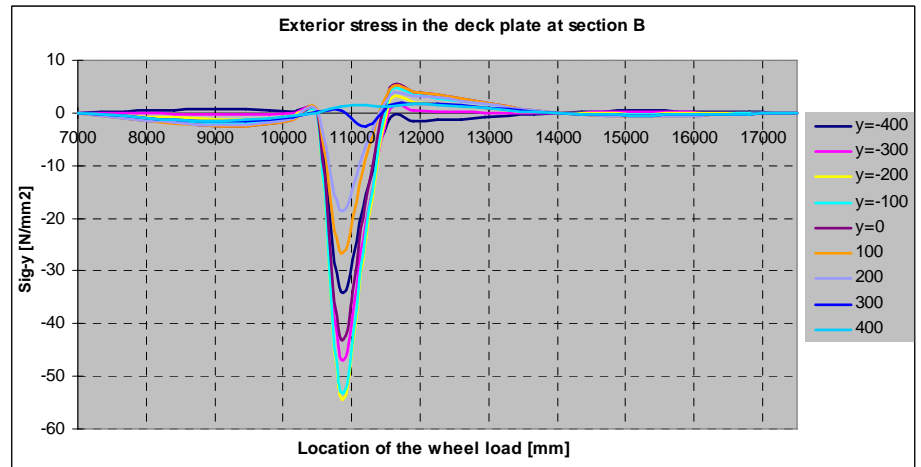
(a) Longitudinal influence line in the interior deck plate at section A



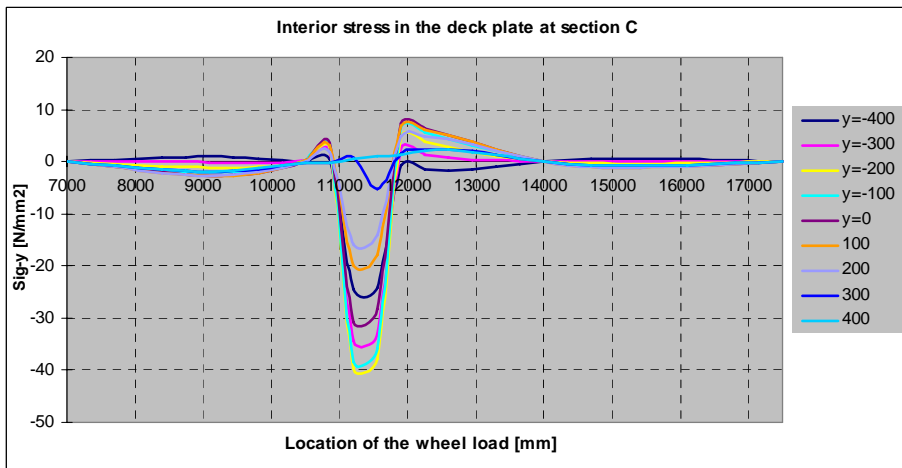
(b) Longitudinal influence line in the exterior deck plate at section A



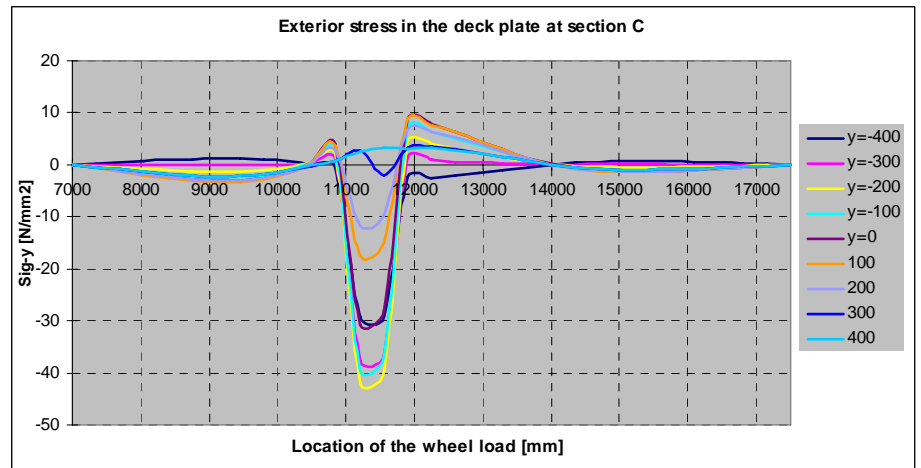
(c) Longitudinal influence line in the interior deck plate at section B



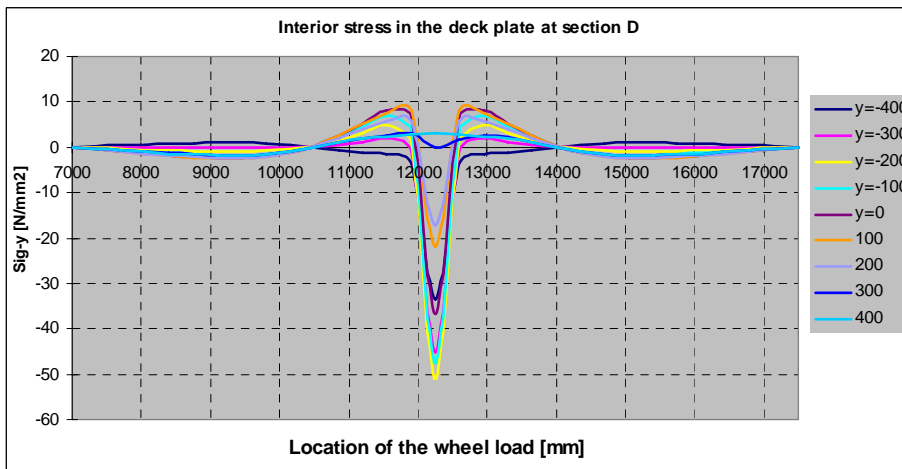
(d) Longitudinal influence line in the exterior deck plate at section B



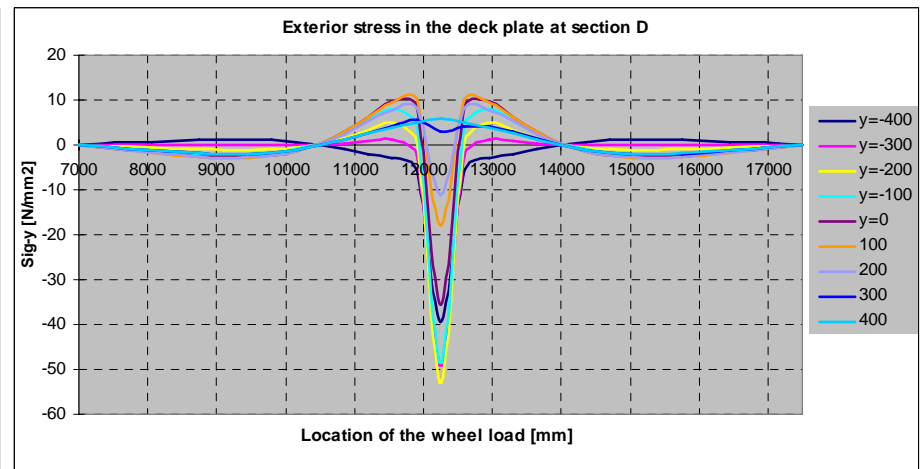
(e) Longitudinal influence line in the interior deck plate at section C



(f) Longitudinal influence line in the exterior deck plate at section C



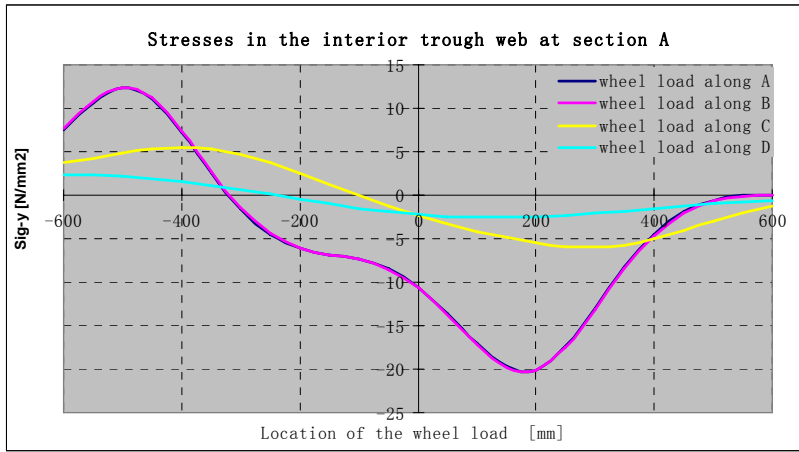
(g) Longitudinal influence line in the interior deck plate at section D



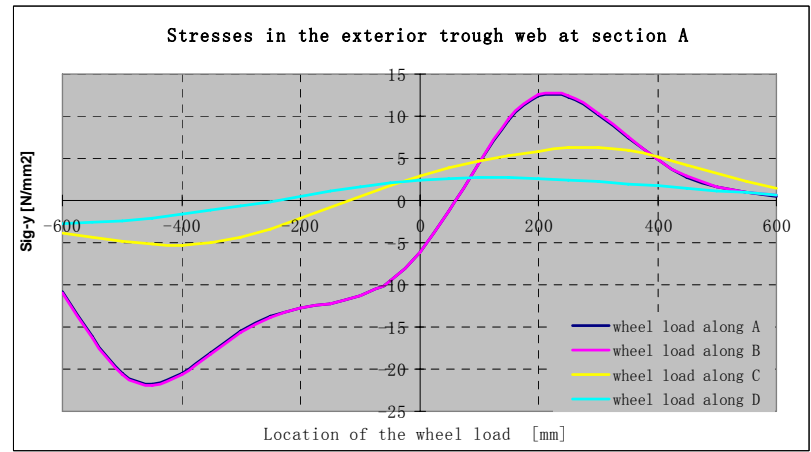
(g) Longitudinal influence line in the exterior deck plate at section D

Transverse influence line under wheel load B

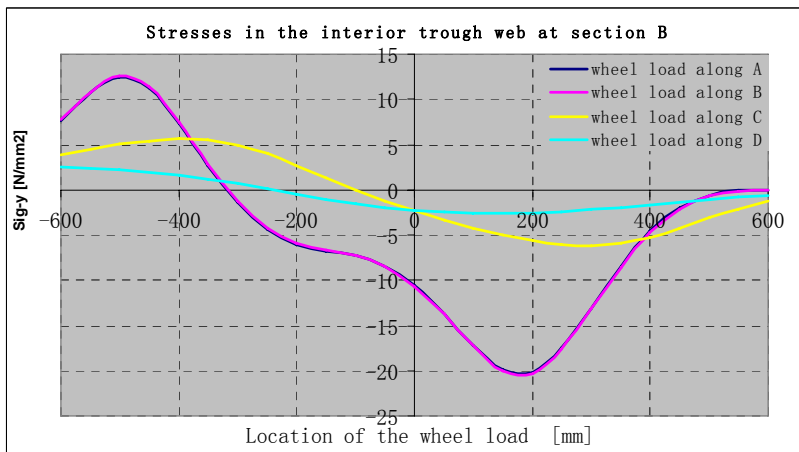
Transverse influence line in the trough web



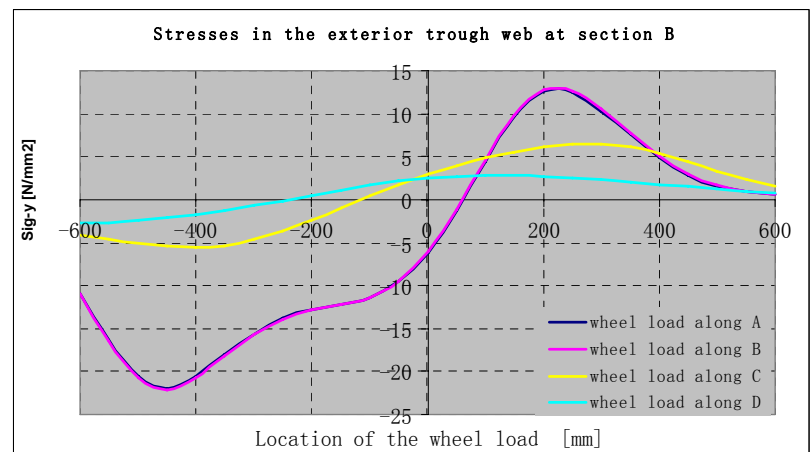
(a) Transverse influence line in the interior trough web at section A



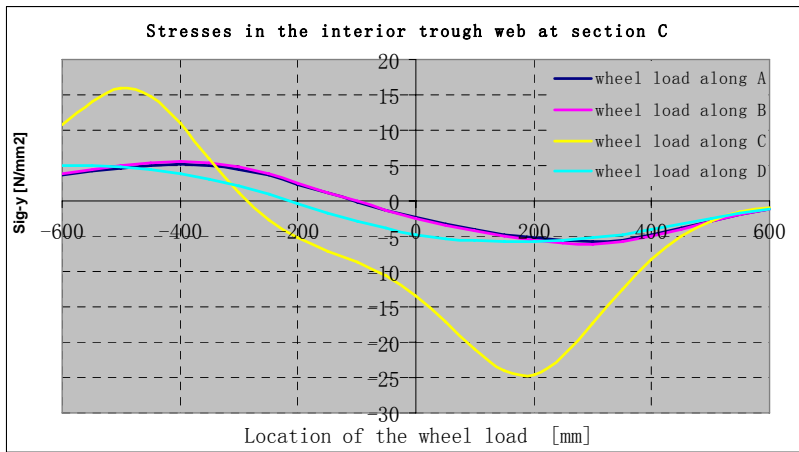
(b) Transverse influence line in the exterior trough web at section A



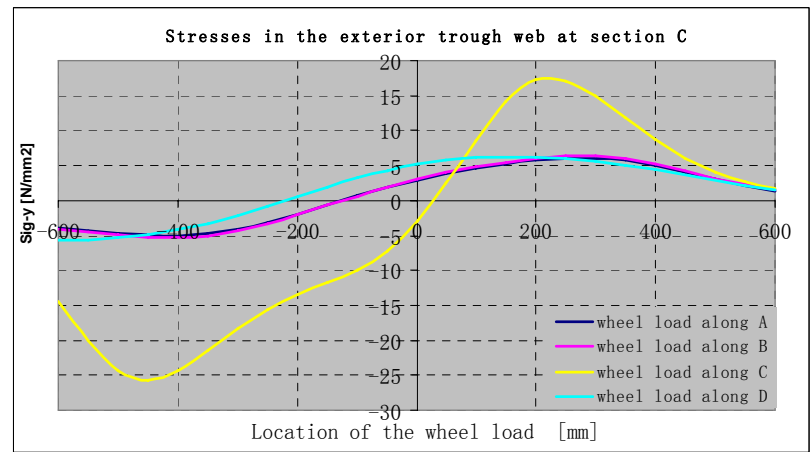
(c) Transverse influence line in the interior trough web at section B



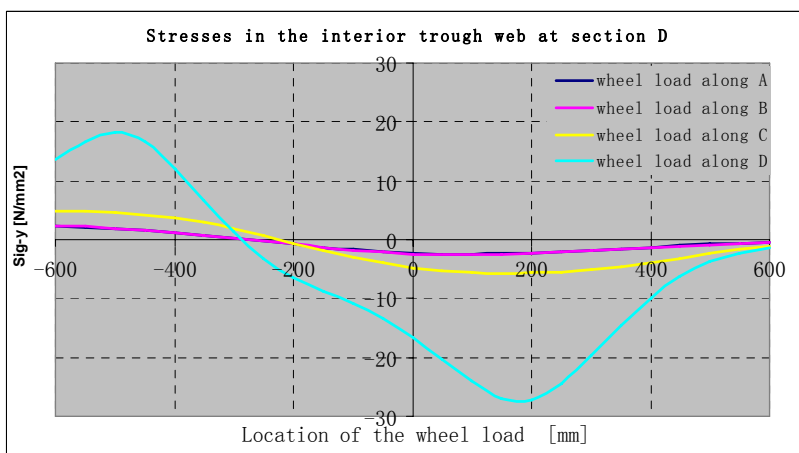
(d) Transverse influence line in the exterior trough web at section B



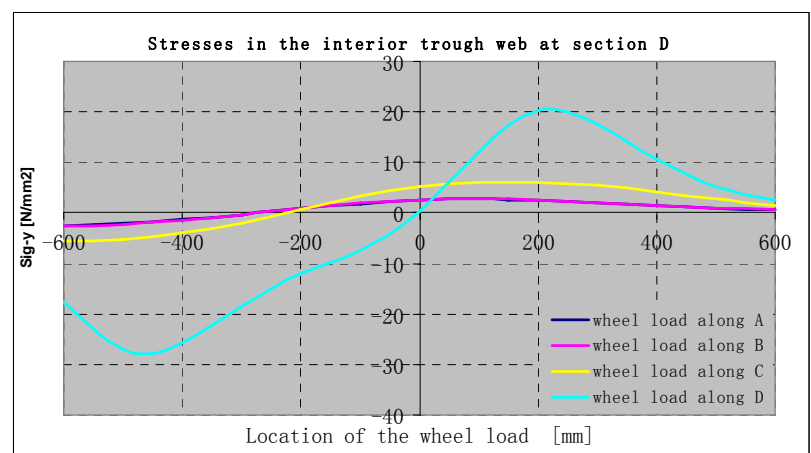
(e) Transverse influence line in the interior trough web at section C



(f) Transverse influence line in the exterior trough web at section C

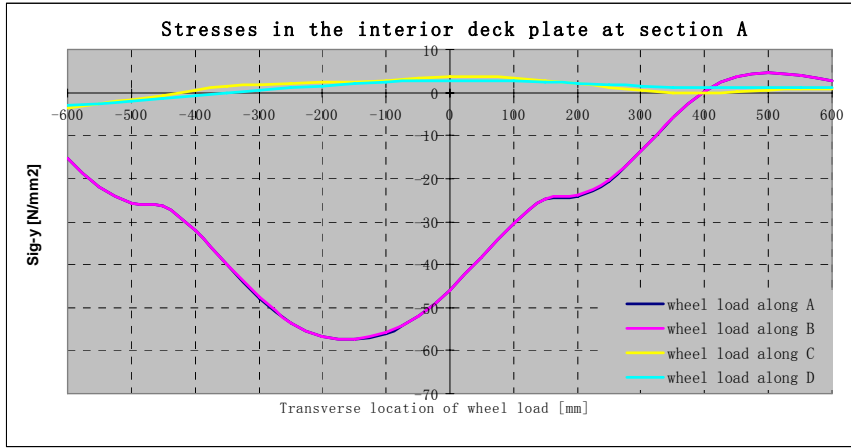


(g) Transverse influence line in the interior trough web at section D

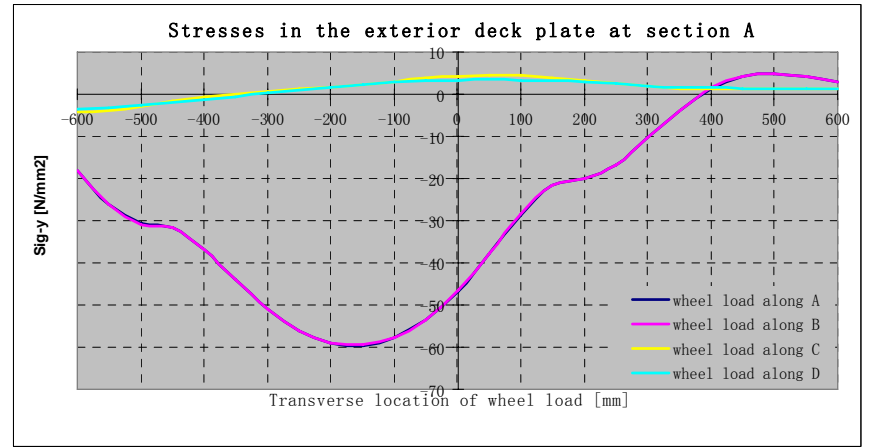


(h) Transverse influence line in the exterior trough web at section D

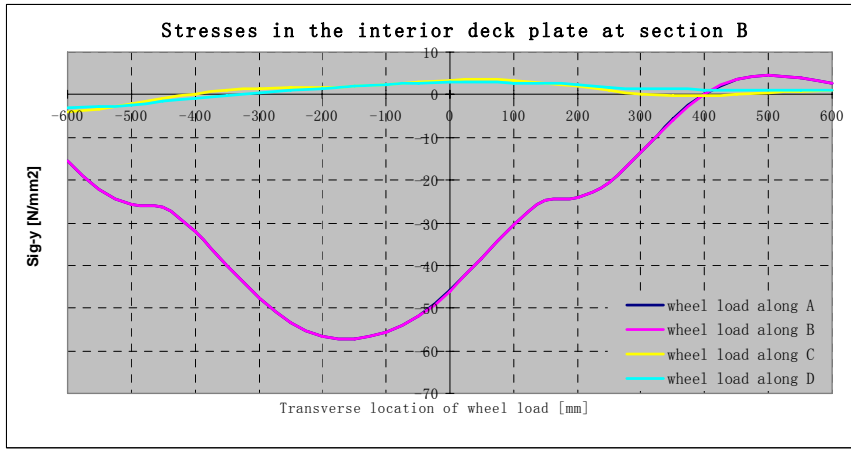
Transverse influence line in the deck plate



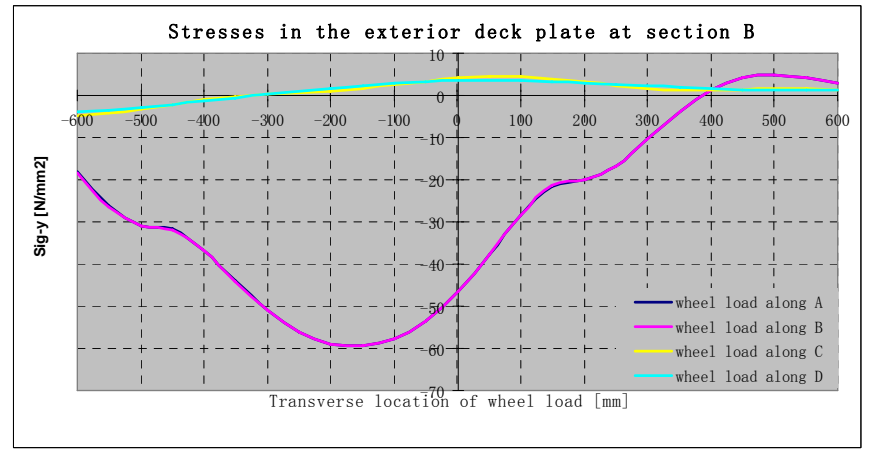
(a) Transverse influence line in the interior deck plate at section A



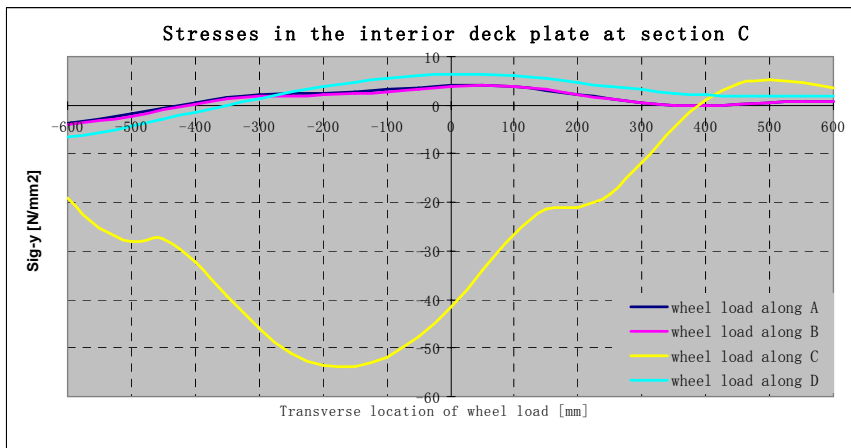
(b) Transverse influence line in the exterior deck plate at section A



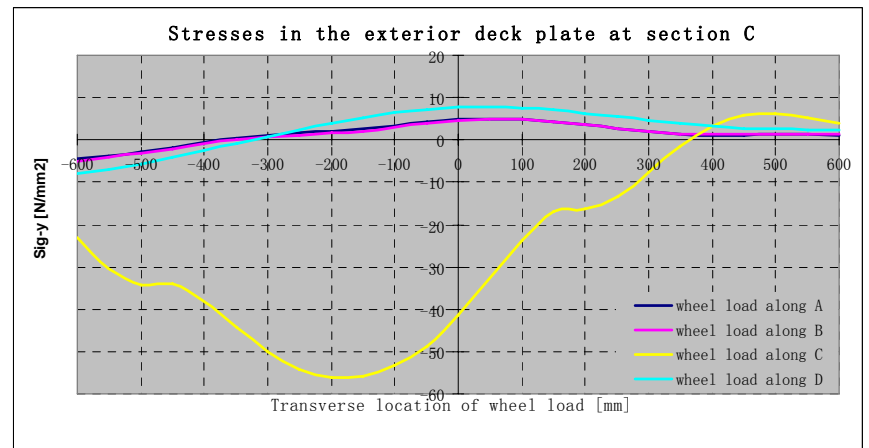
(c) Transverse influence line in the interior deck plate at section B



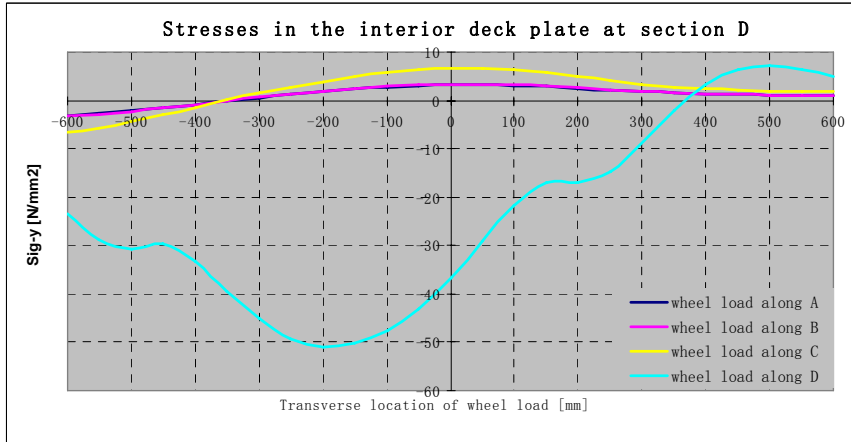
(d) Transverse influence line in the exterior deck plate at section B



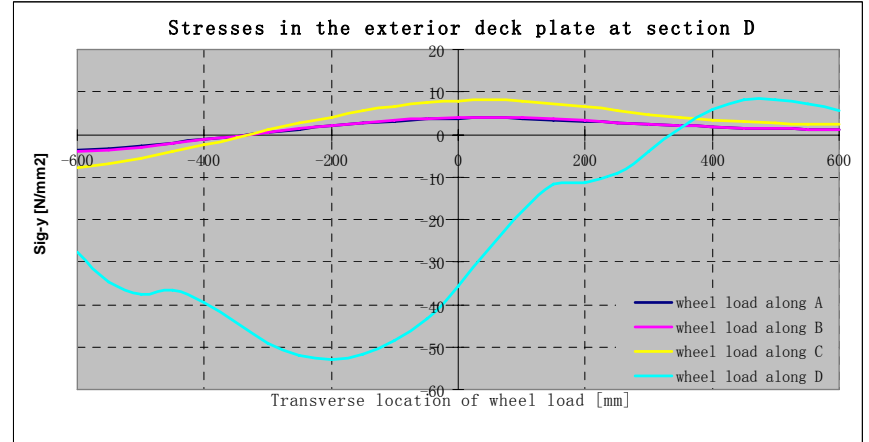
(e) Transverse influence line in the interior deck plate at section C



(f) Transverse influence line in the exterior deck plate at section C



(g) Transverse influence line in the interior deck plate at section D

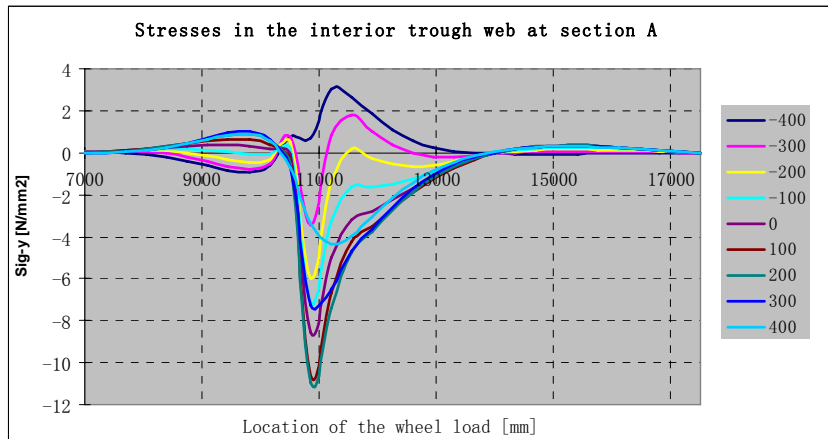


(h) Transverse influence line in the exterior deck plate at section D

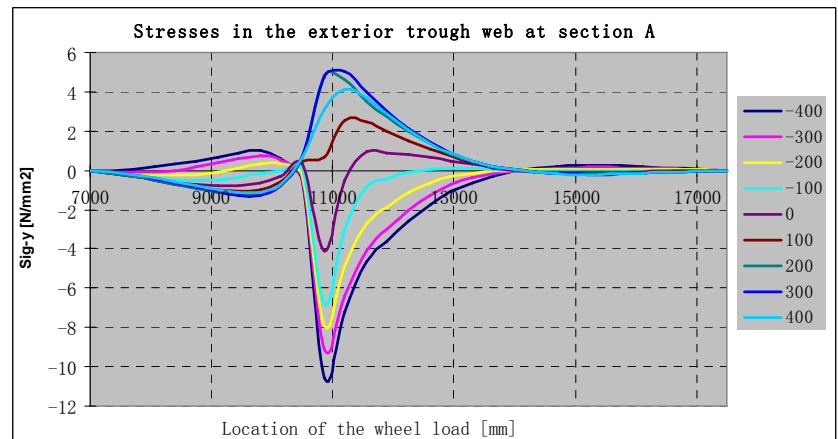
2. Influence lines in model B

Longitudinal influence line under wheel load B

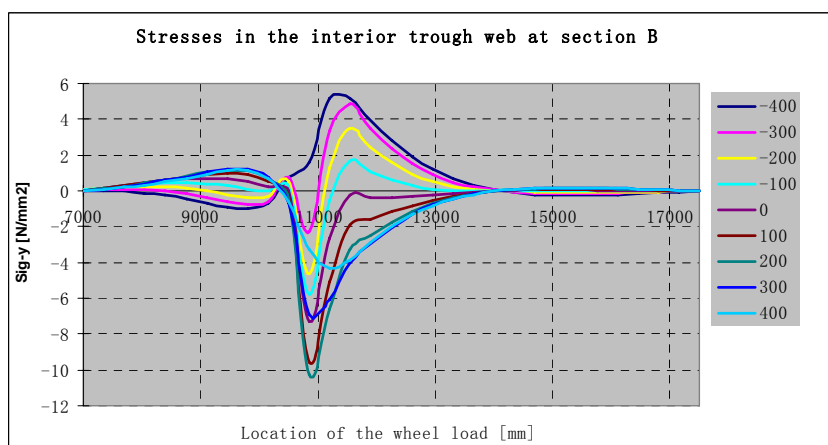
Longitudinal influence line in the trough web



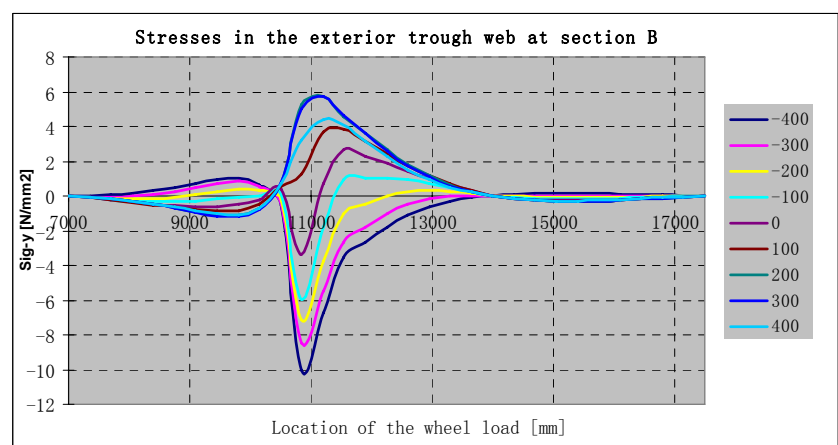
(a) Longitudinal influence line in the interior trough web at section A



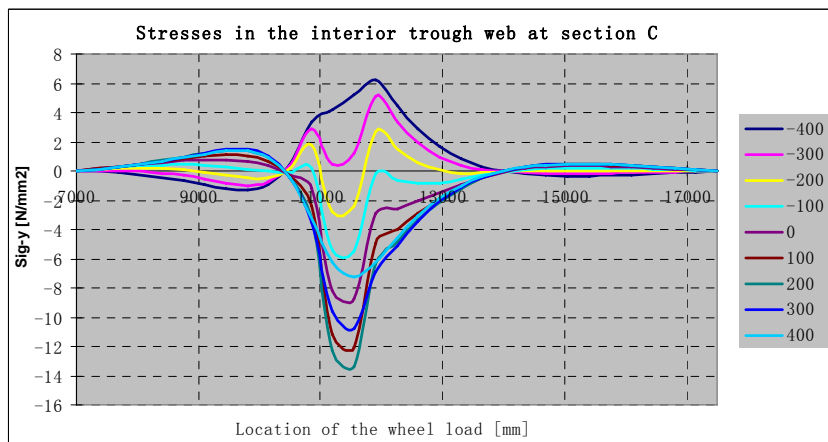
(b) Longitudinal influence line in the exterior trough web at section A



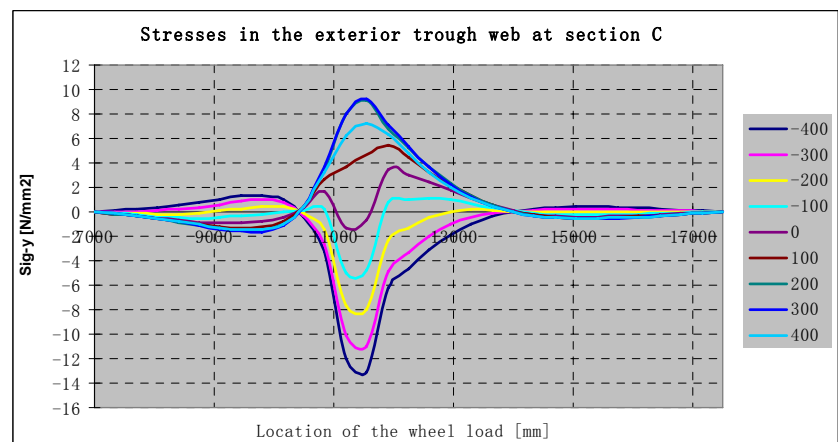
(c) Longitudinal influence line in the interior trough web at section B



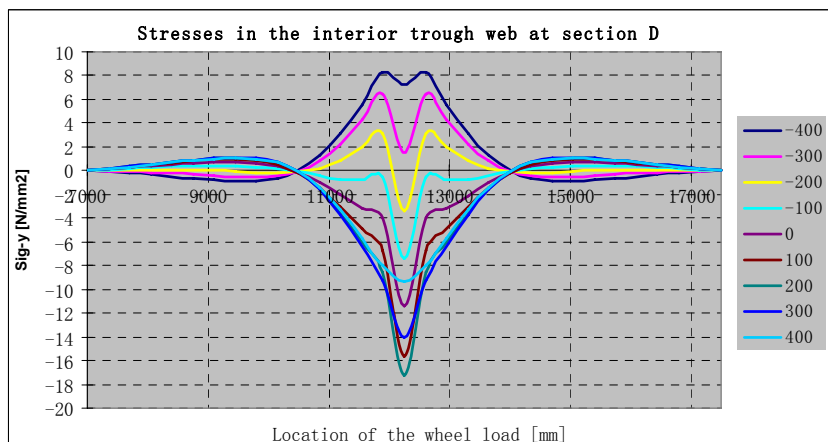
(d) Longitudinal influence line in the exterior trough web at section B



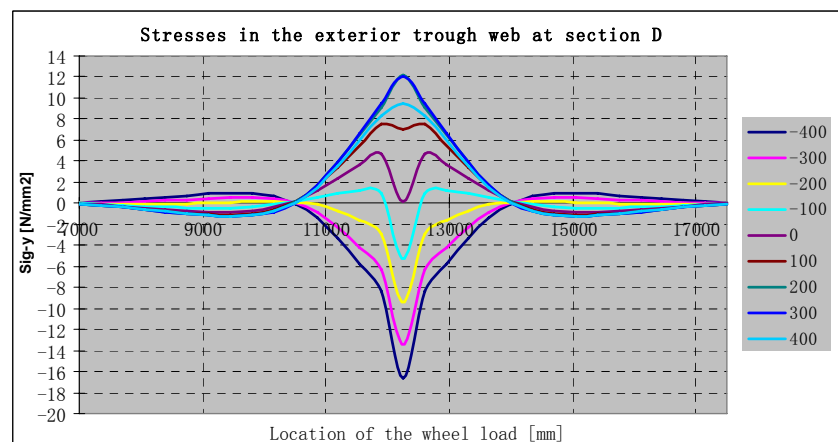
(e) Longitudinal influence line in the interior trough web at section C



(f) Longitudinal influence line in the exterior trough web at section C

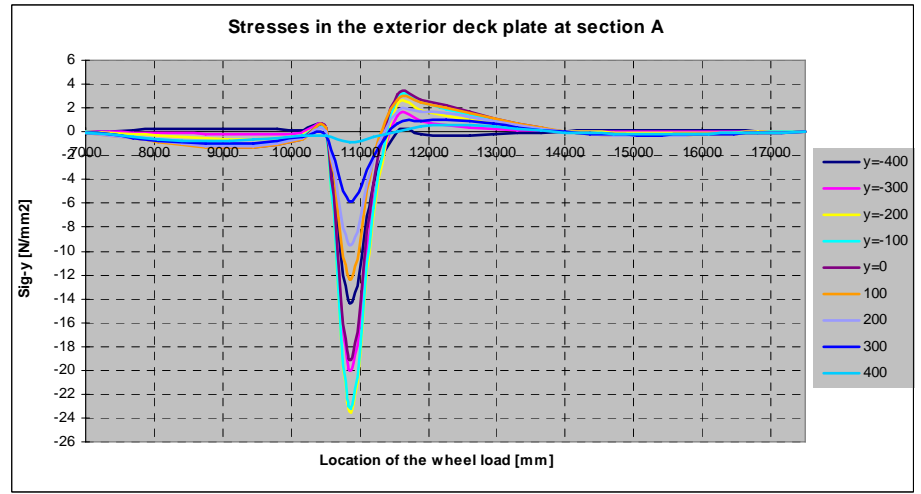
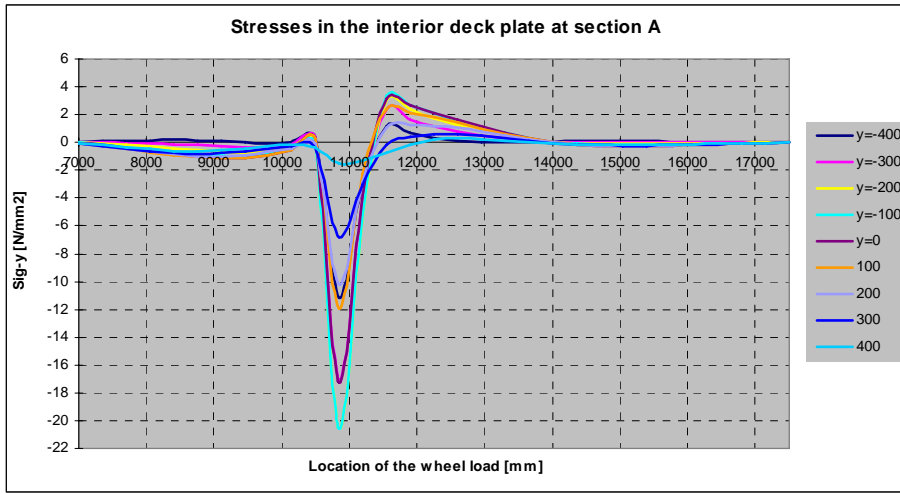


(g) Longitudinal influence line in the interior trough web at section D



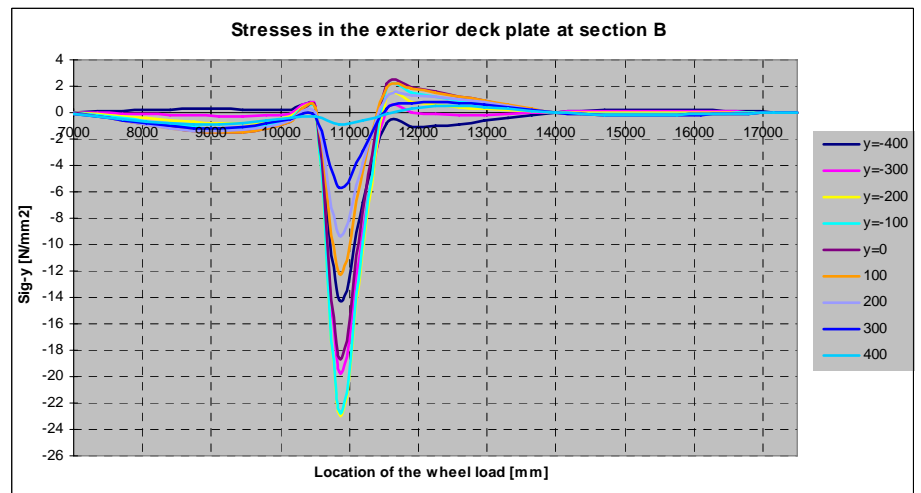
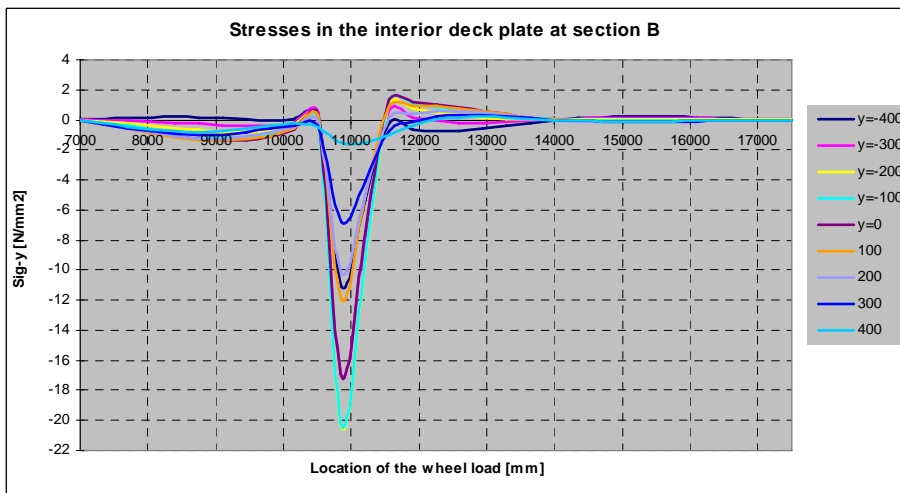
(h) Longitudinal influence line in the exterior trough web at section D

Longitudinal influence line in the deck plate



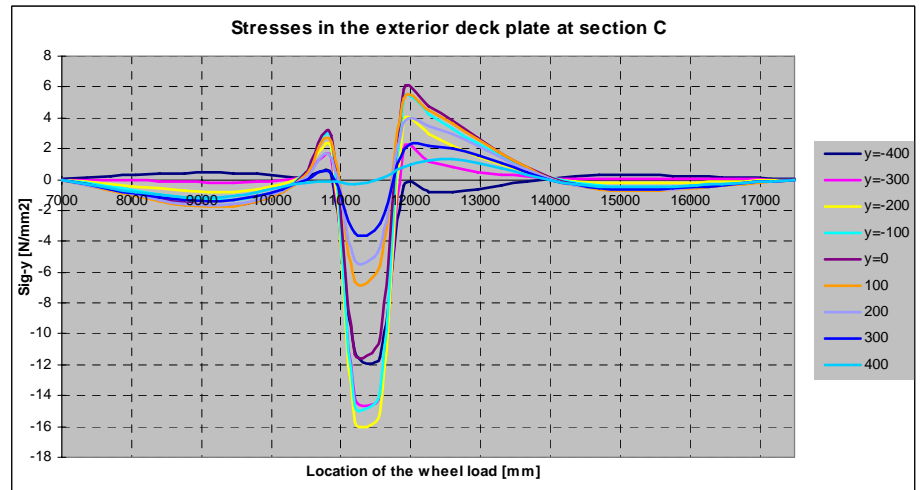
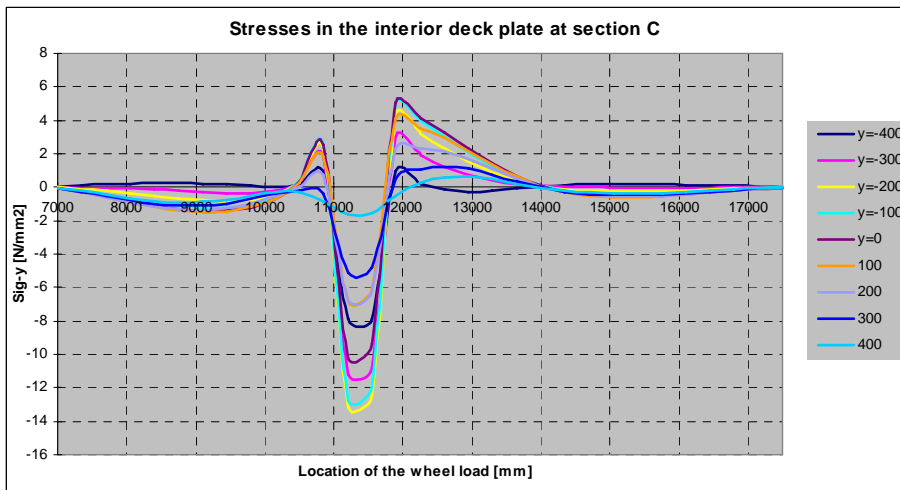
(a) Longitudinal influence line in the interior deck plate at section A

(b) Longitudinal influence line in the exterior deck plate at section A



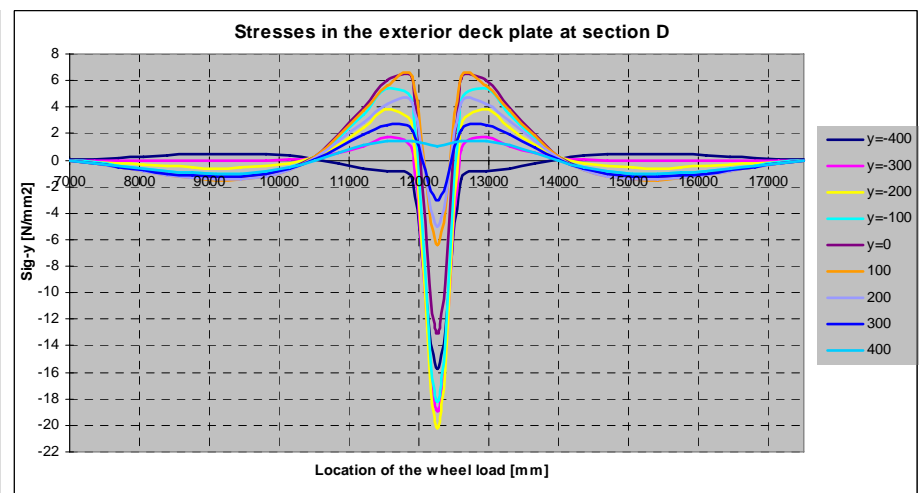
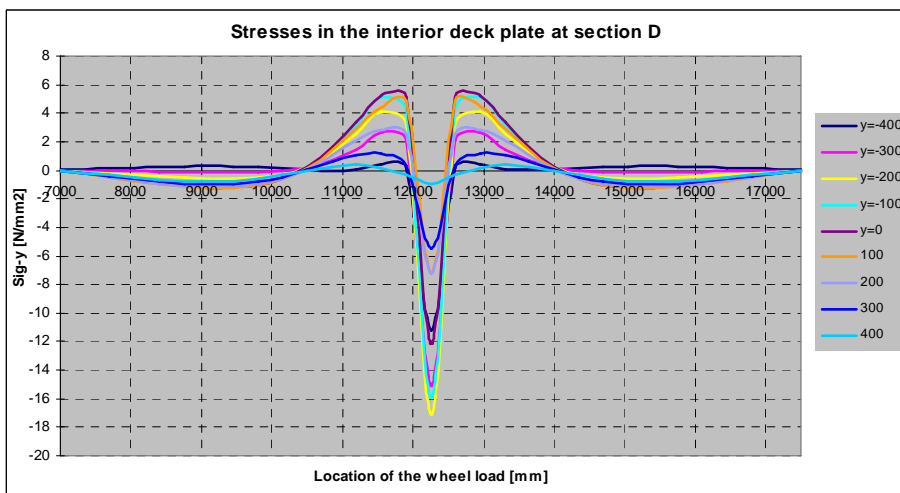
(c) Longitudinal influence line in the interior deck plate at section B

(d) Longitudinal influence line in the exterior deck plate at section B



(e) Longitudinal influence line in the interior deck plate at section C

(f) Longitudinal influence line in the exterior deck plate at section C

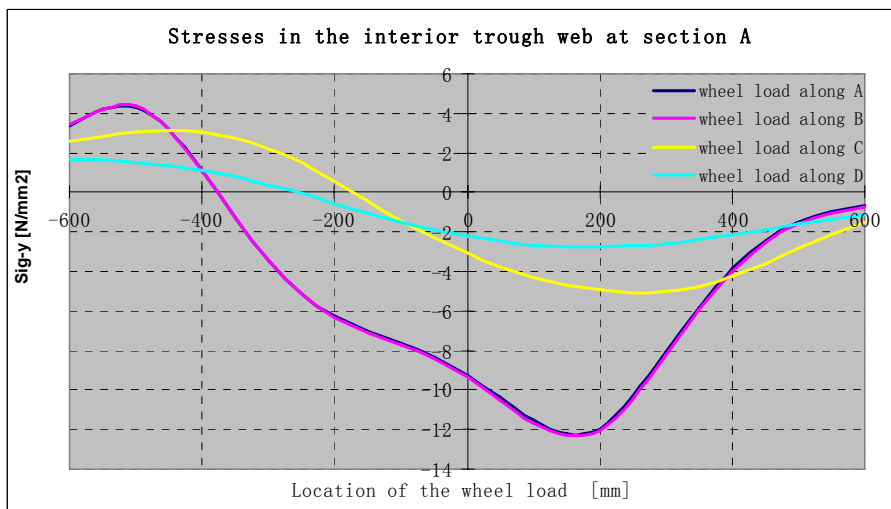


(g) Longitudinal influence line in the interior deck plate at section D

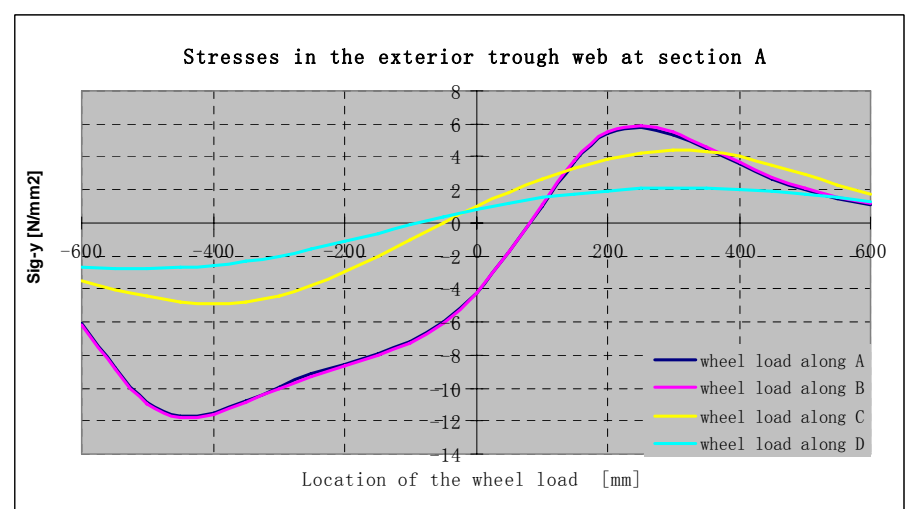
(h) Longitudinal influence line in the exterior deck plate at section D

Transverse influence line under wheel load B

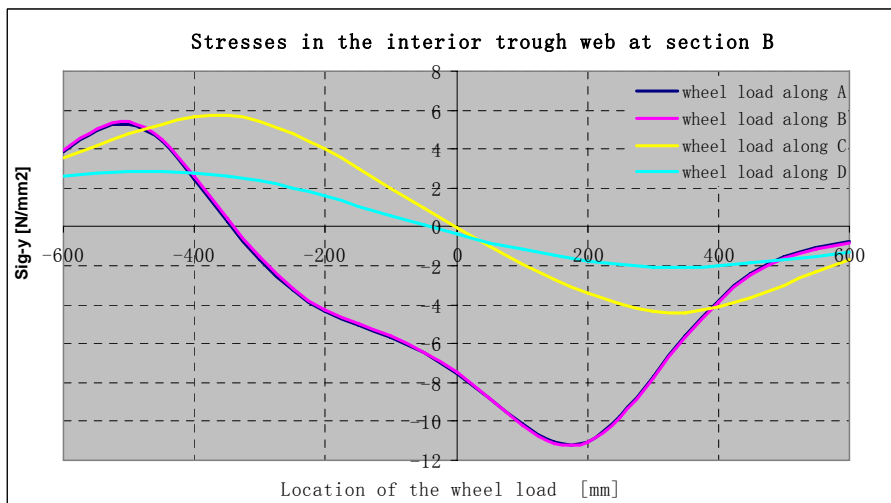
Transverse influence line in the trough web



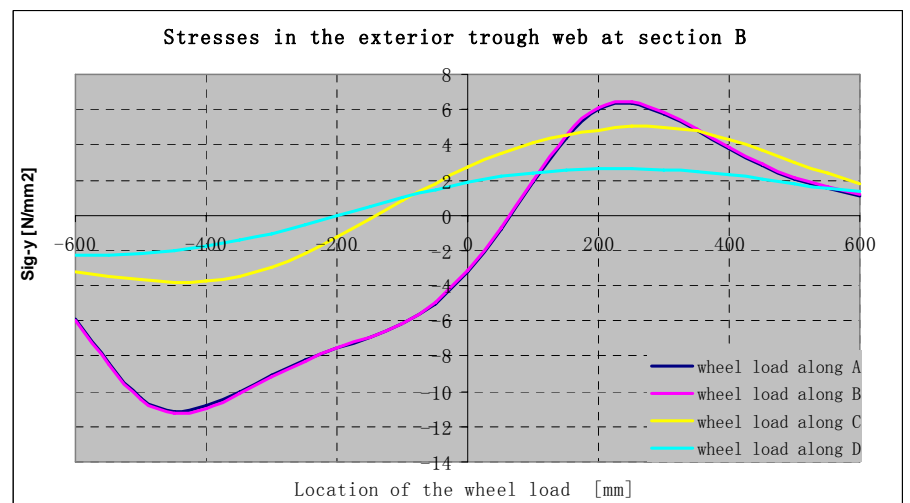
(a) Transverse influence line in the interior trough web at section A



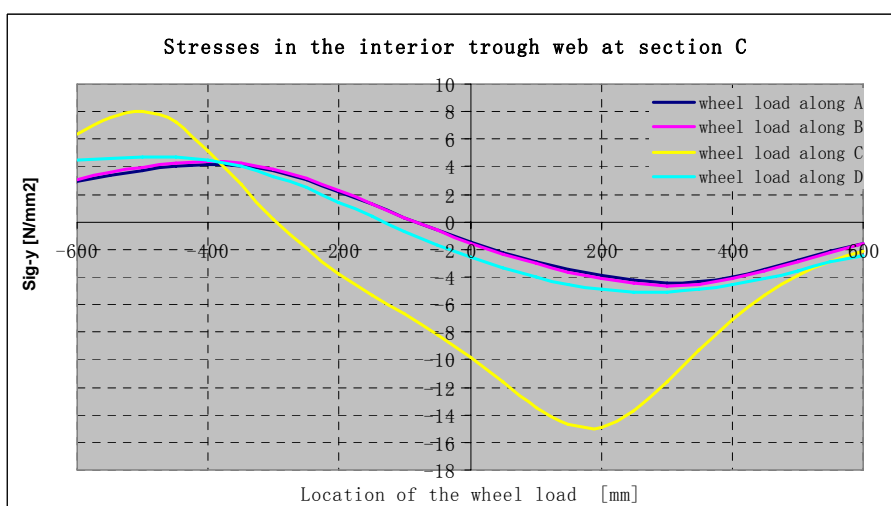
(b) Transverse influence line in the exterior trough web at section A



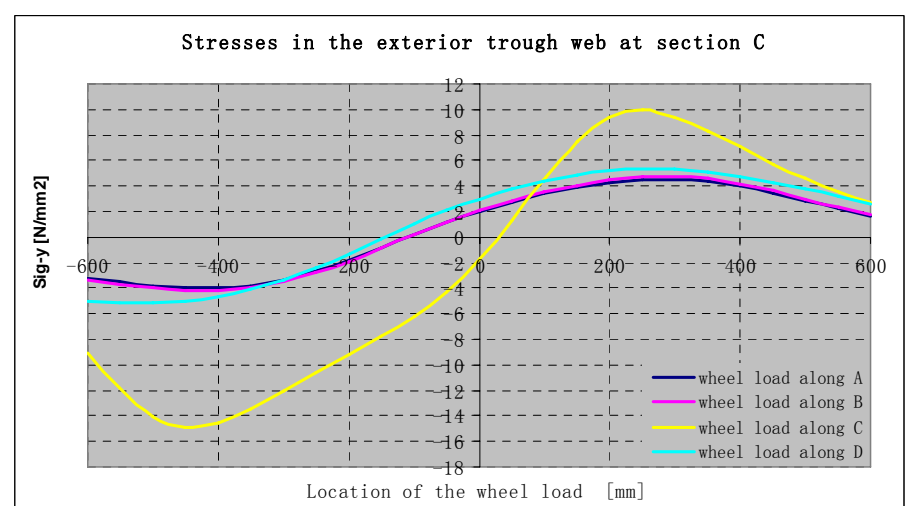
(c) Transverse influence line in the interior trough web at section B



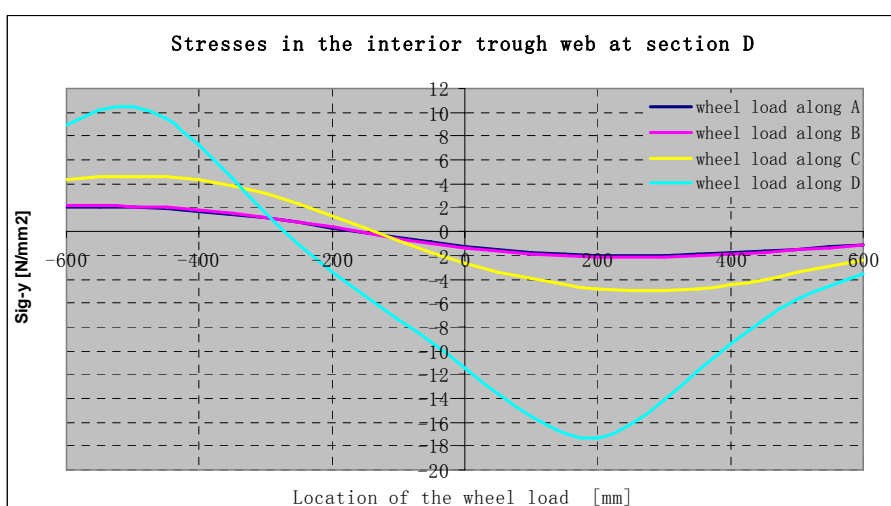
(d) Transverse influence line in the exterior trough web at section B



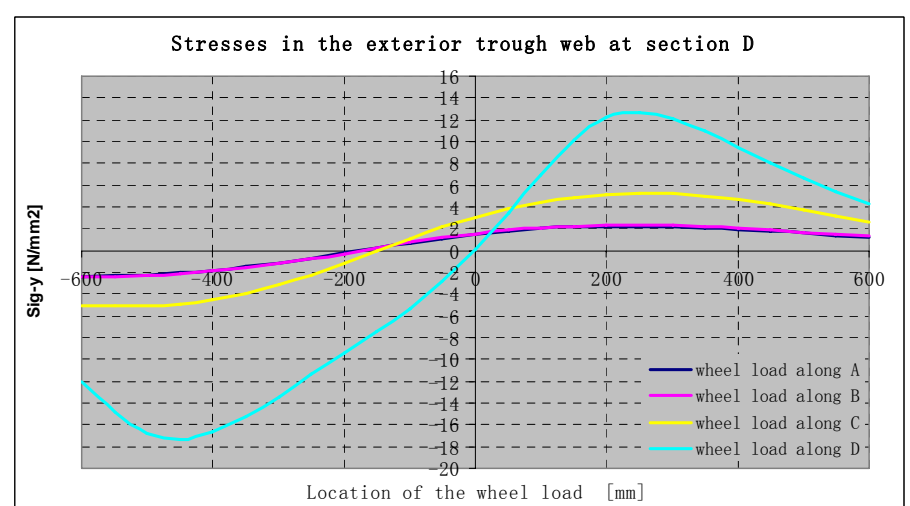
(e) Transverse influence line in the interior trough web at section C



(f) Transverse influence line in the exterior trough web at section C

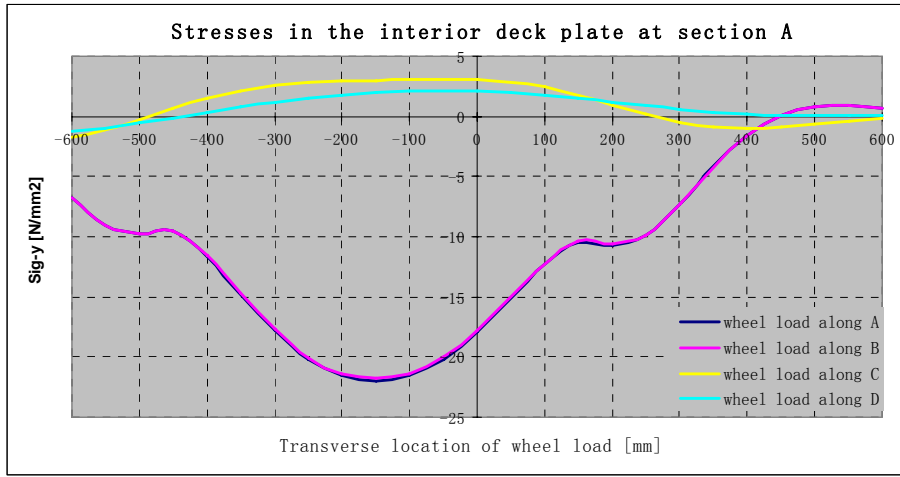


(g) Transverse influence line in the interior trough web at section D

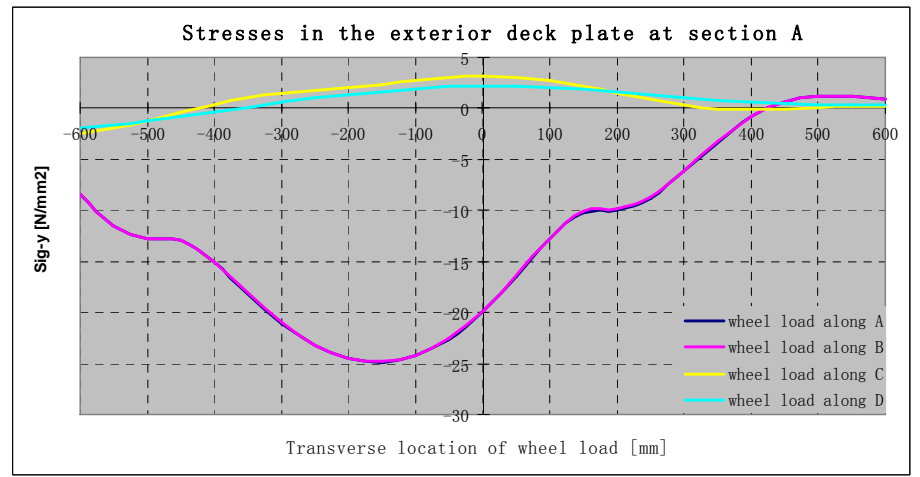


(h) Transverse influence line in the exterior trough web at section D

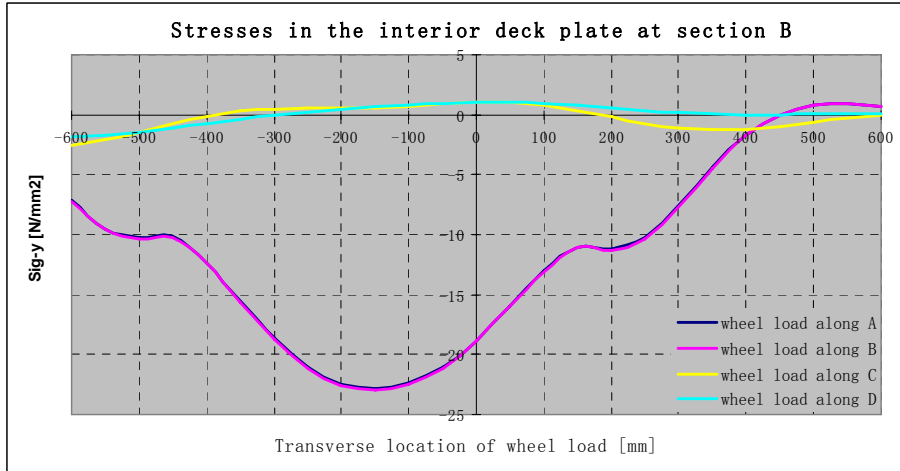
Transverse influence line in the deck plate



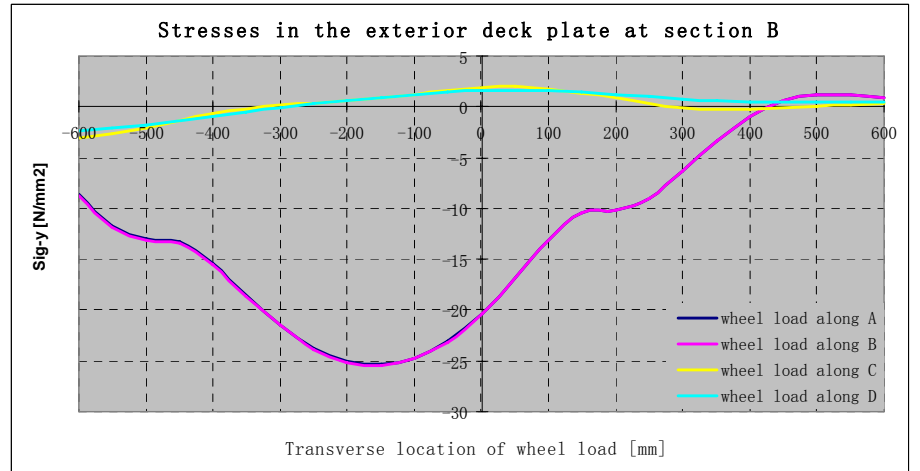
(a) Transverse influence line in the interior deck plate at section A



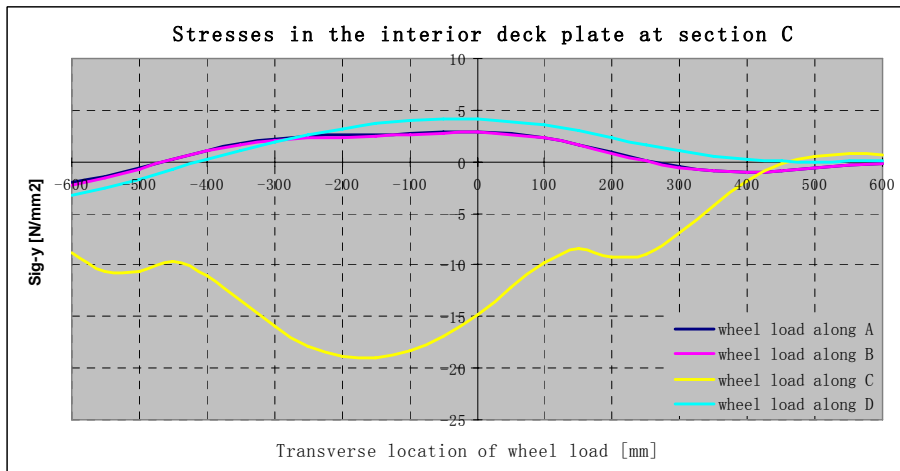
(b) Transverse influence line in the exterior deck plate at section A



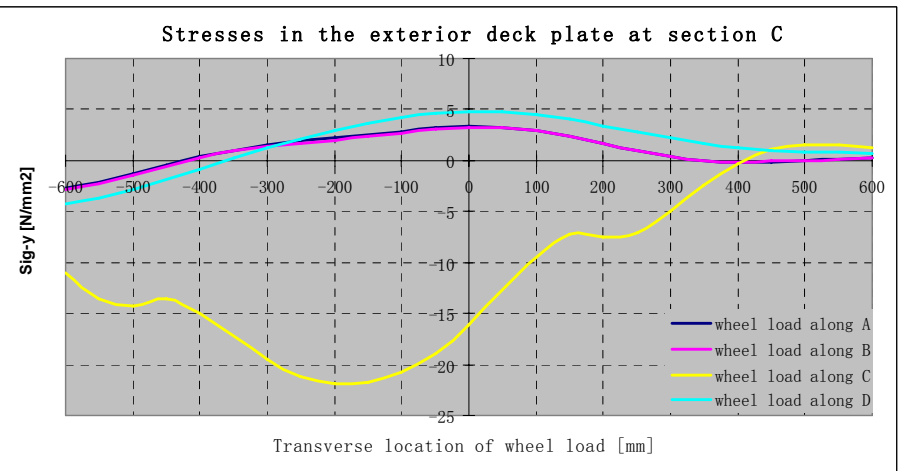
(c) Transverse influence line in the interior deck plate at section B



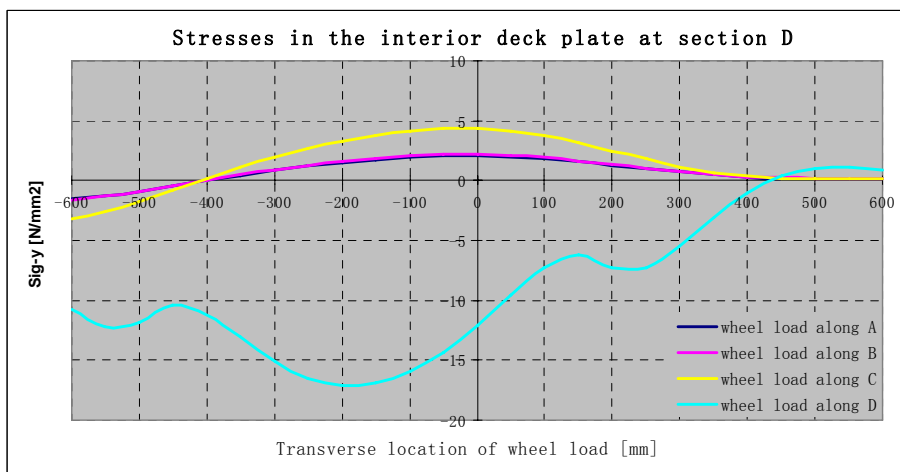
(d) Transverse influence line in the exterior deck plate at section B



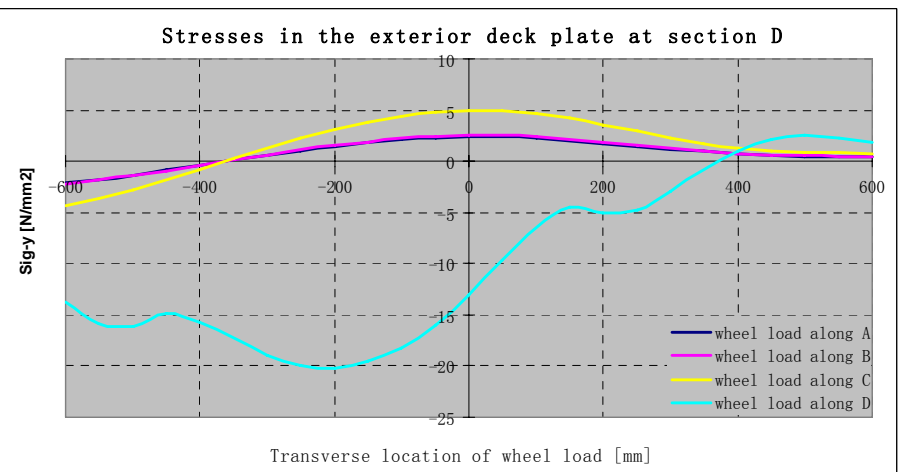
(e) Transverse influence line in the interior deck plate at section C



(f) Transverse influence line in the exterior deck plate at section C



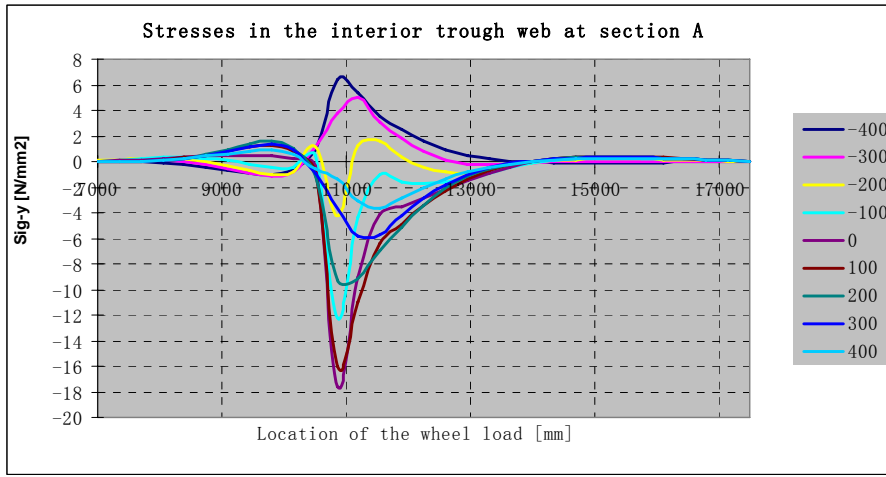
(g) Transverse influence line in the interior deck plate at section D



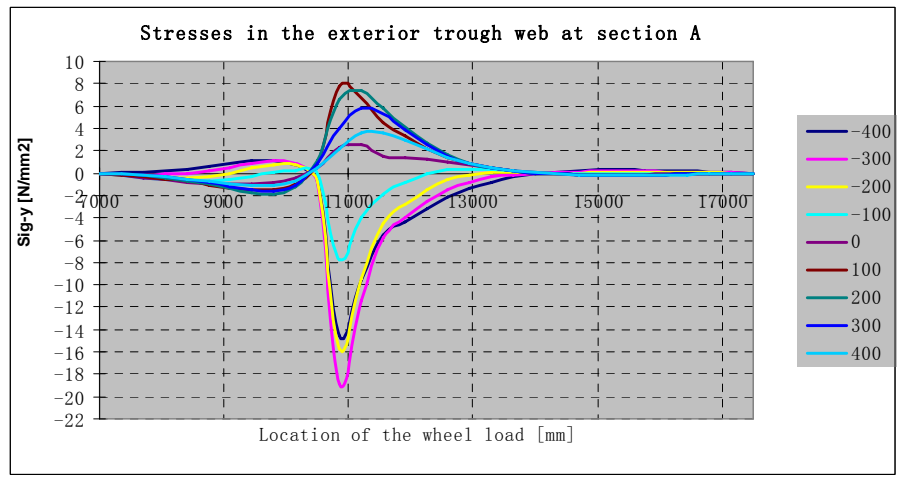
(h) Transverse influence line in the exterior deck plate at section D

Longitudinal influence line under wheel load C

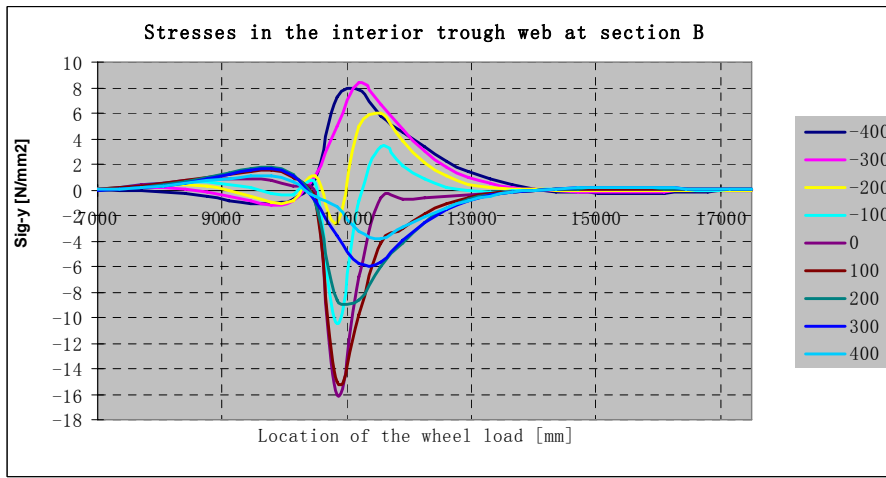
Longitudinal influence line in the trough web



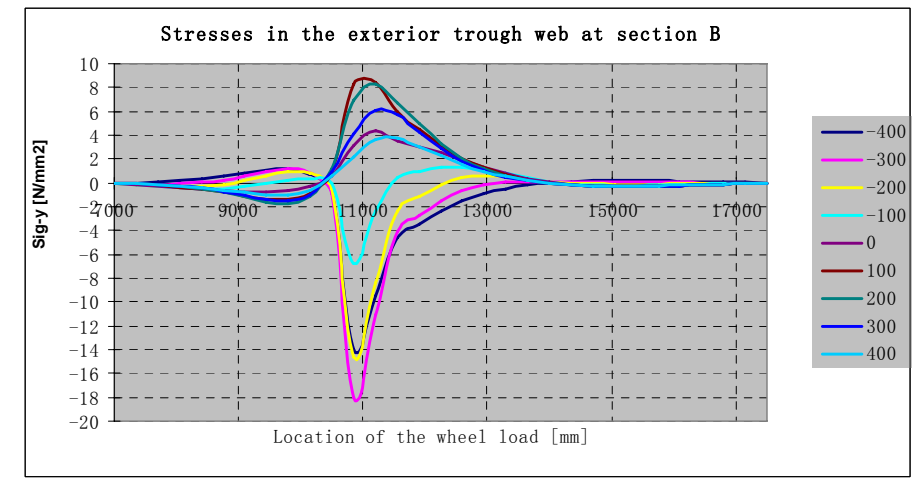
(a) Longitudinal influence line in the interior trough web at section A



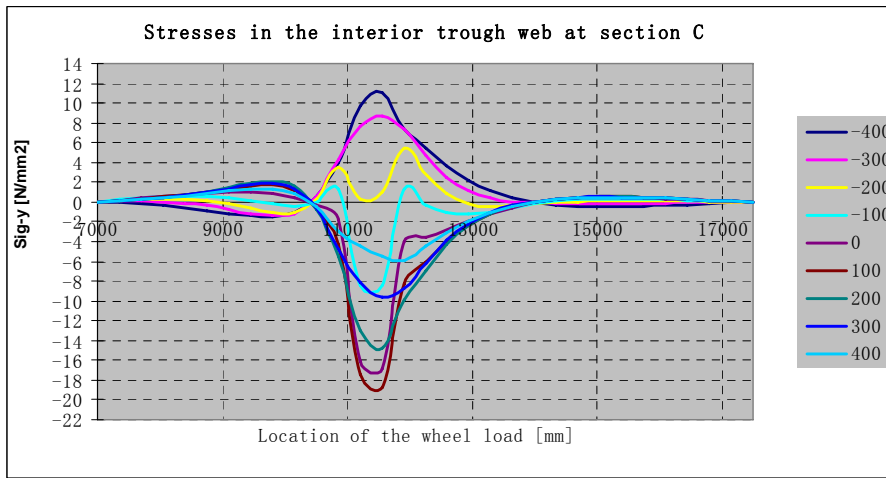
(b) Longitudinal influence line in the exterior trough web at section A



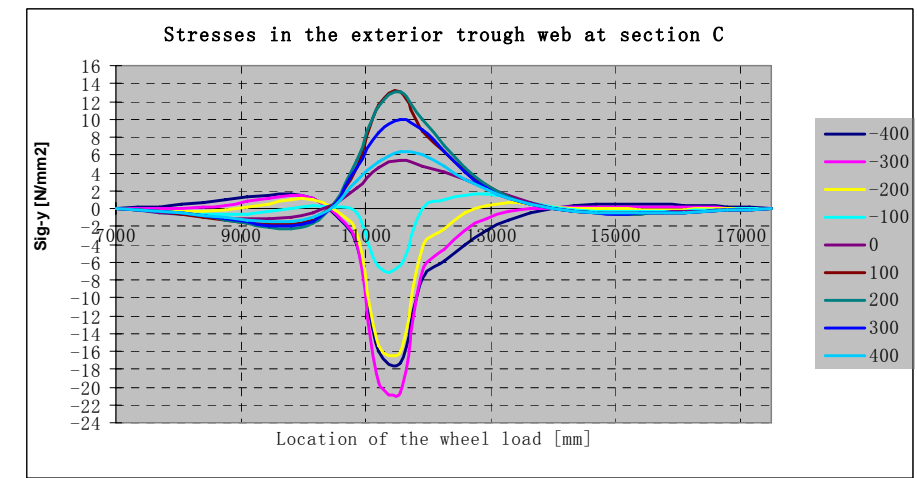
(c) Longitudinal influence line in the interior trough web at section B



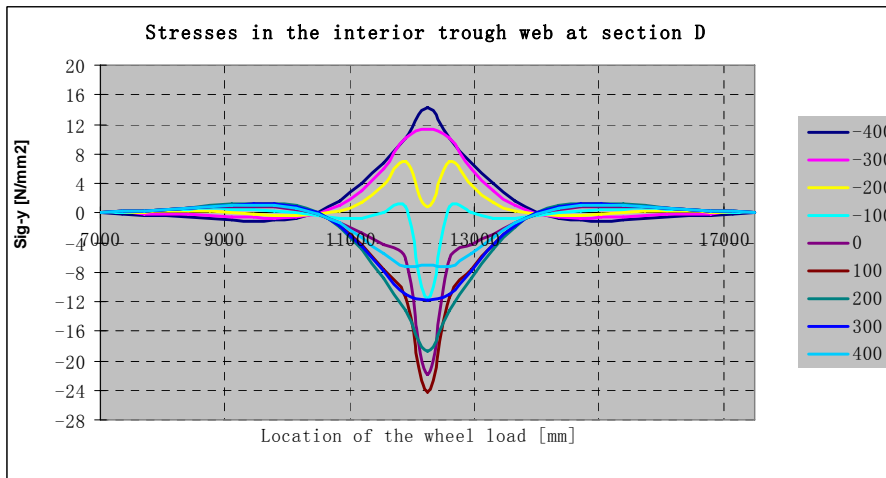
(d) Longitudinal influence line in the exterior trough web at section B



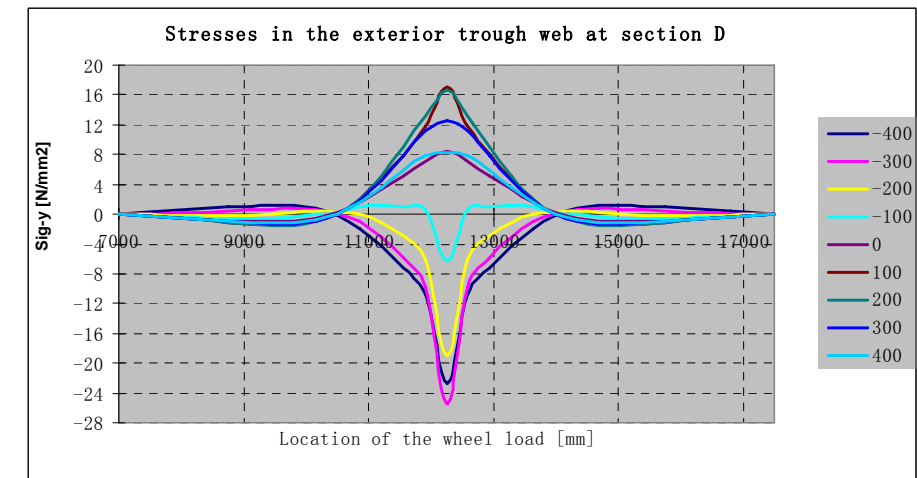
(e) Longitudinal influence line in the interior trough web at section C



(f) Longitudinal influence line in the exterior trough web at section C

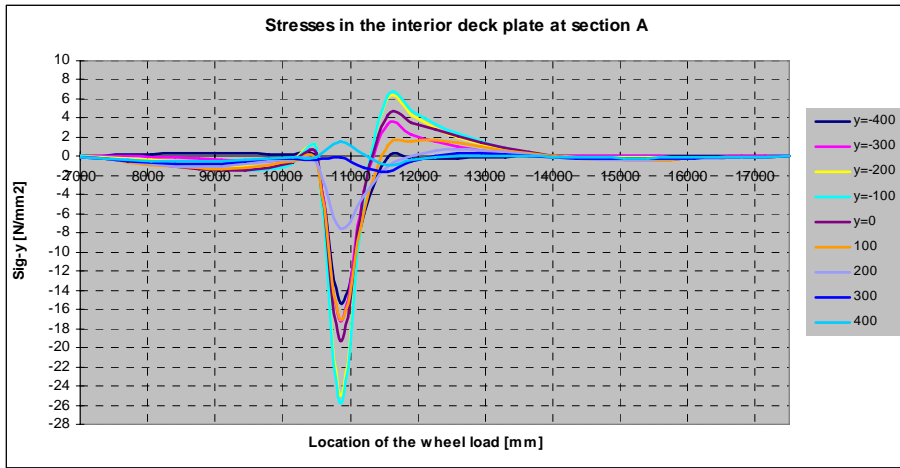


(g) Longitudinal influence line in the interior trough web at section D

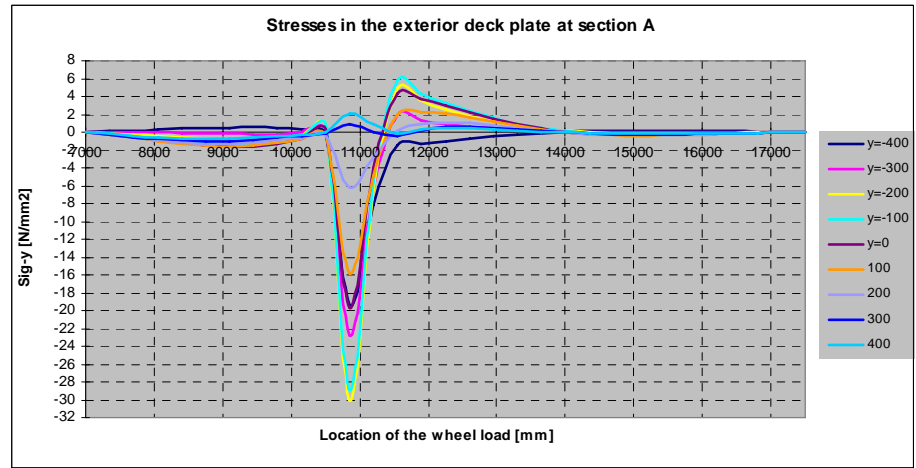


(h) Longitudinal influence line in the exterior trough web at section D

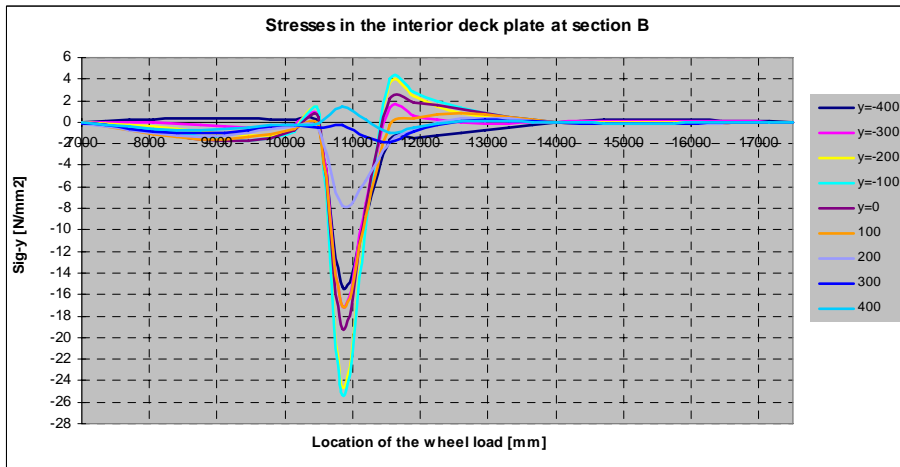
Longitudinal influence line in the deck plate



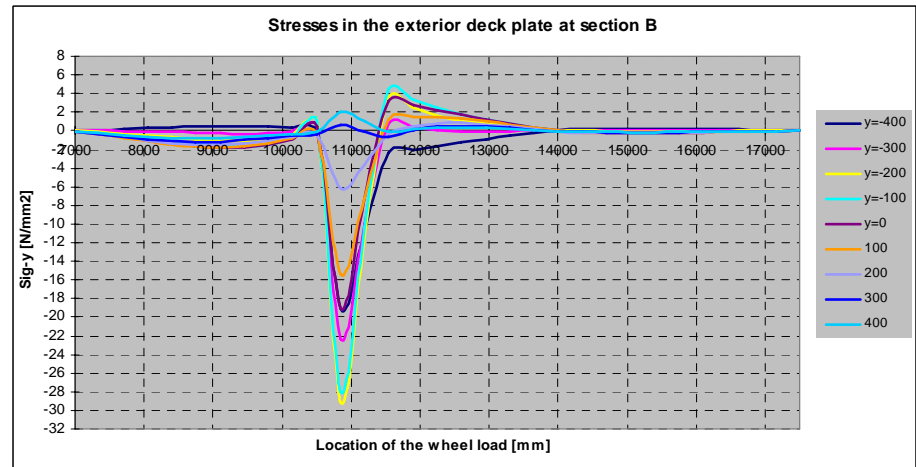
(a) Longitudinal influence line in the interior deck plate at section A



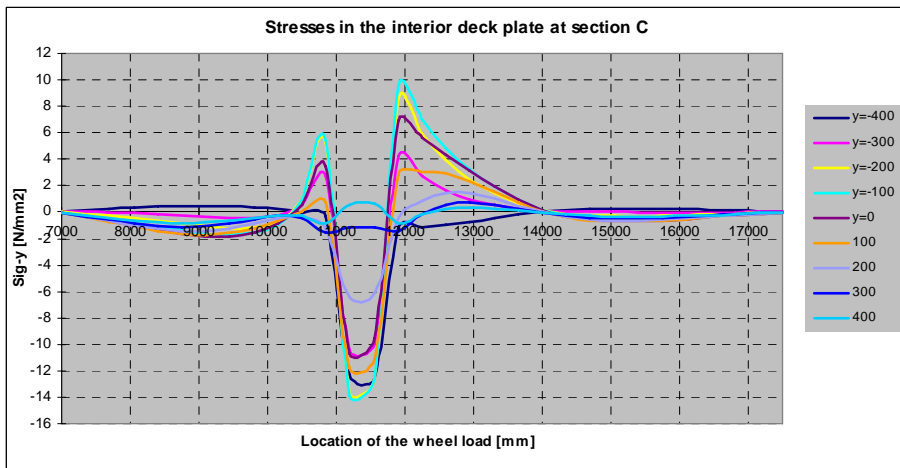
(b) Longitudinal influence line in the exterior deck plate at section A



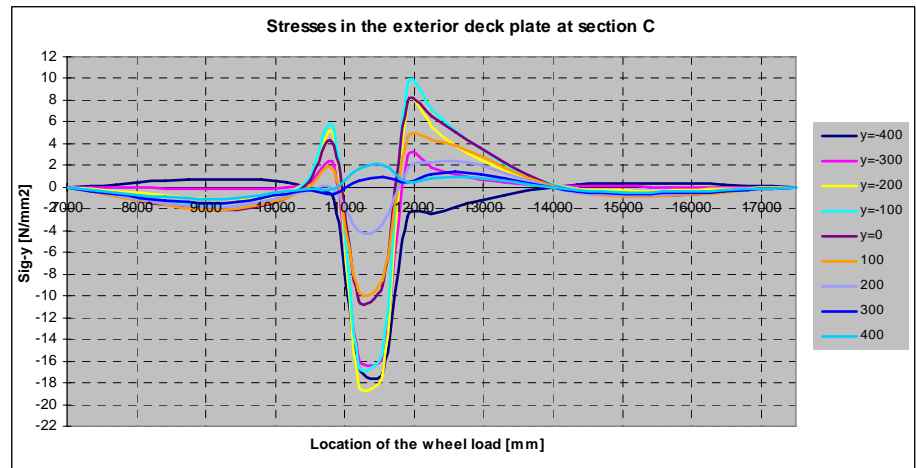
(c) Longitudinal influence line in the interior deck plate at section B



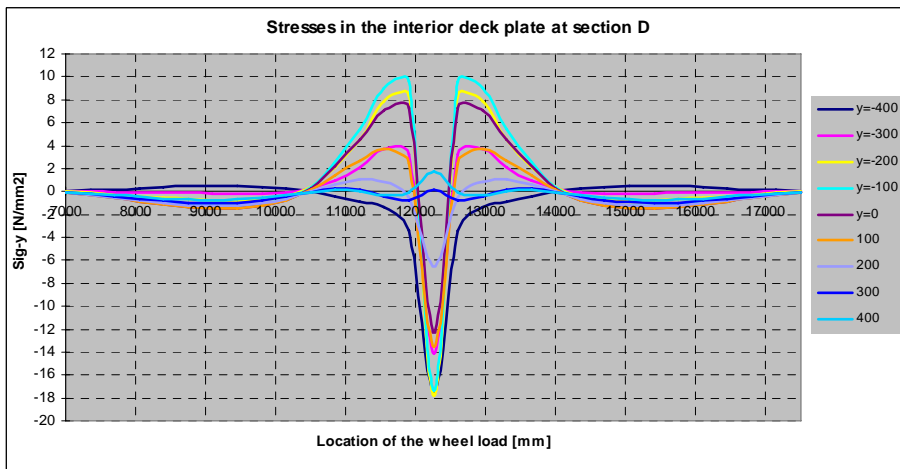
(d) Longitudinal influence line in the exterior deck plate at section B



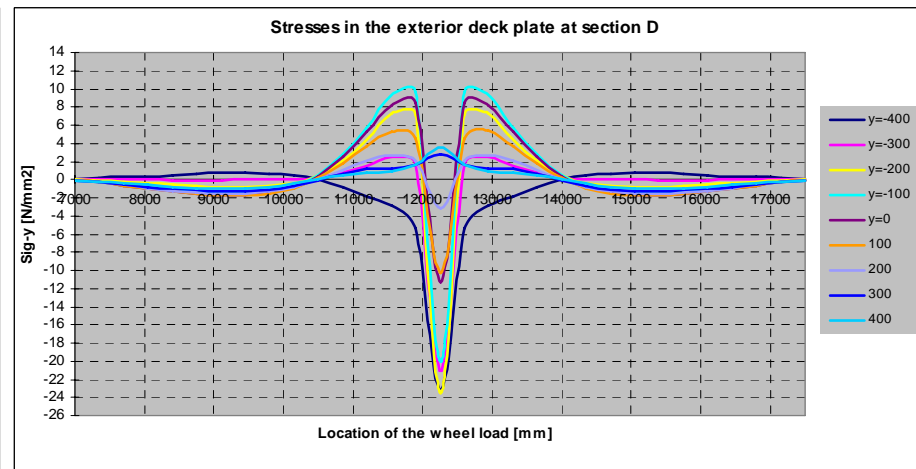
(e) Longitudinal influence line in the interior deck plate at section C



(f) Longitudinal influence line in the exterior deck plate at section C



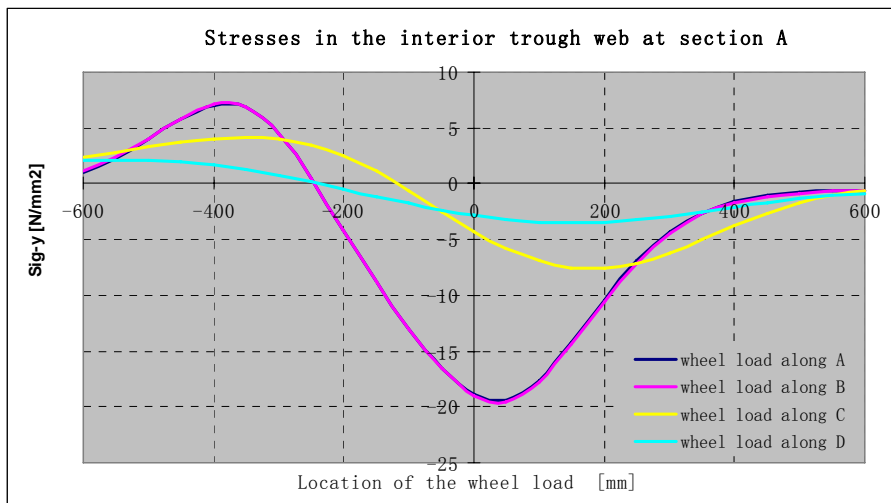
(g) Longitudinal influence line in the interior deck plate at section D



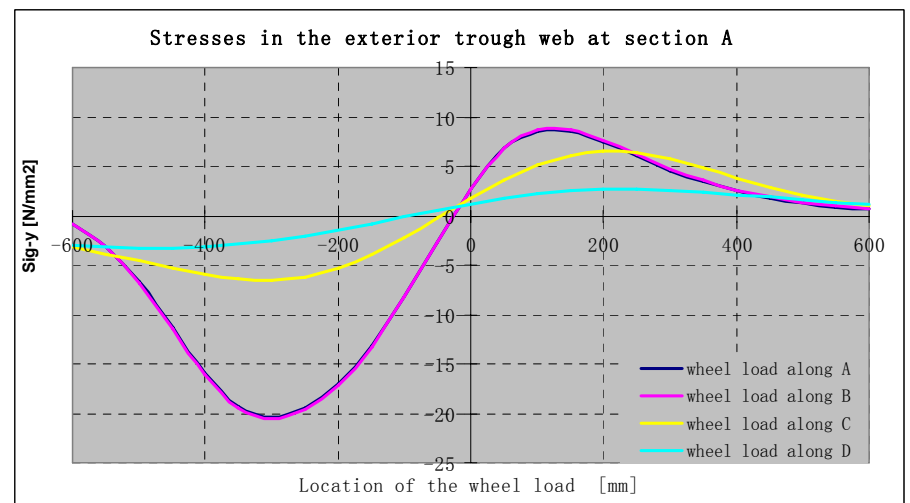
(h) Longitudinal influence line in the exterior deck plate at section D

Transverse influence line under wheel load C

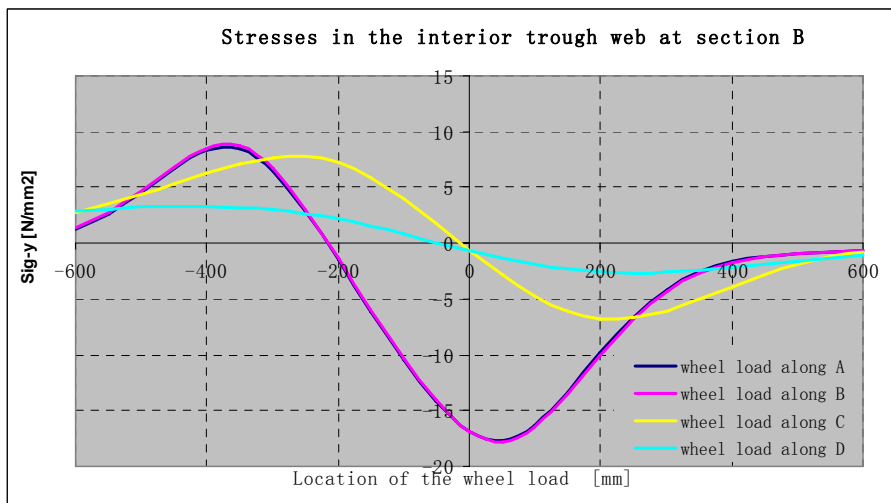
Transverse influence line in the trough web



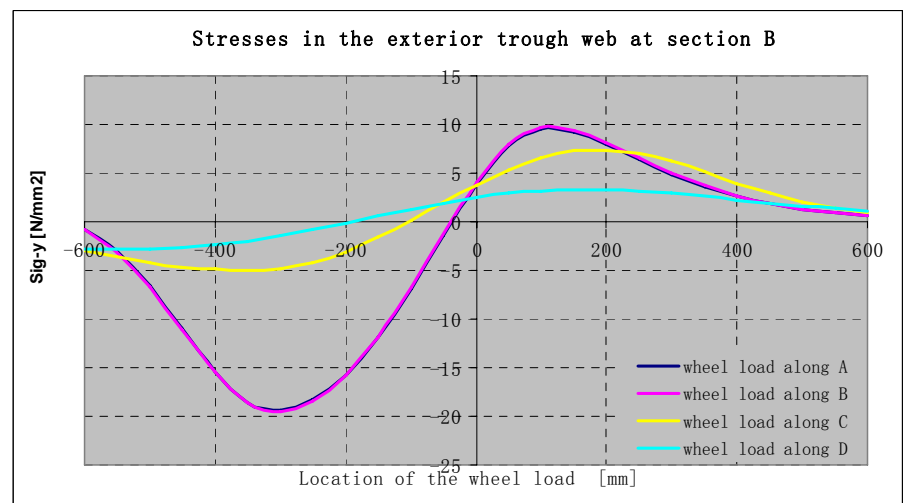
(a) Transverse influence line in the interior trough web at section A



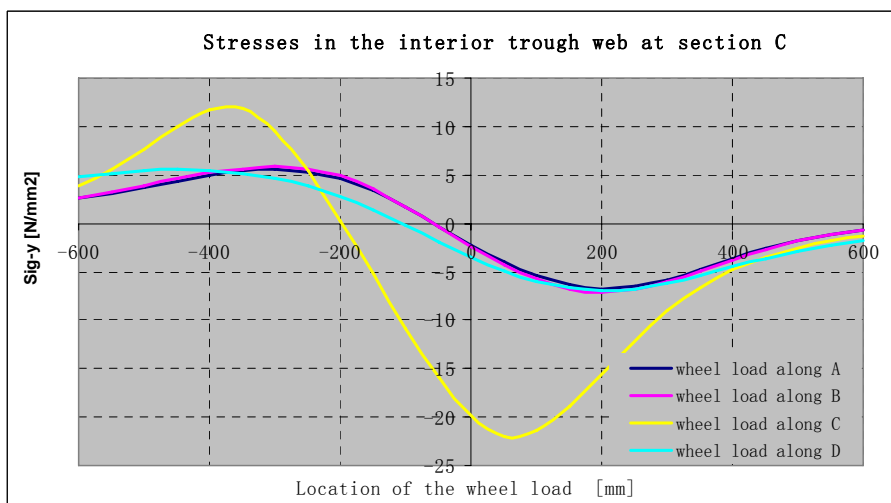
(b) Transverse influence line in the exterior trough web at section A



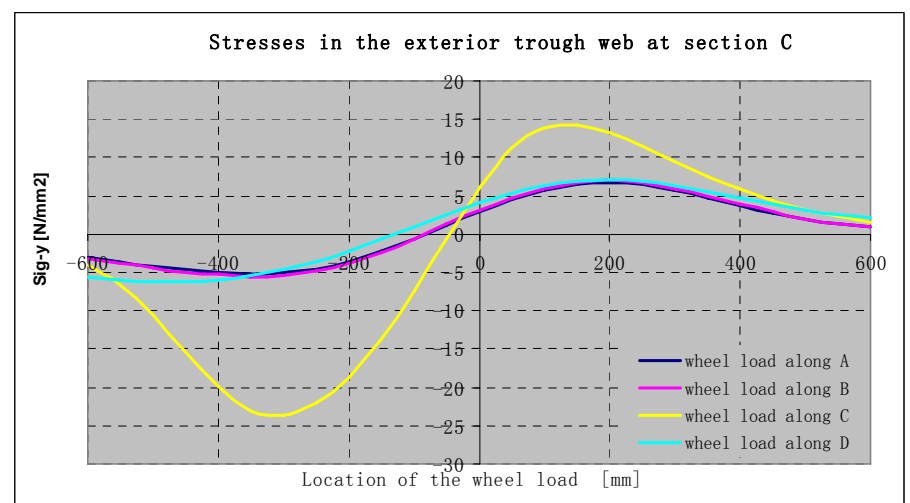
(c) Transverse influence line in the interior trough web at section B



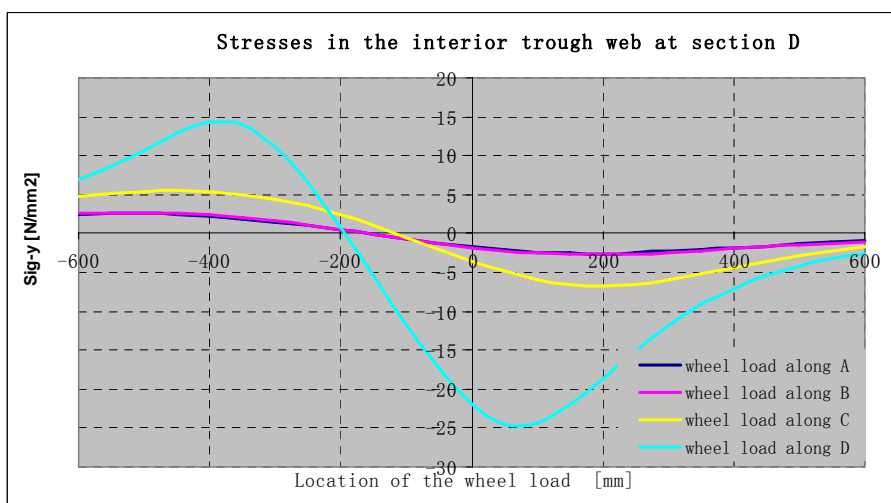
(d) Transverse influence line in the exterior trough web at section B



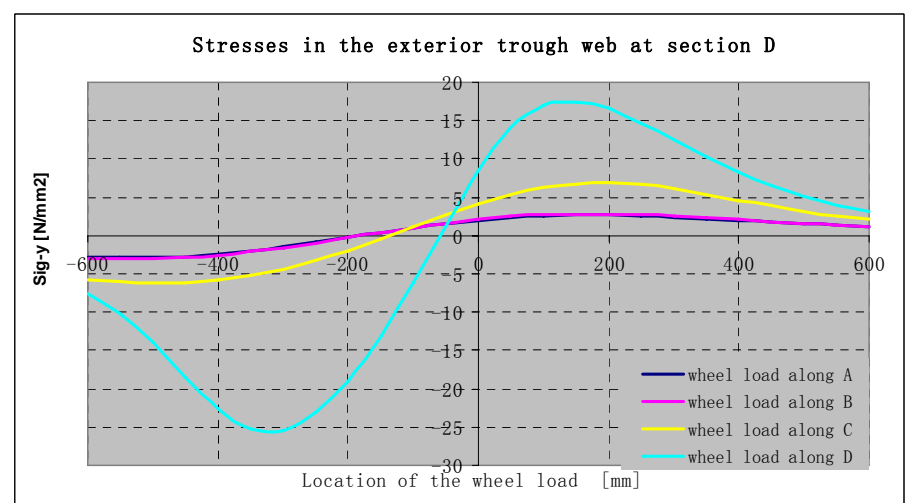
(e) Transverse influence line in the interior trough web at section C



(f) Transverse influence line in the exterior trough web at section C

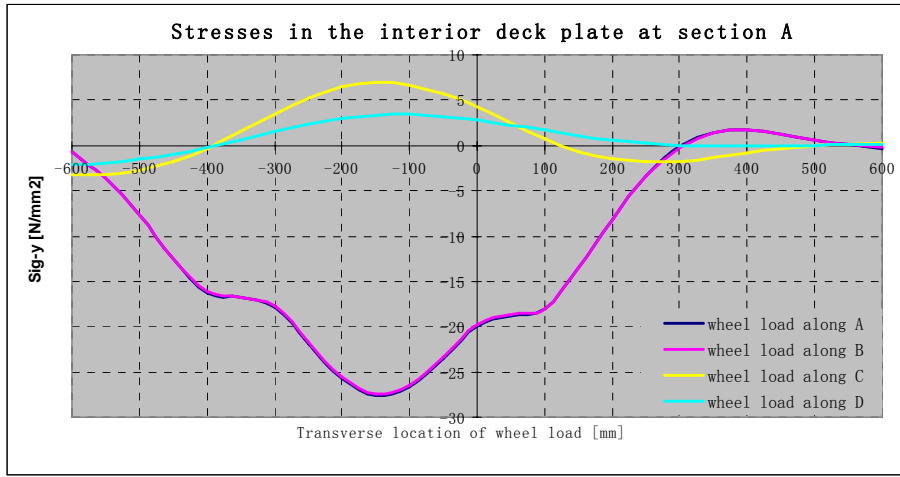


(g) Transverse influence line in the interior trough web at section D

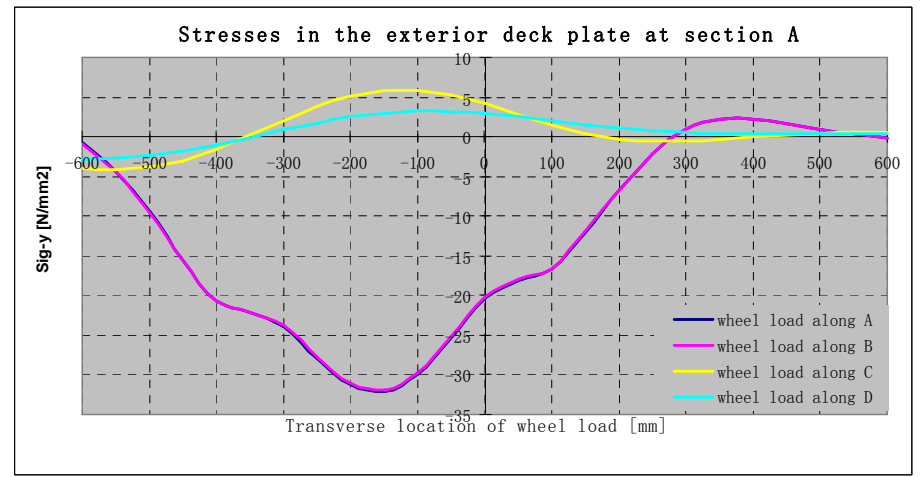


(h) Transverse influence line in the exterior trough web at section D

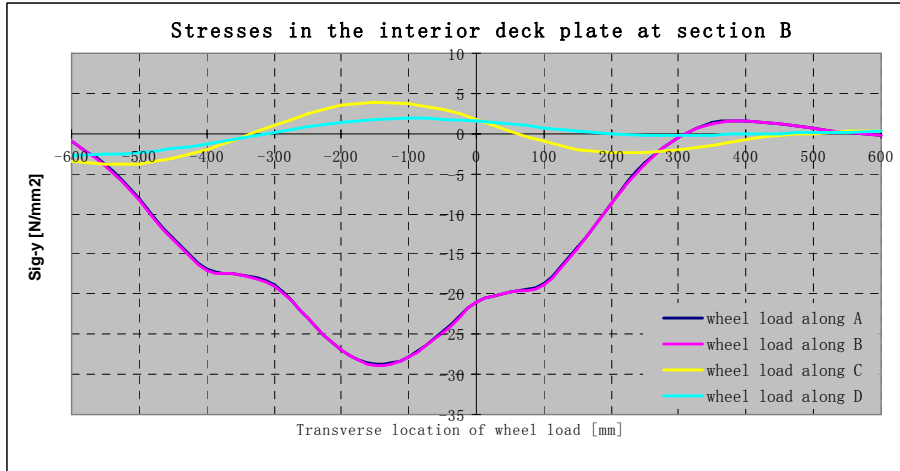
Transverse influence line in the deck plate



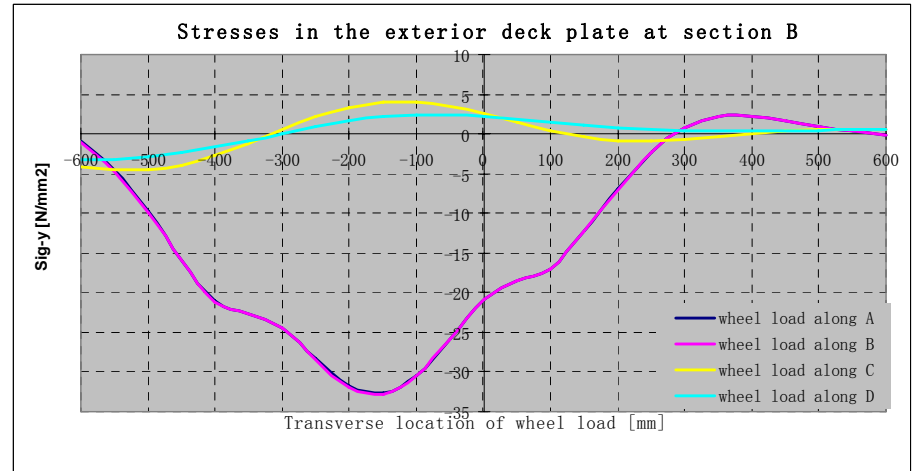
(a) Transverse influence line in the interior deck plate at section A



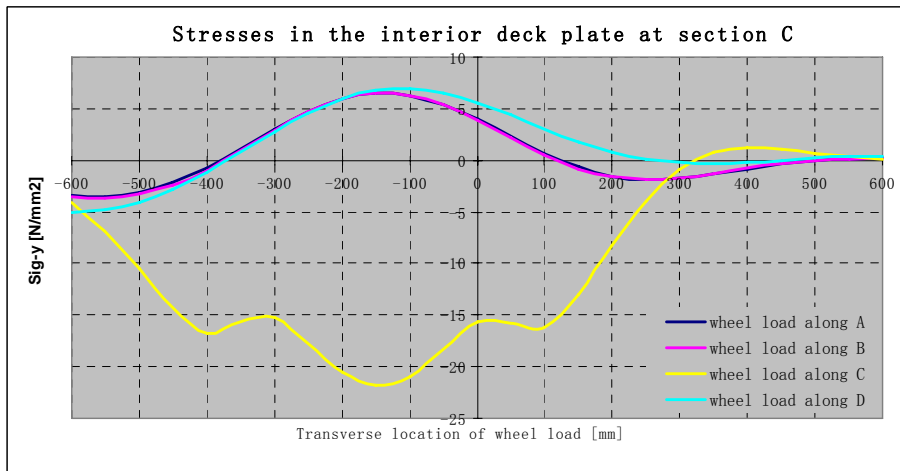
(b) Transverse influence line in the exterior deck plate at section A



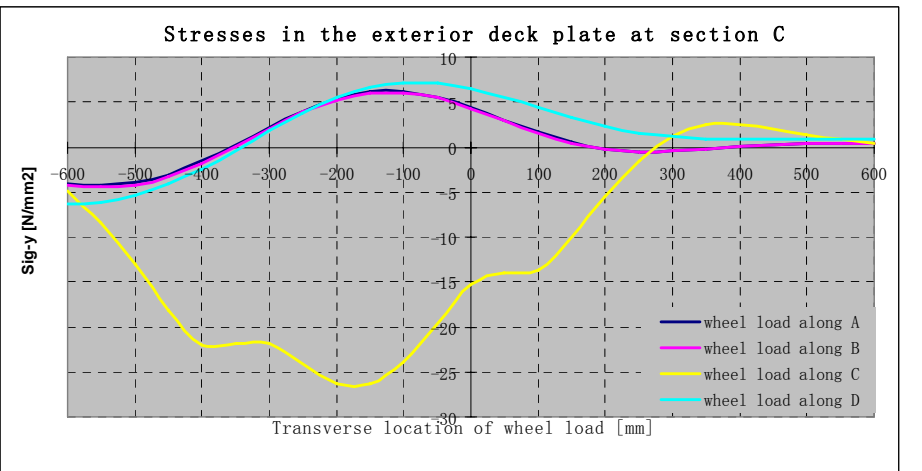
(c) Transverse influence line in the interior deck plate at section B



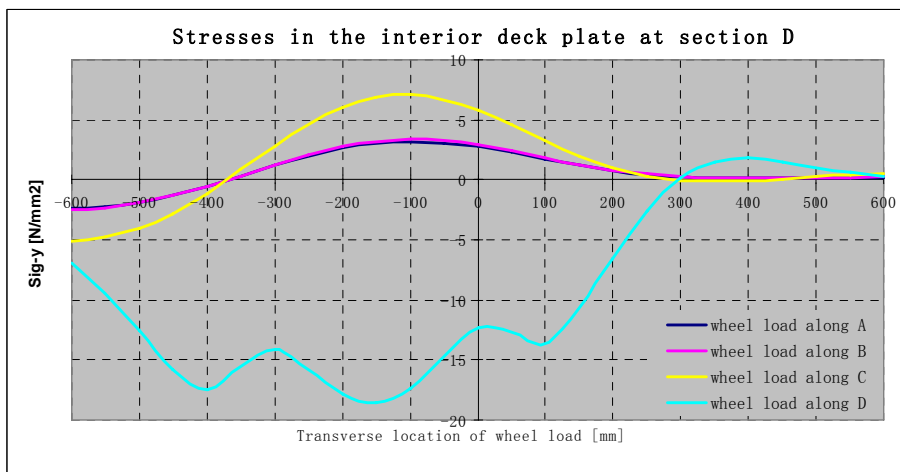
(d) Transverse influence line in the exterior deck plate at section B



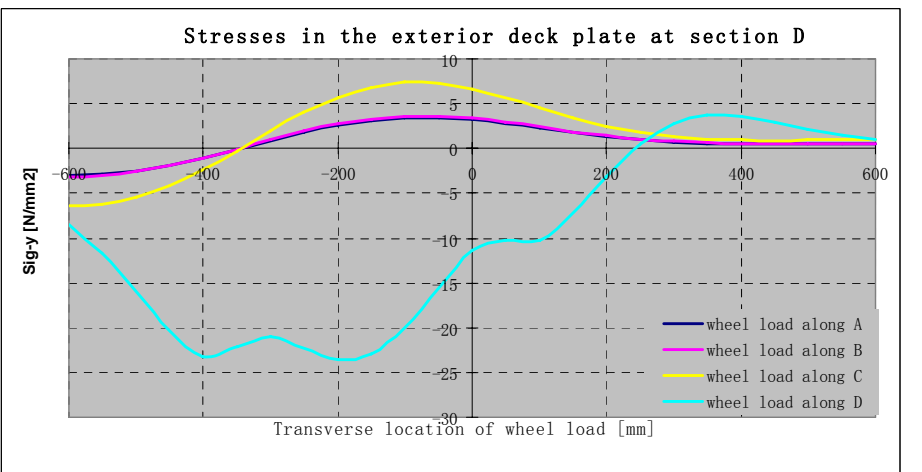
(e) Transverse influence line in the interior deck plate at section C



(f) Transverse influence line in the exterior deck plate at section C



(g) Transverse influence line in the interior deck plate at section D

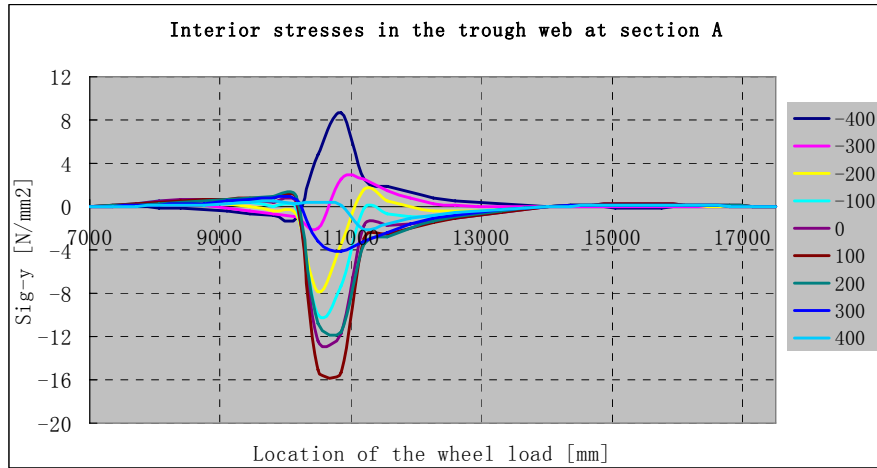


(h) Transverse influence line in the exterior deck plate at section D

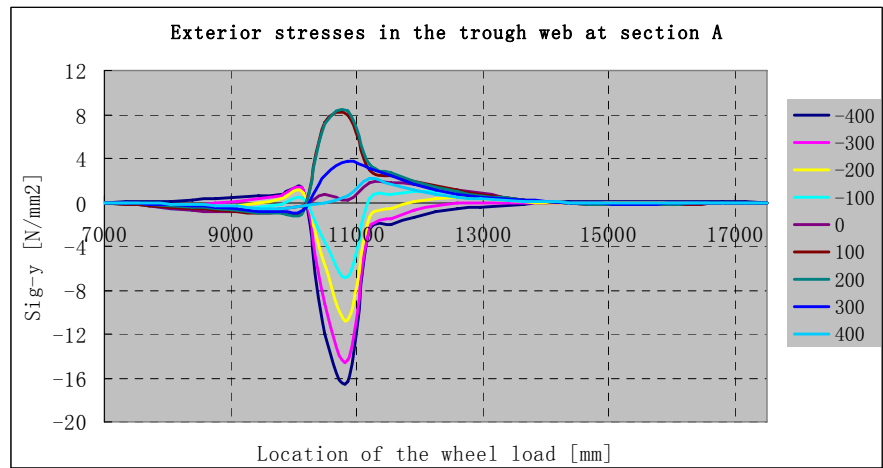
3. Influence lines in model C

Longitudinal influence lines under axle load B

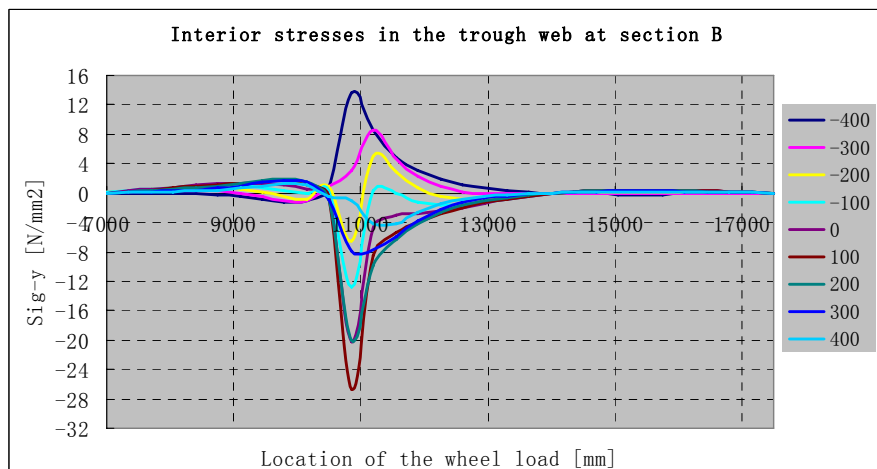
Longitudinal influence line in the trough web



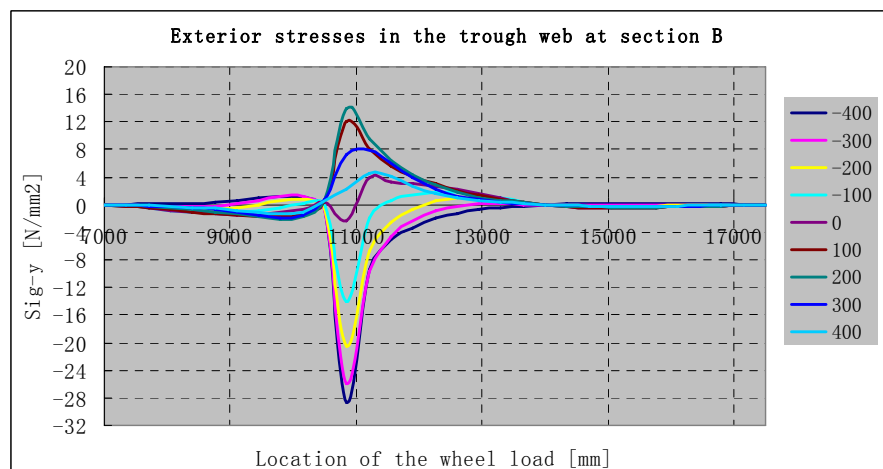
(a) Longitudinal influence line in the interior trough web at section A



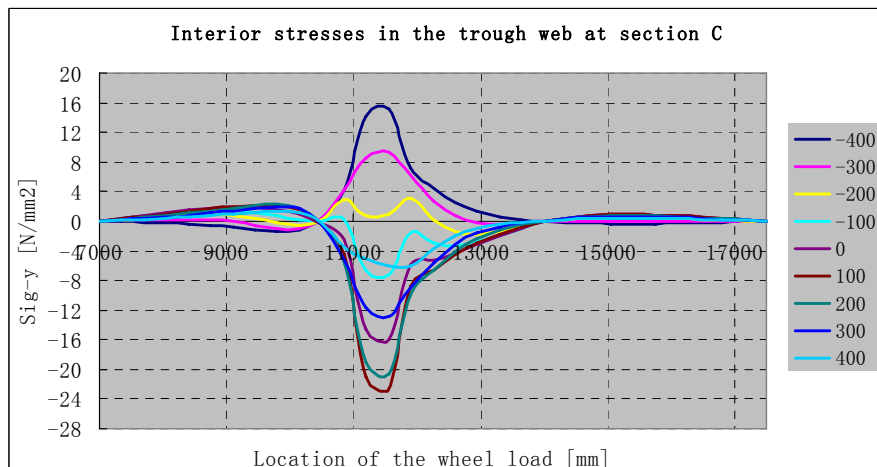
(b) Longitudinal influence line in the exterior trough web at section A



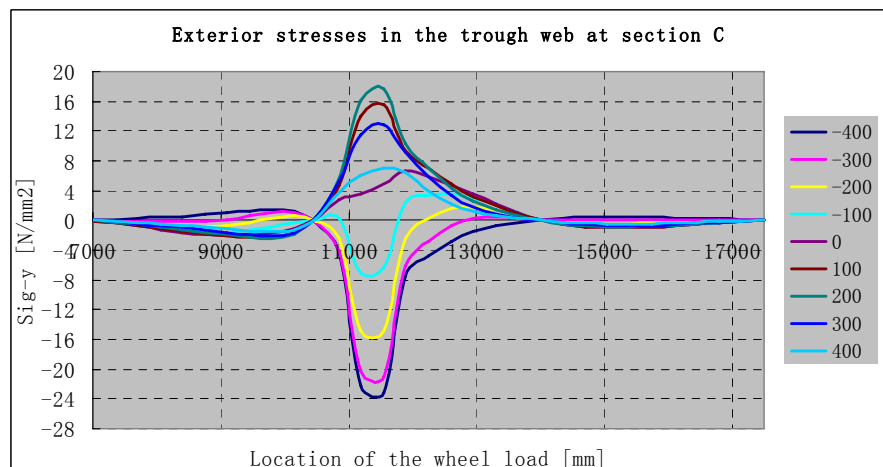
(c) Longitudinal influence line in the interior trough web at section B



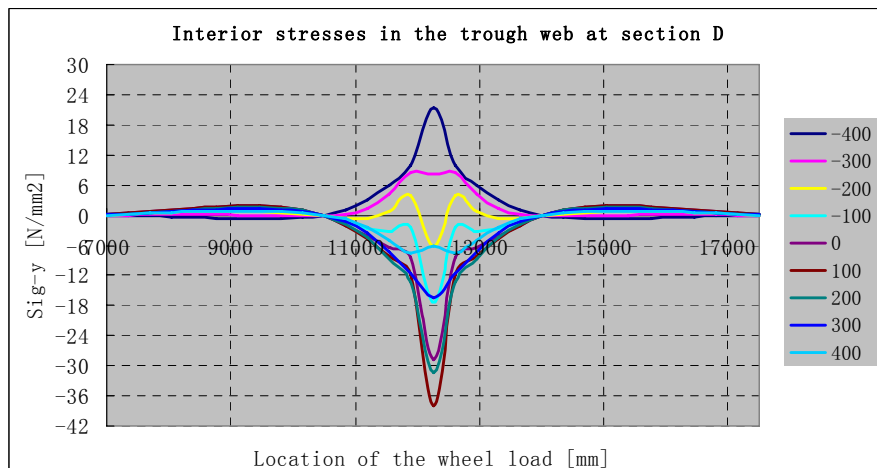
(d) Longitudinal influence line in the exterior trough web at section B



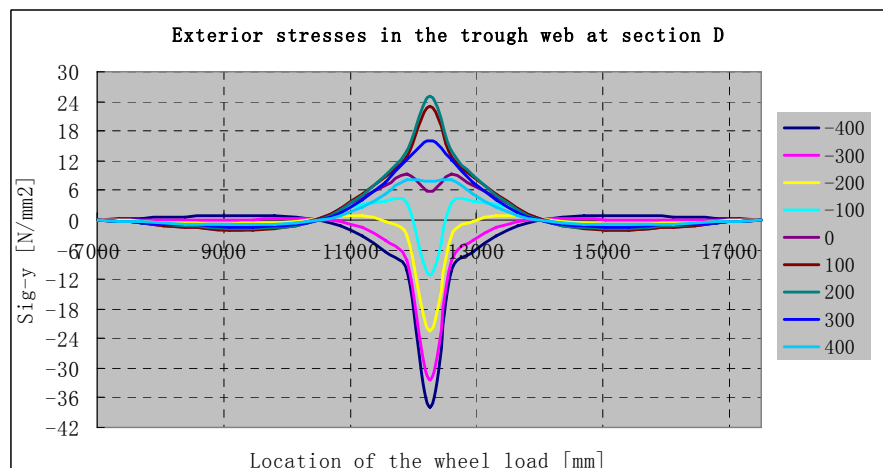
(e) Longitudinal influence line in the interior trough web at section C



(f) Longitudinal influence line in the exterior trough web at section C

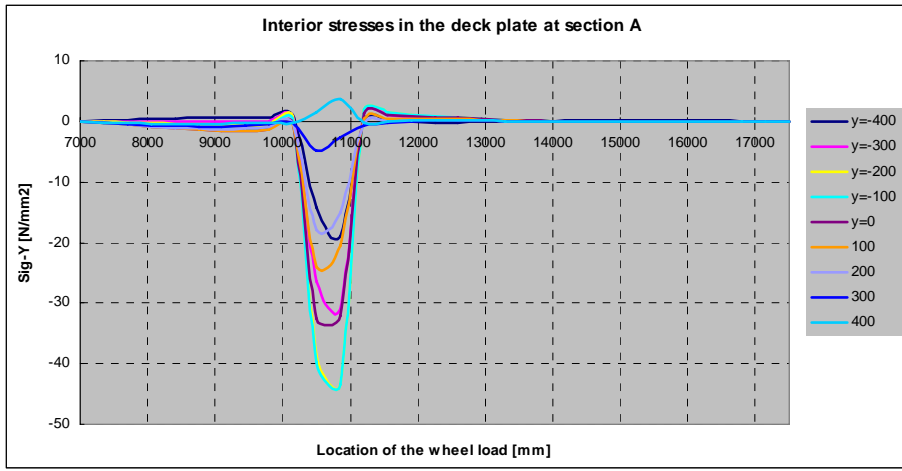


(g) Longitudinal influence line in the interior trough web at section D

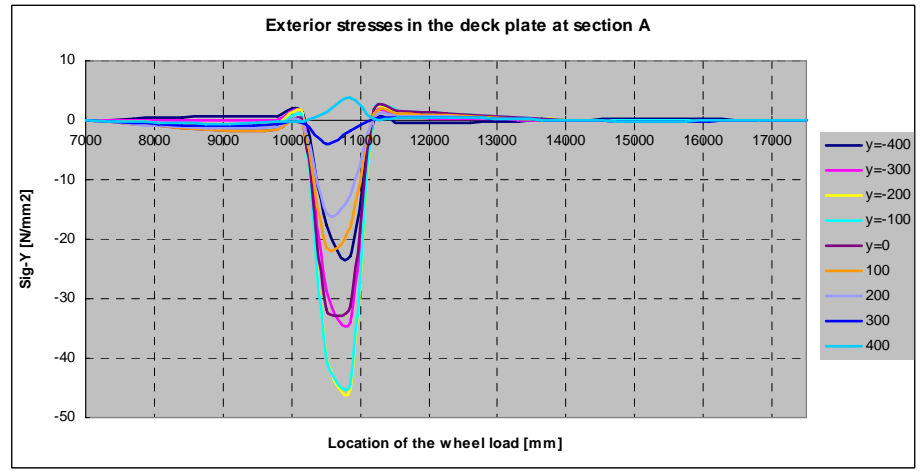


(h) Longitudinal influence line in the exterior trough web at section D

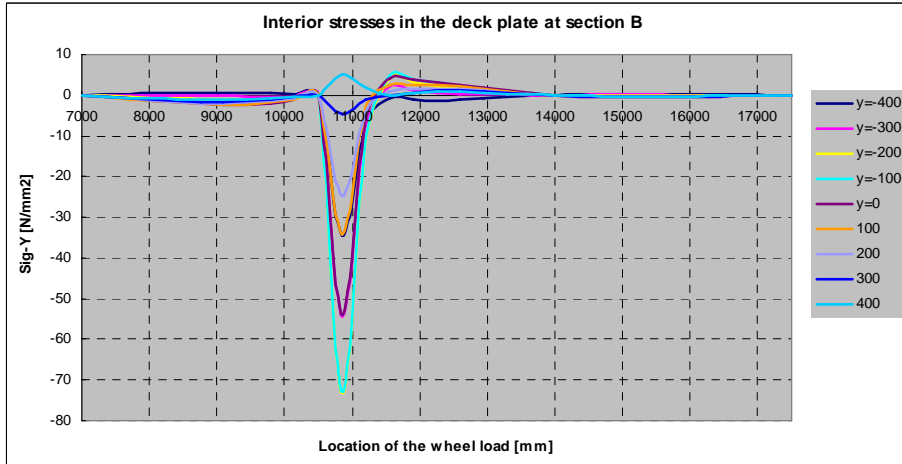
Longitudinal influence line in the deck plate



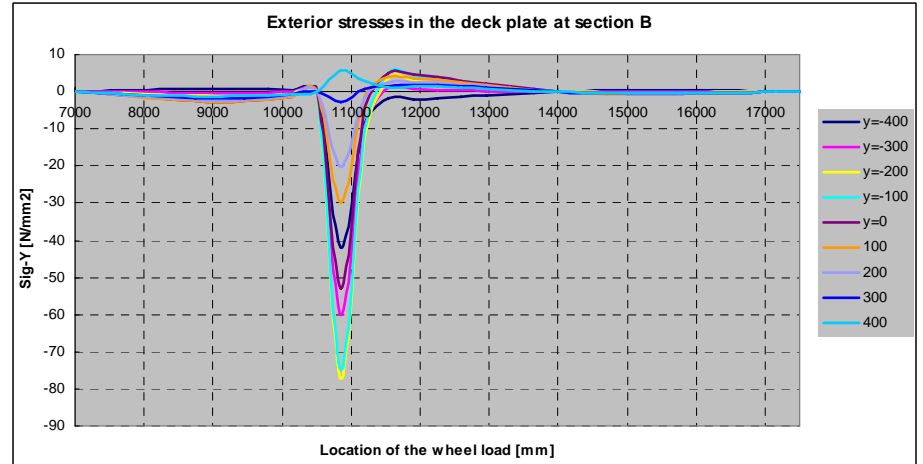
(a) Longitudinal influence line in the interior deck plate at section A



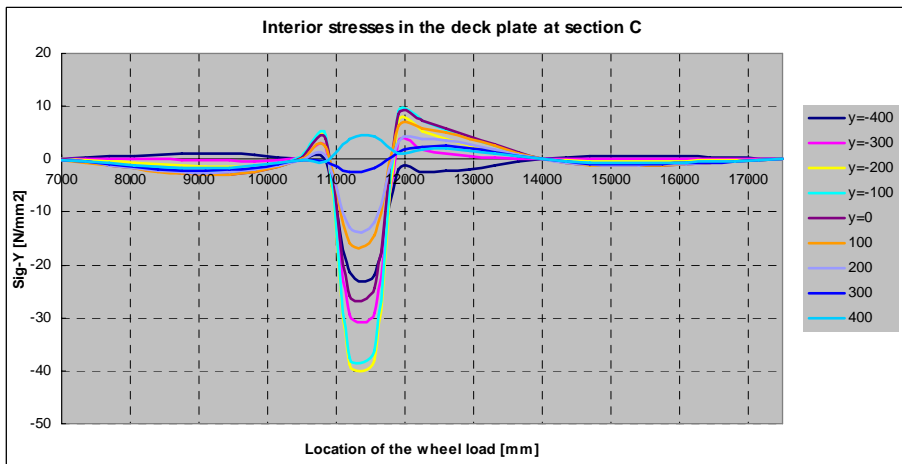
(b) Longitudinal influence line in the exterior deck plate at section A



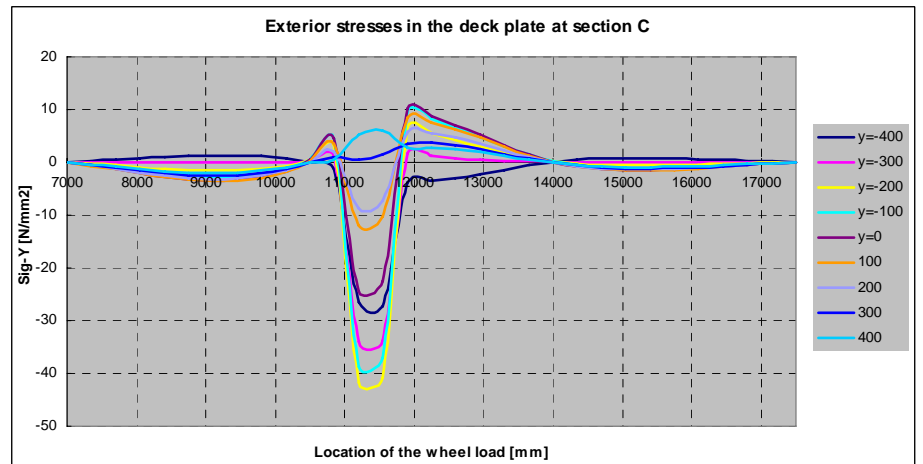
(c) Longitudinal influence line in the interior deck plate at section B



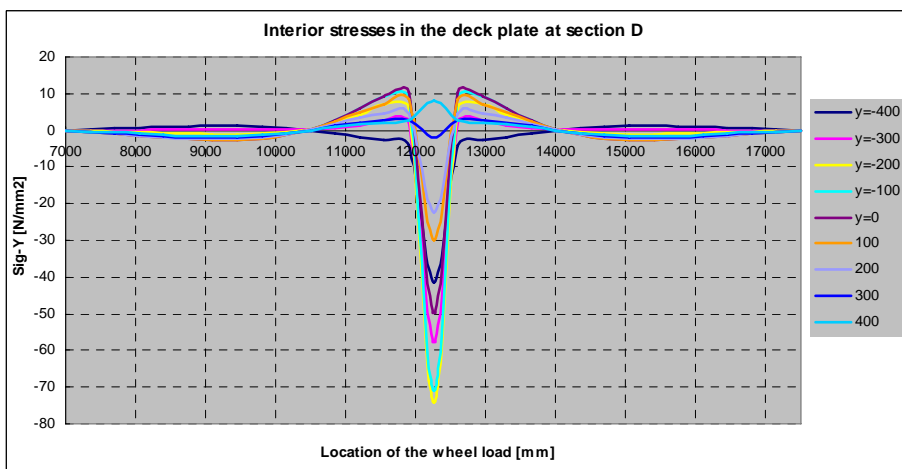
(d) Longitudinal influence line in the exterior deck plate at section B



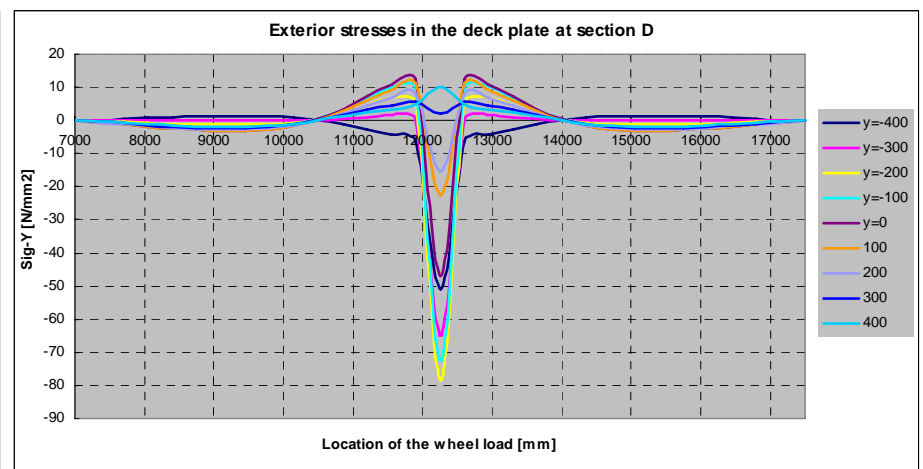
(e) Longitudinal influence line in the interior deck plate at section C



(f) Longitudinal influence line in the exterior deck plate at section C



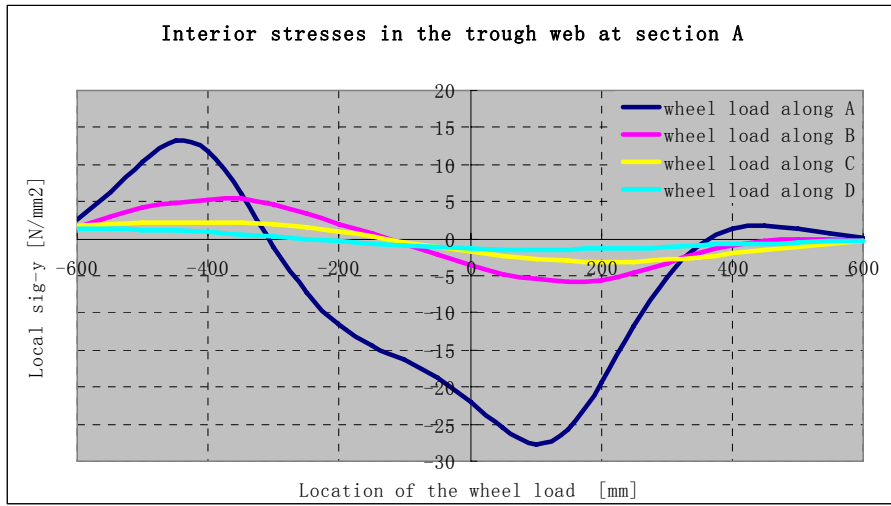
(g) Longitudinal influence line in the interior deck plate at section D



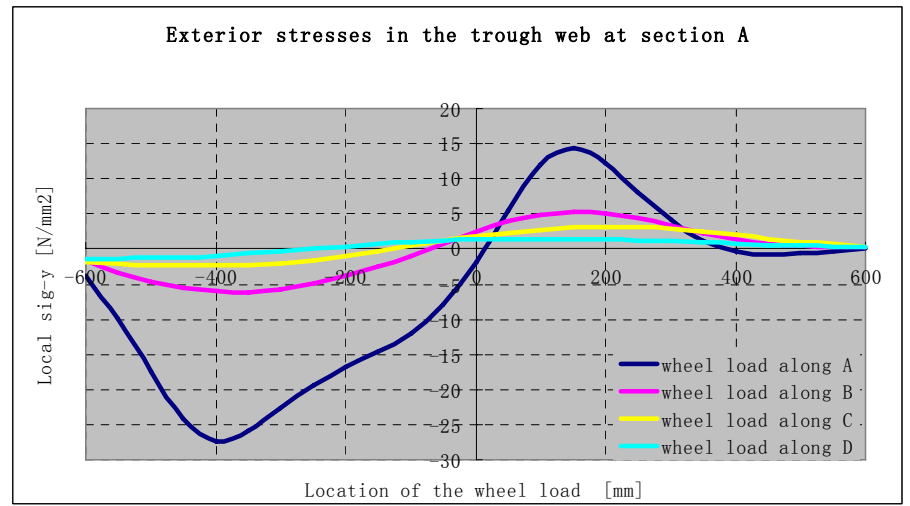
(h) Longitudinal influence line in the exterior deck plate at section D

Transverse influence lines under axle load B

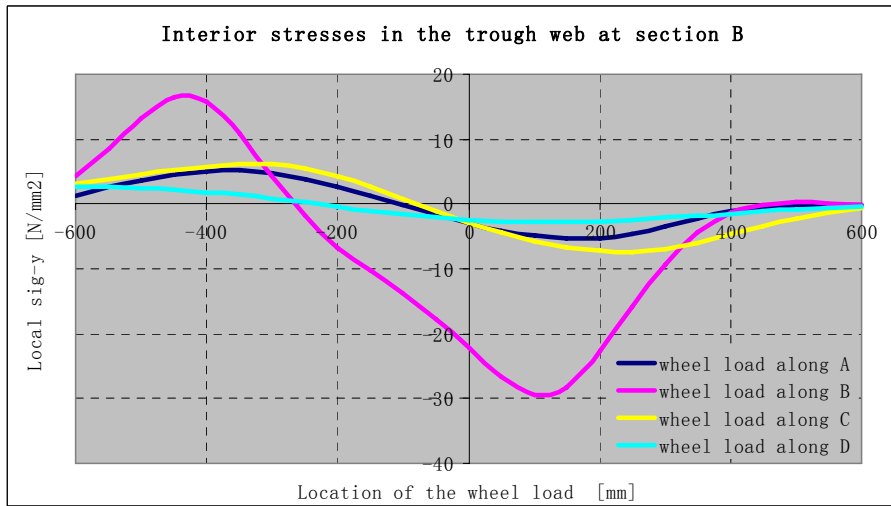
Transverse influence line in the trough web



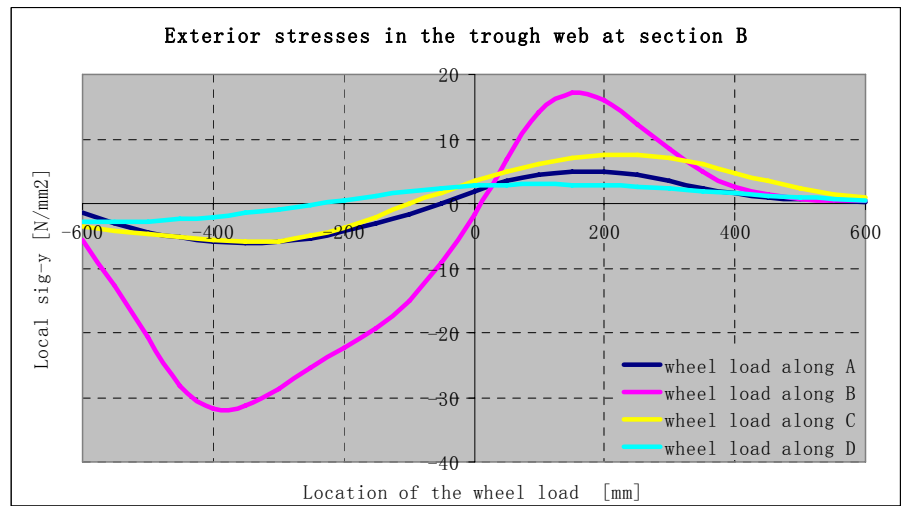
(a) Transverse influence line in the interior trough web at section A



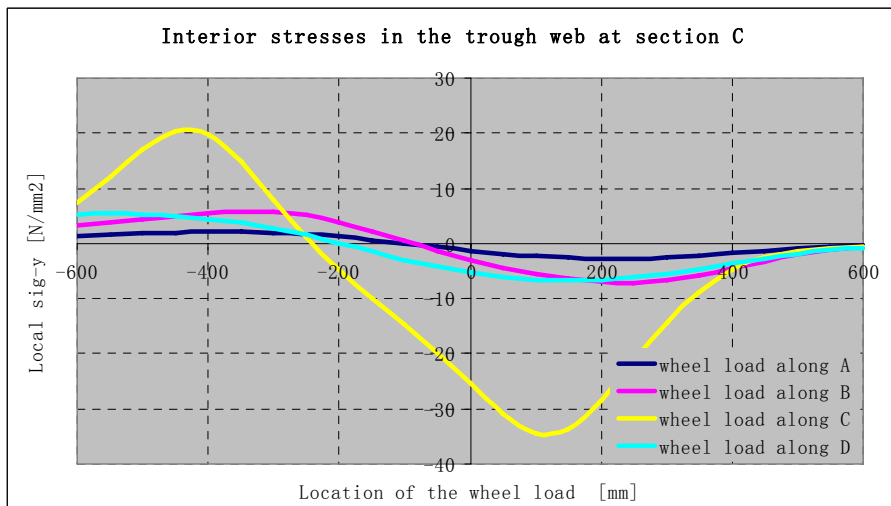
(b) Transverse influence line in the exterior trough web at section A



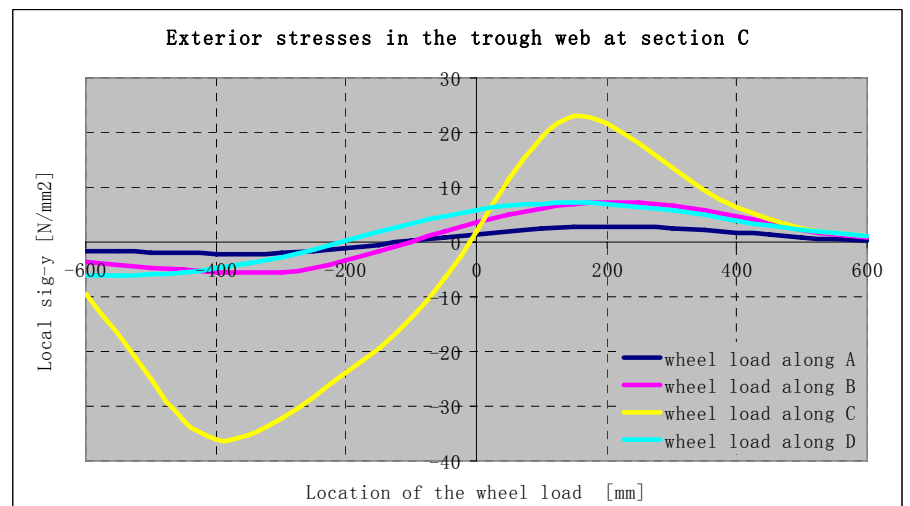
(c) Transverse influence line in the interior trough web at section B



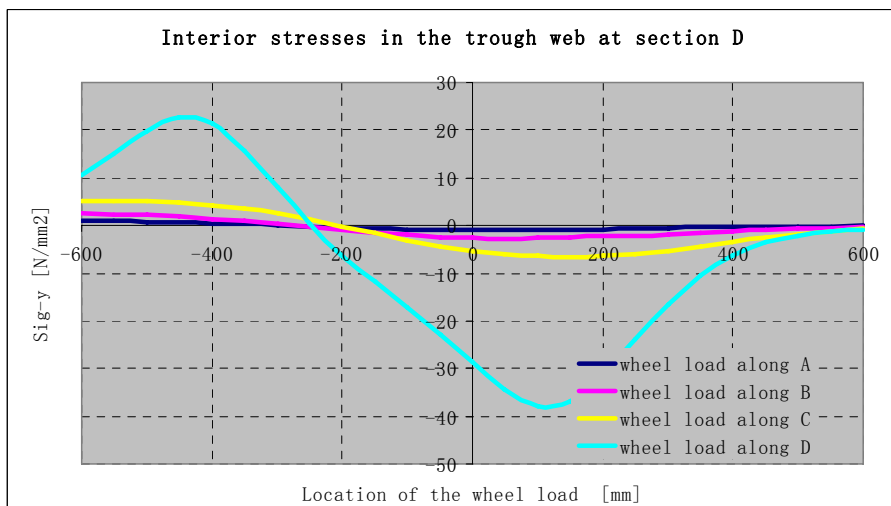
(d) Transverse influence line in the exterior trough web at section B



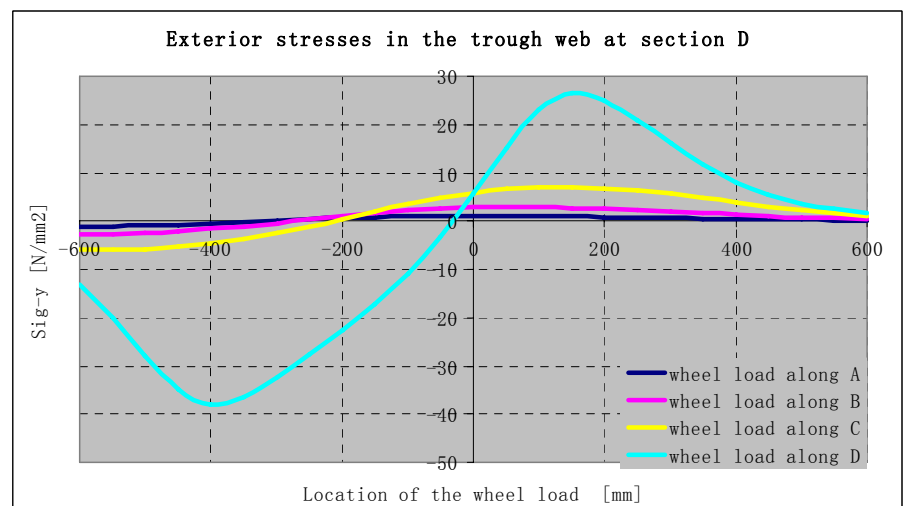
(e) Transverse influence line in the interior trough web at section C



(f) Transverse influence line in the exterior trough web at section C

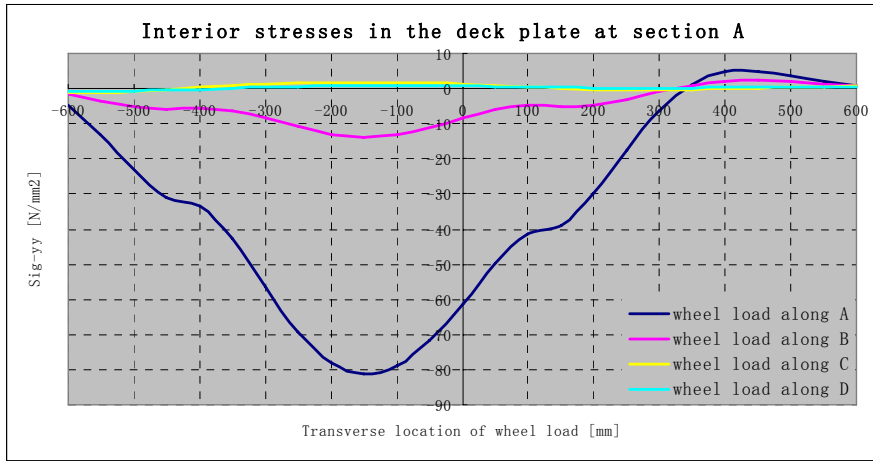


(g) Transverse influence line in the interior trough web at section D

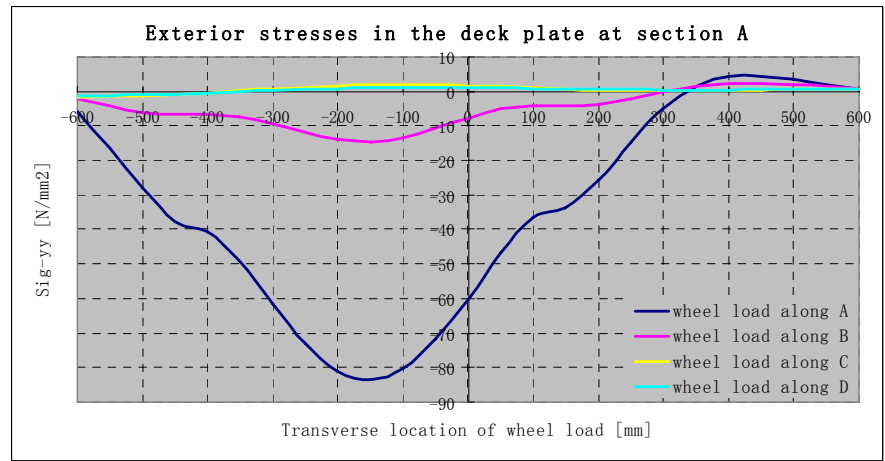


(h) Transverse influence line in the exterior trough web at section D

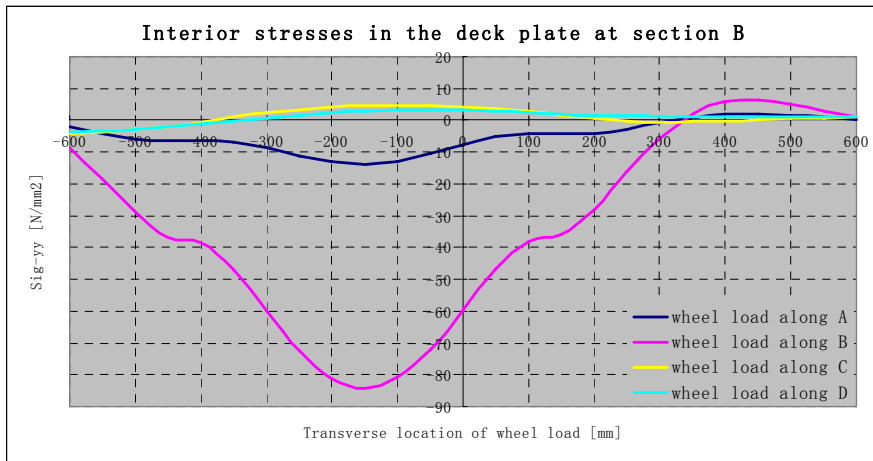
Transverse influence line in the deck plate



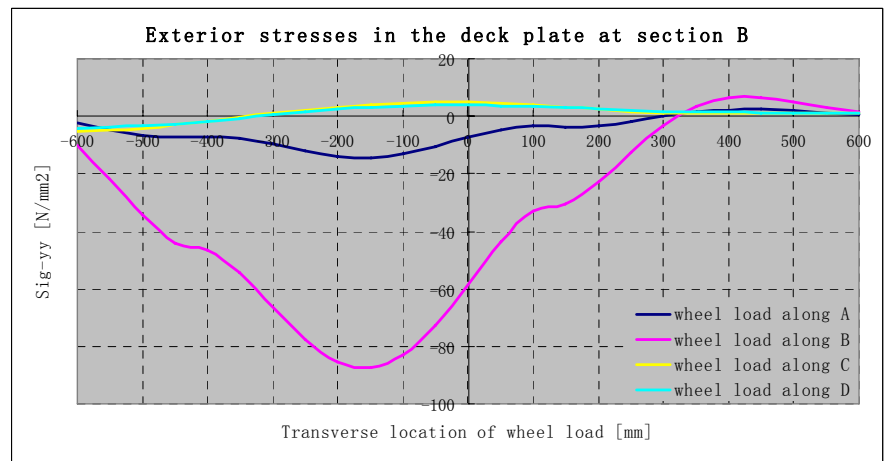
(a) Transverse influence line in the interior deck plate at section A



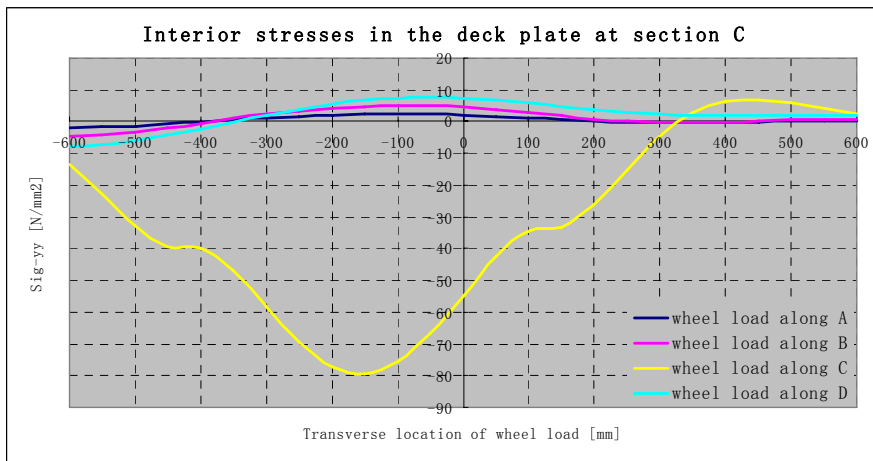
(b) Transverse influence line in the exterior deck plate at section A



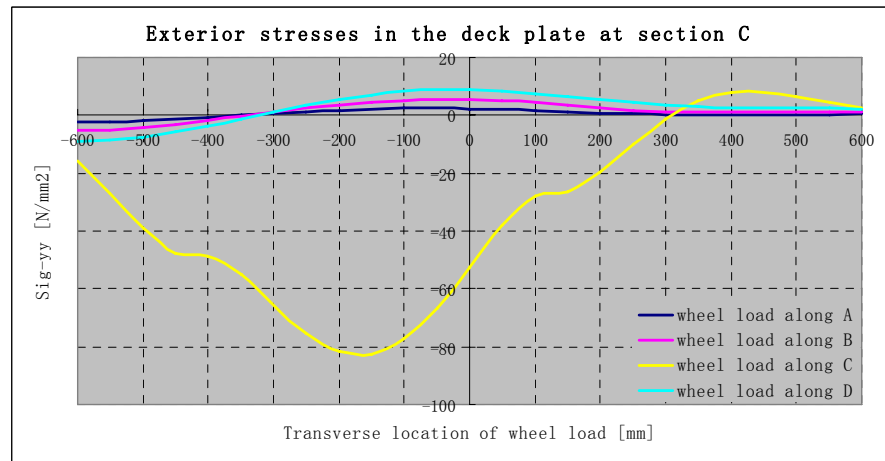
(c) Transverse influence line in the interior deck plate at section B



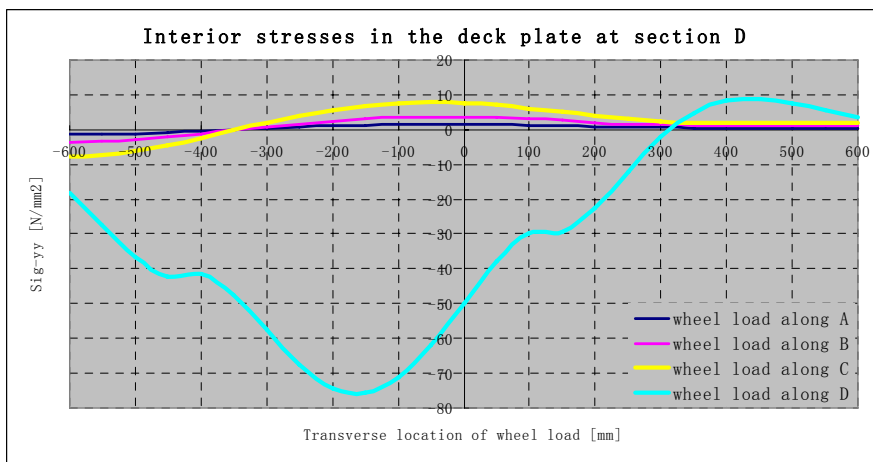
(d) Transverse influence line in the exterior deck plate at section B



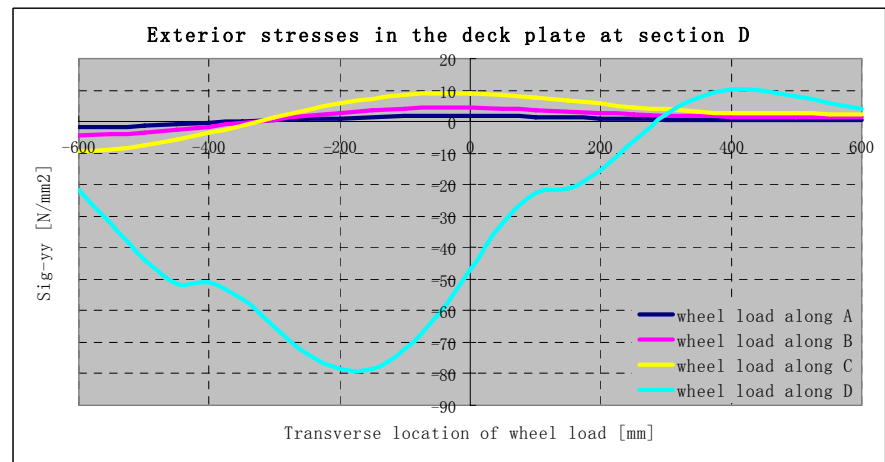
(e) Transverse influence line in the interior deck plate at section C



(f) Transverse influence line in the exterior deck plate at section C



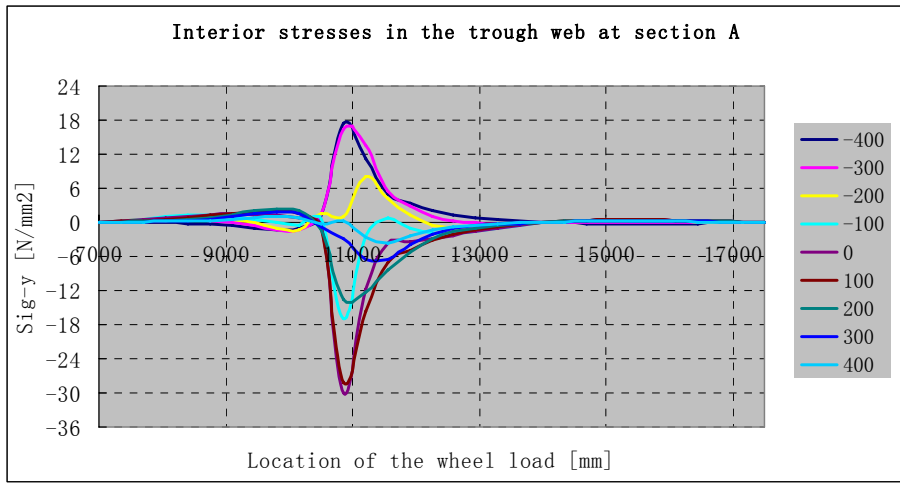
(g) Transverse influence line in the interior deck plate at section D



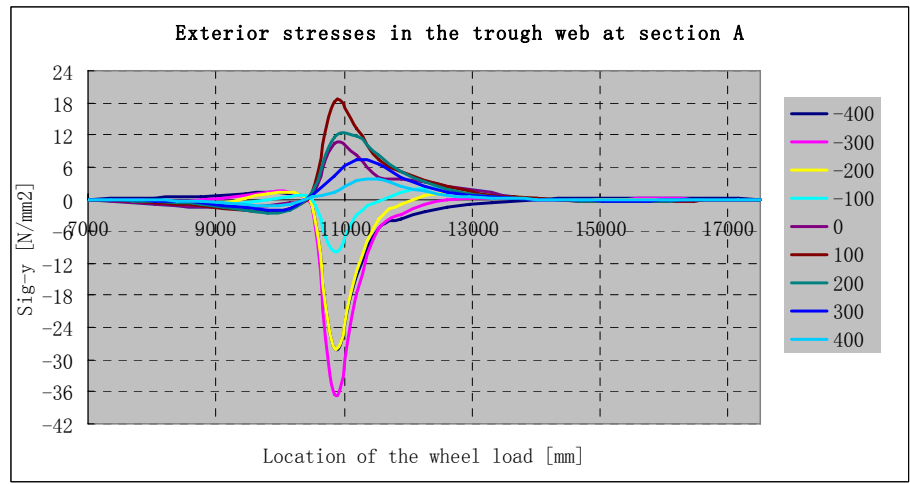
(h) Transverse influence line in the exterior deck plate at section D

Longitudinal influence lines under axle load C

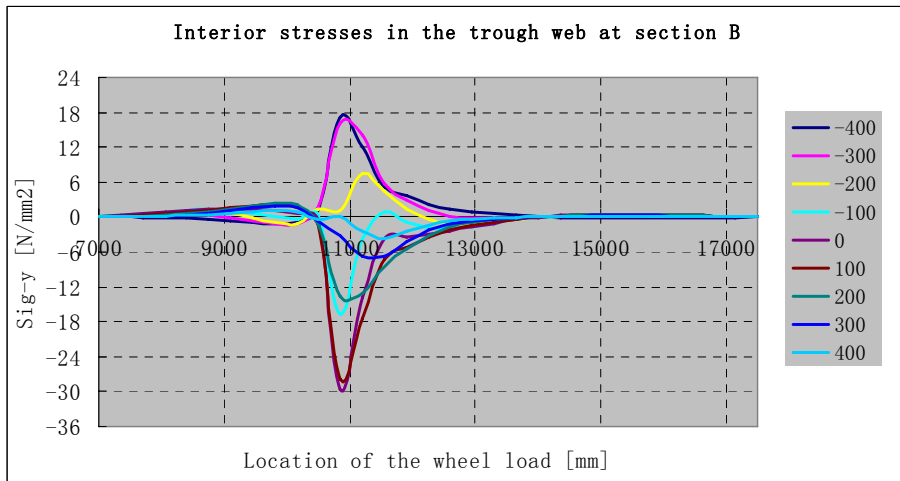
Longitudinal influence line in the trough web



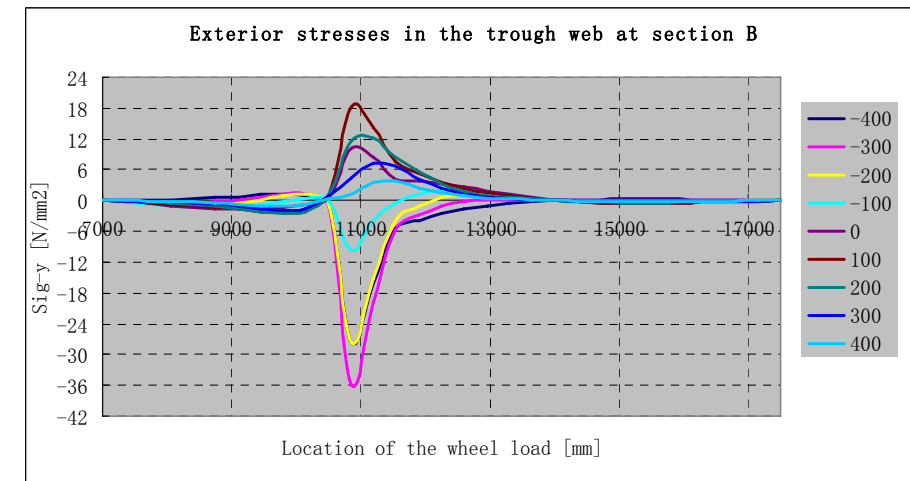
(a) Longitudinal influence line in the interior trough web at section A



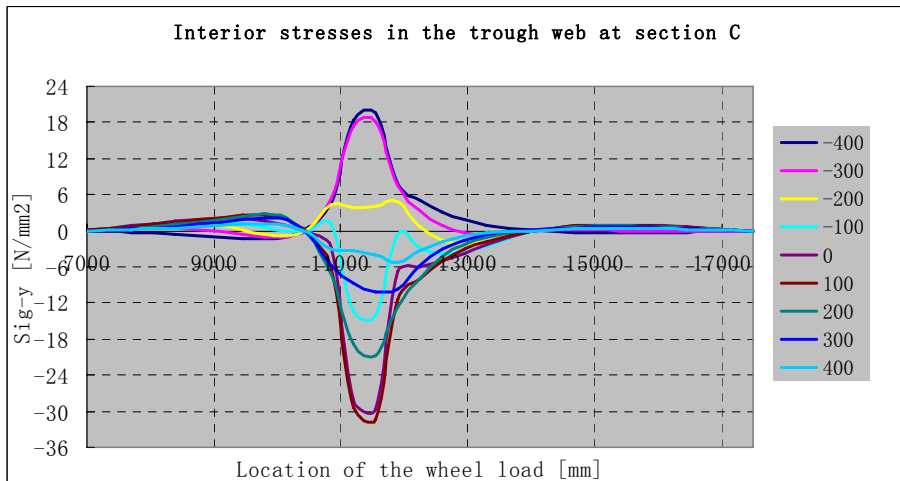
(b) Longitudinal influence line in the exterior trough web at section A



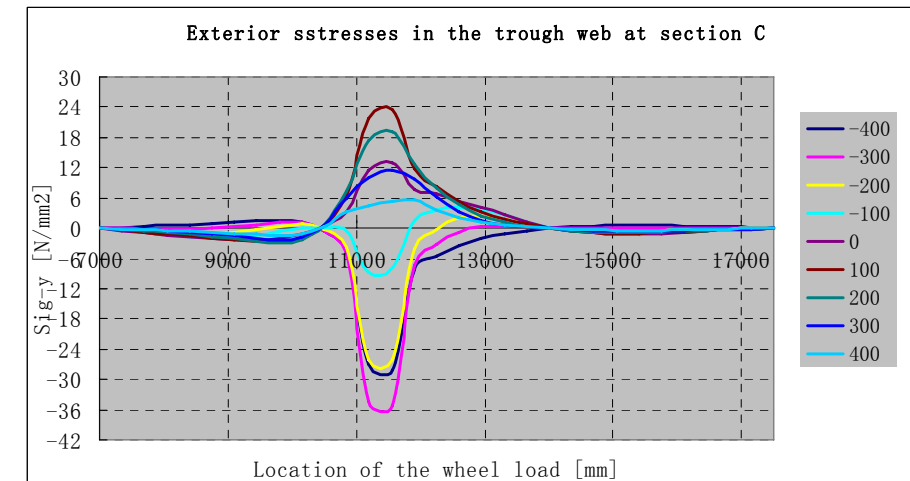
(c) Longitudinal influence line in the interior trough web at section B



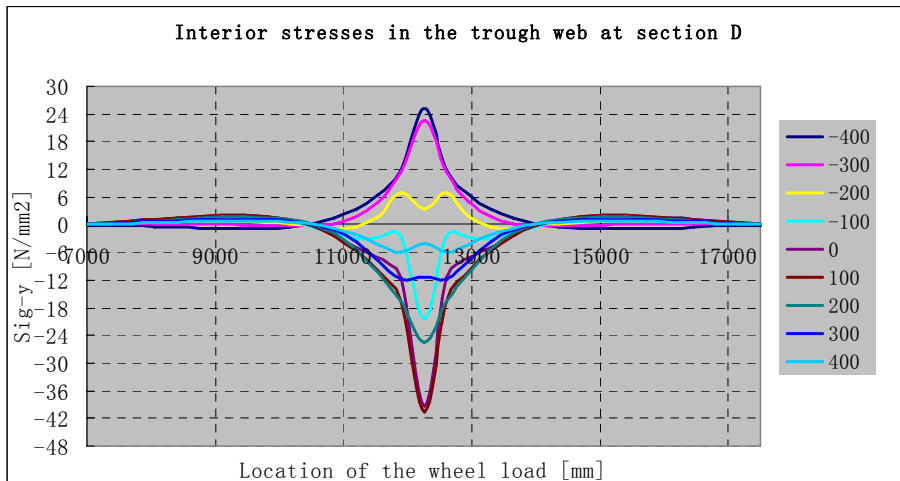
(d) Longitudinal influence line in the exterior trough web at section B



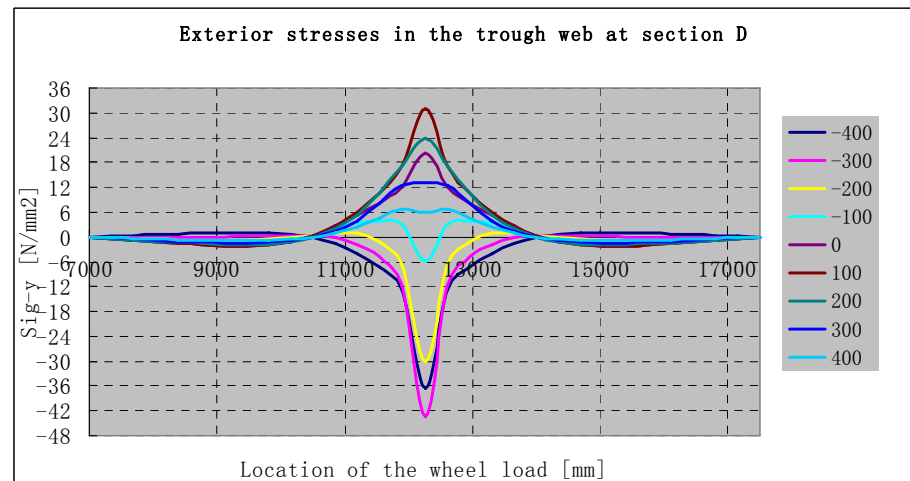
(e) Longitudinal influence line in the interior trough web at section C



(f) Longitudinal influence line in the exterior trough web at section C

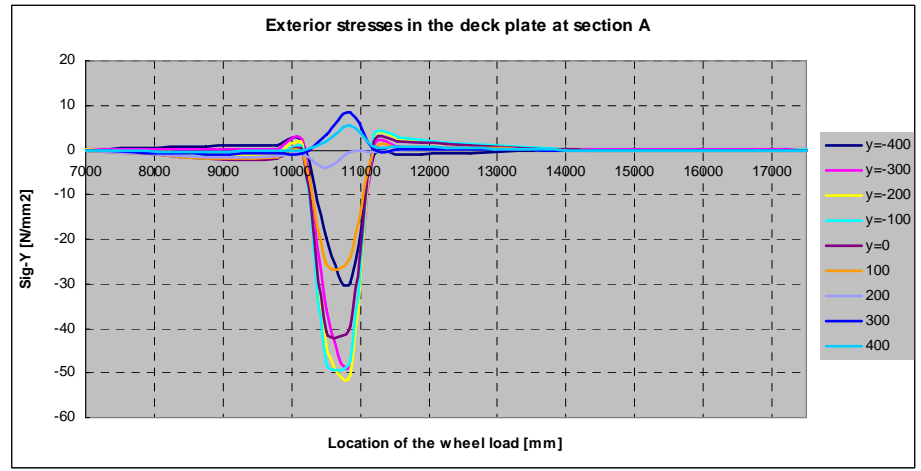
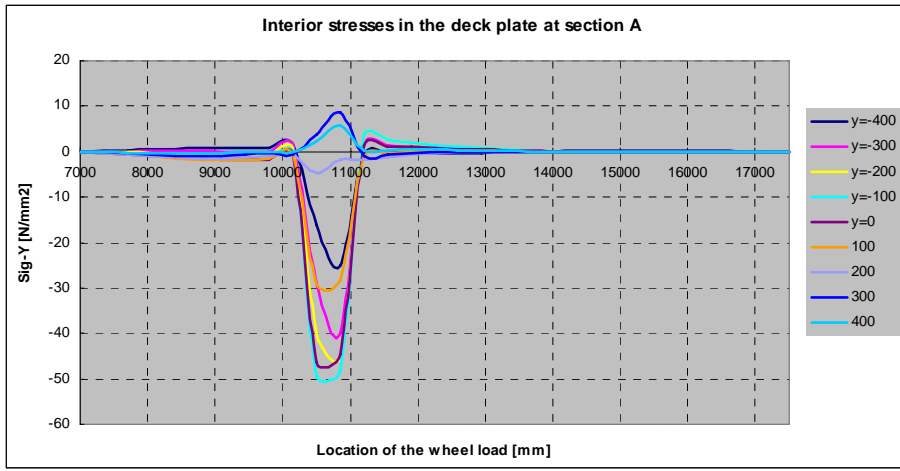


(g) Longitudinal influence line in the interior trough web at section D



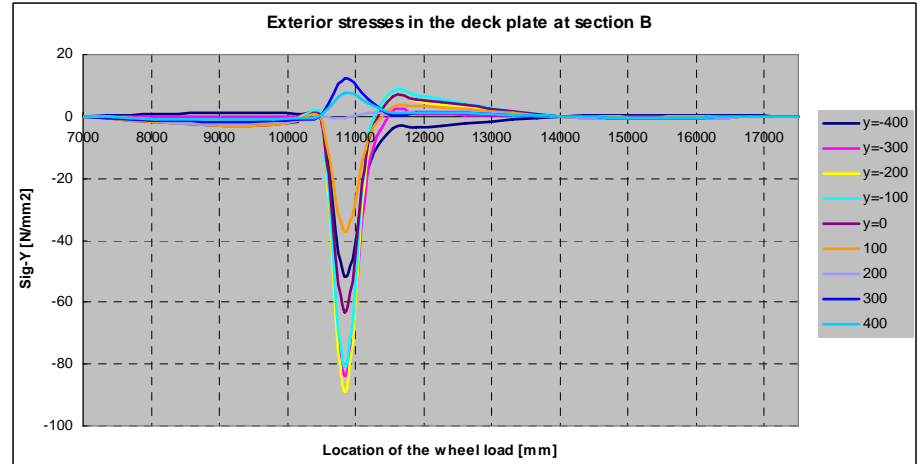
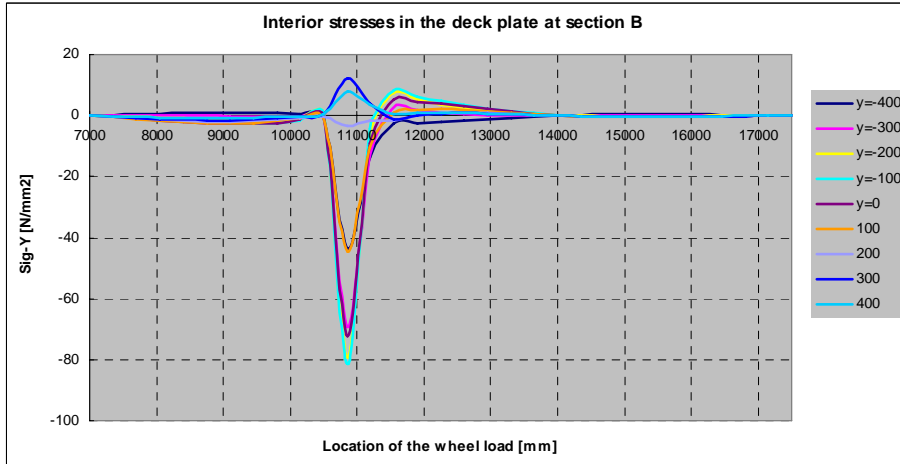
(h) Longitudinal influence line in the exterior trough web at section D

Longitudinal influence line in the deck plate



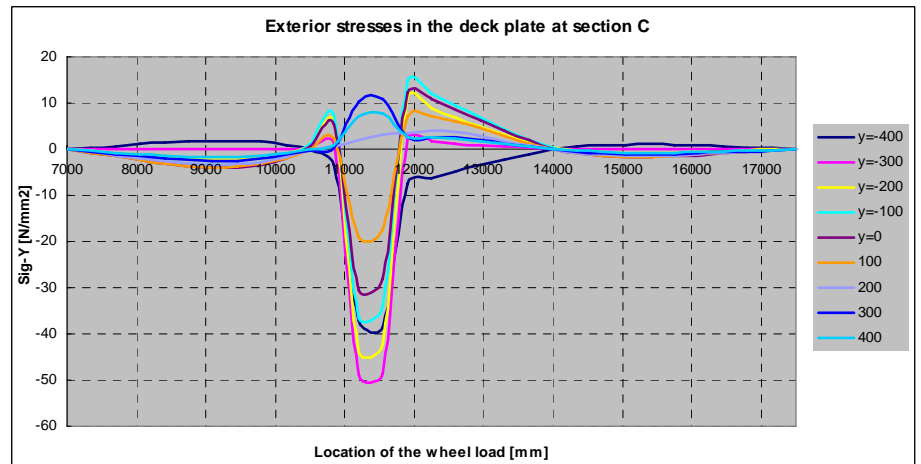
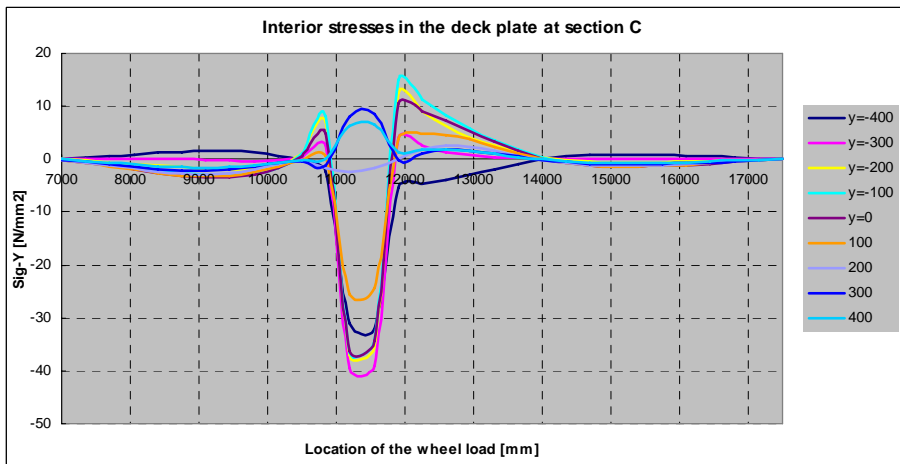
(a) Longitudinal influence line in the interior deck plate at section A

(b) Longitudinal influence line in the exterior deck plate at section A



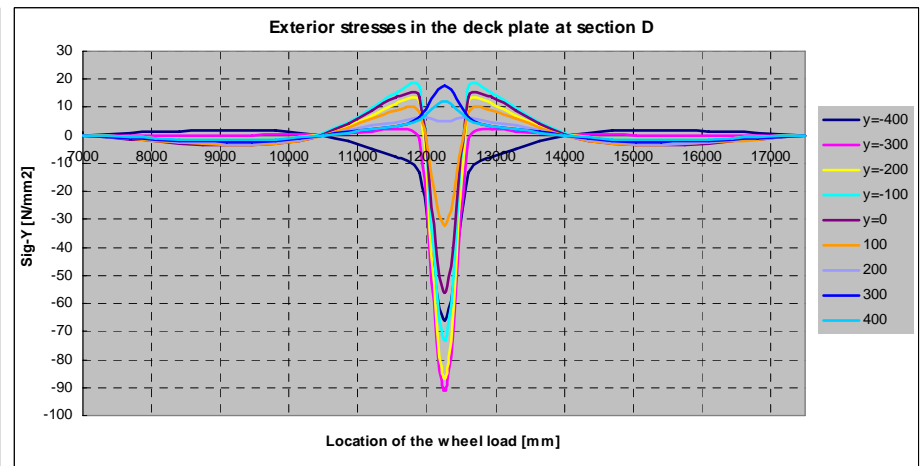
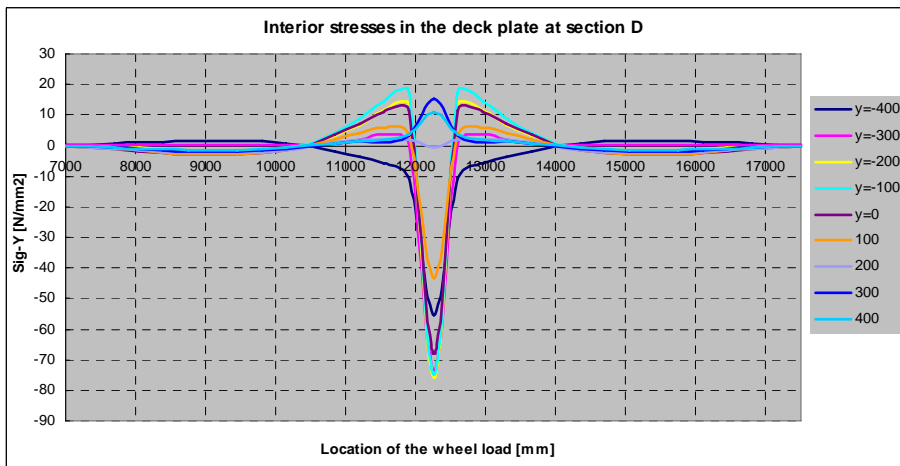
(c) Longitudinal influence line in the interior deck plate at section B

(d) Longitudinal influence line in the exterior deck plate at section B



(e) Longitudinal influence line in the interior deck plate at section C

(f) Longitudinal influence line in the exterior deck plate at section C

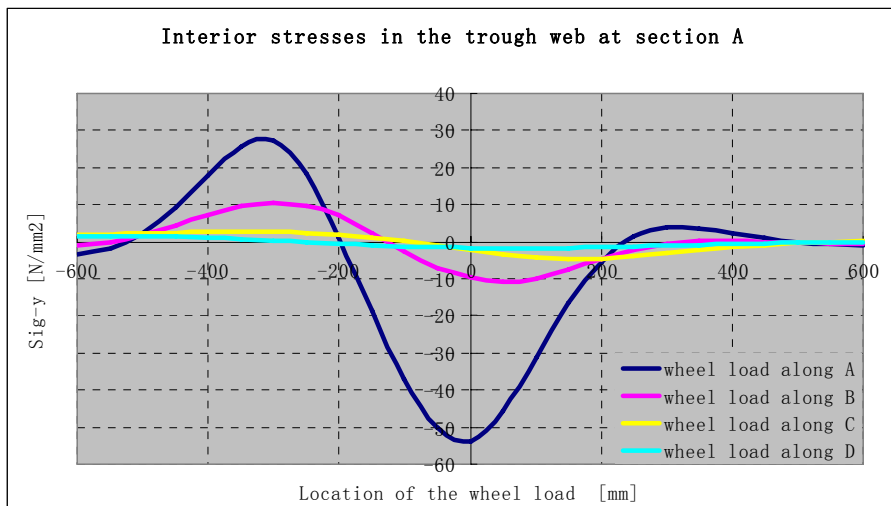


(g) Longitudinal influence line in the interior deck plate at section D

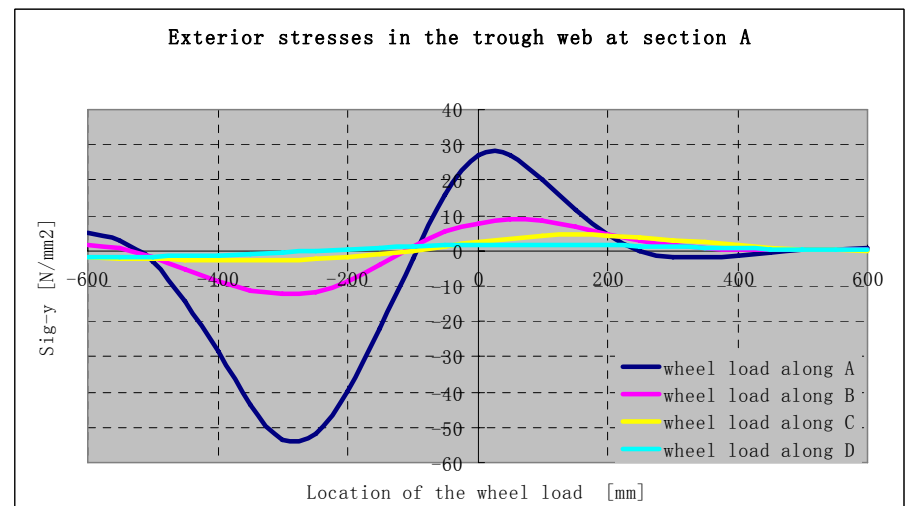
(h) Longitudinal influence line in the exterior deck plate at section D

Transverse influence lines under axle load C

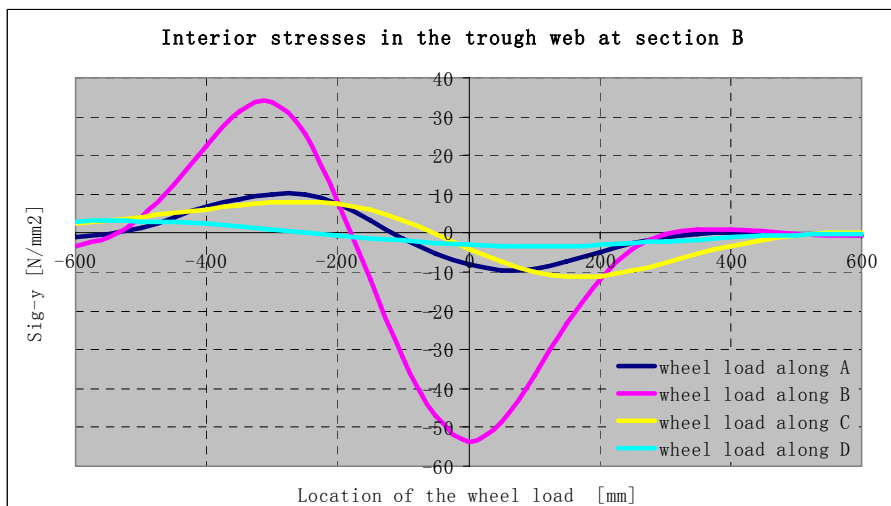
Transverse influence lines in the trough web



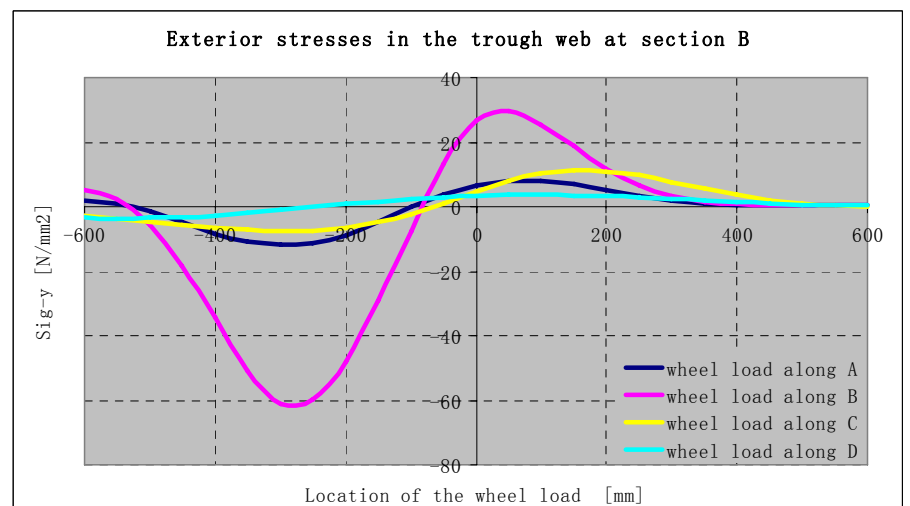
(a) Transverse influence line in the interior trough web at section A



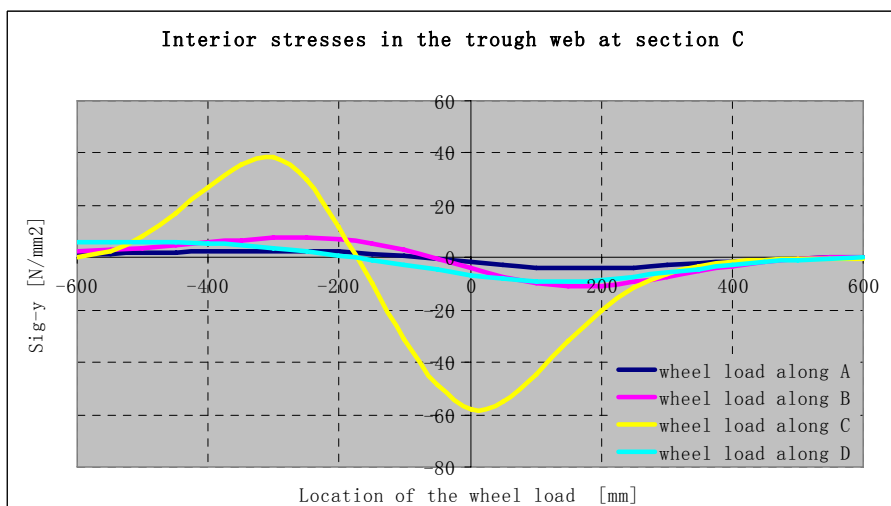
(b) Transverse influence line in the exterior trough web at section A



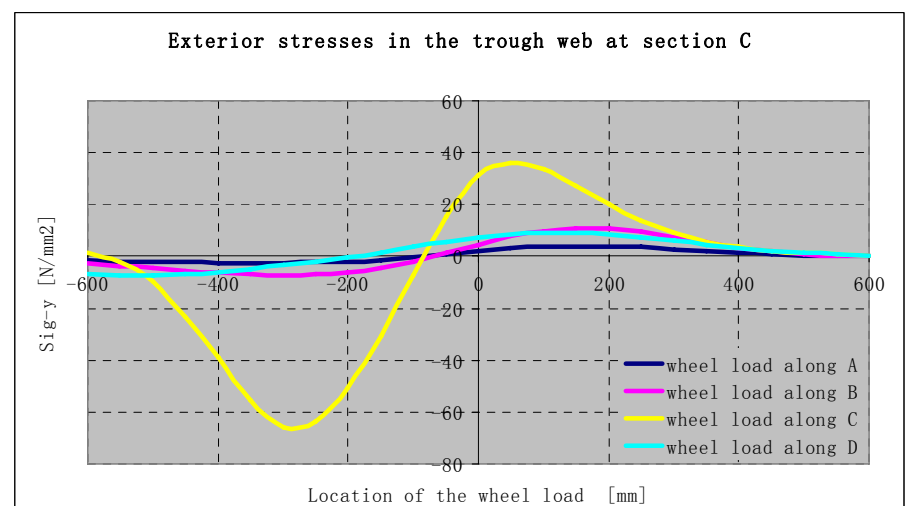
(c) Transverse influence line in the interior trough web at section B



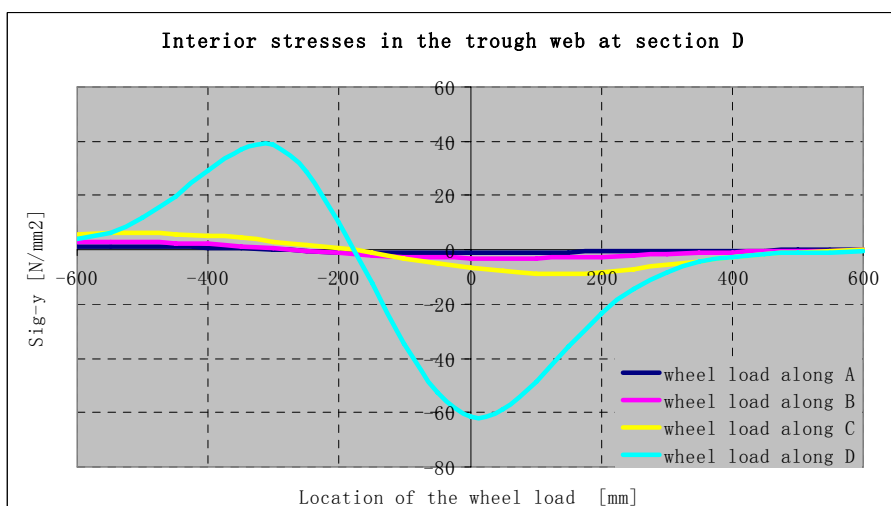
(d) Transverse influence line in the exterior trough web at section B



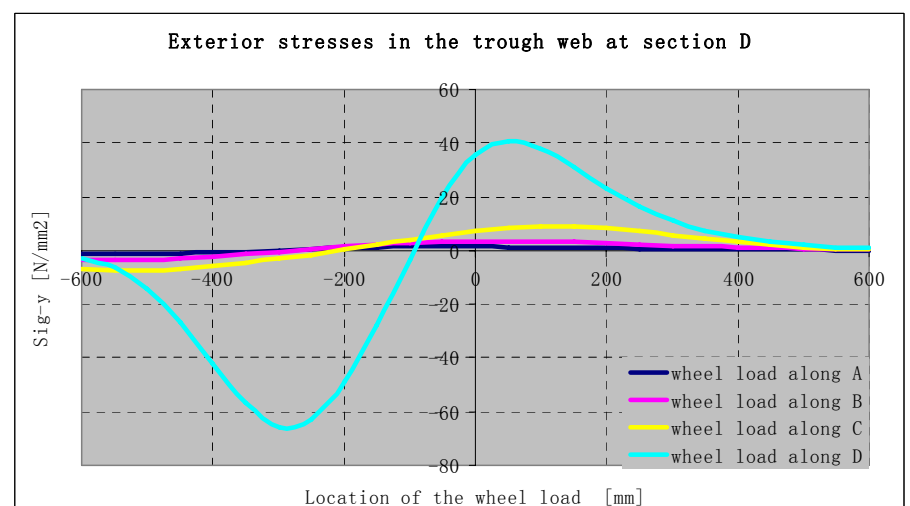
(e) Transverse influence line in the interior trough web at section C



(f) Transverse influence line in the exterior trough web at section C

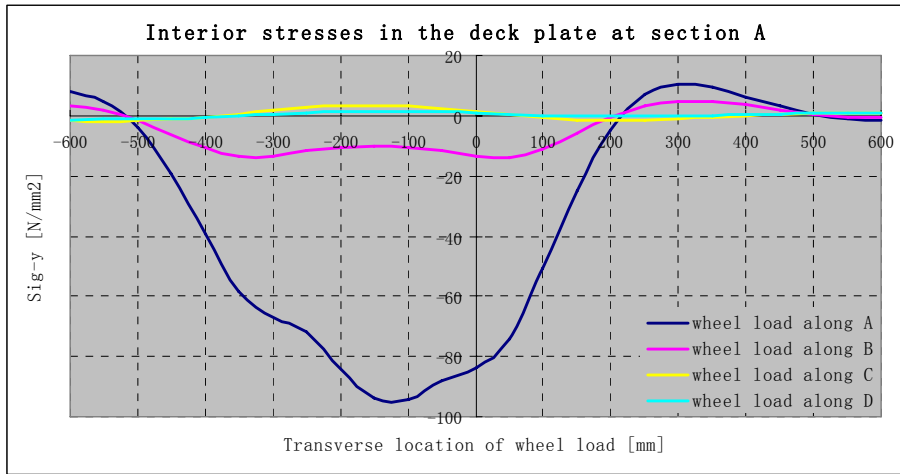


(g) Transverse influence line in the interior trough web at section D

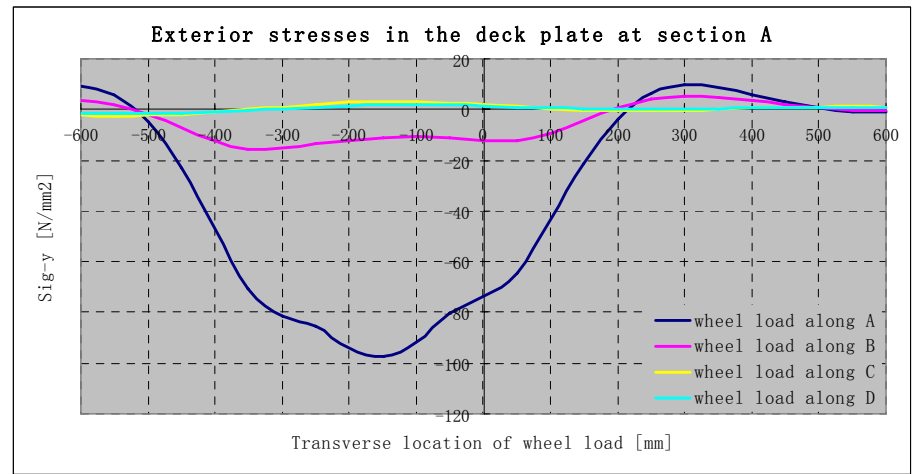


(h) Transverse influence line in the exterior trough web at section D

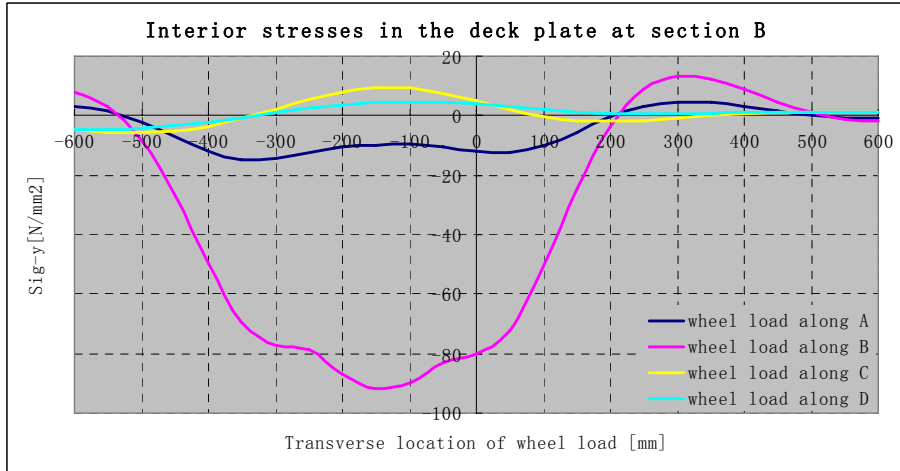
Transverse influence lines in the deck plate



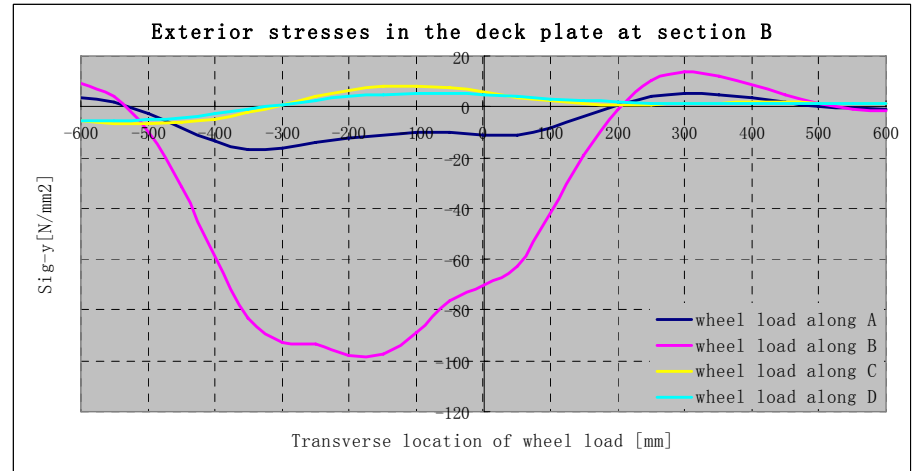
(a) Transverse influence line in the interior deck plate at section A



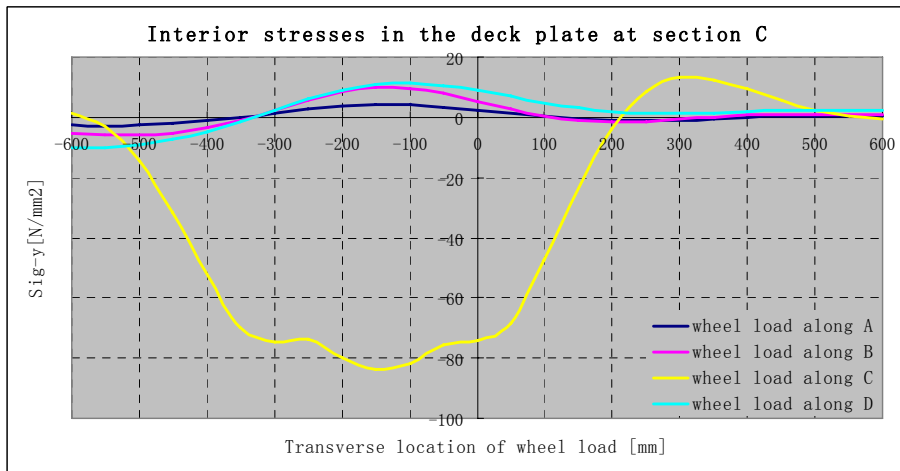
(b) Transverse influence line in the exterior deck plate at section A



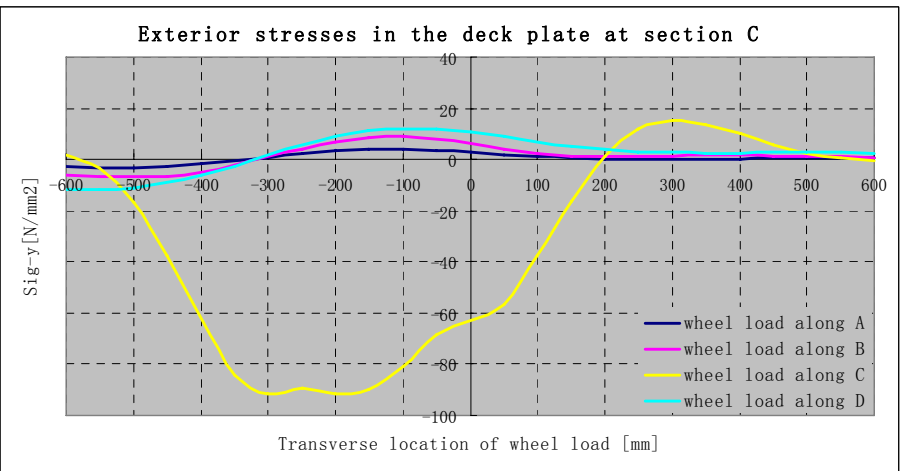
(c) Transverse influence line in the interior deck plate at section B



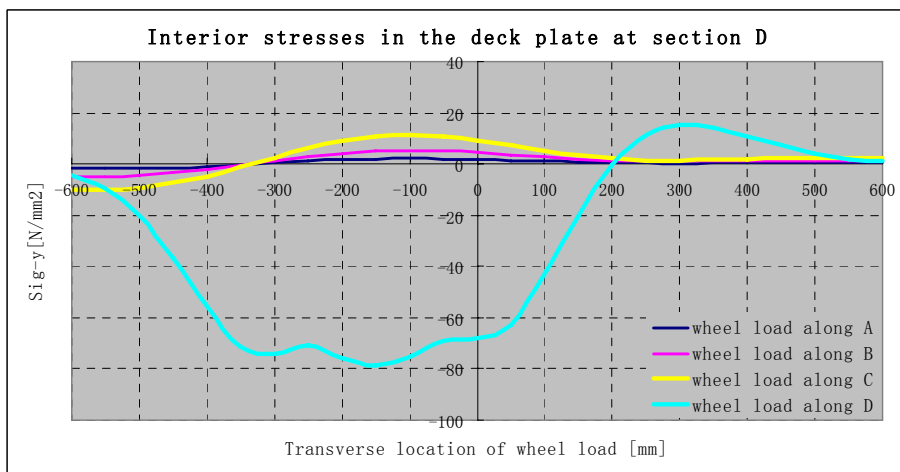
(d) Transverse influence line in the exterior deck plate at section B



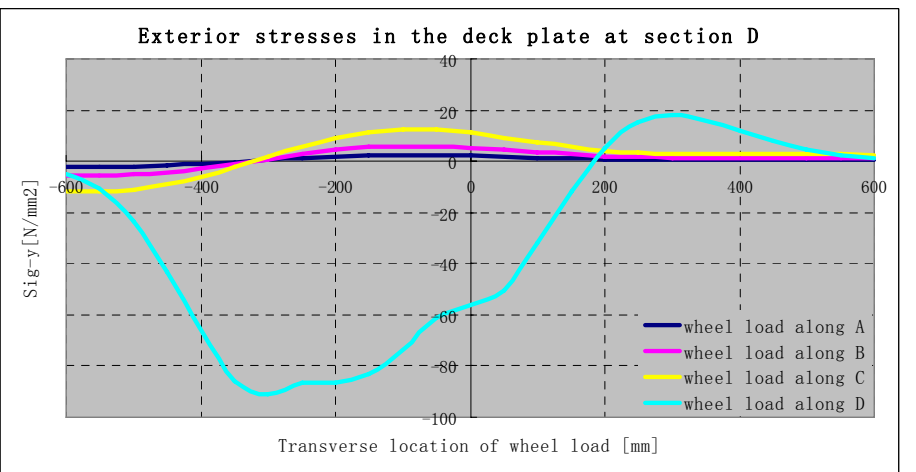
(e) Transverse influence line in the interior deck plate at section C



(f) Transverse influence line in the exterior deck plate at section C



(g) Transverse influence line in the interior deck plate at section D

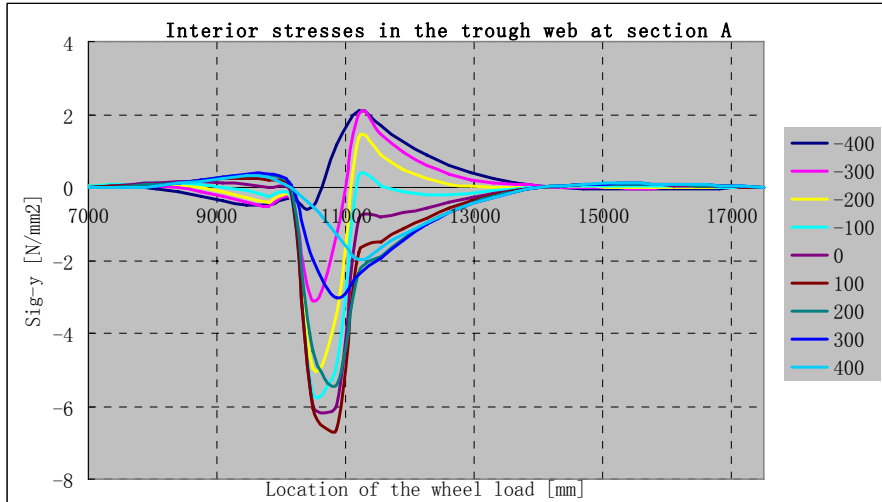


(h) Transverse influence line in the exterior deck plate at section D

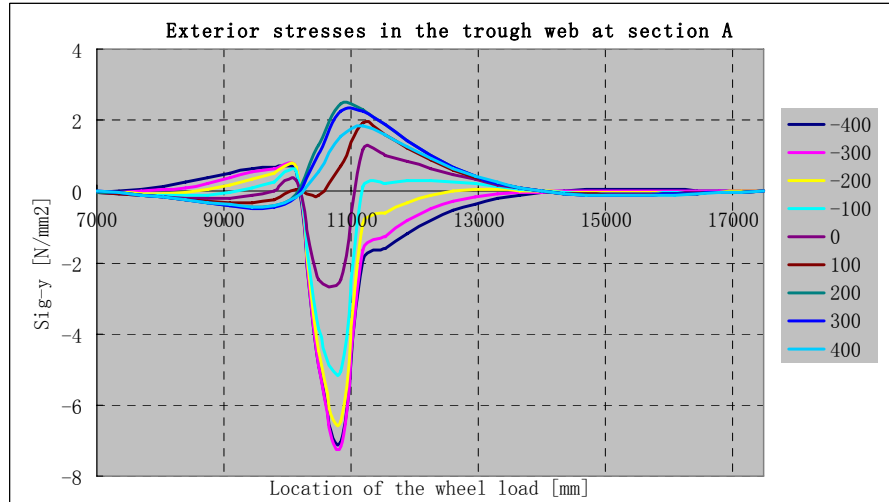
4. Influence lines in model D

Longitudinal influence lines under axle load B

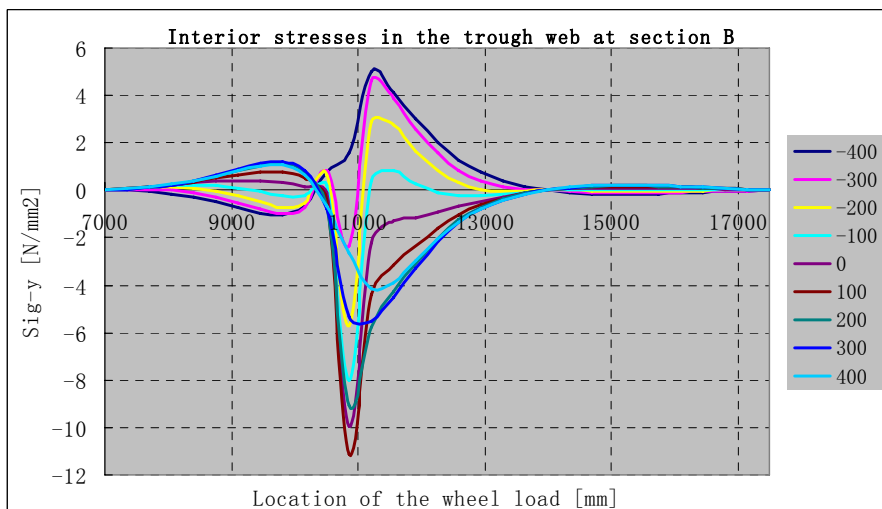
Longitudinal influence line in the trough web



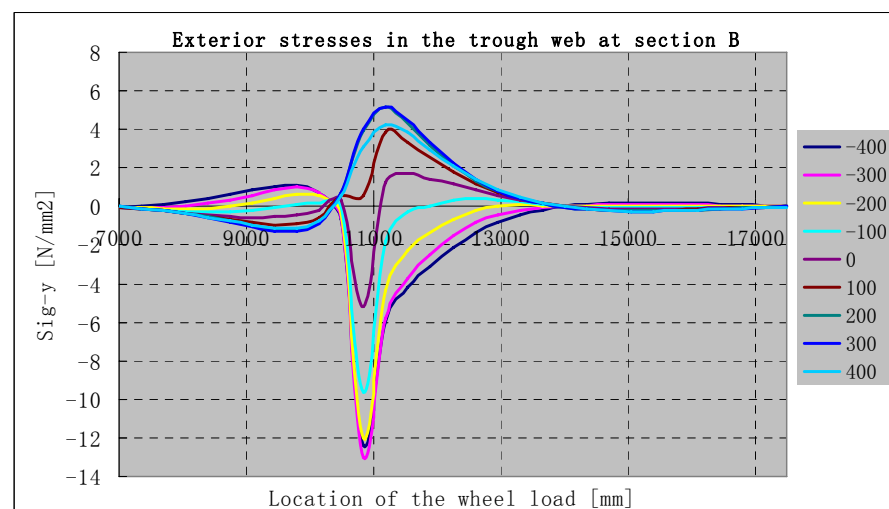
(a) Longitudinal influence line in the interior trough web at section A



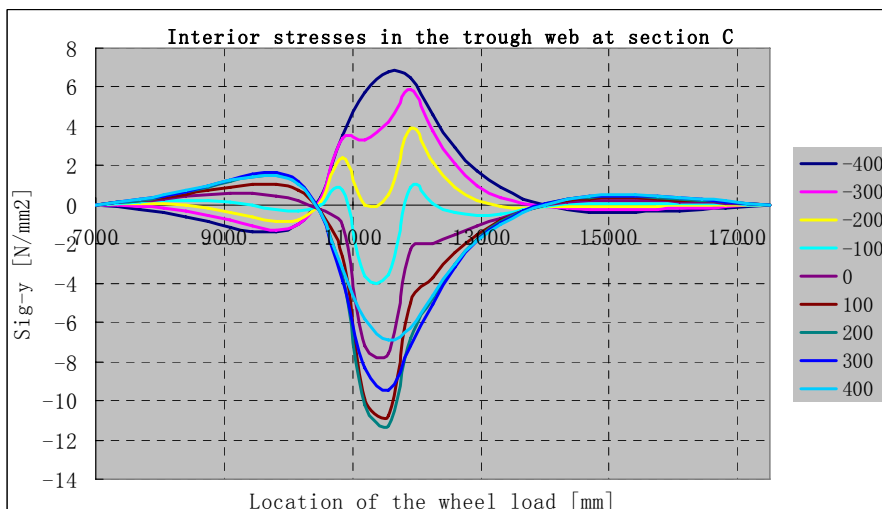
(b) Longitudinal influence line in the exterior trough web at section A



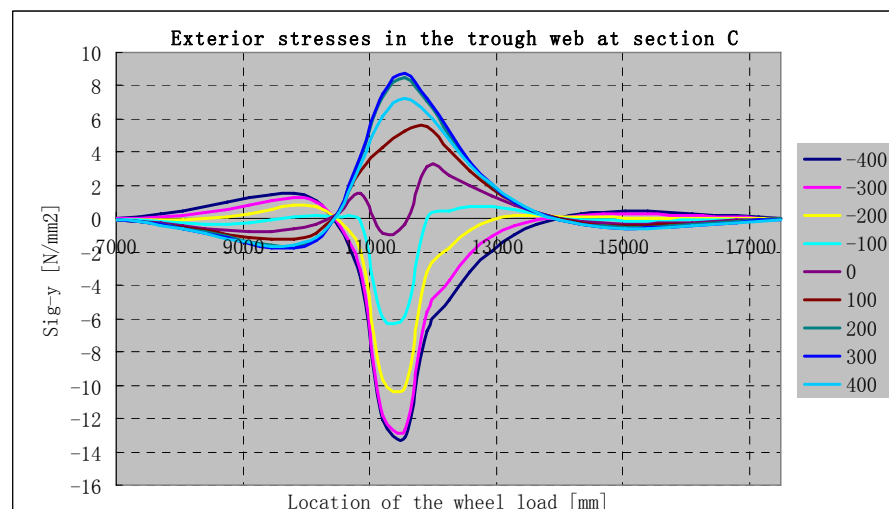
(c) Longitudinal influence line in the interior trough web at section B



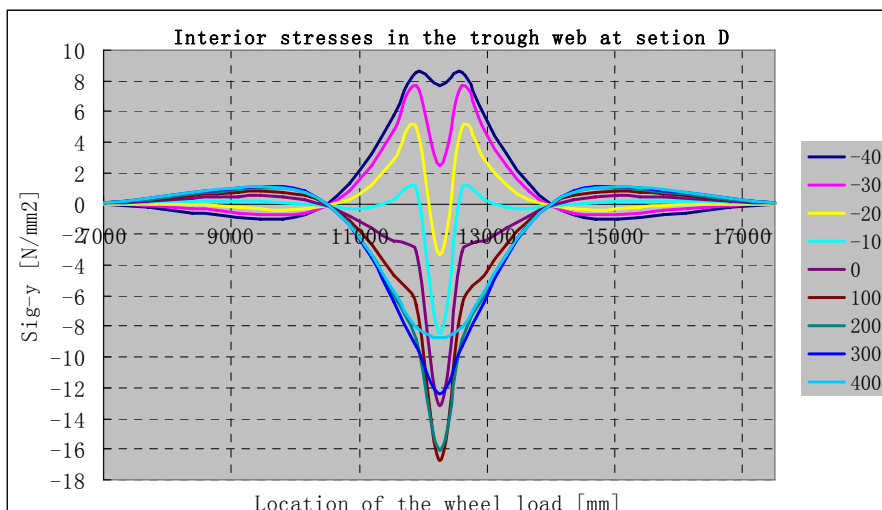
(d) Longitudinal influence line in the exterior trough web at section B



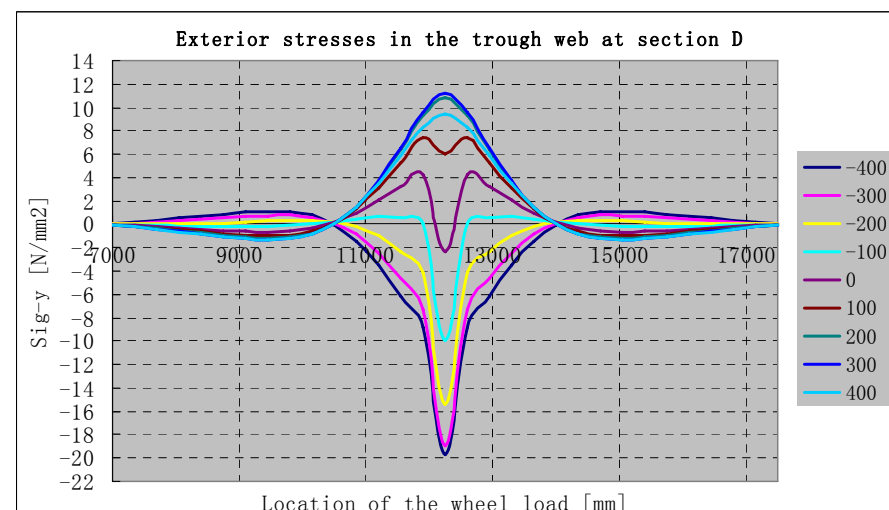
(e) Longitudinal influence line in the interior trough web at section C



(f) Longitudinal influence line in the exterior trough web at section C

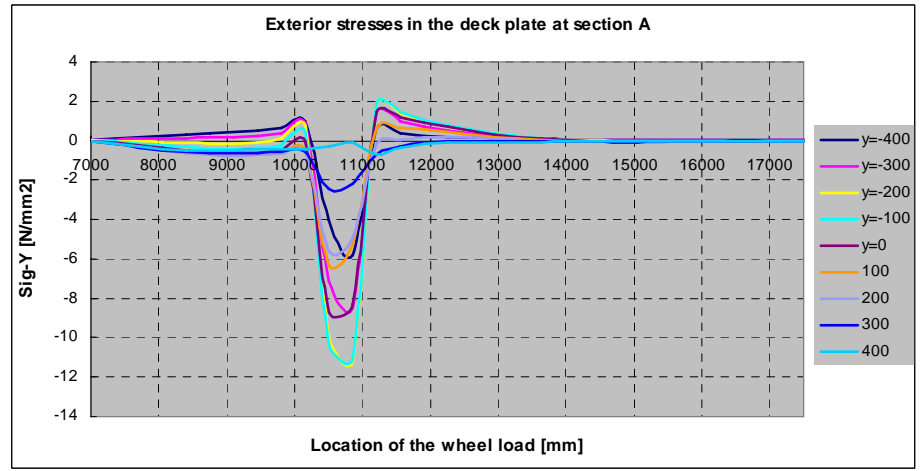
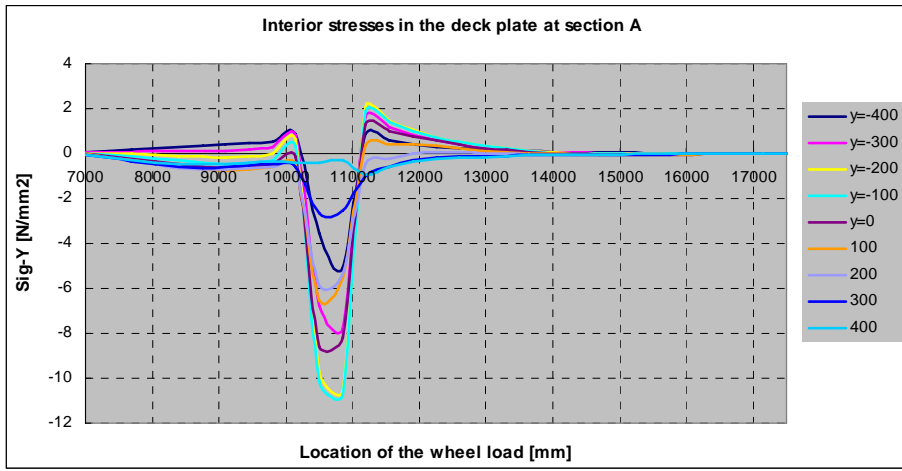


(g) Longitudinal influence line in the interior trough web at section D



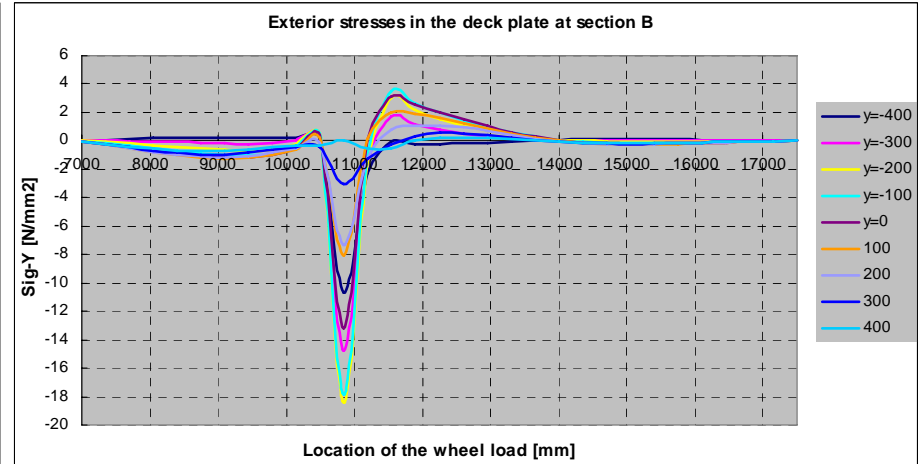
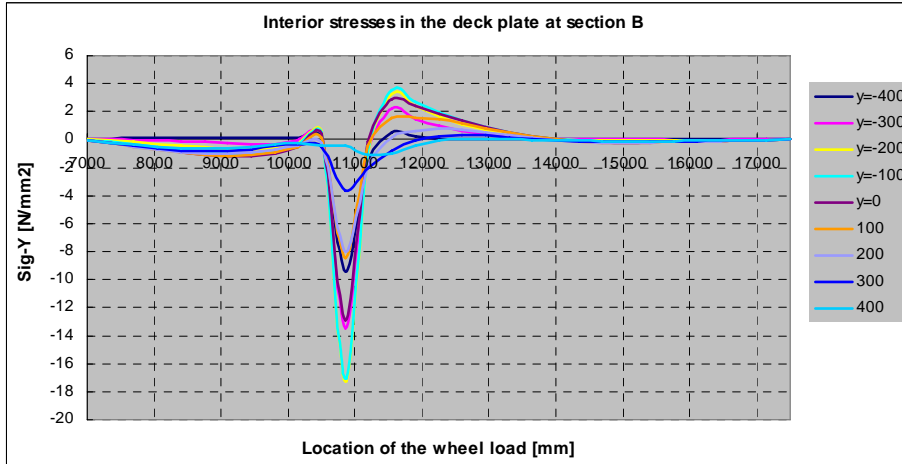
(h) Longitudinal influence line in the exterior trough web at section D

Longitudinal influence line in the deck plate



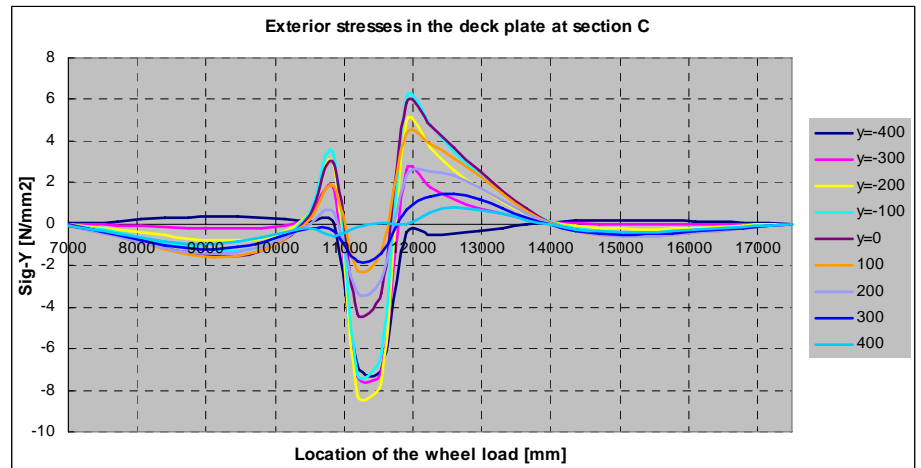
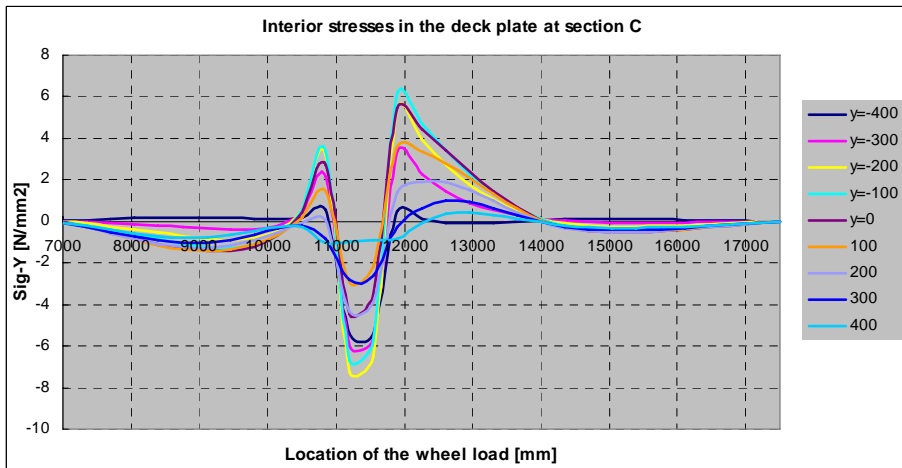
(a) Longitudinal influence line in the interior deck plate at section A

(b) Longitudinal influence line in the exterior deck plate at section A



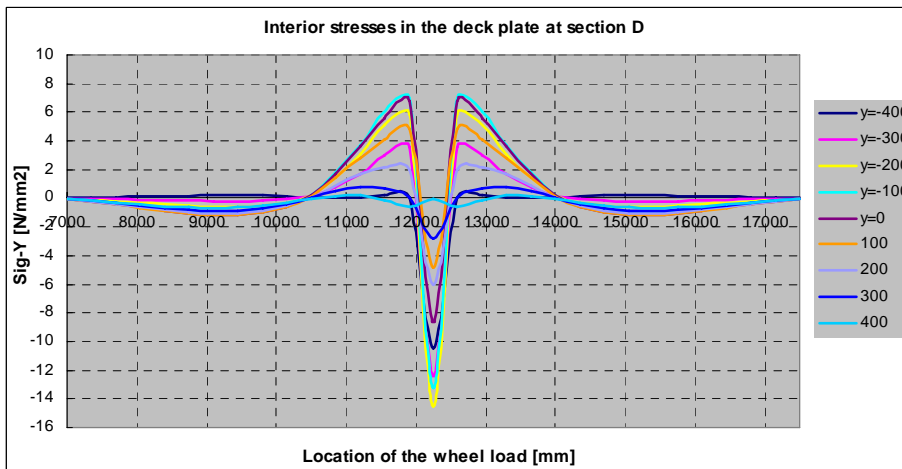
(c) Longitudinal influence line in the interior deck plate at section B

(d) Longitudinal influence line in the exterior deck plate at section B



(e) Longitudinal influence line in the interior deck plate at section C

(f) Longitudinal influence line in the exterior deck plate at section C

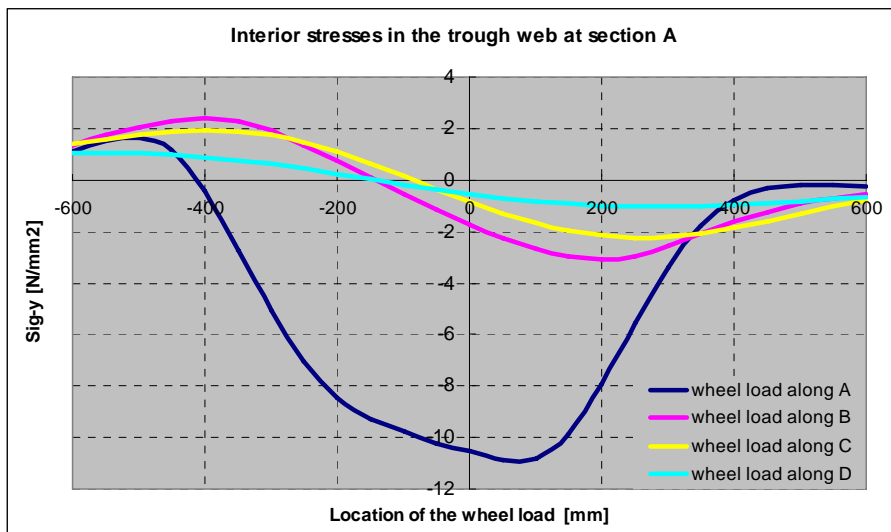


(g) Longitudinal influence line in the interior deck plate at section D

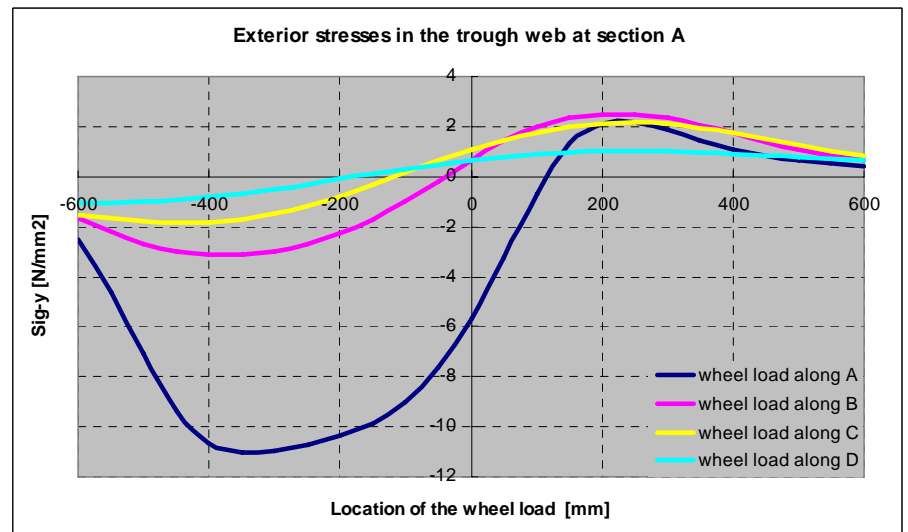
(h) Longitudinal influence line in the exterior deck plate at section D

Transverse influence lines under axle load B

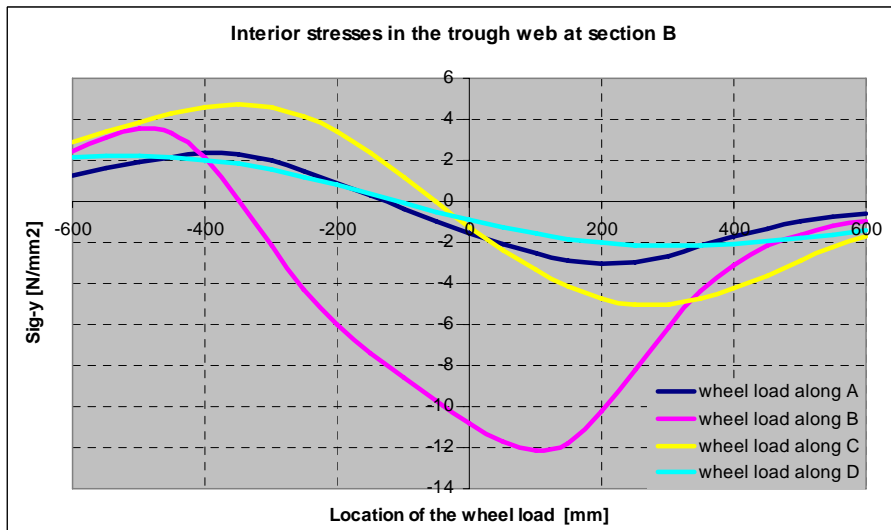
Transverse influence line in the trough web



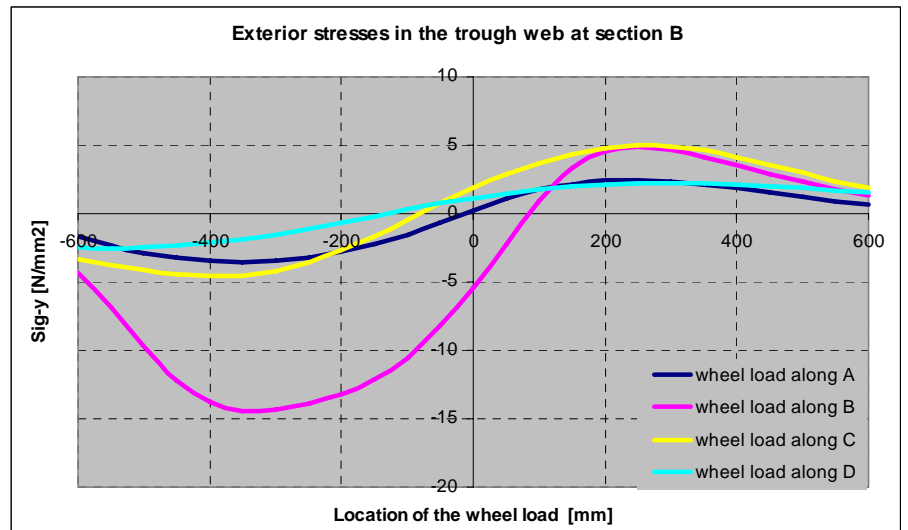
(a) Transverse influence line in the interior trough web at section A



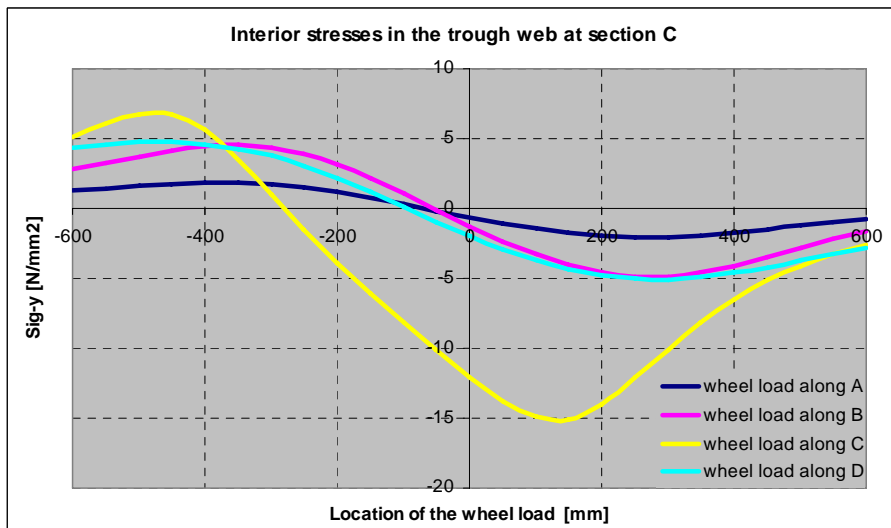
(b) Transverse influence line in the exterior trough web at section A



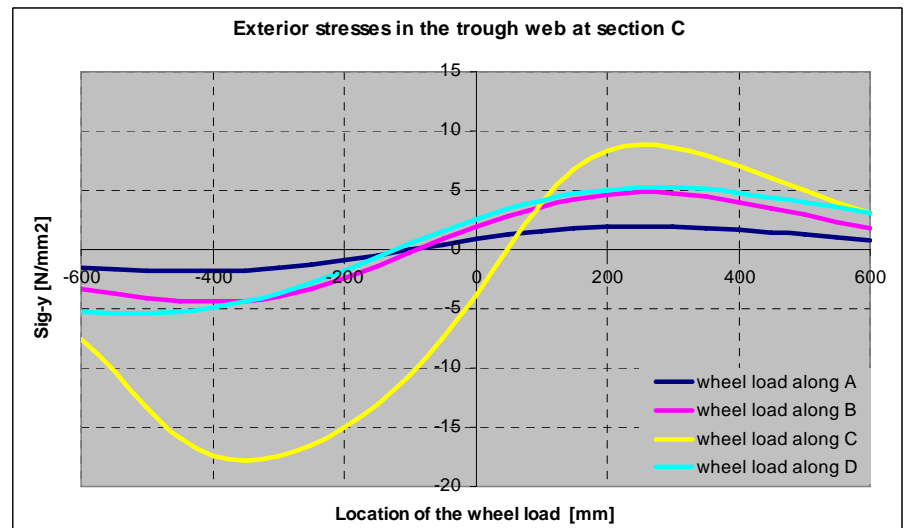
(c) Transverse influence line in the interior trough web at section B



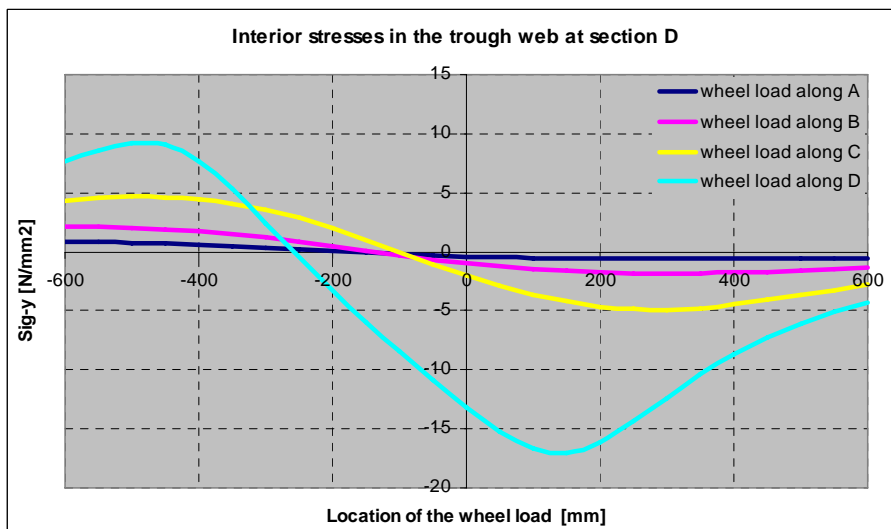
(d) Transverse influence line in the exterior trough web at section B



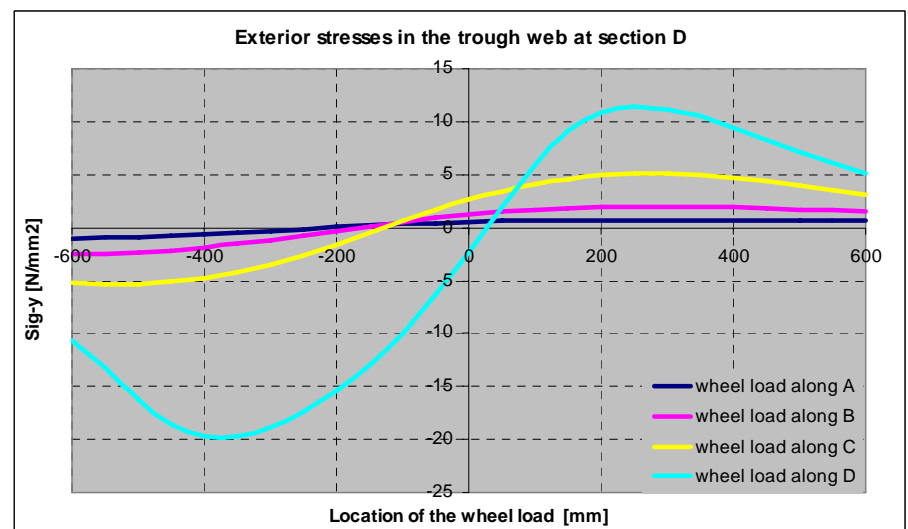
(e) Transverse influence line in the interior trough web at section C



(f) Transverse influence line in the exterior trough web at section C



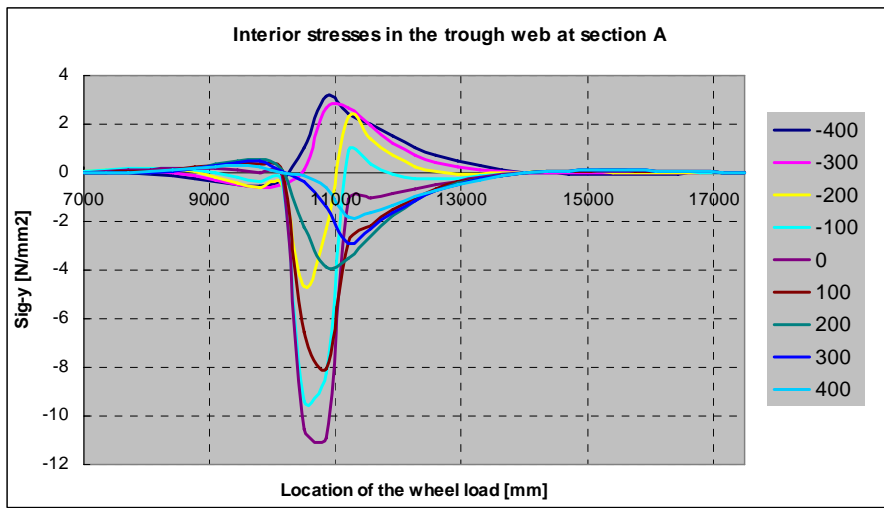
(g) Transverse influence line in the interior trough web at section D



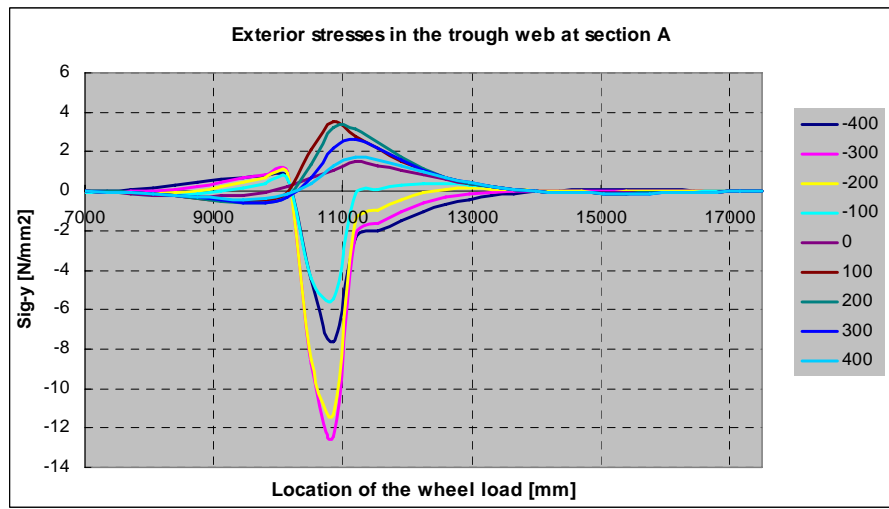
(h) Transverse influence line in the exterior trough web at section D

Longitudinal influence lines under axle load C

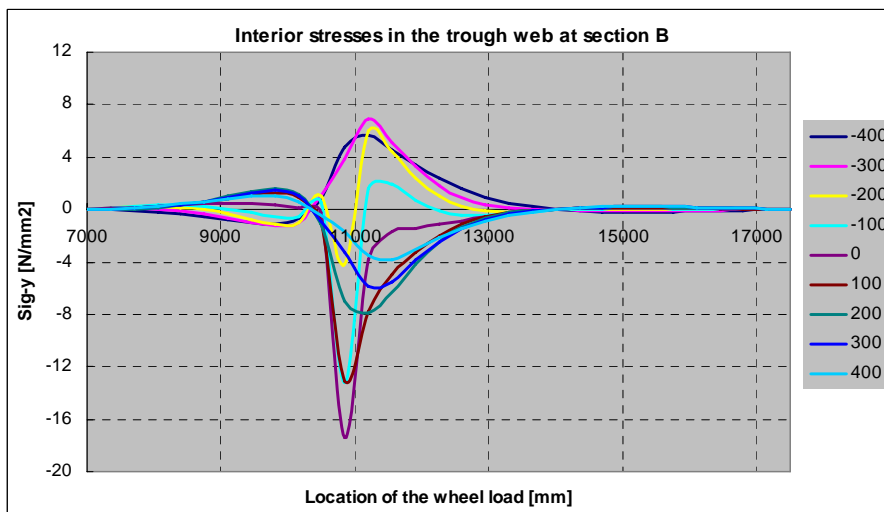
Longitudinal influence lines in the trough web



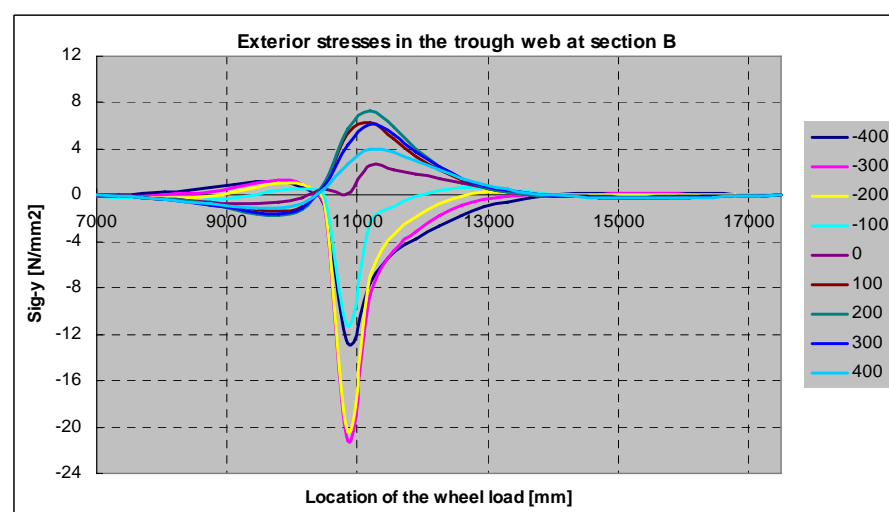
(a) Longitudinal influence line in the interior trough web at section A



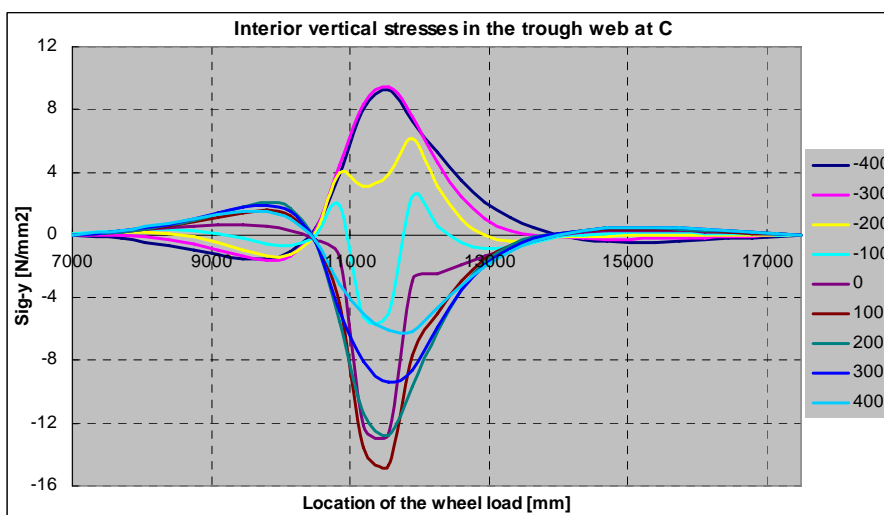
(b) Longitudinal influence line in the exterior trough web at section A



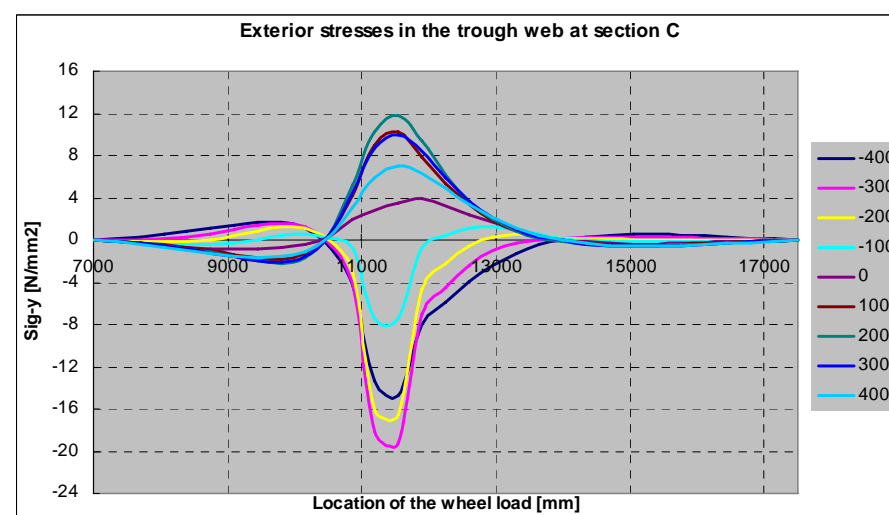
(c) Longitudinal influence line in the interior trough web at section B



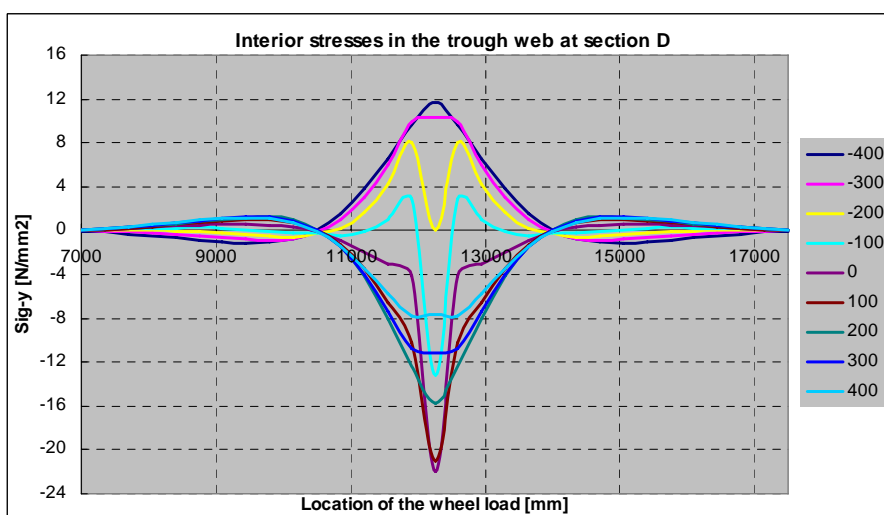
(d) Longitudinal influence line in the exterior trough web at section B



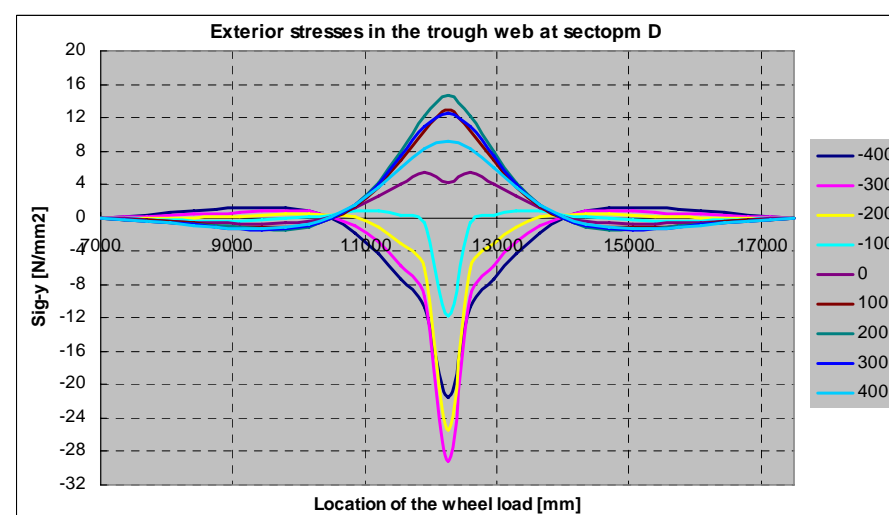
(e) Longitudinal influence line in the interior trough web at section C



(f) Longitudinal influence line in the exterior trough web at section C

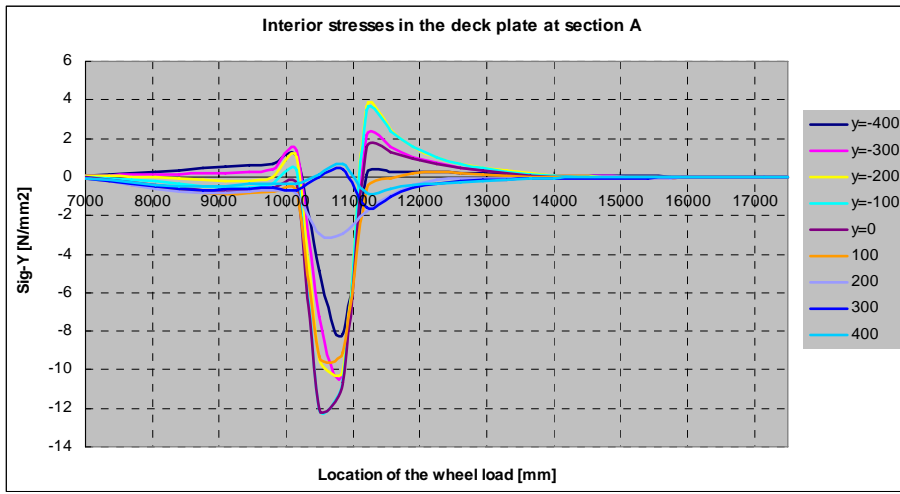


(g) Longitudinal influence line in the interior trough web at section D

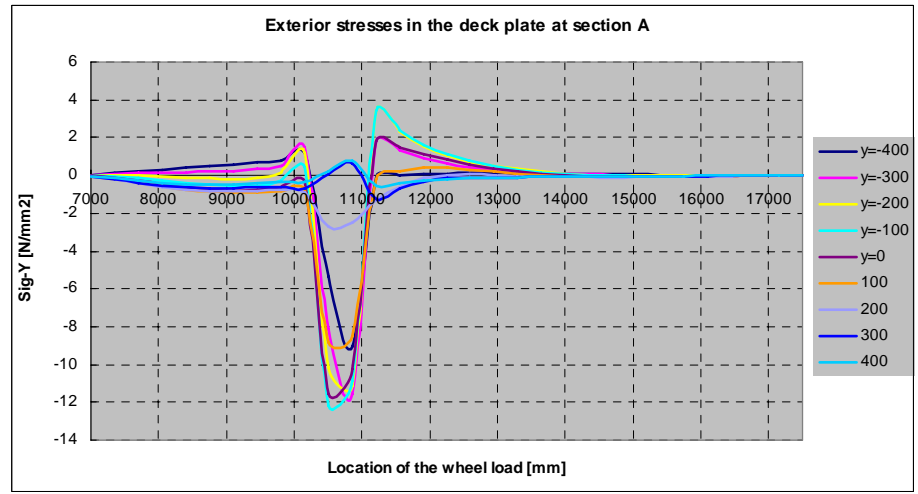


(h) Longitudinal influence line in the exterior trough web at section D

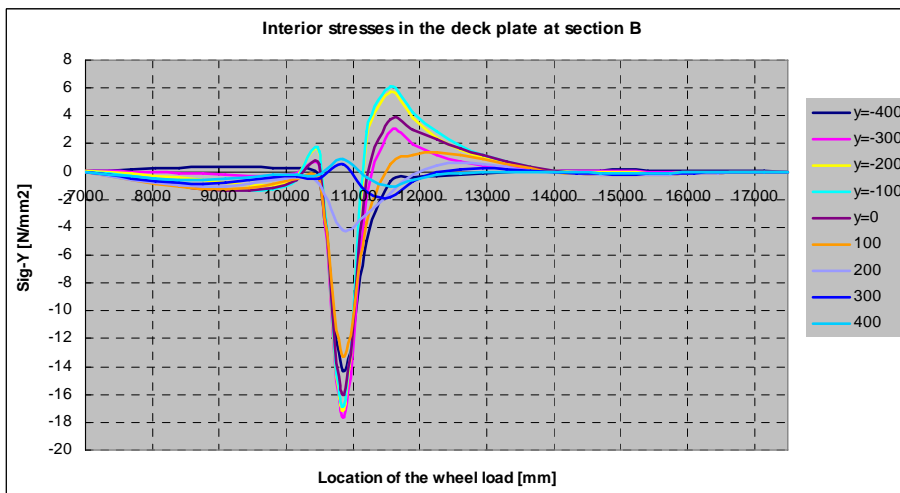
Longitudinal influence lines in the deck plate



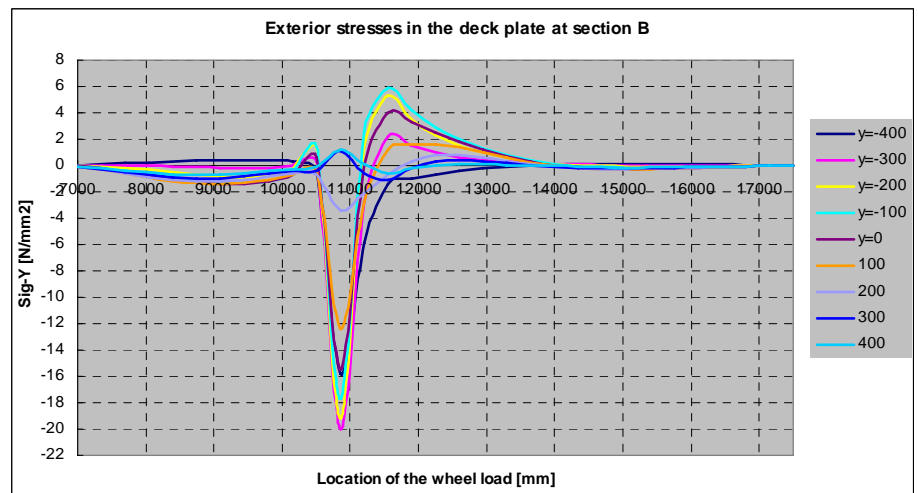
(a) Longitudinal influence line in the interior deck plate at section A



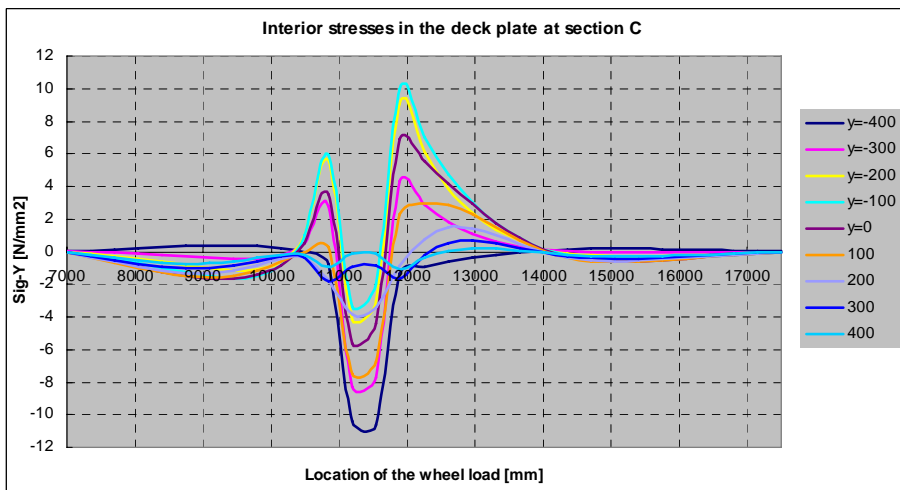
(b) Longitudinal influence line in the exterior deck plate at section A



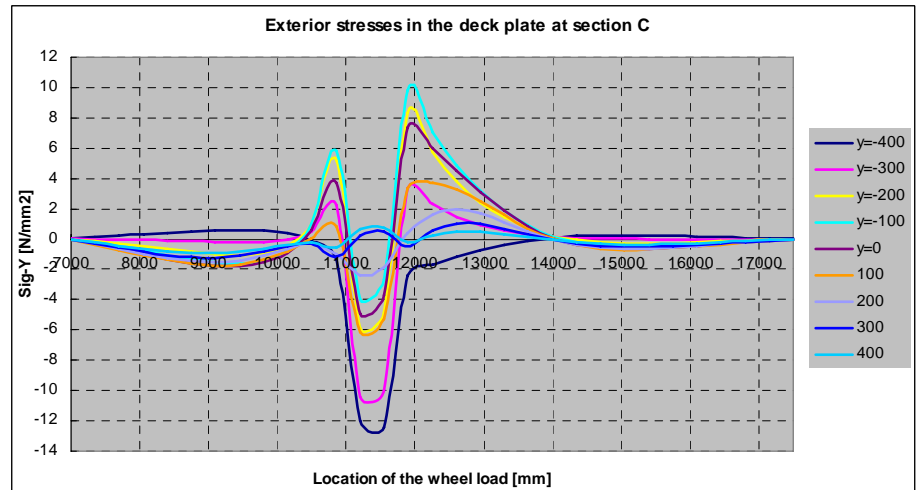
(c) Longitudinal influence line in the interior deck plate at section B



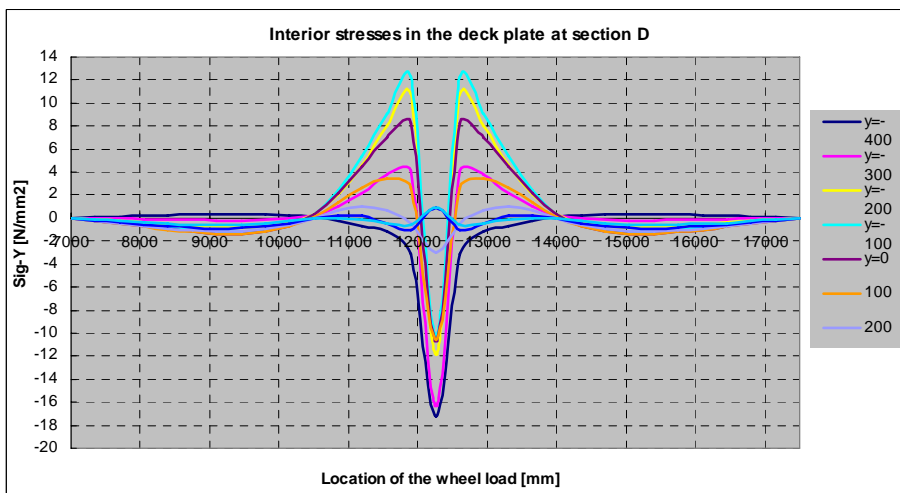
(d) Longitudinal influence line in the exterior deck plate at section B



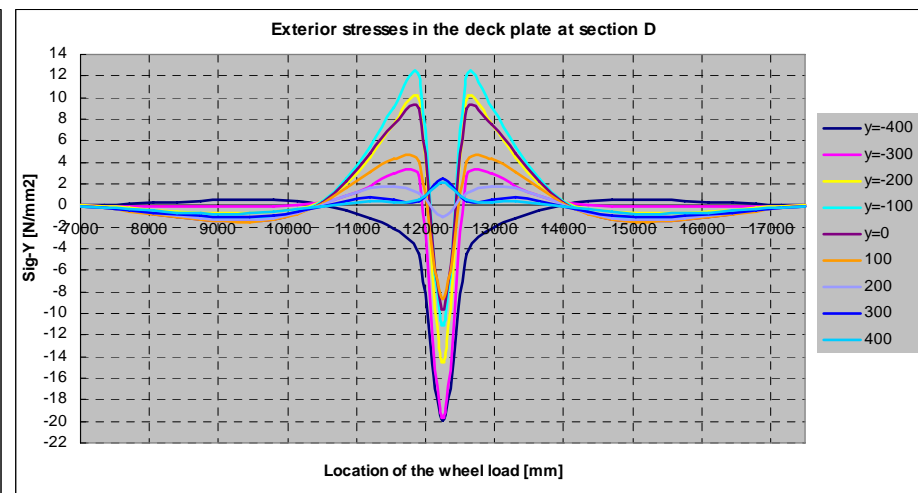
(e) Longitudinal influence line in the interior deck plate at section C



(f) Longitudinal influence line in the exterior deck plate at section C



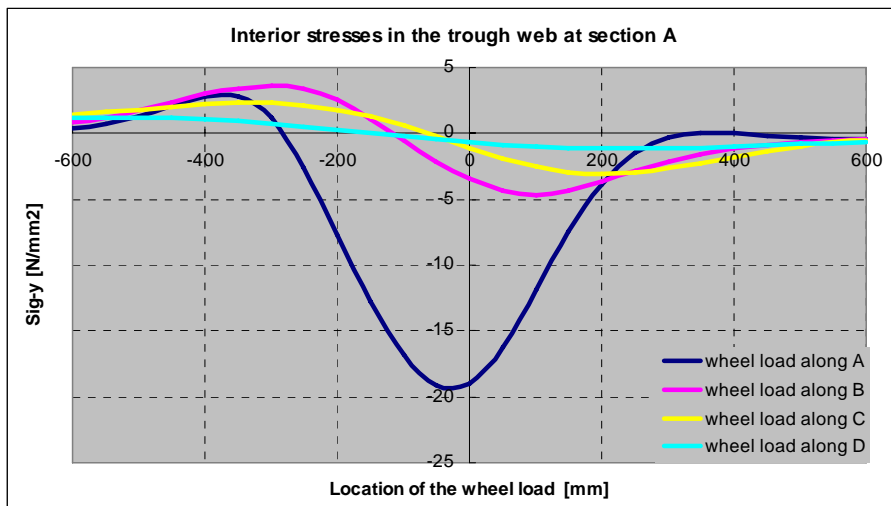
(g) Longitudinal influence line in the interior deck plate at section D



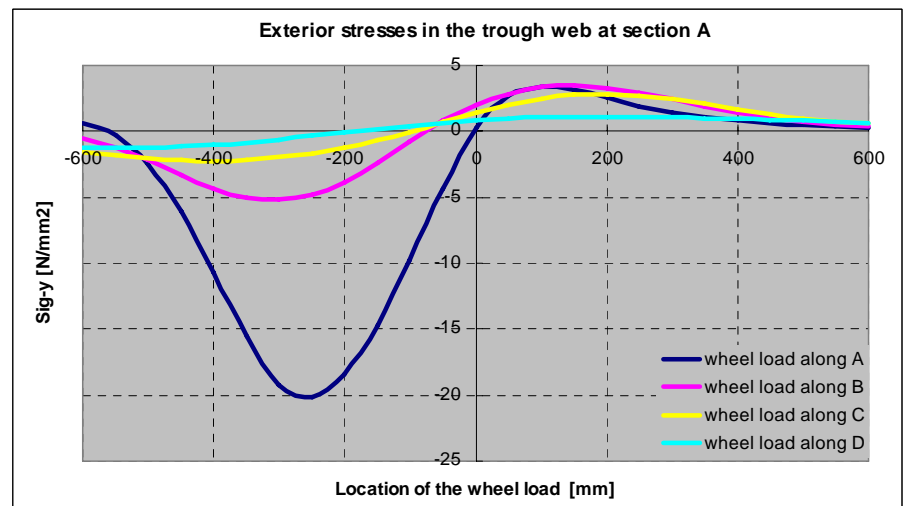
(h) Longitudinal influence line in the exterior deck plate at section D

Transverse influence lines under axle load C

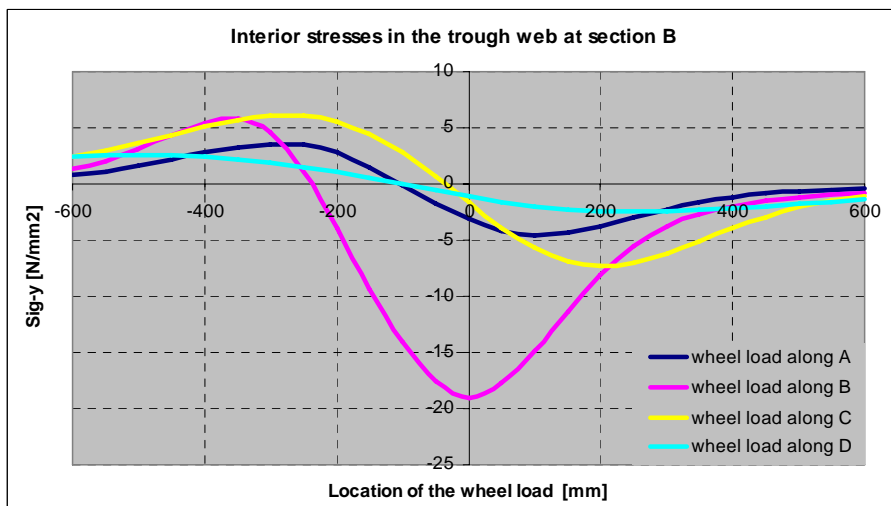
Transverse influence lines in the trough web



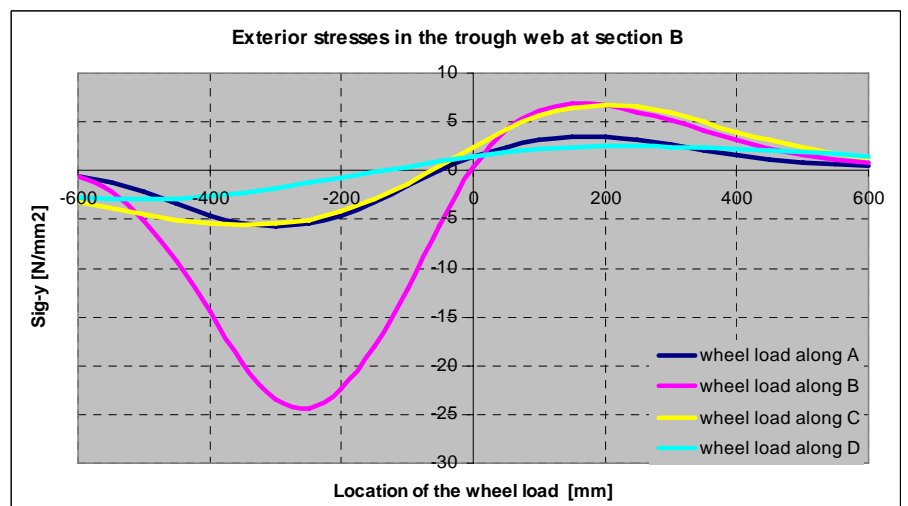
(a) Transverse influence line in the interior trough web at section A



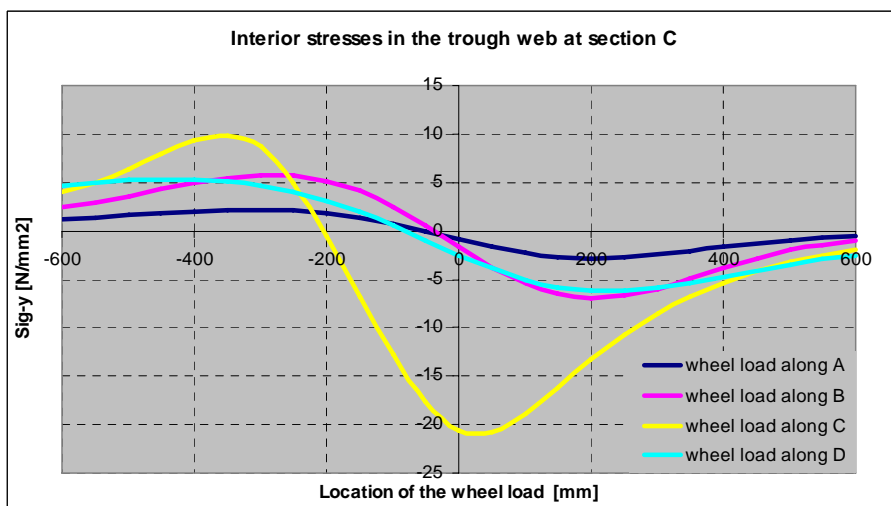
(b) Transverse influence line in the exterior trough web at section A



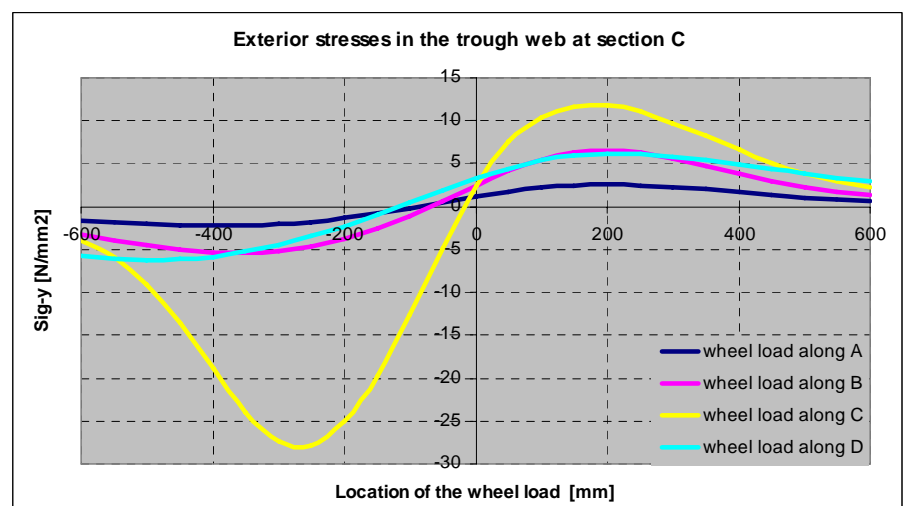
(c) Transverse influence line in the interior trough web at section B



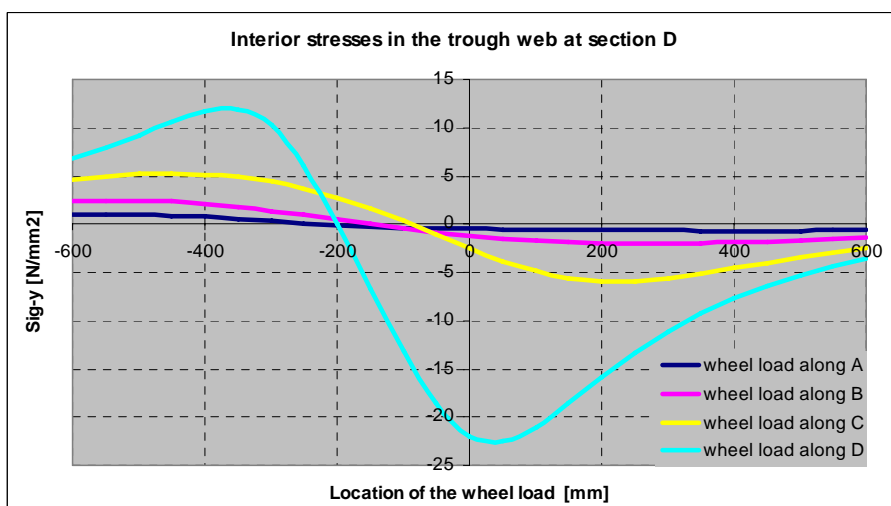
(d) Transverse influence line in the exterior trough web at section B



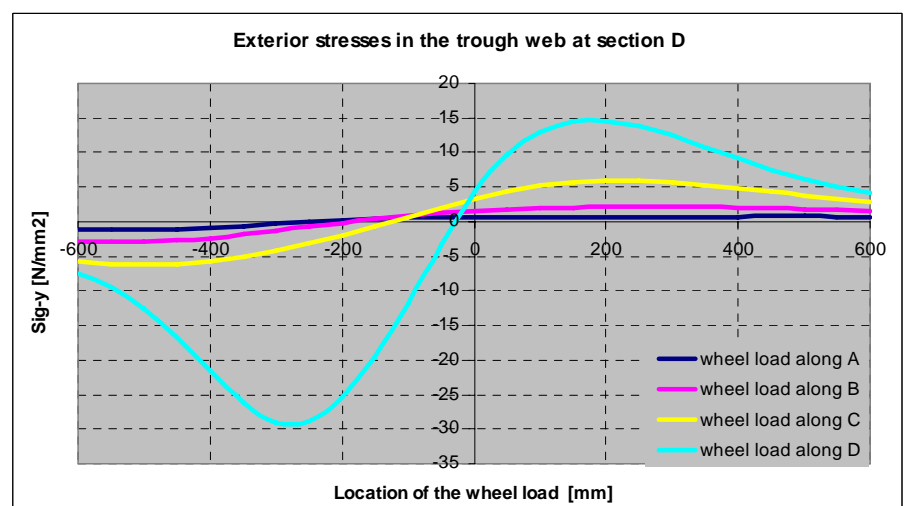
(e) Transverse influence line in the interior trough web at section C



(f) Transverse influence line in the exterior trough web at section C

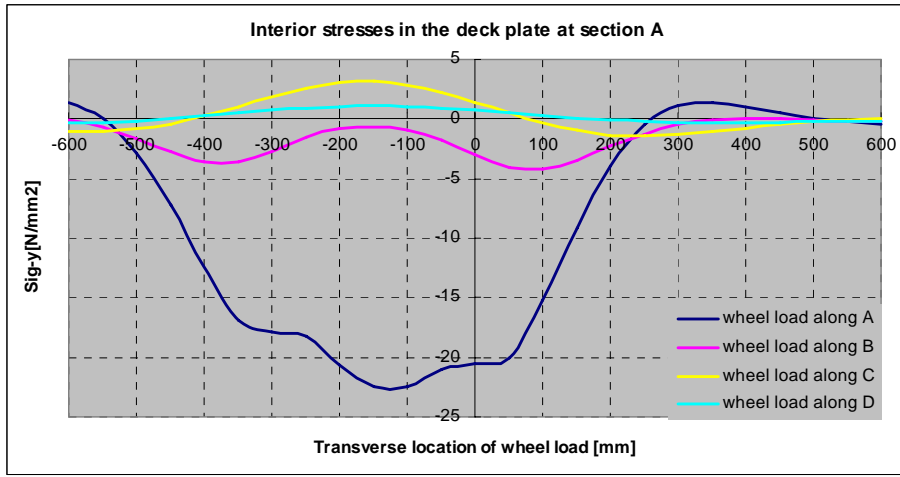


(g) Transverse influence line in the interior trough web at section D

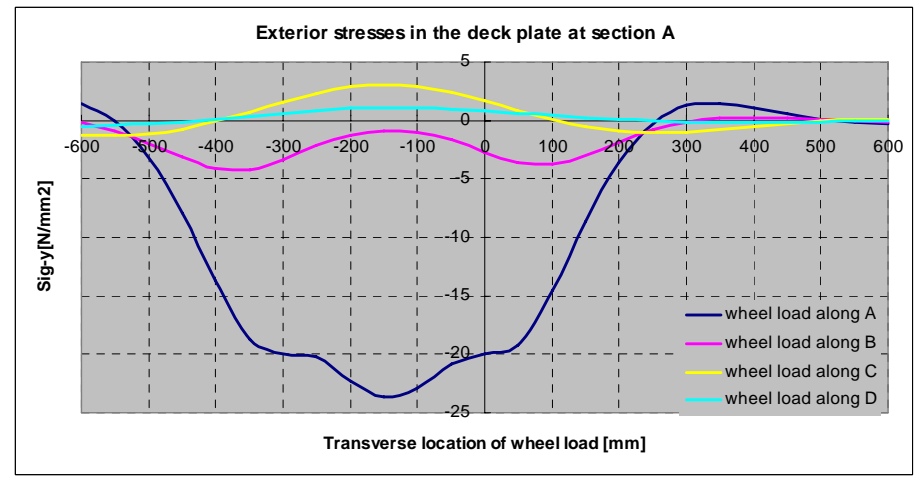


(h) Transverse influence line in the exterior trough web at section D

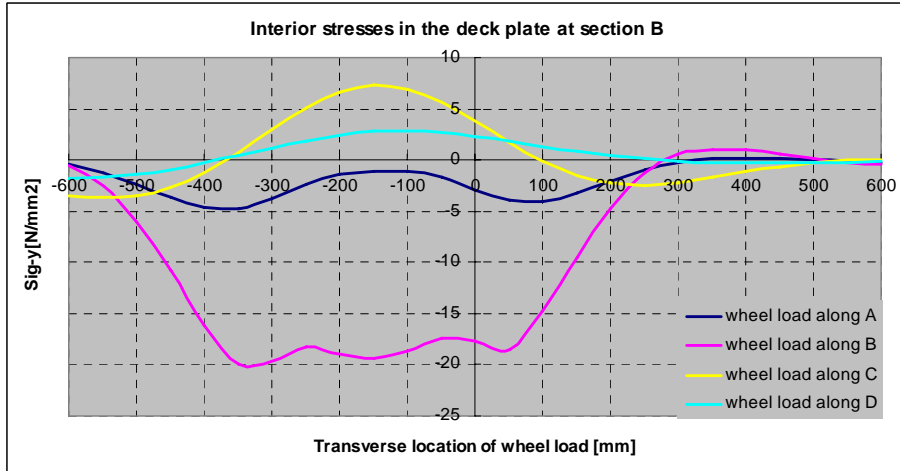
Transverse influence lines in the deck plate



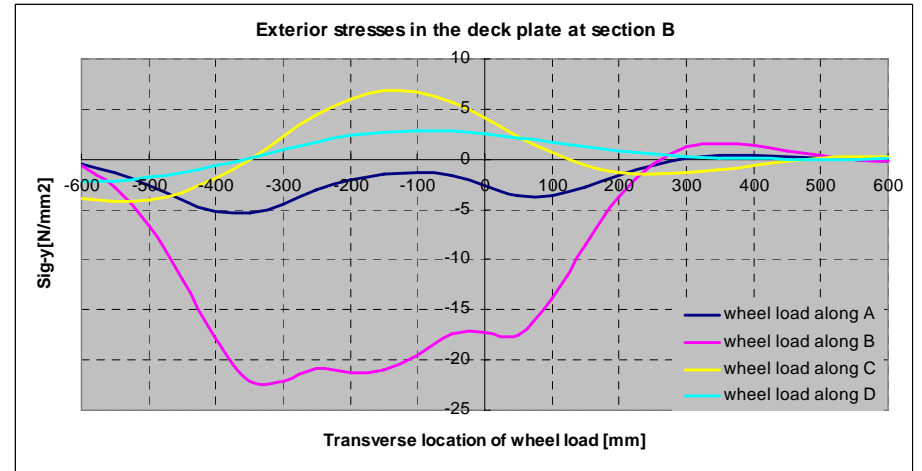
(a) Transverse influence line in the interior deck plate at section A



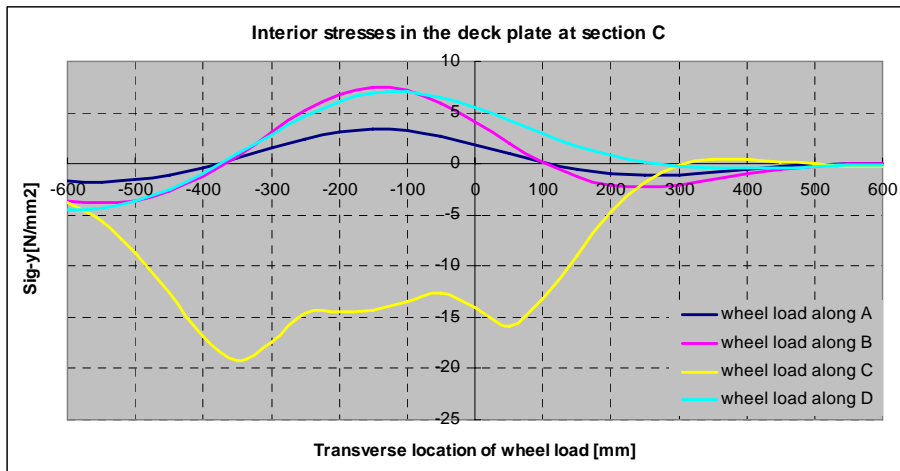
(b) Transverse influence line in the exterior deck plate at section A



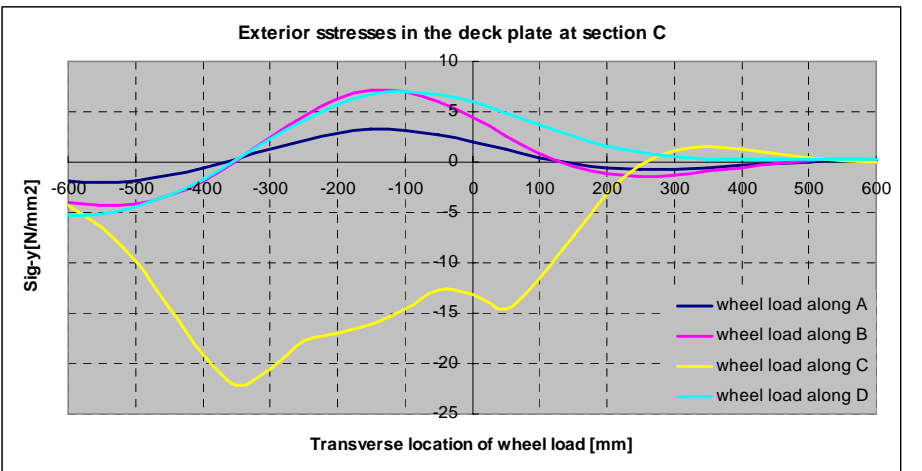
(c) Transverse influence line in the interior deck plate at section B



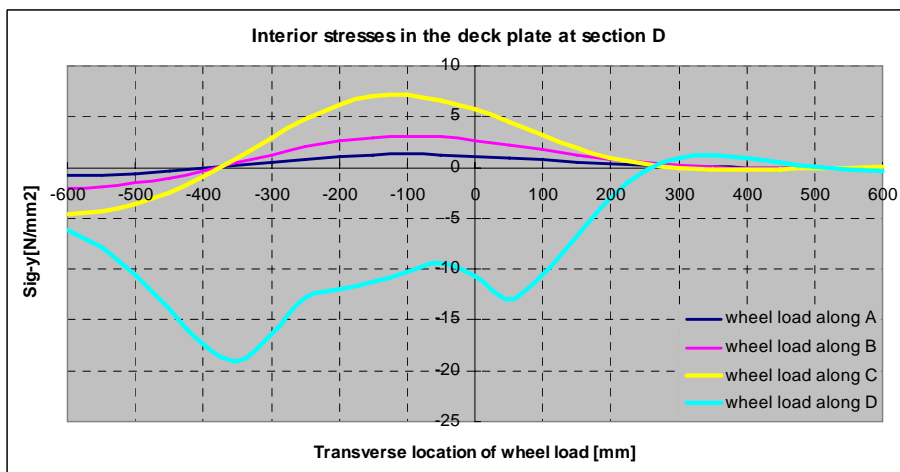
(d) Transverse influence line in the exterior deck plate at section B



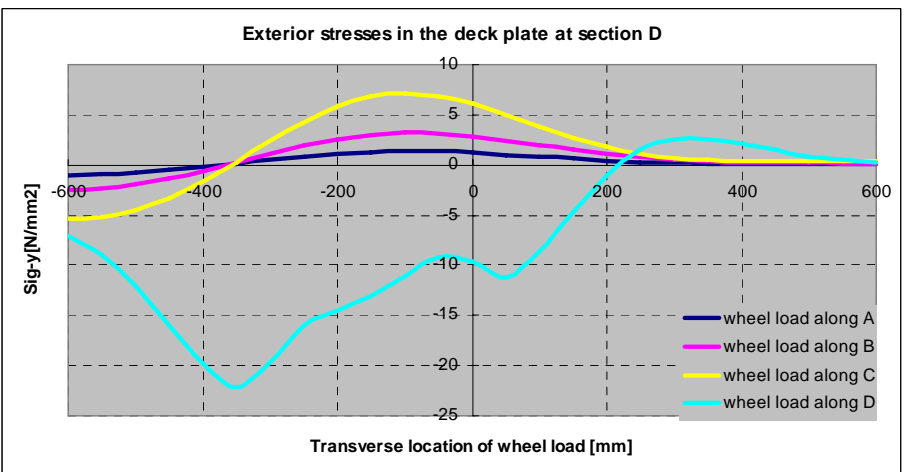
(e) Transverse influence line in the interior deck plate at section C



(f) Transverse influence line in the exterior deck plate at section C



(g) Transverse influence line in the interior deck plate at section D

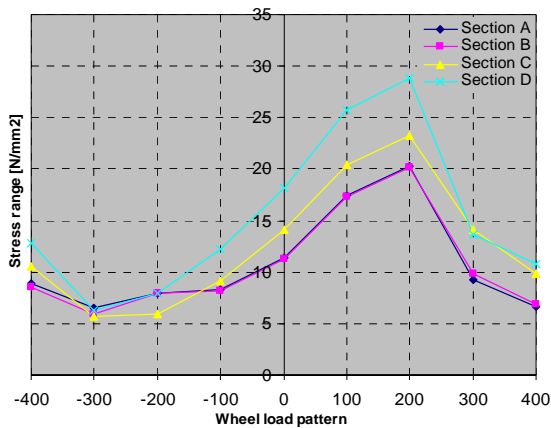


(h) Transverse influence line in the exterior deck plate at section D

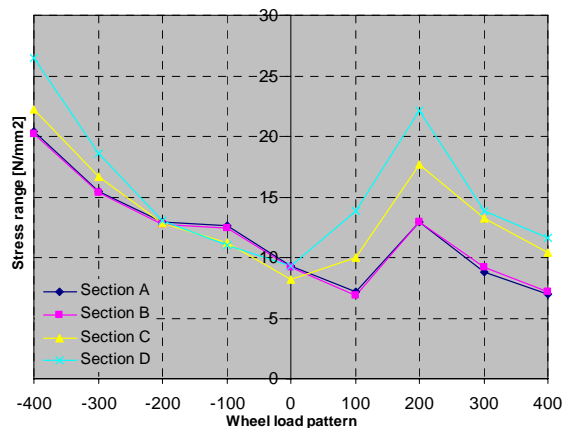
5. Stress ranges in model A

As the most important factor in the fatigue damage calculation, the stress ranges are collected in this part of appendix. The stress ranges are obtained from the longitudinal influence lines.

Stress ranges under axle load B

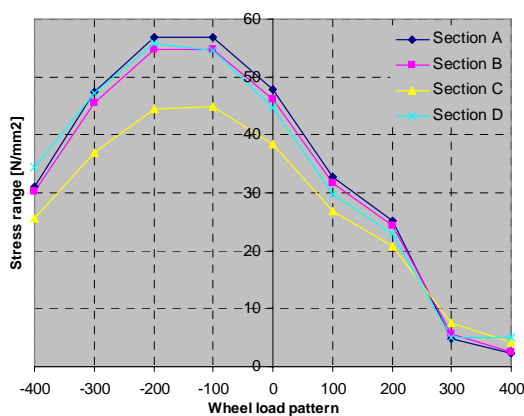


(a) Stress ranges in the interior trough web

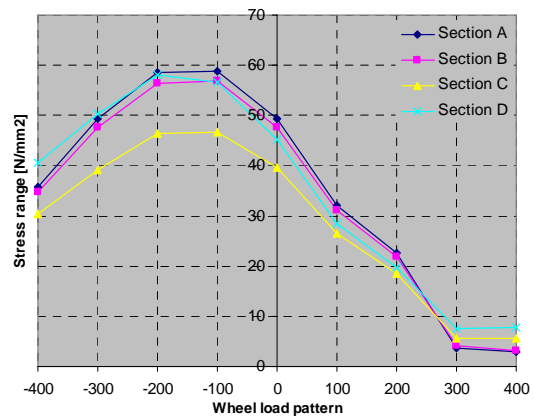


(b) Stress ranges in the exterior trough web

Investigate locations		Wheel load positions y [mm]								
Object locations	Cross sections	-400	-300	-200	-100	0	100	200	300	400
a	A	8.84	6.58	7.96	8.30	11.39	17.41	20.28	9.23	6.62
	B	8.51	5.98	7.92	8.21	11.33	17.30	20.13	9.83	6.85
	C	10.55	5.64	5.90	9.16	14.12	20.41	23.30	14.18	9.84
	D	12.76	6.31	7.91	12.18	18.12	25.80	28.85	13.70	10.80
b	A	20.36	15.49	12.88	12.62	9.31	7.15	12.96	8.78	6.95
	B	20.18	15.34	12.76	12.47	9.24	6.84	12.95	9.19	7.19
	C	22.19	16.68	12.86	11.26	8.20	10.04	17.65	13.27	10.40
	D	26.50	18.56	13.03	11.00	9.34	13.88	22.14	13.86	11.64



(a) Stress ranges in the interior deck plate

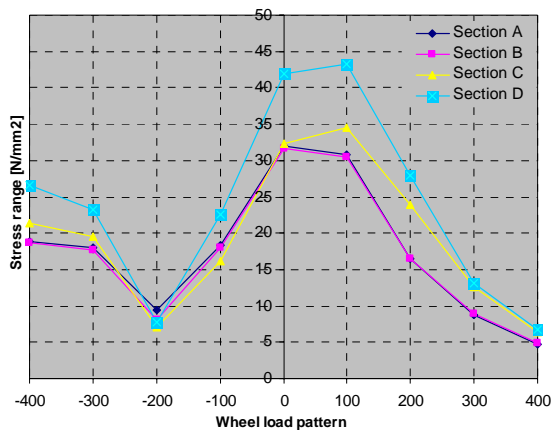


(b) Stress ranges in the exterior deck plate

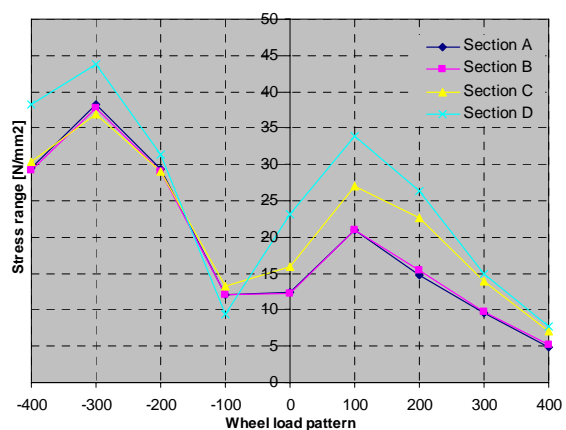
Appendix A

Investigate locations		Wheel load positions								
Object locations	Cross sections	-400	-300	-200	-100	0	100	200	300	400
c	A	31.11	47.38	56.79	56.76	47.76	32.69	25.16	4.88	2.37
	B	30.13	45.60	54.76	54.72	46.16	31.74	24.41	5.68	2.45
	C	25.52	37.02	44.55	44.87	38.34	26.90	20.77	7.52	4.15
	D	34.41	47.25	55.82	54.64	44.75	29.74	22.88	5.01	5.03
d	A	35.73	49.36	58.61	58.84	49.25	31.97	22.54	3.54	3.03
	B	34.65	47.54	56.50	56.81	47.63	31.11	21.89	4.17	3.13
	C	30.43	39.03	46.34	46.73	39.66	26.39	18.57	5.68	5.51
	D	40.59	50.27	57.98	56.55	45.30	28.35	19.59	7.63	7.90

Stress ranges under axle load C

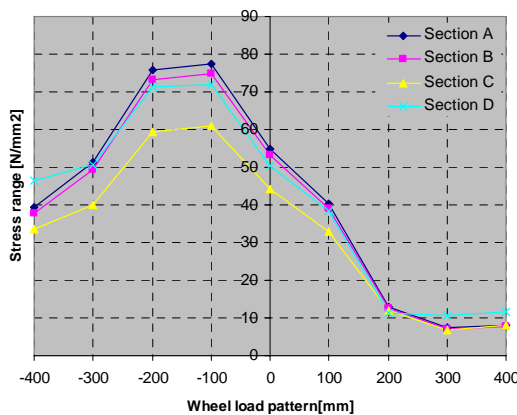


(a) Stress ranges in the interior trough web

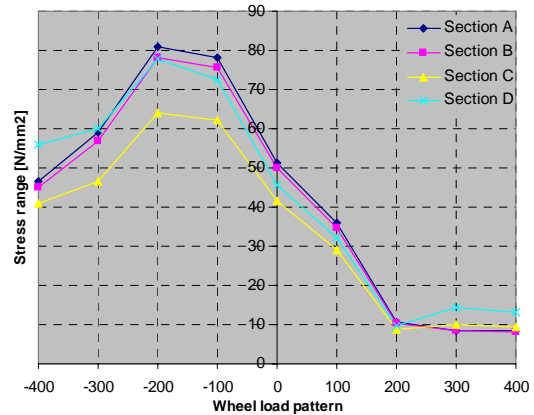


(b) Stress ranges in the exterior trough web

Investigate locations		Wheel load positions y [mm]								
Object locations	Cross sections	-400	-300	-200	-100	0	100	200	300	400
a	A	18.94	17.95	9.48	18.38	31.97	30.83	16.49	8.71	4.69
	B	18.76	17.72	8.14	18.07	31.57	30.49	16.49	9.00	4.89
	C	21.34	19.55	7.10	16.15	32.26	34.47	23.96	12.59	6.47
	D	26.65	23.20	7.82	22.63	41.98	43.28	27.88	13.14	6.71
b	A	29.60	38.22	29.44	12.10	12.39	21.02	14.75	9.49	4.92
	B	29.12	37.74	29.08	12.14	12.19	20.97	15.46	9.77	5.14
	C	30.30	36.88	29.10	13.31	15.95	27.06	22.63	13.89	6.97
	D	38.33	43.74	31.34	9.46	23.08	33.88	26.27	14.97	7.69



(a) Stress ranges in the interior deck plate

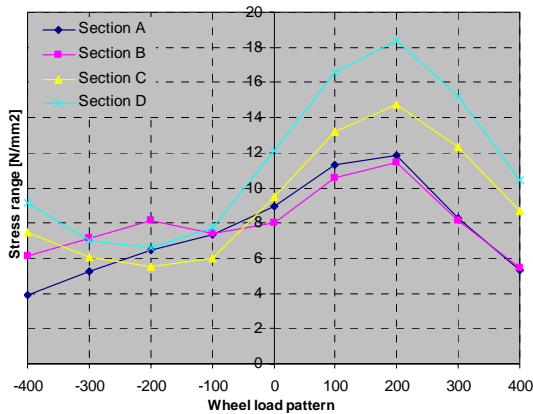


(b) Stress ranges in the exterior deck plate

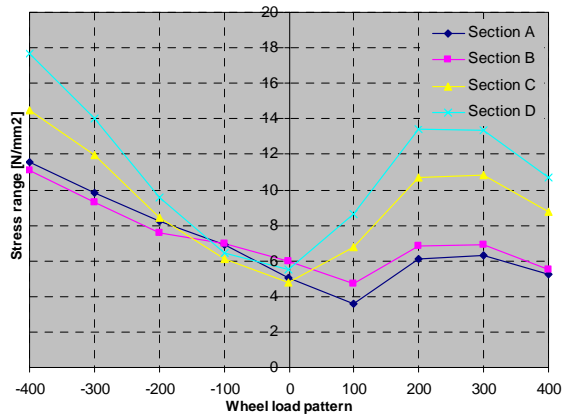
Investigate locations		Wheel load positions								
Object locations	Cross sections	-400	-300	-200	-100	0	100	200	300	400
c	A	39.23	51.29	75.81	77.35	54.80	40.46	12.95	7.32	8.07
	B	37.81	49.42	73.34	74.90	53.11	39.11	12.62	7.03	7.78
	C	33.52	39.89	59.30	61.00	44.17	32.91	11.80	6.89	7.92
	D	46.46	50.50	71.45	71.80	50.35	38.33	11.15	10.75	11.57
d	A	46.71	59.03	80.91	78.09	51.36	35.79	10.50	8.49	8.33
	B	45.14	56.95	78.19	75.62	49.85	34.62	10.18	8.29	8.10
	C	41.01	46.72	64.03	62.20	41.55	28.96	8.80	10.09	9.42
	D	56.03	59.85	77.74	72.55	45.60	32.14	9.67	14.31	13.13

6. Stress ranges in model B

Stress ranges under axle load B

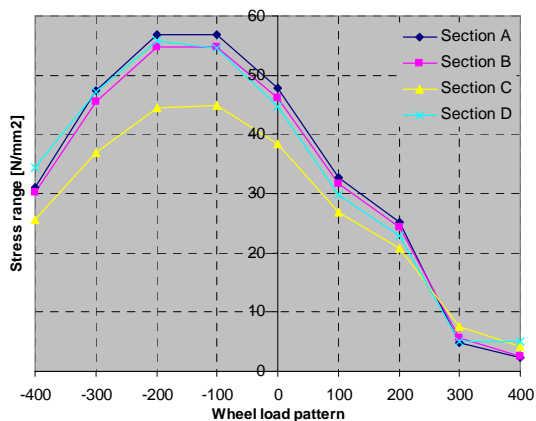


(a) Stress ranges in the interior trough web

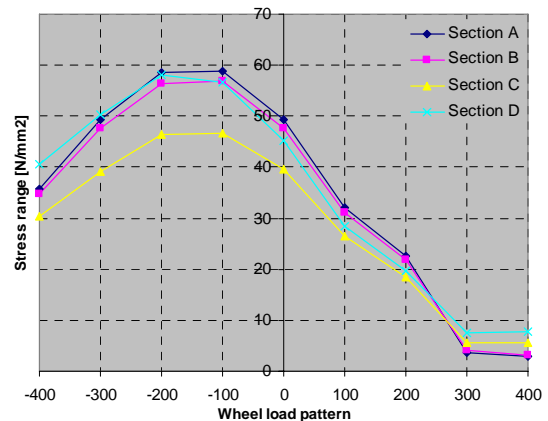


(b) Stress ranges in the exterior trough web

Investigate locations		Wheel load positions y [mm]								
Object locations	Cross section	-400	-300	-200	-100	0	100	200	300	400
a	A	3.92	5.26	6.49	7.36	8.93	11.30	11.85	8.30	5.31
	B	6.14	7.13	8.15	7.43	8.05	10.58	11.42	8.12	5.44
	C	7.46	6.09	5.50	5.96	9.52	13.19	14.77	12.30	8.66
	D	9.17	7.03	6.62	7.75	12.11	16.55	18.39	15.22	10.43
b	A	11.53	9.87	8.23	6.91	5.07	3.59	6.09	6.35	5.28
	B	11.07	9.27	7.56	6.99	5.99	4.74	6.83	6.93	5.50
	C	14.50	11.97	8.47	6.10	4.78	6.79	10.67	10.86	8.77
	D	17.67	13.99	9.58	6.47	5.50	8.64	13.43	13.37	10.71



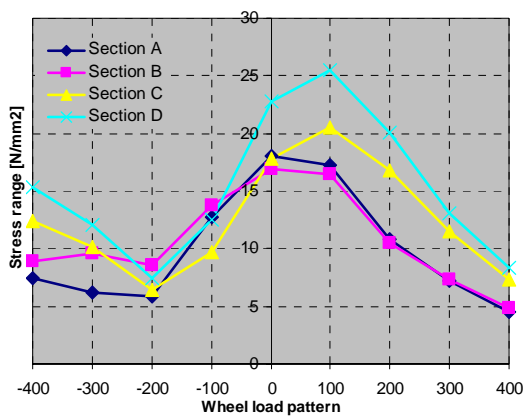
(c) Stress ranges in the interior deck plate



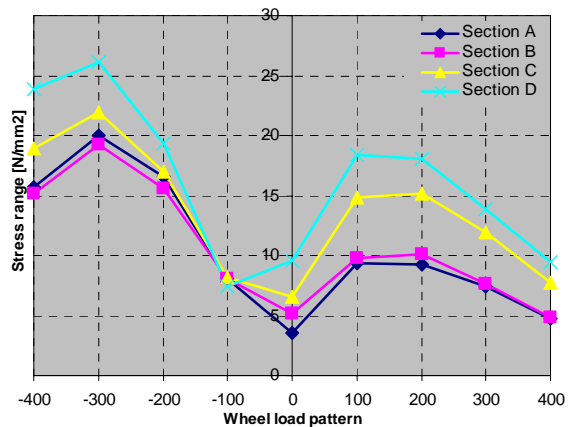
(d) Stress ranges in the exterior deck plate

Investigate locations		Wheel load positions								
Object locations	Cross sections	-400	-300	-200	-100	0	100	200	300	400
c	A	31.11	47.38	56.79	56.76	47.76	32.69	25.16	4.88	2.37
	B	30.13	45.60	54.76	54.72	46.16	31.74	24.41	5.68	2.45
	C	25.52	37.02	44.55	44.87	38.34	26.90	20.77	7.52	4.15
	D	34.41	47.25	55.82	54.64	44.75	29.74	22.88	5.01	5.03
d	A	35.73	49.36	58.61	58.84	49.25	31.97	22.54	3.54	3.03
	B	34.65	47.54	56.50	56.81	47.63	31.11	21.89	4.17	3.13
	C	30.43	39.03	46.34	46.73	39.66	26.39	18.57	5.68	5.51
	D	40.59	50.27	57.98	56.55	45.30	28.35	19.59	7.63	7.90

Stress ranges under axle load C

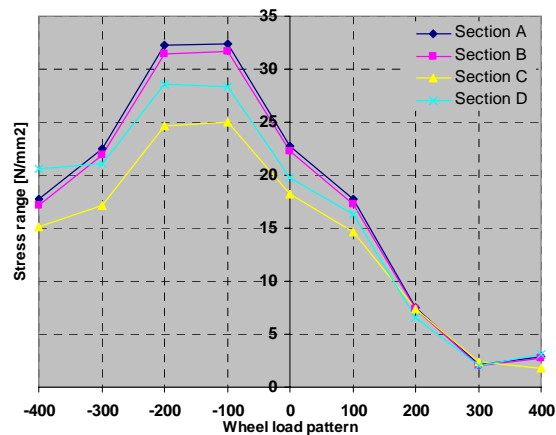


(a) Stress ranges in the interior trough web

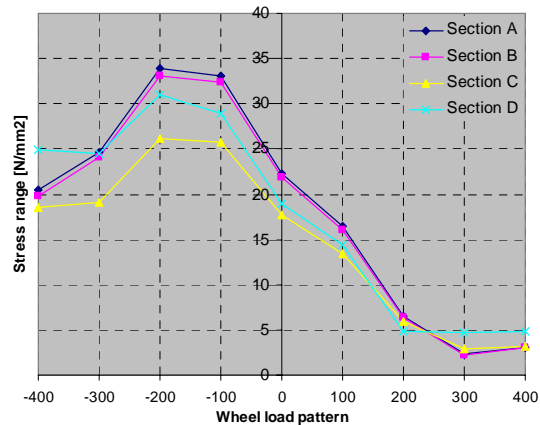


(b) Stress ranges in the exterior trough web

Investigate locations		Wheel load positions y [mm]								
Object locations	Cross section	-400	-300	-200	-100	0	100	200	300	400
a	A	7.42	6.24	5.82	12.74	18.06	17.27	10.78	7.23	4.51
	B	8.93	9.57	8.54	13.78	16.91	16.49	10.51	7.39	4.89
	C	12.44	10.10	6.45	9.72	17.79	20.47	16.80	11.48	7.29
	D	15.34	12.03	7.45	12.48	22.80	25.52	20.03	13.14	8.40
b	A	15.74	20.02	16.53	8.12	3.60	9.32	9.26	7.38	4.77
	B	15.20	19.20	15.58	8.05	5.18	9.78	10.06	7.66	4.85
	C	18.91	21.93	17.00	8.12	6.59	14.86	15.22	11.91	7.77
	D	23.87	26.16	19.37	7.42	9.57	18.38	18.08	13.88	9.45



(c) Stress ranges in the interior deck plate

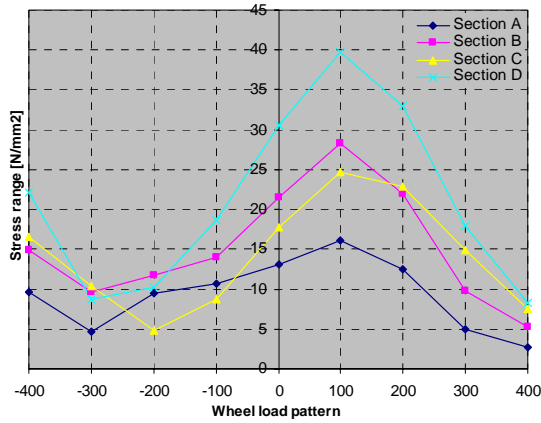


(d) Stress ranges in the exterior deck plate

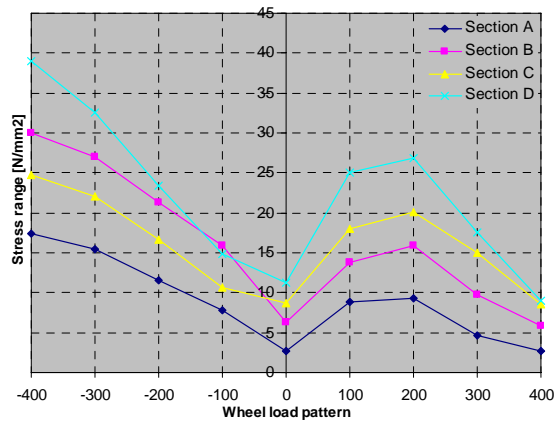
Investigate locations		Wheel load positions								
Object locations	Cross sections	-400	-300	-200	-100	0	100	200	300	400
c	A	17.68	22.52	32.27	32.44	22.79	17.79	7.54	2.14	2.82
	B	17.19	21.94	31.48	31.73	22.24	17.28	7.42	2.07	2.72
	C	15.12	17.14	24.65	25.04	18.17	14.62	7.43	2.39	1.80
	D	20.54	21.12	28.57	28.38	19.74	16.32	6.60	2.06	3.11
d	A	20.45	24.70	33.90	33.05	22.26	16.47	6.52	2.34	3.09
	B	19.86	24.03	33.08	32.33	21.83	16.09	6.41	2.27	3.00
	C	18.53	19.16	26.23	25.76	17.77	13.41	5.99	2.84	3.25
	D	24.87	24.46	31.02	28.99	18.98	14.39	4.83	4.70	4.90

7. Stress ranges in model C

Stress ranges under axle load B

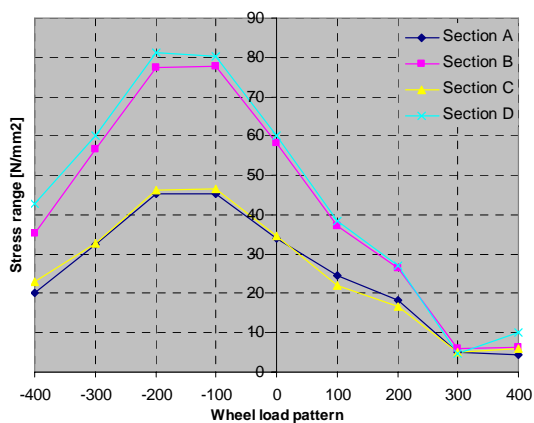


(a) Stress ranges in the interior trough web

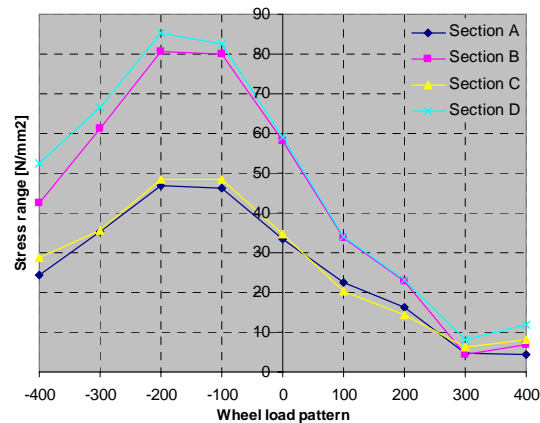


(b) Stress ranges in the exterior trough web

Investigate locations		Wheel load positions y [mm]									
Object locations	Cross sections	-400	-300	-200	-100	0	100	200	300	400	
a	A	9.69	4.61	9.45	10.63	13.08	16.16	12.46	4.94	2.71	
	B	14.86	9.64	11.70	13.94	21.51	28.29	21.94	9.75	5.32	
	C	16.51	10.32	4.75	8.76	17.78	24.63	22.91	14.90	7.49	
	D	22.18	8.70	10.16	18.73	30.58	39.71	33.01	17.86	8.31	
b	A	17.39	15.39	11.49	7.76	2.71	8.83	9.28	4.67	2.76	
	B	30.00	26.98	21.37	15.90	6.27	13.87	15.90	9.73	5.90	
	C	24.69	22.08	16.65	10.72	8.63	17.94	20.12	15.01	8.55	
	D	38.93	32.62	23.41	14.82	11.28	25.00	26.79	17.53	9.06	



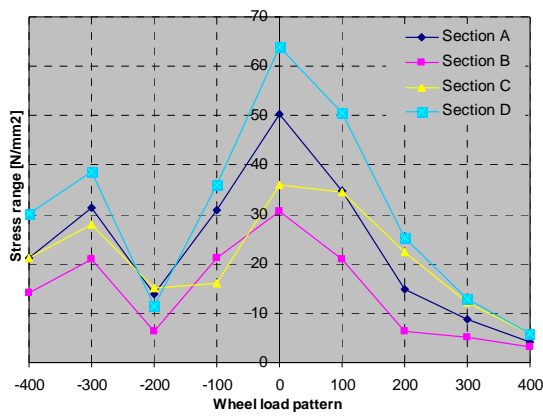
(c) Stress ranges in the interior deck plate



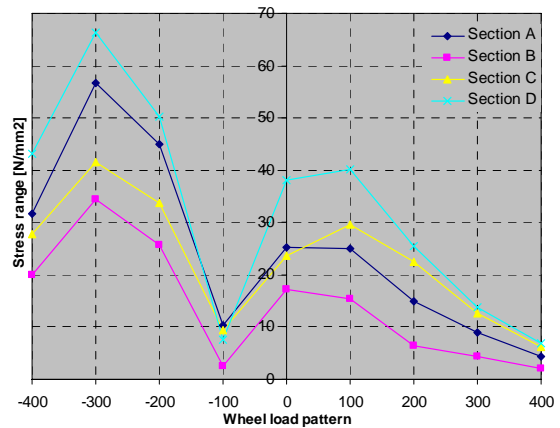
(d) Stress ranges in the exterior deck plate

Investigate locations		Wheel load positions									
Object locations	Cross sections	-400	-300	-200	-100	0	100	200	300	400	
c	A	20.11	32.49	45.32	45.33	33.86	24.41	18.16	4.96	4.31	
	B	35.26	56.53	77.52	77.68	58.25	37.03	26.39	5.83	6.32	
	C	22.95	32.61	46.15	46.72	34.50	22.07	16.72	4.95	6.10	
	D	42.68	60.25	81.22	80.40	60.05	38.48	27.20	4.84	9.95	
d	A	24.27	35.19	46.95	46.36	33.41	22.39	16.30	4.56	4.44	
	B	42.66	61.19	80.66	79.88	58.18	33.65	22.93	4.48	6.90	
	C	28.69	35.67	48.50	48.32	34.55	20.37	14.47	6.32	8.05	
	D	52.40	66.64	85.41	82.65	59.05	34.00	23.21	8.08	12.00	

Stress ranges under axle load C

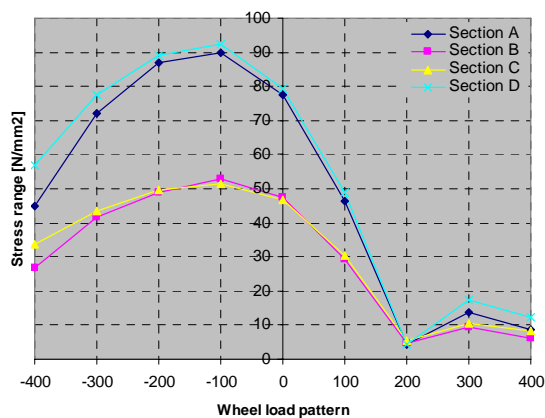


(a) Stress ranges in the interior trough web

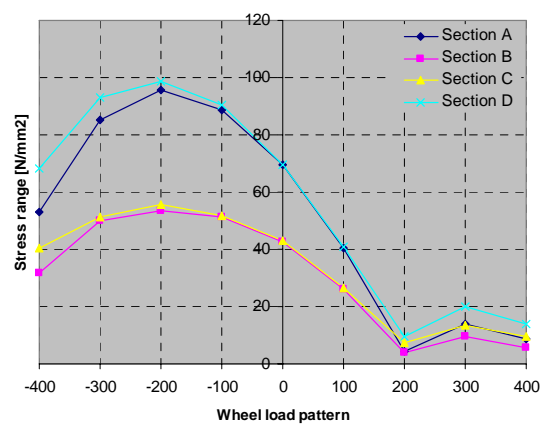


(b) Stress ranges in the exterior trough web

Investigate locations		Wheel load positions y [mm]								
Object locations	Cross sections	-400	-300	-200	-100	0	100	200	300	400
a	A	21.04	31.26	13.77	30.91	50.21	34.83	14.77	8.76	4.23
	B	14.20	20.88	6.43	21.07	30.57	20.98	6.38	5.15	3.06
	C	21.10	27.91	15.09	16.03	36.04	34.63	22.27	12.13	5.72
	D	30.23	38.75	11.35	35.97	63.92	50.52	25.40	12.95	5.89
c	A	31.71	56.71	44.96	10.30	25.28	25.06	15.03	9.03	4.36
	B	20.08	34.42	25.62	2.63	17.26	15.37	6.37	4.42	2.08
	C	27.86	41.44	33.76	9.40	23.71	29.51	22.48	12.74	6.23
	D	43.12	66.28	50.15	7.53	38.03	40.13	25.39	13.72	6.83



(c) Stress ranges in the interior deck plate

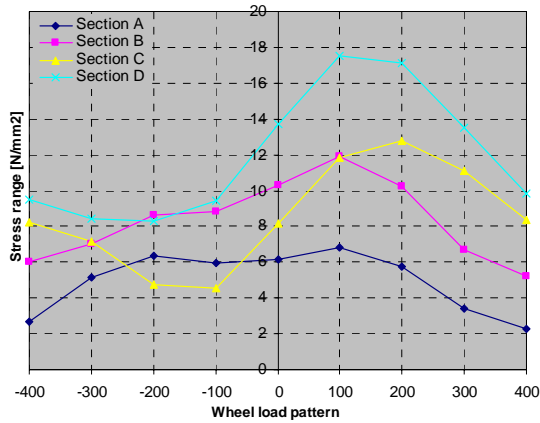


(d) Stress ranges in the exterior deck plate

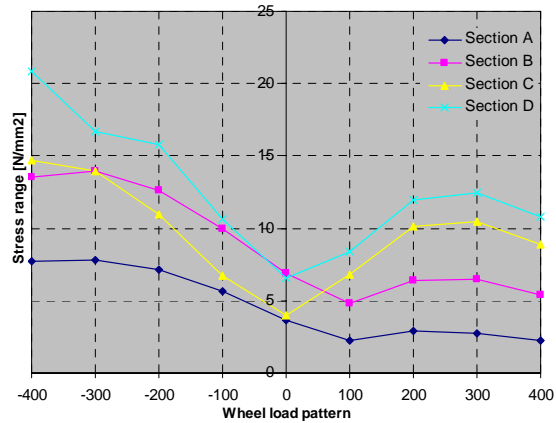
Investigate locations		Wheel load positions								
Object locations	Cross sections	-400	-300	-200	-100	0	100	200	300	400
c	A	44.80	72.26	86.85	89.91	77.42	46.49	4.29	13.65	8.80
	B	26.87	41.69	49.02	52.88	47.63	29.33	4.63	9.57	6.01
	C	33.69	43.45	49.70	51.50	46.75	30.45	5.38	10.67	8.22
	D	56.98	77.57	88.95	92.30	79.45	48.85	4.52	17.39	12.50
d	A	53.05	85.19	95.45	88.85	69.50	40.58	4.18	14.13	8.84
	B	31.93	49.88	53.69	51.17	42.64	26.14	4.05	9.48	5.82
	C	40.40	51.12	55.50	51.60	42.85	26.37	7.34	13.49	9.46
	D	68.17	93.24	98.60	90.55	69.75	40.73	9.55	20.12	13.70

8. Stress ranges in model D

Stress ranges under axle load B

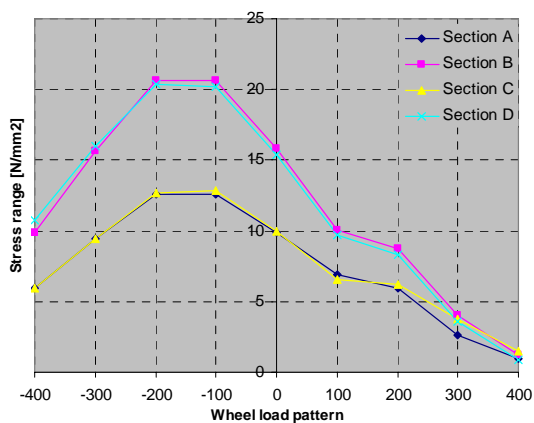


(a) Stress ranges in the interior trough web

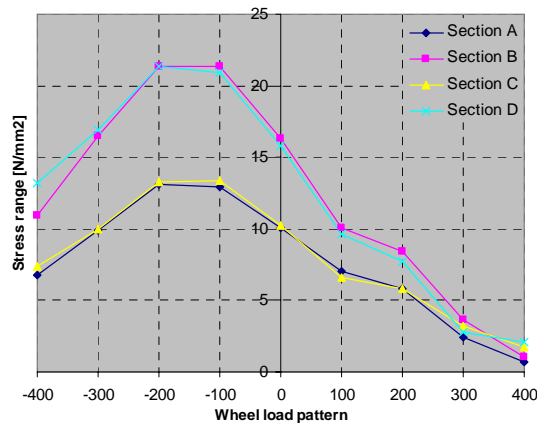


(b) Stress ranges in the exterior trough web

Investigate locations		Wheel load positions y [mm]									
Object locations	Cross sections	-400	-300	-200	-100	0	100	200	300	400	
a	A	2.65	5.15	6.36	5.95	6.14	6.85	5.74	3.40	2.30	
	B	6.00	7.01	8.62	8.82	10.33	11.89	10.21	6.71	5.20	
	C	8.20	7.19	4.78	4.53	8.15	11.82	12.78	11.08	8.38	
	D	9.52	8.42	8.29	9.45	13.69	17.50	17.12	13.52	9.82	
b	A	7.70	7.83	7.14	5.61	3.64	2.24	2.89	2.74	2.28	
	B	13.51	13.99	12.64	10.01	6.88	4.78	6.36	6.51	5.39	
	C	14.68	14.00	10.94	6.72	4.01	6.83	10.15	10.51	8.91	
	D	20.82	16.68	15.77	10.60	6.53	8.41	12.00	12.50	10.76	



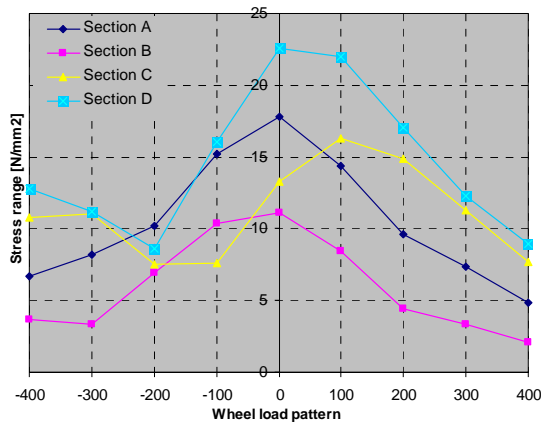
(c) Stress ranges in the interior deck plate



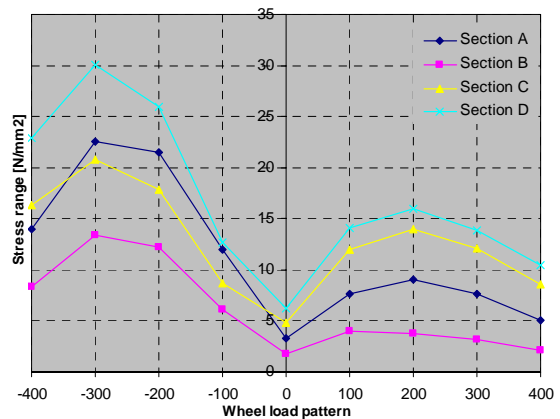
(d) Stress ranges in the exterior deck plate

Investigate locations		Wheel load positions									
Object locations	Cross sections	-400	-300	-200	-100	0	100	200	300	400	
c	A	5.94	9.45	12.59	12.57	9.88	6.93	5.94	2.65	0.93	
	B	9.87	15.68	20.61	20.65	15.79	10.03	8.78	3.99	1.19	
	C	5.98	9.40	12.69	12.87	9.93	6.60	6.25	3.80	1.45	
	D	10.73	15.97	20.37	20.18	15.42	9.74	8.29	3.55	0.88	
d	A	6.77	9.94	13.07	12.95	10.11	7.00	5.81	2.47	0.68	
	B	10.97	16.48	21.38	21.39	16.31	10.10	8.39	3.63	1.01	
	C	7.37	9.98	13.26	13.37	10.22	6.59	5.85	3.24	1.75	
	D	13.16	16.97	21.38	20.94	15.81	9.60	7.71	2.76	2.05	

Stress ranges under axle load C

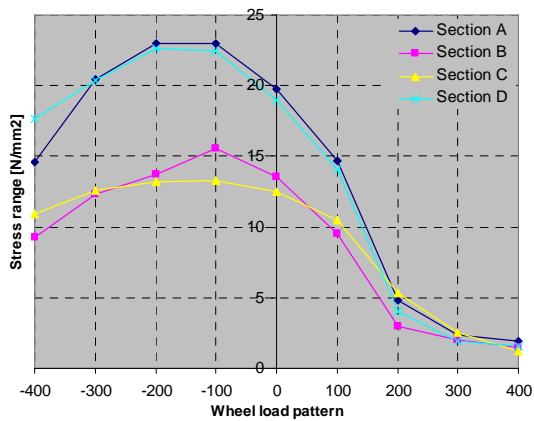


(a) Stress ranges in the interior trough web

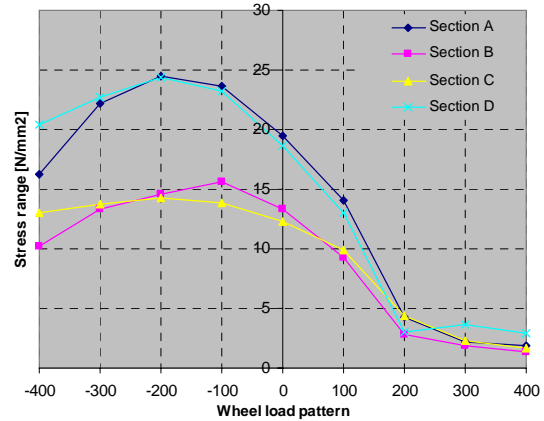


(b) Stress ranges in the exterior trough web

Investigate locations		Wheel load positions y [mm]								
Object locations	Cross sections	-400	-300	-200	-100	0	100	200	300	400
a	A	6.72	8.22	10.22	15.23	17.83	14.37	9.59	7.39	4.82
	B	3.70	3.33	6.95	10.34	11.10	8.45	4.43	3.37	2.10
	C	10.76	11.03	7.50	7.63	13.32	16.30	14.88	11.31	7.67
	D	12.81	11.17	8.58	16.05	22.59	21.99	17.03	12.32	8.92
c	A	14.00	22.51	21.45	11.94	3.32	7.69	9.08	7.65	5.09
	B	8.39	13.37	12.24	6.06	1.77	4.03	3.81	3.20	2.15
	C	16.38	20.81	17.82	8.75	4.86	12.01	14.01	12.05	8.61
	D	22.86	30.01	25.95	12.67	6.28	14.07	16.00	13.90	10.46



(c) Stress ranges in the interior deck plate



(d) Stress ranges in the exterior deck plate

Investigate locations		Wheel load positions								
Object locations	Cross sections	-400	-300	-200	-100	0	100	200	300	400
c	A	14.61	20.47	22.97	22.97	19.74	14.65	4.85	2.34	1.94
	B	9.27	12.30	13.71	15.56	13.59	9.51	2.97	1.98	1.44
	C	10.97	12.57	13.20	13.33	12.47	10.47	5.31	2.52	1.25
	D	17.65	20.37	22.65	22.50	18.96	14.05	4.06	1.96	1.55
d	A	16.25	22.22	24.47	23.61	19.52	14.05	4.24	2.18	1.92
	B	10.25	13.35	14.60	15.64	13.36	9.24	2.78	1.88	1.36
	C	12.98	13.76	14.30	13.83	12.33	9.86	4.39	2.25	1.65
	D	20.41	22.72	24.36	23.20	18.61	13.04	3.05	3.62	2.89

Appendix B Comparison 3D model and 2D model

In the thesis, the comparison between the 3D finite element model and the 2D simplified model is made. It is made in the transverse influence line in the object joint at mid-span of the trough. The complete results and the graphs for each model are presented in this appendix. They are grouped according to each model. First of all, the stress in the mid-span in 3D model is compared to the stress in the bottom level of the simplified model. Then, comparison is made between the stress in the object joint when the wheel load is 350mm away from the mid-span and the stress in the top level of the simplified model.

1. Model A

Geometry of model A

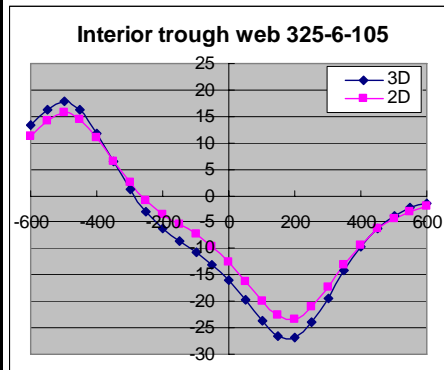
Structural component		Model A
Crossbeam	Height(H_c)	1250
	Length(L_c)	4200
	Distance(D_c)	3500
	Thickness(t_c)	12
Deck plate	Length(L_d)	21000
	Width(B_d)	4200
	Thickness(t_d)	12
Trough	Height(h_t)	325
	Width upper(b_{top})	300
	Width bottom(b_{bot})	105
	Thickness(t_t)	6
Asphalt	Distance(d_a)	600
	Thickness(t_a)	60

The unit of the dimension is mm

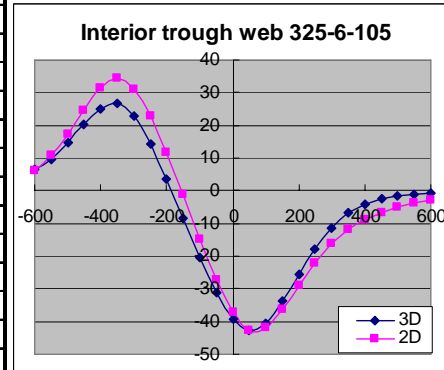
Mid-span (3D model) v.s Bottom level (2D model)

Stress in the trough web

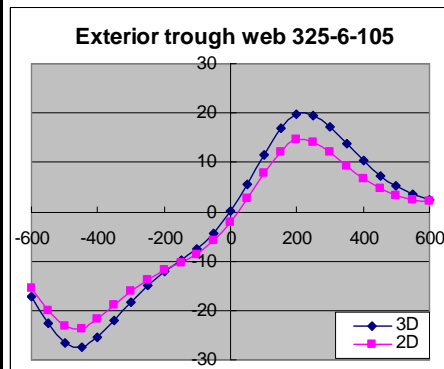
Interior trough web	325-6-105	
	Axle B	
	3D	2D
-600	13.3	11.21
-550	16.3	14.15
-500	17.8	15.62
-450	16.2	14.46
-400	11.9	10.93
-350	6.47	6.58
-300	1.24	2.44
-250	-3.11	-0.98
-200	-6.32	-3.51
-150	-8.64	-5.44
-100	-10.7	-7.27
-50	-13	-9.55
0	-16.1	-12.56
50	-19.8	-16.19
100	-23.6	-19.89
150	-26.5	-22.66
200	-26.8	-23.36
250	-23.9	-21.07
300	-19.3	-17.34
350	-14.2	-13.11
400	-9.61	-9.27
450	-6.08	-6.30
500	-3.71	-4.23
550	-2.27	-2.90
600	-1.44	-2.07



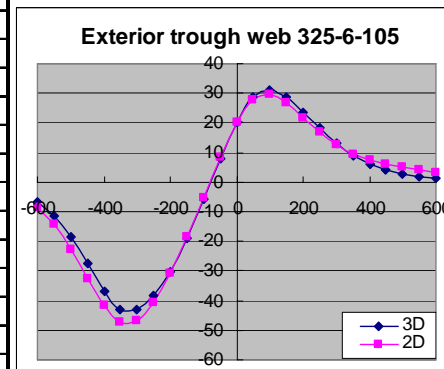
Interior trough web	325-6-105	
	Axle C	
	3D	2D
-600	6.44	6.20
-550	9.77	10.76
-500	14.60	17.27
-450	20.30	24.75
-400	25.20	31.37
-350	26.80	34.31
-300	22.70	31.12
-250	14.30	22.93
-200	3.47	11.64
-150	-8.51	-1.32
-100	-20.40	-14.78
-50	-31.10	-27.26
0	-39.20	-37.28
50	-42.90	-42.84
100	-40.50	-41.87
150	-33.80	-36.39
200	-25.60	-29.09
250	-17.70	-21.93
300	-11.40	-15.95
350	-6.89	-11.67
400	-4.08	-8.65
450	-2.42	-6.55
500	-1.48	-5.02
550	-0.97	-3.84
600	-0.71	-2.84



Exterior trough web	325-6-105	
	Axle B	
	3D	2D
-600	-17.3	-15.59
-550	-22.6	-20.05
-500	-26.5	-23.18
-450	-27.4	-23.74
-400	-25.4	-21.87
-350	-22	-19.02
-300	-18.3	-16.16
-250	-15	-13.74
-200	-12.2	-11.91
-150	-9.92	-10.36
-100	-7.54	-8.55
-50	-4.37	-5.91
0	0.00168	-2.16
50	5.5	2.57
100	11.5	7.71
150	16.9	12.14
200	19.9	14.64
250	19.5	14.13
300	17.1	12.06
350	13.7	9.29
400	10.3	6.69
450	7.36	4.69
500	5.13	3.35
550	3.55	2.52
600	2.46	2.03

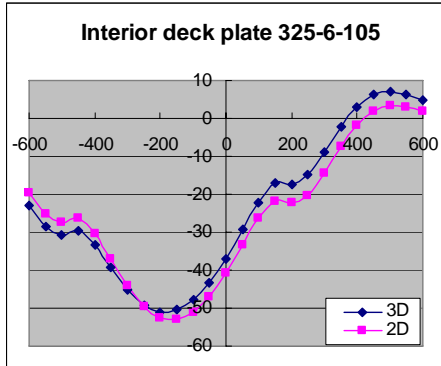


Exterior trough web	325-6-105	
	Axle C	
	3D	2D
-600	-6.73	-8.56
-550	-11.40	-14.44
-500	-18.60	-22.73
-450	-27.60	-32.45
-400	-36.70	-41.63
-350	-42.80	-47.29
-300	-43.20	-46.68
-250	-38.50	-40.67
-200	-30.10	-30.96
-150	-18.80	-18.68
-100	-5.73	-5.16
-50	7.84	8.34
0	20.10	20.12
50	28.50	27.96
100	30.90	29.53
150	28.50	26.61
200	23.70	21.71
250	18.20	16.67
300	13.10	12.45
350	9.06	9.53
400	6.09	7.53
450	4.01	6.13
500	2.60	5.06
550	1.70	4.14
600	1.17	3.28

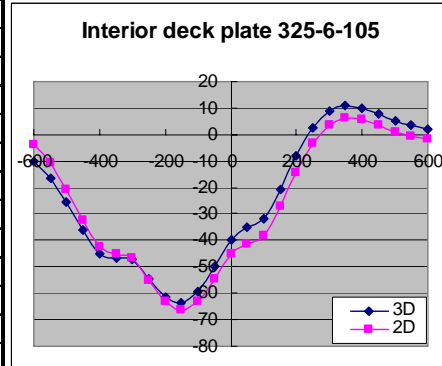


Stress in the deck plate

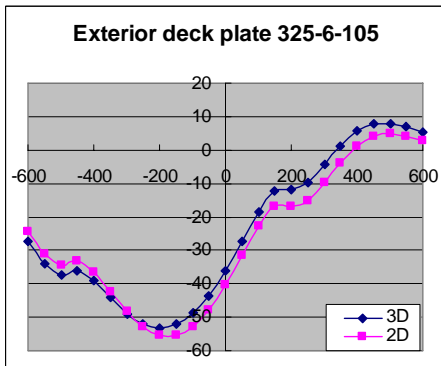
Interior deck plate	325-6-105	
	Axle B	
	3D	2D
-600	-23.10	-19.63
-550	-28.60	-25.31
-500	-30.70	-27.38
-450	-29.60	-26.25
-400	-33.30	-30.29
-350	-39.30	-37.12
-300	-45.20	-44.04
-250	-49.30	-49.54
-200	-51.00	-52.54
-150	-50.40	-53.05
-100	-47.90	-51.28
-50	-43.40	-47.14
0	-37.00	-40.84
50	-29.40	-33.38
100	-22.10	-26.35
150	-17.20	-21.83
200	-17.30	-22.40
250	-14.90	-20.47
300	-8.90	-14.44
350	-2.22	-7.58
400	3.11	-1.74
450	6.15	1.92
500	6.92	3.28
550	6.23	3.05
600	4.92	2.00



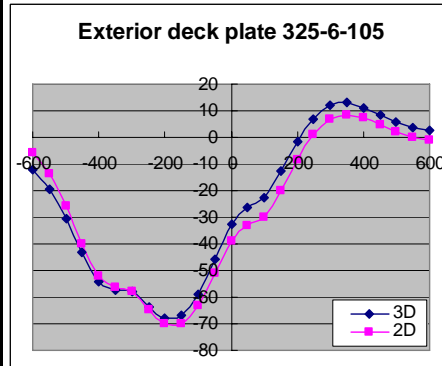
Interior deck plate	325-6-105	
	Axle C	
	3D	2D
-600	-10.20	-3.87
-550	-16.50	-10.45
-500	-25.70	-20.55
-450	-36.30	-32.33
-400	-45.00	-42.29
-350	-46.60	-45.03
-300	-47.30	-46.85
-250	-54.50	-55.25
-200	-61.50	-63.32
-150	-63.60	-66.47
-100	-59.20	-63.02
-50	-49.80	-54.38
0	-39.60	-44.97
50	-35.10	-41.12
100	-31.70	-38.06
150	-20.70	-27.08
200	-8.04	-14.17
250	2.36	-3.23
300	8.69	3.62
350	10.80	6.11
400	9.97	5.49
450	7.80	3.37
500	5.39	1.00
550	3.41	-0.83
600	2.11	-1.75



Exterior deck plate	325-6-105	
	Axle B	
	3D	2D
-600	-27.40	-24.28
-550	-34.20	-31.29
-500	-37.30	-34.29
-450	-36.20	-33.27
-400	-39.20	-36.63
-350	-44.20	-42.46
-300	-49.00	-48.36
-250	-52.20	-53.03
-200	-53.10	-55.37
-150	-52.00	-55.30
-100	-48.90	-52.82
-50	-43.60	-47.75
0	-36.10	-40.28
50	-27.20	-31.43
100	-18.40	-22.78
150	-12.20	-16.92
200	-11.70	-16.86
250	-9.55	-15.11
300	-4.32	-9.85
350	1.31	-3.88
400	5.63	1.05
450	7.86	3.98
500	8.06	4.82
550	6.99	4.21
600	5.44	2.91



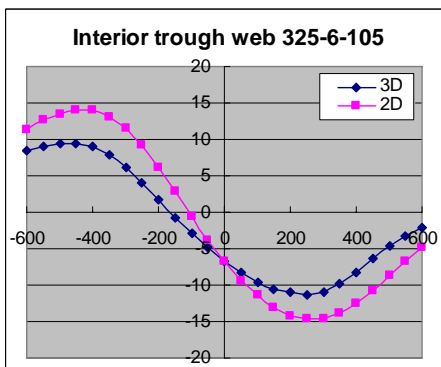
Exterior deck plate	325-6-105	
	Axle C	
	3D	2D
-600	-11.90	-5.90
-550	-19.40	-13.95
-500	-30.40	-25.99
-450	-43.40	-40.15
-400	-54.30	-52.21
-350	-57.40	-56.26
-300	-57.80	-57.76
-250	-63.50	-64.50
-200	-68.00	-70.06
-150	-66.90	-70.14
-100	-59.00	-63.25
-50	-46.00	-51.30
0	-32.80	-39.04
50	-26.40	-33.31
100	-22.80	-29.95
150	-12.80	-19.79
200	-1.71	-8.24
250	7.01	1.28
300	11.90	6.97
350	12.90	8.65
400	11.30	7.47
450	8.67	4.96
500	5.96	2.29
550	3.80	0.21
600	2.39	-0.95



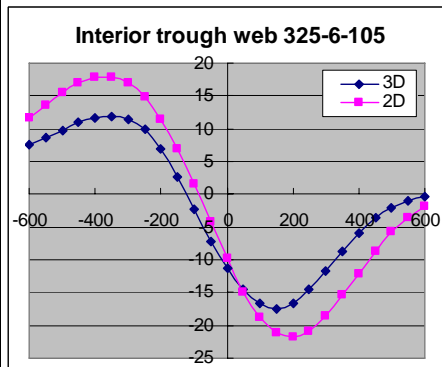
350mm + mid-span (3D model) v.s Top level (2D model)

Stress in the trough web

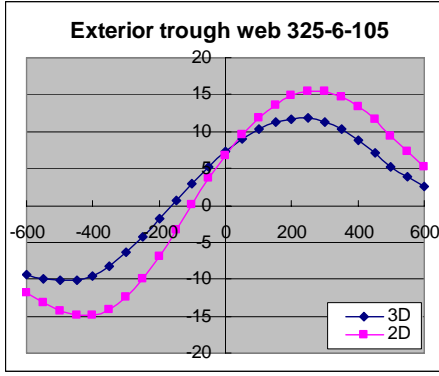
Interior trough web	325-6-105	
	Axle B	
	3D	2D
-600	8.395	11.36
-550	9.07	12.61
-500	9.42	13.55
-450	9.505	14.10
-400	9.1	13.97
-350	7.975	13.16
-300	6.21	11.57
-250	4.015	9.20
-200	1.64	6.22
-150	-0.68	2.88
-100	-2.83	-0.53
-50	-4.825	-3.81
0	-6.665	-6.79
50	-8.285	-9.36
100	-9.58	-11.41
150	-10.5	-13.03
200	-11.05	-14.16
250	-11.25	-14.70
300	-10.9	-14.57
350	-9.805	-13.86
400	-8.23	-12.57
450	-6.425	-10.81
500	-4.67	-8.73
550	-3.185	-6.66
600	-2.04	-4.77



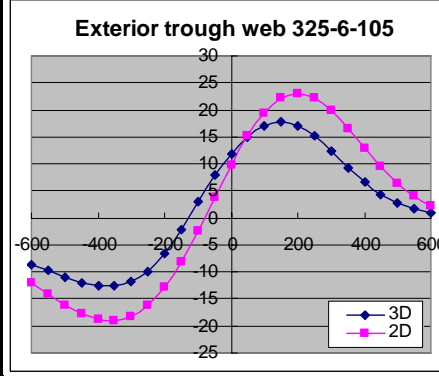
Interior trough web	325-6-105	
	Axle C	
	3D	2D
-600	7.49	11.63
-550	8.59	13.67
-500	9.80	15.50
-450	10.90	17.01
-400	11.65	17.83
-350	11.80	17.95
-300	11.45	17.00
-250	9.92	14.88
-200	6.94	11.52
-150	2.72	7.03
-100	-2.22	1.67
-50	-7.13	-4.13
0	-11.30	-9.83
50	-14.45	-14.89
100	-16.70	-18.72
150	-17.50	-21.19
200	-16.70	-21.80
250	-14.60	-20.88
300	-11.70	-18.60
350	-8.62	-15.46
400	-5.86	-12.04
450	-3.66	-8.64
500	-2.05	-5.75
550	-1.00	-3.49
600	-0.40	-1.93



Exterior trough web	325-6-105	
	Axle B	
	3D	2D
-600	-9.445	-11.84
-550	-10.035	-13.19
-500	-10.2	-14.25
-450	-10.105	-14.90
-400	-9.5	-14.83
-350	-8.25	-14.04
-300	-6.43	-12.43
-250	-4.195	-9.98
-200	-1.77	-6.88
-150	0.6525	-3.40
-100	2.97	0.19
-50	5.165	3.65
0	7.205	6.81
50	8.99	9.56
100	10.4	11.79
150	11.25	13.57
200	11.65	14.84
250	11.8	15.50
300	11.35	15.43
350	10.3	14.74
400	8.77	13.43
450	7.02	11.59
500	5.305	9.41
550	3.82	7.24
600	2.65	5.23

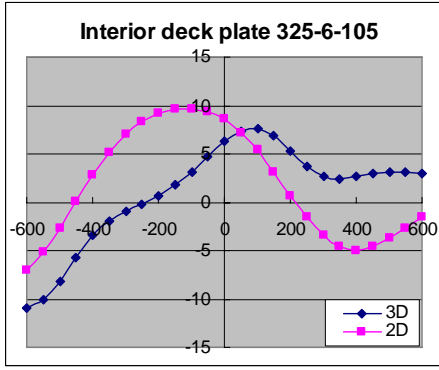


Exterior trough web	325-6-105	
	Axle C	
	3D	2D
-600	-8.57	-11.97
-550	-9.81	-14.13
-500	-11.10	-16.10
-450	-12.15	-17.79
-400	-12.60	-18.77
-350	-12.45	-19.05
-300	-11.75	-18.20
-250	-9.83	-16.12
-200	-6.54	-12.68
-150	-2.10	-8.03
-100	2.97	-2.39
-50	7.90	3.77
0	11.95	9.85
50	15.00	15.31
100	17.05	19.48
150	17.85	22.22
200	17.05	23.00
250	15.10	22.13
300	12.35	19.80
350	9.36	16.54
400	6.65	12.96
450	4.43	9.40
500	2.76	6.33
550	1.63	3.93
600	0.96	2.25

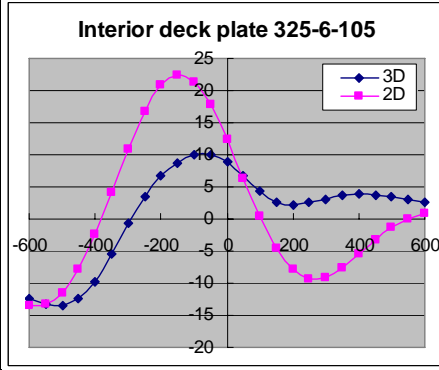


Stress in the deck plate

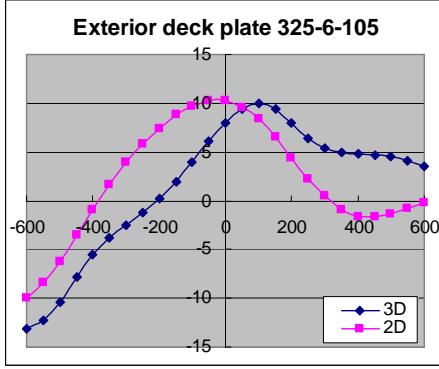
Interior deck plate	325-6-105	
	Axle B	
	3D	2D
-600	-10.95	-7.07
-550	-10.05	-5.14
-500	-8.145	-2.64
-450	-5.685	0.13
-400	-3.45	2.81
-350	-1.895	5.14
-300	-0.908	6.99
-250	-0.1553	8.32
-200	0.6625	9.15
-150	1.76	9.59
-100	3.165	9.69
-50	4.75	9.38
0	6.25	8.56
50	7.325	7.21
100	7.595	5.37
150	6.85	3.14
200	5.315	0.70
250	3.715	-1.59
300	2.73	-3.42
350	2.445	-4.57
400	2.615	-4.94
450	2.93	-4.60
500	3.145	-3.74
550	3.14	-2.63
600	2.945	-1.50



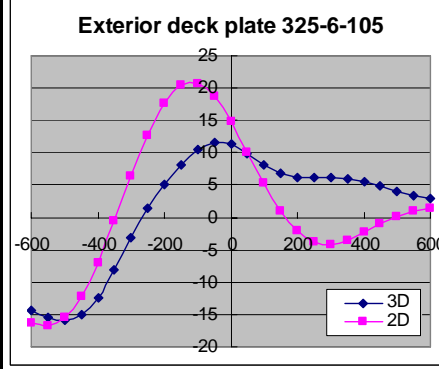
Interior deck plate	325-6-105	
	Axle C	
	3D	2D
-600	-12.35	-13.43
-550	-13.2	-13.35
-500	-13.4	-11.47
-450	-12.4	-7.74
-400	-9.745	-2.36
-350	-5.515	4.14
-300	-0.68	10.84
-250	3.545	16.72
-200	6.65	20.82
-150	8.735	22.33
-100	9.93	21.24
-50	10.065	17.77
0	8.965	12.49
50	6.74	6.37
100	4.255	0.38
150	2.61	-4.56
200	2.155	-7.87
250	2.505	-9.35
300	3.15	-9.13
350	3.685	-7.65
400	3.885	-5.51
450	3.755	-3.29
500	3.425	-1.35
550	3.04	0.06
600	2.68	0.89



Exterior deck plate	325-6-105	
	Axle B	
	3D	2D
-600	-13.15	-10.04
-550	-12.25	-8.45
-500	-10.35	-6.21
-450	-7.87	-3.59
-400	-5.59	-0.91
-350	-3.825	1.63
-300	-2.46	3.89
-250	-1.19	5.83
-200	0.227	7.45
-150	1.93	8.76
-100	3.925	9.75
-50	6.04	10.26
0	8.005	10.28
50	9.44	9.61
100	9.955	8.34
150	9.34	6.55
200	7.905	4.42
250	6.405	2.28
300	5.4	0.45
350	4.94	-0.88
400	4.785	-1.59
450	4.68	-1.72
500	4.465	-1.39
550	4.08	-0.82
600	3.585	-0.21



Exterior deck plate	325-6-105	
	Axle C	
	3D	2D
-600	-14.45	-16.39
-550	-15.5	-16.82
-500	-15.95	-15.56
-450	-15.05	-12.20
-400	-12.4	-7.07
-350	-8.03	-0.62
-300	-3.085	6.31
-250	1.435	12.67
-200	5.165	17.58
-150	8.175	20.42
-100	10.45	20.67
-50	11.65	18.74
0	11.4	14.91
50	9.92	10.18
100	8.045	5.28
150	6.77	1.00
200	6.285	-2.10
250	6.25	-3.81
300	6.255	-4.17
350	6.05	-3.50
400	5.555	-2.29
450	4.855	-0.95
500	4.085	0.22
550	3.405	1.04
600	2.87	1.45



2. Model B

Geometry of model B

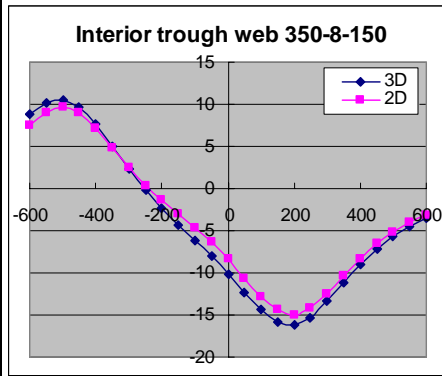
Structural component		Model B
Crossbeam	Height(H_c)	1250
	Length(L_c)	4200
	Distance(D_c)	3500
	Thickness(t_c)	12
Deck plate	Length(L_d)	21000
	Width(B_d)	4200
	Thickness(t_d)	18
Trough	Height(h_t)	350
	Width upper(b_{top})	300
	Width bottom(b_{bot})	150
	Thickness(t_t)	8
Asphalt	Thickness(t_a)	60

The unit of the dimension is mm

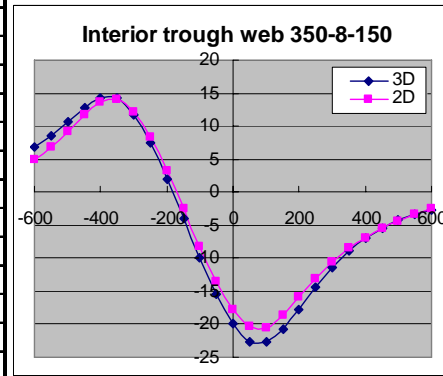
Mid-span (3D model) v.s Bottom level (2D model)

Stress in the trough web

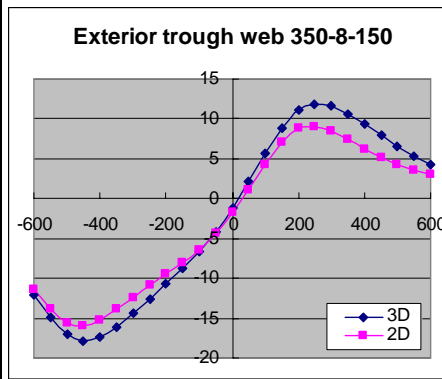
Interior trough web	350-8-150	
	Axle B	
	3D	2D
-600	8.85	7.58
-550	10.10	8.99
-500	10.50	9.63
-450	9.67	8.97
-400	7.63	7.13
-350	5.02	4.84
-300	2.32	2.50
-250	-0.18	0.40
-200	-2.39	-1.41
-150	-4.33	-3.01
-100	-6.16	-4.60
-50	-8.07	-6.36
0	-10.10	-8.40
50	-12.30	-10.61
100	-14.30	-12.75
150	-15.80	-14.39
200	-16.20	-15.01
250	-15.30	-14.13
300	-13.40	-12.48
350	-11.20	-10.37
400	-9.00	-8.33
450	-7.13	-6.57
500	-5.62	-5.16
550	-4.46	-4.03
600	-3.55	-3.13



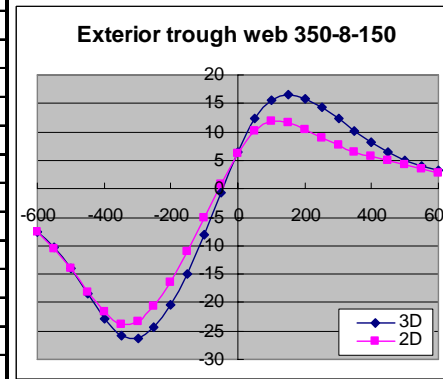
Interior trough web	350-8-150	
	Axle C	
	3D	2D
-600	6.77	4.85
-550	8.47	6.74
-500	10.60	9.10
-450	12.70	11.67
-400	14.30	13.67
-350	14.20	14.06
-300	11.80	12.12
-250	7.42	8.22
-200	1.98	3.18
-150	-4.01	-2.44
-100	-10.00	-8.16
-50	-15.50	-13.45
0	-20.00	-17.82
50	-22.70	-20.42
100	-22.70	-20.44
150	-20.70	-18.63
200	-17.70	-15.96
250	-14.40	-13.07
300	-11.40	-10.55
350	-8.87	-8.50
400	-6.90	-6.88
450	-5.37	-5.54
500	-4.19	-4.42
550	-3.30	-3.44
600	-2.65	-2.58



Exterior trough web	350-8-150	
	Axle B	
	3D	2D
-600	-12.10	-11.34
-550	-14.90	-13.81
-500	-17.00	-15.57
-450	-17.90	-16.03
-400	-17.40	-15.27
-350	-16.10	-13.92
-300	-14.40	-12.38
-250	-12.60	-10.88
-200	-10.70	-9.47
-150	-8.76	-8.05
-100	-6.65	-6.40
-50	-4.17	-4.34
0	-1.22	-1.78
50	2.16	1.19
100	5.69	4.27
150	8.91	7.01
200	11.10	8.79
250	11.90	9.07
300	11.60	8.52
350	10.60	7.41
400	9.30	6.23
450	7.90	5.17
500	6.57	4.30
550	5.37	3.59
600	4.33	2.99

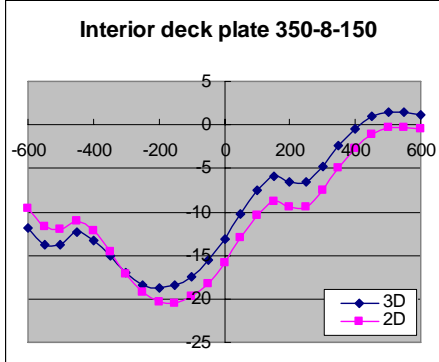


Exterior trough web	350-8-150	
	Axle C	
	3D	2D
-600	-7.55	-7.53
-550	-10.30	-10.46
-500	-14.10	-14.10
-450	-18.50	-18.13
-400	-22.90	-21.73
-350	-25.80	-23.74
-300	-26.30	-23.28
-250	-24.40	-20.58
-200	-20.50	-16.38
-150	-15.00	-11.10
-100	-8.16	-5.22
-50	-0.73	0.73
0	6.47	6.18
50	12.30	10.18
100	15.50	11.76
150	16.50	11.57
200	15.80	10.44
250	14.30	8.93
300	12.30	7.61
350	10.20	6.54
400	8.24	5.68
450	6.52	4.92
500	5.09	4.22
550	3.97	3.52
600	3.14	2.84

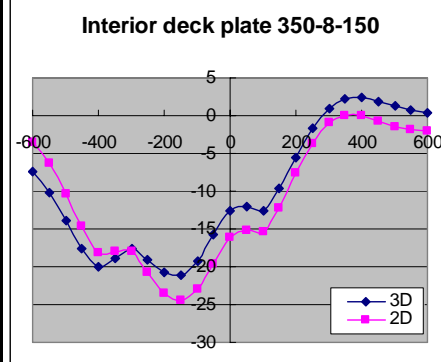


Stress in the deck plate

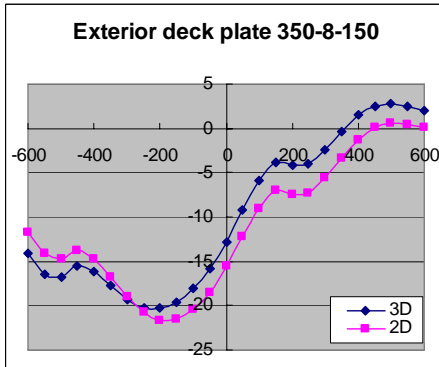
Interior deck plate	350-8-150	
	Axle B	
	3D	2D
-600	-11.80	-9.61
-550	-13.70	-11.70
-500	-13.80	-11.98
-450	-12.40	-10.97
-400	-13.30	-12.14
-350	-15.10	-14.52
-300	-17.00	-17.08
-250	-18.40	-19.15
-200	-18.80	-20.32
-150	-18.50	-20.48
-100	-17.40	-19.76
-50	-15.60	-18.24
0	-13.10	-15.84
50	-10.20	-12.96
100	-7.52	-10.38
150	-5.92	-8.80
200	-6.61	-9.52
250	-6.60	-9.48
300	-4.79	-7.53
350	-2.44	-4.97
400	-0.38	-2.64
450	0.95	-1.07
500	1.48	-0.36
550	1.46	-0.27
600	1.18	-0.49



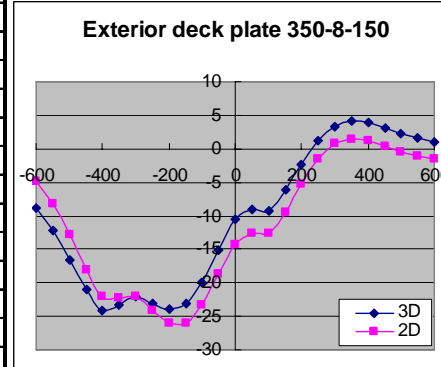
Interior deck plate	350-8-150	
	Axle C	
	3D	2D
-600	-7.46	-3.52
-550	-10.20	-6.27
-500	-13.90	-10.31
-450	-17.60	-14.70
-400	-20.00	-18.08
-350	-18.90	-18.05
-300	-17.50	-17.92
-250	-19.00	-20.68
-200	-20.80	-23.43
-150	-21.10	-24.48
-100	-19.20	-22.93
-50	-15.80	-19.59
0	-12.60	-16.15
50	-12.00	-15.24
100	-12.60	-15.45
150	-9.71	-12.19
200	-5.50	-7.64
250	-1.66	-3.62
300	0.98	-0.98
350	2.19	0.07
400	2.33	-0.04
450	1.92	-0.69
500	1.33	-1.40
550	0.81	-1.88
600	0.44	-2.00



Exterior deck plate	350-8-150	
	Axle B	
	3D	2D
-600	-14.10	-11.70
-550	-16.40	-14.15
-500	-16.80	-14.79
-450	-15.60	-13.83
-400	-16.20	-14.75
-350	-17.80	-16.87
-300	-19.30	-19.07
-250	-20.20	-20.75
-200	-20.30	-21.63
-150	-19.60	-21.50
-100	-18.10	-20.47
-50	-15.80	-18.54
0	-12.80	-15.61
50	-9.26	-12.28
100	-5.94	-9.03
150	-3.78	-6.99
200	-4.12	-7.42
250	-4.06	-7.38
300	-2.39	-5.62
350	-0.30	-3.32
400	1.46	-1.27
450	2.48	0.05
500	2.74	0.55
550	2.48	0.48
600	2.01	0.12



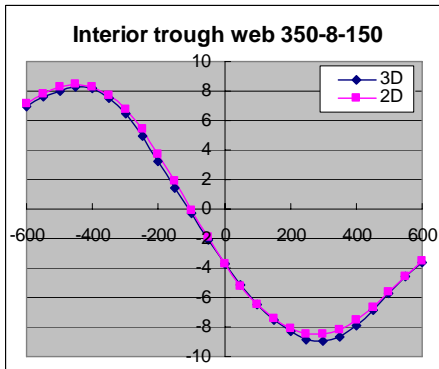
Exterior deck plate	350-8-150	
	Axle C	
	3D	2D
-600	-8.91	-4.88
-550	-12.20	-8.16
-500	-16.50	-12.87
-450	-21.00	-18.04
-400	-24.10	-22.00
-350	-23.40	-22.35
-300	-22.00	-21.98
-250	-23.00	-24.09
-200	-23.90	-26.07
-150	-23.10	-25.93
-100	-19.90	-23.25
-50	-15.10	-18.76
0	-10.60	-14.36
50	-9.03	-12.67
100	-9.18	-12.61
150	-6.22	-9.45
200	-2.26	-5.25
250	1.19	-1.59
300	3.37	0.71
350	4.15	1.50
400	3.90	1.17
450	3.16	0.34
500	2.30	-0.54
550	1.56	-1.17
600	1.04	-1.44



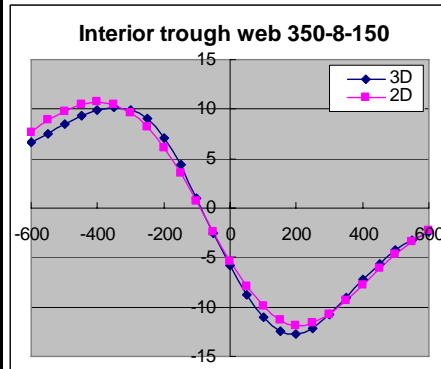
350mm + mid-span (3D model) v.s Top level (2D model)

Stress in the trough web

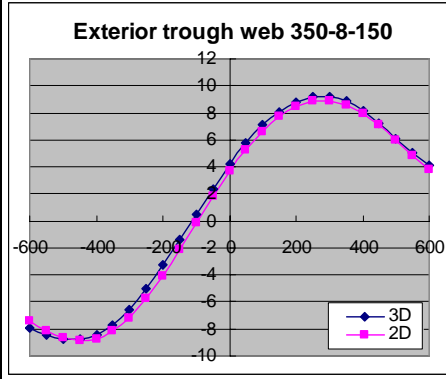
Interior trough web	350-8-150	
	Axle B	
	3D	2D
-600	6.97	7.15
-550	7.59	7.81
-500	8.035	8.26
-450	8.27	8.45
-400	8.15	8.30
-350	7.54	7.74
-300	6.45	6.77
-250	4.985	5.42
-200	3.275	3.75
-150	1.475	1.87
-100	-0.316	-0.06
-50	-2.05	-1.95
0	-3.685	-3.69
50	-5.175	-5.21
100	-6.465	-6.47
150	-7.51	-7.45
200	-8.315	-8.13
250	-8.86	-8.50
300	-8.98	-8.51
350	-8.625	-8.19
400	-7.875	-7.57
450	-6.85	-6.69
500	-5.715	-5.66
550	-4.61	-4.57
600	-3.64	-3.54



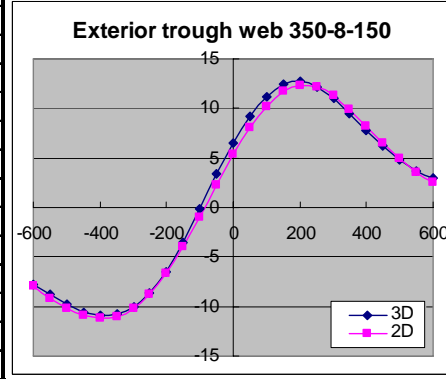
Interior trough web	350-8-150	
	Axle C	
	3D	2D
-600	6.62	7.65
-550	7.535	8.85
-500	8.48	9.83
-450	9.32	10.50
-400	9.915	10.77
-350	10.15	10.54
-300	9.965	9.66
-250	9.005	8.20
-200	7.1	6.15
-150	4.36	3.59
-100	1.03	0.68
-50	-2.495	-2.38
0	-5.835	-5.33
50	-8.71	-7.93
100	-11	-9.94
150	-12.4	-11.29
200	-12.8	-11.85
250	-12.1	-11.63
300	-10.8	-10.73
350	-9.065	-9.34
400	-7.27	-7.75
450	-5.63	-6.13
500	-4.25	-4.61
550	-3.19	-3.33
600	-2.43	-2.31



Exterior trough web	350-8-150	
	Axle B	
	3D	2D
-600	-7.95	-7.41
-550	-8.48	-8.11
-500	-8.745	-8.61
-450	-8.765	-8.83
-400	-8.46	-8.70
-350	-7.72	-8.16
-300	-6.565	-7.17
-250	-5.055	-5.78
-200	-3.3	-4.05
-150	-1.415	-2.11
-100	0.502	-0.10
-50	2.385	1.87
0	4.17	3.69
50	5.77	5.31
100	7.095	6.65
150	8.085	7.70
200	8.77	8.45
250	9.19	8.86
300	9.23	8.91
350	8.865	8.61
400	8.155	7.97
450	7.195	7.07
500	6.12	6.00
550	5.06	4.87
600	4.09	3.79

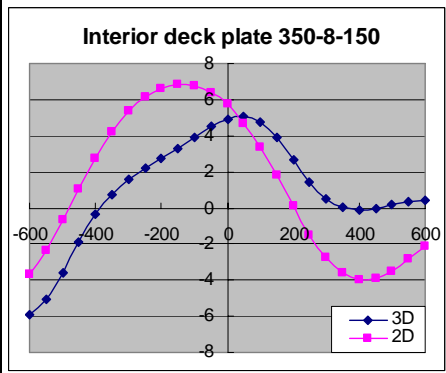


Exterior trough web	350-8-150	
	Axle C	
	3D	2D
-600	-7.775	-7.87
-550	-8.815	-9.13
-500	-9.79	-10.17
-450	-10.55	-10.91
-400	-10.85	-11.23
-350	-10.7	-11.06
-300	-10.05	-10.20
-250	-8.67	-8.74
-200	-6.46	-6.65
-150	-3.52	-4.01
-100	-0.1219	-0.97
-50	3.365	2.24
0	6.525	5.35
50	9.16	8.09
100	11.2	10.26
150	12.5	11.71
200	12.8	12.35
250	12.2	12.17
300	11	11.27
350	9.435	9.86
400	7.755	8.21
450	6.18	6.53
500	4.82	4.95
550	3.74	3.61
600	2.94	2.53

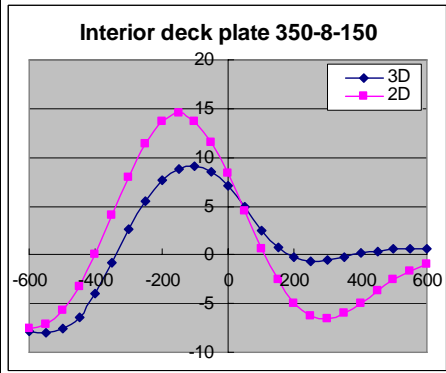


Stress in the deck plate

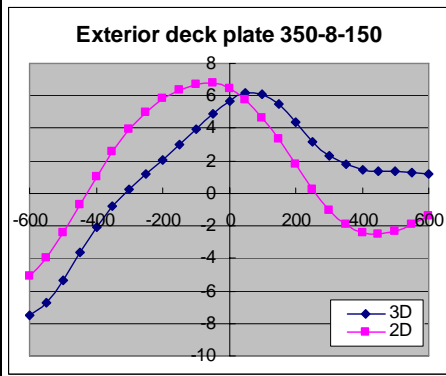
Interior deck plate	350-8-150	
	Axle B	
	3D	2D
-600	-5.94	-3.64
-550	-5.055	-2.32
-500	-3.615	-0.69
-450	-1.92	1.07
-400	-0.3845	2.76
-350	0.766	4.21
-300	1.58	5.36
-250	2.185	6.17
-200	2.725	6.64
-150	3.285	6.83
-100	3.895	6.77
-50	4.485	6.40
0	4.925	5.72
50	5.075	4.69
100	4.765	3.36
150	3.92	1.79
200	2.67	0.11
250	1.4	-1.47
300	0.4825	-2.77
350	0.01084	-3.63
400	-0.1095	-4.02
450	-0.0158	-3.94
500	0.161	-3.49
550	0.3215	-2.84
600	0.426	-2.13



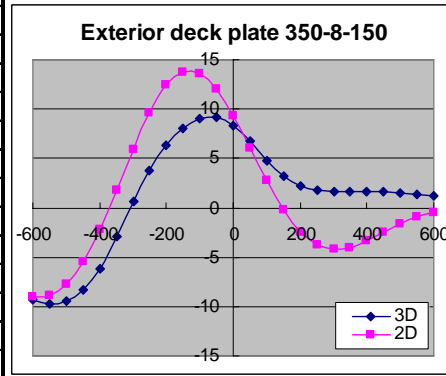
Interior deck plate	350-8-150	
	Axle C	
	3D	2D
-600	-7.815	-7.53
-550	-8.025	-7.14
-500	-7.625	-5.74
-450	-6.34	-3.29
-400	-4.02	0.07
-350	-0.8365	4.00
-300	2.585	7.96
-250	5.51	11.32
-200	7.61	13.72
-150	8.82	14.52
-100	9.15	13.73
-50	8.575	11.53
0	7.105	8.31
50	4.905	4.49
100	2.555	0.69
150	0.7295	-2.57
200	-0.2965	-4.91
250	-0.633	-6.20
300	-0.521	-6.49
350	-0.198	-5.96
400	0.143	-4.95
450	0.4045	-3.74
500	0.5655	-2.59
550	0.639	-1.63
600	0.645	-0.93



Exterior deck plate	350-8-150	
	Axle B	
	3D	2D
-600	-7.46	-5.11
-550	-6.69	-3.93
-500	-5.31	-2.40
-450	-3.63	-0.68
-400	-2.055	1.03
-350	-0.766	2.60
-300	0.2705	3.94
-250	1.175	5.02
-200	2.055	5.84
-150	2.99	6.40
-100	3.975	6.74
-50	4.93	6.78
0	5.715	6.45
50	6.175	5.75
100	6.13	4.68
150	5.49	3.31
200	4.38	1.78
250	3.205	0.28
300	2.305	-1.00
350	1.765	-1.92
400	1.495	-2.44
450	1.4	-2.54
500	1.36	-2.31
550	1.305	-1.88
600	1.215	-1.38



Exterior deck plate	350-8-150	
	Axle C	
	3D	2D
-600	-9.285	-9.09
-550	-9.7	-8.96
-500	-9.49	-7.77
-450	-8.37	-5.46
-400	-6.13	-2.16
-350	-2.94	1.81
-300	0.577	5.94
-250	3.75	9.64
-200	6.27	12.37
-150	8.05	13.68
-100	9.05	13.60
-50	9.18	12.02
0	8.345	9.37
50	6.695	6.11
100	4.765	2.74
150	3.2	-0.23
200	2.245	-2.47
250	1.795	-3.80
300	1.665	-4.26
350	1.665	-4.01
400	1.66	-3.32
450	1.605	-2.45
500	1.49	-1.61
550	1.35	-0.92
600	1.2	-0.43



3. Model C

Geometry of model C

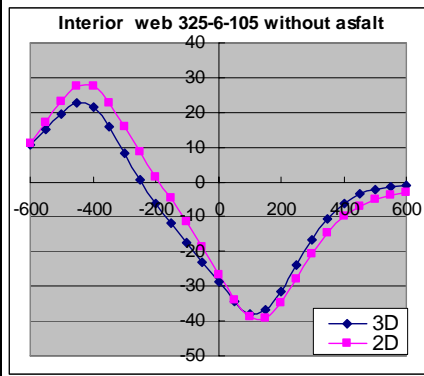
Structural component		Model C
Crossbeam	Height(H_c)	1250
	Length(L_c)	4200
	Distance(D_c)	3500
	Thickness(t_c)	12
Deck plate	Length(L_d)	21000
	Width(B_d)	4200
	Thickness(t_d)	12
Trough	Height(h_t)	325
	Width upper(b_{top})	300
	Width bottom(b_{bot})	105
	Thickness(t_t)	6
Epoxy layer	Distance(d_e)	600
	Thickness(t_a)	8

The unit of the dimension is mm

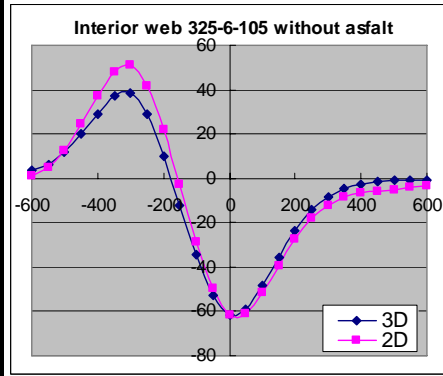
Mid-span (3D model) v.s Bottom level (2D model)

Stress in the trough web

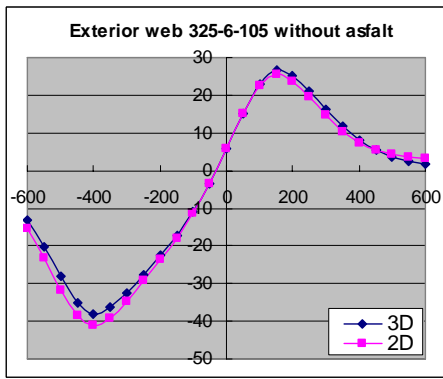
Interior trough web	325-6-105	
	Axle B	
	3D	2D
-600	10.6	11.16
-550	15.1	17.12
-500	19.7	23.19
-450	22.7	27.50
-400	21.4	27.55
-350	15.7	22.84
-300	8.12	15.96
-250	0.509	8.60
-200	-6.21	1.60
-150	-11.9	-4.78
-100	-17.3	-11.32
-50	-22.9	-18.66
0	-28.8	-26.50
50	-34.4	-33.75
100	-37.9	-38.82
150	-36.9	-39.17
200	-31.4	-34.62
250	-23.9	-27.86
300	-16.6	-20.73
350	-10.5	-14.58
400	-6.23	-10.01
450	-3.59	-7.03
500	-2.12	-5.12
550	-1.33	-3.89
600	-0.936	-3.07



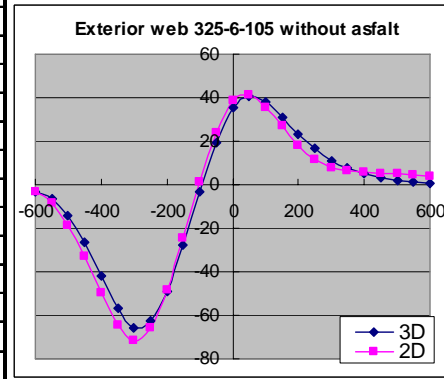
Interior trough web	325-6-105	
	Axle C	
	3D	2D
-600	3.93	0.79
-550	6.35	4.64
-500	11.7	12.64
-450	19.8	24.26
-400	29.2	37.25
-350	37.1	48.06
-300	38.5	51.40
-250	28.7	41.90
-200	10.2	22.20
-150	-12.3	-3.00
-100	-34.7	-28.70
-50	-52.7	-49.90
0	-61.8	-61.70
50	-58.9	-60.88
100	-48.4	-51.68
150	-35.5	-39.40
200	-23.6	-27.24
250	-14.2	-17.96
300	-8.12	-12.14
350	-4.59	-8.69
400	-2.66	-6.83
450	-1.64	-5.80
500	-1.12	-5.05
550	-0.844	-4.23
600	-0.6635	-3.25



Exterior trough web	325-6-105	
	Axle B	
	3D	2D
-600	-13.1	-15.44
-550	-20.1	-23.28
-500	-28.1	-31.61
-450	-35	-38.50
-400	-38	-41.25
-350	-36.4	-39.16
-300	-32.4	-34.64
-250	-27.5	-29.20
-200	-22.5	-23.60
-150	-17.2	-18.02
-100	-11	-11.48
-50	-3.33	-3.54
0	5.69	5.70
50	15.1	15.05
100	23	22.58
150	26.5	25.63
200	25	23.78
250	21	19.54
300	16.1	14.67
350	11.6	10.42
400	7.96	7.37
450	5.38	5.51
500	3.64	4.41
550	2.48	3.73
600	1.73	3.23

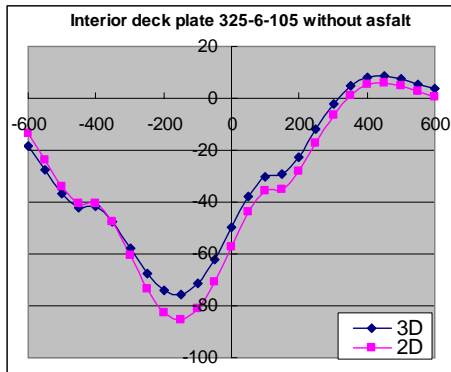


Exterior trough web	325-6-105	
	Axle C	
	3D	2D
-600	-2.98	-3.07
-550	-6.3	-8.38
-500	-14.1	-18.56
-450	-26.5	-33.14
-400	-41.9	-49.75
-350	-57	-64.54
-300	-66	-71.80
-250	-62.9	-65.90
-200	-48.8	-48.60
-150	-27.7	-24.60
-100	-3.45	1.30
-50	19.5	24.10
0	35.7	38.50
50	40.8	41.12
100	37.8	35.52
150	31	26.80
200	23.4	17.96
250	16.5	11.44
300	11.2	7.86
350	7.52	6.15
400	4.93	5.55
450	3.15	5.40
500	1.99	5.21
550	1.3	4.71
600	0.928	3.85

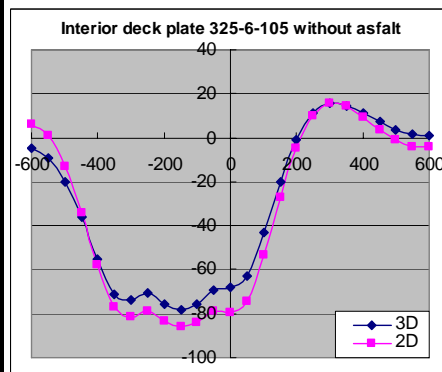


Stress in the deck plate

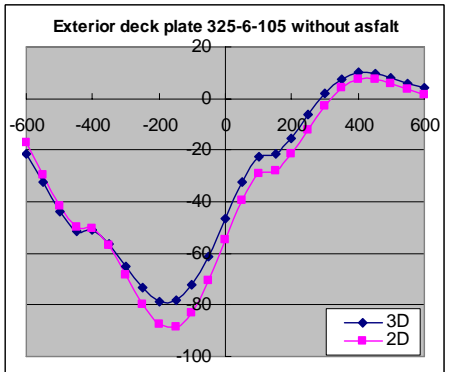
Interior deck plate	325-6-105	
	Axle B	
	3D	2D
-600	-18.2	-13.64
-550	-27.3	-23.83
-500	-36.5	-34.00
-450	-42.3	-40.56
-400	-41.5	-40.59
-350	-47.3	-47.80
-300	-57.6	-60.48
-250	-67.6	-73.35
-200	-74.2	-82.50
-150	-75.6	-85.44
-100	-71.1	-81.20
-50	-61.9	-70.99
0	-49.9	-57.33
50	-37.8	-44.04
100	-30	-35.62
150	-29.3	-35.06
200	-22.5	-28.34
250	-12	-17.41
300	-2.1	-6.68
350	4.91	1.32
400	8.3	5.45
450	8.65	6.14
500	7.37	4.80
550	5.49	2.66
600	3.68	0.58



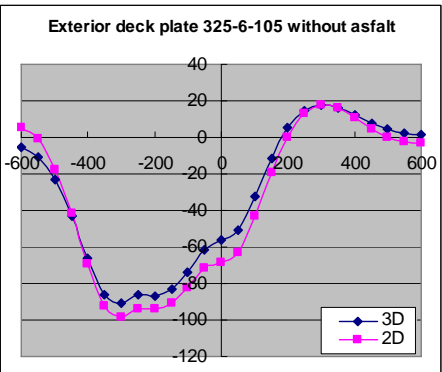
Interior deck plate	325-6-105	
	Axle C	
	3D	2D
-600	-4.58	6.40
-550	-9.22	0.82
-500	-19.9	-12.96
-450	-36.2	-33.84
-400	-55.4	-57.69
-350	-71.3	-77.21
-300	-74.1	-81.70
-250	-70.9	-78.76
-200	-75.6	-83.18
-150	-78.4	-86.07
-100	-75.5	-83.96
-50	-69.3	-79.16
0	-68.1	-79.38
50	-63.1	-74.68
100	-43.2	-53.19
150	-20	-26.93
200	-0.721	-4.82
250	11.2	10.06
300	15.4	15.70
350	14.4	14.21
400	11	9.26
450	7.14	3.55
500	3.88	-1.16
550	1.79	-3.86
600	0.934	-4.40



Exterior deck plate	325-6-105	
	Axle B	
	3D	2D
-600	-21.5	-17.28
-550	-32.4	-29.41
-500	-43.8	-41.57
-450	-51.2	-49.72
-400	-51	-50.25
-350	-56.1	-56.84
-300	-65	-68.19
-250	-73.4	-79.58
-200	-78.5	-87.32
-150	-78.4	-88.80
-100	-72.4	-82.84
-50	-61.2	-70.66
0	-46.8	-54.78
50	-32.4	-39.22
100	-22.7	-29.01
150	-21.4	-27.85
200	-15.3	-21.63
250	-6.24	-12.04
300	2.08	-2.64
350	7.72	4.20
400	10.1	7.48
450	9.79	7.63
500	8.11	5.97
550	5.99	3.62
600	4.05	1.40



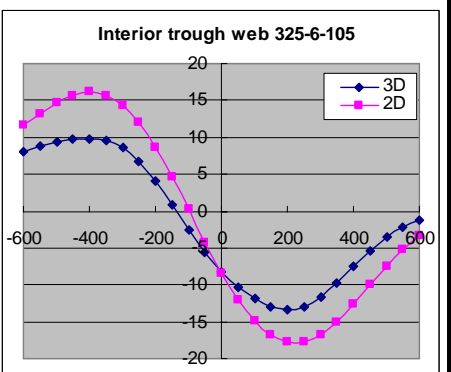
Exterior deck plate	325-6-105	
	Axle C	
	3D	2D
-600	-5.16	5.75
-550	-10.7	-1.09
-500	-23.4	-17.33
-450	-43.1	-41.74
-400	-66.3	-69.58
-350	-86.1	-92.62
-300	-91	-98.71
-250	-86.4	-94.10
-200	-86.7	-93.96
-150	-83.3	-90.79
-100	-73.6	-82.20
-50	-61.2	-71.73
0	-56.1	-68.34
50	-50.5	-63.18
100	-32.1	-43.34
150	-11.5	-19.44
200	5.21	0.26
250	15	13.34
300	17.8	17.94
350	15.9	15.87
400	12	10.78
450	7.78	4.95
500	4.32	0.16
550	2.11	-2.68
600	1.18	-3.46



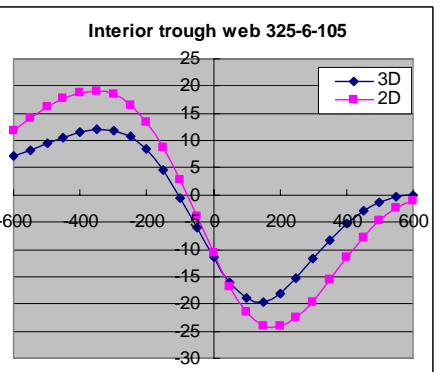
350mm + mid-span (3D model) v.s Top level (2D model)

Stress in the trough web

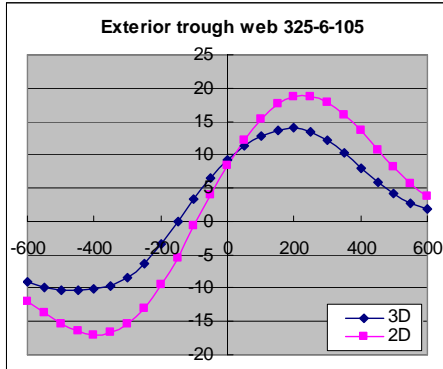
Interior trough web	325-6-105	
	Axle B	
	3D	2D
-600	8.025	11.59
-550	8.85	13.23
-500	9.47	14.67
-450	9.795	15.70
-400	9.855	16.14
-350	9.575	15.70
-300	8.55	14.38
-250	6.66	12.00
-200	4	8.69
-150	0.821	4.67
-100	-2.495	0.25
-50	-5.6	-4.21
0	-8.29	-8.36
50	-10.4	-11.96
100	-11.9	-14.83
150	-12.9	-16.82
200	-13.3	-17.74
250	-12.9	-17.69
300	-11.6	-16.78
350	-9.69	-15.00
400	-7.47	-12.64
450	-5.325	-10.01
500	-3.54	-7.49
550	-2.16	-5.24
600	-1.195	-3.40



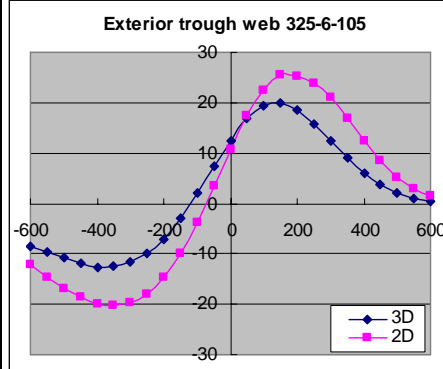
Interior trough web	325-6-105	
	Axle C	
	3D	2D
-600	7.27	11.74
-550	8.235	14.09
-500	9.43	16.22
-450	10.65	17.83
-400	11.65	18.93
-350	12.05	19.13
-300	11.75	18.45
-250	10.7	16.51
-200	8.36	13.33
-150	4.545	8.68
-100	-0.4545	2.81
-50	-5.99	-3.86
0	-11.4	-10.69
50	-16	-16.85
100	-18.85	-21.54
150	-19.55	-24.19
200	-18.25	-24.03
250	-15.35	-22.52
300	-11.75	-19.65
350	-8.22	-15.64
400	-5.205	-11.44
450	-2.89	-7.67
500	-1.295	-4.62
550	-0.368	-2.46
600	0.0251	-1.16



Exterior trough web	325-6-105	
	Axle B	
	3D	2D
-600	-9.1	-12.01
-550	-9.855	-13.77
-500	-10.3	-15.33
-450	-10.4	-16.50
-400	-10.2	-17.06
-350	-9.655	-16.70
-300	-8.355	-15.42
-250	-6.23	-13.00
-200	-3.375	-9.59
-150	-0.039	-5.39
-100	3.4	-0.75
-50	6.595	3.96
0	9.32	8.38
50	11.4	12.25
100	12.85	15.37
150	13.75	17.58
200	14	18.66
250	13.45	18.71
300	12.1	17.82
350	10.2	16.00
400	8.05	13.56
450	5.955	10.79
500	4.185	8.15
550	2.79	5.76
600	1.78	3.80

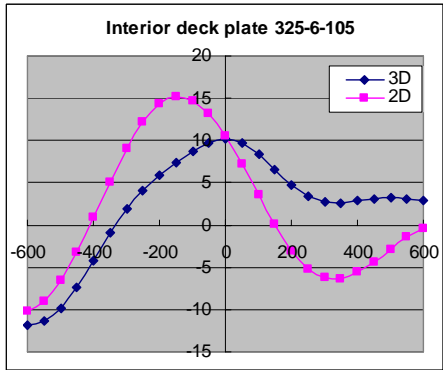


Exterior trough web	325-6-105	
	Axle C	
	3D	2D
-600	-8.415	-12.06
-550	-9.525	-14.51
-500	-10.75	-16.79
-450	-11.95	-18.57
-400	-12.6	-19.87
-350	-12.5	-20.27
-300	-11.6	-19.75
-250	-9.925	-17.89
-200	-7.055	-14.67
-150	-2.915	-9.86
-100	2.12	-3.69
-50	7.45	3.40
0	12.55	10.71
50	16.75	17.36
100	19.35	22.46
150	19.9	25.41
200	18.6	25.37
250	15.85	23.88
300	12.4	20.95
350	8.96	16.76
400	5.99	12.36
450	3.64	8.39
500	1.985	5.16
550	0.9825	2.86
600	0.523	1.45

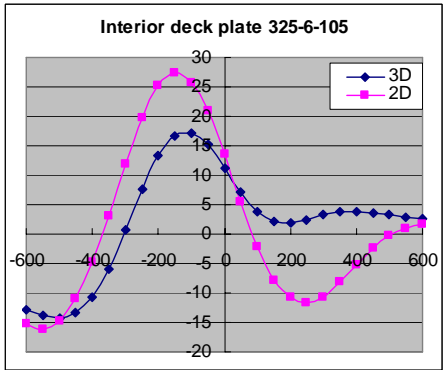


Stress in the deck plate

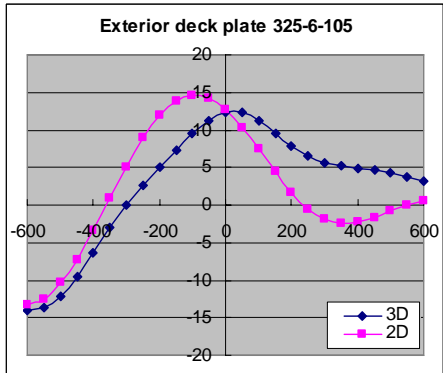
Interior deck plate	325-6-105	
	Axle B	
	3D	2D
-600	-11.8	-10.25
-550	-11.4	-8.96
-500	-9.905	-6.55
-450	-7.385	-3.19
-400	-4.175	0.85
-350	-0.8985	5.07
-300	1.92	8.97
-250	4.135	12.15
-200	5.895	14.35
-150	7.38	15.25
-100	8.66	14.76
-50	9.67	13.17
0	10.15	10.58
50	9.745	7.26
100	8.44	3.60
150	6.54	0.02
200	4.66	-3.02
250	3.33	-5.16
300	2.7	-6.28
350	2.635	-6.37
400	2.86	-5.61
450	3.105	-4.30
500	3.19	-2.84
550	3.075	-1.46
600	2.835	-0.37



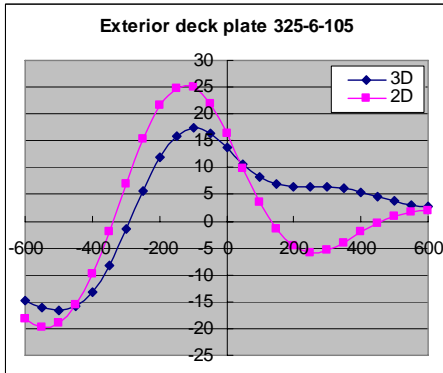
Interior deck plate	325-6-105	
	Axle C	
	3D	2D
-600	-12.75	-15.23
-550	-13.8	-16.14
-500	-14.2	-14.86
-450	-13.25	-10.99
-400	-10.6	-4.79
-350	-5.855	3.19
-300	0.608	11.92
-250	7.54	19.70
-200	13.3	25.20
-150	16.75	27.41
-100	17.25	25.83
-50	15.2	20.96
0	11.3	13.60
50	7.045	5.40
100	3.8	-2.12
150	2.15	-7.81
200	1.89	-10.78
250	2.445	-11.72
300	3.225	-10.68
350	3.75	-8.10
400	3.855	-5.15
450	3.64	-2.40
500	3.28	-0.27
550	2.91	1.06
600	2.62	1.59



Exterior deck plate	325-6-105	
	Axle B	
	3D	2D
-600	-13.95	-13.31
-550	-13.6	-12.44
-500	-12.15	-10.37
-450	-9.585	-7.31
-400	-6.34	-3.41
-350	-3.005	0.89
-300	0.02285	5.13
-250	2.665	8.92
-200	5.065	11.94
-150	7.34	13.87
-100	9.44	14.61
-50	11.15	14.15
0	12.25	12.69
50	12.3	10.33
100	11.3	7.45
150	9.6	4.41
200	7.87	1.67
250	6.525	-0.48
300	5.67	-1.84
350	5.195	-2.38
400	4.895	-2.23
450	4.615	-1.60
500	4.23	-0.80
550	3.755	-0.03
600	3.245	0.58



Exterior deck plate	325-6-105	
	Axle C	
	3D	2D
-600	-14.9	-18.28
-550	-16.15	-19.71
-500	-16.7	-19.05
-450	-15.95	-15.69
-400	-13.25	-9.76
-350	-8.28	-1.88
-300	-1.525	6.95
-250	5.69	15.24
-200	11.85	21.54
-150	15.95	24.87
-100	17.35	24.94
-50	16.35	21.82
0	13.65	16.32
50	10.55	9.75
100	8.19	3.51
150	6.93	-1.47
200	6.52	-4.46
250	6.485	-5.77
300	6.415	-5.38
350	6.05	-3.92
400	5.375	-2.07
450	4.54	-0.32
500	3.735	1.01
550	3.11	1.76
600	2.695	1.95



4. Model D

Geometry of model D

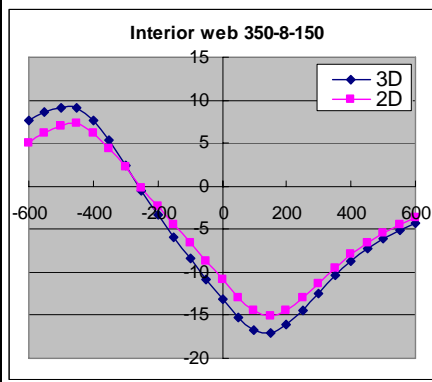
Structural component		Model D
Crossbeam	Height(H_c)	1250
	Length(L_c)	4200
	Distance(D_c)	3500
	Thickness(t_c)	12
Deck plate	Length(L_d)	21000
	Width(B_d)	4200
	Thickness(t_d)	22
Trough	Height(h_t)	350
	Width upper(b_{top})	300
	Width bottom(b_{bot})	150
	Thickness(t_t)	8
	Distance(d_t)	600
Epoxy layer	Thickness(t_a)	8

The unit of the dimension is mm

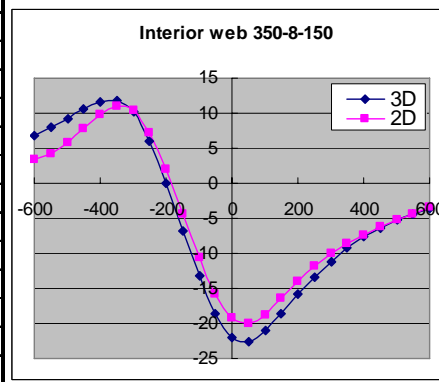
Mid-span (3D model) v.s Bottom level (2D model)

Stress in the trough web

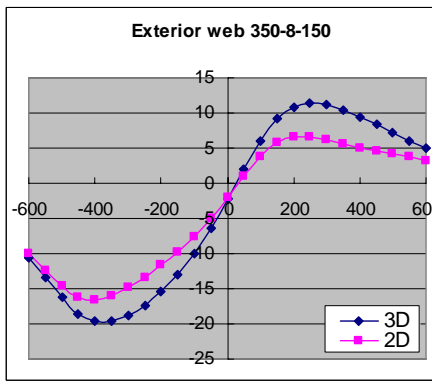
Interior trough web	350-8-150	
	Axle B	
	3D	2D
-600	7.65	5.07
-550	8.59	6.16
-500	9.19	7.05
-450	9.04	7.24
-400	7.68	6.25
-350	5.29	4.42
-300	2.44	2.19
-250	-0.493	-0.14
-200	-3.31	-2.35
-150	-5.94	-4.44
-100	-8.45	-6.53
-50	-10.9	-8.68
0	-13.2	-10.87
50	-15.2	-12.90
100	-16.7	-14.44
150	-17	-15.03
200	-16.1	-14.41
250	-14.4	-13.00
300	-12.4	-11.26
350	-10.4	-9.49
400	-8.69	-7.92
450	-7.26	-6.58
500	-6.09	-5.44
550	-5.11	-4.47



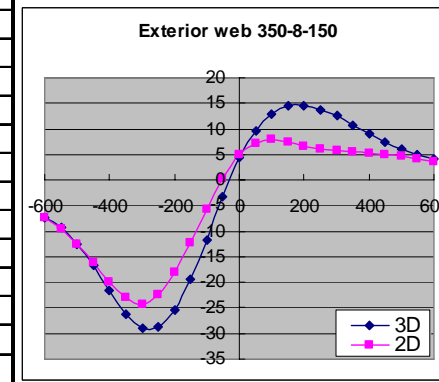
Interior trough web	350-8-150	
	Axle C	
	3D	2D
-600	6.85	3.32
-550	7.93	4.25
-500	9.24	5.78
-450	10.6	7.77
-400	11.7	9.77
-350	11.9	10.95
-300	10.3	10.39
-250	6.1	7.18
-200	0.0563	1.91
-150	-6.7	-4.32
-100	-13.2	-10.58
-50	-18.6	-15.88
0	-22	-19.24
50	-22.5	-19.93
100	-21	-18.74
150	-18.6	-16.42
200	-15.8	-13.94
250	-13.3	-11.73
300	-11.1	-9.93
350	-9.23	-8.51
400	-7.67	-7.32
450	-6.35	-6.27
500	-5.25	-5.27
550	-4.36	-4.31
600	-3.66	-3.36



Exterior trough web	350-8-150	
	Axle B	
	3D	2D
-600	-10.6	-9.97
-550	-13.3	-12.32
-500	-16.2	-14.55
-450	-18.5	-16.16
-400	-19.7	-16.55
-350	-19.7	-15.98
-300	-18.9	-14.85
-250	-17.4	-13.36
-200	-15.4	-11.69
-150	-13	-9.84
-100	-9.95	-7.65
-50	-6.35	-5.04
0	-2.29	-2.09
50	1.99	0.98
100	6.03	3.78
150	9.14	5.77
200	10.8	6.59
250	11.4	6.60
300	11.2	6.18
350	10.5	5.61
400	9.47	5.06
450	8.32	4.58
500	7.16	4.14
550	6.05	3.71
600	5.06	3.27

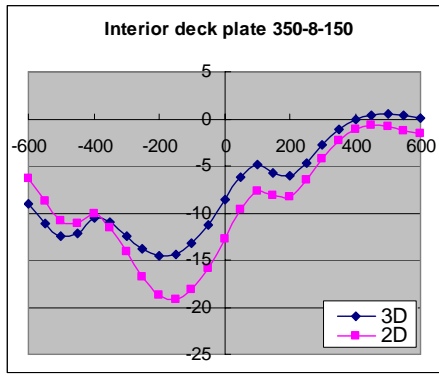


Exterior trough web	350-8-150	
	Axle C	
	3D	2D
-600	-7.42	-7.38
-550	-9.39	-9.55
-500	-12.5	-12.56
-450	-16.7	-16.23
-400	-21.6	-20.03
-350	-26.2	-23.05
-300	-29.1	-24.21
-250	-28.8	-22.42
-200	-25.4	-18.09
-150	-19.5	-12.26
-100	-11.8	-5.78
-50	-3.39	0.32
0	4.29	4.96
50	9.73	7.27
100	12.9	7.86
150	14.4	7.38
200	14.6	6.66
250	13.8	6.05
300	12.5	5.67
350	10.8	5.45
400	9.14	5.26
450	7.54	4.99
500	6.15	4.61
550	5.04	4.09
600	4.2	3.46

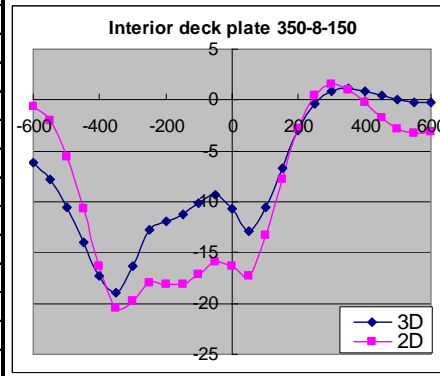


Stress in the deck plate

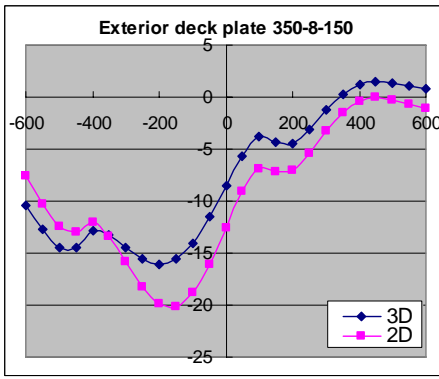
Interior deck plate	350-8-150 Axle B	
	3D	2D
-600	-9.06	-6.36
-550	-11.10	-8.79
-500	-12.50	-10.77
-450	-12.20	-11.05
-400	-10.50	-10.13
-350	-11.00	-11.50
-300	-12.40	-14.17
-250	-13.80	-16.84
-200	-14.50	-18.71
-150	-14.40	-19.17
-100	-13.20	-18.15
-50	-11.20	-15.83
0	-8.65	-12.72
50	-6.25	-9.59
100	-4.86	-7.66
150	-5.78	-8.19
200	-6.08	-8.21
250	-4.67	-6.50
300	-2.77	-4.27
350	-1.11	-2.34
400	-0.03	-1.13
450	0.43	-0.73
500	0.47	-0.85
550	0.32	-1.20
600	0.12	-1.56



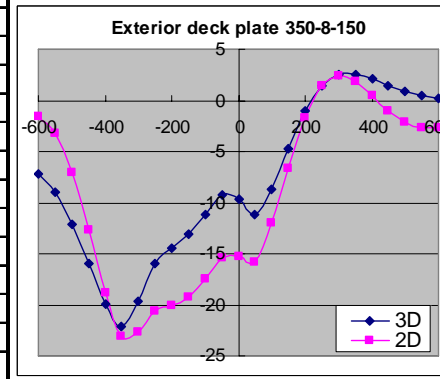
Interior deck plate	350-8-150 Axle C	
	3D	2D
-600	-6.16	-0.63
-550	-7.79	-2.04
-500	-10.5	-5.53
-450	-14	-10.67
-400	-17.3	-16.35
-350	-19	-20.42
-300	-16.3	-19.79
-250	-12.8	-17.95
-200	-11.9	-18.11
-150	-11.3	-18.17
-100	-10.2	-17.13
-50	-9.36	-15.89
0	-10.7	-16.36
50	-12.9	-17.24
100	-10.6	-13.35
150	-6.73	-7.85
200	-2.99	-2.82
250	-0.351	0.44
300	0.93	1.54
350	1.18	1.01
400	0.921	-0.29
450	0.49	-1.71
500	0.0895	-2.78
550	-0.179	-3.27



Exterior deck plate	350-8-150 Axle B	
	3D	2D
-600	-10.4	-7.56
-550	-12.7	-10.24
-500	-14.5	-12.48
-450	-14.4	-12.91
-400	-12.8	-12.04
-350	-13.2	-13.36
-300	-14.4	-15.77
-250	-15.6	-18.26
-200	-16.1	-19.85
-150	-15.6	-20.12
-100	-14	-18.78
-50	-11.5	-16.04
0	-8.52	-12.60
50	-5.61	-9.11
100	-3.76	-6.83
150	-4.33	-7.14
200	-4.48	-7.09
250	-3.06	-5.42
300	-1.24	-3.29
350	0.289	-1.46
400	1.21	-0.36
450	1.51	-0.05
500	1.4	-0.25
550	1.1	-0.68
600	0.776	-1.10



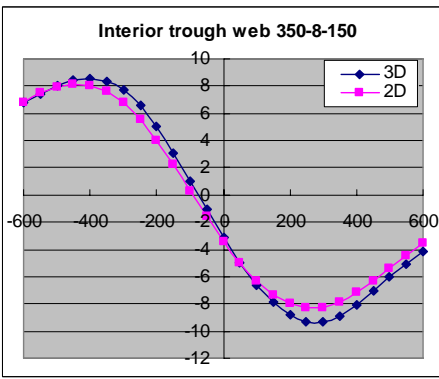
Exterior deck plate	350-8-150 Axle C	
	3D	2D
-600	-7.14	-1.51
-550	-9	-3.17
-500	-12.1	-7.02
-450	-16	-12.62
-400	-19.9	-18.77
-350	-22.1	-23.12
-300	-19.7	-22.65
-250	-16	-20.56
-200	-14.5	-20.05
-150	-13.1	-19.30
-100	-11.1	-17.44
-50	-9.19	-15.36
0	-9.67	-15.27
50	-11.2	-15.89
100	-8.68	-12.03
150	-4.7	-6.58
200	-1.01	-1.69
250	1.48	1.42
300	2.55	2.43
350	2.58	1.84
400	2.1	0.48
450	1.47	-0.99
500	0.889	-2.14
550	0.478	-2.72
600	0.258	-2.69



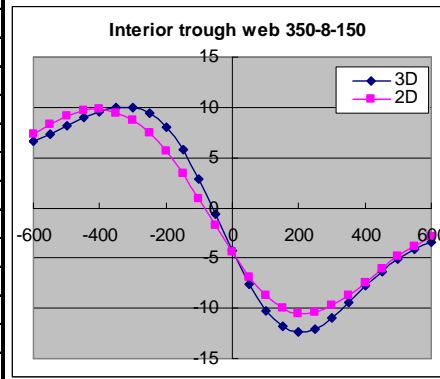
350mm + mid-span (3D model) v.s Top level (2D model)

Stress in the trough web

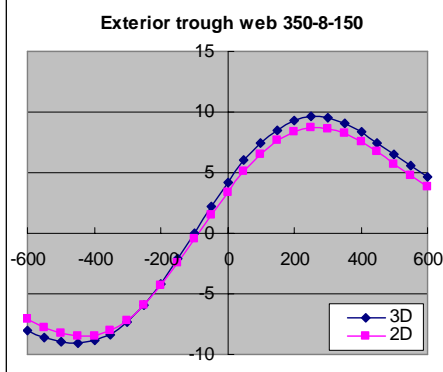
Interior trough web	350-8-150 Axle B	
	3D	2D
-600	6.795	6.85
-550	7.46	7.48
-500	8.02	7.95
-450	8.4	8.17
-400	8.56	8.09
-350	8.375	7.64
-300	7.725	6.81
-250	6.58	5.58
-200	5.005	4.03
-150	3.105	2.25
-100	1.025	0.32
-50	-1.09	-1.59
0	-3.125	-3.40
50	-4.98	-5.00
100	-6.585	-6.34
150	-7.88	-7.36
200	-8.825	-8.02
250	-9.325	-8.32
300	-9.325	-8.25
350	-8.885	-7.86
400	-8.09	-7.20
450	-7.09	-6.35
500	-6.04	-5.42
550	-5.045	-4.47
600	-4.16	-3.58



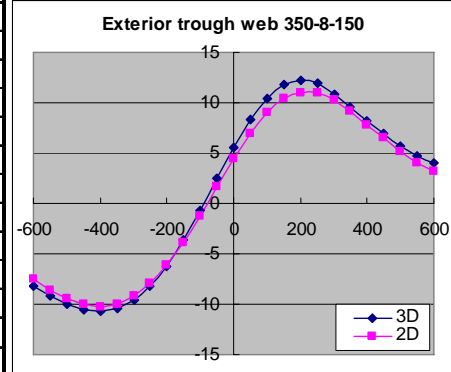
Interior trough web	350-8-150 Axle C	
	3D	2D
-600	6.61	7.29
-550	7.39	8.34
-500	8.205	9.16
-450	8.99	9.67
-400	9.625	9.78
-350	9.985	9.48
-300	9.95	8.70
-250	9.38	7.42
-200	8.05	5.67
-150	5.85	3.49
-100	2.89	0.96
-50	-0.578	-1.75
0	-4.19	-4.44
50	-7.545	-6.85
100	-10.2	-8.77
150	-11.85	-10.01
200	-12.4	-10.57
250	-12	-10.46
300	-10.9	-9.76
350	-9.35	-8.68
400	-7.78	-7.40
450	-6.31	-6.09
500	-5.065	-4.87
550	-4.09	-3.80
600	-3.37	-2.92



Exterior trough web	350-8-150	
	Axle B	
	3D	2D
-600	-8.075	-7.10
-550	-8.635	-7.78
-500	-8.97	-8.28
-450	-9.05	-8.53
-400	-8.865	-8.47
-350	-8.325	-8.04
-300	-7.365	-7.20
-250	-5.975	-5.94
-200	-4.2	-4.35
-150	-2.15	-2.49
-100	0.0322	-0.49
-50	2.2	1.51
0	4.225	3.40
50	5.995	5.10
100	7.44	6.52
150	8.54	7.62
200	9.28	8.34
250	9.62	8.68
300	9.545	8.65
350	9.095	8.26
400	8.365	7.58
450	7.455	6.71
500	6.49	5.74
550	5.55	4.75
600	4.69	3.82

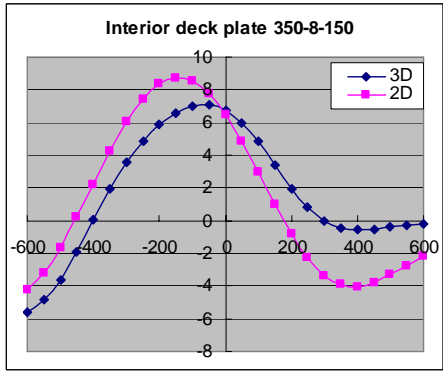


Exterior trough web	350-8-150	
	Axle C	
	3D	2D
-600	-8.18	-7.53
-550	-9.125	-8.62
-500	-9.955	-9.50
-450	-10.5	-10.05
-400	-10.7	-10.22
-350	-10.4	-9.94
-300	-9.545	-9.18
-250	-8.16	-7.90
-200	-6.185	-6.11
-150	-3.64	-3.86
-100	-0.687	-1.22
-50	2.44	1.61
0	5.51	4.44
50	8.275	7.01
100	10.4	9.05
150	11.75	10.39
200	12.2	11.03
250	11.9	10.94
300	10.9	10.24
350	9.645	9.14
400	8.25	7.82
450	6.9	6.47
500	5.71	5.19
550	4.73	4.08
600	3.98	3.14

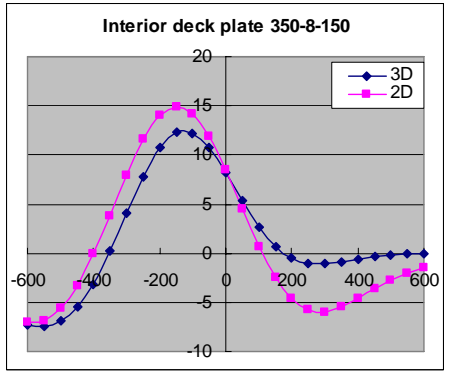


Stress in the deck plate

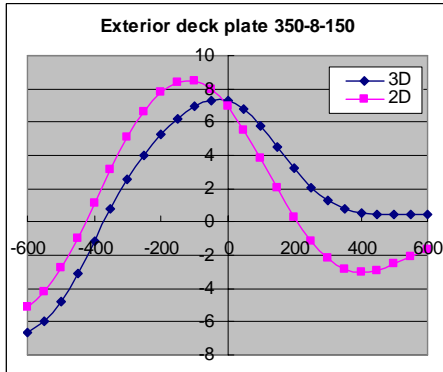
Interior deck plate	350-8-150	
	Axle B	
	3D	2D
-600	-5.59	-4.22
-550	-4.865	-3.17
-500	-3.605	-1.67
-450	-1.89	0.19
-400	0.04885	2.23
-350	1.93	4.24
-300	3.56	6.03
-250	4.865	7.44
-200	5.855	8.38
-150	6.555	8.75
-100	6.96	8.53
-50	7.045	7.76
0	6.745	6.50
50	6.01	4.86
100	4.85	2.97
150	3.42	1.01
200	1.98	-0.80
250	0.8	-2.29
300	-0.0056	-3.35
350	-0.442	-3.92
400	-0.583	-4.04
450	-0.535	-3.79
500	-0.409	-3.31
550	-0.275	-2.74



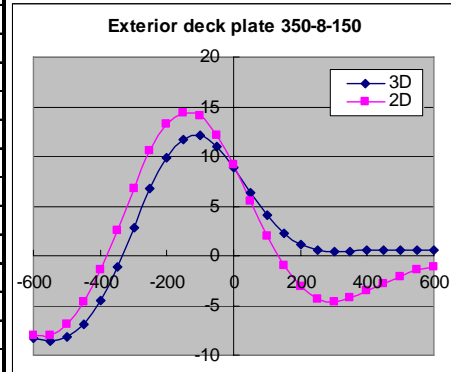
Interior deck plate	350-8-150	
	Axle C	
	3D	2D
-600	-7.235	-7.01
-550	-7.385	-6.81
-500	-6.865	-5.63
-450	-5.485	-3.35
-400	-3.12	-0.11
-350	0.1845	3.81
-300	4.065	7.92
-250	7.835	11.54
-200	10.7	14.04
-150	12.3	14.94
-100	12.25	14.24
-50	10.8	11.94
0	8.235	8.50
50	5.29	4.53
100	2.64	0.73
150	0.688	-2.42
200	-0.4965	-4.63
250	-1.015	-5.78
300	-1.055	-5.97
350	-0.853	-5.49
400	-0.5895	-4.62
450	-0.3505	-3.66
500	-0.171	-2.75
550	-0.0582	-2.02
600	-0.0057	-1.50



Exterior deck plate	350-8-150	
	Axle B	
	3D	2D
-600	-6.625	-5.17
-550	-5.975	-4.22
-500	-4.765	-2.77
-450	-3.08	-0.95
-400	-1.125	1.09
-350	0.8185	3.17
-300	2.56	5.07
-250	4.04	6.65
-200	5.26	7.79
-150	6.225	8.42
-100	6.92	8.47
-50	7.295	7.96
0	7.265	6.95
50	6.77	5.54
100	5.81	3.84
150	4.53	2.03
200	3.205	0.32
250	2.075	-1.12
300	1.265	-2.19
350	0.7665	-2.82
400	0.526	-3.02
450	0.45	-2.89
500	0.444	-2.54
550	0.45	-2.10
600	0.444	-1.64



Exterior deck plate	350-8-150	
	Axle C	
	3D	2D
-600	-8.275	-8.01
-550	-8.535	-7.97
-500	-8.135	-6.89
-450	-6.84	-4.69
-400	-4.51	-1.47
-350	-1.19	2.48
-300	2.775	6.69
-250	6.7	10.50
-200	9.835	13.20
-150	11.7	14.41
-100	12.1	14.02
-50	11	12.14
0	8.915	9.09
50	6.36	5.47
100	4.02	1.94
150	2.26	-1.03
200	1.14	-3.15
250	0.578	-4.32
300	0.4055	-4.61
350	0.4275	-4.26
400	0.498	-3.59
450	0.553	-2.80
500	0.5715	-2.06
550	0.5535	-1.48
600	0.5065	-1.08



5. Model E

Geometry of model E

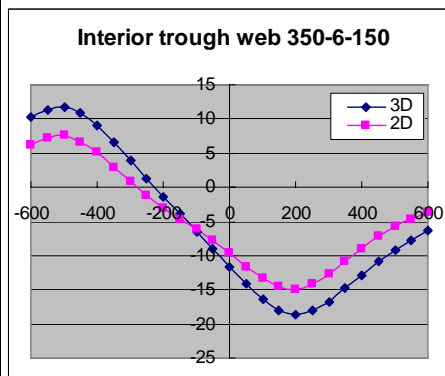
Structural component		Model E
Crossbeam	Height(H_c)	1250
	Length(L_c)	4200
	Distance(D_c)	3500
	Thickness(t_c)	12
Deck plate	Length(L_d)	21000
	Width(B_d)	4200
	Thickness(t_d)	18
Trough	Height(h_t)	350
	Width upper(b_{top})	300
	Width bottom(b_{bot})	150
	Thickness(t_t)	6
Asphalt	Distance(d_a)	600
	Thickness(t_a)	60

The unit of the dimension is mm

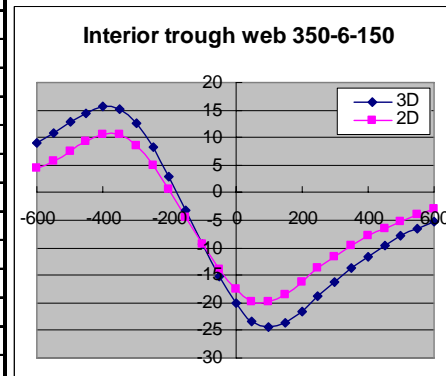
Mid-span (3D model) v.s Bottom level (2D model)

Stress in the trough web

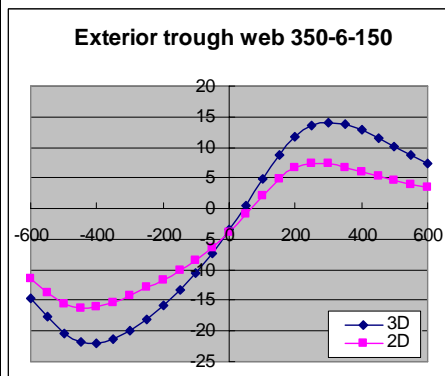
Interior trough web	350-6-150	
	Axle B	
	3D	2D
-600	10.3	6.21
-550	11.4	7.17
-500	11.8	7.52
-450	11	6.67
-400	9.14	5.06
-350	6.67	2.95
-300	3.94	0.79
-250	1.21	-1.22
-200	-1.43	-3.00
-150	-3.96	-4.61
-100	-6.46	-6.20
-50	-8.99	-7.87
0	-11.6	-9.69
50	-14.1	-11.58
100	-16.3	-13.34
150	-18	-14.63
200	-18.7	-14.98
250	-18.1	-14.21
300	-16.7	-12.68
350	-14.8	-10.82
400	-12.8	-8.94
450	-10.9	-7.26
500	-9.19	-5.82
550	-7.69	-4.61
600	-6.38	-3.60



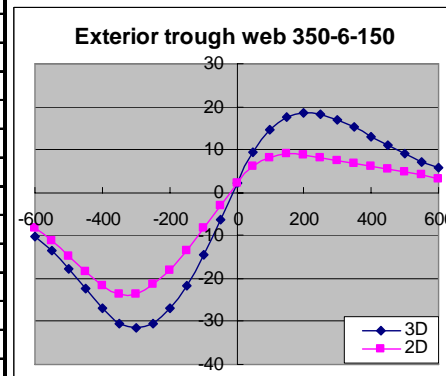
Interior trough web	350-6-150	
	Axle C	
	3D	2D
-600	9.06	4.40
-550	10.8	5.82
-500	12.8	7.51
-450	14.5	9.34
-400	15.6	10.51
-350	15.2	10.49
-300	12.6	8.47
-250	8.26	4.93
-200	2.83	0.49
-150	-3.21	-4.39
-100	-9.36	-9.30
-50	-15.1	-13.81
0	-20	-17.47
50	-23.4	-19.70
100	-24.4	-19.79
150	-23.5	-18.46
200	-21.5	-16.17
250	-18.9	-13.76
300	-16.3	-11.52
350	-13.8	-9.56
400	-11.6	-7.89
450	-9.57	-6.44
500	-7.86	-5.15
550	-6.41	-4.00
600	-5.24	-2.97



Exterior trough web	350-6-150	
	Axle B	
	3D	2D
-600	-14.6	-11.47
-550	-17.7	-13.83
-500	-20.3	-15.68
-450	-21.8	-16.33
-400	-22	-16.14
-350	-21.3	-15.27
-300	-19.9	-14.15
-250	-18.1	-12.92
-200	-15.8	-11.62
-150	-13.3	-10.19
-100	-10.5	-8.50
-50	-7.25	-6.39
0	-3.52	-3.85
50	0.579	-0.96
100	4.8	2.04
150	8.73	4.75
200	11.8	6.62
250	13.5	7.39
300	14	7.30
350	13.7	6.76
400	12.9	6.02
450	11.6	5.28
500	10.2	4.60
550	8.71	3.97
600	7.27	3.38

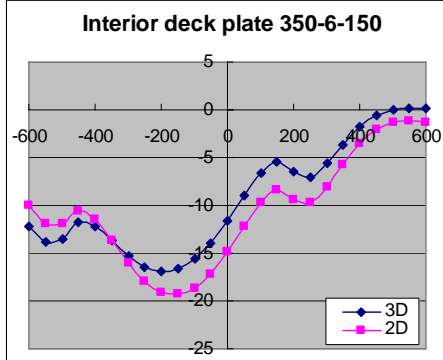


Exterior trough web	350-6-150	
	Axle C	
	3D	2D
-600	-10.2	-8.36
-550	-13.4	-11.26
-500	-17.6	-14.69
-450	-22.4	-18.46
-400	-27	-21.69
-350	-30.5	-23.71
-300	-31.6	-23.53
-250	-30.4	-21.47
-200	-27	-18.03
-150	-21.6	-13.53
-100	-14.4	-8.36
-50	-6.24	-2.97
0	2.12	2.09
50	9.46	6.10
100	14.6	8.21
150	17.5	8.94
200	18.6	8.63
250	18.3	8.04
300	17	7.38
350	15.2	6.74
400	13	6.13
450	10.9	5.48
500	8.92	4.81
550	7.21	4.08
600	5.83	3.33

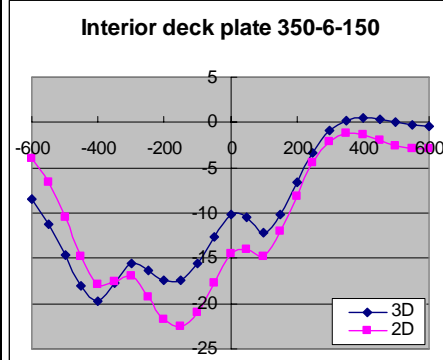


Stress in the deck plate

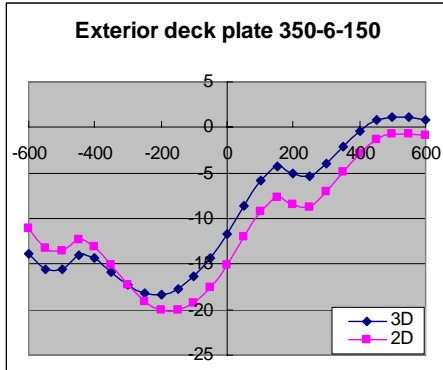
Interior deck plate	350-6-150	
	Axle B	
	3D	2D
-600	-12.2	-9.93
-550	-13.8	-11.88
-500	-13.6	-11.97
-450	-11.8	-10.65
-400	-12.2	-11.52
-350	-13.7	-13.69
-300	-15.3	-16.06
-250	-16.5	-17.93
-200	-16.9	-19.09
-150	-16.6	-19.26
-100	-15.6	-18.64
-50	-13.9	-17.23
0	-11.6	-14.93
50	-8.99	-12.24
100	-6.61	-9.74
150	-5.4	-8.42
200	-6.54	-9.42
250	-7.02	-9.69
300	-5.65	-8.05
350	-3.64	-5.72
400	-1.78	-3.55
450	-0.522	-2.06
500	0.0661	-1.34
550	0.185	-1.17
600	0.0738	-1.29



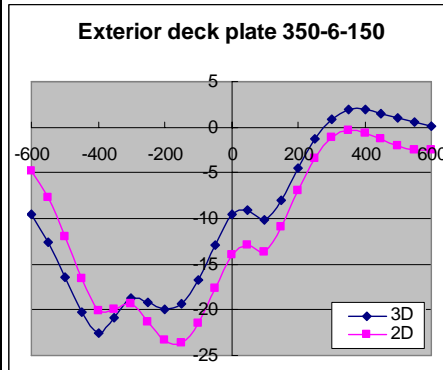
Interior deck plate	350-6-150	
	Axle C	
	3D	2D
-600	-8.42	-3.96
-550	-11.2	-6.61
-500	-14.6	-10.49
-450	-18	-14.77
-400	-19.7	-17.85
-350	-17.8	-17.52
-300	-15.6	-16.99
-250	-16.3	-19.25
-200	-17.4	-21.70
-150	-17.4	-22.45
-100	-15.6	-20.91
-50	-12.6	-17.67
0	-10.1	-14.54
50	-10.4	-14.03
100	-12.1	-14.74
150	-10.1	-12.08
200	-6.67	-8.08
250	-3.34	-4.47
300	-0.949	-2.12
350	0.254	-1.21
400	0.54	-1.34
450	0.356	-1.94
500	0.0174	-2.55
550	-0.291	-2.89
600	-0.484	-2.85



Exterior deck plate	350-6-150	
	Axle B	
	3D	2D
-600	-13.8	-11.09
-550	-15.6	-13.23
-500	-15.6	-13.57
-450	-14	-12.30
-400	-14.4	-13.12
-350	-15.8	-15.13
-300	-17.2	-17.34
-250	-18.2	-19.13
-200	-18.3	-20.01
-150	-17.7	-20.08
-100	-16.4	-19.35
-50	-14.4	-17.62
0	-11.7	-15.09
50	-8.65	-12.06
100	-5.85	-9.26
150	-4.24	-7.67
200	-5.09	-8.48
250	-5.42	-8.71
300	-4.03	-7.11
350	-2.08	-4.88
400	-0.348	-2.81
450	0.763	-1.41
500	1.19	-0.79
550	1.14	-0.71
600	0.869	-0.91



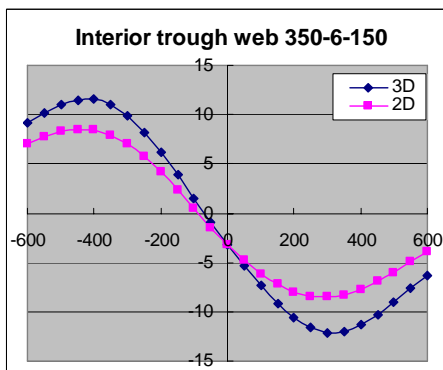
Exterior deck plate	350-6-150	
	Axle C	
	3D	2D
-600	-9.54	-4.81
-550	-12.6	-7.76
-500	-16.5	-11.96
-450	-20.3	-16.61
-400	-22.5	-20.06
-350	-20.9	-19.91
-300	-18.7	-19.34
-250	-19.2	-21.34
-200	-20	-23.32
-150	-19.3	-23.58
-100	-16.7	-21.42
-50	-12.9	-17.64
0	-9.51	-13.96
50	-9.09	-12.98
100	-10.2	-13.62
150	-8.03	-10.89
200	-4.54	-6.93
250	-1.28	-3.44
300	0.936	-1.19
350	1.92	-0.38
400	1.97	-0.61
450	1.55	-1.30
500	0.995	-2.00
550	0.501	-2.44
600	0.157	-2.48



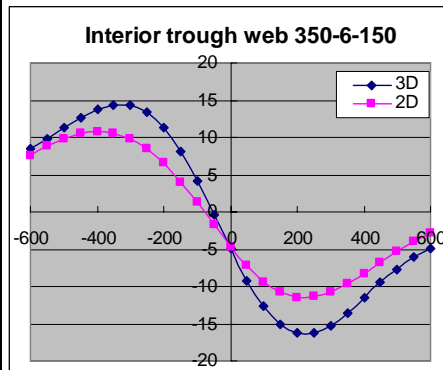
350mm + mid-span (3D model) v.s Top level (2D model)

Stress in the trough web

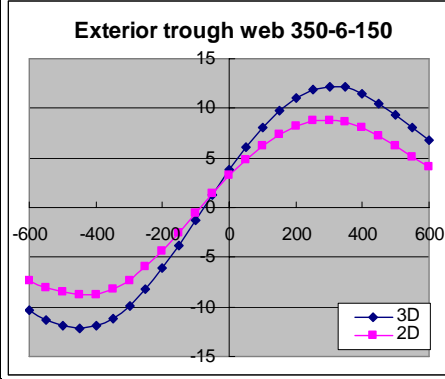
Interior trough web	350-6-150	
	Axle B	
	3D	2D
-600	9.11	7.09
-550	10.1	7.78
-500	10.95	8.29
-450	11.5	8.51
-400	11.6	8.41
-350	11.05	7.91
-300	9.915	7.02
-250	8.245	5.73
-200	6.185	4.13
-150	3.9	2.33
-100	1.525	0.43
-50	-0.86	-1.45
0	-3.185	-3.22
50	-5.385	-4.80
100	-7.39	-6.13
150	-9.13	-7.21
200	-10.6	-7.98
250	-11.6	-8.43
300	-12.1	-8.53
350	-12	-8.29
400	-11.35	-7.76
450	-10.3	-6.95
500	-8.97	-5.98
550	-7.58	-4.93
600	-6.26	-3.89



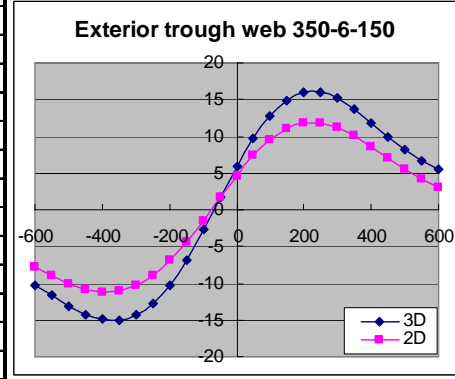
Interior trough web	350-6-150	
	Axle C	
	3D	2D
-600	8.565	7.57
-550	9.89	8.80
-500	11.3	9.83
-450	12.6	10.54
-400	13.7	10.82
-350	14.35	10.60
-300	14.4	9.90
-250	13.45	8.48
-200	11.35	6.52
-150	8.175	4.05
-100	4.115	1.23
-50	-0.4255	-1.74
0	-4.985	-4.66
50	-9.175	-7.26
100	-12.7	-9.35
150	-15.15	-10.75
200	-16.3	-11.52
250	-16.3	-11.40
300	-15.2	-10.80
350	-13.5	-9.64
400	-11.5	-8.22
450	-9.495	-6.70
500	-7.67	-5.25
550	-6.12	-3.94
600	-4.89	-2.84



Exterior trough web	350-6-150	
	Axle B	
	3D	2D
-600	-10.4	-7.29
-550	-11.3	-8.02
-500	-11.85	-8.55
-450	-12.1	-8.81
-400	-11.9	-8.72
-350	-11.2	-8.23
-300	-9.965	-7.32
-250	-8.245	-6.01
-200	-6.135	-4.37
-150	-3.755	-2.51
-100	-1.24	-0.55
-50	1.315	1.39
0	3.805	3.22
50	6.12	4.86
100	8.13	6.27
150	9.765	7.39
200	11	8.22
250	11.85	8.71
300	12.2	8.83
350	12.1	8.61
400	11.5	8.06
450	10.5	7.25
500	9.31	6.24
550	8.01	5.16
600	6.74	4.09

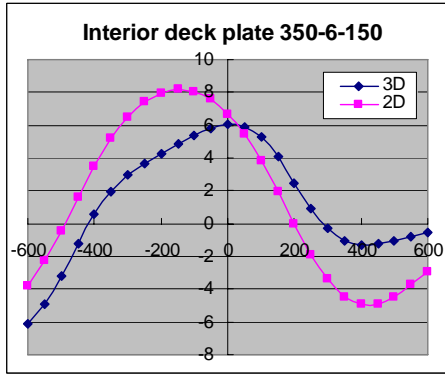


Exterior trough web	350-6-150	
	Axle C	
	3D	2D
-600	-10.2	-7.75
-550	-11.7	-9.02
-500	-13.1	-10.11
-450	-14.3	-10.86
-400	-14.95	-11.18
-350	-15	-11.00
-300	-14.35	-10.30
-250	-12.8	-8.88
-200	-10.25	-6.88
-150	-6.795	-4.35
-100	-2.685	-1.45
-50	1.71	1.64
0	5.935	4.66
50	9.67	7.38
100	12.75	9.57
150	14.9	11.06
200	16	11.89
250	16	11.80
300	15.2	11.20
350	13.7	10.03
400	11.9	8.58
450	10	7.02
500	8.28	5.51
550	6.745	4.16
600	5.49	3.02

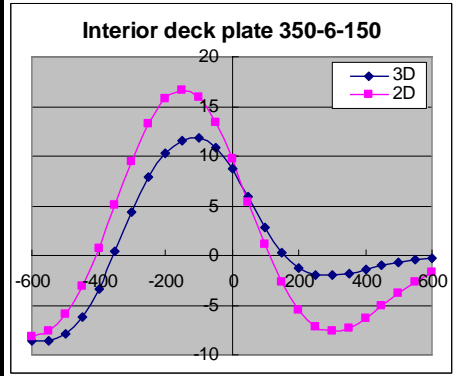


Stress in the deck plate

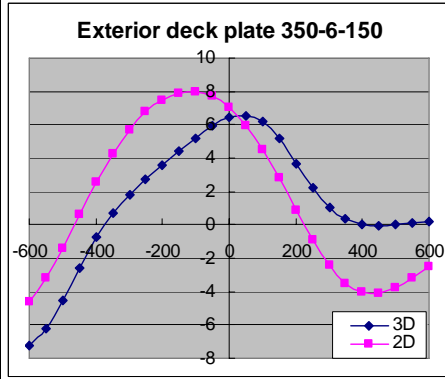
Interior deck plate	350-6-150	
	Axle B	
	3D	2D
-600	-6.08	-3.81
-550	-4.955	-2.30
-500	-3.23	-0.43
-450	-1.24	1.59
-400	0.568	3.50
-350	1.955	5.17
-300	2.96	6.50
-250	3.695	7.43
-200	4.285	7.98
-150	4.835	8.17
-100	5.365	8.04
-50	5.815	7.56
0	6.045	6.69
50	5.925	5.43
100	5.295	3.82
150	4.1	1.95
200	2.48	-0.02
250	0.88	-1.88
300	-0.323	-3.40
350	-1.015	-4.45
400	-1.275	-4.95
450	-1.245	-4.92
500	-1.045	-4.46
550	-0.8005	-3.75
600	-0.579	-2.93



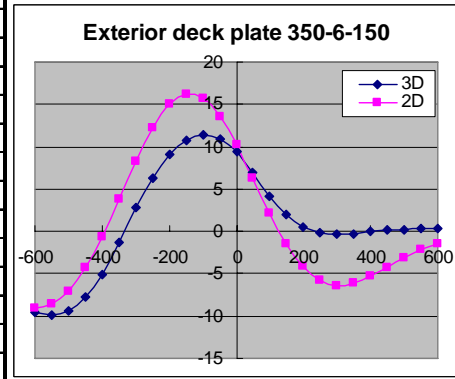
Interior deck plate	350-6-150	
	Axle C	
	3D	2D
-600	-8.535	-8.17
-550	-8.62	-7.60
-500	-7.95	-5.93
-450	-6.25	-3.10
-400	-3.39	0.69
-350	0.407	5.09
-300	4.415	9.49
-250	7.835	13.26
-200	10.25	15.76
-150	11.6	16.66
-100	11.8	15.86
-50	10.8	13.36
0	8.755	9.70
50	5.865	5.40
100	2.795	1.07
150	0.328	-2.69
200	-1.22	-5.48
250	-1.935	-7.14
300	-2.035	-7.66
350	-1.775	-7.27
400	-1.375	-6.28
450	-0.984	-5.01
500	-0.6585	-3.74
550	-0.4185	-2.62
600	-0.262	-1.75



Exterior deck plate	350-6-150	
	Axle B	
	3D	2D
-600	-7.205	-4.63
-550	-6.185	-3.20
-500	-4.53	-1.40
-450	-2.575	0.59
-400	-0.757	2.52
-350	0.7045	4.25
-300	1.845	5.67
-250	2.765	6.75
-200	3.595	7.49
-150	4.405	7.89
-100	5.21	7.99
-50	5.935	7.72
0	6.445	7.06
50	6.575	5.97
100	6.18	4.53
150	5.17	2.78
200	3.7	0.90
250	2.195	-0.90
300	1.035	-2.41
350	0.331	-3.48
400	0.002	-4.04
450	-0.0722	-4.11
500	-0.0112	-3.76
550	0.0845	-3.17
600	0.162	-2.48



Exterior deck plate	350-6-150	
	Axle C	
	3D	2D
-600	-9.625	-9.04
-550	-9.875	-8.63
-500	-9.36	-7.07
-450	-7.8	-4.32
-400	-5.025	-0.57
-350	-1.255	3.84
-300	2.8	8.34
-250	6.375	12.23
-200	9.08	15.03
-150	10.8	16.24
-100	11.4	15.65
-50	10.95	13.56
0	9.38	10.27
50	6.915	6.22
100	4.21	2.14
150	1.99	-1.45
200	0.569	-4.16
250	-0.1395	-5.80
300	-0.3405	-6.40
350	-0.2505	-6.15
400	-0.0566	-5.31
450	0.1245	-4.23
500	0.252	-3.12
550	0.32	-2.15
600	0.336	-1.41



6. Model in F

Geometry of model F

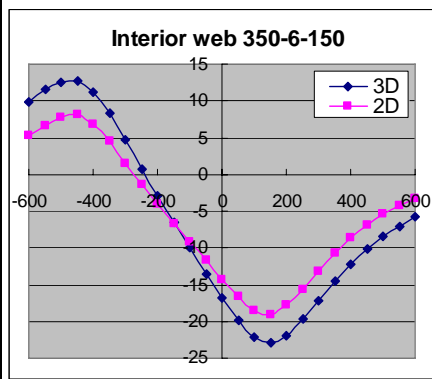
Structural component		Model F
Crossbeam	Height(H_c)	1250
	Length(L_c)	4200
	Distance(D_c)	3500
	Thickness(t_c)	12
Deck plate	Length(L_d)	21000
	Width(B_d)	4200
	Thickness(t_d)	18
Trough	Height(h_t)	350
	Width upper(b_{top})	300
	Width bottom(b_{bot})	150
	Thickness(t_t)	6
Epoxy layer	Distance(d_e)	600
	Thickness(t_a)	8

The unit of the dimension is mm

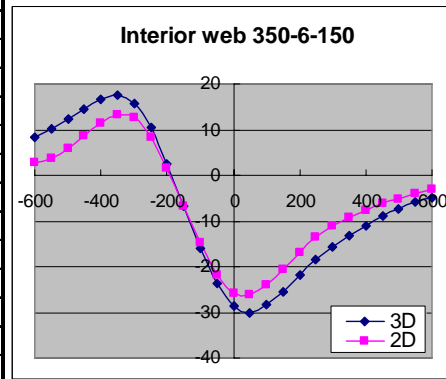
Mid-span (3D model) v.s Bottom level (2D model)

Stress in the trough web

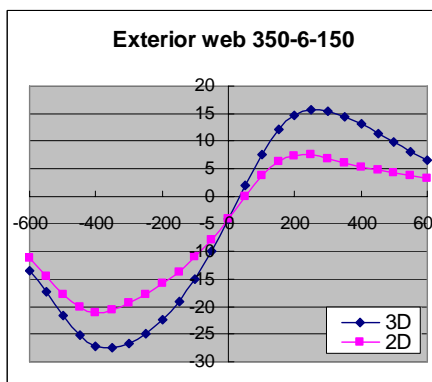
Interior trough web	350-6-150	
	Axle B	
	3D	2D
-600	9.93	5.20
-550	11.5	6.65
-500	12.6	7.83
-450	12.8	8.05
-400	11.2	6.89
-350	8.26	4.51
-300	4.62	1.57
-250	0.799	-1.38
-200	-2.93	-4.12
-150	-6.49	-6.65
-100	-9.97	-9.11
-50	-13.5	-11.65
0	-16.8	-14.27
50	-19.9	-16.67
100	-22.1	-18.47
150	-22.9	-19.00
200	-21.9	-17.81
250	-19.7	-15.75
300	-17.1	-13.18
350	-14.5	-10.75
400	-12.2	-8.61
450	-10.2	-6.86
500	-8.51	-5.45
550	-7.07	-4.28
600	-5.84	-3.30



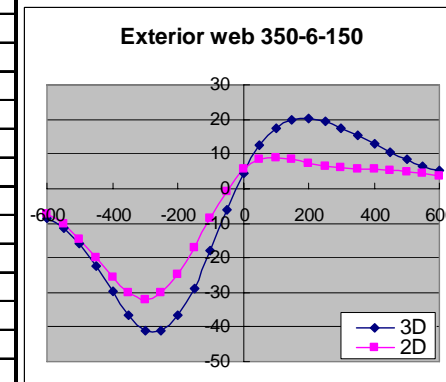
Interior trough web	350-6-150	
	Axle C	
	3D	2D
-600	8.44	2.66
-550	10.1	3.84
-500	12.3	5.87
-450	14.6	8.57
-400	16.7	11.36
-350	17.5	13.11
-300	15.8	12.55
-250	10.5	8.30
-200	2.43	1.50
-150	-6.79	-6.70
-100	-15.9	-14.84
-50	-23.6	-21.70
0	-28.7	-25.70
50	-30	-26.14
100	-28.4	-23.93
150	-25.4	-20.51
200	-21.9	-16.78
250	-18.6	-13.60
300	-15.7	-11.04
350	-13.2	-9.12
400	-11	-7.59
450	-9.02	-6.30
500	-7.36	-5.13
550	-5.99	-4.01
600	-4.89	-2.93



Exterior trough web	350-6-150	
	Axle B	
	3D	2D
-600	-13.4	-11.24
-550	-17.4	-14.55
-500	-21.6	-17.77
-450	-25.1	-20.15
-400	-27.1	-21.11
-350	-27.5	-20.69
-300	-26.7	-19.43
-250	-24.9	-17.78
-200	-22.4	-15.88
-150	-19.1	-13.75
-100	-14.9	-11.09
-50	-9.93	-7.81
0	-4.19	-4.01
50	1.89	0.01
100	7.66	3.73
150	12.2	6.40
200	14.7	7.39
250	15.6	7.45
300	15.4	6.82
350	14.5	6.09
400	13.1	5.39
450	11.4	4.80
500	9.76	4.27
550	8.13	3.78
600	6.67	3.28

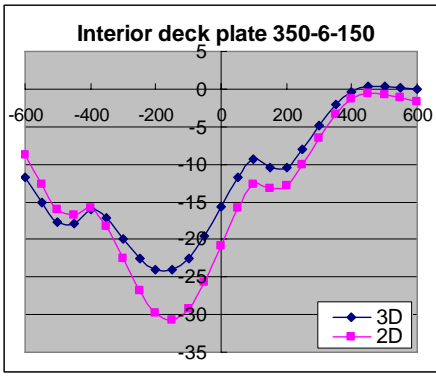


Exterior trough web	350-6-150	
	Axle C	
	3D	2D
-600	-8.57	-7.26
-550	-11.4	-10.28
-500	-16	-14.53
-450	-22.2	-19.83
-400	-29.5	-25.44
-350	-36.4	-30.09
-300	-41	-32.25
-250	-41.2	-30.30
-200	-36.8	-24.90
-150	-28.8	-17.30
-100	-18.1	-8.76
-50	-6.32	-0.70
0	4.59	5.50
50	12.5	8.46
100	17.3	9.07
150	19.7	8.49
200	20.2	7.42
250	19.4	6.60
300	17.6	6.06
350	15.3	5.80
400	12.8	5.59
450	10.4	5.30
500	8.31	4.87
550	6.63	4.27
600	5.35	3.51

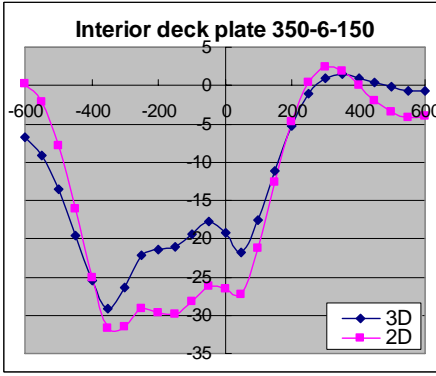


Stress in the deck plate

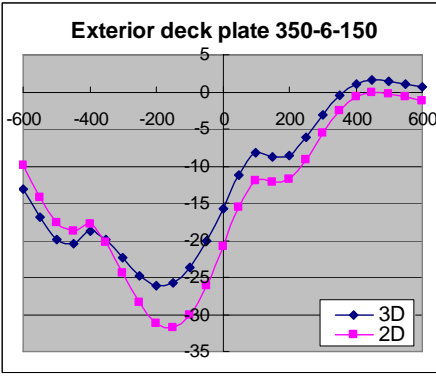
Interior deck plate	350-6-150	
	Axle B	
	3D	2D
-600	-11.8	-8.77
-550	-15.1	-12.68
-500	-17.7	-15.96
-450	-17.9	-16.84
-400	-16	-15.81
-350	-17.2	-18.27
-300	-19.9	-22.53
-250	-22.5	-26.88
-200	-24.1	-29.83
-150	-24.1	-30.68
-100	-22.5	-29.24
-50	-19.5	-25.61
0	-15.6	-20.80
50	-11.8	-15.90
100	-9.38	-12.73
150	-10.4	-13.17
200	-10.4	-12.92
250	-7.98	-10.07
300	-4.85	-6.50
350	-2.16	-3.37
400	-0.42	-1.39
450	0.334	-0.63
500	0.431	-0.71
550	0.227	-1.17
600	-0.0557	-1.66



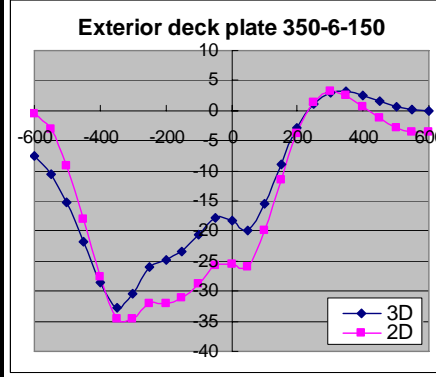
Interior deck plate	350-6-150	
	Axle C	
	3D	2D
-600	-6.69	0.25
-550	-9.22	-2.13
-500	-13.6	-7.76
-450	-19.5	-16.07
-400	-25.5	-25.04
-350	-29.1	-31.70
-300	-26.3	-31.46
-250	-22.1	-29.10
-200	-21.4	-29.64
-150	-21	-29.77
-100	-19.4	-28.21
-50	-17.8	-26.15
0	-19.2	-26.50
50	-21.7	-27.38
100	-17.6	-21.29
150	-11.2	-12.64
200	-5.2	-4.75
250	-0.982	0.45
300	1.05	2.39
350	1.46	1.84
400	1.05	0.08
450	0.388	-1.91
500	-0.215	-3.44
550	-0.597	-4.14
600	-0.719	-3.95



Exterior deck plate	350-6-150	
	Axle B	
	3D	2D
-600	-13.2	-9.90
-550	-16.9	-14.17
-500	-19.9	-17.73
-450	-20.4	-18.78
-400	-18.7	-17.82
-350	-19.9	-20.25
-300	-22.4	-24.36
-250	-24.8	-28.45
-200	-26.1	-31.23
-150	-25.7	-31.79
-100	-23.7	-30.03
-50	-20.1	-26.07
0	-15.7	-20.82
50	-11.2	-15.56
100	-8.23	-12.02
150	-8.78	-12.18
200	-8.63	-11.86
250	-6.15	-9.08
300	-3.1	-5.58
350	-0.546	-2.59
400	1.02	-0.71
450	1.59	-0.04
500	1.5	-0.20
550	1.11	-0.73
600	0.674	-1.29



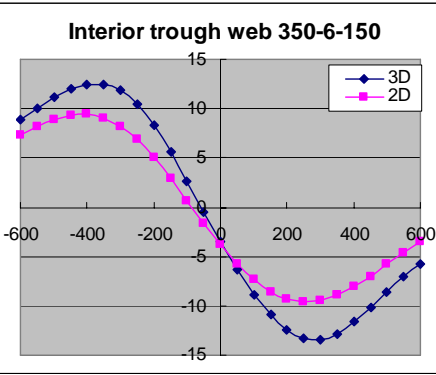
Exterior deck plate	350-6-150	
	Axle C	
	3D	2D
-600	-7.64	-0.46
-550	-10.5	-3.15
-500	-15.3	-9.21
-450	-21.8	-17.98
-400	-28.5	-27.65
-350	-32.8	-34.72
-300	-30.4	-34.67
-250	-26	-31.99
-200	-24.9	-31.97
-150	-23.4	-31.21
-100	-20.7	-28.72
-50	-17.9	-25.71
0	-18.2	-25.48
50	-19.9	-26.06
100	-15.5	-19.98
150	-8.92	-11.43
200	-2.91	-3.70
250	1.16	1.35
300	2.98	3.19
350	3.12	2.57
400	2.44	0.76
450	1.52	-1.29
500	0.698	-2.88
550	0.134	-3.66
600	-0.128	-3.57



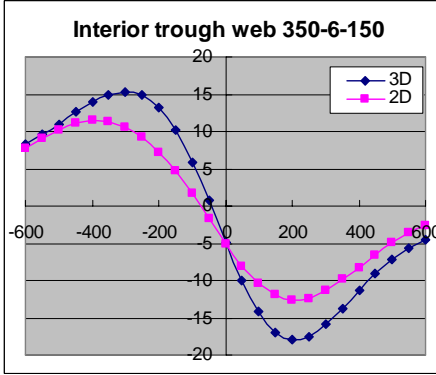
Top level

Stress in the trough web

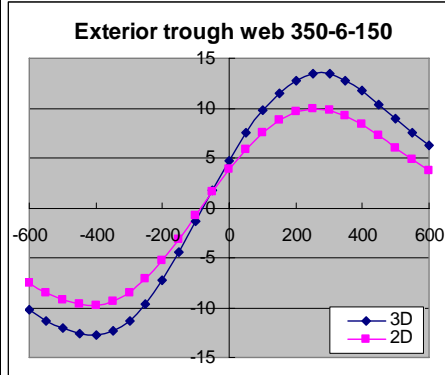
Interior trough web	350-6-150	
	Axle B	
	3D	2D
-600	8.88	7.33
-550	10.05	8.23
-500	11.1	8.93
-450	12	9.37
-400	12.5	9.43
-350	12.5	9.05
-300	11.85	8.18
-250	10.4	6.83
-200	8.3	5.05
-150	5.65	2.95
-100	2.665	0.67
-50	-0.449	-1.63
0	-3.51	-3.80
50	-6.355	-5.73
100	-8.85	-7.33
150	-10.9	-8.54
200	-12.4	-9.31
250	-13.3	-9.62
300	-13.4	-9.48
350	-12.8	-8.94
400	-11.6	-8.06
450	-10.2	-6.98
500	-8.57	-5.79
550	-7.05	-4.61
600	-5.7	-3.52



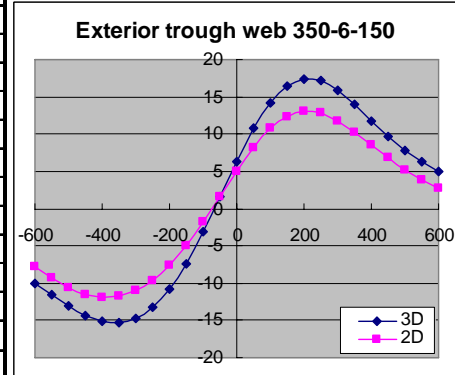
Interior trough web	350-6-150	
	Axle C	
	3D	2D
-600	8.26	7.69
-550	9.575	9.10
-500	11	10.27
-450	12.55	11.14
-400	13.9	11.52
-350	14.95	11.40
-300	15.35	10.58
-250	14.9	9.26
-200	13.25	7.26
-150	10.2	4.67
-100	5.865	1.61
-50	0.684	-1.71
0	-4.82	-5.05
50	-9.995	-8.05
100	-14.2	-10.47
150	-16.9	-11.92
200	-17.95	-12.59
250	-17.5	-12.38
300	-15.9	-11.38
350	-13.7	-9.90
400	-11.3	-8.22
450	-9.04	-6.52
500	-7.1	-4.96
550	-5.57	-3.63
600	-4.44	-2.58



Exterior trough web	350-6-150	
	Axle B	
	3D	2D
-600	-10.25	-7.53
-550	-11.3	-8.47
-500	-12.1	-9.21
-450	-12.6	-9.67
-400	-12.7	-9.77
-350	-12.3	-9.39
-300	-11.3	-8.52
-250	-9.585	-7.15
-200	-7.27	-5.33
-150	-4.475	-3.17
-100	-1.395	-0.82
-50	1.75	1.55
0	4.765	3.80
50	7.47	5.81
100	9.745	7.49
150	11.5	8.78
200	12.8	9.59
250	13.4	9.94
300	13.4	9.82
350	12.8	9.28
400	11.8	8.40
450	10.4	7.28
500	8.97	6.05
550	7.53	4.83
600	6.22	3.70

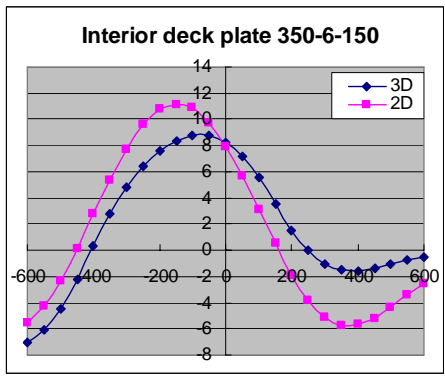


Exterior trough web	350-6-150	
	Axle C	
	3D	2D
-600	-9.96	-7.87
-550	-11.5	-9.32
-500	-13	-10.54
-450	-14.3	-11.46
-400	-15.15	-11.89
-350	-15.3	-11.81
-300	-14.75	-11.02
-250	-13.3	-9.70
-200	-10.85	-7.66
-150	-7.385	-5.01
-100	-3.135	-1.85
-50	1.555	1.59
0	6.325	5.05
50	10.75	8.19
100	14.25	10.73
150	16.5	12.28
200	17.4	13.01
250	17.1	12.82
300	15.8	11.82
350	13.9	10.30
400	11.7	8.58
450	9.62	6.84
500	7.76	5.22
550	6.24	3.85
600	5.07	2.74

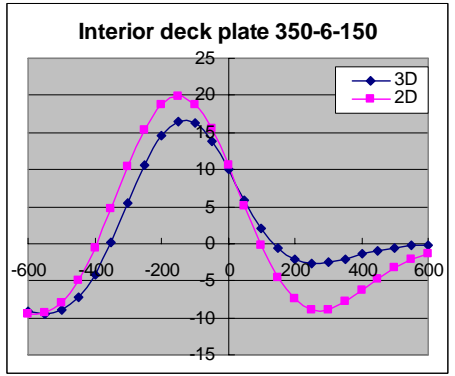


Stress in the deck plate

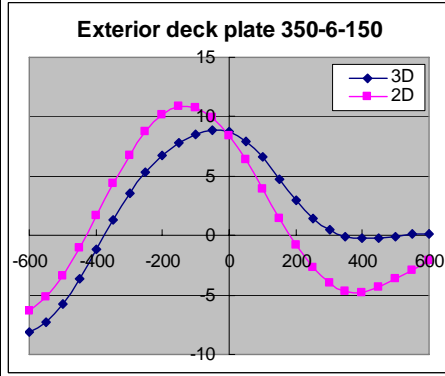
Interior deck plate	350-6-150	
	Axle B	
	3D	2D
-600	-7	-5.55
-550	-6.11	-4.26
-500	-4.48	-2.33
-450	-2.24	0.08
-400	0.3035	2.76
-350	2.745	5.40
-300	4.805	7.75
-250	6.405	9.58
-200	7.57	10.76
-150	8.345	11.16
-100	8.755	10.86
-50	8.745	9.71
0	8.245	7.95
50	7.16	5.68
100	5.515	3.11
150	3.515	0.50
200	1.545	-1.90
250	-0.0311	-3.81
300	-1.045	-5.10
350	-1.515	-5.72
400	-1.565	-5.70
450	-1.345	-5.18
500	-1.03	-4.36
550	-0.728	-3.43
600	-0.4825	-2.52



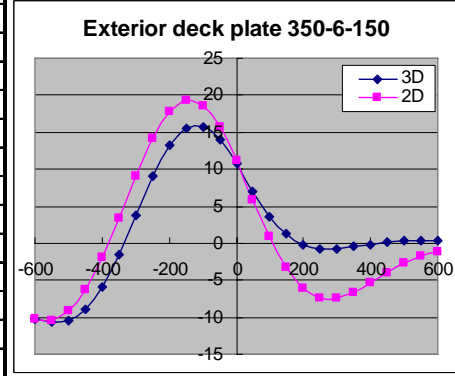
Interior deck plate	350-6-150	
	Axle C	
	3D	2D
-600	-9.105	-9.41
-550	-9.485	-9.38
-500	-8.99	-7.95
-450	-7.3	-4.98
-400	-4.21	-0.63
-350	0.2105	4.71
-300	5.475	10.36
-250	10.6	15.26
-200	14.5	18.66
-150	16.45	19.86
-100	16.2	18.76
-50	13.9	15.46
0	10.1	10.57
50	5.835	5.01
100	2.06	-0.27
150	-0.644	-4.58
200	-2.175	-7.48
250	-2.705	-8.86
300	-2.535	-8.84
350	-2.02	-7.85
400	-1.445	-6.37
450	-0.9355	-4.78
500	-0.552	-3.33
550	-0.301	-2.19
600	-0.166	-1.41



Exterior deck plate	350-6-150	
	Axle B	
	3D	2D
-600	-8.105	-6.40
-550	-7.335	-5.21
-500	-5.8	-3.37
-450	-3.63	-1.01
-400	-1.11	1.66
-350	1.365	4.35
-300	3.525	6.79
-250	5.305	8.79
-200	6.725	10.14
-150	7.81	10.85
-100	8.555	10.75
-50	8.9	9.89
0	8.735	8.38
50	7.96	6.33
100	6.57	3.96
150	4.78	1.48
200	2.96	-0.82
250	1.46	-2.70
300	0.4505	-4.00
350	-0.0857	-4.68
400	-0.2505	-4.76
450	-0.186	-4.36
500	-0.0386	-3.68
550	0.1018	-2.89
600	0.199	-2.11

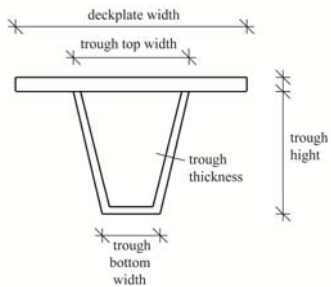
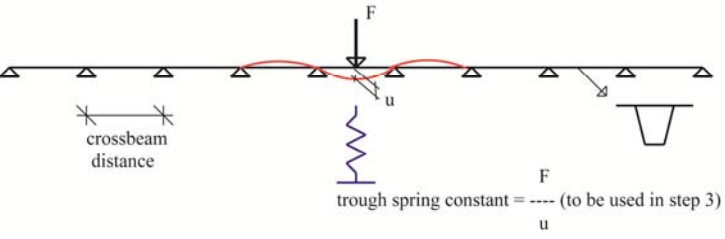


Exterior deck plate	350-6-150	
	Axle C	
	3D	2D
-600	-10.2	-10.33
-550	-10.7	-10.44
-500	-10.4	-9.14
-450	-8.85	-6.27
-400	-5.87	-1.96
-350	-1.495	3.39
-300	3.805	9.08
-250	9.055	14.22
-200	13.2	17.82
-150	15.5	19.33
-100	15.75	18.54
-50	14	15.66
0	10.8	11.17
50	7.005	5.94
100	3.64	0.93
150	1.21	-3.20
200	-0.2155	-6.02
250	-0.7835	-7.42
300	-0.7655	-7.51
350	-0.474	-6.70
400	-0.1425	-5.41
450	0.1255	-4.00
500	0.299	-2.74
550	0.379	-1.76
600	0.384	-1.10



Appendix C Original simplified 2D beam model

During the internship, the Excel Programs developed by Rijkswaterstaat was applied to find out the stresses (in longitudinal direction), stress ranges and fatigue damage in the bottom flange of the trough. The manual of the Excel Programs is presented in this appendix.

Excelprogram	Purpose and explanation	Input	Outcome
1	<p>Calculation of moment of inertia and section modulus of a trough including the deck plate (see Figure 1)</p>  <p>Figure 1 Trough crosssection</p>	<p>Deck plate thickness Deck plate width Trough height Top and bottom width trough Wall thickness trough</p> <p>Example: see appendix B</p>	<p>I_{yy} W_b W_o</p> <p>Example: see appendix B</p>
2	<p>Calculation of the midfield vertical springstiffness of a single trough going over multiple supports (crossbeams).</p> <p>The model used for this step is a simple 2D beam with 10 spans over 11 supports (see figure 2).</p>  <p>Figure 2 2D model</p>	<p>Results of step 1 Crossbeam distance Unit vertical load</p> <p>Example: appendix B</p>	<p>Deflection of the trough due to unit midfield load resulting in unit midfield displacement and a substituting midfield spring stiffness of the trough</p> <p>Example: appendix B</p>
3	<p>Calculation of the amount of the wheel load of the axles A, B and C which is carried by 1 trough.</p> <p>The model used for this step is a 2D beam model of an orthotropic deck cross section which consists of 2 levels (see figure 3a). Both levels consist of 7 troughs with deck plate.</p> <p>The 2 levels are connected by rigid beams to make sure both levels have the same deflections.</p> <p>The bottom level is supported by springs with $\frac{1}{2}$ (translation of the total trough stiffness to the stiffness per trough leg) of the spring stiffness calculated in step 2, representing the vertical stiffness of a trough due to its own bending in longitudinal direction.</p> <p>The bottom level represents the bending stiffness in transverse direction of the deck (and troughs) with a width (in the direction of trough) corresponding with the length of a wheel load (including the spreading of the asphalt). The bottom level therefore represents the cross section of the deck which is directly loaded by the wheel loads and the transverse stiffness of that part of the deck.</p> <p>The top level represents the bending stiffness in transverse direction of the deck (and troughs) with a width (in the direction of troughs) corresponding with half the crossbeam distance minus the length of a wheel load (including the spreading of the asphalt). The top level therefore represents the cross section of the deck which is not directly loaded by the wheel loads and the transverse stiffness of that part of the deck. The width of the top section is an assumption.</p> <p>When the trough deflects due to a load on top of it, the deflection varies along the length of the trough from zero at the crossbeams to a max in the middle of the trough span. This means that the effect of the spreading of the load in transverse direction due to the bending stiffness of the deck also varies along the length of the trough from zero at the crossbeam to a max in the middle of the trough span (see figure 3b). The effective width in this model (which represents the deflections of the middle trough span) is assumed to be 50% of the span.</p> <p>The loads applied are the uniformly distributed single wheel loads (50KN) of the axles A, B and C (with the width of the wheels as contact area length taking account of the spreading of the asphalt) placed centrally over the middle trough on the bottom level.</p> <p>Due to the spreading of the wheel loads in transverse direction the loads are also applied with an offset of 100 mm and 200 mm from the centre of the middle trough.</p>	<p>Crossbeam distance</p> <p>Bottom level:</p> <ul style="list-style-type: none"> - Deck plate thickness - Deck plate width (loaded length including spreading of the asphalt) - Trough height - Top and bottom width trough - Wall thickness trough <p>Top level:</p> <ul style="list-style-type: none"> - Deck plate thickness - Deck plate width - Trough height - Top and bottom width trough - Wall thickness trough <p>Example: appendix B</p>	<p>Spring support forces of the middle trough in the bottom level indicating what part of the wheel loads from axles A, B and C is carried by that middle trough (for the central load situation and reduction factors for the offset situations of +/- 100 and +/- 200 mm. All forces are due to a wheel load of 50 KN</p> <p>Example: appendix B</p>

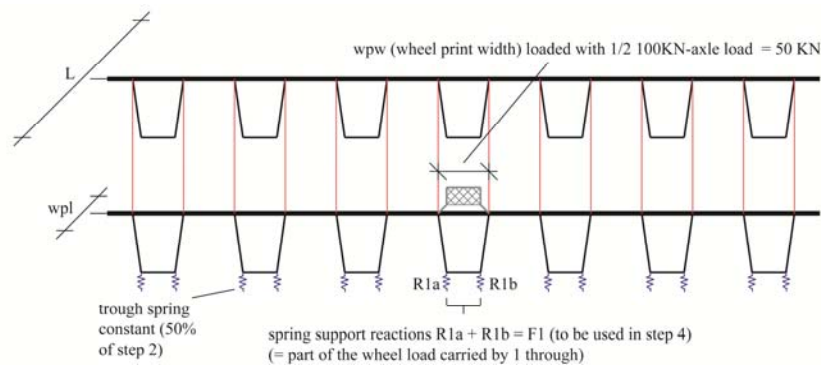


Figure 3a 2D beam model

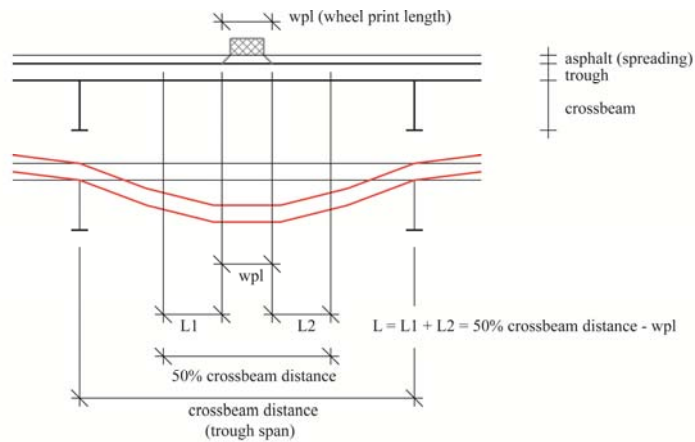


Figure 3b

<p>4</p>	<p>Calculation of the influence lines of the troughs due to a single passing axle load (influence lines for the trough bottom flange stresses at mid span, quarter span, 1/8 span and at the intersection with the crossbeam; reaction force on crossbeam)</p> <p>The model used for this step is a 2D beam model which consists of 2 levels of troughs with 10 spans (see figure 4a). The 2 levels are connected by rigid beams to make sure both levels have the same deflections at the locations of the crossbeams. The 11 (spring) supports of the bottom level represent the crossbeam locations.</p> <p>The bottom level consists of 1 trough (the trough to be reviewed). The top level consists of a number of troughs. The number of troughs to be used in the top level and the spring stiffness of the crossbeams to be used underneath the bottom level should be based on the actual situation. When the trough to be reviewed (bottom level of the model) is in the middle of the span of a crossbeam, the deflection of the crossbeam has an effect on the stresses in the bottom level troughs, and a substituting crossbeam spring should be used. That same deflection of the crossbeam causes the other (top level troughs) also to bend and therefore reduce that deflection. If the trough to be reviewed (bottom level) is in the middle of a crossbeam span it is assumed 50% of the other troughs are effective in reducing the crossbeam deflection (see figure 4b).</p> <p>When, on the other hand, the trough to be reviewed is near a main girder, then the deflection of the crossbeam will be practically zero thus no spring has to be used and, due to the nature of the model the number of troughs on the top level is not of interest (see figure 4c).</p> <p>The loads applied are point loads on many locations along the length of the troughs. Both bottom and top level of the model are loaded (to get the effect of the total axle load on the system). The sum of loads for each load case is 100 KN (axle loads). The bottom level trough is loaded by the part of a wheel load carried by 1 trough derived from step 3. The top level troughs are loaded by the remaining part of the 100 KN axle load.</p>	<p>Trough inertias and section modulus's</p> <p>Individual crossbeam distances</p> <p>Number of troughs for the top level</p> <p>Crossbeam substituting spring stiffness</p> <p>The amount of the wheel load of the axles A, B and C which is carried by 1 trough derived from step 3</p> <p>Example: see appendix B</p>	<p>Influence lines for the stresses in the trough bottom flange at:</p> <ul style="list-style-type: none"> - 1/2 span - 1/4 span - 1/8 span - intersection trough – crossbeam <p>Influence line for the reaction force on crossbeam</p> <p>All influence lines are due to one axle load of 100 KN</p> <p>Example: see appendix B</p>
----------	--	--	--

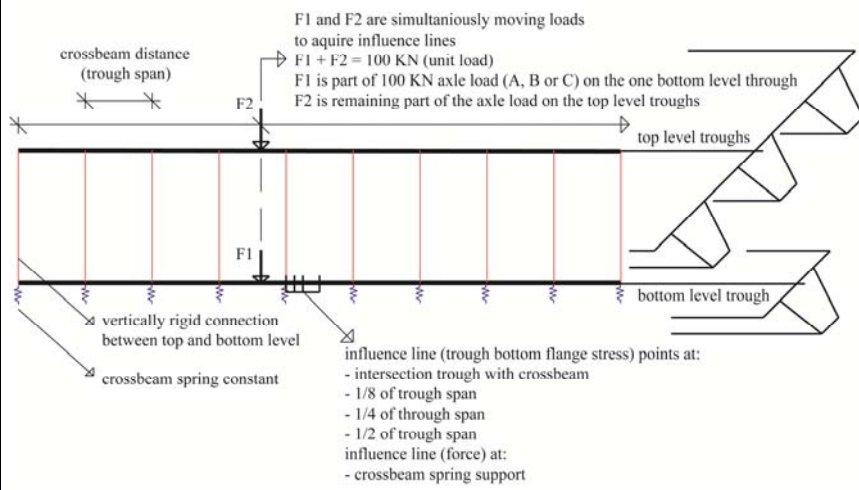


Figure 4a

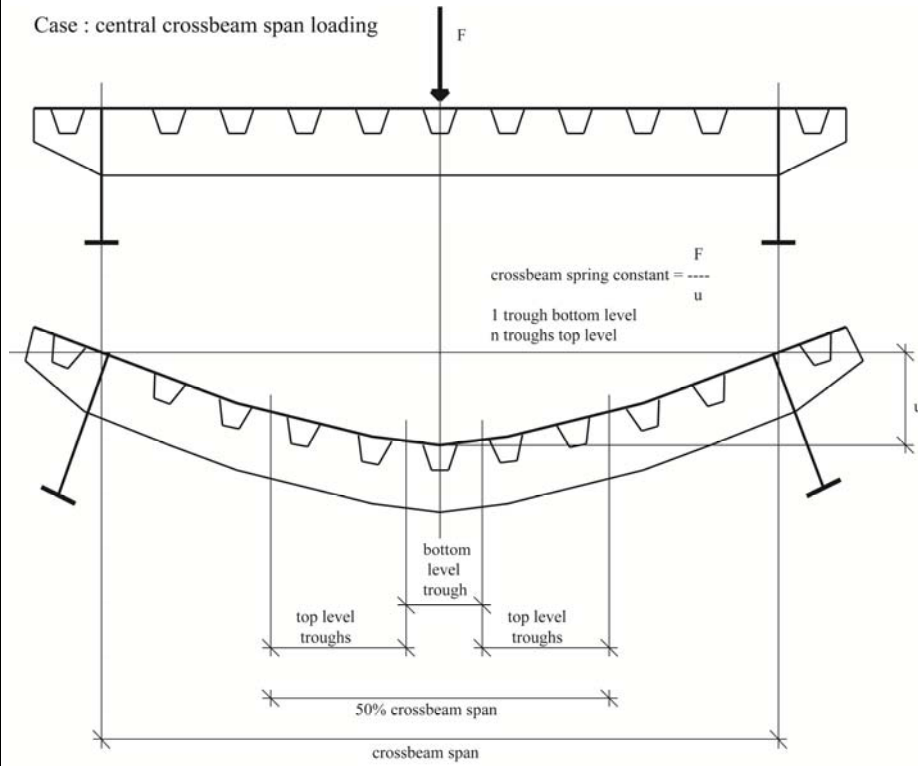


Figure 4b

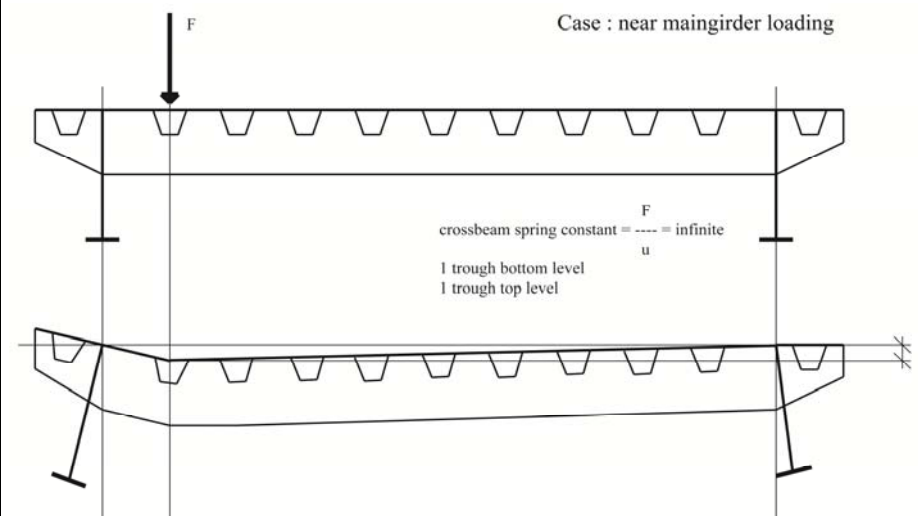


Figure 4c

<p>5</p>	<p>Calculation of the influence lines of the troughs due to a set of passing axle loads representing complete trucks (influence lines for the trough bottom flange stresses at mid span, quarter span, 1/8 span and at the intersection with the crossbeam; reaction force on crossbeam). The trucks used are all the trucks coming from the fatigue load model 1, 2, 3 and 4 of NEN-EN1991-2 + NB. One hundred trucks (taking account of the long distance situation of truck percentages) of fatigue load model 4 of NEN-EN1991-2 + NB are put behind each other, taking account of the reduction of effects due to the transverse spreading of the trucks by 100 and 200 mm. This gives a total stress range spectrum.</p> <p>This is a purely administrative action which needs no further explanation.</p>	<p>Single axle influence lines derived from step 4 Reduction factors for the transverse spreading of the wheels derived from step 3 Definition of trucks from the fatigue models of NEN-EN1991-2+NB (axle loads, type of axles, axle distances) The step interval of moving the trucks over the single axle influence lines.</p> <p>Example: see appendix B</p>	<p>Influence lines for the stresses in the trough bottom flange at:</p> <ul style="list-style-type: none"> - 1/2 span - 1/4 span - 1/8 span - intersection trough – crossbeam <p>Influence line for the reaction force on crossbeam All influence lines are made for all trucks defined in the fatigue models of NEN-EN1991-2 + NB. A total stress range spectrum is made for a 100 trucks of fatigue load model 4 of NEN-EN1991-2+NB for the situation long distance and taking account of the</p>
----------	--	--	---

			transverse spreading of the trucks Example: see appendix B
6	<p>Evaluation of the stress ranges spectrum by means of the reservoir counting method and, based on that, calculation the damage during the lifetime (by means of a classification and the miner rule, based on NEN-EN1991-9+NB and NEN-EN1993-2+NB)</p> <p>This is a purely administrative action which needs no further explanation. For explanation of the reservoir counting method see appendix ..</p>	<p>The total stress range spectrum made for 100 trucks of fatigue load model 4 of NEN-EN1991-2+NB for the situation long distance and taking account of the transverse spreading of the trucks derived from step 5</p> <p>Example: see appendix B</p>	<p>Calculated lifetime damage</p> <p>Example: see appendix B</p>
A	<p>Calculations have been made for the following situations: List of calculations:</p> <ul style="list-style-type: none"> - 9 calculations with fully supported crossbeams spaced at 3500 mm, a 18 mm deck with asphalt and different trough dimensions - 3 calculations with various spring supported crossbeams spaced at 3500 mm, a 18 mm deck with asphalt and trough dimensions 350/150/8 - 6 calculations with fully supported crossbeams spaced at different distances, a 18 mm deck with asphalt and trough dimensions 350/150/8 - 2 calculations with fully supported crossbeams spaced at 2800 mm, a 22 mm deck without asphalt and trough dimensions 350/150/8 		
B	Results of the calculations A in tables and graphs + conclusions concerning the different influences		

Excel Program 1

Calculation of moment of inertia and section modulus of a trough including the deck plate

BEREKENING STATISCHE WAARDEN											
STATISCHE WAARDEN 10 PLAATDELEN											
werk	dek 18 trog 350/150/8 dd3500							N=	0 KN		
profiel	trog in het veld							M=	50 KNM		
locatie								D=	50 KN		
NR	B(mm)	H(mm)	Zo(mm)	Wb(mm ³)	Wo(mm ³)	naam	1= deel van het lijf	Ay(mm ²)	spanning boven	spanning onder	
1	600	18	9	-2.99E+06	-3.74E+06	dek		nvt	-16.7	-13.4	N/mm ²
2	16	342	189	-3.74E+06	9.92E+05	trogbenen	1	5472	-13.4	50.4	N/mm ²
3	150	8	364	9.92E+05	9.64E+05	trog of		nvt	50.4	51.9	N/mm ²
4								nvt			
5								nvt			
6								nvt			
7								nvt			
8								nvt			
9								nvt			
10								nvt			
								5472	tau_gem=	9.1 N/mm ²	
zwaartepunt			89.8 mm ;		0.0898 m						
oppervlak (Ax)			17472 mm ² ;		0.0175 m ²						
dwarskrachtoppervlek (Ay)			5472 mm ² ;		0.0055 m ²						
traagheidsmoment			2.68E+08 mm ⁴ ;		0.0003 m ⁴						
traagheidsstraal			123.9 mm ;		0.1239 m						
eigen gewicht					137.2 kg/m'						
					1.372 KN/m						
alleen waarden copieren naar raamwerk											
							Ax (m ²)	Ay (m ²)	I(m ⁴)	Wb(m ³)	Wo(m ³)
							0.017472	0.005472	0.000268	0.002988	0.000964

Excel Prgoram 2

Calculation of the midfield vertical spring stiffness of a single trough going over multiple supports (crossbeams)

omschrijving	dek 18 trog 350/150/8 dd 3500			
dwarsdragerafstand	3500	mm	3.5	m
statische waarden trog (alleen waarden kopiëren vanuit stap 1)				
Ax (m2)	Ay (m2)	I(m4)	Wb(m3)	Wo(m3)
0.017472	0.005472	0.000268	0.002988	0.000964
resultaat:				
kracht op 1/4 van de overspanning	-100.00	KN		
verplaatsing op 1/4 van de overspanning	-0.00045	m		
veerstijfheid op 1/4 van de overspanning	223408	KN/m		voor de hele trog
veerstijfheid op 1/4 van de overspanning	111704			voor de halve trog
kracht op 1/2 van de overspanning	-100.00	KN		
verplaatsing op 1/2 van de overspanning	-0.00083	m		
veerstijfheid op 1/2 van de overspanning	120190	KN/m		voor de hele trog
veerstijfheid op 1/2 van de overspanning	60095			voor de halve trog

Excel Program 3

Calculation of the amount of the wheel load of the axles A, B and C which is carried by 1 trough

Input result of Excel Program 3 and construction dimensions, output percentage of axle load carried by the middle trough

berekening dekconstructie (dekplaat + troggen) in dwarsrichting (inclusief verdeling belasting over troggen)													
omschrijving:										dek 18 trog 350/150/8 dd 3500			
invoergegevens (geel is in te voeren waarden)													
keuze:										1			
berekening met alleen spreiding asfalt (in deze fase alleen 1 gebruiken)										1			
berekening met spreiding asfalt en buigwerking asfalt los van staal										2			
veerstijfheid trog uit stap 2a										60095.1314 KN/m		uit stap 2	
dekplaatoverspanning tussen 2 troggen										300 mm			
dekplaatoverspanning in 1 trog										300 mm			
dwarsdragerafstand (trogoverspanningslengte)										3500 mm			
percentage trogoverspanningslengte wat bij spreiding over de troggen meewerkt										50 %		1750 mm	
werkende lengte direct buigende deel										420 mm			
werkende lengte spreidende deel troggen										1330 mm			
dikte van de dekplaat										18 mm			
E-modulus dekplaat										210000 N/mm2			
dikte van de trogwand en trogbodem										8 mm			
dikte (asfalt)slijtlaag										0 mm			
E-modulus (asfalt)slijtlaag										2500 N/mm2			
breedte van de trogbodem										150 mm			
hoogte van de trog										350 mm			
resultaat	dek 18 trog 350/150/8 dd 3500							resultaat	dek 18 trog 350/150/8 dd 3500				
	wiel A	wiel B	wiel C	wiel LM1	wiel LM2	wiel C+10	wiel C+20		wiel A	wiel B	wiel C		
	MET spreiding asfalt								ZONDER s				
trog1a	-0.10	-0.11	-0.10	-0.32	-0.46	-0.03	0.02	trog1a	-0.10	-0.11	-0.10		
trog1b	-0.21	-0.23	-0.22	-0.68	-0.95	-0.08	0.03	trog1b	-0.21	-0.23	-0.21		
trog2a	0.57	0.69	0.60	1.94	2.93	0.12	-0.20	trog2a	0.54	0.65	0.57		
trog2b	1.03	1.21	1.08	3.44	5.07	0.27	-0.28	trog2b	0.99	1.15	1.03		
trog3a	-0.68	-1.79	-0.97	-4.05	-9.17	0.86	1.80	trog3a	-0.47	-1.35	-0.68		
trog3b	-2.52	-3.90	-2.89	-10.06	-17.99	0.50	2.49	trog3b	-2.26	-3.35	-2.52		
trog4a	-23.09	-20.86	-22.50	-65.26	-79.44	-19.78	-15.85	trog4a	-23.50	-21.75	-23.09		
trog4b	-23.09	-20.86	-22.50	-65.26	-79.44	-23.27	-21.70	trog4b	-23.50	-21.75	-23.09		
trog5a	-2.52	-3.90	-2.89	-10.06	-17.99	-7.48	-12.73	trog5a	-2.26	-3.35	-2.52		
trog5b	-0.68	-1.79	-0.97	-4.05	-9.17	-3.79	-7.45	trog5b	-0.47	-1.35	-0.68		
trog6a	1.03	1.21	1.08	3.44	5.07	2.05	2.88	trog6a	0.99	1.15	1.03		
trog6b	0.57	0.69	0.60	1.94	2.93	1.19	1.73	trog6b	0.54	0.65	0.57		
trog7a	-0.21	-0.23	-0.22	-0.68	-0.95	-0.38	-0.50	trog7a	-0.21	-0.23	-0.21		
trog7b	-0.10	-0.11	-0.10	-0.32	-0.46	-0.18	-0.25	trog7b	-0.10	-0.11	-0.10		
som	-50	-50	-50	-150	-200	-50	-50	som	-50	-50	-50		
trog4	-46.17	-41.73	-45.00	-130.52	-158.87	-43.05	-37.55	trog4	-47.01	-43.51	-46.17		
%	92	83	90	87	79	86	75	%	94	87	92		
as	-100	-100	-100	-300	-400	-100	-100	as	-100	-100	-100		
trog4	-46.17	-41.73	-45.00	-130.52	-158.87	-43.05	-37.55	trog4	-47.01	-43.51	-46.17		
%	46	42	45	44	40	43	38	%	47	44	46		
			1			0.96	0.83						

2D beam model of an orthotropic deck cross section

aantal knopen	73	maximaal 100
aantal elementen	99	maximaal 100

knopen								
knoop nummer	knoop-coor-dinaat X (m)	knoop-coor-dinaat Y (m)	0 = geen oplegging 1 = oplegging (vast) 2 = oplegging (veer)			veerstijfheid		
			opleg- conditie X	opleg- conditie Y	opleg- conditie PHI	X (KN/m)	Y (KN/m)	PHI KNm/rad
1	0	1	1	0	0			
2	0.15	1	0	0	0			
3	0.45	1	0	0	0			
4	0.75	1	0	0	0			
5	1.05	1	0	0	0			
6	1.35	1	0	0	0			
7	1.65	1	0	0	0			
8	1.95	1	0	0	0			
9	2.25	1	0	0	0			
10	2.55	1	0	0	0			
11	2.85	1	0	0	0			
12	3.15	1	0	0	0			
13	3.45	1	0	0	0			
14	3.75	1	0	0	0			
15	4.05	1	0	0	0			
16	4.2	1	0	0	1			
17	0.225	0.645	0	0	0			
18	0.375	0.645	0	0	0			
19	0.825	0.645	0	0	0			
20	0.975	0.645	0	0	0			
21	1.425	0.645	0	0	0			
22	1.575	0.645	0	0	0			
23	2.025	0.645	0	0	0			
24	2.175	0.645	0	0	0			
25	2.625	0.645	0	0	0			
26	2.775	0.645	0	0	0			
27	3.225	0.645	0	0	0			
28	3.375	0.645	0	0	0			
29	3.825	0.645	0	0	0			
30	3.975	0.645	0	0	0			
31	0	0.5	1	0	1			
32	0.15	0.5	0	0	0			
33	0.45	0.5	0	0	0			
34	0.75	0.5	0	0	0			
35	1.05	0.5	0	0	0			
36	1.35	0.5	0	0	0			
37	1.65	0.5	0	0	0			
38	1.7	0.5	0	0	0			
39	1.75	0.5	0	0	0			
40	1.8	0.5	0	0	0			
41	1.85	0.5	0	0	0			
42	1.9	0.5	0	0	0			
43	1.95	0.5	0	0	0			
44	2	0.5	0	0	0			
45	2.1	0.5	0	0	0			
46	2.2	0.5	0	0	0			
47	2.25	0.5	0	0	0			
48	2.3	0.5	0	0	0			
49	2.35	0.5	0	0	0			
50	2.4	0.5	0	0	0			
51	2.45	0.5	0	0	0			
52	2.5	0.5	0	0	0			
53	2.55	0.5	0	0	0			
54	2.85	0.5	0	0	0			
55	3.15	0.5	0	0	0			
56	3.45	0.5	0	0	0			
57	3.75	0.5	0	0	0			
58	4.05	0.5	0	0	0			
59	4.2	0.5	0	0	1			
60	0.225	0.145	0	2	0		60095.13	
61	0.375	0.145	0	2	0		60095.13	
62	0.825	0.145	0	2	0		60095.13	
63	0.975	0.145	0	2	0		60095.13	
64	1.425	0.145	0	2	0		60095.13	
65	1.575	0.145	0	2	0		60095.13	
66	2.025	0.145	0	2	0		60095.13	
67	2.175	0.145	0	2	0		60095.13	
68	2.625	0.145	0	2	0		60095.13	
69	2.775	0.145	0	2	0		60095.13	
70	3.225	0.145	0	2	0		60095.13	
71	3.375	0.145	0	2	0		60095.13	
72	3.825	0.145	0	2	0		60095.13	
73	3.975	0.145	0	2	0		60095.13	

Excel Program 4

Calculation of the influence lines of the troughs due to a single passing axle load (influence lines for the trough bottom flange stresses at mid span, quarter span, 1/8 span and at the intersection with the crossbeam; reaction force on crossbeam)

Input construction dimensions, results of Excel Program 1 and of Excel Program 3

Programma voor het statisch en qua vermoeiing doorrekenen van troggen					
Invoer	dek 18 trog 350/150/8 dd 3500				
begin		0 mm			0 m
trogoverspanning	1	3500 mm			3.5 m
trogoverspanning	2	3500 mm			3.5 m
trogoverspanning	3	3500 mm			3.5 m
trogoverspanning	4	3500 mm			3.5 m
trogoverspanning	5	3500 mm			3.5 m
trogoverspanning	6	3500 mm			3.5 m
trogoverspanning	7	3500 mm			3.5 m
trogoverspanning	8	3500 mm			3.5 m
trogoverspanning	9	3500 mm			3.5 m
trogoverspanning	10	3500 mm			3.5 m
afstand oplegknopen		100 mm			0.1 m
afstand passtuk in 6		875 mm			0.875 m
Ax trog		0.017472 m ²	uit stap 1		0.017472 m ²
Aytrog		0.005472 m ²			0.005472 m ²
Iz trog		2.68E-04 m ⁴			0.000268 m ⁴
Wb trog		2.99E-03 m ³			0.002988 m ³
Wo trog		9.64E-04 m ³			0.000964 m ³
aantal troggen onder		1 stuks			1 stuks
aantal troggen boven		10 stuks			10 stuks
dwardrager vast (1=ja, 2=veer)		1			
veerstijfheid dwarsdrager		62500 KN/m (N/mm)			62500 KN/m
eenheidsas		100 KN			100 KN
percentage op 1 trog		45 %	uit stap 3		45 %
					F1
				F2	55 KN
hoogte dwarsdrager		1250 mm			
lijfplaatdikte dwarsdrager		12 mm			

2D beam model consists of 2 levels of troughs with 10 spans

Excel 2D-raamwerkprogramma versie 1.27			
Project:	dek 18 trog 350/150/8 dd 3500		
Onderdeel:	invloedslijn troggen		
constructeur:	Frank van Dooren (RWS DI)		
datum:	25-8-2009		
aantal knopen	90	maximaal 100	
aantal elementen	99	maximaal 100	

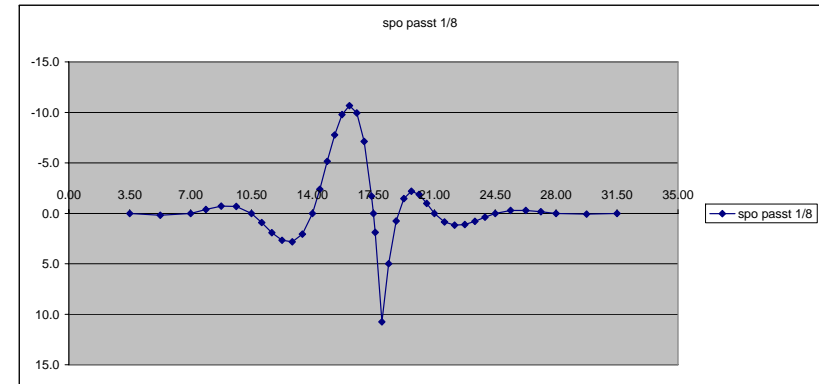


knopen									
knoop nummer	knoop-coor-dinaat X (m)	knoop-coor-dinaat Y (m)	0 = geen oplegging 1 = oplegging (vast) 2 = oplegging (veer)			veerstijfheid			PHI KNm/rad
			opleg- conditie X	opleg- conditie Y	opleg- conditie PHI	X (KN/m)	Y (KN/m)	PHI	
1	0.00	0	1	1	0				
2	3.5	0	0	1	0				
3	5.25	0	0	0	0				
4	7	0	0	1	0				
5	7.875	0	0	0	0				
6	8.75	0	0	0	0				
7	9.625	0	0	0	0				
8	10.5	0	0	1	0				
9	11.08333	0	0	0	0				
10	11.66667	0	0	0	0				
11	12.25	0	0	0	0				
12	12.83333	0	0	0	0				
13	13.41667	0	0	0	0				
14	14	0	0	1	0				
15	14.425	0	0	0	0				
16	14.85	0	0	0	0				
17	15.275	0	0	0	0				
18	15.7	0	0	0	0				
19	16.125	0	0	0	0				
20	16.55	0	0	0	0				
21	16.975	0	0	0	0				
22	17.4	0	0	0	0				
23	17.5	0	0	1	0				
24	17.6	0	0	0	0				
25	17.9875	0	0	0	0				
26	18.375	0	0	0	0				
27	18.8125	0	0	0	0				
28	19.25	0	0	0	0				
29	19.6875	0	0	0	0				
30	20.125	0	0	0	0				
31	20.5625	0	0	0	0				
32	21	0	0	1	0				
33	21.58333	0	0	0	0				
34	22.16667	0	0	0	0				
35	22.75	0	0	0	0				
36	23.33333	0	0	0	0				
37	23.91667	0	0	0	0				
38	24.5	0	0	1	0				
39	25.375	0	0	0	0				
40	26.25	0	0	0	0				
41	27.125	0	0	0	0				
42	28	0	0	1	0				
43	29.75	0	0	0	0				
44	31.5	0	0	1	0				
45	35	0	0	1	0				
46	0.00	0.25	1	0	0				
47	3.50	0.25	0	0	0				
48	5.25	0.25	0	0	0				
49	7.00	0.25	0	0	0				
50	7.88	0.25	0	0	0				
51	8.75	0.25	0	0	0				
52	9.63	0.25	0	0	0				
53	10.50	0.25	0	0	0				
54	11.08	0.25	0	0	0				
55	11.67	0.25	0	0	0				
56	12.25	0.25	0	0	0				
57	12.83	0.25	0	0	0				
58	13.42	0.25	0	0	0				
59	14.00	0.25	0	0	0				
60	14.43	0.25	0	0	0				
61	14.85	0.25	0	0	0				
62	15.28	0.25	0	0	0				
63	15.70	0.25	0	0	0				
64	16.13	0.25	0	0	0				
65	16.55	0.25	0	0	0				
66	16.98	0.25	0	0	0				
67	17.40	0.25	0	0	0				
68	17.83	0.25	0	0	0				
69	18.25	0.25	0	0	0				
70	18.68	0.25	0	0	0				
71	19.10	0.25	0	0	0				
72	19.53	0.25	0	0	0				
73	19.95	0.25	0	0	0				
74	20.38	0.25	0	0	0				
75	20.80	0.25	0	0	0				
76	21.23	0.25	0	0	0				
77	21.65	0.25	0	0	0				
78	22.08	0.25	0	0	0				
79	22.50	0.25	0	0	0				
80	22.93	0.25	0	0	0				
81	23.35	0.25	0	0	0				
82	23.78	0.25	0	0	0				
83	24.20	0.25	0	0	0				
84	24.63	0.25	0	0	0				
85	25.05	0.25	0	0	0				
86	25.48	0.25	0	0	0				
87	25.90	0.25	0	0	0				
88	26.33	0.25	0	0	0				
89	26.75	0.25	0	0	0				
90	27.18	0.25	0	0	0				
91									
92									
93									
94									
95									
96									
97									
98									
99									
100									

elementen												
staaf nummer	profiel-naam	KN_A	KN_B	0 = scharnier 1 = vast		E (KN/m2)	Ax (m2)	voor schuifsp nog geen		Wboven (m3)	Wonder (m3)	
				aansluit- conditie KN_A	aansluit- conditie KN_B			D- verv. Ay (m2)	Iz (m4)			
1	ondertrog	1	2	1	1	2.10E+08	0.017472	0.005472	0.000268	0.002988	0.000964	
2	ondertrog	2	3	1	1	2.10E+08	0.017472	0.005472	0.000268	0.002988	0.000964	
3	ondertrog	3	4	1	1	2.10E+08	0.017472	0.005472	0.000268	0.002988	0.000964	
4	ondertrog	4	5	1	1	2.10E+08	0.017472	0.005472	0.000268	0.002988	0.000964	
5	ondertrog	5	6	1	1	2.10E+08	0.017472	0.005472	0.000268	0.002988	0.000964	
6	ondertrog	6	7	1	1	2.10E+08	0.017472	0.005472	0.000268	0.002988	0.000964	
7	ondertrog	7	8	1	1	2.10E+08	0.017472	0.005472	0.000268	0.002988	0.000964	
8	ondertrog	8	9	1	1	2.10E+08	0.017472	0.005472	0.000268	0.002988	0.000964	
9	ondertrog	9	10	1	1	2.10E+08	0.017472	0.005472	0.000268	0.002988	0.000964	
10	ondertrog	10	11	1	1	2.10E+08	0.017472	0.005472	0.000268	0.002988	0.000964	
11	ondertrog	11	12	1	1	2.10E+08	0.017472	0.005472	0.000268	0.002988	0.000964	
12	ondertrog	12	13	1	1	2.10E+08	0.017472	0.005472	0.000268	0.002988	0.000964	
13	ondertrog	13	14	1	1	2.10E+08	0.017472	0.005472	0.000268	0.002988	0.000964	
14	ondertrog	14	15	1	1	2.10E+08	0.017472	0.005472	0.000268	0.002988	0.000964	
15	ondertrog	15	16	1	1	2.10E+08	0.017472	0.005472	0.000268	0.002988	0.000964	
16	ondertrog	16	17	1	1	2.10E+08	0.017472	0.005472	0.000268	0.002988	0.000964	
17	ondertrog	17	18	1	1	2.10E+08	0.017472	0.005472	0.000268	0.002988	0.000964	
18	ondertrog	18	19	1	1	2.10E+08	0.017472	0.005472	0.000268	0.002988	0.000964	
19	ondertrog	19	20	1	1	2.10E+08	0.017472	0.005472	0.000268	0.002988	0.000964	
20	ondertrog	20	21	1	1	2.10E+08	0.017472	0.005472	0.000268	0.002988	0.000964	
21	ondertrog	21	22	1	1	2.10E+08	0.017472	0.005472	0.000268	0.002988	0.000964	
22	ondertrog	22	23	1	1	2.10E+08	0.017472	0.005472	0.000268	0.002988	0.000964	
23	ondertrog	23	24	1	1	2.10E+08	0.017472	0.005472	0.000268	0.002988	0.000964	
24	ondertrog	24	25	1	1	2.10E+08	0.017472	0.005472	0.000268	0.002988	0.000964	
25	ondertrog	25	26	1	1	2.10E+08	0.017472	0.005472	0.000268	0.002988	0.000964	
26	ondertrog	26	27	1	1	2.10E+08	0.017472	0.005472	0.000268	0.002988	0.000964	
27	ondertrog	27	28	1	1	2.10E+08	0.017472	0.005472	0.000268	0.002988	0.000964	
28	ondertrog	28	29	1	1	2.10E+08	0.017472	0.005472	0.000268	0.002988	0.000964	
29	ondertrog	29	30	1	1	2.10E+08	0.017472	0.005472	0.000268	0.002988	0.000964	
30	ondertrog	30	31	1	1	2.10E+08	0.017472	0.005472	0.000268	0.002988	0.000964	
31	ondertrog	31	32	1	1	2.10E+08	0.017472	0.005472	0.000268	0.002988	0.000964	
32	ondertrog	32	33	1	1	2.10E+08	0.017472	0.005472	0.000268	0.002988	0.000964	
33	ondertrog	33	34	1	1	2.10E+08	0.017472	0.005472	0.000268	0.002988	0.000964	
34	ondertrog	34	35	1	1	2.10E+08	0.017472	0.005472	0.000268	0.002988	0.000964	
35	ondertrog	35	36	1	1	2.10E+08	0.017472	0.005472	0.000268	0.002988	0.000964	
36	ondertrog	36	37	1	1	2.10E+08	0.017472	0.005472	0.000268	0.002988	0.000964	
37	ondertrog	37	38	1	1	2.10E+08	0.017472	0.005472	0.000268	0.002988	0.000964	
38	ondertrog	38	39	1	1	2.10E+08	0.017472	0.005472	0.000268	0.002988	0.000964	
39	ondertrog	39	40	1	1	2.10E+08	0.017472	0.005472	0.000268	0.002988	0.000964	
40	ondertrog	40	41	1	1	2.10E+08	0.017472	0.005472	0.000268	0.002988	0.000964	
41	ondertrog	41	42	1	1	2.10E+08	0.017472	0.005472	0.000268	0.002988	0.000964	
42	ondertrog	42										

Influence lines for the stresses in the troughs and the reaction forces on crossbeams

Resultaat dek 18 trog 350/150/8 dd 3500														
	1	2	3	4	5	6	7	8	9	10	11	12	13	14
	M	M	M	M	M	D	R	N	phi	spo	spo	spo	spo	spdd
	m	stp	passt 1/8	passt 1/4	veld	stp	stp	tussen	stp	stp	passt 1/8	passt 1/4	veld	
	0	0	0	0	0	0	0	0	0	0	0	0	0	0.0
1	3.50	0.00	0.00	0.00	0.00	0.00	0.00	0.00	0.000000	0.0	0.0	0.0	0.0	0.0
2	5.2500	0.23	0.19	0.16	0.08	0.08	0.93	0.54	-0.000004	0.2	0.2	0.2	0.1	0.0
3	7.0000	0.00	0.00	0.00	0.00	0.00	0.00	0.00	0.000000	0.0	0.0	0.0	0.0	0.0
4	7.8750	-0.45	-0.37	-0.31	-0.16	-0.16	-1.83	-1.06	0.000008	-0.5	-0.4	-0.3	-0.2	0.0
5	8.7500	-0.84	-0.69	-0.57	-0.31	-0.30	-3.42	-1.98	0.000015	-0.9	-0.7	-0.6	-0.3	0.0
6	9.6250	-0.81	-0.67	-0.55	-0.30	-0.29	-3.30	-1.91	0.000015	-0.8	-0.7	-0.6	-0.3	0.0
7	10.5000	0.00	0.00	0.00	0.00	0.00	0.00	0.00	0.000000	0.0	0.0	0.0	0.0	0.0
8	11.0833	1.07	0.88	0.73	0.39	0.39	4.35	2.53	-0.000019	1.1	0.9	0.8	0.4	-0.1
9	11.6667	2.24	1.85	1.53	0.82	0.81	9.15	5.30	-0.000040	2.3	1.9	1.6	0.9	-0.1
10	12.2500	3.12	2.57	2.13	1.14	1.13	12.74	7.39	-0.000056	3.2	2.7	2.2	1.2	-0.2
11	12.8333	3.31	2.72	2.26	1.21	1.20	13.50	7.83	-0.000059	3.4	2.8	2.3	1.3	-0.2
12	13.4167	2.40	1.98	1.64	0.88	0.87	9.80	5.68	-0.000043	2.5	2.1	1.7	0.9	-0.1
13	14.0000	0.00	0.00	0.00	0.00	0.00	0.00	0.00	0.000000	0.0	0.0	0.0	0.0	0.0
14	14.4250	-2.80	-2.30	-1.91	-1.02	-1.01	-11.60	-6.73	0.000050	-2.9	-2.4	-2.0	-1.1	0.2
15	14.8500	-6.02	-4.96	-4.11	-2.21	-2.18	-26.02	-15.09	0.000108	-6.2	-5.1	-4.3	-2.3	0.3
16	15.2750	-9.10	-7.49	-6.22	-3.33	-3.30	-41.98	-24.35	0.000163	-9.4	-7.8	-6.4	-3.5	0.5
17	15.7000	-11.45	-9.43	-7.82	-4.19	-4.15	-58.18	-33.75	0.000205	-11.9	-9.8	-8.1	-4.3	0.6
18	16.1250	-12.49	-10.28	-8.53	-4.57	-4.52	-73.36	-42.55	0.000224	-13.0	-10.7	-8.8	-4.7	0.7
19	16.5500	-11.65	-9.59	-7.96	-4.26	-4.22	-86.21	-50.00	0.000209	-12.1	-9.9	-8.3	-4.4	0.6
20	16.9750	-8.34	-6.87	-5.70	-3.05	-3.02	-95.46	-55.37	0.000150	-8.7	-7.1	-5.9	-3.2	0.5
21	17.4000	-2.00	-1.64	-1.36	-0.73	-0.72	-99.82	-57.90	0.000036	-2.1	-1.7	-1.4	-0.8	0.1
22	17.5000	0.00	0.00	0.00	0.00	0.00	-100.00	-58.00	0.000000	0.0	0.0	0.0	0.0	0.0
23	17.6000	-2.00	1.81	1.50	0.81	-41.20	-99.82	-57.90	-0.000036	-2.1	1.9	1.6	0.8	-0.1
24	17.9875	-7.91	10.36	8.61	4.65	-37.48	-96.06	-55.72	-0.000142	-8.2	10.7	8.9	4.8	-0.4
25	18.3750	-11.26	4.80	17.56	9.64	-32.94	-88.14	-51.12	-0.000202	-11.7	5.0	18.2	10.0	-0.6
26	18.8125	-12.50	0.74	11.26	16.64	-27.15	-75.42	-43.75	-0.000224	-13.0	0.8	11.7	17.3	-0.7
27	19.2500	-11.65	-1.41	6.73	25.10	-21.00	-60.05	-34.83	-0.000209	-12.1	-1.5	7.0	26.0	-0.6
28	19.6875	-9.34	-2.11	3.65	16.64	-14.85	-43.42	-25.18	-0.000168	-9.7	-2.2	3.8	17.3	-0.5
29	20.1250	-6.21	-1.80	1.71	9.64	-9.06	-26.93	-15.62	-0.000111	-6.4	-1.9	1.8	10.0	-0.3
30	20.5625	-2.89	-0.95	0.60	4.09	-3.99	-11.99	-6.96	-0.000052	-3.0	-1.0	0.6	4.2	-0.2
31	21.0000	0.00	0.00	0.00	0.00	0.00	0.00	0.00	0.000000	0.0	0.0	0.0	0.0	0.0
32	21.5833	2.40	0.82	-0.44	-3.28	3.25	9.80	5.68	0.000043	2.5	0.8	-0.5	-3.4	0.1
33	22.1667	3.31	1.13	-0.61	-4.52	4.47	13.50	7.83	0.000059	3.4	1.2	-0.6	-4.7	0.2
34	22.7500	3.12	1.06	-0.57	-4.26	4.22	12.74	7.39	0.000056	3.2	1.1	-0.6	-4.4	0.2
35	23.3333	2.24	0.76	-0.41	-3.06	3.03	9.15	5.30	0.000040	2.3	0.8	-0.4	-3.2	0.1
36	23.9167	1.07	0.36	-0.20	-1.46	1.44	4.35	2.53	0.000019	1.1	0.4	-0.2	-1.5	0.1
37	24.5000	0.00	0.00	0.00	0.00	0.00	0.00	0.00	0.000000	0.0	0.0	0.0	0.0	0.0
38	25.3750	-0.81	-0.28	0.15	1.11	-1.09	-3.30	-1.91	-0.000015	-0.8	-0.3	0.2	1.1	0.0
39	26.2500	-0.84	-0.29	0.15	1.14	-1.13	-3.42	-1.98	-0.000015	-0.9	-0.3	0.2	1.2	0.0
40	27.1250	-0.45	-0.15	0.08	0.61	-0.60	-1.83	-1.06	-0.000008	-0.5	-0.2	0.1	0.6	0.0
41	28.0000	0.00	0.00	0.00	0.00	0.00	0.00	0.00	0.000000	0.0	0.0	0.0	0.0	0.0
42	29.7500	0.23	0.08	-0.04	-0.31	0.31	0.93	0.54	0.000004	0.2	0.1	0.0	-0.3	0.0
43	31.5000	0.00	0.00	0.00	0.00	0.00	0.00	0.00	0.000000	0.0	0.0	0.0	0.0	0.0
	51.5000	0	0	0	0	0	0	0	0	0	0	0	0	0.0
		M	M	M	M	D	R	N	phi	spo	spo	spo	spo	spo
		stp	passt 1/8	passt 1/4	veld	stp	stp	tussen	stp	stp	passt 1/8	passt 1/4	veld	veld
max		3.31	10.36	17.56	25.10	4.47	13.50	7.83	0.00	3.43	10.75	18.22	26.04	0.68
min		-12.50	-10.28	-8.53	-4.57	-41.20	-100.00	-58.00	0.00	-12.96	-10.67	-8.85	-4.74	-0.68
verschil		15.81	20.64	26.09	29.67	45.68	113.50	65.83	0.00	16.40	21.41	27.07	30.78	1.36



nog toe te voegen berekening spanning in dwarsdragerlijf uit R, N en phi

omkaderd is het te kopiëren gebied naar 4 b
alleen waarden kopiëren

Excel Program 5

Calculation of the influence lines of the troughs due to a set of passing axle loads representing complete trucks (influence lines for the trough bottom flange stresses at mid span, quarter span, 1/8 span and at the intersection with the crossbeam; reaction force on crossbeam). The trucks used are all the trucks coming from the fatigue load model 1,2,3 and 4 of NEN-EN1991-2 + NB. One hundred trucks (taking account of the long distance situation of truck percentages) of fatigue load model 4 of NEN-EN1991-2 + NB are put behind each other, taking account of the reduction of effects due to the transverse spreading of the trucks by 100 and 200 mm. This gives a total stress range spectrum.

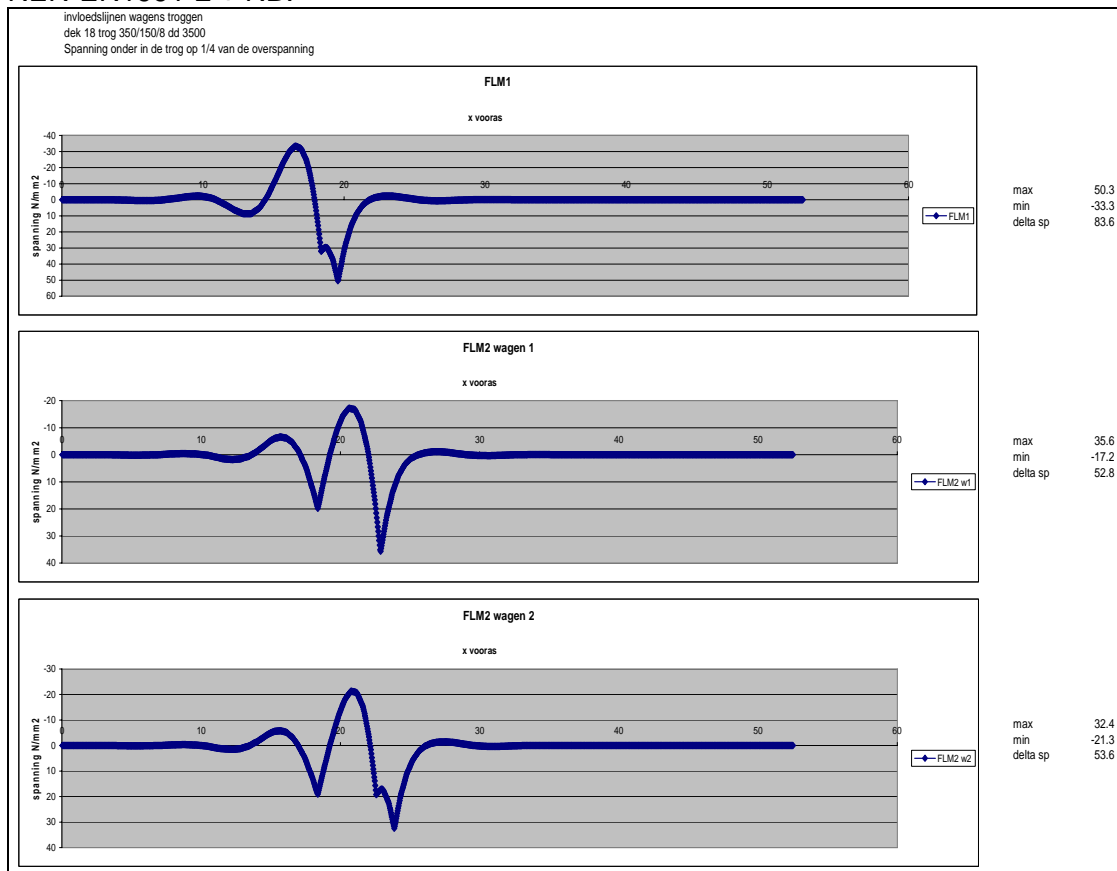
Input construction dimensions and results of Excel Program 4

Vertaling van invloedslijnen (1 puntlast op meerdere posities langs de constructie) naar invloedslijnen van complete wagens	
project	invloedslijnen wagens troggen
onderdeel	dek 18 trog 350/150/8 dd 3500
max aantal wagens	12
max aantal assen	10
basis aslast invloedslijn as A	100
basis aslast invloedslijn as B	100
basis aslast invloedslijn as C	100
basis aslast invloedslijn as LM1	100
aantal invloedspunten uitgangslijn (incl. aanloop en uitloop)	45
dwardragerafstand	3.5 m
stapgrootte van de wagens over de invloedslijn	0.035
aantal stappen	1500
invloedslijn van welk onderdeel	12
	2 = Moment in de trog tpv de dwarsdrager
	3 = Moment in de trog op 1/8 van de overspanning
	4 = Moment in de trog op 1/4 van de overspanning
	5 = Moment in de trog op 1/2 van de overspanning
	6 = Dwarskracht in de trog direct naast het steunpunt
	7 = Reactie op de dwarsdrager
	8 =
	9 =
	10 = Spanning onder in de trog tpv de dwarsdrager
	11 = Spanning onder in de trog op 1/8 van de overspanning
	12 = Spanning onder in de trog op 1/4 van de overspanning
	13 = Spanning onder in de trog op 1/2 van de overspanning
	14 = Spanning in dwarsdragerrijf
gebruik set nummer (1 of 2)	1
set 1	
spreidingsfactor centraal	1
spreidingsfactor +10cm	0.96
spreidingsfactor +20cm	0.83
set 2	
spreidingsfactor centraal	1
spreidingsfactor +10cm	0.9
spreidingsfactor +20cm	0.8

Single axle influence lines derived from step 4

	1	2	3	4	5	6	7	8	9	10	11	12	13	14
	M	M	M	M	M	D	R	N	phi	spo	spo	spo	spo	sp
	m	stp	passt 1/8	passt 1/4	veld	stp	stp	tussen	stp	stp	passt 1/8	passt 1/4	veld	dwarsdr
1	0	0	0	0	0	0	0	0	0	0	0	0	0	0
2	3.50	0.00	0.00	0.00	0.00	0.00	0.00	0.00	0.000000	0.0	0.0	0.0	0.0	0.0
3	5.2500	0.25	0.21	0.17	0.09	0.09	0.93	0.50	-0.000004	0.3	0.2	0.2	0.1	-0.013571
4	7.0000	0.00	0.00	0.00	0.00	0.00	0.00	0.00	0.000000	0.0	0.0	0.0	0.0	0.0
5	7.8750	-0.49	-0.40	-0.33	-0.18	-0.18	-1.83	-0.99	0.000009	-0.5	-0.4	-0.3	-0.2	0.026576
6	8.7500	-0.92	-0.76	-0.63	-0.34	-0.33	-3.42	-1.85	0.000016	-1.0	-0.8	-0.6	-0.3	0.049759
7	9.6250	-0.89	-0.73	-0.61	-0.32	-0.32	-3.30	-1.78	0.000016	-0.9	-0.8	-0.6	-0.3	0.048063
8	10.5000	0.00	0.00	0.00	0.00	0.00	0.00	0.00	0.000000	0.0	0.0	0.0	0.0	0.0
9	11.0833	1.17	0.96	0.80	0.43	0.42	4.35	2.35	-0.000021	1.2	1.0	0.8	0.4	-0.063386
10	11.6667	2.45	2.02	1.68	0.90	0.89	9.15	4.94	-0.000044	2.5	2.1	1.7	0.9	-0.133138
11	12.2500	3.42	2.82	2.34	1.25	1.24	12.74	6.88	-0.000061	3.5	2.9	2.4	1.3	-0.185466
12	12.8333	3.62	2.98	2.48	1.33	1.31	13.50	7.29	-0.000065	3.8	3.1	2.6	1.4	-0.196579
13	13.4167	2.63	2.17	1.80	0.96	0.95	9.80	5.29	-0.000047	2.7	2.2	1.9	1.0	-0.142687
14	14.0000	0.00	0.00	0.00	0.00	0.00	0.00	0.00	0.000000	0.0	0.0	0.0	0.0	0.0
15	14.4250	-3.06	-2.52	-2.09	-1.12	-1.11	-11.60	-6.26	0.000055	-3.2	-2.6	-2.2	-1.2	0.16624
16	14.8500	-6.60	-5.43	-4.51	-2.42	-2.39	-26.02	-14.05	0.000118	-6.8	-5.6	-4.7	-2.5	0.357903
17	15.2750	-9.97	-8.21	-6.81	-3.65	-3.61	-41.98	-22.67	0.000179	-10.3	-8.5	-7.1	-3.8	0.540646
18	15.7000	-12.54	-10.32	-8.56	-4.59	-4.54	-58.18	-31.42	0.000225	-13.0	-10.7	-8.9	-4.8	0.680131
19	16.1250	-13.68	-11.26	-9.34	-5.01	-4.96	-73.36	-39.61	0.000245	-14.2	-11.7	-9.7	-5.2	0.742015
20	16.5500	-12.76	-10.50	-8.71	-4.67	-4.62	-86.21	-46.55	0.000229	-13.2	-10.9	-9.0	-4.8	0.69196
21	16.9750	-9.14	-7.52	-6.24	-3.34	-3.31	-95.46	-51.55	0.000164	-9.5	-7.8	-6.5	-3.5	0.495623
22	17.4000	-2.19	-1.80	-1.49	-0.80	-0.79	-99.82	-53.90	0.000039	-2.3	-1.9	-1.6	-0.8	0.118664
23	17.5000	0.00	0.00	0.00	0.00	0.00	-100.00	-54.00	0.000000	0.0	0.0	0.0	0.0	0.0
24	17.6000	-2.19	1.99	1.65	0.88	-45.13	-99.82	-53.90	-0.000039	-2.3	2.1	1.7	0.9	-0.118664
25	17.9875	-8.67	11.34	9.43	5.09	-41.05	-96.06	-51.87	-0.000155	-9.0	11.8	9.8	5.3	-0.470128
26	18.3750	-12.33	5.26	19.24	10.56	-36.08	-88.14	-47.60	-0.000221	-12.8	5.5	20.0	11.0	-0.66892
27	18.8125	-13.69	0.81	12.33	18.23	-29.74	-75.42	-40.73	-0.000246	-14.2	0.8	12.8	18.9	-0.742498
28	19.2500	-12.76	-1.55	7.37	27.49	-23.00	-60.05	-32.43	-0.000229	-13.2	-1.6	7.6	28.5	-0.692103
29	19.6875	-10.23	-2.31	4.00	18.23	-16.26	-43.42	-23.44	-0.000184	-10.6	-2.4	4.1	18.9	-0.555195
30	20.1250	-6.81	-1.97	1.87	10.56	-9.92	-26.93	-14.54	-0.000122	-7.1	-2.0	1.9	11.0	-0.369235
31	20.5625	-3.16	-1.04	0.66	4.48	-4.37	-11.99	-6.48	-0.000057	-3.3	-1.1	0.7	4.6	-0.171683
32	21.0000	0.00	0.00	0.00	0.00	0.00	0.00	0.00	0.000000	0.0	0.0	0.0	0.0	0.0
33	21.5833	2.63	0.90	-0.48	-3.59	3.56	9.80	5.29	0.000047	2.7	0.9	-0.5	-3.7	0.142687
34	22.1667	3.62	1.24	-0.66	-4.95	4.90	13.50	7.29	0.000065	3.8	1.3	-0.7	-5.1	0.196579
35	22.7500	3.42	1.17	-0.63	-4.67	4.62	12.74	6.88	0.000061	3.5	1.2	-0.6	-4.8	0.185466
36	23.3333	2.45	0.84	-0.45	-3.35	3.32	9.15	4.94	0.000044	2.5	0.9	-0.5	-3.5	0.133138
37	23.9167	1.17	0.40	-0.21	-1.60	1.58	4.35	2.35	0.000021	1.2	0.4	-0.2	-1.7	0.063386
38	24.5000	0.00	0.00	0.00	0.00	0.00	0.00	0.00	0.000000	0.0	0.0	0.0	0.0	0.0
39	25.0833	-0.89	-0.30	0.16	1.21	-1.20	-3.30	-1.78	-0.000016	-0.9	-0.3	0.2	1.3	-0.048063
40	25.6667	-0.92	-0.31	0.17	1.25	-1.24	-3.42	-1.85	-0.000016	-1.0	-0.3	0.2	1.3	-0.049759
41	26.2500	-0.49	-0.17	0.09	0.67	-0.66	-1.83	-0.99	-0.000009	-0.5	-0.2	0.1	0.7	-0.026576
42	26.8333	0.00	0.00	0.00	0.00	0.00	0.00	0.00	0.000000	0.0	0.0	0.0	0.0	0.0
43	27.4167	0.25	0.09	-0.05	-0.34	0.34	0.93	0.50	0.000004	0.3	0.1	0.0	-0.4	0.013571
44	28.0000	0.00	0.00	0.00	0.00	0.00	0.00	0.00	0.000000	0.0	0.0	0.0	0.0	0.0
45	28.5833	0	0	0	0	0	0	0	0	0	0	0	0	0

Influence lines for the stresses in the trough bottom flange and the reaction forces on crossbeams. All influence lines are made for all trucks defined in the fatigue models of NEN-EN1991-2 + NB.

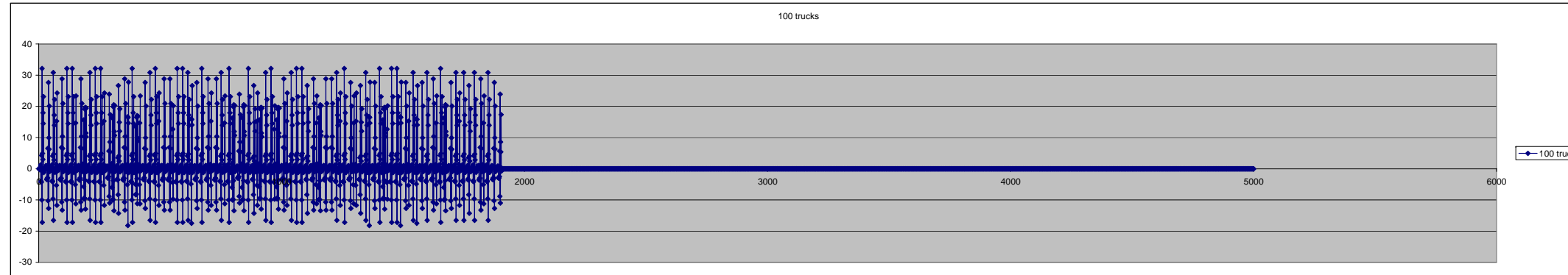


Total stress range spectrum for 100 trucks of fatigue load model 4 of NEN-EN1991+2 + NB

invloedslijnen wagens troggen
dek 18 trog 350/150/8 dd 3500
Spanning onder in de trog op 1/4 van de overspanning

te kopiëren kolom van 0 tot 0

1	0	0
2	0.131242	0.131242
3	0.023624	0.023624
4	0.044021	0.044021
5	-0.380445	-0.380445
6	-0.160243	-0.160243
7	-0.172416	-0.172416
8	1.248641	1.248641
9	-4.131475	-4.131475
10	-4.001566	-4.001566
11	-4.317917	-4.317917
12	4.264426	4.264426
13	-10.01359	-10.01359
14	32.13054	32.13054
15	-17.21247	-17.21247
16	4.906725	4.906725
17	2.961058	2.961058
18	17.93572	17.93572
19	14.51503	14.51503
20	23.13891	23.13891
21	-1.222009	-1.222009
22	0.293482	0.293482
23	-0.068334	-0.068334
24	0	0.125992
25	0	0.00756
26	0	0.013148
27	0	-0.344333
28	0	-0.051154
29	0	-0.051501
30	0	0.999031
31	0	0.861094
32	0	0.920531
33	0	-3.419783
34	0	-3.28359
35	0	-3.477977
36	0	-2.890275
37	0	-2.93411
38	0	6.552664
39	0	-10.25244
40	0	27.66408
41	0	-12.72673
42	0	9.935996
43	0	6.247408
44	0	20.07596
45	0	-0.911229
46	0	0.233863
47	0	-0.043402
48	0	0.125992
49	0	0.022679
50	0	0.04226
51	0	-0.365227
52	0.125992	-0.153833
53	0.00756	-0.165519
54	0.013148	1.198695
55	-0.344333	-3.966216
56	-0.051154	-3.841504
57	-0.051501	-4.1452
58	0.999031	4.093849
59	0.861094	-9.613051
60	0.920531	30.84531
61	-3.419783	-16.52397
62	-3.28359	4.710456
63	-3.477977	2.842616
64	-2.890275	17.21829
65	-2.93411	13.93443
66	6.552664	22.21335
67	-10.25244	-1.173129
68	27.66408	0.281743
69	-12.72673	-0.065601
70	9.935996	0.131242
71	6.247408	-0.385841
72	20.07596	1.420066
73	-0.911229	-5.301039
74	0.233863	15.27609
75	-0.043402	-11.71558
76	0	24.29909
77	0	-0.763389
78	0	0.202997
79	0	-0.059122
80	0	0.131242
81	0	0.007875
82	0	0.013696
83	0	-0.35868
84	0	-0.053286
85	0	-0.053647
86	0	1.040658
87	0	0.996973
88	0	0.958886
89	0	-3.562274
90	0	-3.420407
91	0	-3.622892
92	0	-3.010704
93	0	-3.056364
94	0	6.825692
95	0	-10.67962
96	0	28.81675
97	0	-13.25701
98	0	10.35
99	0	6.507717
100	0	20.91246



Excel Program 6

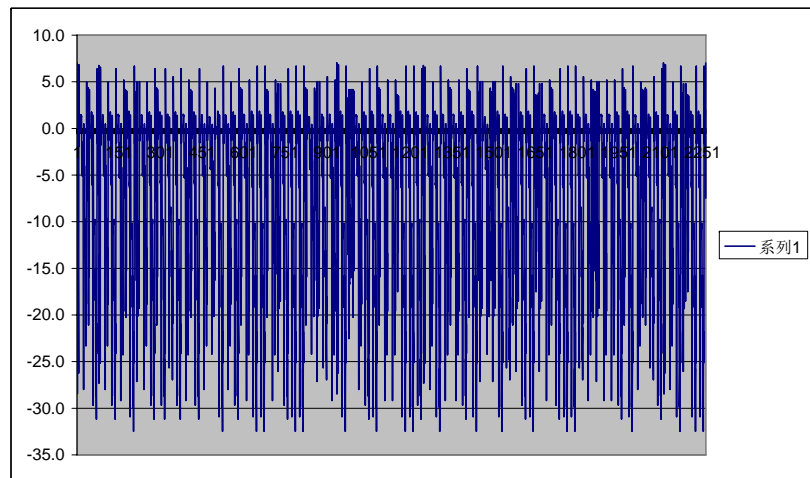
Evaluation of the stress ranges spectrum by means of the reservoir counting method and, based on that, calculation the damage during the lifetime (by means of a classification and the miner rule, based on NEN-EN1991+9 + NB and NEN-EN1993-2 + NB)

Input the total stress range spectrum made for 100 trucks derived from step 5

0	0	0	2347 = aantal gegevens (begin en eindig met 0)
0.18167	0.149586	0.124083	50 = aantal intervallen voor spanningen
0.032701	0.026926	0.022336	sig = tau of sig
0.060935	0.050173	0.041619	10 = detailklasse (= sigma C)
-0.526627	-0.433621	-0.359694	1 = kolom van te gebruiken gegevens
-0.221814	-0.182641	-0.151502	CTRL+SHIFT+R = uitvoeren
-0.238665	-0.196515	-0.163012	dek 18 trog 350/150/8 dd 3500
1.723456	1.419083	1.177145	in kolom A de gegevens van spanning onder trog tpv dwarsdrager plaatsen
-5.710845	-4.702274	-3.900589	in kolom B de gegevens van spanning onder trog op 1/8 dwarsdragerafstand plaatsen
-5.52992	-4.553301	-3.777014	in kolom C de gegevens van spanning onder trog op 1/4 dwarsdragerafstand plaatsen
-5.959997	-4.907423	-4.070763	
-4.244201	-0.111378	4.054314	
-29.20007	-17.76349	-9.471018	
1.283811	19.93603	30.29439	
-11.3245	-16.68585	-15.93776	
-10.73435	-5.29522	4.529286	
-10.78637	-9.653493	2.733593	
-10.125	0.079052	16.59087	
-10.15775	-3.087482	13.42948	
-9.642659	7.42555	21.40583	
-10.0251	-1.609961	-1.131358	
-10.01933	2.107326	0.271442	
-17.627	-0.505602	-0.063203	
-14.50869	0.117724	0.11912	
-27.5749	0.143603	0.007148	
-23.79857	0.008617	0.012431	
-30.03262	0.014986	-0.325552	
-20.19312	-0.392462	-0.048364	
-23.24918	-0.058304	-0.048692	
6.181798	-0.0587	0.944539	
-1.483174	1.13867	0.813898	
0.345342	0.981178	0.86936	
0.174403	1.048038	-3.236487	
0.010465	-3.901679	-3.107722	
0.018201	-3.74645	-3.290246	
-0.476639	-3.966488	-2.731982	
-0.07081	-3.293484	-2.772116	
-0.07129	-3.341867	6.208656	
1.382898	2.647987	-9.682347	
1.191626	-16.52868	26.10722	
1.272828	16.69777	-11.7861	
-4.738534	-12.07543	9.189031	
-4.550011	-12.05044	5.779912	
-4.817243	-12.0976	18.57231	
-3.999889	0.307952	-0.843807	
-4.05865	-5.667658	0.216301	
-1.356612	7.610243	-0.040143	
-26.45005	-1.481157	0.11912	
0.434854	1.571719	0.021442	
-10.79054	-0.402893	0.039955	
-3.764572	0.074772	-0.345306	
-12.45958	0.143603	-0.145442	
-12.45643	0.025849	-0.156491	
-12.74844	0.048167	1.130059	
-8.984166	-0.416276	-3.744566	
-21.54123	-0.175335	-3.625934	
-11.8977	-0.188655	-3.907932	
-17.42326	1.362319	3.892141	
4.610608	-4.514183	-9.092177	
-1.181878	-4.371169	29.08261	
0.219342	-4.711126	-15.30025	
0.174403	-0.106923	4.348114	
0.031393	-17.05295	2.624249	
0.058498	19.13859	15.92724	
-0.505562	-16.01842	12.8923	
-0.212942	-5.083411	20.54959	
-0.229118	-9.267353	-1.086103	
1.654518	0.07589	0.260584	
-5.482411	-2.963983	-0.060674	

Reservoir counting method

min	max	n_i	D_i
4.0	4.8	43	nmb
4.8	5.5	12	nmb
5.5	6.2	9	nmb
6.2	6.9	16	nmb
6.9	7.6	11	nmb
7.6	8.3	17	nmb
8.3	9.0	4	nmb
9.0	9.7	5	nmb
9.7	10.4	3	nmb
10.4	11.1	1	nmb
11.1	11.8	10	nmb
11.8	12.6	16	nmb
12.6	13.3	6	nmb
13.3	14.0	3	nmb
14.0	14.7	1	nmb
14.7	15.4	4	nmb
15.4	16.1		
16.1	16.8		
16.8	17.5	11	nmb
17.5	18.2	15	nmb
18.2	18.9		
18.9	19.6		
19.6	20.3		
20.3	21.1	6	nmb
21.1	21.8	1	nmb
21.8	22.5		
22.5	23.2		
23.2	23.9	9	nmb
23.9	24.6	11	nmb
24.6	25.3	28	nmb
25.3	26.0		
26.0	26.7	1	nmb
26.7	27.4	5	nmb
27.4	28.1		
28.1	28.9	3	nmb
28.9	29.6		
29.6	30.3		
30.3	31.0	4	nmb
31.0	31.7	15	nmb
31.7	32.4	26	nmb
32.4	33.1	12	nmb
33.1	33.8	1	nmb
33.8	34.5	14	nmb
34.5	35.2		
35.2	35.9	4	nmb
35.9	36.6		
36.6	37.4		
37.4	38.1	15	nmb
38.1	38.8		
38.8	39.5	20	nmb



Appendix D Adjusted simplified 2D beam model

After obtaining the stress from the simplified model in MIDAS Civil, a set excel program is applied in order to calculate the fatigue damage in the object joint. The set of excel program consists of two excel documents. In this part of appendix, the manual of the set of excel program is presented.

The description of the five standard trucks in fatigue load model 4. It includes the type of truck, type of axle, axle distance, load of each axle and the percentage of the trucks.

Type voertuig			Verkeerstype			Wiel type
Afbeelding van de vrachtwagen	Afstand tussen de assen	Gelijkwaardige aslast	Lange afstand	Middellange afstand	Lokaal verkeer	
	m	kN	% ¹	% ¹	% ¹	
	4,5	70 130	20,0	50,0	80,0	A B
	4,20 1,30	70 120 120	5,0	5,0	5,0	A B B
	3,20 5,20 1,30 1,30	70 150 90 90	40,0	20,0	5,0	A B C C
	3,40 6,00 1,80	70 140 90 90	25,0	15,0	5,0	A B C C
	4,80 3,60 4,40 1,30	70 130 90 80 80	10,0	10,0	5,0	A B C C C

¹ Percentage vrachtwagens

wagennr	FLM4	FLM4	FLM4												
	1	1	1	2	2	2	3	3	3	4	4	4	5	5	5
	as	as	as												
	type	lokatie	gewicht												
as1	1	0	70	1	0	70	1	0	70	1	0	70	1	0	70
as2	2	-4.5	130	2	-4.2	120	2	-3.2	150	2	-3.4	140	2	-4.8	130
as3				2	-5.5	120	3	-8.4	90	3	-9.4	90	3	-8.4	90
as4							3	-9.7	90	3	-11.2	90	3	-12.8	80
as5							3	-11	90				3	-14.1	80
as6															
as7															
as8															
as9															
as10															
voertuig gewicht	200			310			490			390			450		

bepaling van de volgorde van de vrachtwagens

		200	100	0	-100	200	excentriciteit in mm	
		7	18	50	18	7	7 %	
werkelijk	100							
vrw1	20 %	1.4	3.6	10	3.6	1.4		
vrw2	5 %	0.35	0.9	2.5	0.9	0.35		
vrw3	40 %	2.8	7.2	20	7.2	2.8		
vrw4	25 %	1.75	4.5	12.5	4.5	1.75		
vrw5	10 %	0.7	1.8	5	1.8	0.7		
	100							

		200	100	0	-100	200	excentriciteit in mm	
		7	18	50	18	7	7 %	
gekozen (obv werkelijk)	100							
vrw1	20 %	1	4	10	4	1		
vrw2	5 %	0	1	3	1	0		
vrw3	40 %	3	7	20	7	3		
vrw4	25 %	2	4	12	4	2		
vrw5	10 %	1	2	5	2	1		
	100							

0	0	0	0
0	0	0	0
0	0	0	0
0	0	0	0
0	0	0	0

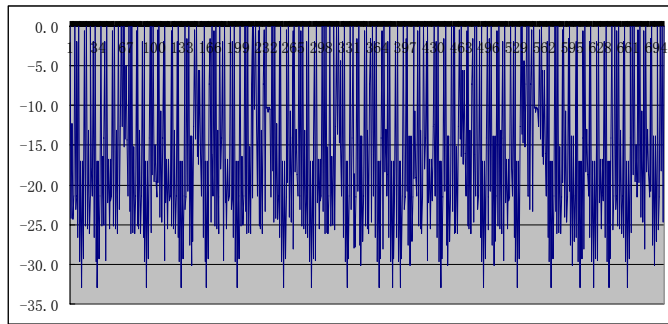
vrw nr

		200	300	400	500	600	excentriciteit in mm (ingevoerd in uitleg1)		
vrw1	20 %	1	4	10	4	1	100		
vrw2	5 %	0	1	3	1	0			
vrw3	40 %	3	7	20	7	3			
vrw4	25 %	2	4	12	4	2			
vrw5	10 %	1	2	5	2	1			
1									
2									
3									
4									
5									
6									
7									
8									
9									
10									
11									
12									
13									
14									
15									
16									
17									
18									
19									
20									
21									
22									
23									
24									
25									
26									
27									
28									
29									
30									
31									
32									
33									
34									
35									
36									
37									
38									
39									
40									
41									
42									
43									
44									
45									
46									
47									
48									
49									
50									
51									
52									
53									
54									
55									
56									
57									
58									
59									
60									
61									
62									
63									
64									
65									
66									
67									
68									
69									
70									
71									
72									
73									
74									
75									
76									
77									
78									
79									
80									
81									
82									
83									
84									
85									
86									
87									
88									
89									
90									
91									
92									
93									
94									
95									
96									
97									
98									
99									
100									

The arrangement of the one hundred trucks taking account of the transverse spreading which pass the orthotropic deck one after another.

In this step, the evaluation of the stress ranges spectrum by means of the reservoir counting method is carried out. Based on this, the fatigue lifetime damage is calculated (by means of a classification and the miner rule, based on NEN-EN 1991-9/NB and NEN-EN 1993-2/NB)

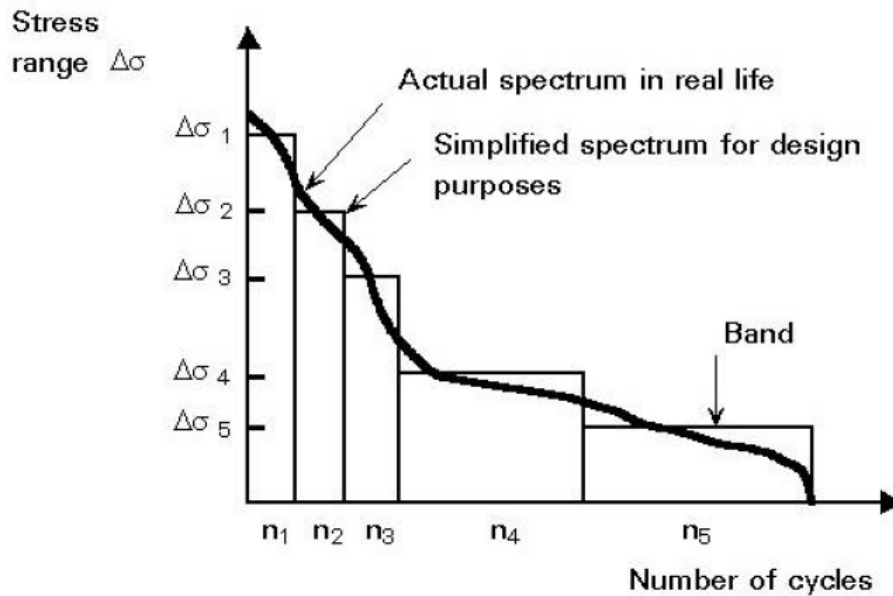
min	max	n_i	D_i
4.0	4.6		
4.6	5.2	1	nbn
5.2	5.8	6	nbn
5.8	6.4		
6.4	6.9		
6.9	7.5		
7.5	8.1		
8.1	8.7	2	nbn
8.7	9.2		
9.2	9.8	2	nbn
9.8	10.4		
10.4	11.0	3	nbn
11.0	11.5		
11.5	12.1	3	nbn
12.1	12.7	36	nbn
12.7	13.3		
13.3	13.9	12	nbn
13.9	14.4		
14.4	15.0		
15.0	15.6	1	nbn
15.6	16.2	1	nbn
16.2	16.7		
16.7	17.3		
17.3	17.9		
17.9	18.5	2	nbn
18.5	19.1	1	nbn
19.1	19.6	14	nbn
19.6	20.2		
20.2	20.8	2	nbn
20.8	21.4		
21.4	21.9	4	nbn
21.9	22.5	3	nbn
22.5	23.1	1	nbn
23.1	23.7	5	nbn
23.7	24.2	3	nbn
24.2	24.8	8	nbn
24.8	25.4	2	nbn
25.4	26.0	4	nbn
26.0	26.6	9	nbn
26.6	27.1	14	nbn
27.1	27.7		
27.7	28.3	1	nbn
28.3	28.9		
28.9	29.4		
29.4	30.0	3	nbn
30.0	30.6	4	nbn
30.6	31.2		
31.2	31.7		
31.7	32.3		
32.3	32.9	15	nbn



By means of the reservoir counting method, the stress ranges spectrum is derived from the stress history due to one hundred tucks.

Appendix E Stress spectra

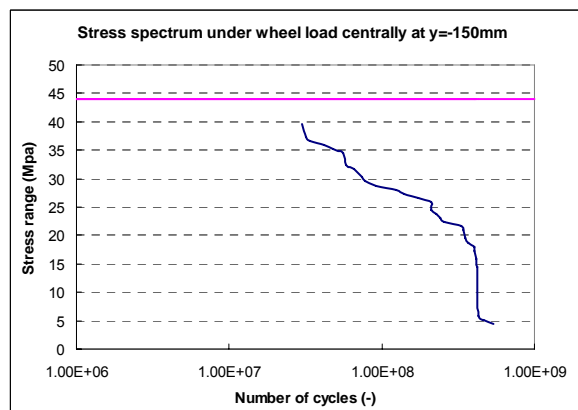
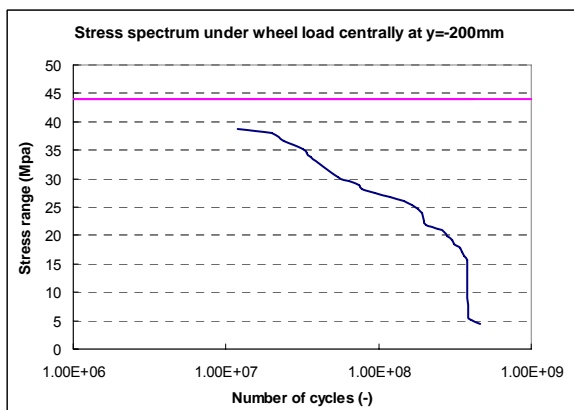
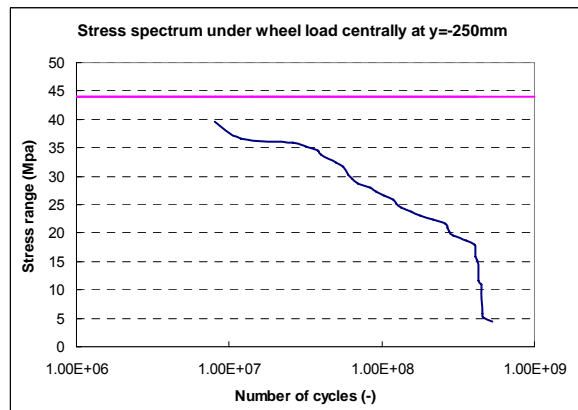
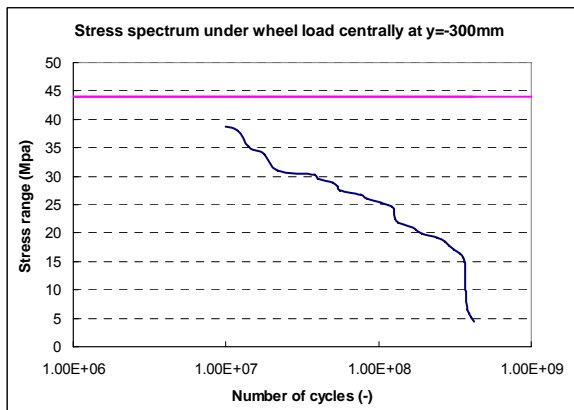
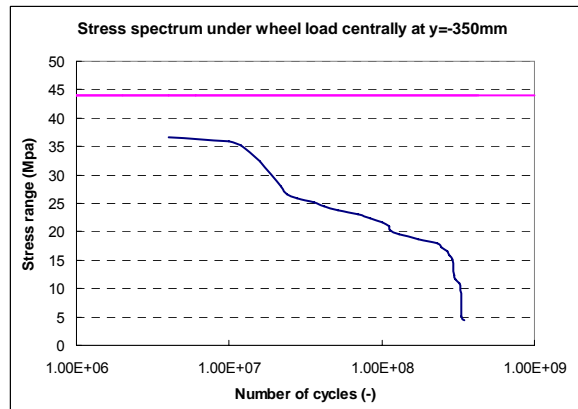
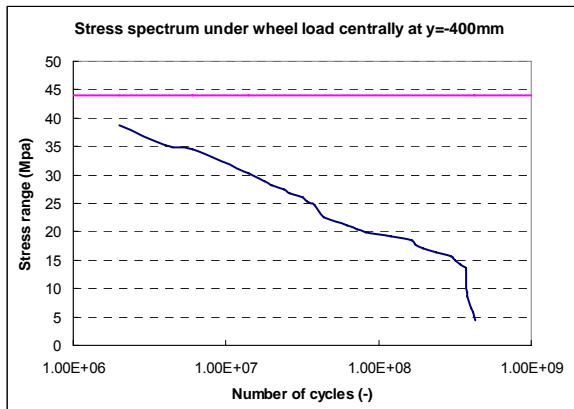
For variable amplitude loading the life is estimated by calculation of the total damage done by each cycle in the stress spectrum. For practice the stress spectrum is simplified into a representative number of stress ranges. The figure below is presented as an example. The vertical axle defines the stress range $\Delta\sigma_R$ which fluctuates at the location of crack initiation. The horizontal axle gives the number of cycles N corresponds to the stress range.

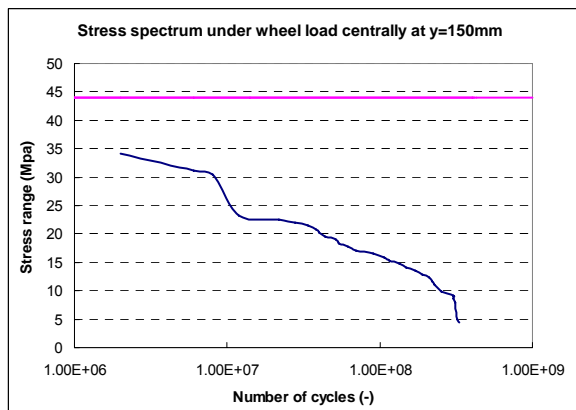
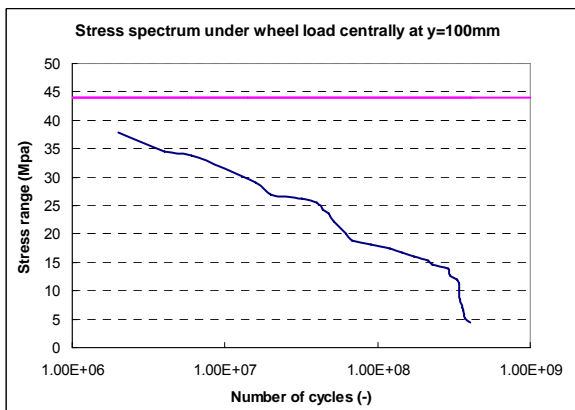
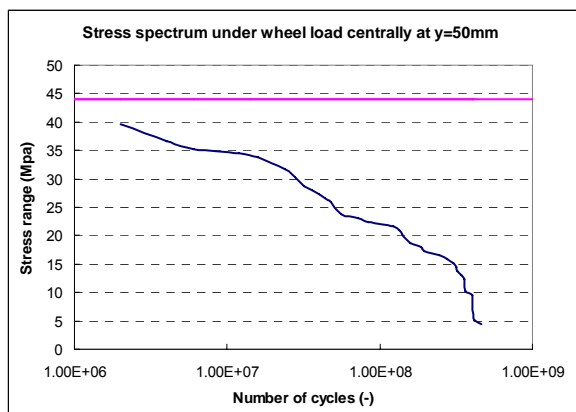
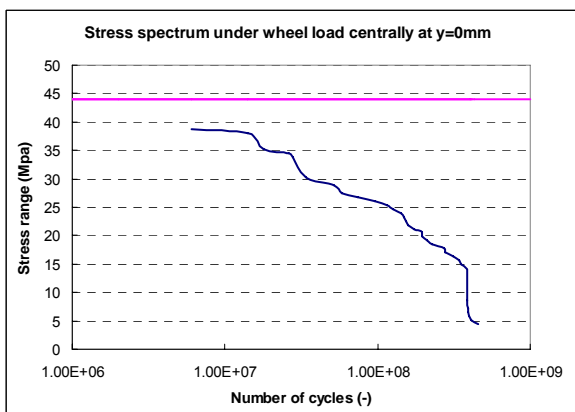
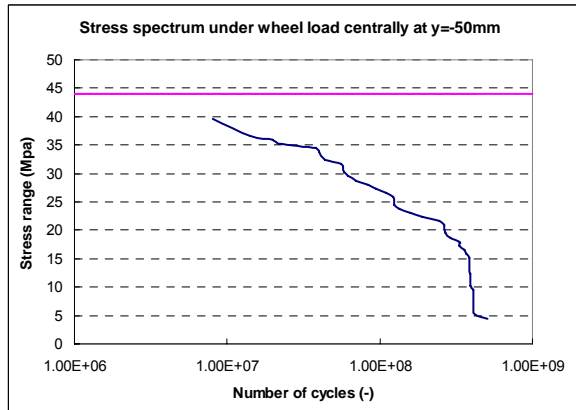
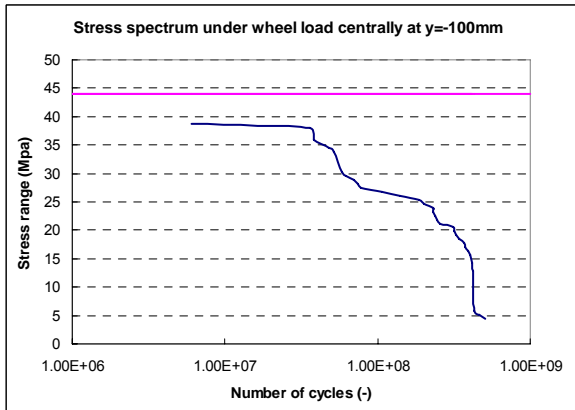


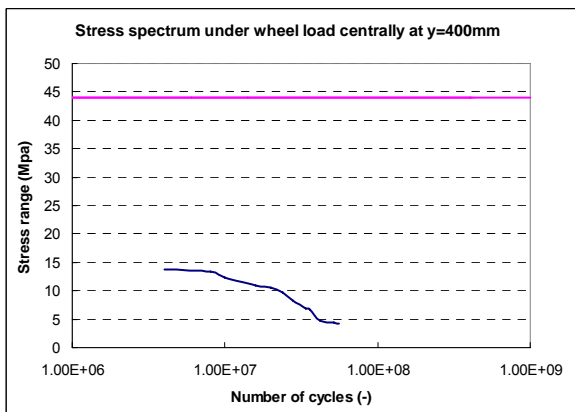
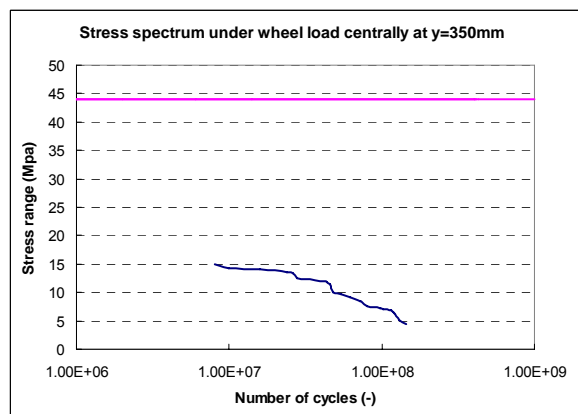
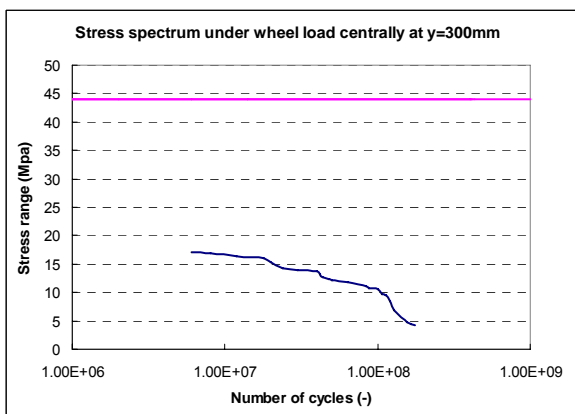
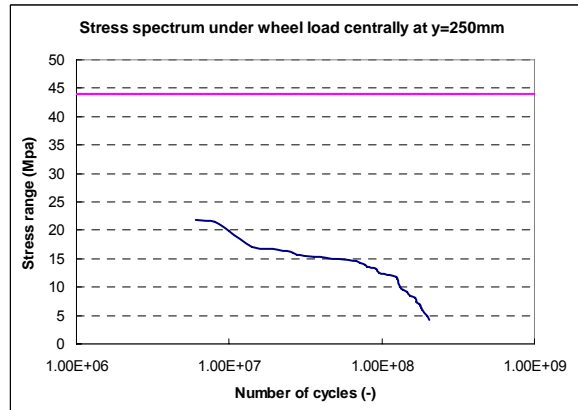
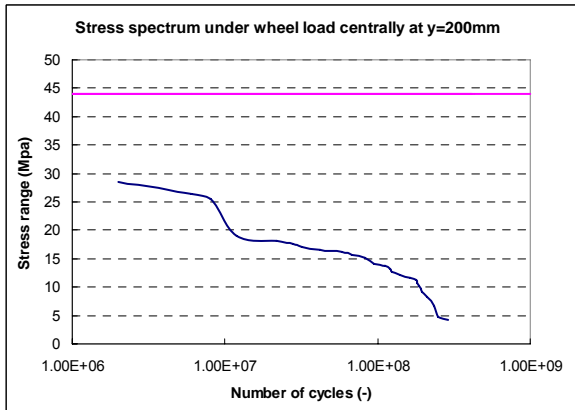
In this appendix, the stress spectra obtained with the help of the 2D model for model B and model D are presented. The stress spectrum is drawn separately for each location of the central line of the wheel load. The stress spectrum curve is in blue color. Besides, the cut-off limit for each kind of detail category is also drawn. The stress range, smaller than this cut-off limit, has no influence on the lifetime fatigue damage. The detail category for the crack in the deck plate is 125. And its cut-off limit is 44N/mm^2 (pink line). Compared to the detail category in the deck plate, the detail category in the trough web is 100, 90 or 50. Therefore, the cut-off limit in the trough web is smaller than in the deck plate which is 35.2 N/mm^2 (pink line) 31.7 N/mm^2 (yellow line) and 17.6 N/mm^2 (red line) respectively.

Model B

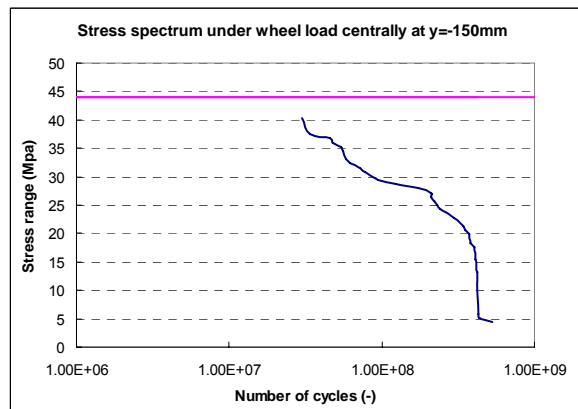
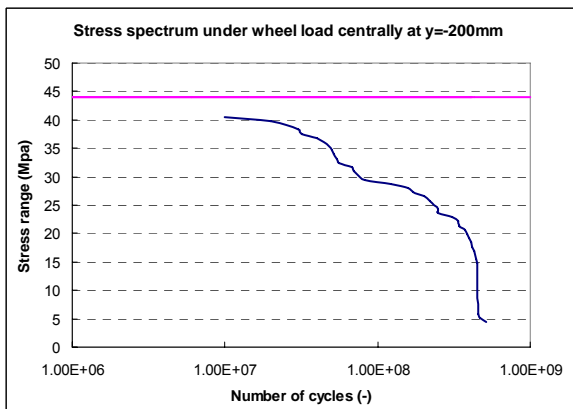
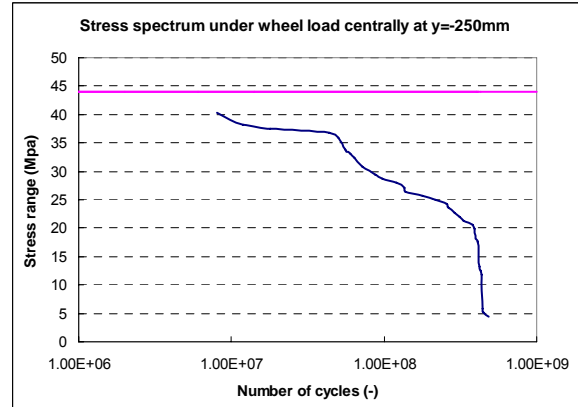
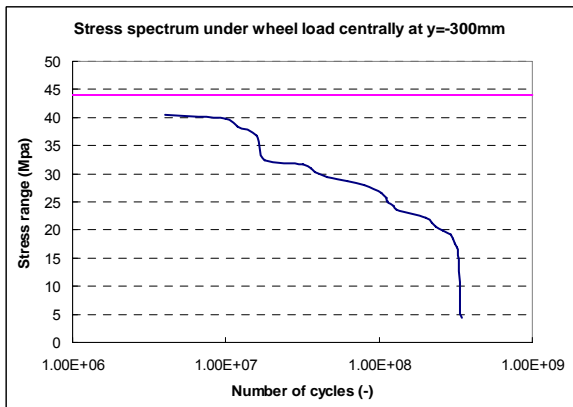
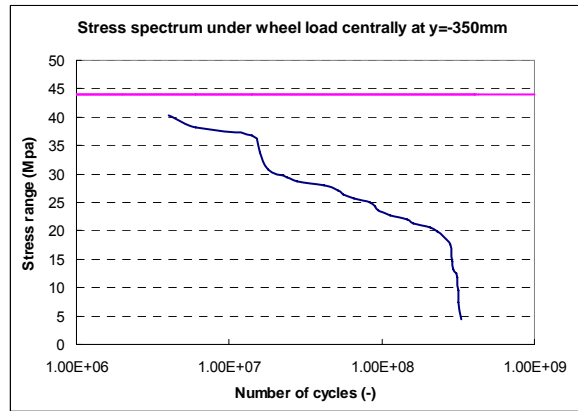
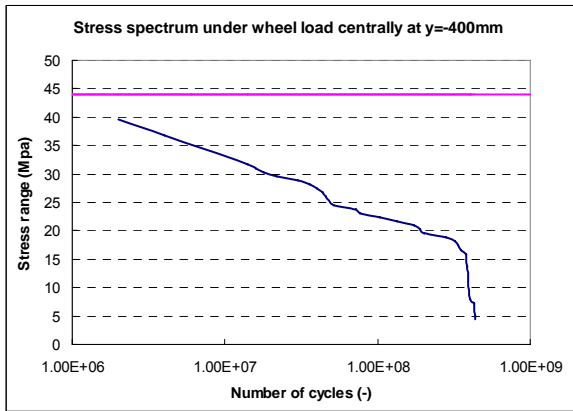
Bottom surface of the interior deck plate

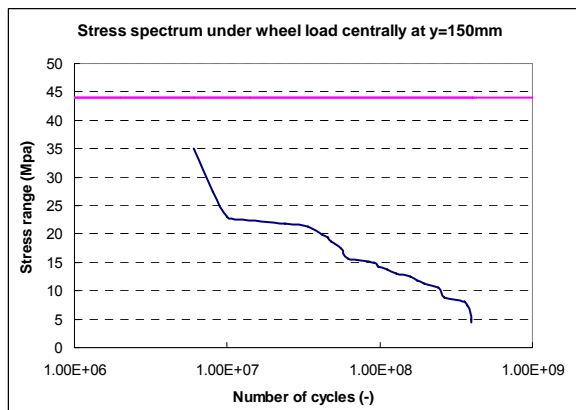
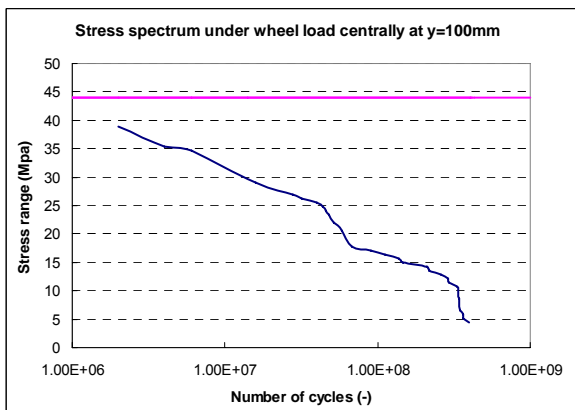
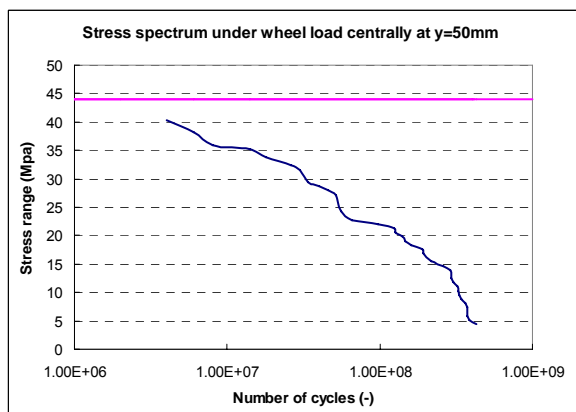
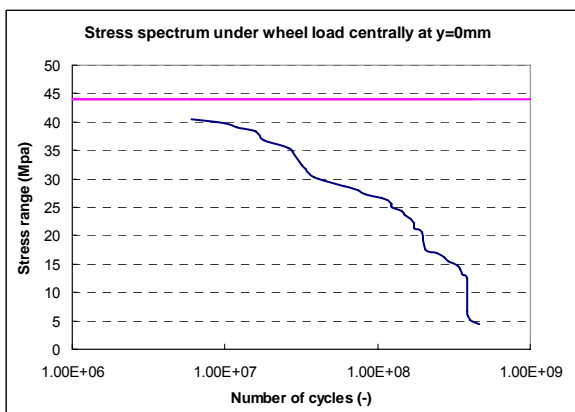
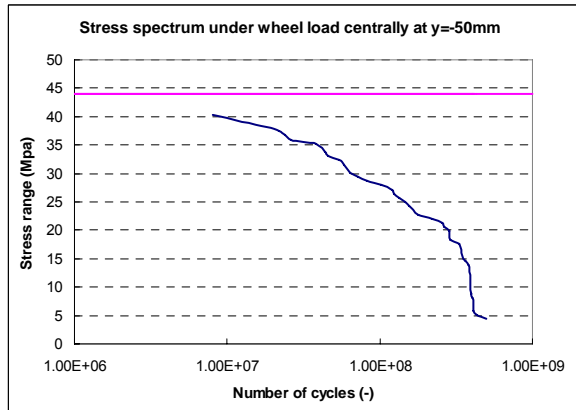
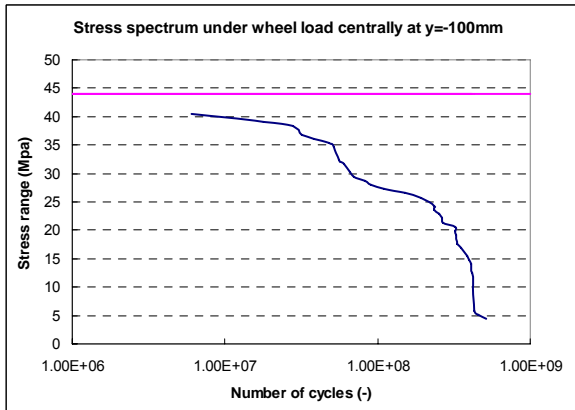


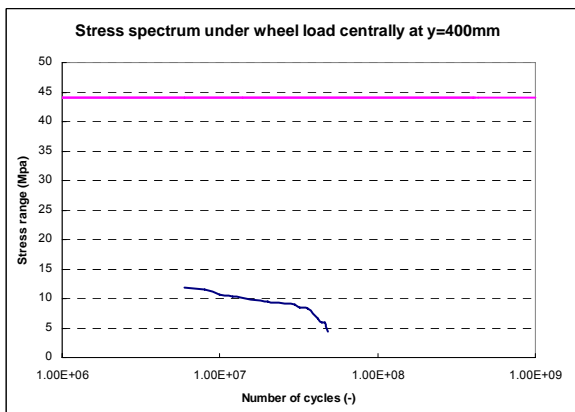
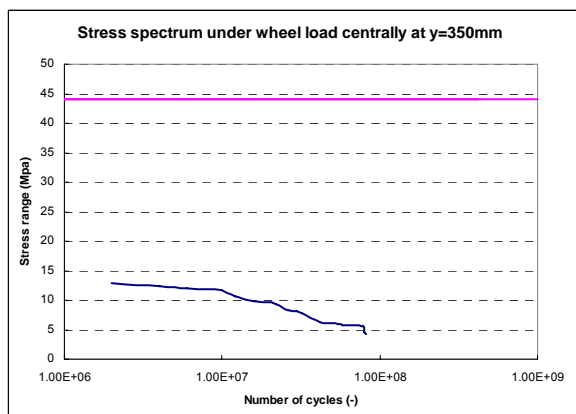
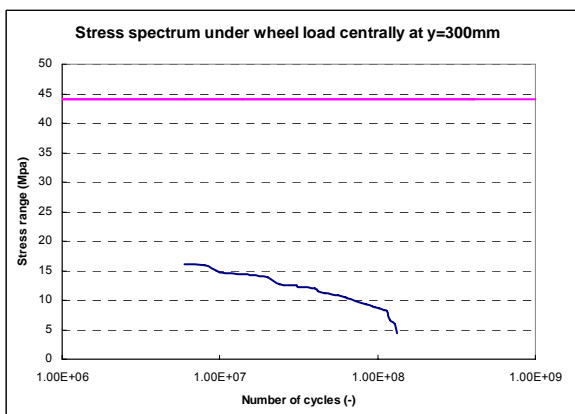
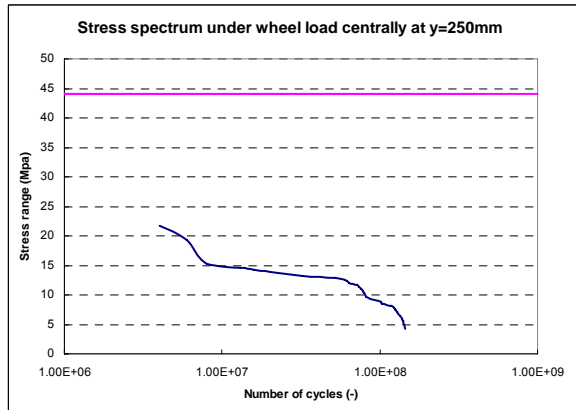
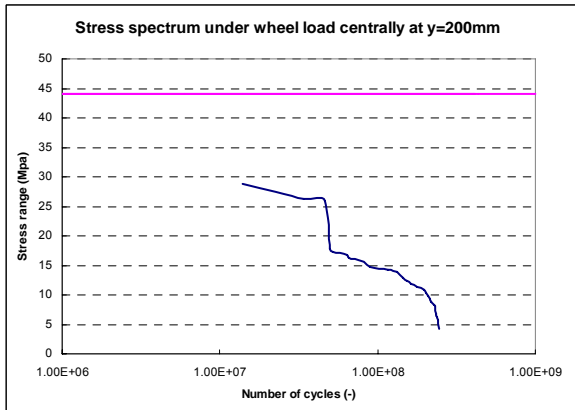




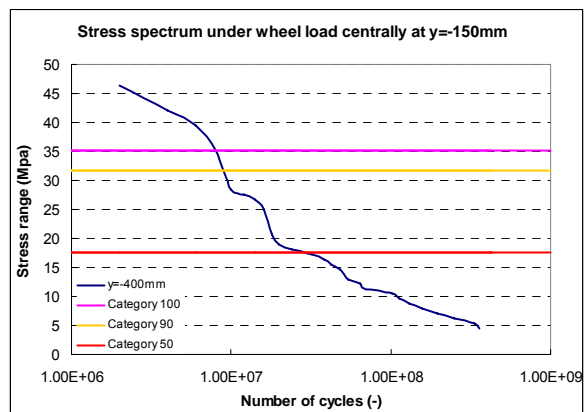
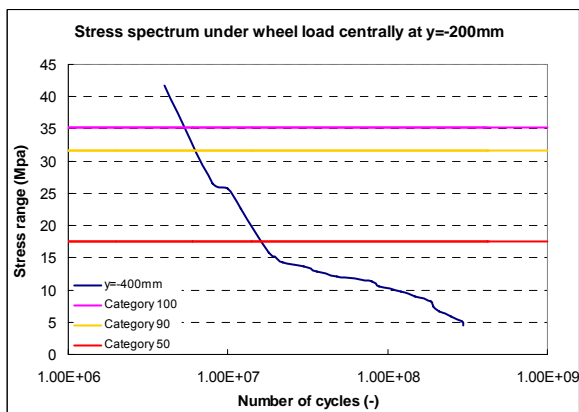
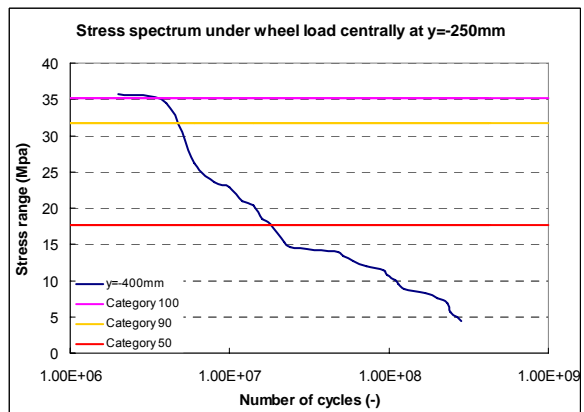
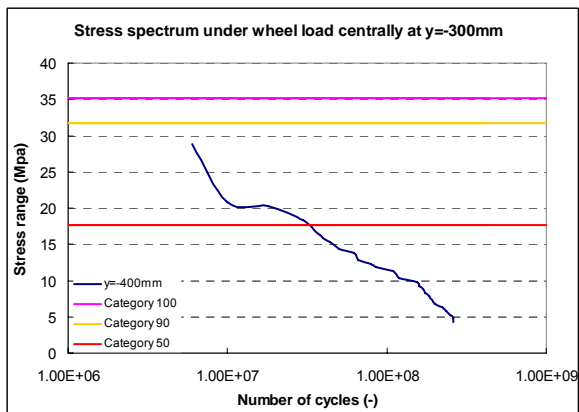
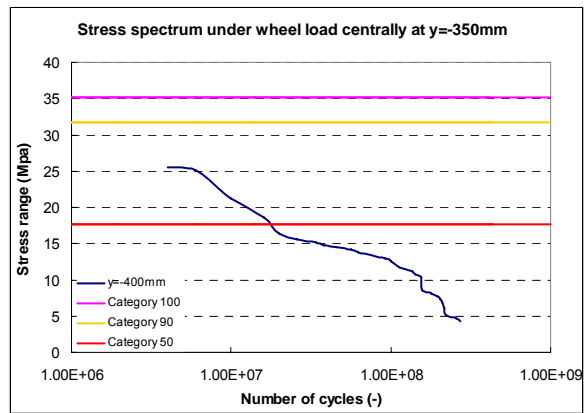
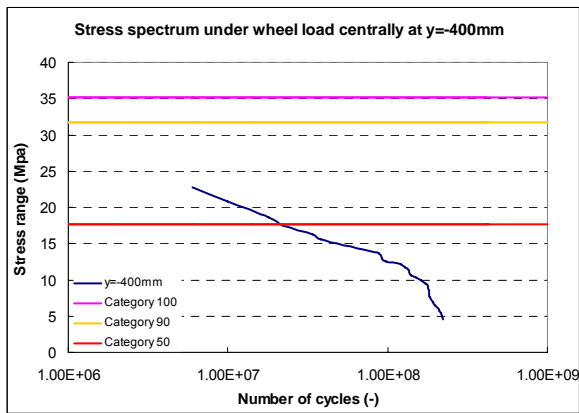
Bottom surface of the exterior deck plate

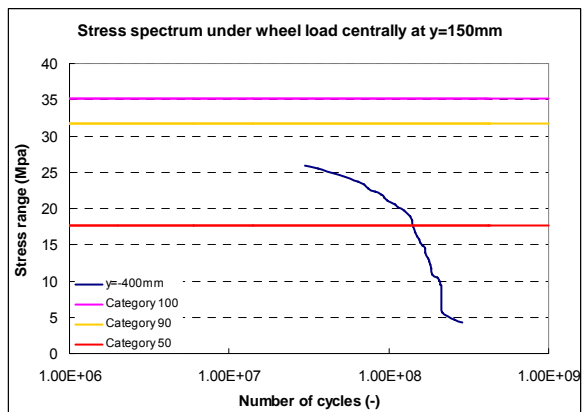
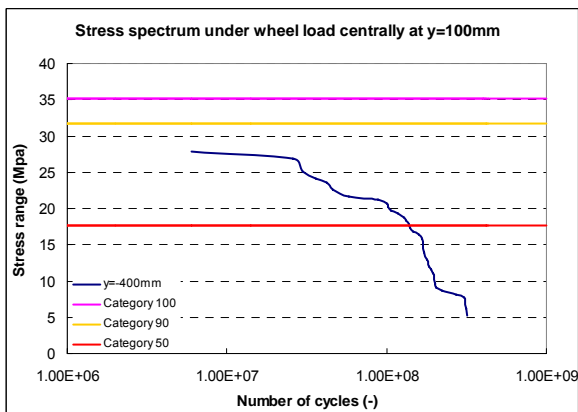
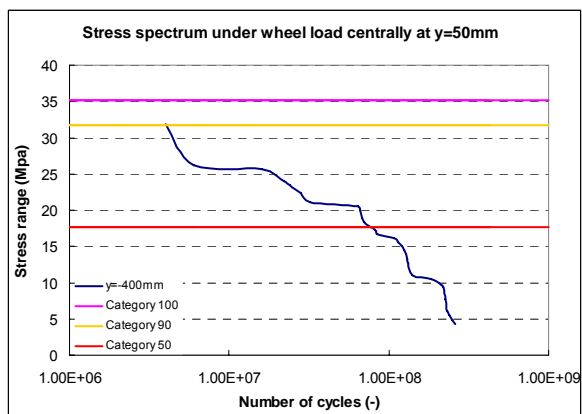
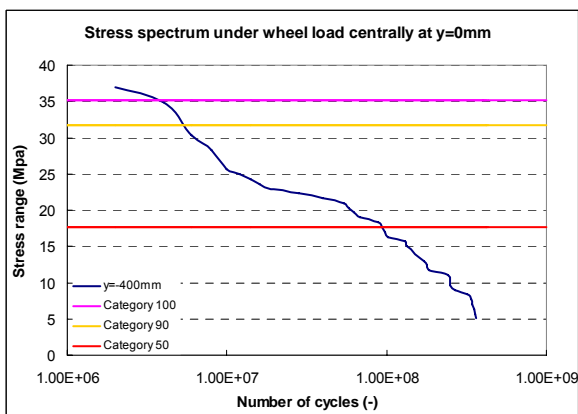
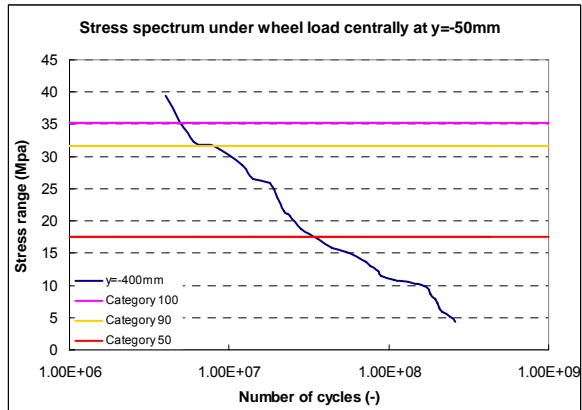
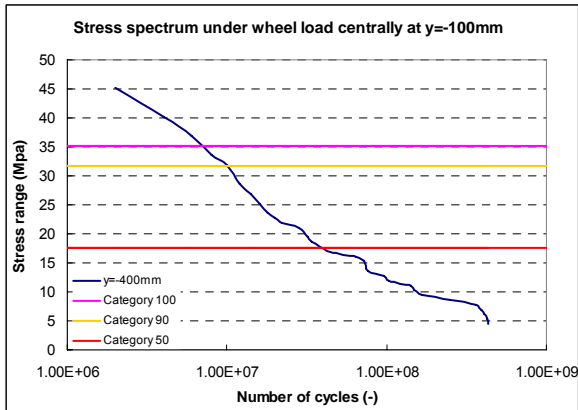


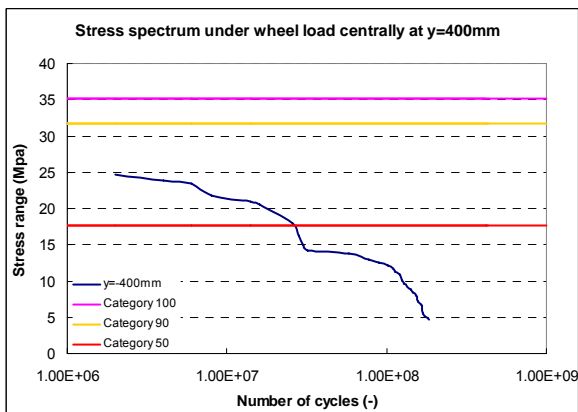
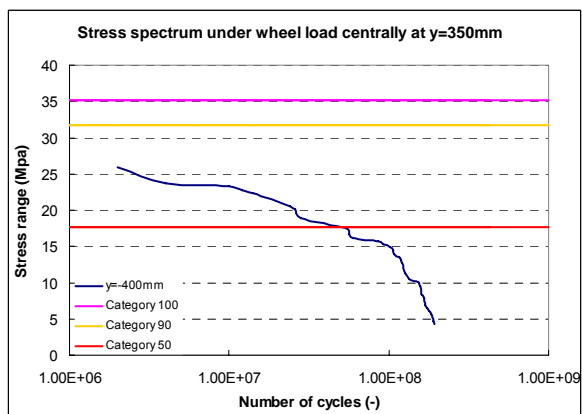
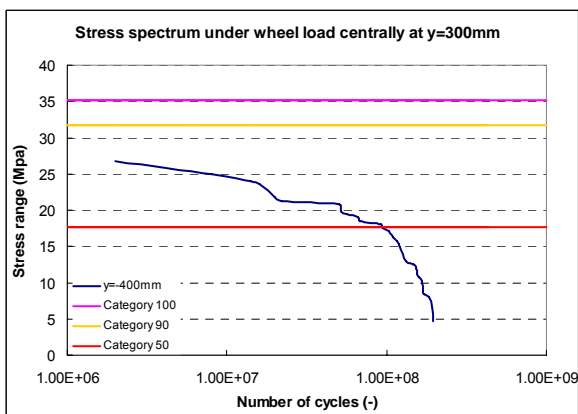
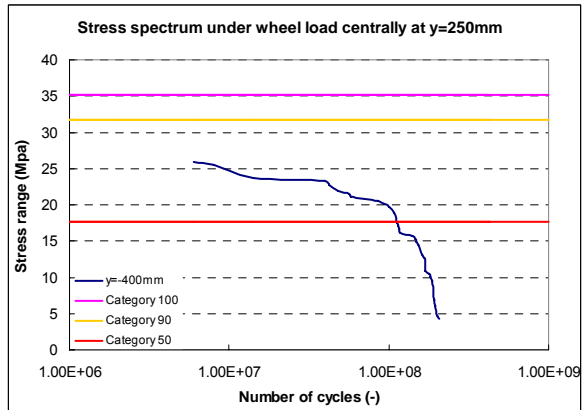
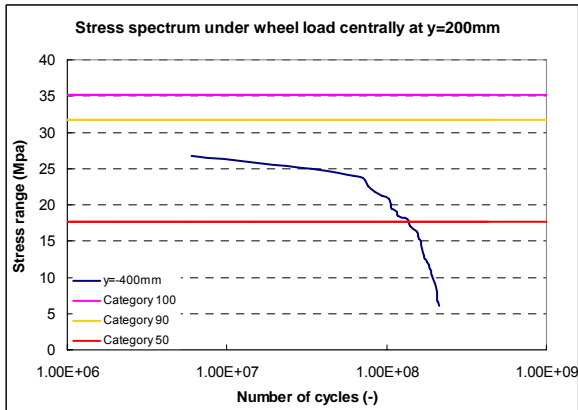




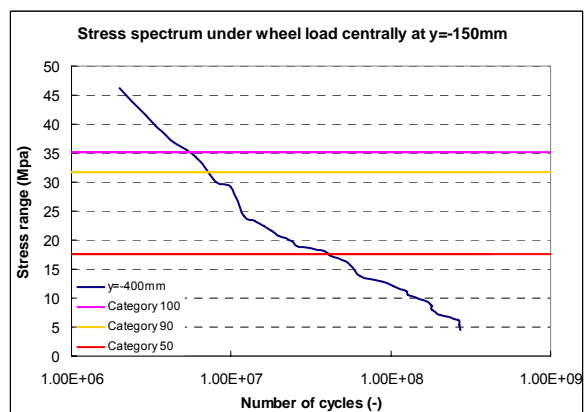
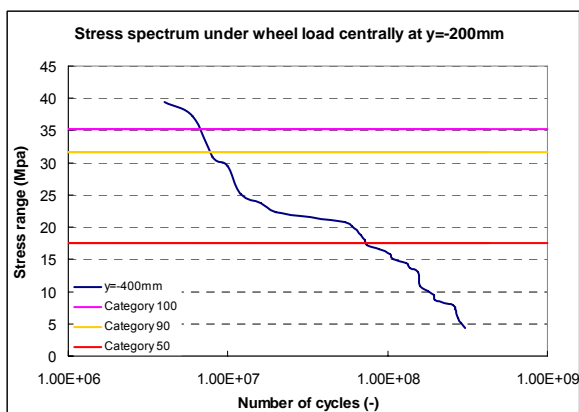
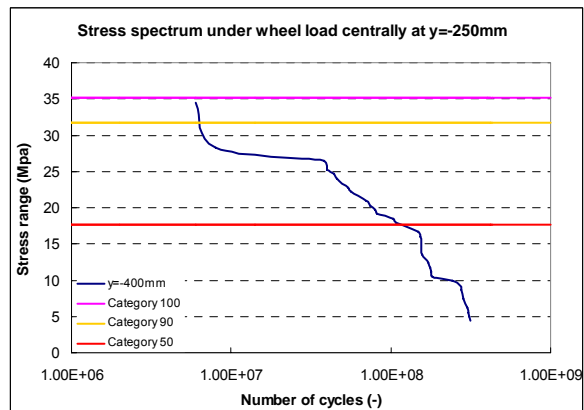
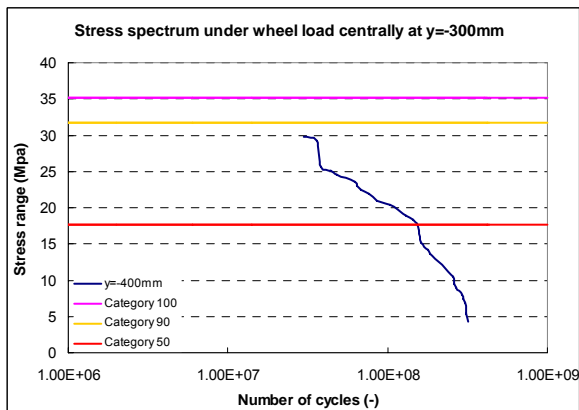
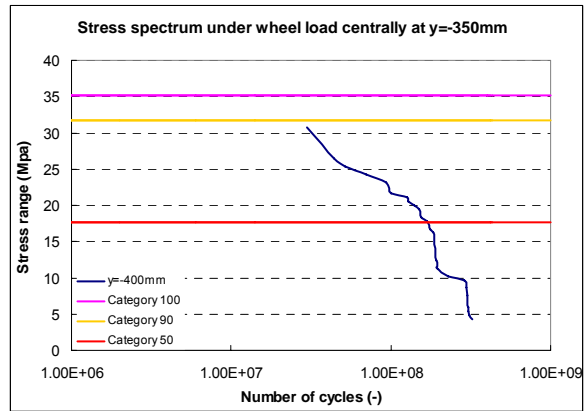
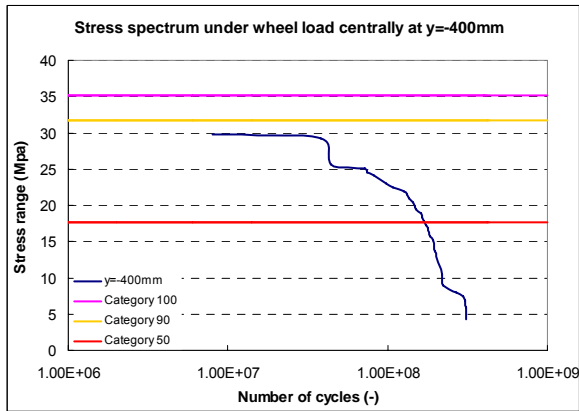
Interior surface of the trough web

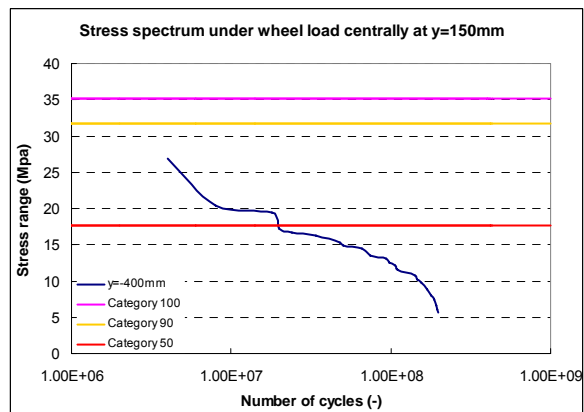
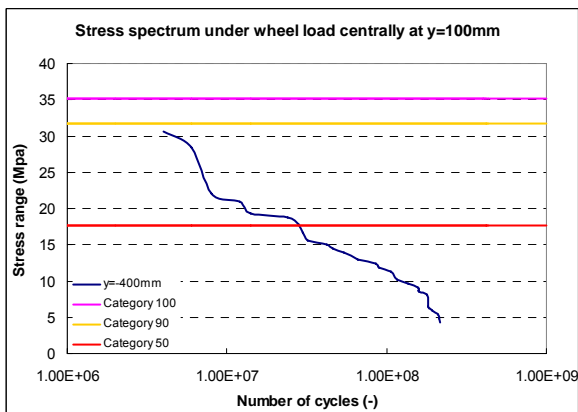
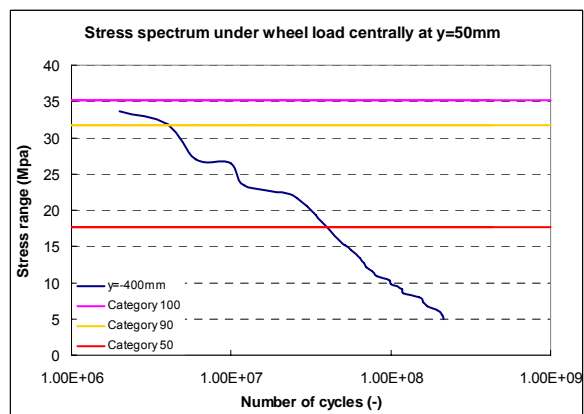
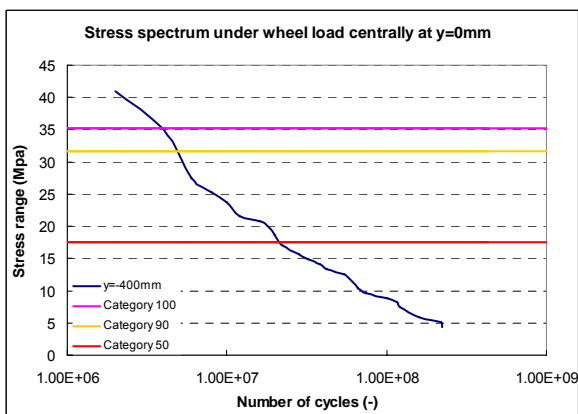
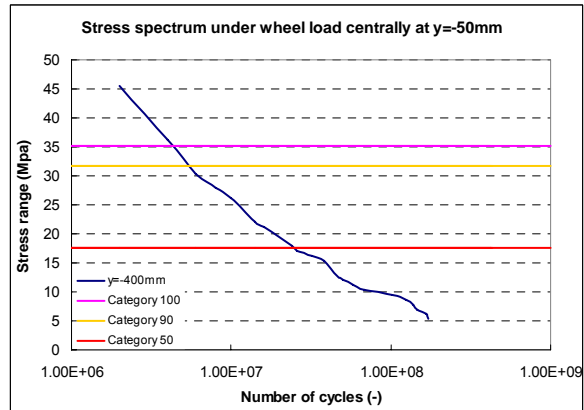
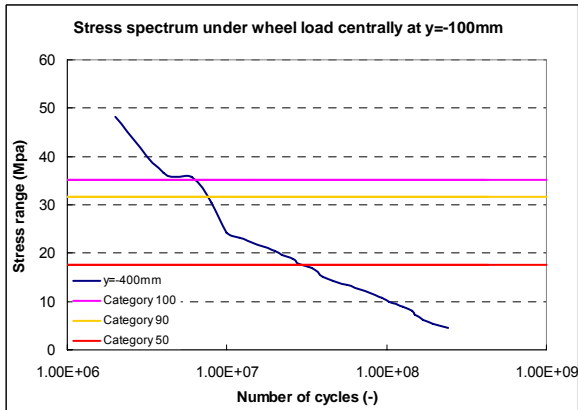


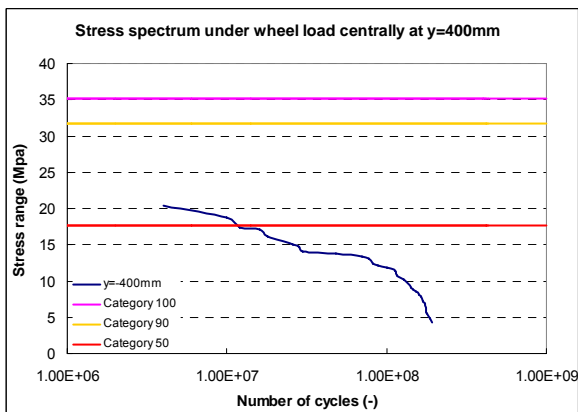
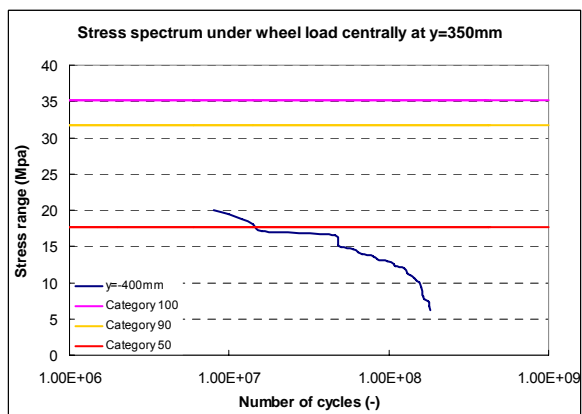
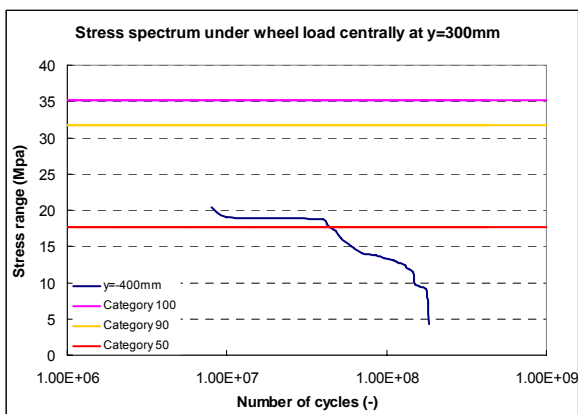
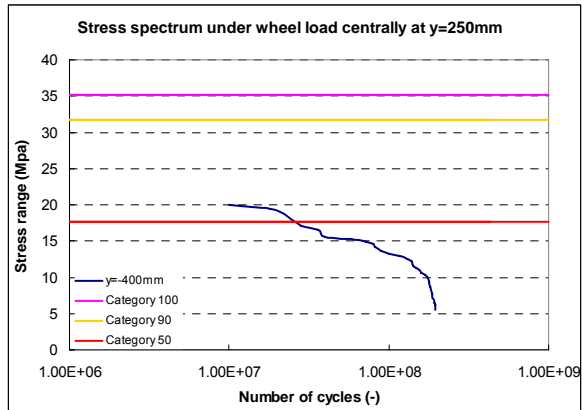
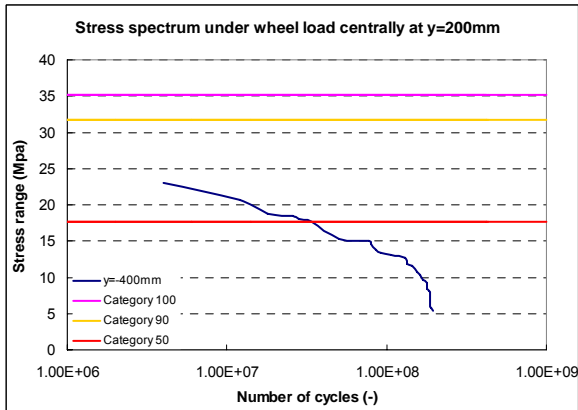




Interior surface of the trough web

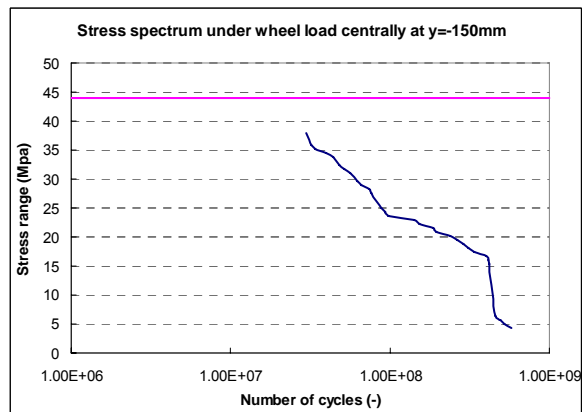
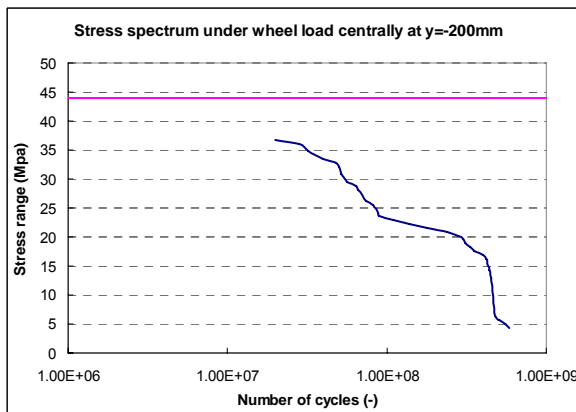
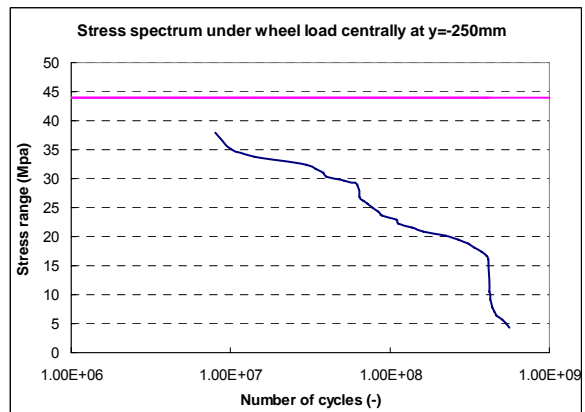
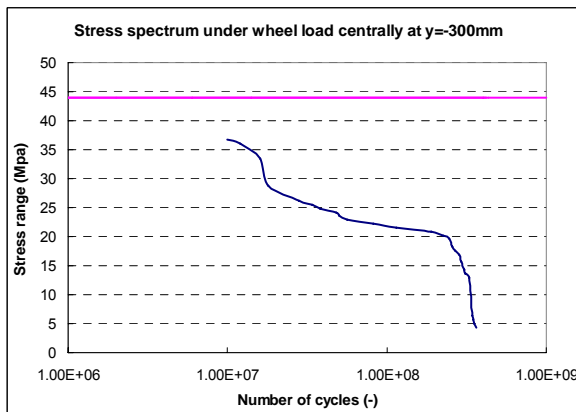
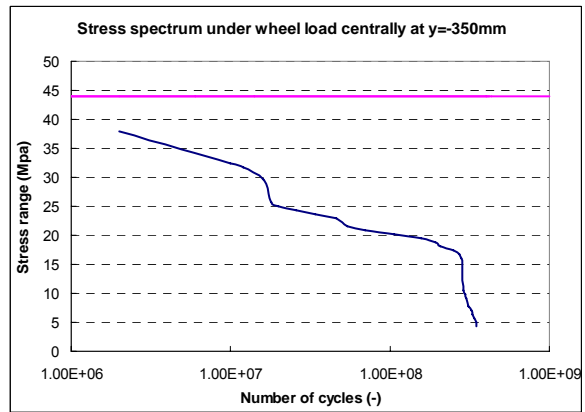
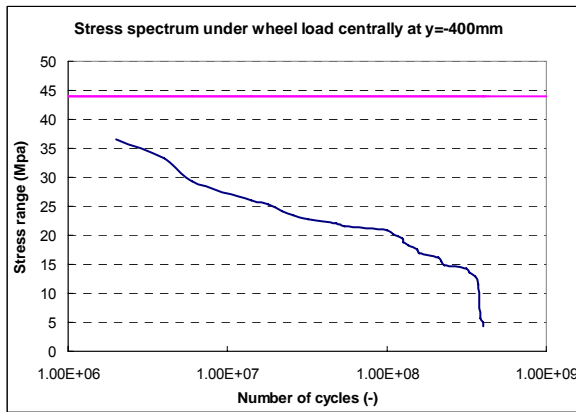


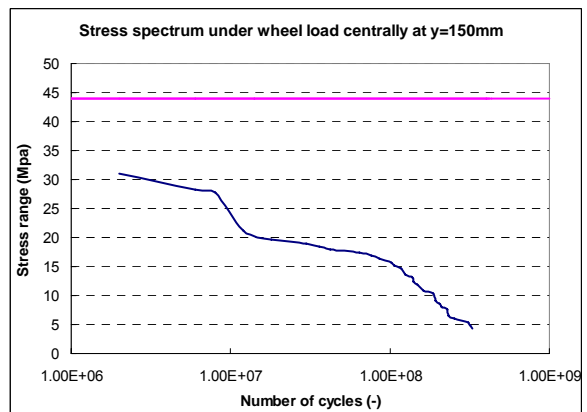
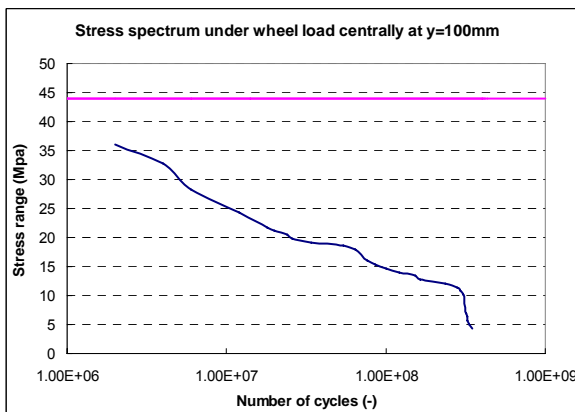
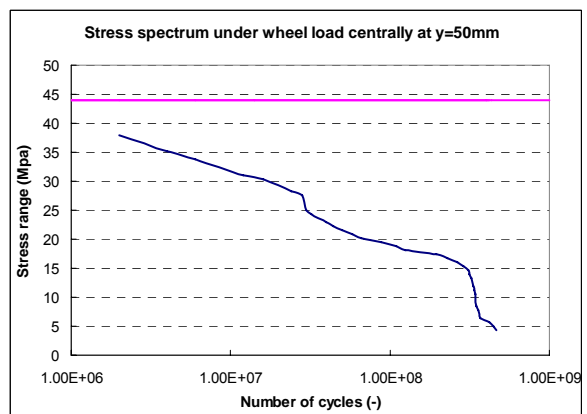
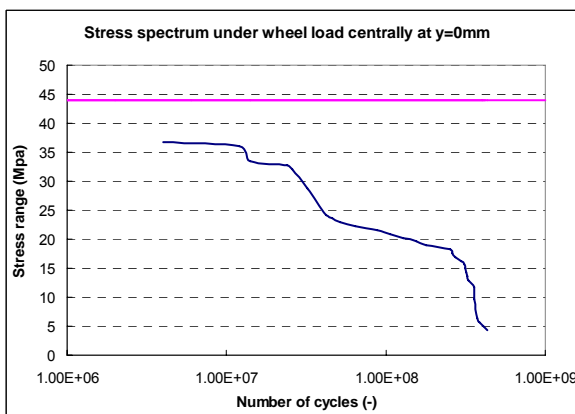
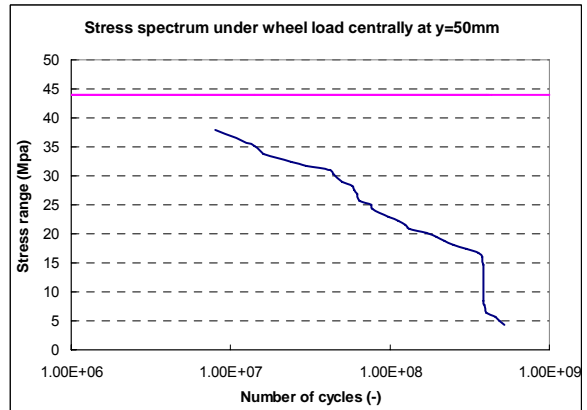
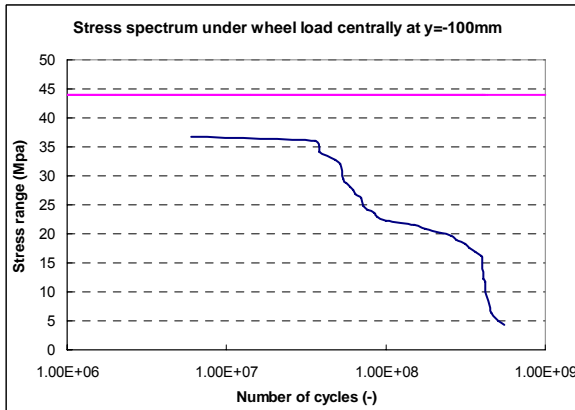


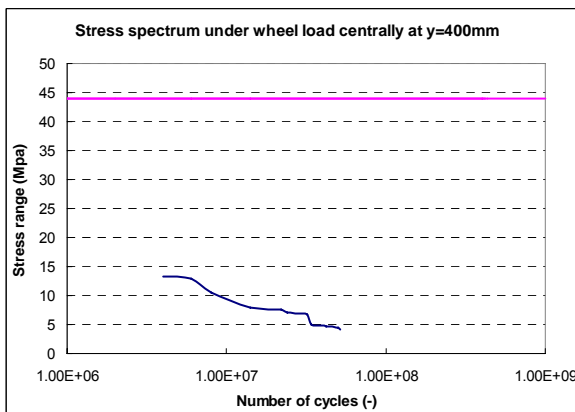
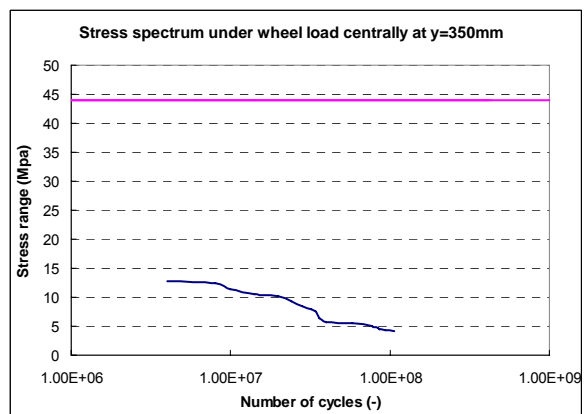
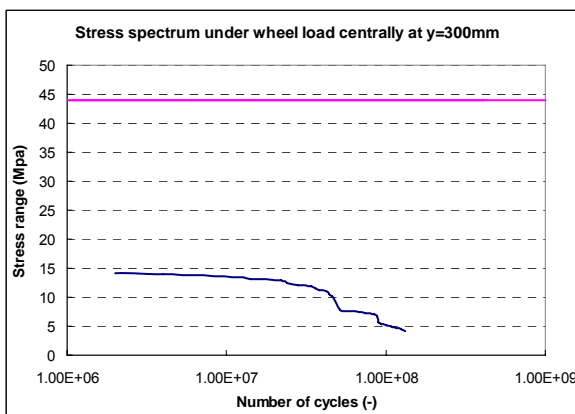
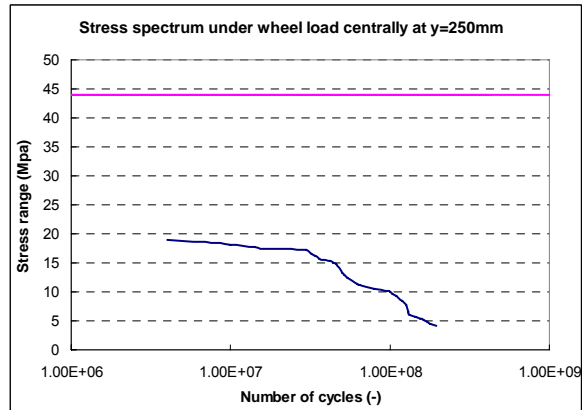
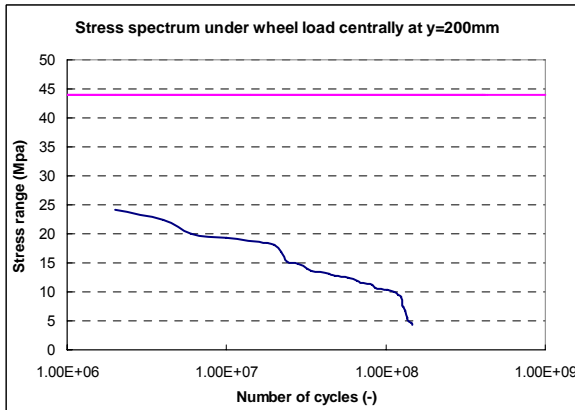


Model D

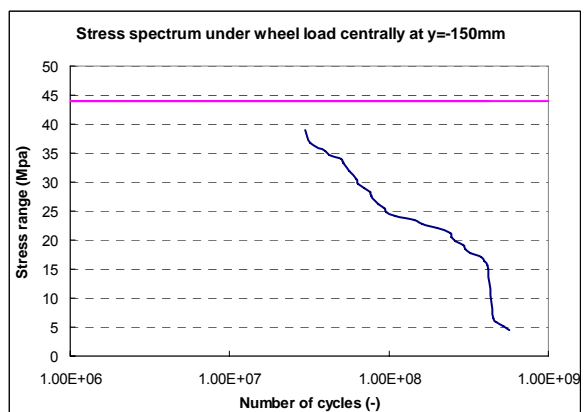
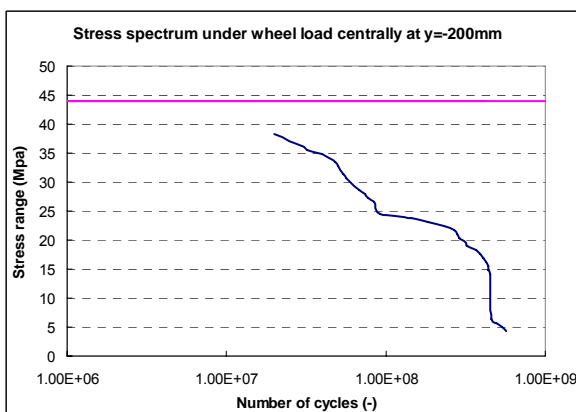
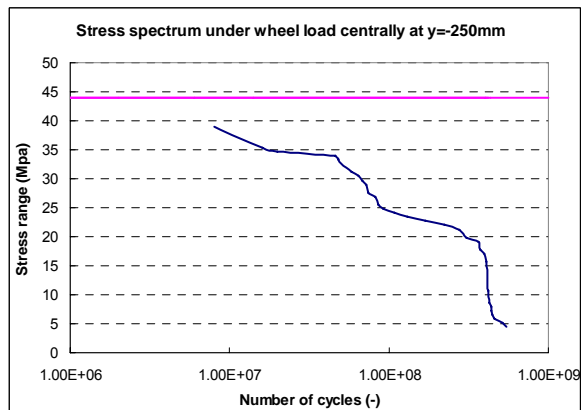
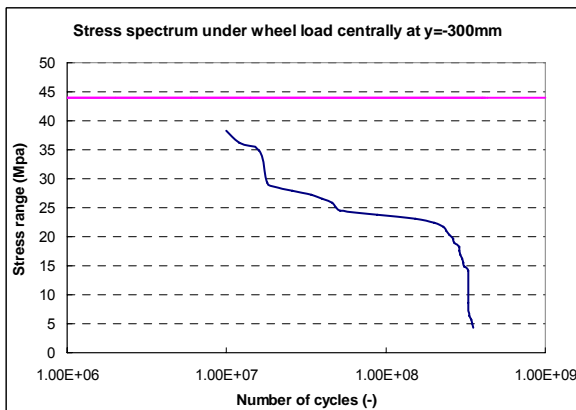
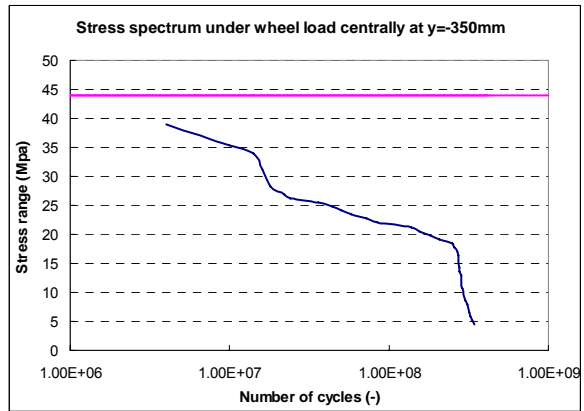
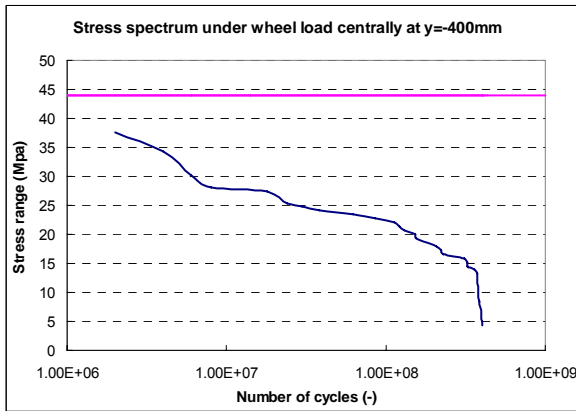
Bottom surface of the interior deck plate

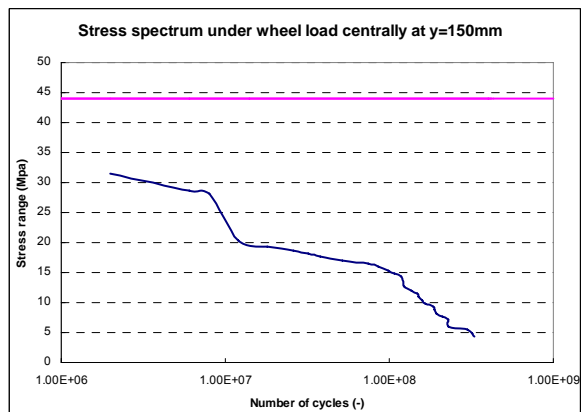
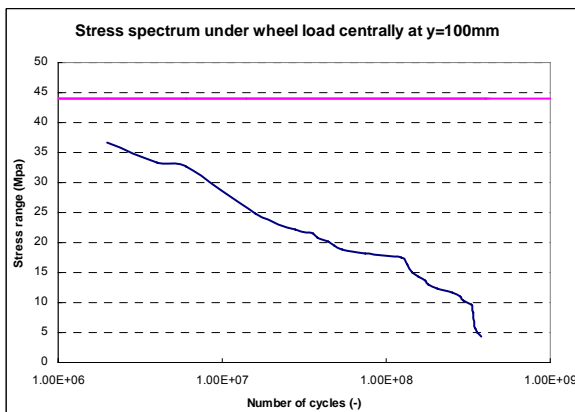
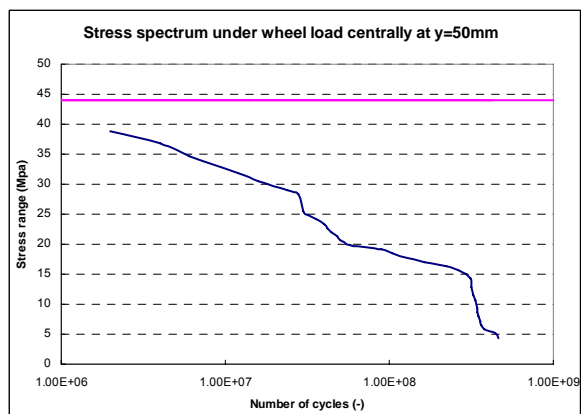
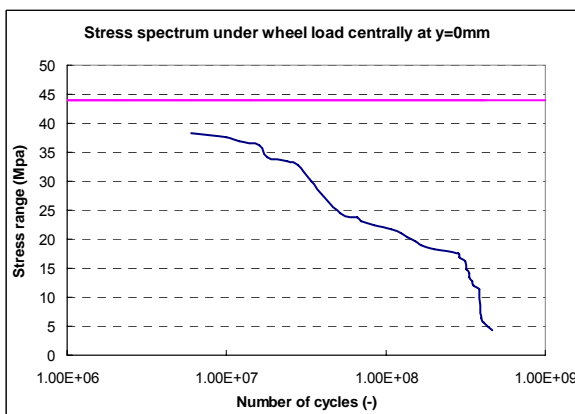
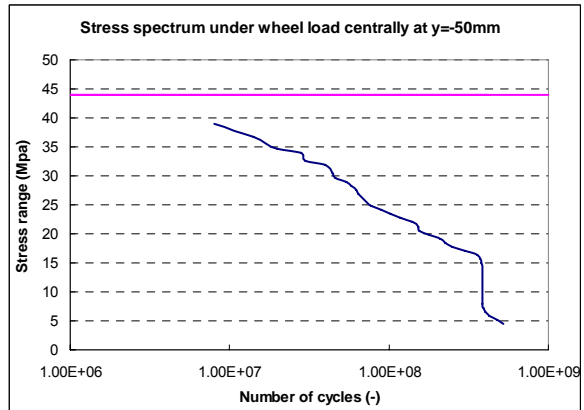
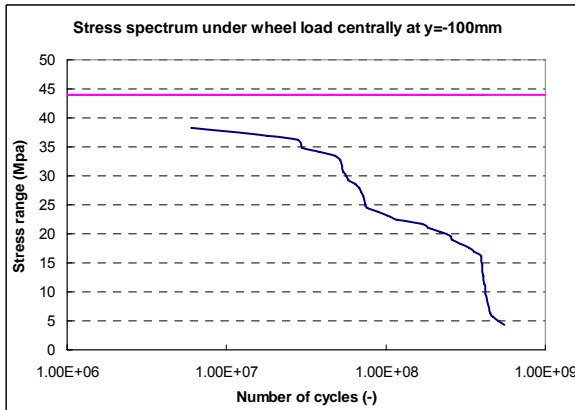


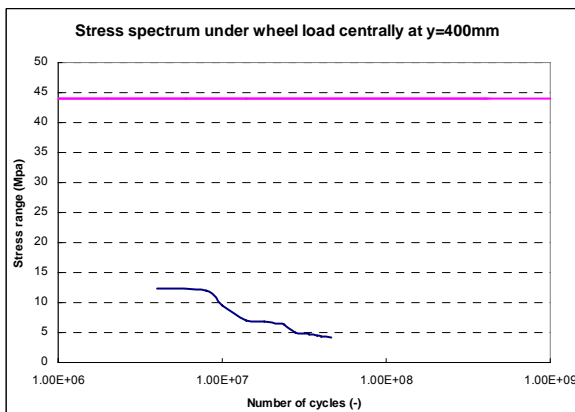
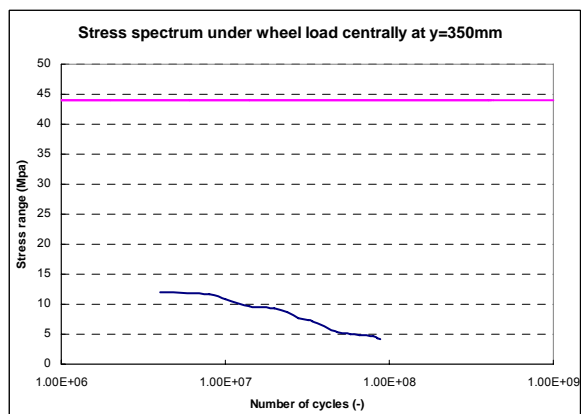
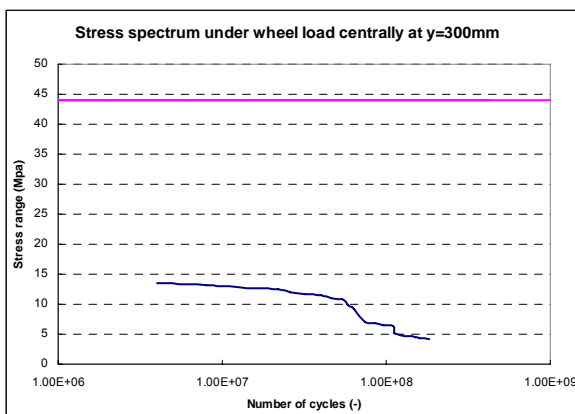
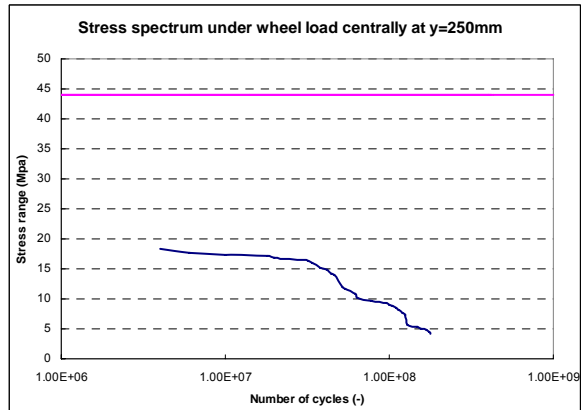
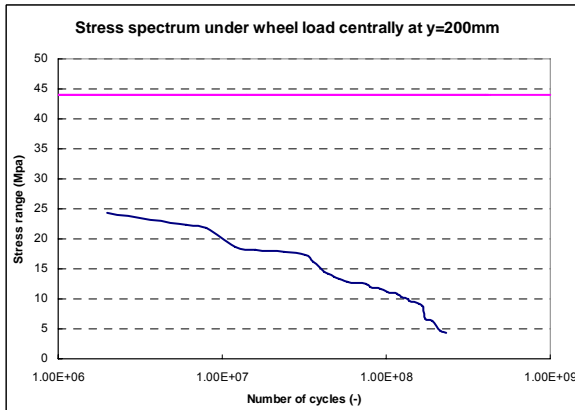




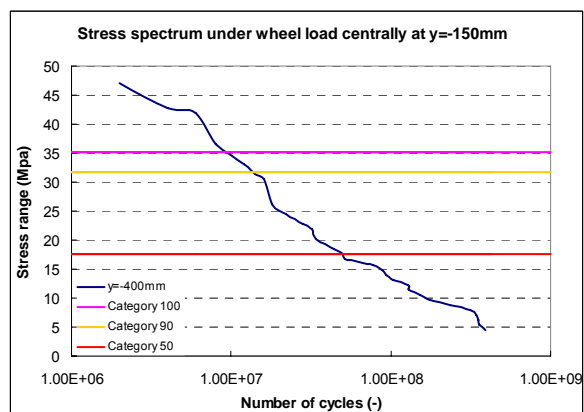
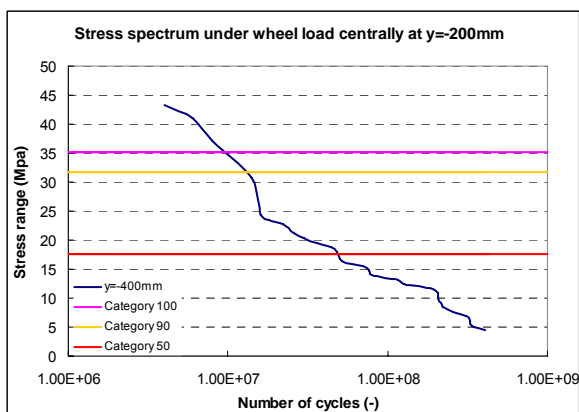
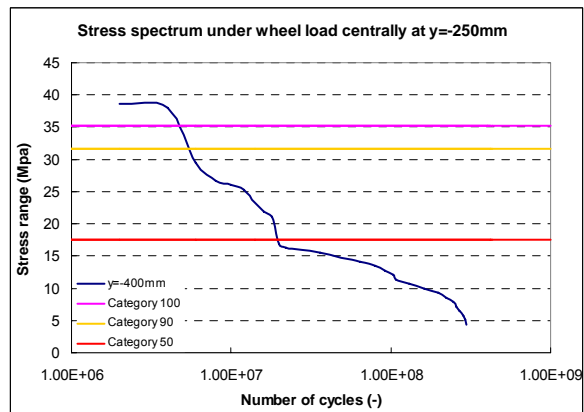
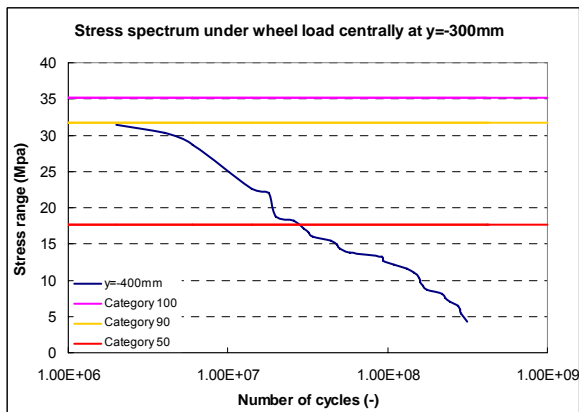
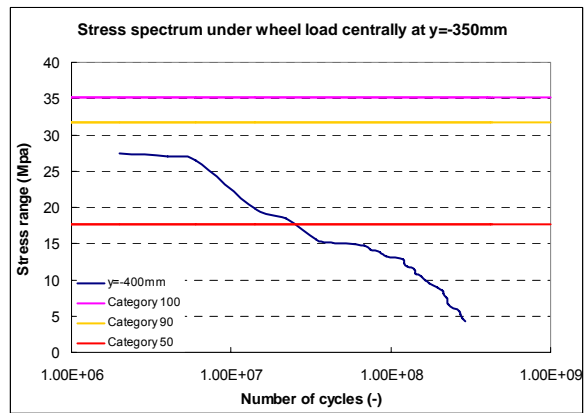
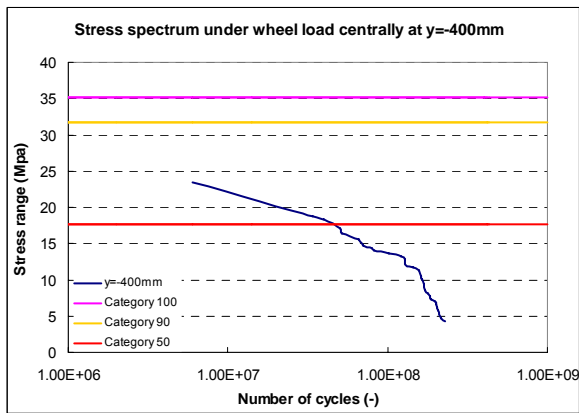
Bottom surface of the exterior deck plate

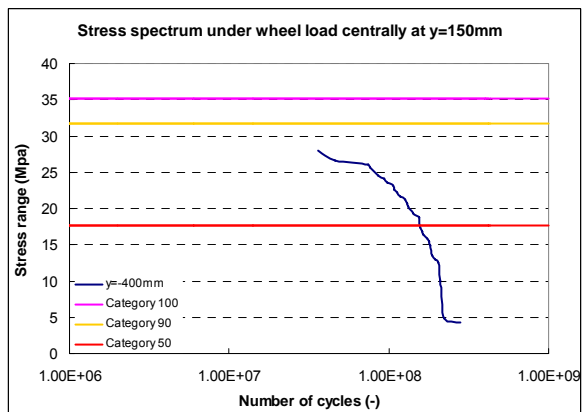
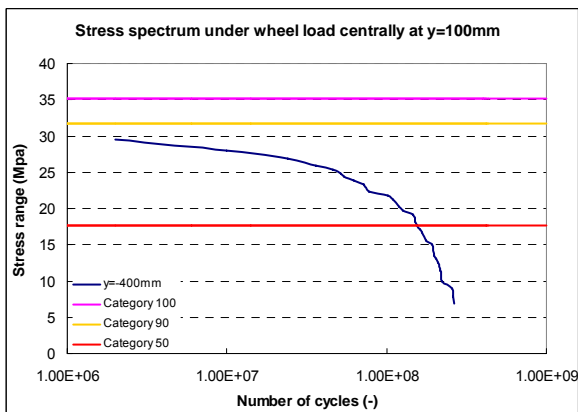
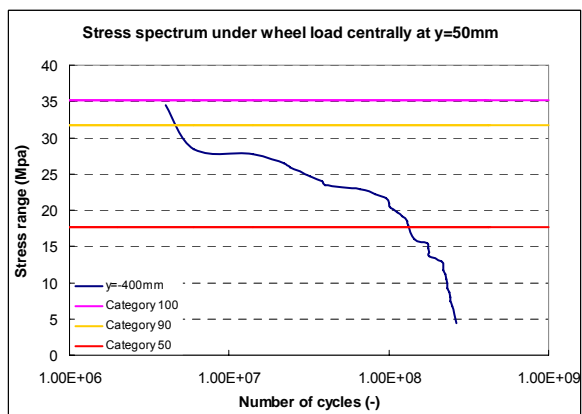
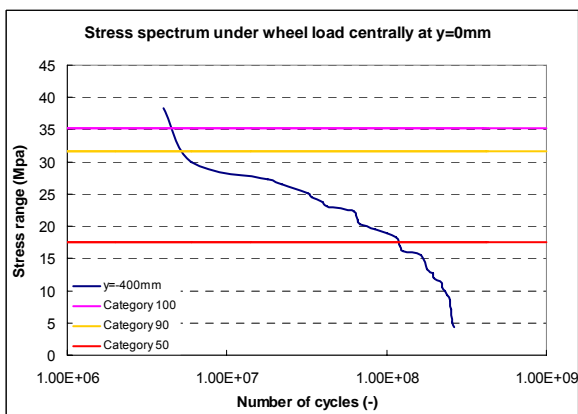
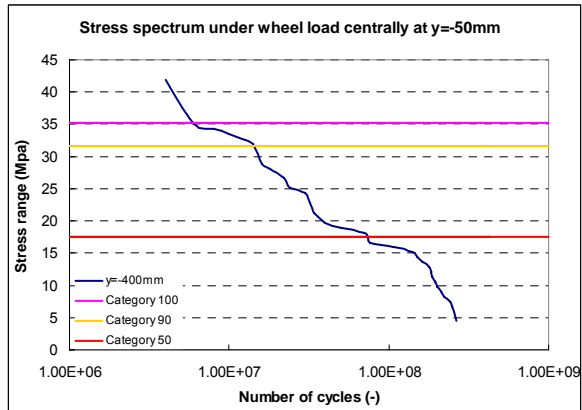
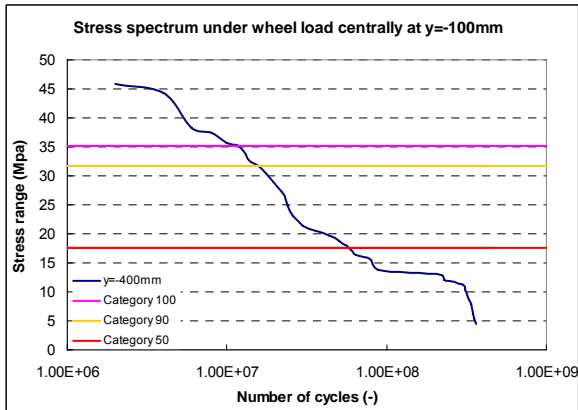


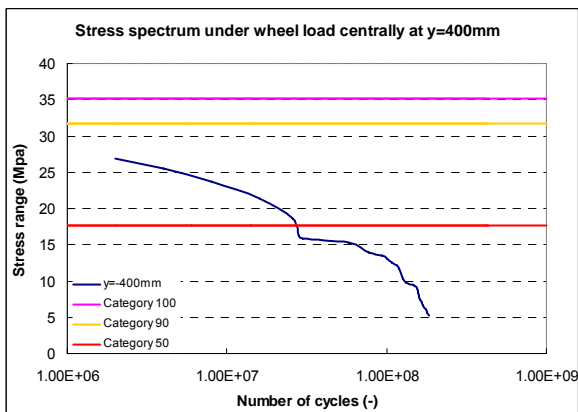
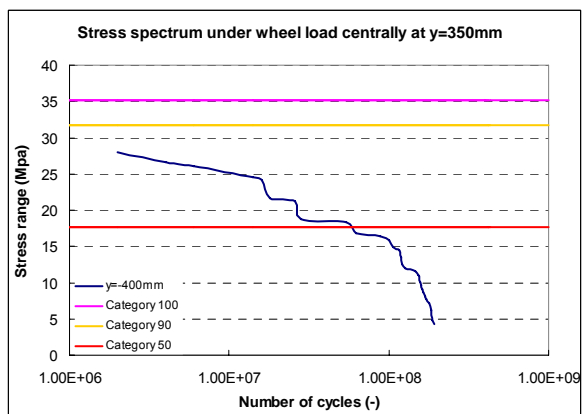
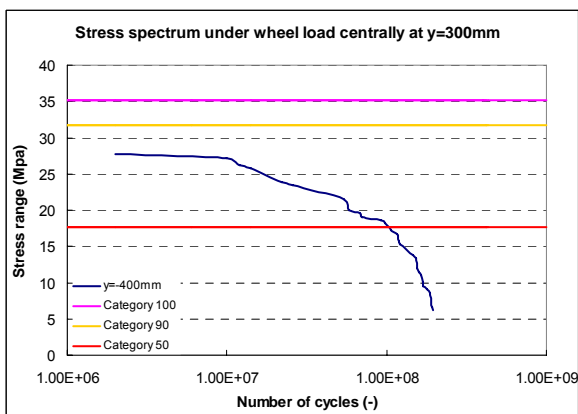
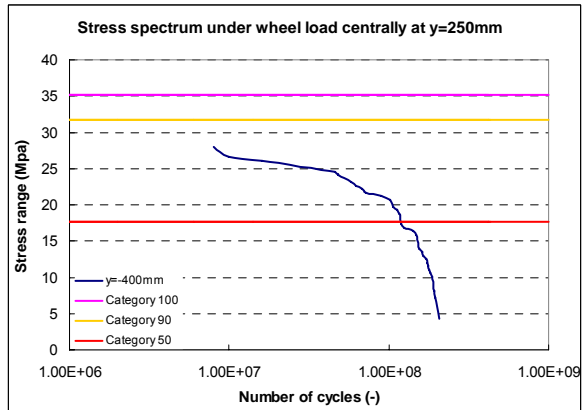
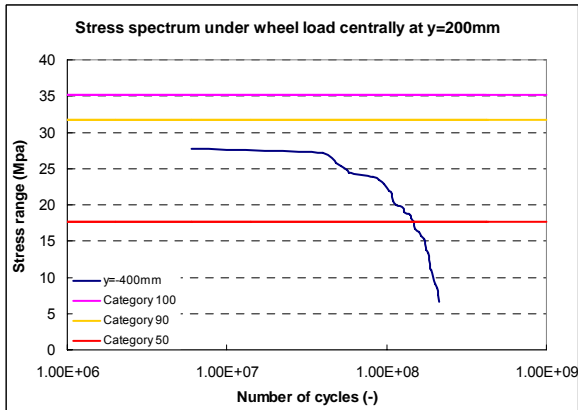




Interior surface of the trough web







Exterior surface of the trough web

